Michael McIntyre

Variations of local heat transfer coefficient in piped flow of viscous liquids.

Submitted for the degree of Doctor of Philosophy.

January 1973.

SUMMARY.

Measurements were carried out to determine local coefficients of heat transfer in short lengths of horizontal pipe, and in the region of a discontinuity in pipe diameter. Laminar, transitional and turbulent flow regimes were investigated, and mixtures of propylene glycol and water were used in the experiments to give a range of viscous fluids.

Theoretical and empirical analyses were implemented to find how the fundamental mechanism of forced convection was modified by the secondary effects of free convection, temperature dependent viscosity, and viscous dissipation.

From experiments with the short tube it was possible to determine simple empirical relationships describing the axial distribution of the local Nusselt number and its dependence on the Reynolds and Prandtl numbers. Small corrections were made to account for the secondary effects mentioned above. Two different entrance configurations were investigated to demonstrate how conditions upstream could influence the heat transfer coefficients measured downstream.

In experiments with a sudden contraction in pipe diameter the distribution of local Nusselt number depended on the Prandtl number of the fluid in a complicated way. Graphical data is presented describing this dependence for a range of fluids indicating how the local Nusselt number varied with the diameter-ratio. Ratios up to 3.34:1 were considered.

With a sudden divergence in pipe diameter, it was possible to derive the axial distribution of the local Nusselt number for a range of Reynolds and Prandtl numbers in a similar way to the 'convergence' experiments. Difficulty was encountered in explaining some of the measurements obtained at low Reynolds numbers, and flow visualization

techniques were used to determine the complex flow patterns which could lead to the anomalous results mentioned.

Tests were carried out with divergences up to 1:3.34 to find the way in which the local Nusselt number varied with the diameter ratio, and a few experiments were carried out with very large ratios up to 14.4.

A limited amount of theoretical analysis of the 'divergence' system was carried out to substantiate certain explanations of the heat transfer mechanisms postulated.

ACKNOWLEDGEMENTS.

The author is indebted to Professor A.J. Ede for his guidance and encouragement in the preparation of the thesis.

He also wishes to thank the Director of the National Engineering Laboratory, East Kilbride, (Department of Trade and Industry) for the opportunity of pursuing this research, for the loan of equipment, financial support and advice on technical problems.

Further thanks are due to the Senate and Staff of the University of Aston in Birmingham for providing the extensive facilities which made the work possible.

PREFACE.

In preparing this thesis it was decided that particular consideration should be given to the background of the reader who, in some cases, may be familiar with the terminology of heat-transfer but have a practical rather than formal appreciation of the subject. It is hoped that part 2. of the thesis will present a sufficient background to the underlying problems without being pedantic.

The theoretical aspects of the work are presented in a single section, part 11. of the thesis. In practice the analytical work was carried out in small sections, each supporting some particular aspect of the experimental investigations. To position each section of the theory within the text at the appropriate stage of an empirical argument would have meant a loss of continuity in the development of the theory. The method of presnntation chosen leads to a certain number of unavoidable cross-references when reading the thesis.

The figures appropriate to a particular part of the text are contained at the end of that part, and are denoted with a number; which is the same as the part number, followed by a period then a further number, which gives the position in sequence. Occasionally a figure is placed within the text where appropriate. A similar numbering system is used for the most important equations within each part of the thesis.

As far as possible, the numerical data given has been specified in metric units. As a guide to the International System of Units, the following publication was referred to -

B.S.I. publication number PD5686.

A series of data sheets have been made available by the Engineering Sciences Data Unit which provide the designer with information on a range of topics connected with heat transfer in tubes. Preferred results have been correlated from a review of the literature, and relationships for calculating coefficients of heat transfer in tube configurations are proposed, together with an estimate of their reliability. These references provide a much more satisfactory source than the older text books, but have not been considered in this thesis because they do not represent an original source of experimental data, and because the results of this work are supplementary to them - Refs: K.14.

NOMENCLATURE.

The following definitions are generally applicable, but sometimes the text contains symbols which have a local definition and these may or may not appear in the list below. All fluid properties are evaluated at the local bulk temperature of the fluid unless otherwise stated.

c,C	Specific heat capacity at constant pressure.
D	Inside diameter of tube.
e	Electrical resistivity of tube material.
E	Mechanical dissipation paramoter $(\mu \bar{u}^2)/(q r_w)$.
f	Friction factor (see text)
F	Volume flow-rate.
g	Gravitational acceleration.
Gr	Grashof number = $(8\ g\ \rho^2 \beta\ (t_w - t_b) r_w^3\ )/(\mu^2)$.
h	Local coefficient of heat transfer $q/(t_w - t_b)$.
h_∞	Value of h at large axial distances.
h_m	Mean value of h from $\frac{1}{L}\int_0^L h\ dx$
H	Specific Enthalpy.
I	Electrical current in tube wall (A)
k,K	Thermal conductivity.
l	Prandtl's mixing length.
L	An axial (scalar) length of tube.
m	Mass flow-rate.
M	The ratio of two viscosities (see text).
M_{wall}	The local ratio of (viscosity of fluid at bulk temp)/(viscosity at tube wall). (μ_b/μ_w).
Nu	Local Nusselt number.
Nu_∞	Nusselt number at large axial distances.
Nu_m	Mean Nusselt number from $\frac{1}{L}\int_0^L Nu\ dx$.
Nu_o	Defined in text, but generally the value of Nu for a corresponding fluid having constant viscosity and density, and no mechanical dissipation.
p	Static pressure.
P	Electrical power generation.
Pr	Prandtl number $(\mu C/K)$

q	Heat flux at tube wall.
Q	Rate of heat transfer.
Q'	Rate of heat transfer per unit length.
r, R	Radius from tube axis.
Re	Reynolds number $(\rho \bar{u} D/\mu)$.
s	Circumferential distance around tube wall.
S	Diameter ratio (D_2/D_1).
t, T	Temperature.
$u, \bar{u}$	(x-wise) axial velocity, and mean axial velocity.
v	(r or y - wise) velocity along a radius.
V	Applied voltage.
w	(z-wise) circumferential velocity.
x	axial distance downstream direction measured from either onset of heating or from change in tube diameter.
X	Dimensionless axial distance. Either $(x/2r_w)$ or $(x/r_w)/(RePr)$ (always defined in text).
y	Distance from tube wall $(r_w - r)$.
Z	Circumferential distance.

Subscripts:

1,2	Upstream, downstream of diameter change.
b, bulk	Evaluated at mixed mean temperature.
eff	Effective value of parameter.
i	At inner surface.
M, mean	A mean value of the parameter.
o	Evaluated at conditions at the inlet of tube; a reference value of the parameter; or value at outer surface.
t	turbulent component of parameter.
w, wall	Evaluated at the wall temperature.
x	Value at distance x.

β	Temperature coefficient of thermal expansion.
Γ	The Gamma factorial function.
ϵ	Signifies a parameter having a small numerical value.
θ	Dimensionless temperature function $(t - t_n)/(qr_w/K)$ where t_n is some reference temperature i.e. t_b or t_o.
μ	Viscosity.
ζ	Viscosity variation parameter whose value depends on fluid properties and heat flux.
ρ	Density.
σ	Prandtl number.
τ	Shear stress.
ω	Vorticity.

Other Greek symbols appearing in the text are defined locally, for example ϕ can be a mechanical dissipation parameter, or a general mathematical function. ψ can be the stream function or a general mathematical function.

CONTENTS.

1.1. INTERNAL FLUID FLOWS WITH HEAT TRANSFER.

Heat transfer by convection is encountered frequently in engineering processes, and often plays a fundamental part in the operation of plant and machinery. The term 'convection' is used to describe the mode of energy transfer by which heat is transported in a fluid through the motion of the fluid particles. The process is one of 'free' or 'natural convection' when the movement is caused by density differences, and of 'forced convection' when the motion is imparted by an external source of friction force. In practice, these mechanisms are seldom independent of each other, but in many applications 'forced convection' predominates, and this is the case with the experiments described in this thesis.

Internal fluid flows constitute a particularly important class of forced convection systems in engineering. The design of mechanisms often depends crucially on the existence of reliable heat transfer information, and in some cases considerable capital investments are represented by large heat exchangers, so that overspecification is expensive. A list of typical applications serves to illustrate the scope of this subject - heat exchangers in generating plant, cooling passages in electrial machinery, boiler tubes, gas turbine cooling passages, space heating systems, exhaust systems for internal combustion engines, hydraulic controls, bearings, and so on.

This work is concerned with internal fluid flows of the most common type, namely those bounded by circular tubes, where the tube is maintained at a higher temperature than the entrained fluid.

1.2. THE TYPE OF FLUID.

A wide range of fluids is utilised in forced convection applications. Most of these may be classified as being characteristically gaseous, aqueous or viscous; typical examples for instance could be air, water and oil, respectively. The outstanding physical property which distinguishes these fluids is the viscosity, and the relevant orders of magnitude might be .015, 1.0, and 50 centipoise (cP).

From a review of research into heat transfer in tubes (as in part 3) it became apparent that considerable attention has been given in the past to air and water, whereas comparatively little work has been done using viscous fluids; no doubt this is because of the natural abundance of air and water. Since the rate of heat transfer by forced convection is known to be highly dependent on the viscosity of the fluid, it is not possible to extrapolate experimental data derived using low viscosity fluids into the highly viscous region reliably.

One of the main objectives of this work has been the investigation of forced convection in highly viscous fluids, and much of the experimental data is unique in this respect. In many ways this may be viewed as a logical extension of the work of Ede (Ref: H.1, H.2) who studied similar experimental configurations using air and water as the heat transfer media.

In the couse of these investigations a particular kind of internal fluid flow pattern was encountered; this may be briefly described as being a localised region of the fluid in which the flow is stalled and disturbed. The phenomenon is usually termed 'separation' and is well known, however, despite the considerable volume of publications on the subject of heat transfer in separation, no previous works could be found dealing with viscous fluids. It was intended that this research would help to extend the state of the art in this direction, as well as providing a detailed investigation of some particular tube configurations.

1.3. THE TUBE GEOMETRY.

An extensive range of circular ducts is encountered in heat transfer applications, the simplest and most important being long, straight lengths of uniform diameter tube. Most arrangements also incorporate other shapes, which may be described generally as embodying changes in cross-section or direction. Additionally the straight, uniform duct may be included in very short lengths.

A considerable amount of research effort has been applied to heat transfer in long tubes, and notwithstanding this, publications continue to appear regularly on this topic. At the present time more productive research may be carried out with the other duct geometries mentioned, particularly if the experimental configuration is kept simple and possesses near similitude with a variety of practical systems.

The tube geometries chosen for these investigations were the short, straight tube, and the tube with a change in cross-section. In the latter case a sudden, discontinuous increase or decrease in diameter was considered, since it is known that in this kind of disturbed flow region extremely high rates of heat transfer are possible. In practice, situations of this type arise in the cooling passages of electrical machinery or hydraulic controls, and in multifarious heat exchangers there can be found component parts which at least approximate to the configuration mentioned.

With a little appreciation of the underlying mechanisms of heat transfer it becomes apparent that the sudden convergence or divergence in diameter bears close similarity to other realistic applications, such as a stepped plate, or an exterior surface with certain types of sharp projection. It may even be possible to consider an external, axial flow around a convergence as being qualitatively similar to an internal flow through a divergence. The implication here is that an appreciation of a much wider range of practical, heat transfer problems may be gained than is first realised, as a result of investigating the discontinuous tube described.

Six values of the ratio upstream to downstream diameter were selected in the range 3.3 to 0.3. No special significance was attributed to the actual values used, provided the effects of this ratio upon heat transfer could be determined. Hence, it appeared reasonable to choose diameter ratios at least near to some of those encountered in similar work on gaseous and aqueous fluids, thus facilitating a direct comparison of the results obtained. The range of ratios could be extended as the investigations proceeded, should this become desirable, but the ratio 3.3 was a reasonably practical maximum to impose, even though some applications are bound to exist outside the range considered. This point is taken up later in the thesis.

The unique diameter ratio of unity corresponds to the short, uniform tube or the long, uniform tube depending on the system of heating i.e. for a tube having a discontinuity in the axial distribution of the heat source the situation is analogous to the short tube. In these experiments only the short tube was to be considered.

In selecting experimental tubes three factors have to be considered, the type of material, the quality of the tube surfaces or roughness, and the dimensions of the tube. The material is determined largely by practical considerations, and does not influence the convection process. The tube dimensions are also chosen on practical grounds, but the diameter may well be related to the convection process in some way which can only become clear with hindsight. The actual sizes chosen were of the same order of magnitude as would be encountered in a typical heat exchanger - insofar as one can generalise. The roughness may affect the fluid flow pattern, however, it is sufficient at this stage to say that the tube surfaces were hydraulically smooth, as is the case in the majority of real applications. These points will be further discussed in part 5.

1.4. TRANSFER MECHANISMS OF HEAT AND MOMENTUM.

Any discussion on convective heat transfer must of necessity include a description of the fluid flow. It is usual for heat to be transferred from a solid boundary to an adjacent fluid medium, and the mechanism is simple to illustrate qualitatively. Moving particles of fluid change position relative to the boundary and pass through regions of different temperature level. Heat is gained or lost by a particle through the process of conduction, the amount depending on the velocity and direction of the particle relative to the boundary. The greater the rate of interchange of particles between the space near to and distant from the boundary, the greater the amount of heat transferred.

It is evident that a highly disturbed flow will transfer heat more effectively than one which moves smoothly, parallel to the boundary. Furthermore, a fast moving flow will be more effective in transferring heat than a slow one.

Steady, forced flows may be defined as characteristically 'laminar' or 'turbulent.' The former refers to those in which the molecules of fluid slide smoothly over each other and the motion appears not to change with time. Turbulent flows are very disturbed, and the molecules move randomly throughout the fluid. At a given point in the flow, the velocity is time dependent in magnitude and direction, however, it is usually possible to consider the actual velocity as being made up of a mean velocity with superimposed velocity fluctuations. This means the main, mean velocity component has magnitude and direction which is not time dependent.

For a given geometry at the boundary, both laminar and turbulent flow may exist, but the existence of either depends largely on the magnitude of the mean velocity. Generally, turbulence occurs in 'fast' flows and lamination in 'slow' flows. For a given fluid, and above a certain mean velocity, the turbulent regime can be sustained. Near to this critical velocity there is often a 'transitional' flow regime in which regions of the flow oscillate between turbulence and lamination.

In studying a particular forced convection system it is necessary to specify the type of heating, so in an effort to generalise on the temperature conditions at the boundary two realistic situations are found useful. First, the boundary may be maintained at a constant, uniform temperature throughout the entire surface, and second, a uniform rate of heating per unit area (or uniform heat-flux) may be used as the constraint. These conditions are somewhat idealised, and in reality something between the two is to be expected, however, experience has indicated that there is little to choose between either with regard to the applicability of the experimental results. The first constraint is similar to the kind of boundary condition found on a tube in an evaporator or condensor, and the second kind appears in equipment where the heat source is electrical, radiant or nuclear. In the present work the uniform heat flux condition was selected, primarily because of certain advantages in the construction and operation of the experimental apparatus.

1.5. A DESIRABLE RANGE OF FLOW RATE.

From a previous knowledge of flow in plain tubes it was possible to estimate the minimum velocity at which full turbulence was likely to occur. This may be given approximately by the formula

$$\text{Velocity} = 10^4 \times \text{Viscosity}/(\text{Density} \times \text{Diameter}).$$

It was desirable that heat transfer measurements be made in the laminar, transitional and turbulent regimes. In practice the range of flow-rate must be limited by the maximum, attainable pressure drop in the tube, at the other end of this range no obvious, practical limitation exists. The pressure drop is known to be proportional to the square of velocity, so that when viscous fluids are used the system pressure is likely to be high. From the above equation it is seen that by increasing the viscosity by a factor of 20, and for a similar range of experimental results, with respect to the flow-regime, the system pressure must be increased by 400 times.

It was decided initially that the maximum flow rate required be given approximately by twice that value necessary for full turbulence, the fluid being ten times as viscous as water. The maximum system pressure thus obtained was of the order 700kN/m^2.

2. FUNDAMENTALS AND HISTORICAL BACKGROUND.

2.1. INTRODUCTION.

It is desirable at this stage to give an account of the earlier works concerned with heat transfer in tubes, the purpose being to introduce some of the fundamental concepts which arise in work of this nature, and to present the background from which the current research has evolved. This section begins with an explanation of some important principles encountered in convective heat transfer (2.2.).

2.2. EXPERIMENTAL AND THEORETICAL FUNDAMENTALS.

2.2.(i) DIMENSIONLESS GROUPS.

In forced convective heat transfer, analysis may proceed on theoretical or empirical lines. In general however, the information required is obtained by conducting experiments, then determining correlations between various groups of significant parameters. Usually, measurements of the coefficient of heat transfer, h, are carried out, this variable being defined by Newton's Law of cooling, $q = h\Delta t$. In the latter expression q is the heat flux, and Δt the temperature difference between the heated surface and the fluid medium.

The following dimensionless groups of parameters are encountered frequently in fluid mechanics and heat transfer, and will occur throughout this thesis.

Nusselt number $Nu = \frac{hD}{K}$, Reynolds number $Re = \frac{\rho \bar{u} D}{\mu}$,

Prandtl number $Pr = \frac{\mu c}{K}$, Grashof number $Gr = \frac{g \rho^2 D^3 \beta \Delta t}{\mu^2}$,

Dimensionless distance $X = x/D$,

where $\Delta t = q/h$ or $(t_w - t_b)$,

t_w = the temperature at the inner tube surface,

t_b = bulk, or mixed mean temperature of the fluid

$= 2 \int_0^1 (u/\bar{u})(r/r_w)t \; d(r/r_w)$,

$u, \bar{u}$ = axial velocity of fluid, and the mean velocity,

$\bar{u} = 2 \int_0^1 (r/r_w) \, u \; d(r/r_w)$,

$D = 2r_w$ or inner diameter of the tube,

x = distance from the onset of heating.

In convective heat transfer the value of the dependent variable Nu can often be obtained from an expression of the kind

$$Nu = f(Re, Pr, Gr, X) \qquad (2.1)$$

where the functionality is determined experimentally. The uniqueness of this kind of relationship depends on the validity of the initial assumptions made regarding the significance of certain experimental variables. In this research, consideration was given to frictional heating in the fluid, the temperature dependence of the viscosity, and the way in which these phenomena could affect the value of Nu. The above expression excludes any such dependence.

2.2.(ii) THE ENERGY AND MOMENTUM EQUATIONS.

The derivations of the energy and momuntum (or Navier-Stokes) equations are given in many standard text books (e.g. Ref K.1). For steady, incompressible, axi-symmetrical flow through a tube with axi-symmetrical temperature distribution, these equations are stated -

$$\rho u \frac{\partial H}{\partial x} + \rho v \frac{\partial H}{\partial r} - \frac{1}{r}\frac{\partial}{\partial r}\left[r K \frac{\partial t}{\partial r}\right] - \frac{\partial}{\partial x}\left[K \frac{\partial t}{\partial x}\right] - \mu\phi - u\frac{\partial p}{\partial x} - v\frac{\partial p}{\partial r} = 0 \qquad (2.2)$$

where

$$\phi = 2\left(\left(\frac{\partial u}{\partial x}\right)^2 + \left(\frac{\partial v}{\partial r}\right)^2\right) + \left[\frac{\partial v}{\partial x} + \frac{\partial u}{\partial r}\right]^2 - \frac{2}{3}\left[\frac{\partial v}{\partial r} + \frac{v}{r} + \frac{\partial u}{\partial x}\right]^2 \qquad (2.3)$$

and

$$\rho u \frac{\partial u}{\partial x} + \rho v \frac{\partial u}{\partial r} = -\frac{\partial p}{\partial x} + 2\frac{\partial}{\partial x}\left[\mu \frac{\partial u}{\partial x}\right] + \frac{1}{r}\frac{\partial}{\partial r}\left[\mu r\left(\frac{\partial v}{\partial x} + \frac{\partial u}{\partial r}\right)\right] \qquad (2.4)$$

with

$$\rho v \frac{\partial v}{\partial r} + \rho u \frac{\partial v}{\partial x} = -\frac{\partial p}{\partial r} + 2\frac{\partial}{\partial r}\left[\mu \frac{\partial v}{\partial r}\right] + \frac{\partial}{\partial x}\left[\mu\left(\frac{\partial v}{\partial x} + \frac{\partial u}{\partial r}\right)\right] + 2\frac{\mu}{r}\left[\frac{\partial v}{\partial r} - \frac{v}{r}\right] \qquad (2.5)$$

The equation of continuity is $\frac{\partial u}{\partial x} + \frac{\partial v}{\partial r} + \frac{v}{r} = 0$. (2.6)

Some of the theoretical work carried out in this research required the use of the above equations, but the well known boundary-layer simplifications of Prandtl were applied for the analyses associated with unidirectional flows. The energy equation, unlike that of Prandtl, retains a first order approximation for the dissipation function ϕ, as follows:

$$\rho u \frac{\partial t}{\partial x} + \rho v \frac{\partial t}{\partial r} = \frac{1}{r}\frac{\partial}{\partial r}\left(\frac{K}{c} r \frac{\partial t}{\partial r}\right) + \frac{\mu}{c}\left(\frac{\partial u}{\partial r}\right)^2 . \qquad (2.7)$$

The single momentum equation becomes

$$\rho u \frac{\partial u}{\partial x} + \rho v \frac{\partial u}{\partial r} = -\frac{dp}{dx} + \frac{1}{r}\frac{\partial}{\partial r}\left(\mu r \frac{\partial u}{\partial r}\right) . \qquad (2.8)$$

The specific heat capacity is assumed to be constant, which is a reasonable approximation for most liquids.

2.2.(iii) THE LAMINAR REGIME.

In the investigation of laminar flows (in a uniform tube laminar flow is known to be present when $Re < 2,500$) the axial velocity distribution in the fluid must be specified at the tube entrance. For most applications an adequate description of this flow condition would be that the velocity profile is 'developed' or 'undeveloped'. The former condition implies a parabolic radial distribution, and the latter implies uniform distribution. During laminar heat-transfer the thermal conductivity is assumed to be constant, since variations with temperature are of the order $\frac{1}{4}$% per Kelvin.

2.2.(iv) THE TURBULENT REGIME.

For Reynolds numbers above 2,500 in a straight tube, the flow is usually turbulent. It is well understood (Ref: K4.) that full turbulence can be sustained when Re is approximately

4,000 to 10,000, and that for intermediate Re a transitional regime occurs. When the geometry of the system is altered the numbers quoted have little relevance, so when discontinuous tubes are encountered, as in this research, the possibility of a more complicated flow regime with different, critical Reynolds numbers, must be considered.

In the theoretical analysis of turbulent flow, it is usual to treat the system as a laminar one, for convenience, but to replace the viscosity and thermal conductivity by 'effective' properties which have an added turbulent component: viz:

μ(effective) = μ(laminar) + μ(turb), K(effective) = K(laminar) + K(turb.),

or $\mu_{eff} = (\mu + \mu_{turb})$, $K_{eff} = (K + K_{turb})$.

The Reynolds analogy can be used to determine the relationship between μ_{turb} and K_{turb}. This states that the rate of transport of heat by turbulence is the same as the rate of transport of momentum (for unit heat flux and stress). Therefore $\frac{1}{q_y}\cdot\frac{\partial}{\partial y}(\rho c t) = \frac{1}{\tau_{xy}}\frac{\partial}{\partial y}(\rho u)$

or $$\left(\frac{\mu_{turb}\, C}{K_{turb}}\right) = 1 \quad .$$

A model of turbulent flow near to a heated surface was developed in 1910 by Prandtl, and successive improvements by Von Karman in 1939 (Ref: C.5) and later by Martinelli, 1941 (Ref: C.6) produced a workable theory which enabled coefficients of heat transfer to be calculated for fluids with different Prandtl numbers. The theory was applied to long tubes and was reliable for moderately high Prandtl numbers ($\widetilde{30}$). The model referred to made allowance for the fact that turbulent eddies are damped by viscous action near to a surface. A laminar sub-layer was hypothesised, and a fully turbulent mainstream. In between these two extremes, a buffer layer was inserted which was only partially turbulent.

In 1925 Prandtl proposed the 'mixing length theory' which has benn widely used in the analysis of turbulent flows. The properties μ_{turb} and K_{turb} are calculated from the following formula -

$$\left(\frac{\mu_{turb}}{\rho}\right) = \left(\frac{K_{turb}}{\rho C}\right) = \ell^2 \left|\frac{du}{dy}\right|$$

, where ℓ is proportional to the width of the mixing region, or width of the boundary layer.

The equations of momentum and energy become greatly simplified for turbulent flow near a wall, because streamlines are almost parallel. Hence -

$$\rho u C \frac{\partial t}{\partial x} = \frac{\partial}{\partial r}\left(K_{eff} \frac{\partial t}{\partial r}\right) + \mu_{eff}\left(\frac{\partial u}{\partial r}\right)^2 \qquad (2.9)$$

with $$\frac{dp}{dx} = \frac{\partial}{\partial r}\left(\mu_{eff} \frac{\partial u}{\partial r}\right). \qquad (2.10)$$

2.2.(v) SEPARATED FLOWS.

Flow in tubes may often be considered as boundary-layer flow since the axial velocity component usually predominates. If the flow is disturbed by a discontinuity in the tube's geometry a localised region of the fluid may experience an adverse pressure gradient which causes large transverse velocity components. The axial velociety may be reversed locally, and a standing eddy (indicated by closed streamlines) formed downstream of the discontinuity. This kind of flow is termed 'separated', and separation can have a considerable effect on the local coefficient of heat transfer.

In general, the boundary-layer equations cannot be used to analyse this sort of problem, only a solution of the full equations will suffice.

The early experiments of Boelter (Ref: H.15) on forced convection with air in tubes having different entrance configurations, gave evidence as to the general character of heat transfer during separation. The local coefficient of heat transfer becomes very high, about four times greater than its non-separated value. The location of the maximum value is probably near to the point of boundary-layer reattachment, i.e. the point downstream of the separation 'bubble' at which the direction of the flow reverses on the heat-transfer surface, and the entire domain becomes a boundary layer. The magnitude of the local coefficient of heat transfer falls away sharply as the distance from the position of the maximum value increases.

The length of the separated region remains reasonably constant at high Re and is about seven times the height of the discontinuity causing separation when this is a sharp projection or downward step in the flow direction. At low Re, though how low cannot be defined, the length of the region could well increase with reducing Reynolds number, but this must remain intuitive for the present.

Separation may also be caused by an upward step in the flow direction, or by various forms of cavity. Even smooth directional changes such as occur in a diffuser, around a bend, or in cross-flow, over a cylinder can cause separation. The latter was the subject of many early heat-transfer researches (see Knudsen and Katz Ref: K.3) but such configurations have little relevance in this work and will not be discussed.

Because of its importance in aerodynamic applications, the study of separated heat transfer has tended to be limited to gaseous media and in particular with supersonic velocities. Some recent investigators (Ref: H.1, H.9, H.14, H.17) have used water, but no previous data is available for viscous fluids.

2.2.(vi) THE PRANDTL NUMBER AND VISCOUS FLUIDS.

Before proceeding with a discussion on heat transfer in tubes, it should be pointed out that viscous fluids generally have a high Prandtl number. Since it is sometimes convenient to utilise dimensionless groups, the terms 'viscous fluids' and 'fluids with high Prandtl number' are often used synonymously in this sense.

2.3. THE LONG STRAIGHT TUBE.

2.3.(i) DESCRIPTION.

The long straight tube is defined as one in which the axial velocity gradient is zero, and the axial temperature gradient is constant. In practice, this implies a length of at least 100 diameters in the turbulent regime, or (0.05 Re Pr) diameters in the laminar regime (e.g. see Kays Ref: K.5)

2.3.(ii) LAMINAR HEAT TRANSFER.

This elementary problem has been solved theoretically yielding $Nu_{\infty} = 4.36$, and experimental corroboration has been obtained (Ref: C.1).

2.3.(iii) TURBULENT HEAT TRANSFER.

Considerable interest has been shown in turbulent heat-transfer in long tubes. Theoretical and experimental analyses have been carried out, some of which will be discussed.

Numerous papers on the subject were published prior to 1936. McAdams (Ref: K.2) gives a comprehensive review of these. Most of the experimental data was correlated with equations of the form $Nu_{\infty} = B.Re^{m}.Pr^{n}$, where B, m and n are constants. Some controversy existed as to the best reference temperature for determining the fluid properties, but this was of little consequence since the temperature differences $(t_w - t_b)$ employed were usually small, and the physical properties varied insignificantly. The values of the experimental constants which best suited the data available were found by McAdams to be $B = 0.023$, $m = 0.8$ and $n = 0.4$, for the following conditions: $Re > 10,000$, $0.7 < Pr < 100$. The value of Nu_∞ can be estimated with $\pm$ 30% accuracy from this exponential relationship, which is remarkable when consideration is given to the comparatively crude apparatus utilised in the early researches.

Little data existed at the time for experiments with viscous fluids. In 1928 Morris and Whitman (Ref: A.5) did some tests on oils with viscosities up to 55 cP. The mean rate of heat transfer was determined for a steam-heated tube 150 diameters long. The temperature differences $(t_w - t_b)$ were in the range 15 to 70 K. It was recommended that the following constants be used, $m = 0.83$, $n = 0.37$, and it was pointed out that with viscous liquids, the high dependence of viscosity on temperature made the choice of reference temperature an important issue.

In 1932 Sherwood (Ref: A.7.) conducted some experiments similar to those of Morris and Whitman, incorporating a range of viscous fluids. The bulk temperature was used for determining the properties, and it was concluded that the value of Nu_∞ should be given by $Nu_\infty = 0.023\, Re^{0.8}\, Pr^{0.4}$. This is in agreement with the equation already quoted, which was based largely on data obtained with non-viscous fluids. Sherwood suggested that the exponent of Re could possibly increase slightly with increasing Pr.

In 1933 Colburn made some recommendations (Ref: A.8) on how to correlate the experimental results for a long tube with heat transfer, and supported his hypothesis with existing data. Nu_∞ was supposed to be proportional to $Pr^{\frac{1}{3}}$, and the reference temperaturefor determining the physical properties was taken as the average of the wall temperature and the bulk temperature. It was further suggested that the viscosity-temperature dependence be taken into account by making Nu_∞ a function of (viscosity at bulk temp.)/(viscosity at reference temp.).

In 1936 Sieder and Tate (Ref: D.1) reconsidered some earlier experimental data obtained from tests to determine the mean rate of heat transfer to oils in a long steam-heated tube. Colburn's conclusions were simplified for practical reasons and the ensuing relationship proposed was $Nu = 0.027\, Re^{0.8} . Pr^{\frac{1}{3}} . M_{wall}^{0.14}$, where M_{wall} was (viscosity at the wall)/(viscosity at bulk temp.), and all other properties were estimated at the bulk temperature. This expression has gained wide acceptance by virtue of its simplicity and is still in use today despite the fact that experimental deviations of $\pm$ 30% were evident in the original correlation. A graph of the Sieder and Tate results is given in figure 2.1. The authors could not substantiate the selection of the exponent 0.14 in the turbulent regime but conjectured its value from results obtained with laminar flow.

In the theoretical analysis of turbulent heat-transfer in long tubes, the work of Martinelli (Ref: C.6.) in 1941 is outstanding as the first refined analysis. It was no doubt based on the earlier analyses of Prandtl and Von Karman (mentioned in 2.2.(iv)) which were fairly crude attempts. Martinelli made use of Prandtl's mixing length theory, and after an approximate integration of the momentum and energy equations calculated Nu_∞ to be given by

$$Nu_\infty = \frac{(f/2)^{\frac{1}{2}}\, Re\, Pr}{5\, \mathfrak{D} \left\{ Pr + \log(1 + 5\, Pr) + 0.5\, Pr \log\left[\frac{Re}{60} \left(\frac{f}{2} \right)^{\frac{1}{2}} \right] \right\}}$$

where all the properties are determined at the bulk temperature, and

$$f = \tau_{wall} / (\tfrac{1}{2} \rho \bar{u}^2), \quad \text{the friction factor,}$$

$$\mathfrak{D} = \frac{(\text{wall temp} - \text{bulk temp})}{(\text{wall temp} - \text{temp at centre of tube})}$$

Martinelli claimed $\pm$ 20% accuracy in the range

$$Re > 10^5 \quad , \quad 0.5 < Pr < 350$$

It is possible that this was an overoptimistic estimate of reliability particularly when high values of Pr are encountered. As the diagram (Figure 2.2) indicates, with Pr = 100, 95% of the temperature drop $(t_w - t_b)$ occurs in the region of the laminar sublayer. Some special consideration should be given in such an extreme case.

2.3.(iv) TRANSITIONAL HEAT TRANSFER.

In the transitional region $(2,500 < Re < 10,000)$ comparatively little research has been carried out. This is probably due to the erratical behaviour of the tube temperature, which is a consequence of the very disturbed flow pattern and accompanies transition. McAdams (Ref: K.2) made some tentative suggestions but Colburn (Ref: A.8) attempted the first significant correlation of experimental data.

Colburn showed that the mean value of Nu_{∞}, with respect to time, changed smoothly from the characteristically low values associated with laminar flow, to the characteristically high values associated with turbulent flow, as the Reynolds number increased from 2,500 to 10,000. It is interesting to note that the data for fluids having a low viscosity did not correlate nearly as well as the data for viscous fluids.

Sieder and Tate (Ref: D.1.) included much experimental data for the transition region in their work on viscous liquids. They showed that plotting

$$(Nu_{\infty}/Pr^{\frac{1}{3}}) \text{ versus } Re$$

gave a unique relationship when the tube length was great.

The experiments of Norris and Sims (Ref: A.9.) dealt with cooling, rather than heating, in the transitional region. It was shown that for fluids with Pr in the range 35 to 140, the value of Nu_{∞} could be estimated from $Nu_{\infty} = 0.0067\ Re.Pr^{0.2}$, when $3,500 < Re < 11,000$.

The maximum experimental errors were approximately 5%, and the tests carried out were repeatable. This work indicated that useful heat-transfer information can be obtained with transitional flow, despite the fluctuating temperatures.

2.4. THE SHORT STRAIGHT TUBE.

2.4.(i) DESCRIPTION.

In the early research, little attention was given to the measurement of local coefficients of heat transfer, and consequently when short lengths of tube were encountered mean Nusselt numbers, dependent on the overall tube length, were postulated. These will be written Nu_m in this thesis. In general, the local Nusselt number, Nu, is dependent on the axial position, and the measurement of this axial profile is more complicated than the measurement of Nu_m.

Consider a fluid entering a uniformly heated section of tube. At onset of heating, $x = 0$, there is a heat flux but no heat has penetrated the fluid. This implies that $Nu = \infty$ by definition. Further downstream at $x = x_1$, a temperature profile has developed within the fluid therefore $Nu = Nu_1$, which is less than infinite. Hence, Nu must fall with increasing axial distance.

The function Nu(x), must be dependent, amongst other things, on whether a developed or undeveloped velocity profile is present at the onset of heating.

2.4.(ii) LAMINAR HEAT TRANSFER.

Theoretical analyses, for the short tube with laminar flow, have been thoroughly investigated since Graetz solved the boundary-layer equations in 1885 (e.g. see Knudsen Ref: K.3.) for a tube at constant temperature, with fully developed velocity. The resulting eigenvalue series in X, Re and Pr converges slowly at high Prandtl numbers and small distances, as do the solutions for other boundary conditions, such as uniform flux with undeveloped velocity at the inlet (Ref: C.13, C.14, C.15, C.16, C.17).

The above-mentioned solutions have been found useful with gaseous media, but unsuitable for viscous media. In 1928 Leveque (Ref: C.18) discovered an asymptotic solution to the uniform tube-temperature problem, for high Pr.

$$Nu = 1.077 \left\{\frac{2r_w}{x} Re\ Pr\right\}^{\frac{1}{3}}$$

The simplifying assumption made was that the velocity profile could be linearised near the wall. This was founded on the observation that 'temperature boundary-layers' are always much thinner than 'velocity boundary-layers' at high Prandtl numbers. The uniform flux problem was solved much later (Ref: C.13).

Most of the early experimental data is quoted in terms of Nu_m, and can only be compared with the local value Nu through the following integral.

$$Nu_m = \frac{1}{L}\int_0^L Nu(x)\ dx.$$

Some of the references already quoted, - Sherwood, Colburn and Sieder - have made use of Nu_m, and the difference should be appreciated as this discussion progresses.

In 1948 Cholette (Ref: B.14) provided some of the earliest measured local coefficients of heat transfer in the laminar regime. The rate of heat transfer to air was measured for a tube heated with a series of small, steam compartments. These rather crude measurements are given in figure: 2.4 , which indicates the variation in the local coefficient of heat transfer, h, with axial distance from the start of heating, X, for different values of Re. For Re $<$ 2,500 the values of h fall rapidly with increasing axial distance, from a high initial value. After approximately 40 diameters the decrease becomes much more gradual.

When viscous fluids are considered, it is necessary to take account of the viscosity-temperature dependence in estimating Nu. Figure 2.3 illustrates how the axial velocity profile is affected by variations in the viscosity. In 1933 Colburn's Synthesis (Ref: A.8) of a variety of experimental data resulted in a viscosity correction of the form $\frac{Nu_m\ (\mu\text{variable})}{Nu_m\ (\mu\text{constant})} = \left(\frac{\mu_b}{\mu_{ref}}\right)^{\frac{1}{3}}$

where μ ref is the viscosity at the average of the wall and bulk temperatures. No rigorous test was made of this proposition, and the work of Sieder and Tate (Ref: D.1) superseded it. Sieder proposed the relationship already discussed in 2.3.(iii) in connection with turbulent flow - $\frac{Nu_m\ (\text{variable})}{Nu_m\ (\text{constant})} = M_{wall}^{0.14}$.

This correction to the Nusselt number gave reasonable results when M_{wall} was varied up to 10. Graphical representation of this relationship is given in figure 2.1.

The way in which free convectional effects modify the flow through a tube is illustrated qualitatively in figure 2.3. In assessing the contribution of free convection to the value of Nu_m Colburn realised the significance of the Grashof number. A tentative estimate of Nu_m was given by Nu_m(with free convec.) = Nu_m (without free convec.) $(1 + 0.015\ Gr^{\frac{1}{3}})$. The properties contained in Gr were evaluated at Colburn's reference temperature, and the equation was considered valid for $Gr > 25{,}000$. Sieder and Tate made a similar suggestion but chose to evaluate properties at the bulk temperature. In 1943 Kern and Othmer pointed out the limitations (Ref: E.2) in such expressions by investigating free and forced convection in horizontal tubes with three oils. The main conclusion reached was that previous correlations were inadequate, and the right hand side of Colburn's equation should contain a function of Reynolds number.

2.4.(iii) TURBULENT HEAT TRANSFER.

McAdams (Ref: K.2) survey of the early research into short tubes with turbulent flow, led to the conclusion that Nu_m could be determined from

$$Nu_m = Nu\left(1 + C\left[\frac{L}{2r_w}\right]\right),$$

where L is the overall tube length, and C is a coefficient, the value of which depends largely on conditions upstream of the tube entrance, but is also a weak function of Reynolds number. Such relationships were reasonable substitutes in the absence of measured, local coefficients of heat transfer.

Cholette's work (described in the preceding section) constituted one of the earliest attempts at measuring local coefficients of heat transfer, h. Figure 2.4 shows how h varied with axial distance for air in a short tube fitted with a 'bellmouth' entrance to establish uniform velocity. In the initial part of the tube the flow developed as a laminar boundary layer, which broke down into turbulence at some distance from the inlet. The characteristic 'dip' in the 'h versus distance' curves can be attributed to the transition from laminar to turbulent flow.

In 1948 Boelter, Young and Iverson (Ref: H.15) measured local values of h for a similar experimental configuration to that of Cholette. In this case the measurements also included data obtained with a 'calming length' fitted to the inlet, which established a fully developed velocity distribution. Figure 2.5 illustrates some of the results, and indicates how the absence of velocity development causes a smooth reduction in h, from a high initial value, to low final value, h_∞, after approximately 40 diameters distance.

No investigations were carried out by the early researchers into the effects of free convection, or viscosity-temperature dependence, on the value of h.

2.5. THE DISCONTINUOUS TUBE.

Boelter, Young and Iverson (Ref: H.15) passed air through a steam-heated tube, which was constructed so that local coefficients of heat transfer could be measured. Different devices were fitted to the inlet of the tube, so that h could be determined downstream of bends, bellmouths, orifices, sharp edged inlets, calming lengths and other configurations. Two of the arrangements have close similarity with the sudden divergence and convergence in diameter, the subjects of this research, and these were described as "the orifice type entrance" and "the right-angle edge type entrance". The studies of Boelter et.al. did much to stimulate the current interest into heat transfer with regions of separated flow, and in tubes with complicated forms.

Figure 2.6 shows 'h versus axial distance' for Re = 27,000. Despite the crude nature of the measurements, the very high coefficients of heat transfer arising near to the inlet of the tube highlighted the value of having data on local coefficients. Where thermal stress in the tube material, or economy of size are important criteria, the design process is more effective when local, rather than mean, values for Nu are available.

The presence of a maximum in h as a function of length was pronounced in the case of the orifice-entrance, but more difficult to explain in the case of the right-angle entrance. Boelter reasoned a priori that a stagnant pocket of air, near to the inlet, caused low coefficients of heat transfer by insulating the mainstream from the tube. Slightly downstream, the flow was supposed to develop in a similar way to the 'short tube', yielding a high value of h which reduced rapidly with increasing distance.

FIGURE 2.1.

THE EXPERIMENTS OF SIEDER AND TATE ON HEATING AND COOLING OILS.

HIGH REYNOLDS NUMBER CORRELATION.*

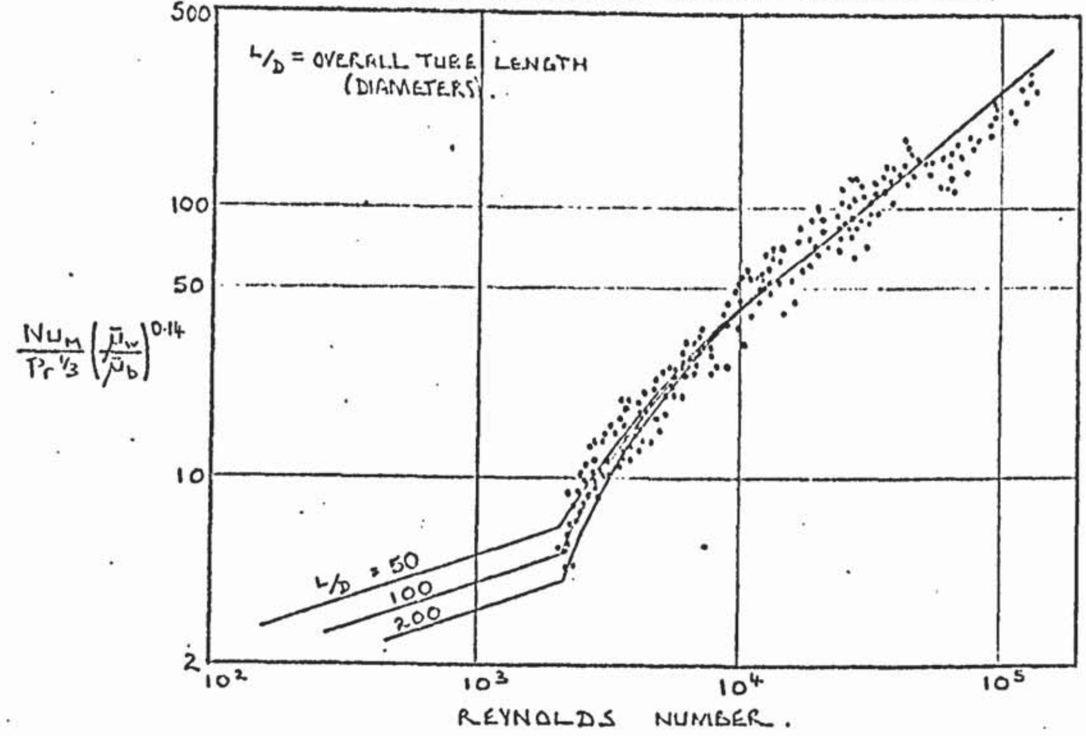

$$\frac{\bar{\mu}_w}{\bar{\mu}_b} = \frac{(\mu \text{ AT WALL TEMP.})}{(\mu \text{ AT AVERAGE TEMP. INLET—OUTLET})}$$

Nu_M = NUSSELT NUMBER - MEAN VALUE FOR A LONG TUBE.

* THE AUTHORS RELIED MAINLY ON OTHER SOURCES FOR DATA USED IN HIGH Re CORRELATION.

LOW REYNOLDS NUMBER CORRELATION.

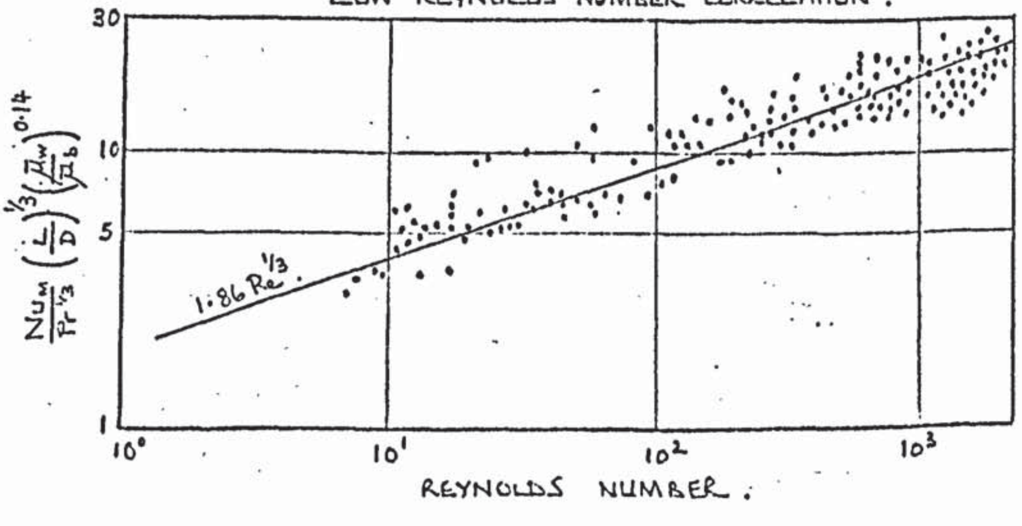

THE EFFECT OF VISCOSITY VARIATION ON Nu AT LOW VALUES OF Re.

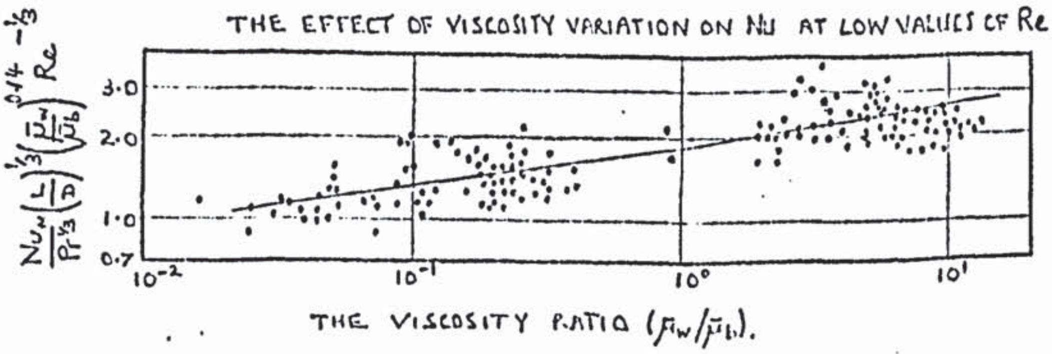

THE VISCOSITY RATIO ($\bar{\mu}_w/\bar{\mu}_b$).

FIGURE 2.2.

RADIAL TEMPERATURE DISTRIBUTION IN TUBE ACCORDING TO MARTINELLI. Re - 10,000 ..

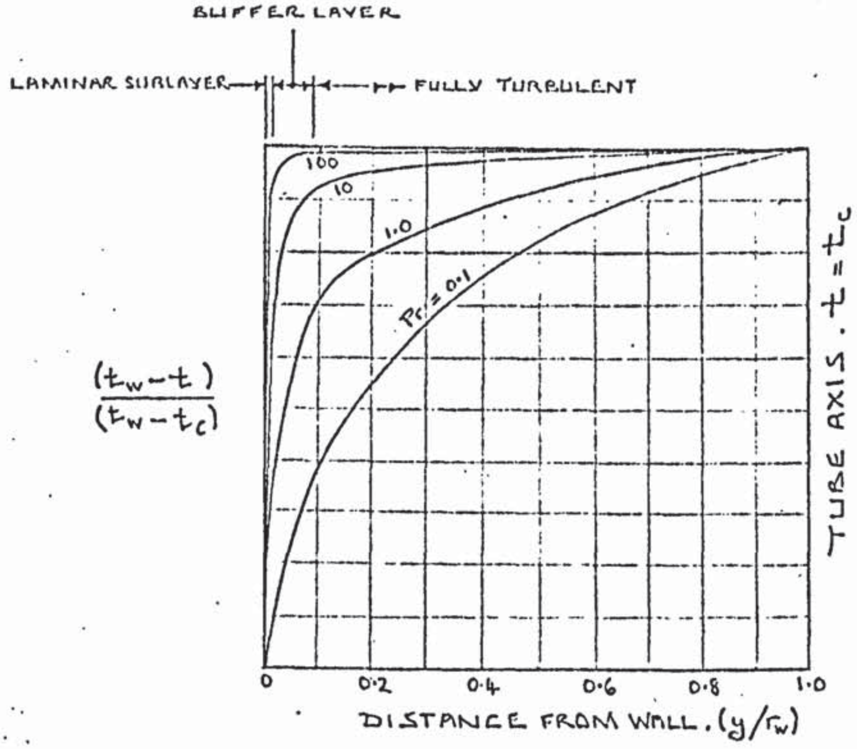

FIGURE 2.3.

ILLUSTRATION OF HOW THE AXIAL VELOCITY DISTRIBUTION IS MODIFIED BY TEMPERATURE DEPENDENT VISCOSITY AND BY FREE CONVECTION.

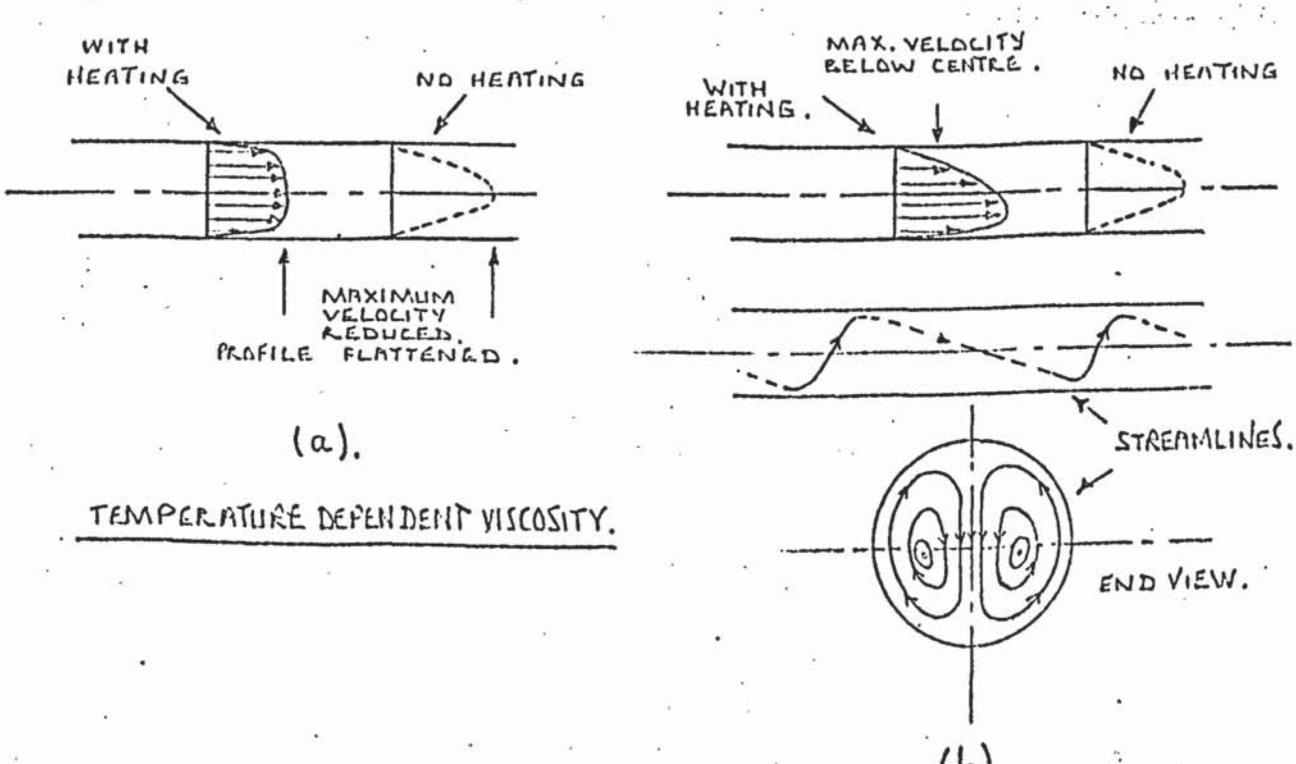

(a).

TEMPERATURE DEPENDENT VISCOSITY.

(b).

FREE CONVECTION PRESENT.

FIGURE 2.4.

HEAT TRANSFER TO AIR FROM CHOLETTE. BELLMOUTH ENTRANCE.

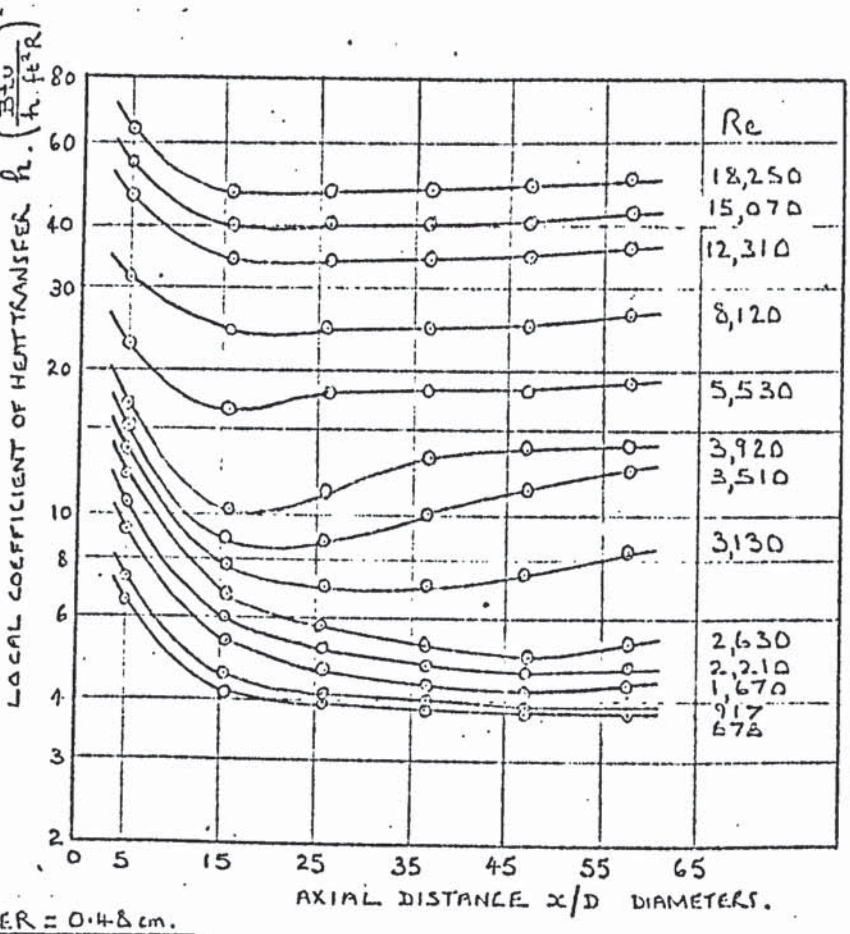

TUBE DIAMETER = 0·48 cm.

FIGURE 2.5.

HEAT TRANSFER TO AIR FROM BOELTER. BELLMOUTH AND CALMING LENGTH.

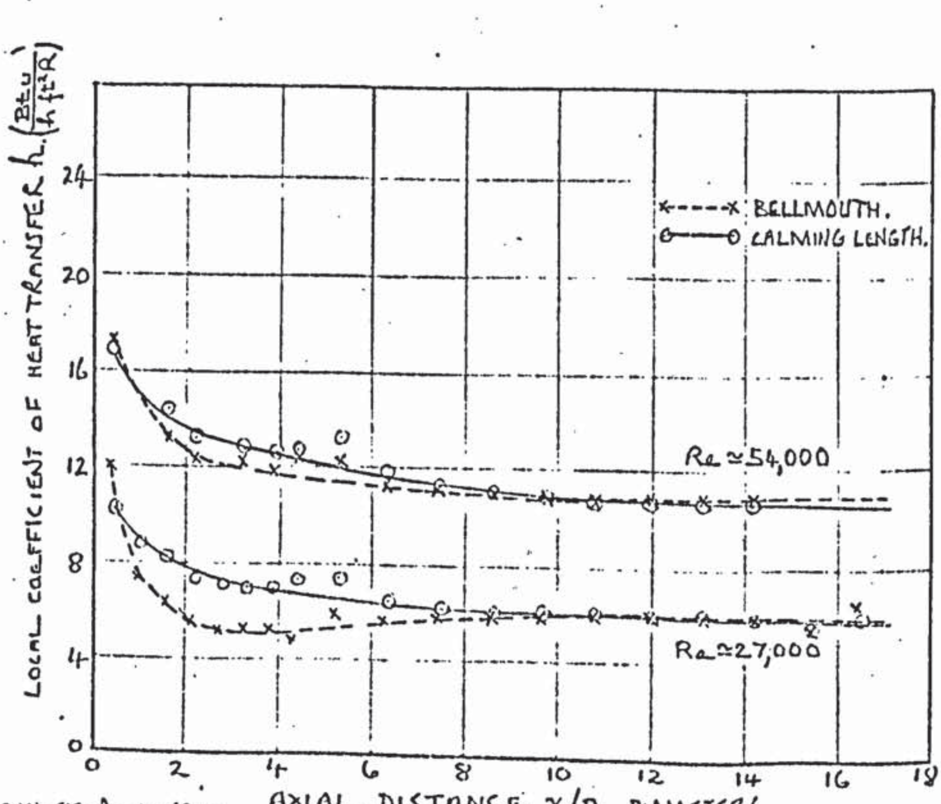

TUBE DIAMETER = 11·53 cm.

* UNITS FROM ORIGINAL SOURCE. $\left(\frac{Btu}{h\ ft^2\ K}\right) = 5{\cdot}678\left(\frac{W}{m^2\ K}\right)$

FIGURE 2.6.

HEAT TRANSFER FOR DIFFERENT ENTRANCE CONFIGURATIONS FROM BOELTER.

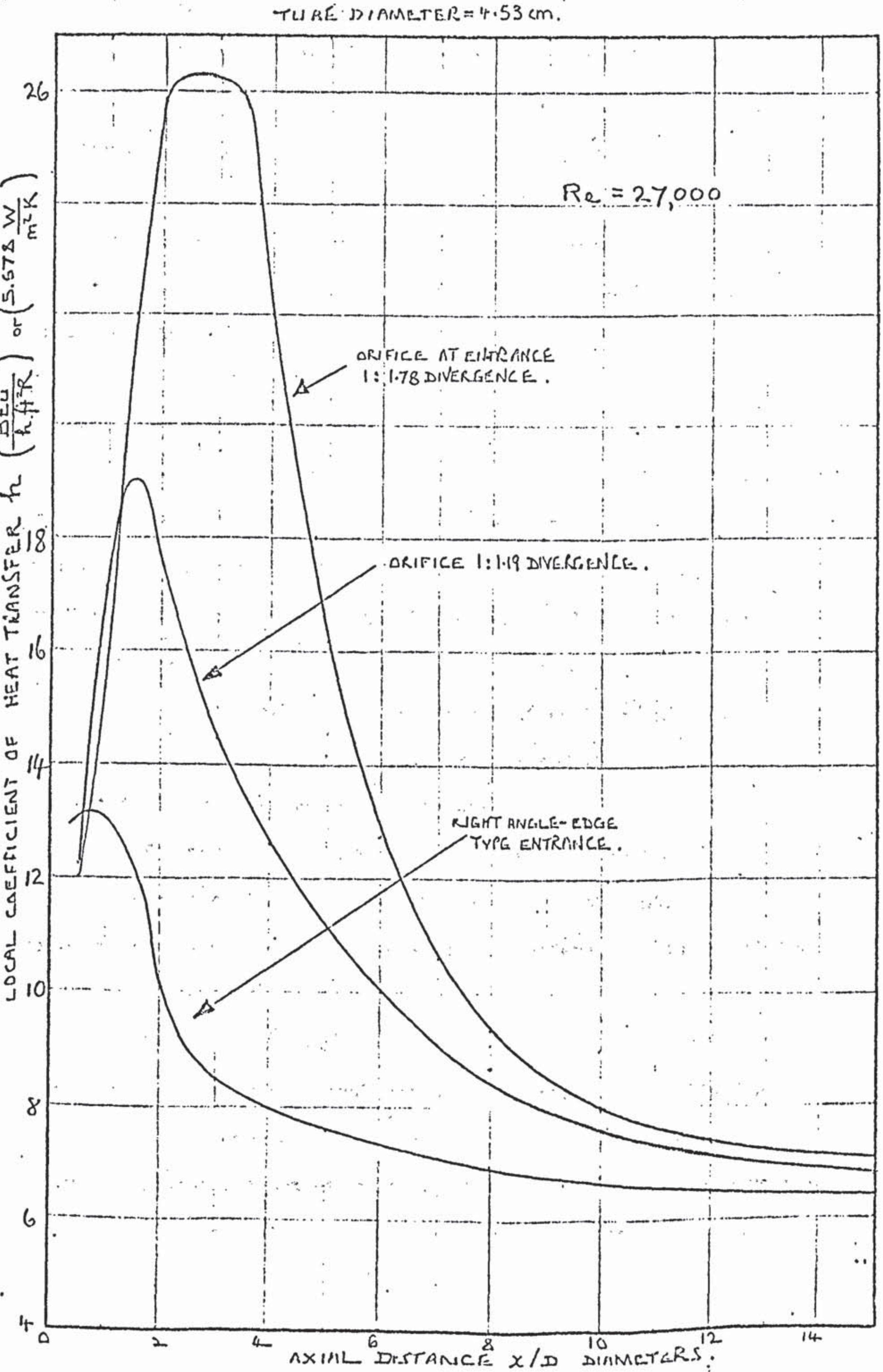

3. LITERATURE SURVEY.

3.1. Introduction.

A survey of recent work on convective heat transfer in tubes was carried out, which encompassed numerous related topics. This part of the thesis is sub-divided into eight sections, each dealing with a particular aspect of the survey, and containing a discussion on those publications which have dealt specifically with a particular problem relevant in this research. It should be noted that in the following the term 'non-viscous' is used to indicate a low viscosity.

3.2. THE LONG STRAIGHT TUBE.

3.2(i) 'NON-VISCOUS' FLUIDS.

During the last twenty years a considerable volume of literature has been published on the experimental findings of researchers who measured Nu_∞ for long tubes, with gaseous or aqueous heat-transfer media, in the fully turbulent flow regime. In references (A1, A2, A6, B1, B2, B3, B5, B6, B8, B9, B10, B12, E11) attempts have been made to obtain a correlation between Nu_∞, Re and Pr, although in some of the cases quoted this did not constitute the main objective of the work.

For moderate temperature differences, so that the properties of the fluid remained substantially constant, the experimental data in most of the aforesaid references was correlated in the following way.

$$Nu_\infty = B.Re.^m\ Pr.^n\ .$$

The usual practice was to evaluate the properties of the fluid at the local, bulk temperature and for the parameters B, m and n to be given suitable, constant values. Typical values of the parameters are 0.023, 0.8 and 0.4 respectively, these being the values most often used in practice, and which were postulated by McAdams (Ref. K2.) as described in part 2.3(iii). Despite the confidence of each worker in his own experimental data, and this was expressed as a tolerance on Nu_∞ number of between 2% and 15%, the suggested values of the parameters B, m and n varied between sources as follows -

B - 0.018 to 0.031
m - 0.77 to 0.87
n - 0.333 to 0.420

Two recent (1964) papers by Allen and Eckert (Ref. B10.) and Malina and Sparrow (Ref. B1.) commented on the results of almost identical experiments with water in long, electrically heated tubes. The precision obtained was undoubtedly very good, the measurements of coefficients of heat transfer, h_∞, being repeatable within a 2% tolerance. The possibility of the variation in the physical properties of water with temperature affecting Nu_∞ was considered, even though such effects would have probably been small. For a given Re and Pr the ratio $(Nu_\infty)/(0.023.Re^{0.8}.Pr^{0.4}.)$ was plotted against the temperature difference employed in calculating h, that is $(t_w - t_b)$. Hence, departures of the experimental Nu_∞ from the McAdams equation were indicated, and the effects of property variations could be eliminated by repeating the measurements for different values of the heat flux, then extrapolating the data to the 'zero heat-flux' condition. Figure 3.1. illustrates this procedure with the results of both Allen and Malina. The way in which the ratio $(Nu_\infty)/(0.023.Re^{0.8}.Pr^{0.4}.)$ varies with Re is also shown; the work of Allen was based on water with Pr = 8, and that of Malina with Pr = 3. In Allen's results the equation of McAdams is shown to underestimate Nu_∞ by 11% at Re = 10,000 increasing to 20% at Re = 100,000. In Malina's results the underestimation increases from 2% to 11% in the same range of Re.

In conclusion, the dependence of Nu_∞ on Re, as given by the McAdams equation, must be inadequate, furthermore there is some indication that the dependence on Pr is unreliable. The accuracy of the McAdams equation in the calculation of Nu_∞ for water can be expressed as a 20% tolerance.

In 1961 Ede (Ref. A.1.) recorded values of Nu_∞ for both water and air. The data was derived whilst conducting various experiments on more complicated configurations and with tubes having a range of diameter. The tubes were heated electrically, and particular emphasis was placed on the accuracy of thermocouple, flowmeter, and heat flux measurements. Small temperature differences were used in order to minimise variations in the properties of the fluids. Similar observations were made regarding the reliability of the McAdams formula as were made later on by Allen and by Malina. For water, the ratio $(Nu_\infty)/(0.023\ Re^{0.8}Pr^{0.4})$ increased with Re from approximately 1.0 at Re = 10,000 to 1.1 at Re = 100,000. The Prandtl number of the water was nominally 8. The results for air were somewhat different, in that the McAdams formula overestimated Nu_∞ by approximately 20% to 25% in the same range of Re. Clearly the Pr dependence as indicated by McAdams is unsatisfactory where accurate values of Nu_∞ are required. Ede showed that the theoretical formula of Martinelli (described in 2.3(iii)) gave a much better indication of the Pr dependence of Nu_∞, but even this was far from satisfactory. The results of Ede are shown in Figure 3.2 .

It is concluded that any further research into forced convection in long tubes with 'non-viscous' fluids would not be particularly productive at this time.

3.2(ii) VISCOUS FLUIDS.

From the early researches, discussed in 2.3(iii), two empirical relationships emerged for correlating data on turbulent Nu with viscous liquids. For a fluid having constant physical properties they both look very similar. The McAdams equation was

$$Nu_{\infty} = 0.023\ Re^{0.8}Pr^{0.4},$$

and the Sieder and Tate equation (which assumes constant viscosity in this discussion)

$$Nu_{\infty} = 0.027\ Re^{0.8}Pr^{\frac{1}{3}}.$$

In 1955 Hartnett (Ref. B2.) used a long, electrically heated tube, to measure coefficients of heat transfer for an oil with Pr in the range 60 to 200. The maximum experimental error in measuring Nu_{∞} was assessed at 10%. The values obtained for Nu_{∞} were approximately 10% higher than the Sieder and Tate equation predicts at Re = 50,000, but the difference reduced to 0% at Re = 10,000. The McAdams equation overestimated Nu_{∞} by up to 20% approximately, and was found unsuitable. The viscosity of the oil did vary considerably with temperature in these tests, but Nu_{∞} was corrected to give the equivalent constant property value with the 'Sieder and Tate factor' $(M_{WALL})^{0.14}$ - as discussed in 2.3(iii). Since no attempt was made to justify this procedure, there is an inherent weakness in the arguments presented in this research, though the reliability of the results was probably not seriously impaired.

Friend and Metzner (1958) pointed out that simple equations of the form $Nu_{\infty} = B.Re^{m}Pr^{n}$ may not be satisfactory for correlating experimental data when Pr varies over a wide range of values, and that no satisfactory experimental or theoretical analysis existed at that time to justify such a supposition. Experiments were conducted to measure Nu with a steam-heated tube, and a number of sugar-based fluids were used to provide a wide range of Pr. (Ref. A4.) The Prandtl number of the sugar solutions was shown to be only a weak function of temperature in these experiments. Although the reliability of the experimental results was not good (about 20% tolerance on Nu_∞) the work was interesting because it showed how Nu_∞ could vary with Pr whilst Re remained constant. With Re = 10,000, Pr was varied from approximately 50 to 600. The results are shown in Figure: 3.3 . Two equations were given to represent the experimental data, the first being a rather crude, semi-theoretical formula which showed no improvement over the second, more conventional form of equation - $Nu_\infty = 0.022\ Re^{0.8}Pr^{0.42}$. The exponent of Re was never justified experimentally, and since the reliability of the correlation, with respect to the Pr term, can be shown to be

$$\frac{\Delta Nu}{Nu} = \Delta n \log\left(\frac{Pr_{max}}{Pr_{min}}\right) ,$$

where Δn = error in Pr exponent, ΔNu = error in Nu,

a reduction of 20% in the exponent 0.42 (or 0.33) would be equivalent to 21% variation in Nu_∞, which is about the same as the reliability of the results. The insensitivity of Nu_∞ to the Pr exponent is evident from this calculation.

In 1964 Malina and Sparrow (Ref. B1.) extended their experiments with water (See 3.2(i)) to include oils with Prandtl numbers 48 and 75. The ratio of ($Nu_\infty / 0.023\ Re^{0.8}Pr^{0.4}$) was determined for the 'zero heat-flux' condition over a range of Re. With Pr = 48, the ratio was found to vary from 0.94 at Re $\simeq$ 14,000, to 1.11 at Re = 43,000. The values for Pr = 75 were 0.97 at Re $\simeq$ 12,000, and 1.07 at Re $\simeq$ 28,000. Hence the ratio increased with Re and the rate of increase was greater for higher Prandtl numbers. It appears that a suitable form of expression for calculating Nu would be

$$Nu_\infty = B.\ Re^{\gamma_1(Pr)} Pr^{\gamma_2(Re)} .$$

Sufficient experimental data has been provided to enable the value of Nu_{∞} to be estimated with viscous fluids, and little purpose would be served by pursuing this line of research. A possible exception to this statement would be in the transitional flow regime where experimental data is sparse.

As a final comment it is suggested that when equations of the McAdams kind are utilised, the exponent of Re should certainly be greater than the value 0.8 - which is encountered frequently in the heat-transfer literature - when viscous fluids are to be considered. Furthermore, a suitable value for the exponent of Pr has not been satisfactorily established; although typical values of 0.4 and $\frac{1}{3}$ to appear equally reliable. The latter follows because few experimenters have utilised highly viscous fluids, and a simple exponential relationship does not necessarily provide an adequate means of correlating the experimental parameters.

3.3. THE SHORT STRAIGHT TUBE.

3.3(i) 'NON-VISCOUS' FLUIDS.

Themeasurement of local coefficients of heat transfer inthe entrance region of tubes has been the objective of many experiments following the early works of Cholette (Ref. B14.) and Boelter (Ref. H 15.). Particular attention has been given to gaseous and aqueous media, and the flow has nearly always been turbulent. References (B1, B2, B3, B4, B5, B6, B7, B8, B9, B10, B11, B12, C2, E1, E11 ,) relate to such experiments.

For 'non-viscous' fluids in the laminar regime few data are reported on local coefficients of heat transfer. Apart from the experiments of Kays and of Kroll (Ref. C1.), most of the research effort has been concerned with 'secondary effects' such as the influence of free convection - references B7, B13, E1, fall into this category.

In 1953 Kays (Ref: C1 .) carried out a theoretical analysis of heat transfer to air in short tubes, with undeveloped flow at the inlet. To support the theory a comparison was made with empirical data. These were derived with steam heated and electrically heated tubes. The results were presented as a graph of Nu versus (RePr)/($x/2r_w$), as in Figure: 3.4. The local Nusselt number was greater for uniform heating than for uniform temperature at the tube wall, the extent being 20% to 40% . At small axial distances Nu for the 'undeveloped' case exceeded the 'fully developed' values by a bout 40%, but this difference diminished with increasing axial distance.

The results of Kays were applicable only to fluids with Pr $\approx$ 1. In such fluids the temperature profile develops at a similar rate to the velocity profile, so one would expect the difference between the 'developed' and 'undeveloped' Nu to become less than stated as the Prandtl number increases above unity.

In 1966 McComas and Eckart (Ref: E.1) reported the results of experiments on electrically heated horizontal tubes with a long calming length. Local coefficients of heat transfer were obtained for a range of Re from 100 to 900, with air as the medium. Figure 3.5 shows Nu versus distance from the onset of heating with Re $\approx$ 740 and 220. With the lower Reynolds number Nu reduced rapidly with increasing distance to a minimum value, which was of the same order as the fully developed Nusselt number 4.36. This minimum was reached > 60 diameters downstream with Re $\simeq$ 740, and 5 to 10 diameters with Re $\approx$ 220. Further downstream with Re $\simeq$ 220, the value of Nu increased with distance, the rate of increase depending on the heat-flux imposed (this is indicated by the value of Gr in figure 3.5). The latter phenomenon was attributed to the secondary effects of free convection (a subject discussed later in this section).

The considerable influence of free convection on the coefficient of heat transfer - for laminar forced flow of 'non-viscous' fluids - makes data for the case of pure forced convection of doubtful practical value, except where fine-bore tubes are encountered. For this reason, the objectives of researchers in this area have centred mainly on the 'mixed' convection process.

In turbulent flow, local measurements have been obtained with gases and water. References B.1, B.2, B.3, B.5, B.8, B.9, B.10, B.11, and B.12 report results of this kind.

Mills (Ref: B.12) measured local values of h for air passing through a brass tube, heated with an electrical winding. Various entrance configurations were investigated, including a long calming length upstream, and a bellmouth entrance. Figure 3.6 summarises these results. The localcoefficient of heat transfer, h, with the calming length, reduced from a high initial value to a constant limiting value in the first 6 diameters downstream, and this development length did not appear to vary significantly with Re in the range 16,670 to 102,600. The value of h $\frac{1}{4}$ diameter downstream was $\tilde{1.8}$ times the limiting value h_∞. With the bell-mouth fitted the h - functions were found to be quite different. Initially, h was found to reduce much more rapidly than with the calming length, until a minimum was reached which was less than h_∞. This initial length reduced from $\tilde{15}$ diameters at Re = 10,240, to $\tilde{1.5}$ diameters at Re = 107,800. Further downstream, h increased with distance until the limiting value h_∞ was reached. The overall effect of fitting the bellmouth was to increase the length of the development region, and reduce the 'average' value of h in this region of the tube. The characteristic 'dip' in the latter functions was explained by Mills as being caused by the transition from laminar to turbulent flow at the tube-inlet, the onset of turbulence occurring at the minimum value of h.

Wolf (Ref: B.8) measured values of h for air and CO_2 in 3 tubes which were heated electrically. A calming length was fitted upstream, and large temperature differences (tube-gas) were utilised (> 200K). The physical properties of the gases varied substantially with temperature. To facilitate the comparison of the results obtained, the values of Nu measured were corrected to give equivalent values for particular, nominal Reynolds numbers. A further correction was made to account for the differences in $(t_w - t_b)$ between measurements, which included an allowance for variations in the physical properties. For this purpose the parameter β^* was derived, as a measure of the intensity of heat transfer, and Nu was corrected to nominal values of β^*. (The reader is referred to the original text for details. Variable properties are considered later in part 3.4). Figure 3.7 shows $Nu_b^{R\beta}$ (the corrected value of Nu) versus (axial distance) for air and CO_2. The general shape of these functions is similar to those measured by Mills, but the value of $Nu_b^{R\beta}$ continues to reduce gradually at large distances. This was attributed to the increase in thermal conductivity of the gas with increasing bulk temperature. A reduction in the rate of heat transfer (as indicated by a proportional reduction in β^*) caused the rate of change of $Nu_b^{R\beta}$ with distance to increase, although the magnitude at any position was greater (mainly because properties were evaluated at the local bulk temperature).

With water as the entrained fluid, most of the works have considered moderate temperature differences ($t_w - t_b$), and the secondary effects of free convection and property variations in some of these cases has been found negligible. References B.1, B.2, B.3 and B.5 fall into this category.

In 1955 Aladev (Ref: B.5) measured h for a horizontal tube enclosed in a steam jacket. The conditions at the tube-entrance were not well defined, being something between fully developed and undeveloped. The results of these experiments, although crude, have been quoted in several standard text books. After taking measurements for a range of Re, unique functions of ($Nu/Pr^{0.4}$) versus (Re) were plotted for particular axial locations and from these results graphs of (h/h_∞) versus (distance) were derived for selected Reynolds numbers - as shown in figure 3.8(i). The magnitude of (h/h_∞), at distances of the order $\frac{1}{2}$ diameters, can be seen to reduce appreciably as Re is increased, from a ratio of $\tilde{2}$ at Re = 10,000 to a ratio of $\tilde{1}.1$ at Re = 100,000.

In 1955 Hartnett (Ref: B.2) presented data for water, but in these experiments electrical heating was applied to a vertical tube having a long calming length. Figure 3.8(ii) shows a comparison with the results of Aladev. The temperature development length was much shorter than given by the latter, and the measured values of (h/h_∞) in the entrance region were much lower. The experiments of Hartnett were not so crude as those of Aladev and are probably more reliable, but the effects of the different inlet conditions might well account for some of the disparity between the results.

A comparison can be made between the values of h - in a short tube with calming length - for gases and for water, by referring to the results of Mills (Fig: 3.6) and Hartnett (Fig: 3.8(ii)). Although the thermal entrance length was 10 to 15 diameters in both cases, the ratio (h/h_∞) at 0.5 diameters according to Mills was 1.8 to 1.6 with Re = 16,670 to 102,600, and with water the ratio was 1.5 to 1.2 with Re = 16,900 to 44,300. A substantial difference is indicated between the (h) versus (distance) functions for water and gas.

In 1965 Stone (Ref: B.3) conducted a detailed investigation of h in the entrance region of an electrically heated tube, with water as the fluid. Various complex methods of correlating the experimental data were attempted, but his general conclusions were that a unique function of (h/h_∞) versus (distance) could be specified, independent of Re (but not Pr) representing his results with a maximum error of ± 20%. The range of Re encompassed was 10,000 to 100,000. The shape of this function was shown to be highly dependent on the length of the unheated region upstream, and figure 3.9 illustrates these findings. Considering the substantial deviations permissible with the Stone (h/h_∞) functions, the results of Hartnett (Fig: 3.8(ii)) are in reasonable agreement, the majority of the latter data falling within 0 and - 20%. It seems probable that the correlations of Stone should have incorporated the effects of Re in a different way. It is clear from figure 3.9 that (h/h_∞) could be increased appreciably by shortening the calming length, and a comparison with the results of Aladev (Fig: 3.8(i)) indicates the likely reason for the disparity between the latter data and that of Hartnett.

In 1964 Malina (Ref: B.1) produced experimental data of (h/h_∞) for water in short tubes, heated electrically. The limited range of results was derived meticulously, and good repeatability was obtained. Figure 3.10 shows (h/h_∞) versus (distance) for

Re = 14,500 to 101,300. The results are similar to those of Hartnett (Ref: B.2), the thermal entrance lengths were slightly shorter and the magnitude of (h/h_∞) was in reasonable agreement at all values of Re.

3.3.(ii) 'VISCOUS' LIQUIDS.

It was clear from a survey of a wide number of sources that only a small amount of experimental data was available on local heat transfer in the entrance-region of a tube, for high Prandtl number fluids.

In the turbulent regime, Hartnett (Ref: B.2) used an electrically heated tube with a long calming length to determine the distribution of h for oil. The range of Prandtl number covered by the tests was 60 to 480, and the Reynolds number varied from 1,600 to 47,000. The maximum Re attainable with the apparatus was limited by the available pressure drop to 2,000 for Pr = 480, 10,000 for Pr = 206 25,000 for Pr = 107 and 47,000 for Pr = 61. The limited amount of experimental data derived by Hartnett is shown in figure 3.20, where (h/h_∞) is plotted versus axial distance. These results may be compared to the data obtained with water by Hartnett (discussed earlier) which are given in figure 3.8(ii). It can be concluded that the effect of increasing Pr was to reduce the value of (h/h_∞) in the entrance-region; although the distance downstream at which the fully developed value of 1.00 was reached was apparently independent of Pr.

Another limited investigation of the short tube was carried out by Malina (Ref:B.1) whose experiments have been described earlier (Parts 3.2.(i) and 3.3.(i)) as well defined and reliable. Prandtl numbers of 3 (water), 48 and 75 (oil) were considered, and the different values of (h/h_∞) measured at small axial distances are compared in figure 3.10. The values of (h/h_∞) were slightly lower than those reported by Hartnett, but were in qualitative agreement. No comparison could be made below Re = 12,000 since Malina did not present data in this range. The length of the development region was approximately the same from both sources.

Malina pointed out that the values of h presented were up to $\tilde{3}\%$ greater than would have been obtained with a fluid having constant physical properties. In general the results indicated that the value of h tended to the limiting h_∞ more rapidly as Re was increased for a given Pr. It was further shown that the development was more rapid as Pr was increased for a given Re.

In practice, it is probable that transitional and turbulent flows having low Re, in the range Re = 2,500 to 15,000 (say), will occur frequently because of limitations on the available pressure drop when handling a viscous medium. This is also the region in which the thermal development at the entrance of a tube is slowest, and local measurements most beneficial to the designer. It can be concluded that no satisfactory experimental work has been carried out for such conditions. Undoubtedly, the reason for avoiding the transitional Reynolds numbers is the difficulty which might occur in conducting experiments with an unstable flow regime. However, it is not always possible to select a satisfactory design point in this respect, and experimental data would be valuable. A few results presented by Hartnett (figure 3.20) give some credence to this argument.

With laminar flows the experimental data available was limited, and such data as exists has usually been obtained in order to justify a theoretical analysis, or to provide a method of determining the way in which the secondary effects of free convection and viscosity-temperature dependence would modify the value of Nu estimated for a system in which no such secondary effects arise. It was decided to classify the references consulted in terms of the main objective of the work, e.g. the effects of free convection on the forced convective process. These references will be discussed in parts 3.4. to 3.6.

3.4. VARIABLE FLUID PROPERTIES.

The rate of heat transfer to a piped fluid is likely to influence the shape of the axial velocity profile, and therefore must have some effect on the Nusselt number. In a gaseous medium the properties ρ, K and μ could vary appreciably with the radial temperature distribution at high heat fluxes. For forced convection in a viscous liquid the most significant variations are concerned with the radial changes in viscosity with temperature. In general the analysis of problems of gaseous heat transfer with property-variations has differed from the case of liquids, accordingly it has been decided to review only those works concerned with liquid media. References C.2, C.3, D.6, D.7, D.9 and J.6 discuss methods of estimating Nu for gases with variable properties.

In the turbulent regime few authors have attempted to determine the effect of viscosity-variations on the Nusselt number. Hartnett (Ref: B.2) and Davies (Ref: B.6) are examples of authors who have attempted to compensate for viscosity-variations (with water and oil) by using a relationship of the kind:-

$$Nu_{\infty}\ (\text{variable}\ \mu) = (\mu_b/\mu_w)^{0.14}.\ Nu_{\infty}\ (\text{with constant}\ \mu)$$

which was proposed by Sieder and Tate (Ref: D.1) as discussed previously. This equation was not justified by the users since the viscosity corrections made were small. Aladev attempted to derive a similar method for correlating experimental data obtained with water and arrived at the following expression: -

$$\frac{Nu_{\infty}\,(\text{variable})}{Nu_{\infty}\,(\text{constant})} = (Pr_b/Pr_w)^{\frac{1}{4}} \simeq (\mu_b/\mu_w)^{\frac{1}{4}}.$$

The expression was used primarily to account for the apparent differences in Nu obtained with heating and cooling. The range of $(Pr_b/Pr_w)^{\frac{1}{4}}$ was approximately 0.9 to 1.1.

Allen (Ref: B.10) carried out experiments heating water, and showed that the correction factor $(\mu_b/\mu_w)^{0.14}$ was valid only with Re = o (10^5). The limited amount of data presented indicated that a more suitable correction factor would be $(\mu_b/\mu_w)^{f(Re)}$ where $0 \rightarrow f(Re) \rightarrow 0.14$ as $10^4 \rightarrow Re \rightarrow 10^5$. The ratio $(Nu_{\infty}\,(\text{variable})/Nu_{\infty}(\text{constant}))$ never exceeded 1.15, and a greater range of values might have demonstrated that part of the correction could have been absorbed by limitations on the experimental method.

The results of Malina (Ref:B.1), which were obtained with water and oil (Pr = 48 and 75), showed a similar trend to those of Allen over a comparable range of Re. A correction factor was proposed of the kind $(\mu_b/\mu_w)^n$ to compensate for the effect of viscosity variations on Nu_{∞}. The value of n was shown to be in the range 0.05 to 0.08 for most of the experimental data, and the value 0.05 was recommended. Once again the variations in viscosity were small, however, and the ratio $(Nu_{\infty}(\text{variable})/(Nu_{\infty}(\text{constant}))$ never exceeded 1.1.

No experimental evidence could be found which enabled the effects of viscosity-variations on Nu in the entrance-region to be determined.

With laminar flow the effects of viscosity-variations on Nu are amenable to mathematical analysis. Yang (Ref: D.3) solved a simplified version of the boundary-layer equations for uniform heat-flux, with fully developed flow at the inlet of the tube, and viscosity dependent on temperature. The equations were solved analytically using an iterative integral technique. The complicated form of the results make it difficult to draw general conclusions, but the ratio of (Nu with variable viscosity)/(Nu with constant viscosity) was of approximately the same magnitude as $(\mu_b/\mu_w)^{0.14}$. The value of Nu tended to the constant property value at small axial distances but increased above the latter (for heating) with increasing distance. The value of Nu was raised as the heat flux increased, or as the rate of change of μ with temperature increased. $(1/\mu)$ was assumed to be linear in temperature.

Rosenberg (Ref: D.8) solved the boundary-layer equations numerically for laminar flow in a tube, with the constant wall temperature condition. The inertial terms were retained in the solution because the flow conditions considered were undeveloped and developed at the inlet. The viscosity was related to temperature by one of two equations viz:

$$\mu = (C_1 + C_2T)^{-1} ,$$

or $$\log (\mu) = C_3/T + C_4.$$

(C's are constant).

Results were calculated for a range of Pr up to 1,000, and it was shown that the flow became 'fully developed' in a very short axial distance when viscous fluids were considered. The viscosity dependence of Nu was shown to be mainly a function of (μ_w/μ_o), but a weak function of $(x/r_w)/(\text{RePr})$ —— $\mu_o = \mu$ at inlet $\simeq \mu_b$.

A comparison with the relationship : -

$$Nu_m \text{ (variable viscosity)} = (\mu_b/\mu_w)^{0.14} . \; Nu_m \text{(variable viscosity)}$$

(proposed by Sieder and Tate) demonstrated that the above expression enabled Nu_m to be estimated for a short pipe within $\sim 2\%$ of the calculated result, in the range $1 < (\mu_b/\mu_w) < 100$. The magnitude of Nu_m was consistently 15% less than the empirical equation proposed by Sieder and Tate, but this has not been considered in assessing the effects of viscosity ratio.

Test (Ref: D.5.) analysised the same problem as was discussed by Rosenberg using a similar numerical technique but the initial equations were more general. The effects of several terms in the energy and momentum equations on the local Nusselt number were evaluated before eliminating them as being small and obtaining the final solutions. The equation of state for viscosity was -

$$\log_{10} \log_{10} (\mu/\rho + 0.8) = 9.1 - 3.16 \log_{10} T.$$

Although mathematically rigorous, the results could not be generalised easily, and the increased complexity of the solution led to large truncation errors. The local Nusselt numbers calculated were compared with the results of some experimental data derived from a steam-heated tube with a calming length upstream. The entrained fluid was oil. The relationship (for local values) between Nu and (μ_b/μ_w) was ascertained and the Sieder and Tate correction was found to overestimate Nu considerably. The following relationship was proposed:

$$Nu \text{ (variable } \mu) = Nu \text{ (constant } \mu). (\mu_b/\mu_w)^{0.05}.$$

Insufficient data was presented to determine the magnitudes of the viscosity-ratio which were investigated.

Shannon (Ref: D.10) combined an experimental and analytical investigation of laminar heat transfer with variable viscosity. The flow was fully developed at the inlet, and a viscous liquid, ethylene glycol, was used as the medium. In this analysis uniform heat-flux was imposed by electrical heating of the tube. The range of Re was 6 to 300, and Pr varied from 26 to 500. The experimental data was not presented, and only a vague description of the numerical method is discussed. The conclusions were that experiment agreed well with theory, and that the effects of viscosity variations could be estimated as follows:

For a liquid with viscosity $\mu = \mu_{ref.} \exp(-\text{constant}(T-T_{ref}))$,
or for the case $\mu \doteq \mu$ (ethylene glycol),

$$Nu\ (\text{variable}\ \mu) = Nu\ (\text{constant}\ \mu).(\mu_b/\mu_w)^m,$$

where $m = 0.14$ at large axial distances, but increases to $\tilde{0.3}$ at small axial distances. The axial distance referred to was a dimensionless distance defined by $(x/D)/(RePr)$. In the numerical work (μ_b/μ_w) had a maximum value of 100, whilst in the experiments the maximum value attained was $\tilde{6}$.

The magnitude of Nu obtained experimentally consistently underestimated the theoretical results by 0 - 15%.

Petukhov (Ref: D.2) investigated the case of undeveloped laminar flow of viscous liquid in a constant temperature tube. Experiments were carried out for heating oil which had a variable viscosity, and the main parameters were in the following ranges:- $44 < Re < 2{,}100$, $130 < Pr < 3{,}900$, $1 < (\mu_o/\mu_w) < 12.5$ (where μ_o = inlet value $\mu \simeq \mu_b$). The dependence of Nu_m on (μ_o/μ_w) was compared with the equation of Sieder and Tate and the latter was found to be in reasonable agreement with the final proposal that

$$Nu_m(\text{variable}) = Nu_m(\text{constant})\ (\mu_o/\mu_w)^{1/6}\ .$$

The difference between the exponents 0.14 and 1/6 was small, and both were equally reliable for the range of the parameters stated above.

The local values of Nusselt number were correlated using the similar equation:

$$Nu\ (variable) = Nu\ (constant)(\mu_o/\mu_w)^{1/6}.$$

The experimental data used to arrive at the above expressions showed a maximum deviation from the estimated Nu of $\pm$ 15% of Nusselt number.

The preceding discussion indicated that there is still considerable disagreement between sources as to the effects of the viscosity-temperature relationship on the local Nusselt number for both turbulent and laminar flow of liquid in heated tubes.

It should be pointed out here that quite different expressions to those discussed have been proposed for the related problem of cooling liquids in tubes, a subject not directly relevant to the present work.

3.5. FREE CONVECTIONAL EFFECTS IN HORIZONTAL TUBES.

The effects of free convection on the heat-transfer coefficient in forced laminar flow can be appreciable whether the tube is horizontal, inclined or vertical. Several investigations have been carried out for the first and last cases, but the horizontal tube is probably the most common configuration in practice as well as being the least amenable to analysis, and therefore consideration has been given to this in these experiments.
The bouyancy forces in a horizontal tube are transverse to the direction of pumped flow primarily, but in a vertical tube the forced and free components are co-axial either aiding or opposing each other depending on the direction of the flow. In forming correlations for the value of Nusselt number, in horizontal flow, attempts have been made at drawing an analogy with expressions proposed for the simpler case of vertical flow (usually with no

sound basis.)

References E.4, E.5, E.13 and E.16 to E.22, deal with experimental and theoretical values for the Nusselt number in a vertical tube. No further comment will be made on these works since the problem was considered to be fundamentally different and discussion would tend to confuse rather than simplify the issue. An exception to the latter statement is the work of Martinelli (Ref: E.4) who determined values for Nu_m using a combined theoretical and empirical approach.

The main result of Martinelli will simply be stated. An equation was derived for heated flow travelling upwards in a tube as follows:-

$$Nu_m = 1.75F_1 \left[(\pi Re_m Pr_m D)/(4L) + 0.0722\, F_2 (Gr_w Pr_w D/L)^{\frac{3}{4}} \right]^{\frac{1}{3}}$$

where F_1 is a correction factor which allows arithmetic rather than logarithmic temperature differences to be used, and F_2 is a function which compensatps for the reduction in bouyancy forces, in the axial direction, as the bulk temperature increases. The forced and buoyant terms are seen to be additive, the net result being that Nu_m increases above the normal 'forced' value as the free convection parameter Gr_w (w - properties at wall) increases.

Aladev (Ref: E.11) attempted to find an equation for Nu_m, with $Re < 2,300$, which would satisfy a horizontal or vertical tube carrying water. The experimental analysis was fairly crude and applicable only to a tube 60 diameters long. The condition of uniform wall temprrature was approximated. The form of the equation for the horizontal case reduced to -

$$Nu_m = 0.74\ (Re_m^{0.2}\ Gr_m^{0.1}\ Pr_m^{0.3})$$

The form of the expression must be discounted because it demonstrates that the contribution of free convection to Nu_m is the same for all values of Re_m. (This criticism was made by Kern of the Colburn equation. Part 2.4.(ii)).

Other workers have used water as the medium. Martin (Ref: E.15) considered the local parameter Nu in the entrance-region of a constant-temperature tube with developed and undevelped flow at the inlet. A slightly modified version of the Colburn equation was found to represent the experimental data adequately, viz: $Nu = Nu_o\,(1 + 0.127\,Gr^{0.145})$ for $Gr > 10^7$.

(Nu_o = Nu when $\beta = 0$).

Once again the equation is unlikely to be valid for conditions outside the range of the experiments, there being no consideration of tube length, Pr or Re in the free convective factor.

Jackson (Ref: E.14) experimented with air in a horizontal, steam heated tube. The correlation of results was based on the following expression:-

$$Nu_m = 2.67\left[(\pi Re_m Pr_m D/4L)^2 + (0.0087)^2\,((Gr_w Pr_w)^{3/2}\right]^{1/6}$$

for the laminar regime, which was based on the work of Martinelli and represented a vectorial addition of the forced and free convective components in such a way that the asymptotic cases of pure forced flow, and pure free flow, could be accommodated. Hence the omission of L in the last term. The weakness in this expression is that the thickness of the temperature layer increases with length when forced flow predominates, and therefore the free convective term (a function of the rate of secondary recirculation) must contain a length dependent parameter for such conditions. It is difficult to envisage any simple addition of forced and free components, such as the one postulated, which could satisfy both the asymptotic cases and also the intermediate states, when both components are significant.

Edo (Ref: A.1) whose experiments, for water in long tubes with uniform heat-flux, have already been discussed, considered the case when $Nu \rightarrow Nu_\infty$. The value of Nu_∞ in laminar forced flow is 4.36 and was therefore independent of length. For water with $Pr \sim 8$, the values of Nu_∞ with free convection were found to agree reasonably with -

$$Nu_\infty = 4.36\ (1 + 0.06\ Gr_\infty^{0.3}).$$

The expression was considered valid for the particular fluid, and was restricted to the case when forced flow predominated with $Gr_\infty < 10^7$. The data are presented in figure 3.2.

Brown (Ref: E.6) considered the case of water in a tube at approximately constant wall temperature. The significant groups of parameters used in correlating values of Nu_m were slightly different than had been hypothesized earlier. It was assumed that

$$Nu_m = f\ (Re_m Pr_m D/L,\ Gr_m).$$

The approach to the problem was influenced by the works discussed previously, but the analysis was largely empirical. The philosophy behind the final form of solution for the problem is not at all clear, but the best fit to the experimental data was found to be given by:

$$Nu_m = 1.75(\mu_b/\mu_w)^{0.14} \left[(\pi Re_m Pr_m D/4L) + 0.012((\pi Re_m Pr_m D/4L) Gr_m^{\frac{1}{3}})^{4/3}\right]^{\frac{1}{3}}$$

The introduction of Re into the free convective term was not adequately explained, and it is difficult to see how the free component of Nu_m could increase with Re_m for a fixed value of Gr_m.

Oliver (Ref: E.3) carried out experiments on mixed convection with forced flow predominating, in a tube heated by a water jacket. The heat-transfer liquids were glycerol-water, ethyl alcohol, and water. A resulting equation for estimating

Nu_m was stated thus -

$$Nu_m = 1.75\ (\mu_b/\mu_w)^{0.14} \left[(\pi Re_m Pr_m D/4L) + 0.00056\ (Gr_m Pr_m L/D)^{0.7}\right]^{\frac{1}{3}}$$

After surveying some of the works already discussed, Oliver showed that the experimental data was correlated more reliably, and agreed more closely with previous data, if the term containing Gr_m also included tube length. When the length was incorporated, as above, the intention was to demonstrate that the effects of free convection were more pronounced in long tubes than in short tubes. This had not been considered in any of the earlier equations, where the effect of increased length, on the free contribution to Nu_m, was either not apparent or caused a reduction in magnitude.

A novel approach at correlating the experimental parameters in mixed convection was discussed by Shannon (Refs: E.7 and D.10). Tests were carried out with water at the ice-point, and with ethylene glycol. An electrically heated test section was used, and local measurements of Nu were made. When plotting the experimental values of Nu versus distance, Shannon noted that the effects of free convection on Nu became more pronounced at large axial distances and hence the free convective contribution to Nu increased as Nu reduced. It was further assumed that with low flows and high heat-fluxes, the value of Nu would tend to be proportional to $(GrPr)^{\frac{1}{4}}$. The latter is typical of laminar natural convective systems, but Shannon was influenced by reference J.10 in particular. The hypothesis was made that

$$(Nu - Nu_o) = f\left(\frac{(GrPr)^{\frac{1}{4}}}{Nu_o}\right)$$

where Nu_o = the value of Nu with $\beta = 0$.

The value of f was found to be zero when the independent variable was less than 2, but a very considerable amount of 'scatter' was apparent when an attempt was made to correlate the experimental results graphically, as above.

It was found that widely different arguments had been presented in an attempt to define how Nu could be estimated for horizontal tubes, in the case of forced convection with some free convection superimposed. No single approach to the subject was shown to be reliable outside the experimental range, the logic behind the proposed equations was seldom acceptable, and very large errors, possibly of the order 100%, could be incurred when utilising any of the equations hypothesized above. A detailed review, and analysis of the literature, would perhaps lead to a better understanding of the problem, but the latter was not a major objective of this study. It was decided to rationalize on the problem without being influenced by previous analyses, if and when the need arose during the work of this author.

Some theoretical investigations have been conducted which show a continuing development towards the state when all the important groups of parameters required to define Nu, with mixed convection, are known; even if a formal solution of the equations is not obtained. The theoretical approach is likely to prove extremely useful in determining the solutions to problems which have apparently eluded the empiricists.

Morton (Ref: E.8) sought a solution to the problem of mixed convection in a long tube with uniform heat-flux. Forced laminar flow predominated so that $Nu_\infty = 4.36$, with no secondary flow. The energy and momentum equations were solved using a perturbation series which was valid for small values of the group $(Re\ Ra)_\infty$. The result was considered accurate when $(Re\ Ra)_\infty < 3{,}000$, which meant Nu_∞ was modified by 10% at the most. The parameter Ra had a perculiar, impractical definition which can be reduced into a more recognisable form to give:

$$(Re\ Ra)_\infty \equiv Gr\ Pr\ r_w\ (dt_w/dx)\ /\ (8\ (t_w - t_b)\ )_\infty\ .$$

$$\equiv Nu_\infty\ Gr_\infty\ /4.$$

Hence the result:-

$$Nu_\infty = 4.36\ (1 + f_1(Pr)\ (Re_\infty\ Ra_\infty\ )^2 ++\ )$$

can be expressed

$$Nu_\infty = 4.36\ (1 + f_2(Pr)\ (Nu_\infty\ Gr_\infty\ )^2 ++\ )$$

which leads to

$$Nu_\infty = (1 - (1 - 7.44.\ 10^{-8}\ (GrPr)^2_\infty\ )\ )^{\frac{1}{2}}\ /\ (8.54.\ 10^{-9}(GrPr)^2_\infty\ )$$

where $f_2 \simeq Pr^2\ /\ 3$ for $Pr > 50$

Mori (Refs: E.9 and E.10) improved on the solution of Morton using a boundary-layer analysis, so that the results were valid for larger values of the complex $(Re\ Ra)_\infty$ (i.e. values $> 10^4$). The final equation proposed was

$$Nu_\infty = f_3\ (Pr)\ (Re\ Ra)^{1/5}_\infty$$

where $f_3 \simeq 0.842$ for $Pr = 1$.

Values of Nu_∞ several times greater than 4.36 could be calculated. Some experiments were carried out with air in the region of $(Re\ Ra) = 10^5$, and good agreement with theory was demonstrated. The unusual parameters chosen to define the problem $(Re\ Ra)$ tend to obscure the true meaning of the result. In order to measure these parameters experimentally the problem must be overspecified, as will be obvious from the following.

Substituting the more conventional parameters into the equation above, for $Pr = 1$, $Nu_\infty = 0.842\ (Nu_\infty\ Gr_\infty\ )^{1/5}\ /\ 4^{1/5}$,

which is $Nu_\infty = 0.596\ Gr_\infty^{\frac{1}{4}}$.

It is now clear that the result obtained by Mori simply represents the limiting case when free convection predominates. This is clear because the reduced equation is very similar to other well known relationships for free convection on the outside of a tube or vertical surface. (see for example Ref: K.2 where $0.59\ Gr^{\frac{1}{4}}$ is proposed.)

Faris (Ref: J.11) carried out a similar boundary-layer solution, using the perturbation technique, for fully developed heat-transfer with uniform flux at the wall. The resulting equation given was $Nu_{\infty} = 4.36\ (1 + f_4\ (Pr)\ (Gr_*^2\ Pr^2\ Re_*\ )_{\infty}\ )$.

Once again the equations were formulated in terms of unconventional parameters, obscuring the meaning of the result. The limit of accuracy was specified in terms of Morton's parameters as being $(Re\ Ra)_{\infty} < 3{,}000\ Re^{\frac{1}{2}}$. The starred variables above had definitions different to those commonly used. Rewriting the equation in terms of more conventional parameters -

$$Nu_{\infty} = (1 - (1 - 5.17\ 10^{-8}(GrPr)^2/Re\ )_{\infty}^{\frac{1}{2}})/(0.593\ 10^{-8}(GrPr)^2/Re)_{\infty}$$

This indicates that initially Nu_{∞} increases with (GrPr) and reduces with increasing Re, which is as would be expected. The result must always be limited to those cases where free convection does not dominate in calculating Nu_{∞}, because the trend changes to one of Nu_{∞} increasing with Re increasing, and Nu_{∞} reducing with Gr increasing.

Cheng (Ref: E.24) produced a numerical solution of the problem posed by Morton and Mori, but in this case rectangular channels were considered. From the analysis the authors produced a graphical relationship between Nu_{∞} and the parameter (Re Ra) which was a unique relationship for a given channel. (The parameter was defined in a similar way to Morton and Mori.) The solution became unstable for large values of (Re Ra), but the method could be used to produce similar results in a circular tube for an intermediate range of (Re Ra), between the ranges of Morton and Mori.

Siegwarth (Ref: J.10) discussed the equations governing mixed convection in a horizontal tube. An approximate result was obtained for fully developed laminar flow, with uniform heat-flux, using an approximate integral procedure. The case considered was for $Pr \longrightarrow \infty$, and it was shown that

$$Nu_\infty = 0.471\ (Gr\ Pr)_\infty^{\frac{1}{4}} \quad .$$

The result would clearly be invalid for low values of $(Gr\ Pr)_\infty \sim 10^4$, since a lower limit of 4.36 exists. The result agrees within 22% of that derived from the formula proposed by Mori, which was derived specifically for the case when free convection begins to dominate.

Some recent papers not reviewed are given in references J.9 and J.12.

3.6. THEORETICAL HEAT TRANSFER IN TUBES.

Theoretical analyses for combined convection, and for the types of separated flow encountered herein, are discussed in parts 3.5. and 3.7. The main purpose of this section is to illustrate the scope of the many papers published on laminar or turbulent heat-transfer in tubes, without secondary effects or a geometrical discontinuity. The result of each of these theoretical works can be described as being an approximate integral solution, an eigenvalue-series solution, a numerical solution or an asymptotic solution whose convergence depends on the magnitude of Pr. The following table lists most of the publications acquired during the literature survey.

Name.	Ref	Date	Type Sol'n	Type Flow	Local/ F.D.	Turb. Model	Wall Bound	Fluid	Inlet Flow
Bankston	J.6	1970	Num.	L/T	Loc.	I6	UHF	Gas	Dev.
Mizushina	J.8	1970		T		Inv.			
Haberstroh	C.20	1968	Int	T	F.D.	Vel.	UHF	Gas/W	Dev.
Sherwood	I.3	1968		T		Inv.			
Hishida	C.19	1967	Int	T	Loc.	Vel.	CT	Gas/W	Dev.
Son	I.4	1967		T		Inv.			
Popovich	I.5	1967		T		Inv.			
Patankar	I.7	1966		T		Inv.			
Hubbard	I.8	1966		T		Inv.			
Sparrow	C.4	1958	Series	T	Loc.	C2/3	UHF	Gas/V	Dev.
Reynolds	J.5	1958	Series	T	Loc.	I10	UHF	Gas	Dev.
Hunziker	C.9	1958	Series	T	F.D.	Vel.	UHF	Gas	Dev.
van Driest	I.6	1956		T		Inv.			
Deissler	C2/3	1955	Int.	T	Loc.	C2/3	UHF/CT	Gas/V	Dev.
Reichardt	I.10	1951		T		I10			
Manohar	C.8	1969	Num.	L	Loc.		UHF/CT	Gas/W	Undev.
Shannon	D.10	1968	Num.	L	Loc.		UHF	Visc.	Dev.
Test	D.5	1967	Num.	L	Loc.		CT	Visc.	Dev.
Rosenberg	D.8	1965	Num.	L	Loc.		CT	Gas/V	Undev.
Roy	C.12	1965	Int.	L	Loc.		UHF	Gas/V	Dev.
Chi Tien	C.17	1963	Asymp series	L	Loc.		CT	Visc.	Undev.
Yang	D.3	1961	Int.	L	LLoc.		UHF/CT	Gas	Dev.
Mercer	C.7	1960	Series	L	Loc.		CT	Gas/W	Dev.
Sellars	C.13	1955	Asymp/ Series	L	Loc.		UHF/CT	Gas/V	Dev.
Kays	C.1	1953	Num.	L	Loc.		CT	Gas	Undev.
Yih	C.16	1951	Series	L	Loc.		CT/VT	Gas/V	Dev./ Undev.
Martin	J.14	1972	Int.	L	Loc.	—	UHF	W/V	Undev.
Siegel	C.4	1958	Series	L	Loc.		UHF	Gas/W	Dev.
Butterworth	C.21	1970	Num.	L	Loc.		UHF	V	Undev.

Num. - Numerical, Int. - Integral, Asymp. - Asymptotic,

L - Laminar, T - Turbulent, Loc. - Local and fully developed conditions calculated.

F.D. - Fully Developed conditions calculated,

Vel. - Effective turbulent properties estimated from shape of a velocity profile,

Inv. - Investigation into turbulence,

UHF - Uniform heat-flux,

VHF - Variable heat-flux,

CT - Constant wall temperature,

VT - Variable wall temperature,

W - Water or aqueous fluids considered,

V/Visc. - Viscous fluids considered,

Dev. - Developed flow at tube-entrance,

Undev. - Undeveloped flow at tube-entrance.

Parts of references C.2, C.3, I.6 and C.13 were considered in conjunction with the theoretical work included in this thesis. Their relevance will be apparent later on (in part 11).

In turbulent flow, the models for deriving the effective component of viscosity, defined by van Driest and Deissler, were considered for incorporation into this theoretical work. These can be stated thus -

$\mu_t = \rho A^2 y^2 (du/dy)(1 - \exp(-(\rho B^2 y^2 (du/dy)/\mu)^{\frac{1}{2}}))^2$, from van Driest,

and from Deissler -

$\mu_t = \rho A^2 y^2 (u/y)(1 - \exp(-\rho B^2 y^2 (u/y)/\mu))$.

A and B are constants.

Both expressions were arrived at by different reasoning, but appear remarkably similar. The values of μ_t in the above formulae were intended to apply when y was small i.e. in the region of a surface, where $(du/dy) \xrightarrow{\sim} (u/y)$. The equations have the appearance of 'Prandtl's mixing-length' formula multiplied by a damping factor. The damping factor being an attempt at demonstrating that transverse eddies must be damped close to a surface, and as $u \to 0$ in the 'laminar' sub-layers the turbulence is suppressed by viscous action. Expanding the exponential, and assuming terms in y^4 become small near to the wall, both formulae reduce to

$$\mu_t = C.\rho^2 \ (du/dy_o)^2 \, y^4/\mu \ . \qquad (C \text{ constant})$$

As $Pr \to \infty$ this latter expression becomes sufficiently reliable for estimating the radial temperature distribution because the thermal layer is extremely small. The velocity distribution could not be determined in this way however, the complete expression for μ_t would be required. The dependence of μ_t on the exponent of y becomes crucial, therefore, as $Pr \to \infty$. No adequate justification for the selection of the damping factor could be found, and no attempt has been made to find empirical proof at large values of Pr. For moderate values of Pr of the order unity, the form of the damping factor was likely to be comparatively unimportant. In references I.8, I.9 and J.8, the authors proposed that the exponent of y should be closer to 3 than 4, based on an analysis of Nu_∞ (and Sh_∞ for mass transfer experiments) - measurements derived with high Prandtl (or Schmidt - mass transfer) number fluids. There is clearly some doubt as to the limiting behaviour of μ_t near to a heated surface, and this was recognised during the theoretical work carried out and described herein.

In the laminar regime, Sellars modified the result of Leveque (discussed in part 2.) to determine the distribution of Nu for a fluid having a high Pr, where the boundary condition of uniform heat-flux was imposed. Appendix B describes the procedure used by Sellars but for a different problem. The result can be stated - $Nu = 1.639\ (r_w\ Re\ Pr/x)^{\frac{1}{3}}$.

This equation can be considered valid provided Nu is no less than ~ 10; but the solution is asymptotic for large values of the bracketed term which is the case most likely to occur with liquids having a high Prandtl number. For example, with Pr = 100 and Re = 1,000, the equation will be reliable for all axial distances less than ~ 500 diameters from the onset of heating.

3.7. SEPARATED FLOWS AND HEAT TRANSFER.

The sharp leading edge, at a sudden convergence in tube diameter, causes a separated region of flow to occur just downstream, sometimes known as the vena contracta. This distinguishes the configuration from developed or undeveloped flow at the entrance of a short tube, and a different distribution of Nu is likely to occur close to the discontinuity. Little experimentation has been carried out in this area. References B.11, B.12, H.1 and H.24 contain data for air and water, but the results most relevant to the present research are given by Grass (Ref: H.24) and Ede (Ref: H.1) using water as the medium.

Grass considered an electrically heated tube with a 2:1 convergence ratio, and the section upstream was unheated. Figure 3.11 shows the axial distribution of $(Nu/Pr^{0.4})$ downstream of the discontinuity. The shape of these functions, derived for different Reynolds numbers downstream, is qualitatively similar to measurements obtained with the short tube, as discussed earlier. However, the initial values of Nu close to the convergence were very much higher.

A more detailed study of the convergence system was carried out by Ede, in which three separate diameter ratios were investigated for a wide range of Reynolds number. The tubes were electrically heated so that uniform heat generation per unit length was imposed upstream and downstream of the discontinuity. The results are summarised in figure 3.17. The data presented for the 2:1 convergence compared favourably with the results of Grass. It was demonstrated that the Nusselt number close to the convergence reduced considerably as the diameter ratio was reduced to 1.25:1. An increase in the diameter ratio to 3.33:1 also caused a reduction in Nu close to the discontinuity, but to a lesser extent, and the general trend was for the value of Nu to increase in the region 3 to 20 diameters downstream.

Several attempts have been made to generalise on the heat transfer process in regions of separated flow. Chapman (Ref: H.21) produced an analysis for a laminar boundary-layer of gas which separated from a surface, causing a separation 'bubble', then reattached further downstream. (The analysis was complex and the reader is referred to the original text.) It was concluded that the coefficient of heat transfer in the separated region was less than that for an equivalent attached region by a factor of approximately 2. Larson (Ref: H.20) attempted to obtain experimental corroboration of Chapman's theory, and extended his work into the turbulent region. Electrically heated models were investigated having various contours, both two-dimensional and axi-symmetric. It was concluded that for laminar separation of air the separated coefficient of heat transfer was 35% to 50% of the corresponding attached value. With turbulent flow, however, it was found that very high coefficients of heat transdfer occurred in the reattached region of the boundary layer. It was demonstrated that for turbulent flow - $Nu \propto Re^{0.8}$ when attached, and $Nu \propto Re^{0.6}$ when separated. Seban (Ref: H.11 and H.13) conducted some similar experiments with air-flow over two dimensional bodies containing a sudden step in the otherwise smooth surface. The flow was found to separate at the step, then reattach at a distance of 6 step-heights downstream. This was indicated by a sudden increase in the local coefficient of heat transfer, and by local measurements of velocity distribution.

In references J.2 and J.3 attempts were made at measuring the intensity of the turbulent velocity fluctuations in the region of a discontinuity; both a stepped plate and pipe-orifice were investigated. Whereas these works provide a deeper understanding of the mechanisms involved in separation, the work is of the preliminary nature, and is not of particular practical value. Future developments in this area could prove to be useful to the theoretician interested in separated heat transfer, a subject which is outside the scope of the present studies.

The theoretical investigations of Mills (Ref: H.16) and Macagno (Ref: H.17) provide some insight into the flow patterns for the sudden divergence in tube diameter. In both cases stable laminar motion was considered, and a numerical solution of the momentum equations was sought. The usual boundary-layer approximations were not invoked since large radial velocities were likely to occur downstream of the discontinuity. Mills investigated a pipe-orifice and Macagno a sudden increase in tube diameter. The range of flow rates considered was limited in both cases by the computational stability of the numerical method employed. Mills performed calculations up to Re = 50 downstream, and Macagno extended the range to Re = 200. In both cases the diameter ratio was 1:2. Neither author attempted to solve the energy equations to yield the coefficients of heat transfer. The streamlines calculated indicated that a captive annular eddy was formed downstream of the discontinuity, and the length of this separated region increased from ~ 1 diameter at Re = 50, to ~ 4.5 diameters at Re = 200 (downstream values). It could be postulated that the distance to the point of reattachment would correspond approximately to the position of the maximum local value of Nu, but this statement is speculative and no evidence was found to support this conclusively. It should be stated here that the flow pattern is likely to be unstable, having a point of inflection in the axial velocity profile, and the critical Reynolds number for the onset of turbulent instability has not been considered in the above investigations.

Filetti (Ref: H.8) carried out a detailed investigation of heat transfer downstream of an abrupt enlargement in the cross section of a flat duct, and the heat transfer medium was air. Local heat-transfer rates were measured using heat-meters, and the channel walls were maintained at a lower temperature than the entrained air. The duct width increased in the ratio 1:2.1 and 1:3.1 for the two configurations studied. It was shown that a region of separation occurred on either side of the downstream section, but the length of each region differed since the flow pattern was asymmetrical. The Reynolds number was varied from $\tilde{70},000$ to $\tilde{200},000$ (based on hydraulic diameter). It was demonstrated that the average distance to the point of reattachment was independent of Re and was equal to $\tilde{6}$ step heights. In the separated region Nu was comparatively small rising to a peak at the point of reattachment, then reducing with increasing distance downstream. The maximum value of Nu was proportional to Re^n where $n = 0.689$ for the short separated length and 0.593 for the long separated length.

Several workers have reported data for configurations similar to the divergence experiments in this thesis. Air has been used in some of these. Zemanick (Ref: J.1) investigated local heat transfer downstream of a sudden increase in tube diameter; the section upstream was unheated, and the section downstream was heated directly by applying a voltage to the tube. Three diameter ratios were utilised, 0.43:1, 0.54:1 and 0.82:1. The results of the tests are recorded in figure 3.13. The axial distribution of the ratio-- local Nusselt number to Nusselt number at large axial distances - is shown. A well defined peak occurred in the functions which has been discussed previously as being typical of separated flows at high values of Re. The maximum value of Nu was measured at 7 and 9 step heights downstream for each of the diameter ratios, and this was independent of Re except at the lower values of Re. The maximum value of Nu could be estimated approximately from

$$Nu_{max} = 0.2\ Re_1^{\frac{2}{3}} ,$$

where Re_1 is the value of Re upstream.

Emerson (Ref: H.7) measured local coefficients of heat transfer downstream of a 1:1.7 divergence ratio using air. The tubes were heated electrically so that uniform heat generation per unit length was achieved upstream and downstream of the discontinuity. In these experiments a most detailed investigation of the apparatus and instrumentation was carried out. It was shown that longitudinal conduction of heat in the tube material can have a profound effect on the accuracy of measured values of h when small values of the latter are considered (such is the case with gases in convection.) A tube was manufactured with a thickness of only 0.05mm for use in the experiments to minimise the conduction problem. The results incorporated several geometries for causing separation, but only the divergence will be discussed here. Figure 3.15 shows how h varied downstream of the divergence, for a range of Re (downstream) of 14,500 to 105,000. Less than $\frac{1}{2}$ diameter downstream a minimum occurred in the h - distance function, and it was suggested that the 'high' values upstream of the minimum were 'artificial' values caused by conduction in the tube-wall.

The maximum value of h was measured a $2\frac{2}{3}$ diameters downstream, (or 13 step heights). In an attempt to relate this to the distance at which reattachment occurred, flow visualization tests were carried out with a transparent 'mock up'. Droplets of oil were placed on the inner tube-wall and the position of zero shear stress located by observing the displacement of the drops. Figure 3.16 illustrates that the point of reattachment was slightly more than 2 diameters downstream (or $9\frac{1}{2}$ step heights). The maximum value of h was apparently downstream of the separated region. The effect of changing the heat transfer rate in the upstream leg (keeping the downstream value constant) is indicated in figure 3.16. An increase of 70% in the rate of heat transfer upstream caused a reduction of $\widetilde{15}$% in the value of h in the region of the maximum value. It was suggested by Emerson that the peak Nu would probably be located at the point of reattachment if the lateral temperature profile within the air upstream had been uniform (or zero heat-transfer upstream).

A few experiments have been carried out with water in a sudden divergence, at high Reynolds numbers. Grass (Ref: H.24) fitted orifices to the inlet of an electrically heated tube, and measured h downstream. The ratios of orifice to tube diameter employed were 1:1.25, 1:1.67 and 1:2.5. Figure 3.12 summarises these results. It is clear that the position of the peak Nusselt number moved downstream as the orifice size was reduced, and in the case of the 1:1.25 ratio, the peak value occurred too close to the discontinuity to permit the value to be measured. The position of the peak was apparently independent of Re, and was located 2.6 diameters downstream ($8\frac{1}{2}$ step heights) with 1:2.5 ratio, and 1.7

diameters ($8\frac{1}{2}$ step heights) with 1:1.67 ratio.

A similar experimental configuration was investigated by Krall (Ref: H.9) using water. For Reynolds numbers above 10,000, the value of h was measured for 1:1.5, 1:2, 1:3 and 1:4 orifice to tube diameter ratios. The ratio of Nu_x to the fully developed value of Nu_{fd} at large distances (or Nu/Nu_∞) is shown in figure 3.14. It is difficult to draw a comparison with the results of Grass, which were somewhat incomplete, however, small differences were observable. The position of maximum Nu was 1.5 to 2.5 diameters downstream for all the geometries considered. For the ratios 1:2 and 1:3 this distance was $1\frac{3}{4}$ to $2\frac{1}{4}$ diameters, which is rather less than the 2.6 diameters obtained by Grass with the 1:2.5 ratio. Although a direct comparison of the maximum Nu was not possible, the evidence suggests a reasonable agreement between the two sources. The maximum value of Nu for all the divergences could be expressed as $0.398\ Re_1^{\frac{2}{3}}$, (where Re_1 is the orifice Reynolds number).

The most detailed investigation of the divergence system with water has been carried out by Ede (Ref: H.1). The configurations included sudden increases in tube diameter, the divergence ratios studied being 1:1.25, 1:2 and 1:3.33. Uniform heat generation per unit length was imposed upstream and downstream of the discontinuity, and careful instrumentation of the apparatus allowed reliable measurements of h to be determined in the region of the divergence. A wide range of Re was covered extending to much lower values than were employed hitherto. The experimental findings are summarised in figures 3.18 and 3.19. Figure 3.18 gives the axial distribution of $(Nu/Pr^{0.4})$ for the three divergences, the Reynolds number downstream ranged from 3,000 to 50,000. The functions were derived by interpolating the extensive experimental data in such a way that the small axial variations in fluid properties (caused by the increasing bulk temperature) were eliminated.

The location of the peak Nu was 1 diameter downstream of the discontinuity for the 1:1.25 ratio, increasing to $2\frac{1}{4}$ diameters for the 1:2 ratio and 3 diameters for the 1:3.33 ratio (or 10, 9 and $8\frac{3}{4}$ step heights respectively.) The distance in diameters was approximately equal to the diameter ratio. The ratio (maximum Nu/Nu_{∞}) increased with the diameter ratio, and could be expressed approximately by $15.3\ Re^{-0.22}$.(dia.downstream/dia.upstream) according to Ede.

Figure 3.19 shows the results derived for the lower Reynolds numbers. Reducing Re it was found that the temperature measurements became unstable and it proved impossible to obtain reliable data. A transition region occurred until Re downstream reduced to the order 10^2. As Re decreased, the trend was for the peak Nu to move downstream, and the ratio (maximum Nu/Nu_{∞}) became much smaller. With Re of the order 10^2 the peak in the Nu-distance function vanished, for the lowest divergence ratio, and a sudden drop to a minimum was evident just downstream of the step. The value of this minimum was considerably less than Nu_{∞}.

Flow visualization tests carried out by Ede showed that at high values of Re the flow entered the downstream leg as a jet surrounded by a region of pronounced recirculation. The jet expanded to fill the tube. When the flow was laminar far downstream, the laminar distribution was very slow in developing, and the flow pattern close to the discontinuity was similar to the fully turbulent case to very low values of Re ($\ll$ 2,000 downstream). With laminar flow upstream, the flow through the divergence was stable for very low Reynolds numbers ($\tilde{1}00$). However, an intermediate regime was evident in which the laminar flow broke down and became unstable several diameters downstream.

No experimental or theoretical work could be traced which dealt with viscous fluids in stepped tubes. It was apparent that little or no work had been carried out for heat transfer in the region of a sudden geometrical discontinuity, where the heat-transfer medium possessed a high Prandtl number. A comparison between the results of Emerson (Ref: H.7) and Ede (Ref: H.1) indicates the effect of increasing Pr from $\tilde{0}.7$ to $\tilde{8}.0$. Interpolating the data of Ede to give equivalent results for a 1:1.7 sudden divergence, as used by Emerson, significant differences are evident. For water, the maximum value of (Nu/Nu_{∞}) was 4.3 to 2.5 reducing as Re increased from 5,000 to 50,000. This maximum was located $\tilde{2}.0$ diameters downstream.. For air, the value of $Nu/Nu_{\infty})$ was maximum $\tilde{2}.9$ diameters downstream and the magnitude was 2.5 to 2.8 in the range Re = 14,500 to 105,000. No definite relationship between $(Nu/Nu_{\infty})_{max}$ and Reynolds number was established. Increasing Pr from 8 to 500 say, could lead to very significant departures from the 'non-viscous' results discussed in this section, and there is no reasonable justification for applying the data obtained with water or air when viscous fluids are encountered.

3.8. THE EFFECTS OF DISSIPATION.

The dissipation of mechanical energy into heat is likely to play an important part in the convection process when the shear stress is high in the region of the thermal boundary-layer, and the working temperature differences $(t_w - t_b)$ is small. In general, this is likely to be the case (for moderate Re, say 10^3 to 10^5) when either the viscosity is small and velocity high, or the viscosity is high and the velocity moderate. The former is common with gases and the latter with oils.

The width of the thermal and momentum boundary-layers are comparable in magnitude with gases, but the thermal layer is much thinner with fluids having a high Prandtl number, so the theoretical treatment of the two cases must differ considerably. The analysis of dissipative heat-transfer for gas flowing over a plate is well known, and is treated in many standard text books (e.g. Ref: K.5). Few references were found which discussed dissipation with viscous fluids in tubes. References J.14 and C.21 provide an explanation of how Nu increases when dissipation becomes significant, and a limited amount of experimental work was done to demonstrate the phenomenon. In general, the effects of dissipation on Nu were pronounced when Pr >> 100. It was intended to attempt a theoretical assessment of such effects for the simplest configuration herein i.e. the short tube.

Kudryashev (Refs: F.1 and F.2) analysed heat transfer with dissipation for the laminar flow of non-viscous fluids in the entrance region of a tube. The flow was fully developed at the entrance and the tube was at constant temperature. Two solutions of the energy equation were sought, the first was for the case when wall temperature was constant and equal to the inlet temperature of the fluid. The second solution assumed a constant wall temperature, which was higher than the inlet temperature of the fluid, and no dissipation was present. The general solution was assumed to be the sum of both particular solutions, and the local Nusselt number was finally expressed:-

$$\mathrm{Nu} = \frac{8\,D + \sum_{n=0}^{\infty} H_n \exp\left(-2\,k_n^2\; x/(r_w \mathrm{RePr})\right)}{5\,D/6 + \sum_{n=0}^{\infty} G_n \exp\left(-2.k_n^2\; x/(r_w \mathrm{RePr})\right)}$$

where the first five values of coefficients G, H and constants k in the above series are given in references F.1 and F.2.

$$D = \mathrm{Re}^2\,\mathrm{Pr} \,/\, \left((8gr_w^2\,\rho^2/\mu^2)(c\,(t_w - t_o)/2r_w) \right),$$

t_o = inlet temperature.

The above result converges rapidly as Pr tends to zero, and would be found suitable for application with gases. It is interesting to note that the value of Nu tends to 9.6 at large axial distances, which can be compared with the non-dissipative limit of 3.65.

The analysis of fully developed heat-transfer, with dissipation, in long tubes is discussed in references F.3 and F.4. The procedures described enable the value of Nu to be determined for a tube of generalised cross-section, and can thus be extended to circular tubes. The boundary conditions considered (in Ref: F.3) appertain to a linear axial distribution of wall temperature, and internal heat generation is permitted within the fluid (such as might occur with nuclear heating). The result for a circular tube is expressed:-

$$\mathrm{Nu} = \frac{48}{11} F$$

$$\text{where } F \qquad = F\left(\frac{\mu \bar{u}^2}{q r_w}\right)$$

In the attempt at generalising on the problem, the function F was derived in a complicated form, and for fully developed heat transfer in laminar tube-flow, it is just as convenient to integrate the energy equation from first principles. This is carried out in part 11. It can be concluded from the above analysis that the parameter $(\mu \bar{u}^2/qr_w)$ is a significant group in estimating the contribution of dissipation to Nu_∞.

In turbulent tube-flow, the effects of shearing rate on the value of Nu apparently have not been assessed for a viscous medium. The solution of this problem is likely to indicate that the main contribution of viscous dissipation occurs in the laminar sub-layers at the tube wall where high shear stresses can arise. In the mainstream, velocity and temperature gradients are small, and good thermodynamic mixing is inevitable. The model of turbulence proposed must have some effect on the dissipative energy, and some difficulty in justifying the solution is likely to occur.

No empirical data on dissipative heating could be found which would be of value in these investigations.

3.9. TUBE WALL CONDUCTION.

Although the temperature distribution in the heat-transfer medium is of prime interest in work of this nature by definition, it is recognised that a solid-liquid interface is present in practice, and that before reliance can be placed on the temperatures measured at the surface of the tube, the heat-transfer processes within the tube-wall itself should be probed. For instance, the relationship between the temperatures at the inner and outer surfaces of the tube must be influenced by the properties and thickness of the material, and the distribution of the heat generated electrically within the material. Further, the heat-flux at the solid-liquid interface can only be truly uniform for a linear axial temperature distribution inside and outside the tube.

In references G.1, G.2, and J.7, attempts have been made at solving the temperature distribution within a solid wall, and within the heat transfer medium entrained, simultaneously. In each case the mathematical techniques employed were sophisticated, and the distribution of velocity and temperature in the fluid was simple. This kind of formal approach to the problem was considered to be of little practical value in these experiments, and a more direct and elementary approach was sought, as described in a later section of the thesis.

FIGURE 3.1.

COMPARISON BETWEEN THE RESULTS OF MALINA AND ALLEN.

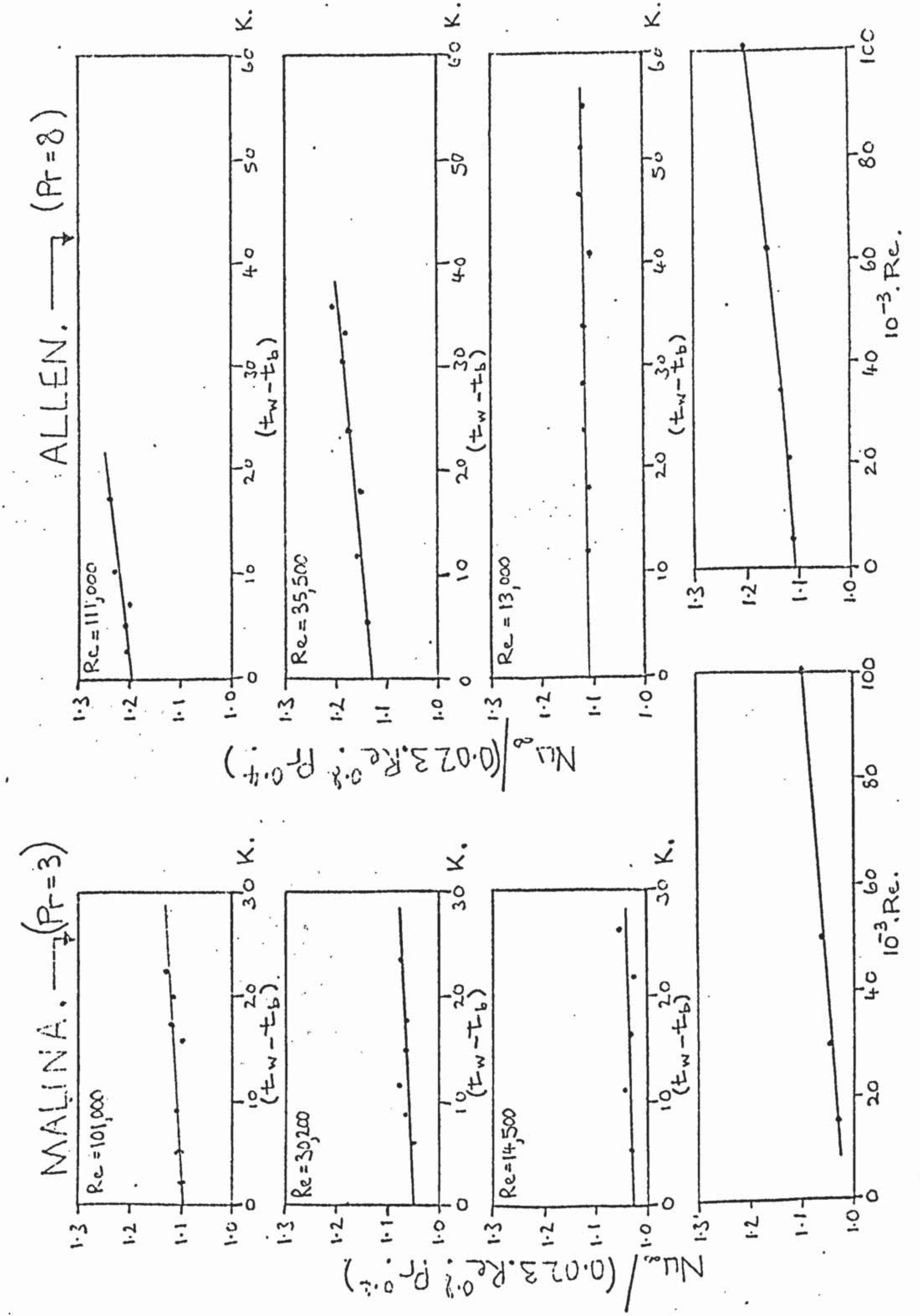

FIGURE 3.2.

THE RESULTS OF EDE FOR EXPERIMENTS WITH LONG ELECTRICALLY HEATED TUBES.

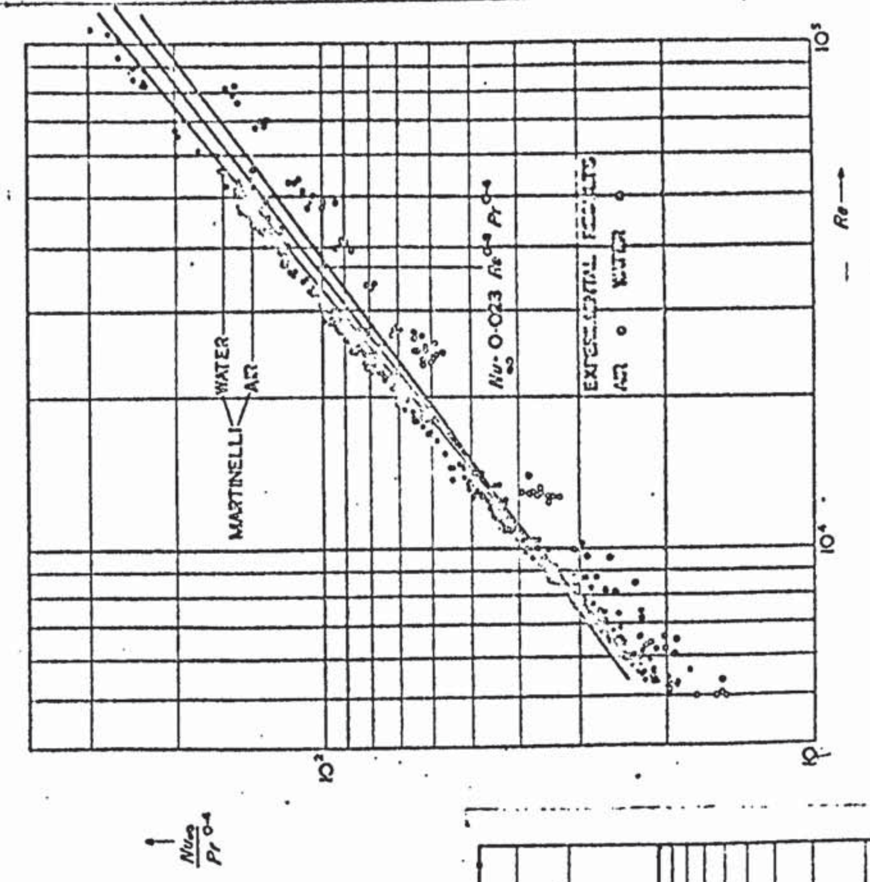

Results for turbulent flow.

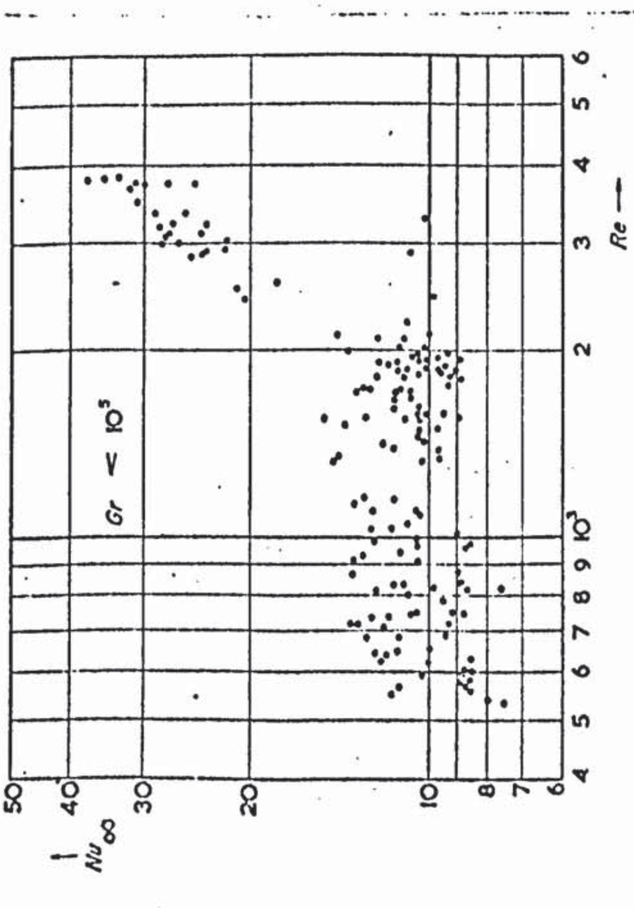

Results for low Reynolds numbers with the Grashof number less than 10^5.

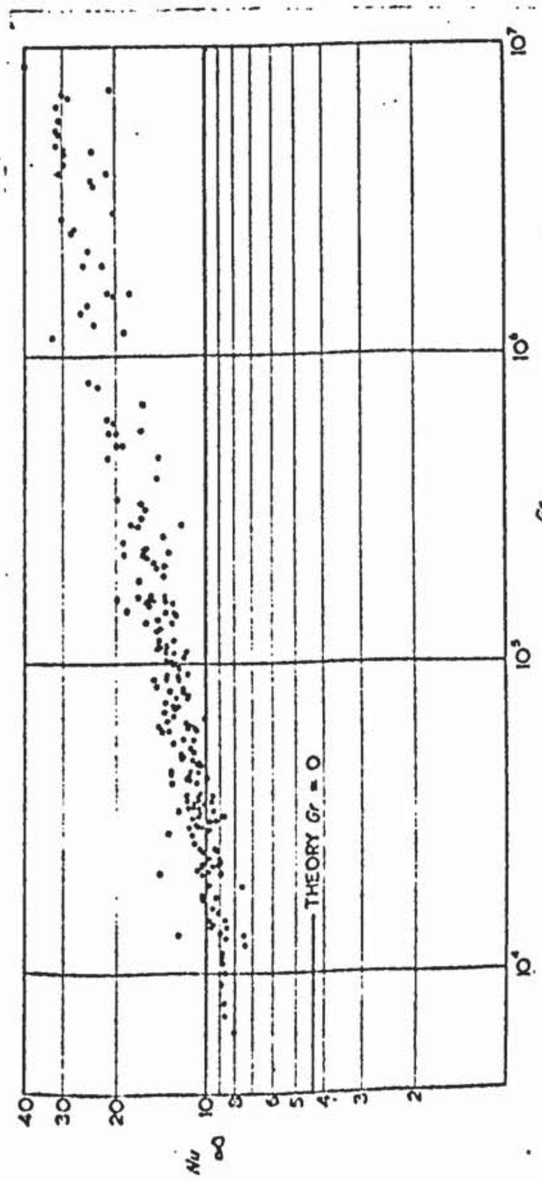

Results for laminar flow correlated against Grashof number.

FIGURE 3.3.

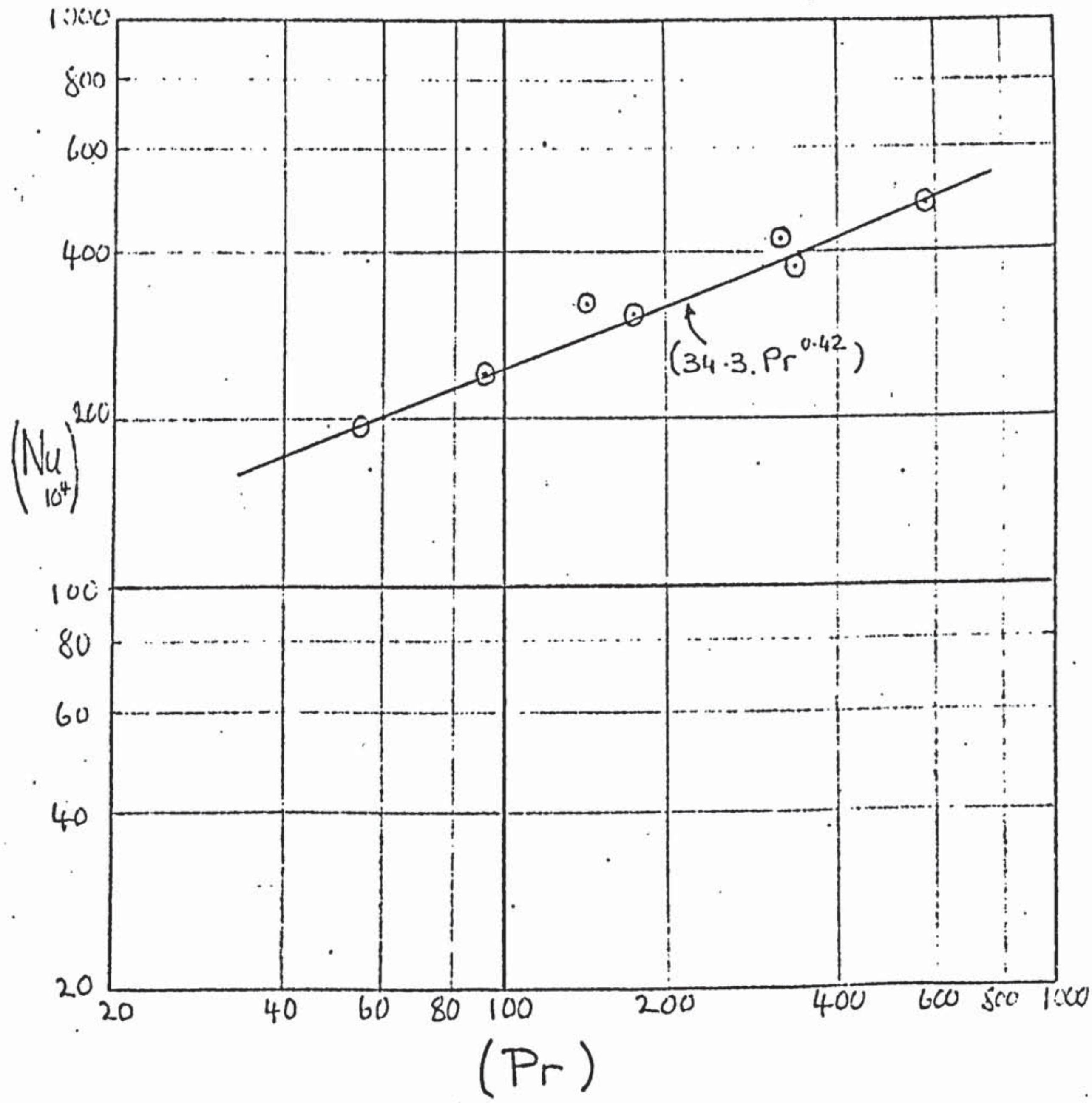

THE VARIATION IN (Nu_∞) WITH (Pr) WHEN $Re = 10^4$

FRIEND AND METZNER.

$Nu_{10^4} = Nu_\infty$ AT $Re = 10^4$.

FIGURE 3.4.

SUMMARY OF KAYS RESULTS.

LAMINAR HEAT-TRANSFER. DEVELOPED AND UNDEVELOPED FLOW OF LOW PRANDTL NUMBER FLUIDS WITH UNIFORM HEAT-FLUX AND CONSTANT TUBE TEMPERATURE.

LOCAL NUSSELT NUMBERS.

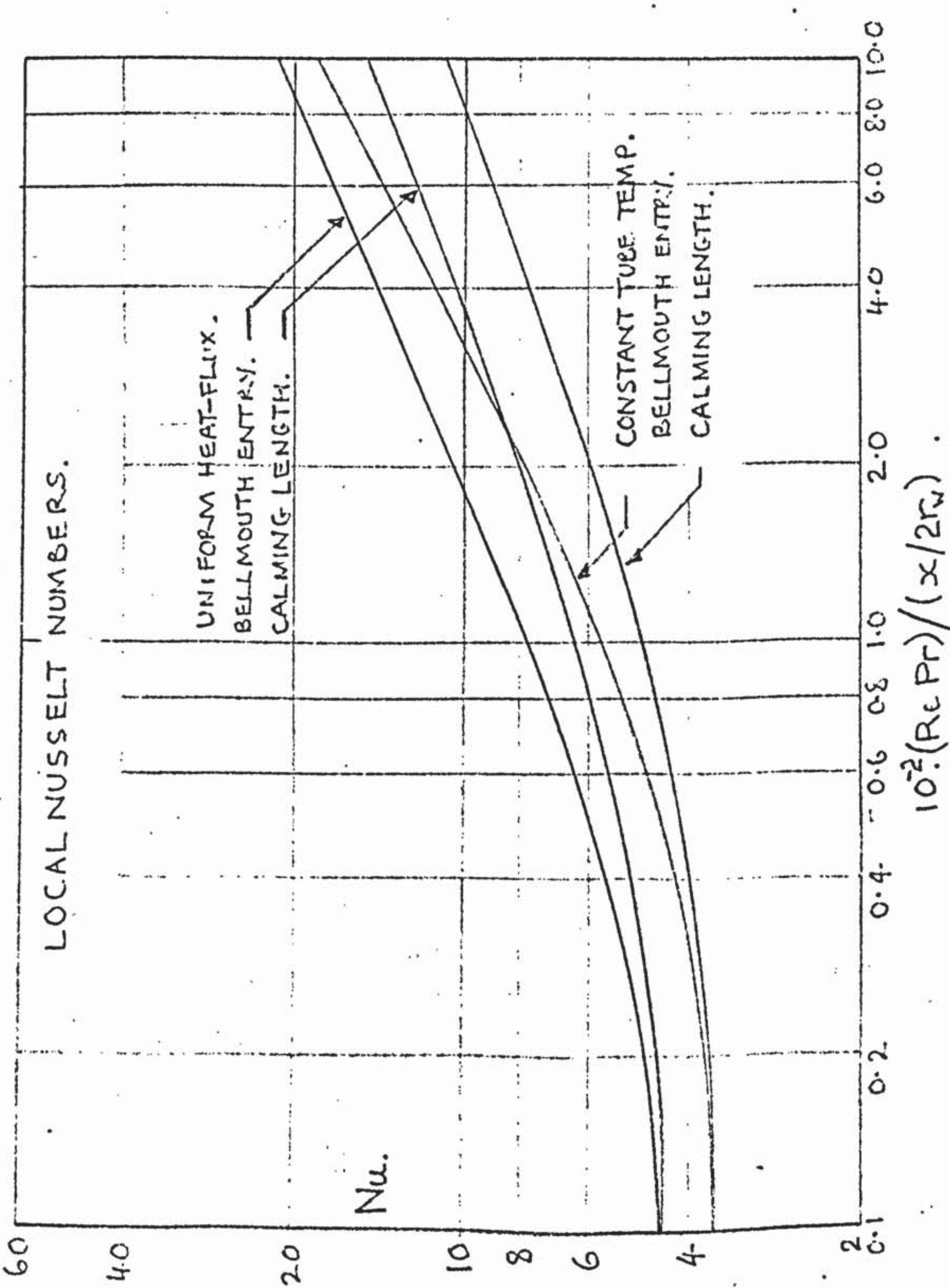

FIGURE 3.5.

THE RESULTS OF McCOMAS AND ECKERT FOR LOCAL COEFFICIENTS OF HEAT TRANSFER WITH LAMINAR TUBE-FLOW (HORIZONTAL).
HEAT-TRANSFER MEDIUM — AIR.
DEVELOPED FLOW AT ENTRANCE.

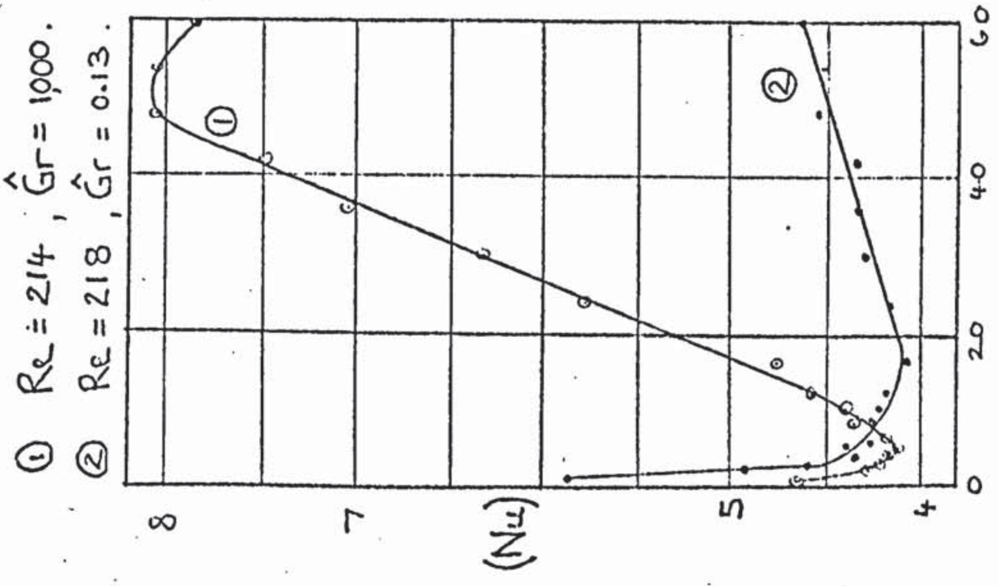

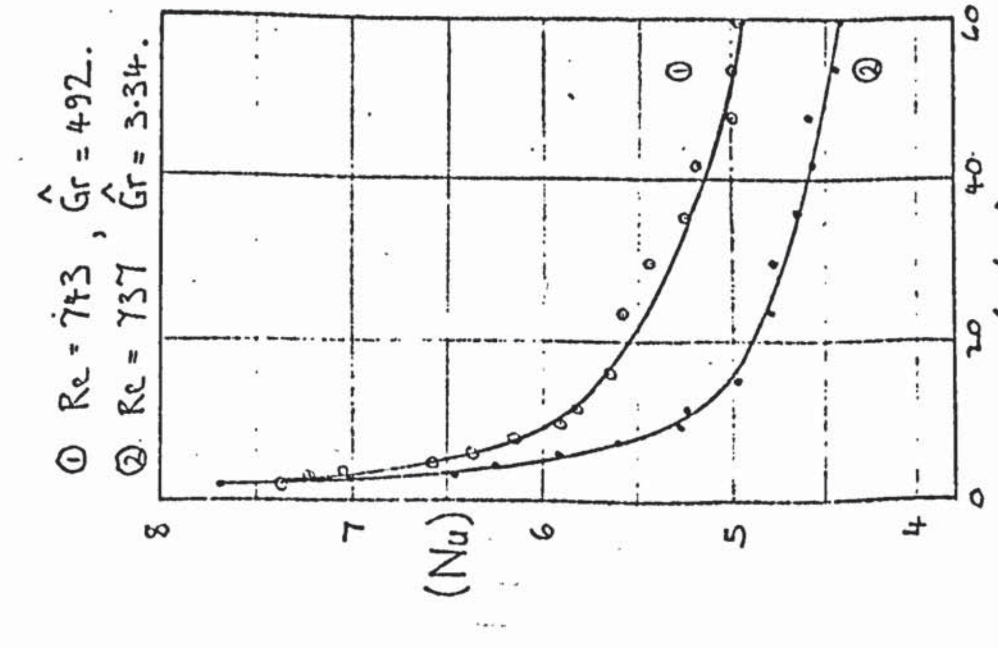

.FIGURE 3.6.

THE EXPERIMENTAL RESULTS OF MILLS FOR AIR IN HEATED TUBES.

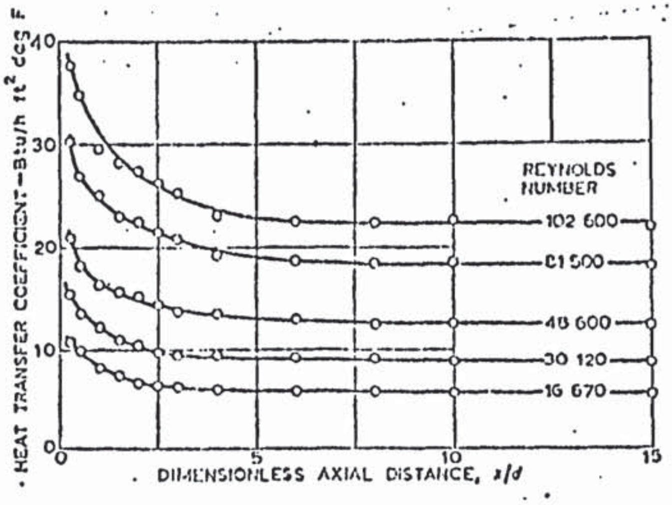

Local heat transfer coefficients for long calming section entry

$$\left(1 \frac{\text{Btu}}{\text{ft}^2\,\text{h}\,^\circ\text{F}} = 5{\cdot}678 \frac{\text{W}}{\text{m}^2\,\text{K}} \right)$$

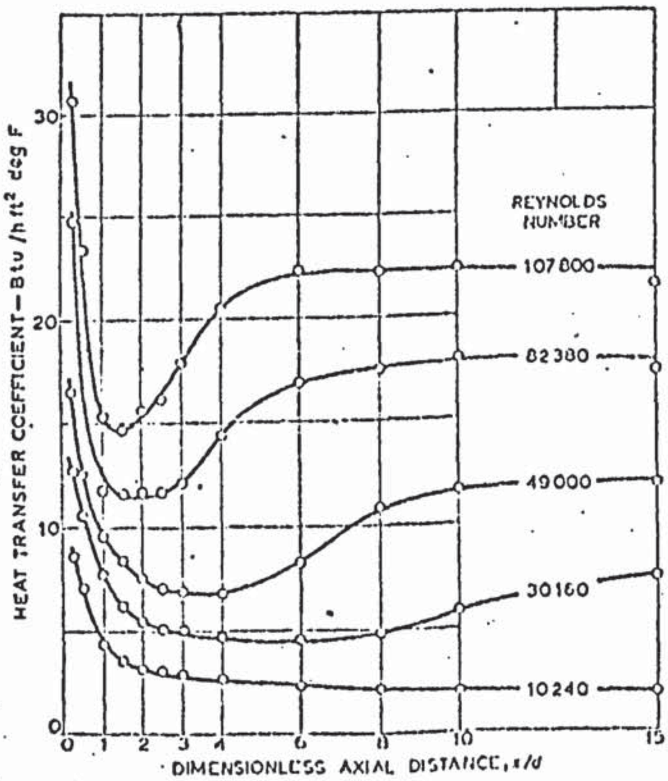

Local heat transfer coefficients for bellmouth entrance

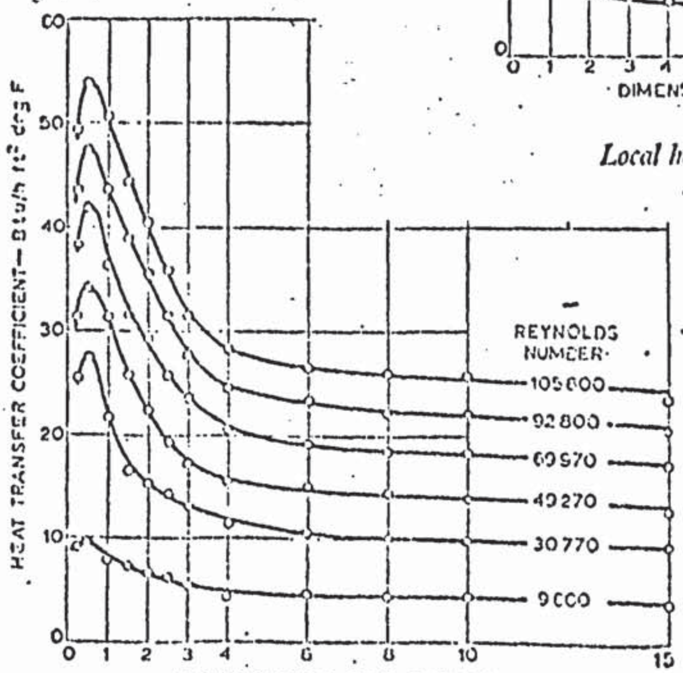

Local heat transfer coefficients for sharp 90° edge entrance

x = DISTANCE FROM ONSET OF HEATING.

d = TUBE DIAMETER.

FIGURE 3.7.

THE EXPERIMENTAL RESULTS OF WOLF FOR HEAT TRANSFER TO AIR AND CARBON DIOXIDE. WITH CALMING LENGTH.

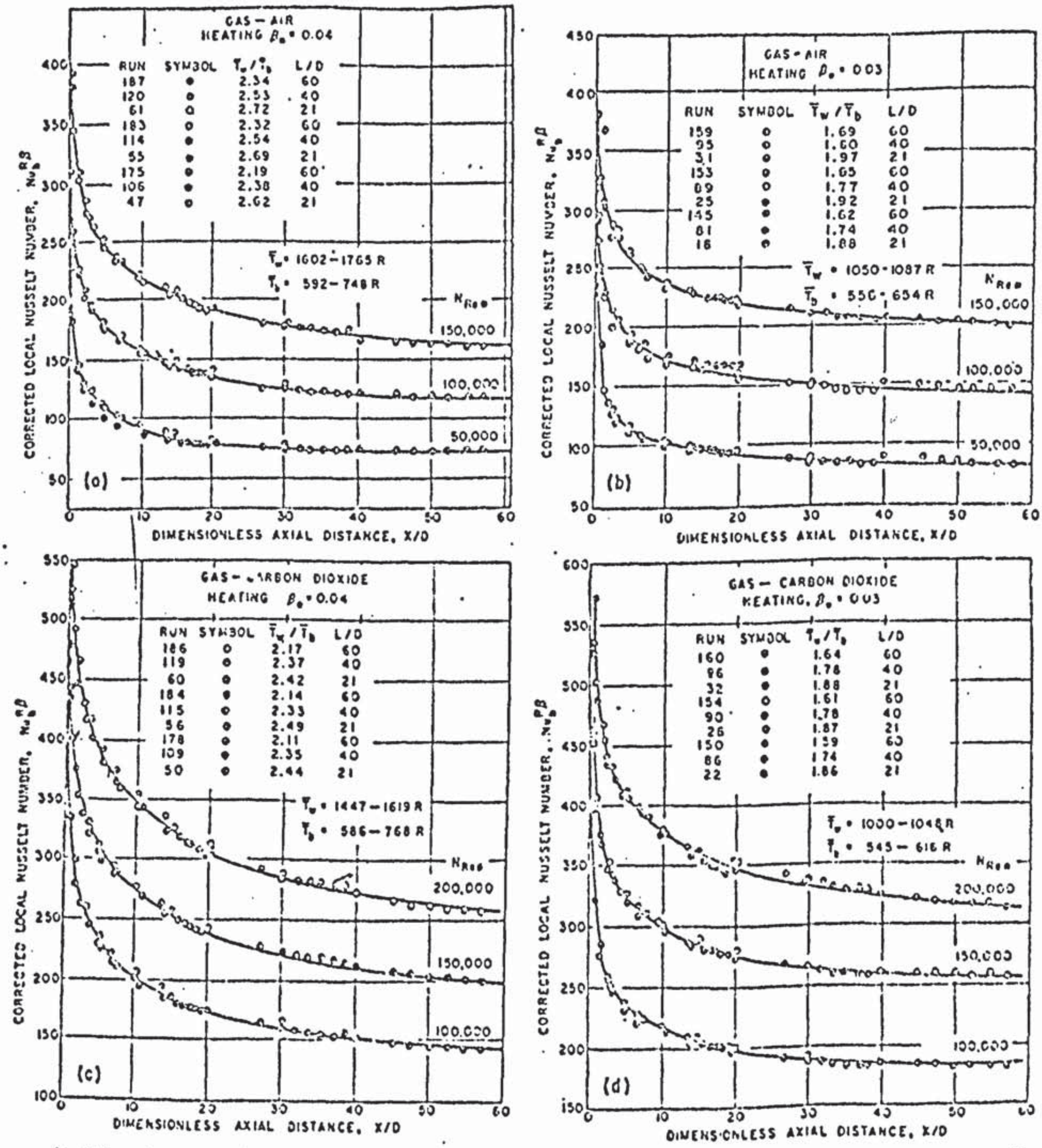

Variation of corrected local Nusselt number with x/D for air and carbon dioxide; uniform initial temperature profile, fully developed initial velocity profile, constant heat flux

$Nu_b^{R\beta}$ = NUSSELT NUMBER CORRECTED TO NOMINAL VALUES OF Re AND β. (AT LOCAL BULK TEMP.)

$$\beta_* = \left[\frac{q_w \sqrt{\tau_w/\rho_w}}{g\, C\, \tau_w \cdot t_w} \right]$$

FIGURE 3.8:

3.8 (i).

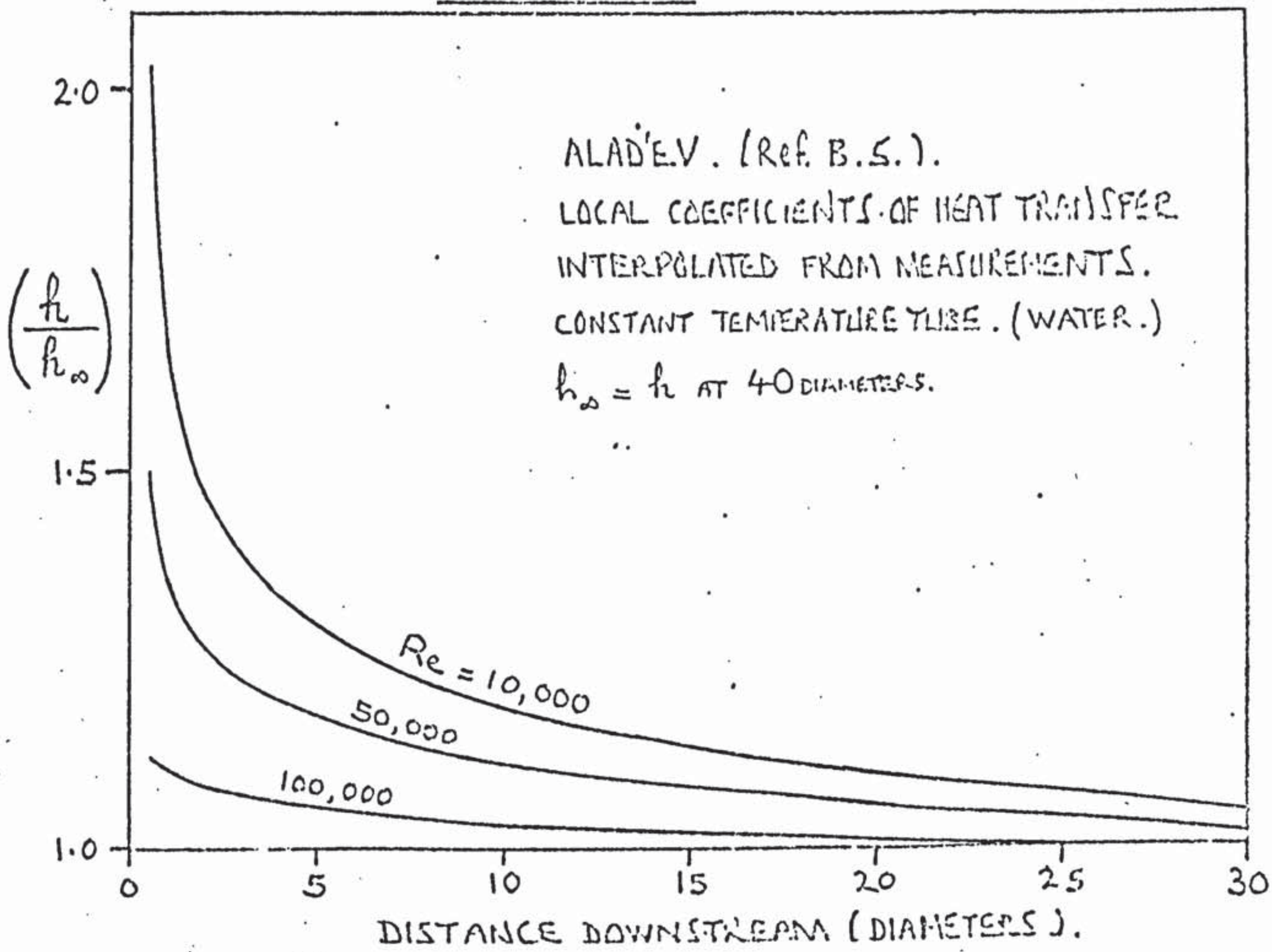

3.8 (ii).

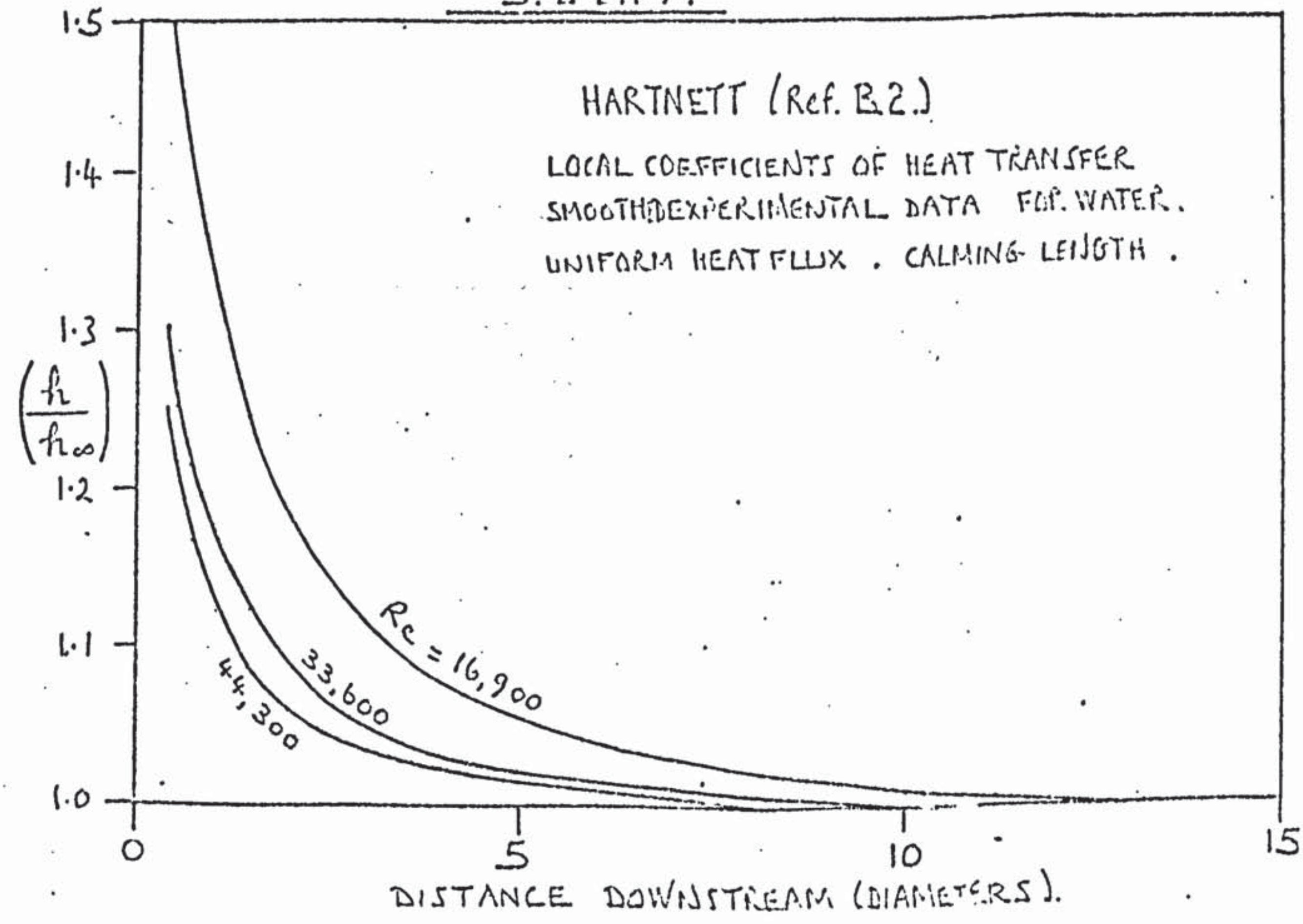

FIGURE 3.9 .

THE EXPERIMENTAL RESULTS OF STONE (Ref B.3.). (h/h_∞) VERSUS (DISTANCE): SHOWING THE EFFECT OF CALMING LENGTH.

SMOOTHED AND INTERPOLATED DATA. EXPERIMENTAL SCATTER ±20% MAX.

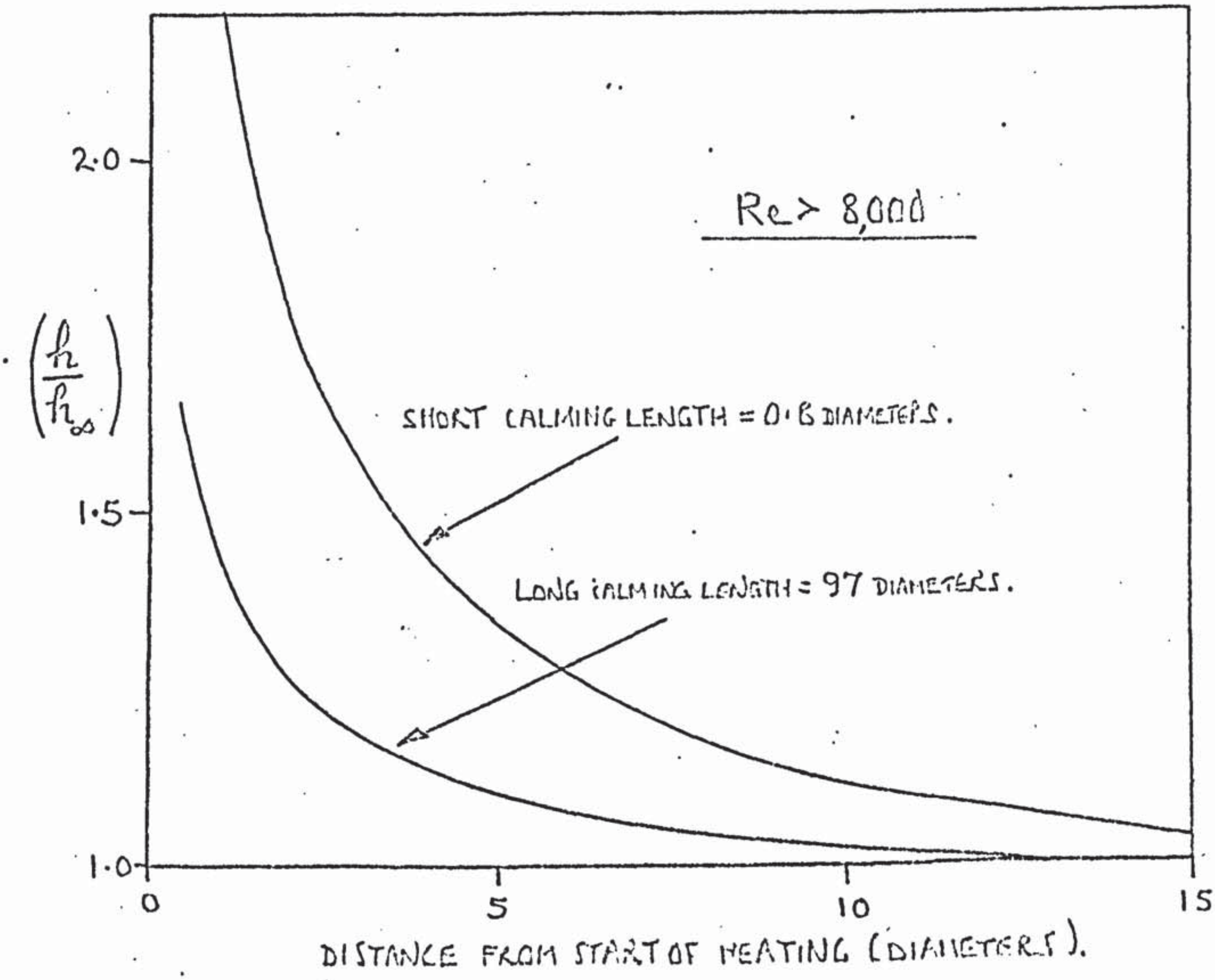

FIGURE 3.10.

MEASURED VALUES OF (h/h_∞) IN THE ENTRANCE REGION OF A TUBE WITH CALMING LENGTH. RESULTS FOR WATER AND TWO OILS.
MALINA (Ref.: B.1.).

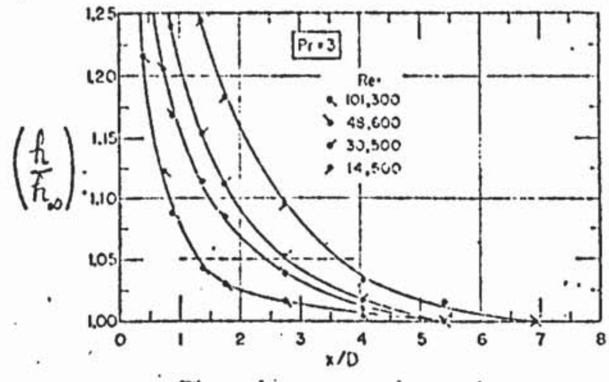

Thermal entrance region results, water, Pr = 3.

TUBE HEATED ELECTRICALLY.

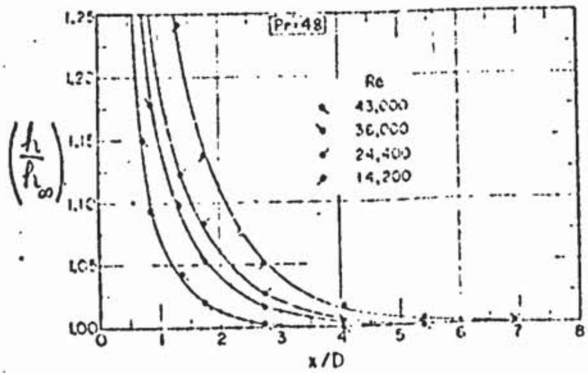

Thermal entrance region results, oil, Pr = 48.

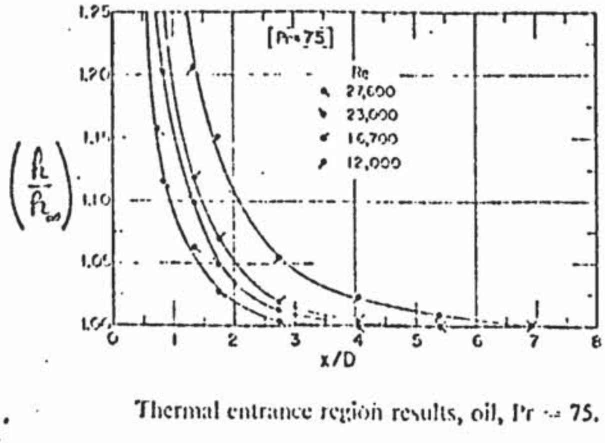

Thermal entrance region results, oil, Pr = 75.

h_∞ = FULLY DEVELOPED VALUE.
h = LOCAL VALUE.
x = DISTANCE FROM ONSET OF HEATING.
D = TUBE DIAMETER.

FIGURE 3.11

HEAT TRANSFER DOWNSTREAM OF A SUDDEN REDUCTION OF 2:1
IN TUBE DIAMETER ACCORDING TO GRASS.
UPSTREAM SECTION UNHEATED.

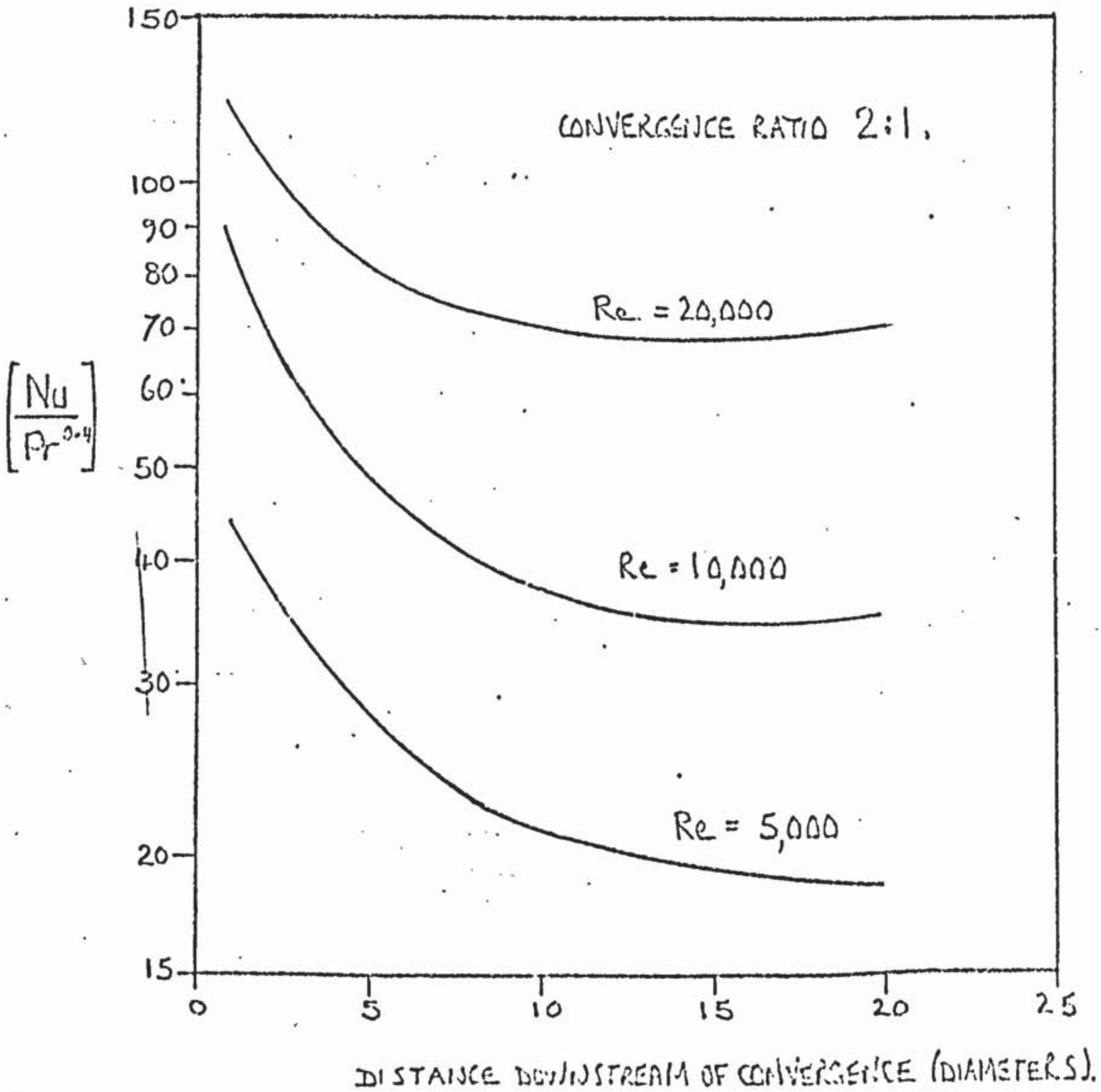

FIGURE 3.12.

HEAT TRANSFER DOWNSTREAM OF A SUDDEN DIVERGENCE IN TUBE DIAMETER. UPSTREAM SECTION UNHEATED. (GRASS).

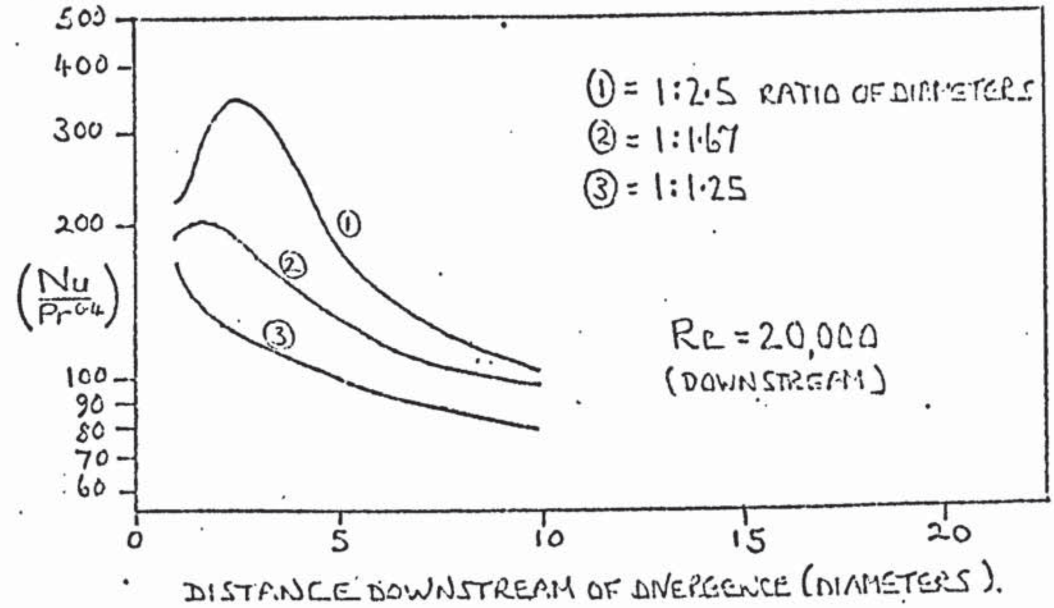

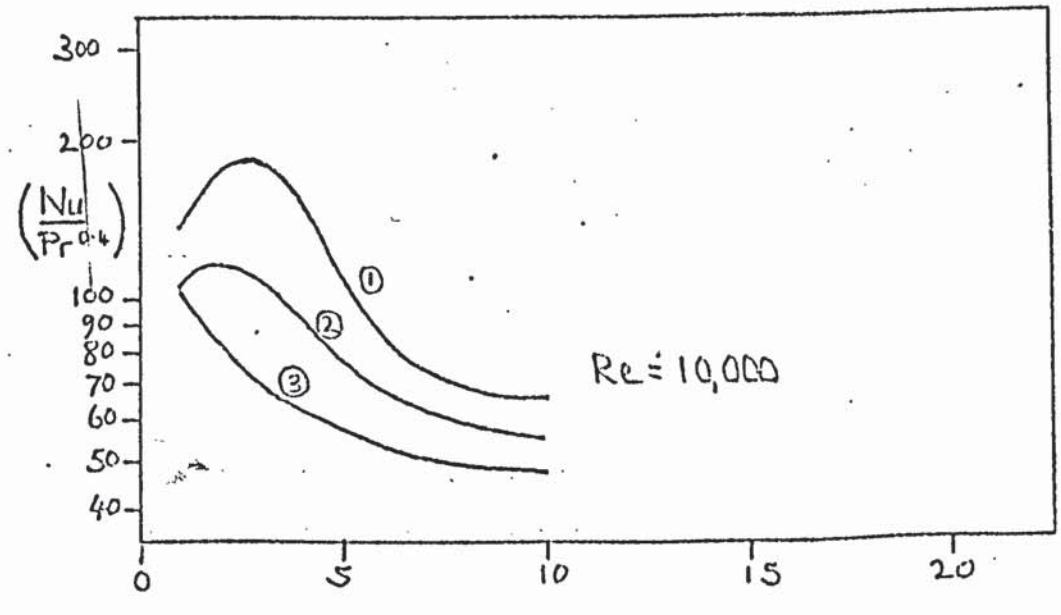

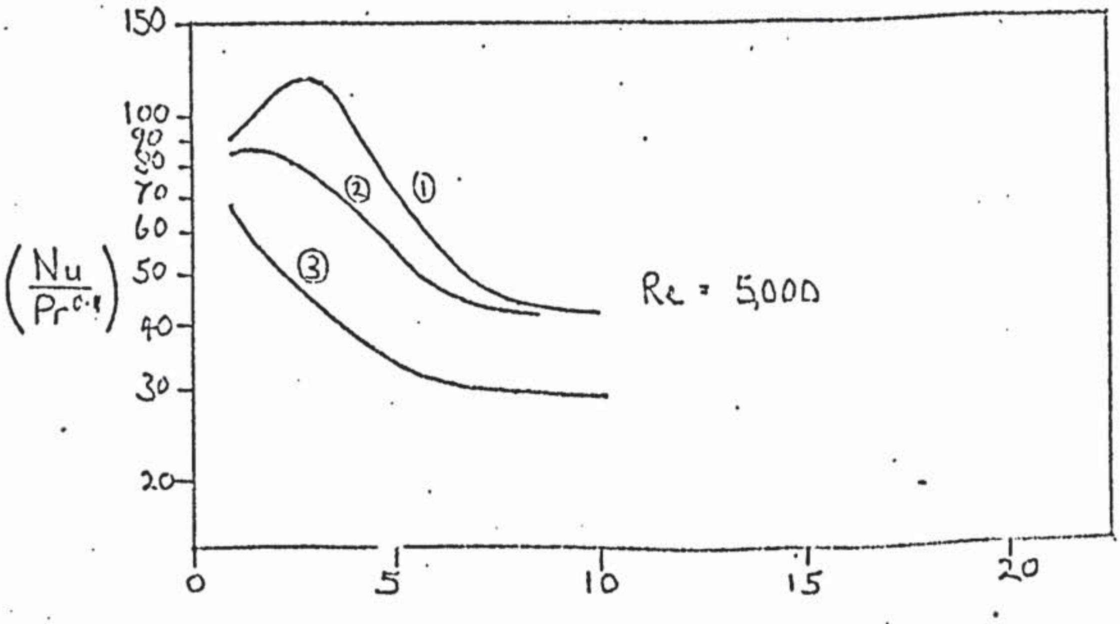

FIGURE 3.13.

Nu_{fd} = THE VALUE OF Nu AT LARGE AXIAL DISTANCES.

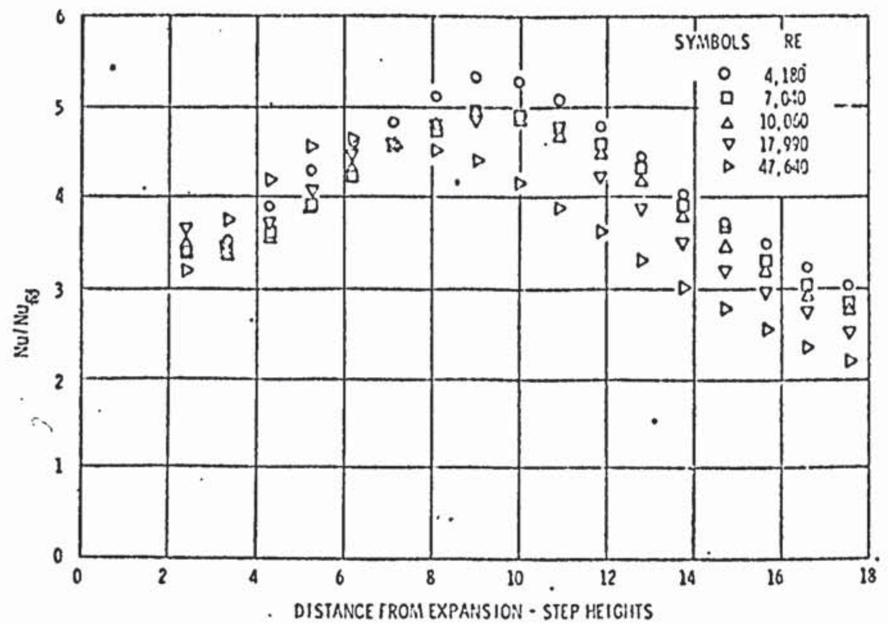

Axial distribution of local to fully developed Nusselt number ratio, $d/D = 0.43$

d = DIAMETER UPSTREAM.
D = DIAMETER DOWNSTREAM.

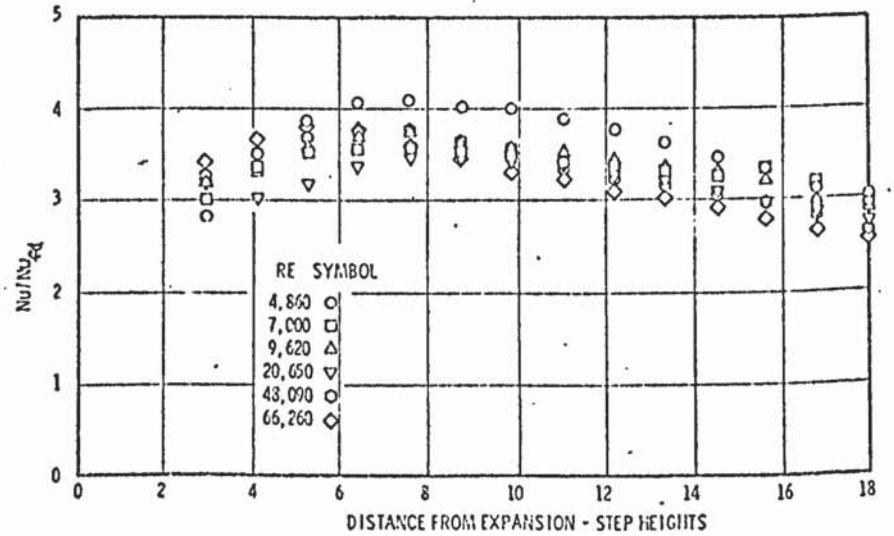

Axial distribution of local to fully developed Nusselt number ratio, $d/D = 0.54$

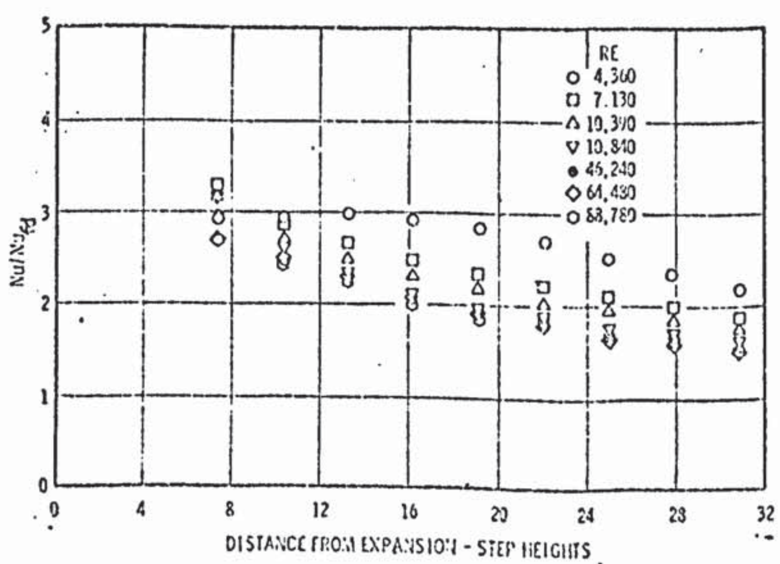

Axial distribution of local to fully developed Nusselt number ratio, $d/D = 0.82$

HEAT TRANSFER DOWNSTREAM OF A SUDDEN DIVERGENCE, FROM ZEMANICK.

FIGURE 3.16.

HEAT TRANSFER DOWNSTREAM OF AN ORIFICE IN A TUBE, FROM KRALL.

d_o = ORIFICE DIAMETER D = TUBE DIAMETER Nu_{fd} = VALUE OF Nu_x AT LARGE DISTANCES.
$Nu_x \equiv Nu$.

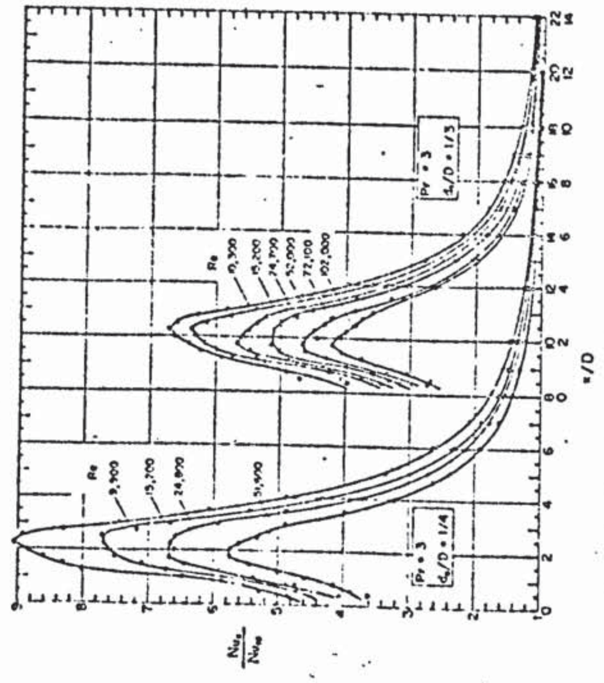

Local heat-transfer results in the separated, reattached, and redevelopment regions; Pr = 3, $d_0/D = 1/3$ and $1/4$

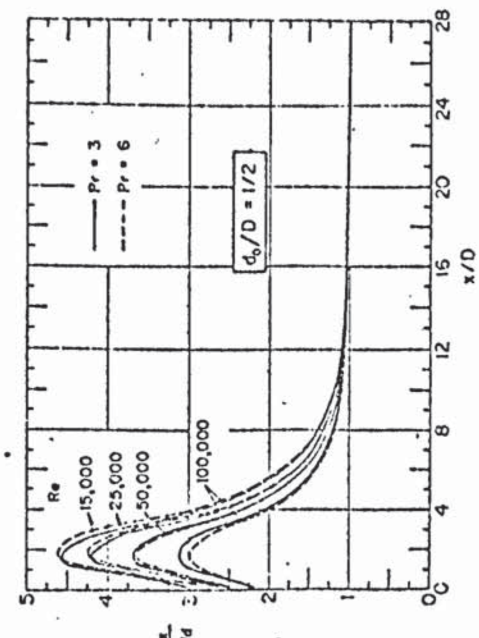

Comparison of heat transfer results for Pr = 3 and Pr = 6

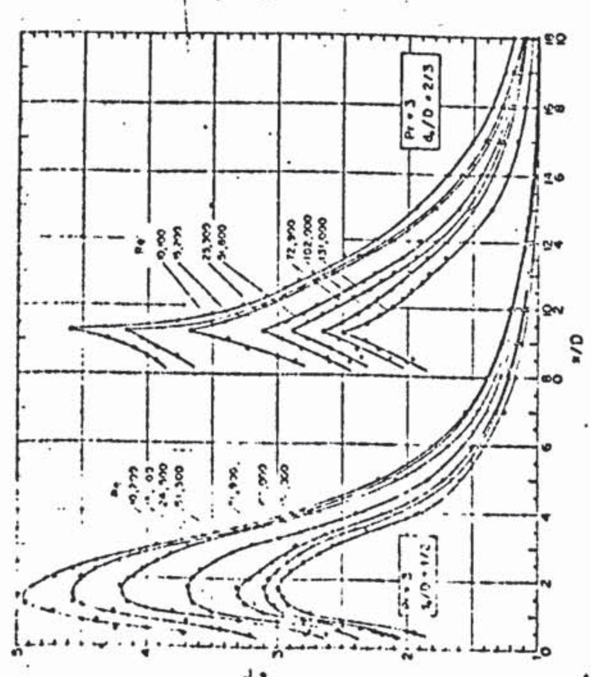

Local heat-transfer results in the separated, reattached, and redevelopment regions; Pr = 3, $d_0/D = 2/3$ and $1/2$

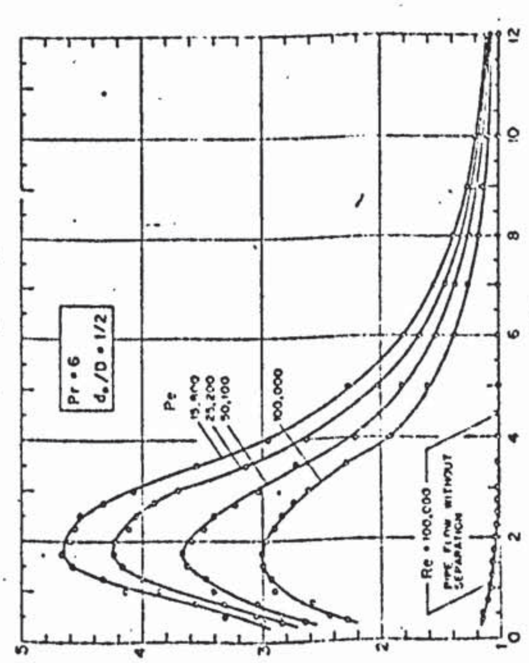

Local heat-transfer results in the separated, reattached, and redevelopment regions; Pr = 6, $d_0/D = 1/2$

FIGURE 3.15

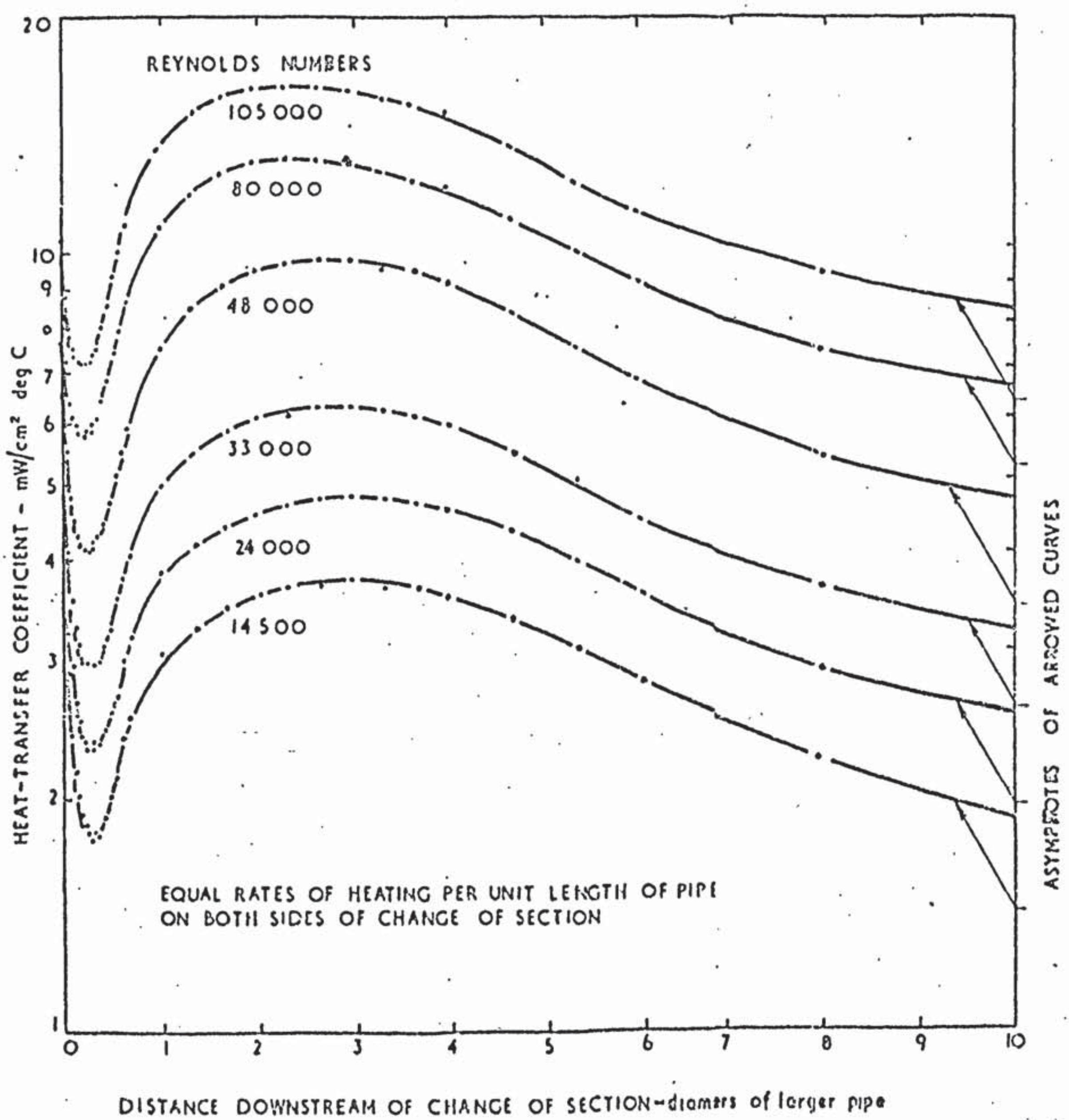

LOCAL HEAT-TRANSFER COEFFICIENTS WIT AIR IN A 3-inch DIA PIPE DOWNSTREAM FROM A STEP CHANGE FROM $1\frac{3}{4}$ inch DIA (EMERSON).

FIGURE 3.16

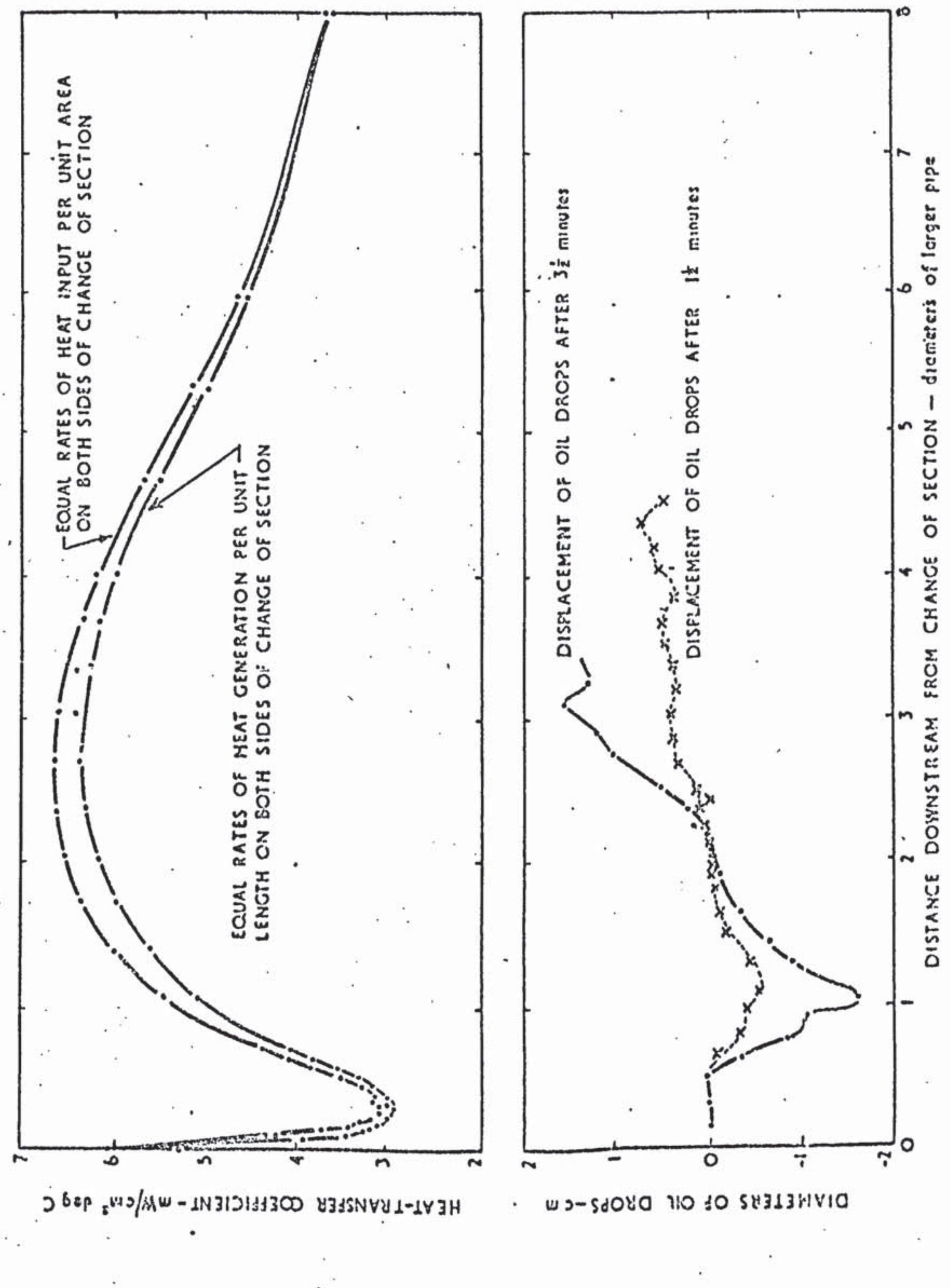

HEAT TRANSFER AND OIL-DROP TESTS AT REYNOLDS NUMBER=32000, 1¼ inch DIA PIPE ENLARGING TO 3-inch DIA ([illegible]).

FIGURE 3.17.

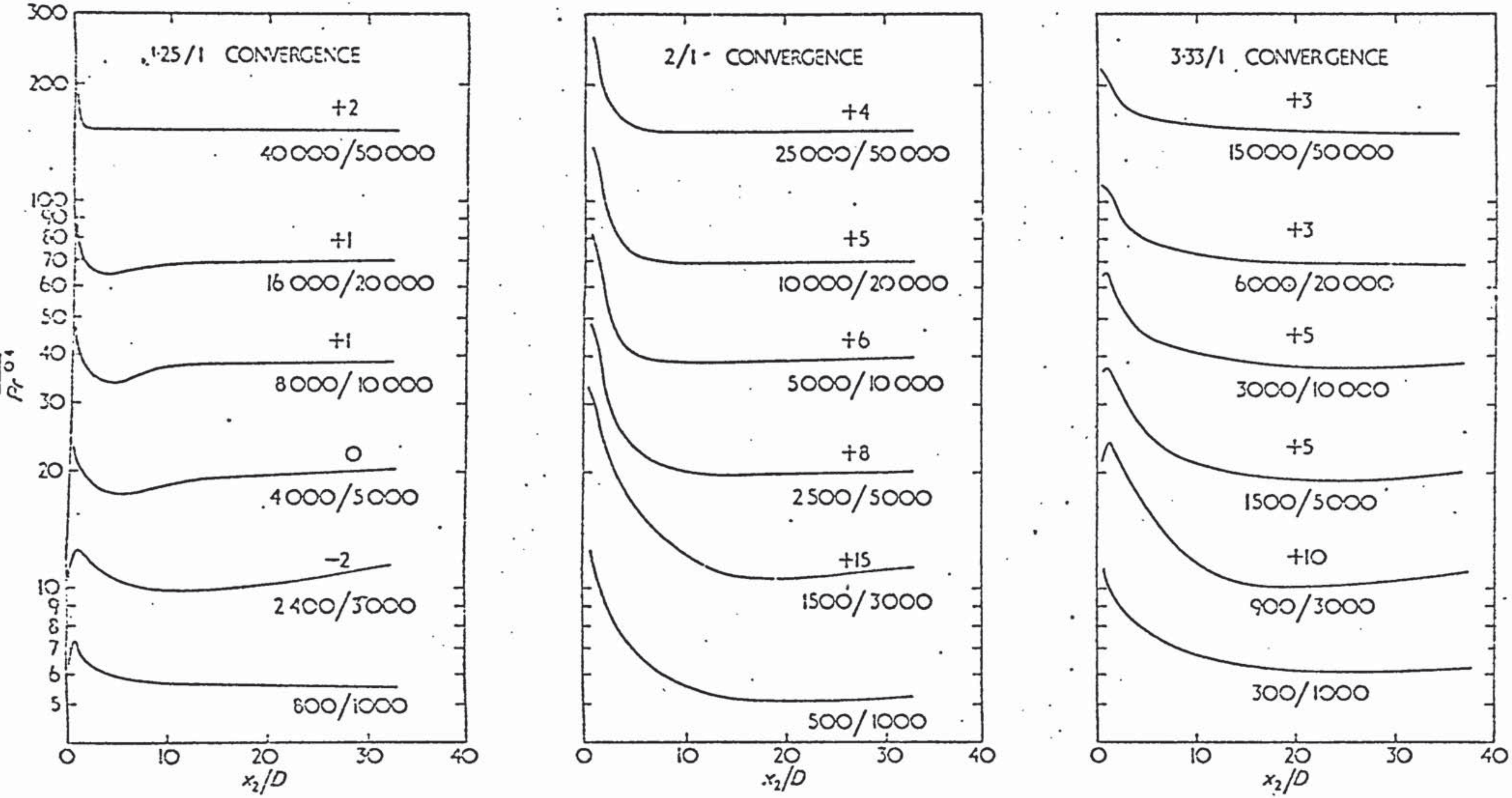

EXTRA DIAMETERS EQUIVALENT TO EXTRA HEAT TRANSFER PRODUCED BY CHANGE OF SECTION SHOWN ABOVE CURVE
REYNOLDS NUMBER BEFORE AND AFTER CHANGE OF SECTION SHOWN BELOW CURVE

EFFECT OF AN ABRUPT CONVERGENCE INTERPOLATED FROM CROSS-PLOTS OF EXPERIMENTAL DATA (E.D.E.).

FIGURE 3.18

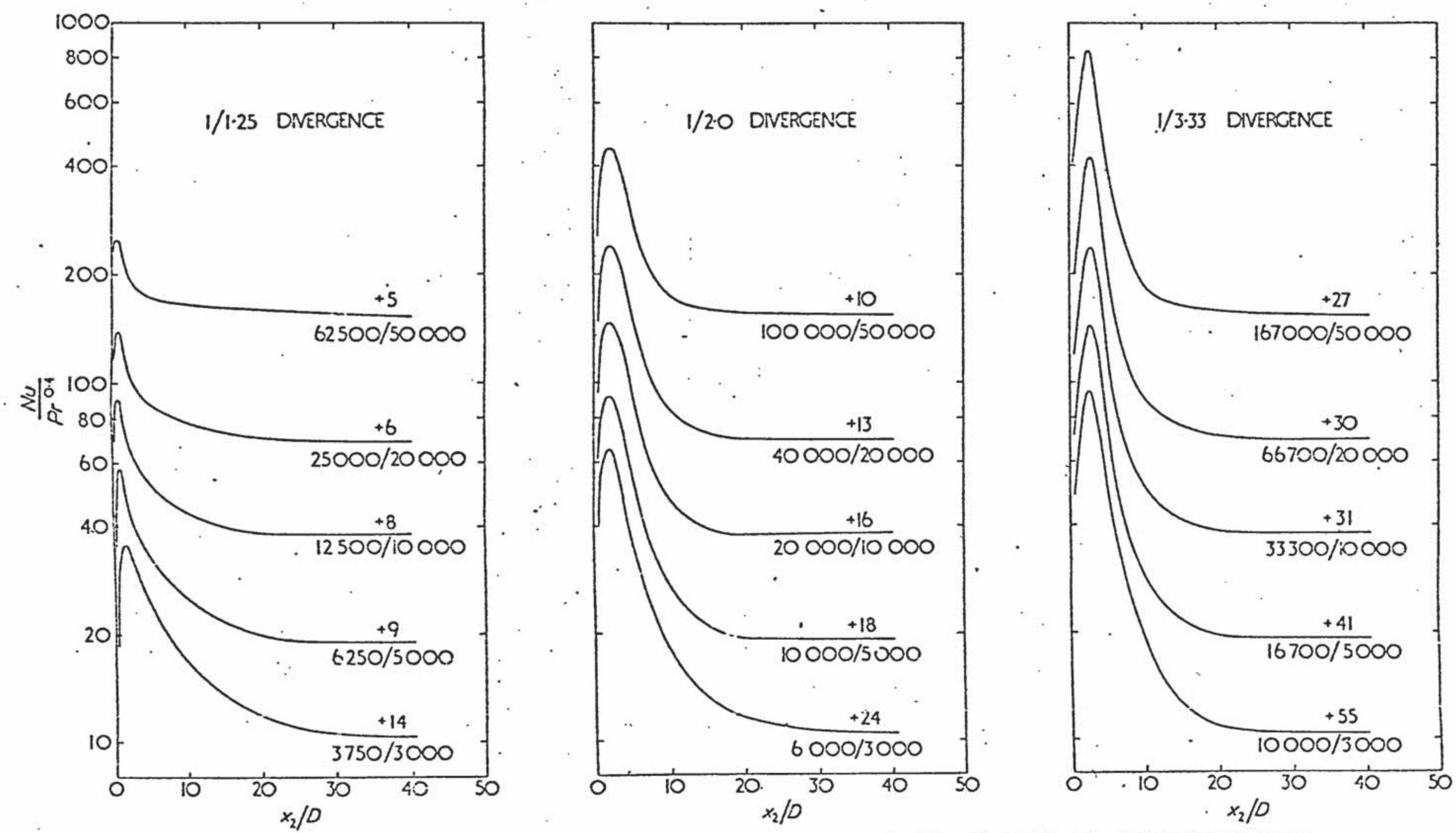

EXTRA DIAMETERS EQUIVALENT TO EXTRA HEAT TRANSFER PRODUCED BY CHANGE OF SECTION SHOWN ABOVE CURVE
REYNOLDS NUMBER BEFORE AND AFTER CHANGE OF SECTION SHOWN BELOW CURVE

EFFECT OF AN ABRUPT DIVERGENCE INTERPOLATED FROM CROSS-PLOTS OF EXPERIMENTAL DATA (ED2).

FIGURE 3.19.

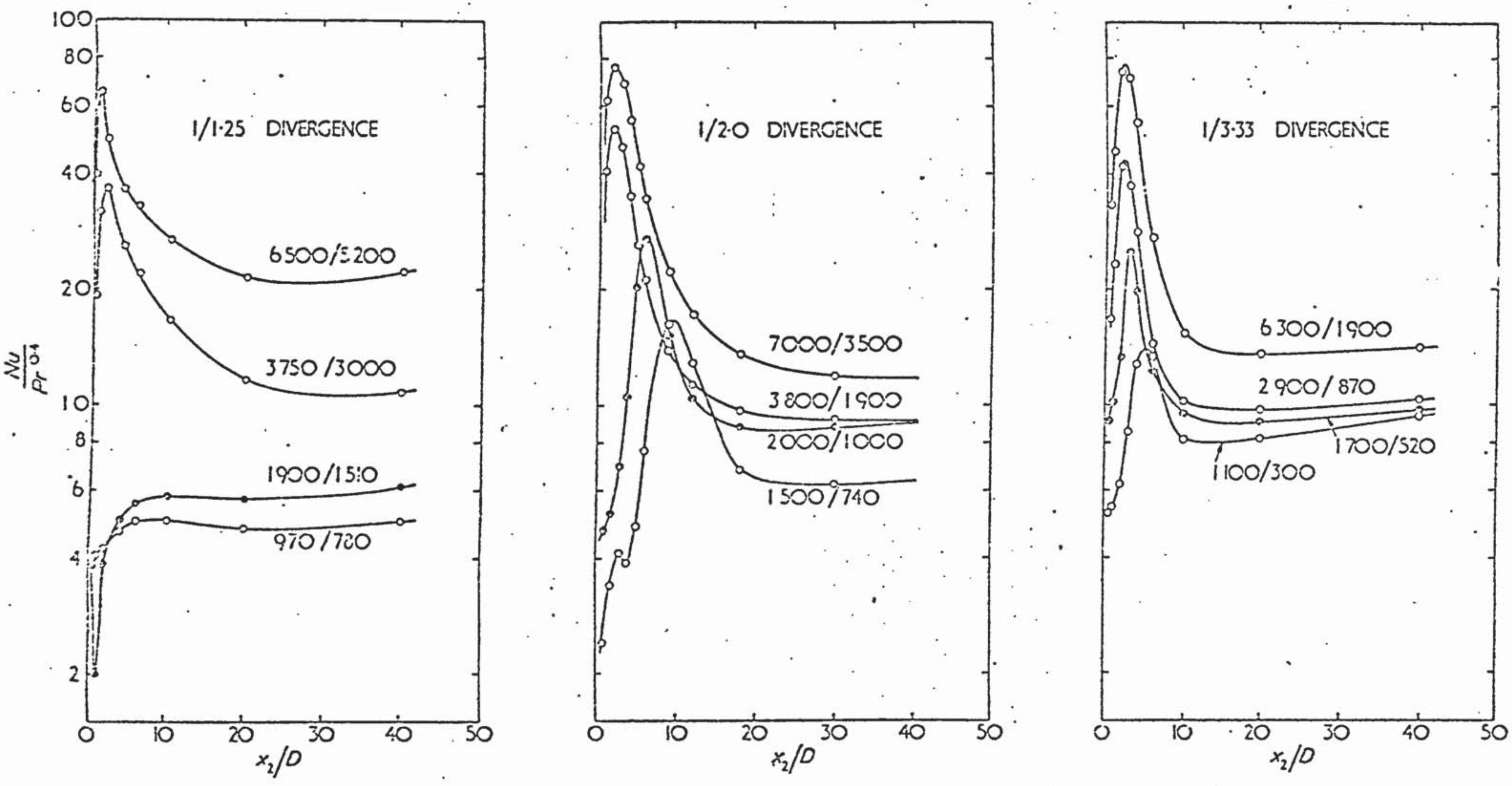

REYNOLDS NUMBER BEFORE AND AFTER CHANGE OF SECTION SHOWN BESIDE EACH CURVE

EFFECT OF AN ABRUPT DIVERGENCE AT LOW REYNOLDS NUMBER, EXPERIMENTAL DATA (EDE).

FIGURE 3.20.

RESULTS OF HARTNETT (Ref: B2). DISTRIBUTION OF HEAT TRANSFER COEFFICIENT IN THE ENTRANCE-REGION OF AN ELECTRICALLY HEATED TUBE WITH CALMING LENGTH FITTED UPSTREAM. DATA FOR OIL.

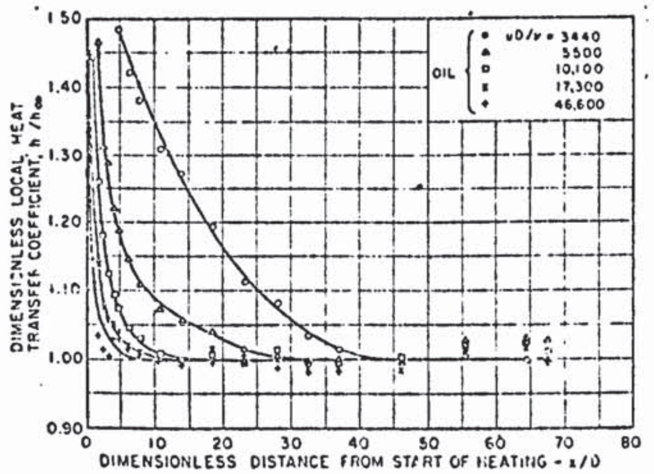

THERMAL-ENTRY-LENGTH RESULTS FOR OIL FLOW IN THE TRANSITION REGION

h = LOCAL COEFFICIENT OF HEAT TRANSFER.

h_∞ = THE VALUE OF h AT LARGE AXIAL DISTANCES.

x = DISTANCE FROM ONSET OF HEATING.

D = TUBE DIAMETER.

4. A RESTATEMENT OF OBJECTIVES.

4.1. This research was carried out under the terms of a Ministry of Technology (now Department of Trade and Industry) contract for the National Engineering Laboratory, East Kilbride. The project represents part of a wider project initiated at NEL to investigate those little explored areas of the heat-transfer field in which disturbed regions of flow arise, or where fluids of viscous or non-newtonian nature occur - particularly in piped flows.

At this stage of the thesis the objectives of the work can be stated in greater detail. The subjects of investigation were selected after a survey of previous research (3) and with consideration for the constraints of the contract. The following contains a summary of these objectives.

4.2. It was proposed that an investigation be carried out passing highly viscous fluids through horizontal tubes, the range of viscosities being 1 to 50 cP. Heat transfer by forced convection was to be studied for Reynolds numbers between 100 and 20,000, and the experimental configurations were to be as follows. First, a short, uniform diameter tube having either developed or undeveloped flow at the start of heating; second, tubes having a sudden increase in diameter, the proposed ratios of diameters being 1:3, 1:2 and 4:5; third, tubes having a sudden decrease in diameter, the proposed ratios being 3:1, 2:1 and 5:4.

The investigations were to include an assessment of the way in which the rate ofheat transfer is affected by the variation in viscosity with temperature, the presence of natural convection, and the viscous dissipation of mechanical energy in the fluid.

5. DESCRIPTION OF THE APPARATUS.

5.1. THE CONFIGURATION.

The basic functions of the apparatus will be described in this paragraph. First, it was necessary to supply a steady flow of fluid to the section of tubing under investigation. The temperature of this fluid was to be constant with respect to time, and both the temperature and rate of flow were to be continuously variable between certain specified limits. Second, the temperature of the tube was to be controllable, so that the level could be set at some value above that of the fluid. Third, a means had to be provided for measuring the temperature at any required point on the inner surface of the tube, the bulk temperature of the fluid at any axial location, the rate of flow of the fluid, and the rate of heat transfer from the tube to the fluid.

The schematic diagram, figure 5.3 , shows the apparatus which was employed in all the heat-transfer experiments described in this thesis. The test-section, or experimental tube, was heated electrically by a direct current passing longitudinally through the material, heat being generated within the wall of the tube. The entire test-section with its fittings was enclosed in a rectangular, wooden box which was lined with 4cm. of polystyrene sheet. The box was firmly packed with polystyrene beads, about 5 mm. in diameter, so that at least 15 cm. of insulation was provided in all directions away from the test-section. Polystyrene was considered to be a good insulator, its conductivity being only 1/600 times that of the tube material, and 1/10 times that of the fluid in the tube. Calculations carried out in 5. 6. indicated that less than 5% of the heat generated was dispersed by conduction through the polystyrene. The condition of uniform heat-flux at the inner surface of the tube was therefore well approximated, and the magnitude of the flux could be derived by measurement of the electrical power dissipated in the tube.

The electrical power supply was 415 volts - 3 phase a/c. A stabilised voltage controller permitted the selection of 0 to 415 volts and ensured that the output would not vary by more than ± 1% of the voltage setting. In order to match the voltage and current requirements at the test-section, the voltage was transformed to give a 0 to 30 v supply. A metal rectifier and smoothing unit was inserted to convert this into direct current, and the range of operating conditions established was 0 to 30 v. d/c, 0 to 1000A, or 0 to 30 kW. (All specifications for the components are given in Appendix (A)).

The general layout of the electrical equipment was such that no loops occurred in the alternating current circuitry, thereby avoiding the possibility of stray e.m.f's being induced into the instrumentation. The choice of direct current heating followed similar reasoning; if the tube were heated by an alternating current then it would be difficult to eliminate the possibility of stray voltages being induced in the thermocouples situated on the test-section.

The leads carrying the current to the test-section comprised 7 cm^2. of copper. An insignificant amount of heat was generated within the copper because of the high electrical conductance. The potential difference over the test-section was measured close to the points where the leads made contact with the tube, and the current was given by the volt drop across a calibrated shunt in series with the positive lead.

The heat-transfer fluid was drawn from the reservoir by a centrifugal pump, circulated through the test-section, then returned to the reservoir (figure 5.3). The main filter was situated at the pump outlet, its primary purpose being the protection of the turbine-flowmeters. Downstream of the filter some of the flow was passed through a branch-pipe which was connected directly to the reservoir, hence bypassing the test-section. The quantity bled off was controlled by the 'bypass-valves', and these enabled a suitable operating point to be chosen for the pump independent of the test-section requirement. The temperature of the fluid discharged from the pump was dependent to some extent on the setting of these valves. The main flow, to the test-section, was controlled by the 'inlet-valves'. After this point, the flow was diverted into one of two parallel pipelines, each incorporating a turbine-type flowmeter, the capacity being different in each case, (details in Appendix (A)). A secondary filter having a finer mesh was included in the line with the smaller flowmeter.

After passing through a 180 degree bend, the fluid entered the test-section. Mixing boxes (see figure 5.3) were situated at the inlet and outlet ends of the tube, to enable the bulk temperature to be measured. The inlet-end box also served to baffle irregularities in the flow following the 180 degree bend upstream. (More details of the mixing boxes are given in 5.4.). A restriction was applied at the outlet end of the test-section (the back-pressure valve), its function being to maintain a system pressure higher than atmospheric throughout, hence eliminating the possibility of air-leakage into the heat-transfer fluid. All connections with the reservoir were submerged, and the tank was fitted with a rubber-edged lid to minimise the hygroscopic absorption of water from the atmosphere by the fluid.

The line diagram given in figure 5.4 shows the dimensions of the system and sizes of the connecting pipework.

To ensure that the temperature of the test-section never approached a dangerous level, a thermostatic control was affixed to the tube. The thermostat was connected via a relay to the circuit breaker in the tube's power supply, and a suitable, maximum temperature level could be selected at which the power switched off.

A water-cooler was situated between the pump outlet and the main filter, and this facilited the transfer of heat out of the system so that a suitable, steady temperature could be maintained in the heat-transfer fluid at the entrance of the test-section. The heat exchanger was a 'shell and tube' type with the water contained in the tube side. The water supply was provided by a cooling-tower circuit. The tower was capable of dissipating 88 kW, whilst delivering $6\frac{kg}{s}$ of water at 24°C, with an atmospheric wet-bulb temperature of 21°C. In practice, water temperatures of 10 to 15 °C could be obtained, since the maximum dissipation required was approximately 30 kW and the atmospheric temperature typically 5 to 20°C.

5.2. DESIGN CONSIDERATIONS.

5.2. (i) INTRODUCTION.

To simplify the problem of designing the apparatus it was necesaary to write a specification which would help to initiate the calculations involved in the selection of the components, e.g. the pump, heat exchanger, flowmeters, and so on. The following specification was in keeping with the general objectives of this research.

(1) The fluid used should be ten times as viscous as water (or have a nominal viscosity of 10 cP).

(2) The experimental tube should be nominally 2.5 cm. diameter and at least 200 diameters in length.

(3) With the maximum rate of flow, and with 100 diameters of the tube heated, the maximum temperature difference between the tube and fluid should be 4CK approximately.

(4) The maximum Re should be nominally 20,000.

(5) The electrical power supply should be limited to a maximum of 30 kW, or 30 v and 1000 A.

The statement (5) must be added to the specification since part of the apparatus (for the provision of a high current at a low voltage level) was already made available at the outset. Some elementary calculations showed these limitations to be no obstacle in the ensuing experiments, and this will be illustrated shortly, (part 5.2.(iii)).

Prior to discussing the design-calculations, the problems associated with the selection of the heat-transfer media will be outlined. Part 5.2.(ii) deals with this topic.

5.2.(ii) THE HEAT-TRANSFER FLUID.

In the selection of the heat-transfer medium the viscosity range to be considered was 1 to 50 cP (as discussed in part 4), and the fluids had to exhibit newtonian behaviour (that is, shear strain being directly proportional to shear stress). Light oils were considered first, but it eventually became apparent that glycols had certain advantages, and subsequently propylene glycol mixtures were selected.

The dependence of viscosity on temperature varies considerably from one fluid to another, so initially it was thought the best approach would be to utilise at least three oils in the experiments, each having a particular kind of viscosity-temperature dependence. For purposes of comparison, one of the fluids was to have a viscosity which was almost independent of temperature, hence consideration was given to a silicone based fluid (silicone fluids exhibit less viscosity variation with temperature than any other known fluid).

The advantages of propylene glycol mixtures over light oils, in the context of this research, becomes apparent from the following description. Propylene glycol is often used as a heat-transfer fluid, it is completely miscible with water, it is non-toxic, it has a boiling point much higher and a freezing point much lower than those of water, dry propylene glycol is non-corrosive, and the viscosity of water-glycol mixtures ranges from 1 cP to 56 cP at 20°C. In changing the composition of a water-glycol mixture the viscosity changes, and also the temperature dependence of the viscosity changes. It would appear, therefore, that no advantages would accrue from having several oils rather than several glycol mixtures as far as the experimental objectives are concerned, and obvious operational advantages can be derived from handling liquids with the same base (ie. propylene glycol.)

Silicone oil was considered for use in experiments on 'constant viscosity', viscous liquids, but this aspect of the work was found to be unjustifiably expensive. The cost of a suitable silicone oil is about £4.8 per kg, and such an investment should only be made after examining the cost effectiveness of the research, which in this case was qualitatively estimable from the experimental data derived with propylene glycol. The rate of change of viscosity with temperature for a 10 cP fluid at 20°C is approximately 0.2 cP per degree K for silicone oil, and 0.4 cP per degree K for water-glycol. Even for silicone oil the variations in viscosity with temperature are therefore comparatively large. It was observed in the 'glycol' experiments that quite substantial viscosity variations were necessary before any measurable changes in the coefficient of heat-transfer were detected. This implied that under certain conditions glycol could be considered as having a near constant viscosity. Such was the case when small heat fluxes were applied and the viscosity of the glycol was not greater than approximately 10 cP.

5.2(iii) CALCULATIONS.

The following calculations are included to exemplify the design process, the selection of the components was of couse based on repetitious calculations and tempered by practical limitations. The final scheme, containing detailed specifications of the components, had to be analysed to give the performance characteristics of the apparatus. The calculations herein show how this analysis was carried out.

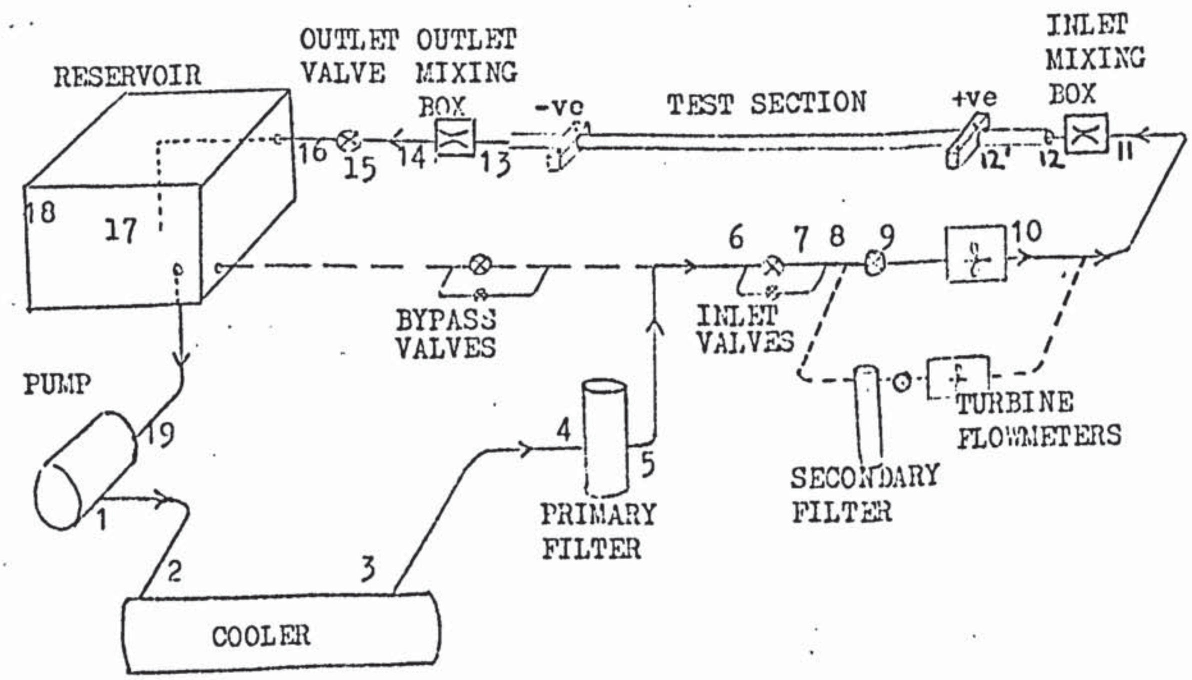

The first requirement is for an assessment of the pressure distribution in the system. The estimates are made assuming the heat-transfer fluid to be 61½% (by weight) propylene glycol and the specification in 5.2(i) is to be observed. The following assumptions are made (see the diagram above) -

1. $p_{18} = 0 = p_{19}$
2. There is no 'bypass' flow.
3. All valves are open, except the bypass valves.
4. The properties of the fluid are constant with temperature and are estimated at 20 °C reference temperature, i.e.

$$\rho = 1.04\ 10^3 \frac{kg}{m^3}, \quad \mu = 10cP, \quad c = 3360 \frac{J}{kg\ K}, \quad K = 0.337 \frac{W}{mK}$$

5. The test-section is perfectly insulated.

The pressure drop in any length of tube or fitting is estimated on the basis of the Fanning equation, and all fittings are given an 'effective' length, L diameters, to conform with this. A detailed explanation can be found in McAdams book (p 145 Ref: K2.).

Hence, $\frac{dp}{dL} = 2f\rho\bar{u}^2$

where $f = 0.046\ Re^{-0.2}$

with
- L = tube, or effective length (diameters)
- $(2r_w)$ = local diameter,
- $\bar{u}$ = mean velocity,
- f = friction factor,
- Re = local Reynolds number.

From McAdams -

for a 90 degree bend	$L_{bend} \simeq 32$ diameters,
for an open valve	$L_{valve} \simeq 7$ diameters,
for a tee-junction	$L_{tee} \simeq 90$ diameters.

For the test-section, $L_{12,13} = 200$, $(2r_w)_{12,13} = 2.5$ cm,

and $$\frac{dp}{dL}_{12,13} = 0.096 \frac{\mu^2}{\rho\,(2r_w)^2_{12,13}} \cdot Re^{1.8}_{12,13}$$

so that $(p_{12} - p_{13}) = 0.00295\ Re_{12,13}^{1.8}\ \frac{N}{m^2}$

For the valves, $(2r_w)_{6,7} = 4.5$ cm, $(2r_w)_{8,9} = 3$ cm,

$(2r_w)_{15,16} = 2.5$ cm,

so that $(p_6 - p_7) = 0.320\ 10^{-4}\ Re_{6,7}^{1.8}\ N/m^2$,

$(p_8 - p_9) = 0.718\ 10^{-4}\ Re_{8,9}^{1.8}\ N/m^2$,

and $(p_{15} - p_{16}) = 1.04\ 10^{-4}\ Re_{15,16}^{1.8}\ N/m^2$.

The total pressure drop in the valves, referred to $Re_{12,13}$ at the test-section, is $\Delta p_{valves} = 0.000167\ Re_{12,13}^{1.8}\ \frac{N}{m^2}$.

For the ancillary pipework including bends the appropriate dimensions are -

Position	1 – 2	3 – 4	5 – 6	7 – 8	9 – 11	14 – 15	16 – 17
$(2r_w)$ cm	6	6	4.5	4.5	3	2.5	2.5
L_{pipe} Dia	10	36	27	41	143	24	67
L_{bends} Dia	32	32	122	0	64	0	32
$L_{effective}$ Dia	42	68	149	41	207	24	99

The pipe between 9 and 11 includes the flowmeter, but since the pressure drop in turbine-type flowmeters is usually very small its influence was neglected.

Application of Fanning's pressure-drop equation yields -

$(p_1 - p_2) = 1.08\ 10^{-4}\ Re_{1,2}^{1.8}\ N/m^2$,

$(p_3 - p_4) = 1.75\ 10^{-4}\ Re_{3,4}^{1.8}\ N/m^2$,

$(p_5 - p_6) = 6.80\ 10^{-4}\ Re_{5,6}^{1.8}\ N/m^2$,

$(p_7 - p_8) = 1.83\ 10^{-4}\ Re_{7,8}^{1.8}\ N/m^2$,

$(p_9 - p_{11}) = 21.3\ 10^{-4}\ Re_{9,11}^{1.8}\ N/m^2$,

$(p_{14} - p_{15}) = 3.55\ 10^{-4}\ Re_{14,15}^{1.8}\ N/m^2$,

$(p_{16} - p_{17}) = 14.7\ 10^{-4}\ Re_{16,17}^{1.8}\ N/m^2$, The total pressure drop in the ancillary pipework, referred to the test-section Re is therefore -

$$\Delta p_{pipes} = 0.00351 \; Re^{1.8}_{12,13} \; \frac{N}{m^2} \; .$$

For the cooler, the pressure drop was estimated from the manufacturers' specification, and the latter may be stated in the following way -

$(p_2 - p_3)_{spec.} = 48 \; kN/m^2$, when mass flow rate = 4.0 kg/s, viscosity $\mu_{spec.} = 72$ cP, and density $\rho_{spec.} = 0.85 \; 10^3 kg/m^3$.

This data may be put into the same form as the Fanning equation and an effective length, L_{cooler}, determined. It can be inferred that $(p_2 - p_3) = G. \frac{\mu^2}{\rho} Re^{1.8}_{12,13}$, where G is a constant containing L_{cooler}.

G is determined from the data in the specification just quoted, giving

$$(p_2 - p_3) = 0.0565 \; 10^{-4} \; \frac{\mu^2}{\rho} \; Re^{1.8}_{12,13} \; \frac{(N/m^2) \; (10^{-3} \; kg/m^3)}{(cP^2)} \; .$$

hence $$(p_2 - p_3) = 0.000665 \; Re^{1.8}_{12,13} \; \frac{N}{m^2} \; .$$

For the mixing boxes, it was difficult to obtain a reliable estimate of the pressure drop. It was assumed that the arrangement resembled a venturimeter with a contraction ratio of 3:1, this being a guess at the value which would be required for adequate mixing. The well known pressure-drop equation is given by Owczarek (p. 446 Ref: K8.) and states -

$$(p_{11} - p_{12}) = (p_{13} - p_{14}) = \frac{\mu^2}{\rho (2r_w)_{13,14}} \; Re^2_{13} \left\{ \frac{1}{2} \left(\frac{1}{C_d^2} - 1 \right) (S^2 - 1) \right\}$$

Where S = 3, the contraction ratio,

and $C_d = 0.95$, the estimated coefficient of discharge.

Hence $$(p_{13} - p_{14}) = 0.000134 \; Re^2_{12,13} \; .$$

For convenience, this may be approximated in the region of $Re_{12,13} = 20{,}000$ by $(p_{11} - p_{12}) = (p_{13} - p_{14}) \simeq 0.000973\ Re_{12,13}^{1.8}$.

The pressure drop through the filter $(p_4 - p_5)$ can be reasonably set at zero, but the outlet-end kinetic loss should be assessed, $(p_{17} - p_{18})$. The loss of kinetic energy gives $(p_{17} - p_{18}) = \rho \dfrac{\bar{u}_{17}^2}{2}$, where $\bar{u}_{17}$ is the outlet velocity.

Hence $\qquad (p_{17} - p_{18}) = 0.0000768\ Re_{17}^2$,

or approximately, $\qquad (p_{17} - p_{18}) \simeq 0.000558\ Re_{12,13}^{1.8}$.

Finally the pressure drop requirement at the pump, and hence the maximum system pressure, is

$$(p_1 - p_{19}) = p_1 = (p_{12} - p_{13}) + \Delta p_{valves} + \Delta p_{pipes} + (p_2 - p_3) + (p_{11} - p_{12}) + (p_{13} - p_{14}) + (p_{17} - p_{18})$$

or

$$p_1 = 0.00980\ Re_{12,13}^{1.8}\ \frac{N}{m^2}.$$

To determine the maximum $Re_{12,13}$ which could be obtained with the apparatus, the system pressure drop $(p_1 - p_{19})$ must be matched to the pump's 'pressure-flow rate' characteristic. For a centrifugal pump running at a small fraction of its maximum flow rate the pressure is almost constant (falling slightly with increasing flow rate). For the pump utilised in the apparatus the 'pressure-flow rate' characteristic can be approximated by a constant 717 kN/m^2. The maximum $Re_{12,13}$ which can be obtained with the apparatus is therefore

$$Re_{12,13} = \left(\frac{717{,}000}{0.00980}\right)^{1/1.8} = 23{,}410.$$

The second requirement is for an assessment of the bulk-temperature distribution in the system (denoted t). The following additional assumptions are made -

6. The entire apparatus is perfectly insulated.

7. The test-section is made up of 100 diameters of unheated tube followed by 100 diameters of heated tube.

8. The required temperature at the inlet of the tube is 25°C.

9. The maximum power dissipated in the tube is 30 kW.

For the maximum flow rate condition $Re_{12,13} = 20{,}000$, and noting that Pr = 100 (from the properties in assumption 4.), the approximate temperature difference between the heated half of the test section and the fluid, Δt_{tube}, can be found.

$$\Delta t_{tube} = \frac{VI}{\pi (2r_w)_{12,13} L_{12,13} K \ Nu_m}$$ where Nu_m is the mean Nu number for the test section given by the well known equation (discussed in 2.3(iii)) $Nu_m = 0.027 \ Re_{12,13}^{0.8} \ Pr^{\frac{1}{3}}$,

and becomes $Nu_m = 346$

Hence, $$\Delta t_{tube} = \frac{30{,}000}{\pi \ 0.025 \ 100 \ 0.337 \ 346} \text{ K}$$

or $$\Delta t_{tube} = 32.75 \text{ K}.$$

The initial specification in 5.2(i) required 40K approximately, but the value 32.75K can be considered sufficiently high for experimental purposes.

The temperature of the fluid at the start of heating is given by

$$t_{12'} = t_{12} + \frac{(p_{12} - p_{12'})}{\rho C} .$$

Hence $$t_{12'} = 25 + \frac{0.001475 \ (20.000)^{1.8}}{1.04 \ 10^3 \ 3360} \ {}^{\circ}\text{C},$$

or $$t_{12'} = 25.023 \ {}^{\circ}\text{C}.$$

At the outlet end of the test-section, t_{13} is given by

$$t_{13} = t_{12'} + \frac{4V.I}{Re_{12,13}\ Pr\ \pi\ K\ (2r_w)_{12,13}} + \frac{(p_{12'} - p_{13})}{\rho\ c}$$

$$\text{or } t_{13} = 25.023 + \frac{4\ \ 30,000}{20,000\ 100\ \pi\ 0.337\ 0.025} + 0.023\ ^{\circ}C$$

$$t_{13} = 27.314\ ^{\circ}C.$$

The reservoir temperature, t_{18}, is obtained as follows

$$t_{18} = t_{13}\ \frac{(p_{13} - p_{18})}{\rho\ c}$$

where $(p_{13} - p_{18}) = 0.00346\ Re^{1.8}_{12,13}$ from the pressure drop calculations, hence

$$t_{18} = 27.314 + \frac{0.00346\ (20,000)^{1.8}}{1.04\ 10^3\ 3360}\ ^{\circ}C\ ,$$

$$t_{18} = 27.369\ ^{\circ}C.$$

It is assumed that the temperature at the pump inlet is the same as the reservoir temperature

$$t_{19} = 27.369\ ^{\circ}C.$$

At the pump outlet the temperature is given by

$$t_1 = t_{19} + \frac{(p_1 - p_{19})}{\rho c}\left(\frac{1}{\bar{\eta}} - 1\right),$$ where $\bar{\eta}$ = the hydraulic efficiency of the pump,

$$\text{so that } t_1 = 27.369 + \frac{0.00980\ (20,000)^{1.8}}{1.04\ \ 10^3\ \ 3360}\left\{\frac{1}{0.30} - 1\right\}\ ^{\circ}C,$$

$$t_1 = 27.731\ ^{\circ}C.$$

The estimate for pumping efficiency was 30%, which appears to be a low value because of the operating conditions; the pump-power was 1/5th the rated load. It is as well to underestimate the efficiency to ensure that the temperature rise is at least as great as would be achieved in practice.

The temperature at the inlet to the cooler, t_2, is derived in the same way as $t_{12'}$, hence

$$t_2 = 27.732\ ^{\circ}C.$$

At the outlet end of the cooler the temperature, t_3, is obtained from t_{12} at the test-section as follows -

$$t_3 = t_{12} - \frac{(p_3 - p_{12})}{\rho C}$$

where $(p_3 - p_{12})$ is the sum of the pressure drops calculated between (3) and (12).

Therefore $$t_3 = 25 - 0.046\ ^{\circ}C$$

$$t_3 = 24.954\ ^{\circ}C.$$

The heat which the cooler must dissipate, Q_{cooler}, is given by $$Q_{cooler} = \frac{\pi Re\ Pr}{2} K\,(r_w)_{12,13}\,(t_2 - t_3)$$

$$Q_{cooler} = 36.76\ kW.$$

As a check, the pumping power, Q_{pump}, and test-section power, Q_{test} can be utilised. $\bar{Q}_{cooler} = Q_{test} + Q_{pump}$,

therefore $$\bar{Q}_{cooler} = 30\ kW + \frac{(p_1 - p_{19})}{\eta}\,\frac{\pi}{2}\,\frac{\mu}{\rho}\,(r_w)_{12,13}\ Re_{12,13}\ ,$$

and $$\bar{Q}_{cooler} = 36.80\ kW$$

A small, 'rounding off' error is evident in Q_{cooler}.

The overall coefficient of heat transfer of the cooler is not easy to assess, therefore the size necessary to dissipate $\bar{Q}_{cooler}$ (that is the number of tubes, diameter of tubes, tube-spacing and so on) was best determined by the manufacturer. The following information was specified - the density, specific heat, viscosity, thermal conductivity and temperature at the inlet and outlet of the cooler on the glycol side, also the inlet temperature on the water side. The cooler in this apparatus was incorporated on the basis of the specification given in the appendix (A).

The figures given refer to a much more viscous fluid (72 cP) so that the temperature difference between oil and water, or the temperature rise on the water side, appear much greater than they would be for a less viscous fluid (say 10 cP).

Supposing a 2.5 K rise in the temperature of the cooling water, Δt_{water}, then the required rate of flow is given by a simple heat balance -

$$\text{water mass-flow rate} = \text{glycol mass flow rate} \times \frac{C\,(t_2 - t_3)}{C_{water}\,\Delta t_{water}}$$

$$= 3.93 \left(\frac{kg}{S}\right) \times \frac{3.36\ 10^3\ 2.78}{4.18\ 10^3\ 2.5}$$

Water mass-flow rate = 3.51 kg/s.

To check whether the cooling flow rate can be attained, the maximum flow must be calculated for the water-supply system. The cooling water was supplied to the heat exchanger from a constant head tank with a fall of 4.6 m, through a 5 cm pipe, the outlet end being open to the drain. An estimate of the maximum flow rate possible under these conditions is as follows -

Say z = the head of water,

Δp_c = the pressure drop on the water side of the cooler,

$\dot{m}$ = mass-flow of water,

subscript w' - refers to the cooling flow.

Now $$g\,\rho_{w'}z = \frac{\rho_{w'}\bar{u}_{w'}^2}{2} + 2f\left(\frac{z}{2r_w}\right)_{w'}\rho_{w'}\bar{u}_{w'}^2 + \Delta p_c,$$ is the energy equation, and Δp_c can be obtained with reference to the Fanning equation putting $\Delta p_c = N\bar{u}_{w'}^{1.8}$ where N is a constant. N is determined from the manufacturers specification (appendix (A)) which states $\Delta p_c)_{spec.} = 13.8\ kN/m^2$ when $\dot{m}_{spec.} = 3.79\ kg/s$ for water. Hence,

$$\Delta p_c = 4.22\ 10^3\ \bar{u}_{w'}^{1.8}\ \left(\frac{N}{m^2}\right)\left(\frac{s}{m}\right)^{1.8}$$

Inserting the value $\rho_{w'} \simeq 10^3$ kg/m^3 gives

$$45{,}200 = 500\,\bar{u}_{w'}^2 + 1{,}605\,\bar{u}_{w'}^{1.8} + 4{,}220\,\bar{u}_{w'}^{1.8}\,,$$

or $\quad \bar{u}_{w'} = 2.95$ m/s,

so that $\quad \dot{m}_{w'} = 5.80$ kg/s.

This is nearly twice the estimated requirement.

The next step is to determine the true dimensions of the test-section, and these are readily obtained from consideration of the electrical resistance of the tube. The nominal tube size chosen in the initial specification, 5.2(i), was 2.5 cm. The actual sizes of the experimental tubes were to some extent limited by the ability of the manufacturer to supply them. Ideally, an infinitely thin wall thickness is desirable to eliminate thermal conduction. Unfortunately this implies negligible electrical conduction. A compromise (further discussed in part 5.3) was reached which led to the selection of stainless steel for the test-section material; this has one of the lowest thermal conductivities of the more common metals, i.e. nominally 15.5 W/mK. The electrical resistivity of stainless steel (type 321 AISI) is approximately $e = 0.72\ 10^{-6}\,\Omega$m. For a 2.5 cm. bore the wall thickness, Δ, is calculated as follows:

If the maximum dissipation of heat is required, then $V = 30$ volts and $I = 1{,}000$ amp. The thickness necessary for a 100 diameter length is given by $\dfrac{V}{I} = \dfrac{e\,L}{\pi(2r_w + \Delta)\Delta}$; which in this case becomes

$$\frac{30}{1{,}000} = \frac{0.72\ 10^{-6}\ 2.5}{\pi(0.025 + \Delta)\Delta}$$

or $\qquad \Delta = 0.072$ cm.

The value of Δ stated is the optimum size, but small departures from the calculated value are acceptable in practice.

5.3. THE EXPERIMENTAL TUBES AND FITTINGS.

5.3.(i) SPECIFICATIONS.

Having designed the apparatus it was necessary to select the actual experimental tubes which would give a desireable range of operating conditions. The specification of these tubes is as follows:-

Experiment	Inner dia. (cm)	Wall thickness/ Variation. (cm)	Length (m)	Roundness (cm)
Short tube	2.616	0.121/0.004	5.2	0.0056
Divergence & Convergence Ratio 3.34:1	1.709	0.265/0.010	1.8	0.0020
	5.715	0.0952/0.005	2.8	0.0300
Ratio 1.99:1	2.555	0.159/0.002	2.8	0.0015
	5.088	0.0788/0.002	2.8	0.0074
Ratio 1.25:1	2.557	0.118/0.010	2.5	0.0040
	3.189	0.103/0.004	3.1	0.0038

All tubes: Material - AISI Type 321 stainless steel

Straightness - 1 in 600

Surface finish of the bore - 3 μm

Method of manufacture - cold drawn and seamless

The above measurements were taken on samples cut from both ends of each tube because in the manufacture of cold drawn seamless tubing the dimensional variations normally increase with the distance between the sampling points. Stainless steel was chosen because of its relatively low thermal and electrical conductivities in comparison with other common metals, also its high resistance to corrosion. The low conductivities imply that the tube wall need not be unreasonably thin in order to obtain a given heat flux, also the distortion of the temperature distribution in the tube, due to the axial conduction of heat, is minimised because of the high thermal resistance.

The surface finish of the inner tube surfaces was such that they could be described as hydraulically smooth up to Reynolds numbers of the order 10^5, that is the frictional force was independent of the roughness at the surface according to the findings of Moody (these are well known, e.g. Ref: K3.).

When two tubes were connected in series, the selection of the tube wall thicknesses was such that the heat generated per unit length was the same for both tubes. This was a matter of practical convenience, since the condition stated gave rise to a nearly linear rise in the bulk temperature of the fluid, a similar surface temperature for each tube, and a practical thickness to diameter ratio for each tube. No other criterion appeared to have any advantage over the one chosen, and by keeping the copper leads well away from the diameter discontinuity, the possibility of distorting the temperature distribution in this region was eliminated.

5.3. (ii) THE TUBE FITTINGS.

The fittings for connecting the test-sections to the mixing-boxes, and to each other (in the case of a diameter discontinuity), are shown in figures 5.5. and 5.6.

The brass fittings utilised to produce a sudden change in diameter were of high electrical conductivity to transfer the potential from the upstream to the downstream tube with a minimal volt drop. The brass was brazed to the stainless steel ensuring an even distribution of solder in the process, thereby achieving a good electrical contact. In between the two parts of each fitting a good electrical contact and hydraulic sealing were established by the insertion of a thin, brass shim which was compressed by eight, small securing bolts, these being evenly tensioned around the periphery of the flanges. Functional tests indicated no unevenness of heating close to a fitting which would have indicated a poor electrical contact. Voltage drops measured across the 3.34:1 fitting were entirely negligible being of the order 5×10^{-4}v.

The copper leads were attached to the test-sections using the copper straps shown in figures 5.7. The contact area was machined to the tube outside diameter whilst the upper and lower portions were separated by 0.008cm., this amount being allowed for the compression strain when tightening the strap.

5.3.(iii) END EFFECTS.

It has been said (5.3 ii) that a high electrical conductivity was desirable in certain fittings attached to the test-sections. This implied high thermal conductivity as well, which was clearly undesirable, since these fittings could act as a sink and distort the heat flux at the inner surface of the tube. In the case of the short-tubes experiments, a practical solution was found by fixing a heater to the copper strap (to be discussed in 5.5). The brass fittings joining two tubes of different diameter could not be dealt with in this way, and it was necessary to try to analyse the system thermetically to discover the extent of the problem, and the implication of ignoring this 'end effect' altogether.

In part 3.8. it is pointed out that there is no generalised procedure available for handling this kind of conduction problem, and an analysis must be carried out.

Assume that the system shown in figure 5.1. closely resembles the region of a diameter discontinuity, and say that -

(a) The following take on constant values:

> the fluid temperature throughout,
> the coefficient of heat transfer on all inside surfaces,
> all the physical properties of the fluid and tube,
> the tube and fitting thicknesses.

(b) The tube and fitting walls are thin.

(c) The exterior surfaces are ideally insulated.

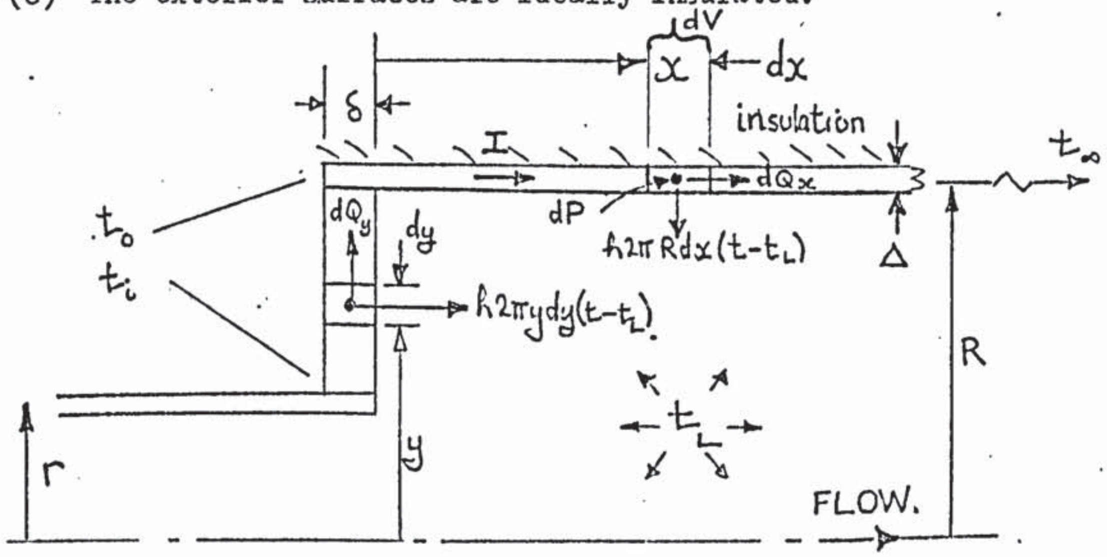

h = coefficient of heat transfer at inner surface.

Figure 5.1.

The problem is to determine how the temperature in the tube upstream t_1, effects the temperature distribution in the downstream tube. The diagram below indicates this.

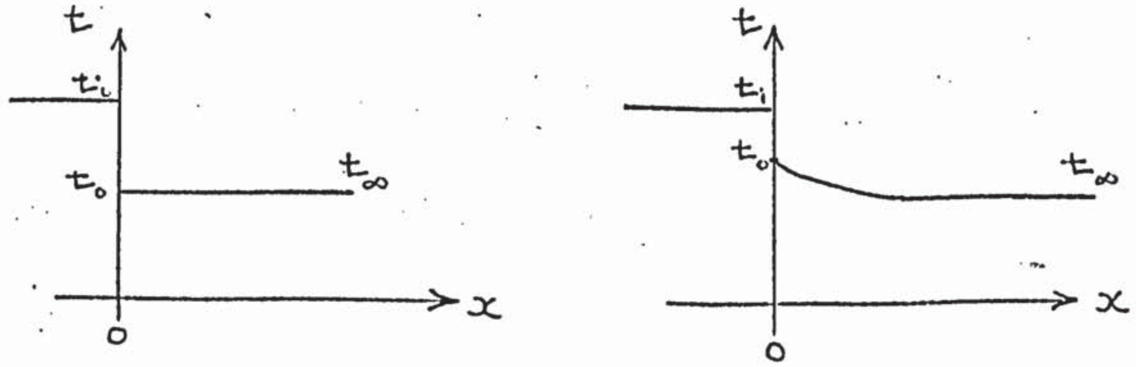

No conduction through fitting. Conduction through fitting.

Considering conduction in the tube wall; thermal conductivity K_t.

Put $\phi = (t - t_L) = \phi(x)$, for a thin wall.

so that
$$\left(\frac{I\,\frac{dv}{dx}}{2\pi R K_t \Delta}\right) + \phi'' = \left(\frac{h}{K_t \Delta}\right)\phi \,, \qquad (5.1)$$

and since $$\phi_\infty = \left(\frac{I\,\frac{dv}{dx}}{2\pi R h}\right) \qquad (5.2)$$

then $$\phi'' + \left(\frac{h}{K_t\Delta}\right)\left(\phi_\infty - \phi\right) = 0 \qquad (5.3)$$

now $\phi(0) = \phi_o$, and $\phi(\infty) = \phi_\infty$, so that

$$(\phi - \phi_\infty) = (\phi_o - \phi_\infty)\exp\left(-\left[\frac{h}{K_t\Delta}\right]^{\frac{1}{2}} x\right). \qquad (5.4)$$

ϕ_o may be derived in terms of ϕ_1 by considering conduction in the fitting; conductivity k_f.

Now $\phi = \phi(y)$ for a thin wall,

hence $$\phi'' + \frac{\phi'}{y} - \frac{h}{k_f\delta}\phi = 0 \qquad (5.5)$$

The solution of this equation is

$$\phi = A.I_o\left(\left(\frac{h}{k_f\delta}\right)^{\frac{1}{2}} y\right) + B.K_o\left(\left(\frac{h}{k_f\delta}\right)^{\frac{1}{2}} y\right) \qquad (5.6)$$

with $$\frac{d\phi}{dy} = \left(\frac{h}{k_f\delta}\right)^{\frac{1}{2}}\left(A.I_1 - B.K_1\right). \qquad (5.7)$$

I_n and K_n are Modified Bessel's Functions of the first and second kind, and order n.

By matching $\phi(y)$ and $\phi'(y)$ at $y = R$ with $\phi(x)$ and $\phi'(x)$ at $x = 0$, the relationship $\phi = f\left(\phi_1, \phi_\infty, \frac{x}{R}, \frac{h}{k_f\delta}, \frac{h}{K_t\Delta}, \frac{r}{R}\right)$ may be found.

A simple result may be obtained as $\frac{r}{R} \to 1$, as follows:-

In the fitting $\phi'' \gg \frac{\phi'}{y}$,

hence $$\phi'' = \left(\frac{h}{k_f\delta}\right)\phi.$$

Now since $\phi(R) = \phi_o$, $\phi'(R) = \phi'_o$,

and $$\phi = M.\exp\left(\left(\frac{h}{k_f\delta}\right)^{\frac{1}{2}} y\right) + N.\exp\left(-\left(\frac{h}{k_f\delta}\right)^{\frac{1}{2}} y\right), \qquad (5.8)$$

then $$\phi_1 = \phi_o\cosh\left(\frac{h}{k_f\delta}\right)^{\frac{1}{2}}(R - r) - \phi'_o\left(\frac{k_f\delta}{h}\right)^{\frac{1}{2}}\sinh\left(\frac{h}{k_f\delta}\right)^{\frac{1}{2}}(R - r). \qquad (5.9)$$

Now $\phi_o(y)$ and $\phi_o'(y)$ may be matched with $\phi_o(x)$ and $\phi_o'(x)$

i.e. $$\phi_o(y) = \phi_o(x),$$

and $$\phi_o'(y) = \frac{K_t\Delta}{k_f\delta}\ \phi_o'(x).$$

But $\phi_o'(x)$ is known to be

$$\phi_o'(x) = \pm(\phi_\infty - \phi_o)\left(\frac{h}{K_t\Delta}\right)^{\frac{1}{2}}, \text{ -ve. when } r > R,$$

therefore all terms in ϕ_0 and ϕ_o' may be replaced by ϕ_∞ and ϕ_1, giving (after reverting to "t" notation):

$$\frac{t - t_L}{t_\infty - t_L} = 1 + Z\exp\left\{-\left(\frac{hR}{K_t}.\frac{R}{\Delta}\right)^{\frac{1}{2}}.\frac{x}{R}\right\} \qquad (5.10)$$

where

$$Z = \frac{\left(\dfrac{t_1 - t_L}{t_\infty - t_L}\right) - \cosh\left\{\left(\dfrac{hR}{k_f}.\dfrac{R}{\delta}\right)^{\frac{1}{2}}.\left(1 - \dfrac{r}{R}\right)\right\}}{\cosh\left\{\left(\dfrac{hR}{k_f}.\dfrac{R}{\delta}\right)^{\frac{1}{2}}\left(1 - \dfrac{r}{R}\right)\right\} \pm \left(\dfrac{K_t\Delta}{k_f\delta}\right)^{\frac{1}{2}}\sinh\left\{\left(\dfrac{hR}{k_f}.\dfrac{R}{\delta}\right)^{\frac{1}{2}}\left(1 - \dfrac{r}{R}\right)\right\}}$$

Clearly, the fittings which would permit the greatest distortion of the heat flux in the downstream-tube for this apparatus would be those having 1.25:1 ratio, since $\left(\frac{r}{R}\right)$ would be a minimum. Also, the experime nts most likely to be affected would be those where small heat-transfer coefficients were encountered, such as when utilising fluids of low viscosity at low Reynolds numbers.

Before estimating the temperature distribution for a typical case, it should be mentioned that the above equation is valid for $r > R$ with a difference sign in the denominator.

The following data applies in the case of the 1.25:1 convergence-ratio - $R = 1.27$ cm., $r = 1.59$ cm., $\delta = 0.1$ cm., $\Delta = 0.5$ cm., $K_t = 15.5\ \frac{W}{mK}$, $k_f = 100\ \frac{W}{mK}$.

Assuming a typically small value for the coefficient of heat transfer of 100 $\frac{W}{m^2K}$, the temperature difference required is given within 1% by the limiting case as $\frac{hR}{k_f}\frac{R}{\delta}\left(1-\frac{r}{R}\right) \rightarrow 0$, that is

$$\frac{t - t_L}{t_\infty - t_L} \simeq 1 + \left[\frac{(t_1 - t_L)}{(t_\infty - t_L)} - 1\right] \exp\left\{-\left(\frac{hR}{K_t}\cdot\frac{R}{\Delta}\right)^{\frac{1}{2}}\frac{x}{R}\right\} \quad , \qquad (5.11)$$

giving $\frac{(t - t_\infty)}{(t_1 - t_\infty)} = \exp\left\{-1.02\,\frac{x}{R}\right\}$, which becomes 0.1 as $\frac{x}{R} \rightarrow 2.26$

Hence $(t_{\frac{x}{R} = 2.26} - t_\infty) = 0.1\,(t_1 - t_\infty)$. (5.12)

Now rewriting in terms of Nu_1' and Nu_2', the Nusselt numbers upstream and downstream away from the discontinuity, yields

$$\frac{(t_{\frac{x}{R} = 2.26} - t_\infty)}{(t_\infty - t_L)} = 0.1\left[\frac{Nu_2'}{Nu_1'} - 1\right] = \epsilon_{2.26} \quad \text{say.}$$

Making the further assumption that $Nu' \propto Re^{\frac{1}{3}}$ (which seems plausible in view of the previous discussion on laminar heat-transfer in part 2.3.(ii),) the equation becomes

$\epsilon_{2.26} = 0.1\left[\left(\frac{r}{R}\right)^{\frac{1}{3}} - 1\right]$, where $\epsilon_{2.26}$ is the approximate error incurred by neglecting axial conduction in the determination of the local coefficient of heat transfer. The greatest error would occur when $\left(\frac{r}{R}\right) = 3.34$, giving $\epsilon_{2.26} = 5\%$.

The result of this analysis can be stated simply; in this, the most severe case likely to be encountered during experimentation, the effects of 'end-conduction' on heat transfer in the downstream tube are probably confined to an initial length of one diameter. In most experiments this length is likely to be much less.

It is worth noting that the typical value for the coefficient of heat transfer, h, was given approximately by the numerical equation $h \simeq 10.Nu_1 \frac{W}{m^2K}$ for propylene glycol, where a low value of 10 was alloted to Nu_1 (the local value of Nu near to the diameter-discontinuity). A similar equation for gaseous media (where the thermal conductivity is approximately one tenth that of glycol) would be $h_{gas} \simeq 1.\ Nu_1 \frac{W}{m^2K}$.

This would yield a value for $\left(\frac{x}{R}\right)$ of 7.2, when $(t - t_L)$ reaches 95% of its limiting value $(t_\infty - t_L)$. It would appear that the present experimental configuration is inadequate for investigating heat transfer with gases, since axial conduction could lead to erroneous results when determining h in the region of the first 3.6 tube diameters downstream of the diameter discontinuity.

5.4. THERMOCOUPLES AND VOLTAGE MEASUREMENTS.

The thermocouples were made from 3m lengths of 0.0027 cm. diameter Nichrome and Constantan which yield a high voltage-temperature gradient whilst having a low thermal conductivity. The cold junctions were formed by soft soldering each wire to a copper lead then setting each pair in paraffin wax, contained in a 0.5 cm. diameter, glass tube. These glass tubes were immersed in Dewar flasks filled with water and ice chips. The copper leads were connected to a vernier potentiometer via a selector switch, and the thermocouple e.m.f.'s were measured by comparison with a standard cell, the voltage being given as the potentiometer setting corresponding to a null reading galvanometer. The hot junctions were formed by resistance-welding the two wires either in-parallel or in-line. The latter configuration was required for the couples positioned inside the mixing boxes, and the former was required in all other applications. The mixing-box junctions were bead-shaped, but the test-section junctions were flattened into a spade-shape for fixing to the meter surfaces.

The diagram (figure 5.8) shows how a cruciform array of ten thermocouples was positioned in each mixing box so that local temperatures in the flow could be measured downstream of the venture-type mixing tube. The flow was considered to be adequately mixed when the ten local temperature measurements were the same. A range of mixing tubes was available with throat diameters from 0.3 to 1.3 cm., and a suitable size could be chosen to produce a high Reynolds number at the throat, therby causing a leveling of the temperature in the fluid whilst minimising the pressure drop necessary for mixing to occur.

The greater part of each mixing box was manufactured from 'Tufnol' and 'Perspex' plastics, which are both good thermal and electrical insulators. The test-section was thus isolated so that practically no loss of heat or current could occur through the ends of the experimental tube. A transparent section was incorporated into the boxes to permit observation of the fluid during the experiments, thus enabling incipient fouling or air bubbling to be detected. Sealing was effected by the use of rubber O - rings, between the demountable parts, p.t.f.e. tape was compressed between the threaded joints, and silicone-rubber (which cured at room temperature) was used as a sealant around the thermocouple leads.

The method of affixing thermocouples to the outer surface of the test-section was as follows. At a given axial location the periphery of the tube was covered with a strip of adhesive, cellophane tape of thickness 0.005 cm. This served to insulate the thermocouple electrically whilst presenting negligible thermal resistance, so that the temperature drop across the tape was immeasurably small (an estimate being 0.025% of the temperature difference used in calculating the coefficient of heat transfer). The thermocouple wire was bound firmly onto the surface of the tube with several layers of the adhesive tape, so that, at a given axial position a minimum of 5 cm. of the lead encircled the tube. Since the peripheral region described was almost isothermal, the possibility of heat-conduction in the leads affecting the readings was avoided.

The voltage supplied at the test-section was measured with the same potentiometer as the thermocouple e.m.f.'s. A voltage divider, ratio 50:1, was included into the circuit to reduce the potential to a manageable level. The volt drop in the calibrated shunt was measured directly with the vernier potentiometer, the resistance being only $5 \mu\Omega$.

5.5. FUNCTIONAL TESTS AND CALIBRATION OF THERMOCOUPLES.

Calibration of the thermocouples was carried out in strict adherence to the National Physical Laboratory recommendations (given in "Calibration of Temperature Measuring Instruments" H.M.S.O. 1955, code 48/120/12). Six sample thermocouples were taken from the test-section and the 'hot' junctions set in paraffin wax in glass tubes. These tubes were immersed in a uniform-temperature, recirculating water-bath (as described on page 28 of the publication) and the thermocouple readings were recorded for bath temperatures of 10 to 90°C, in approximately 4K increments. The bath temperature, which was continually rising at a slow rate, was measured with N.P.L. mercury-in-glass thermometers to an accuracy of $\pm$ 0.02 K. The calibration was checked at six monthly intervals.

The reliability of the calibration could be expressed as a tolerance of ± 2 μv, or ± 0.05 K. This differed from the accuracy of the standard because of non-uniformities in the thermocouple wire.

The method of fixing the thermocouples to the test-section was investigated by positioning three hot junctions in close proximity on the tube, using three separate techniques, as below -

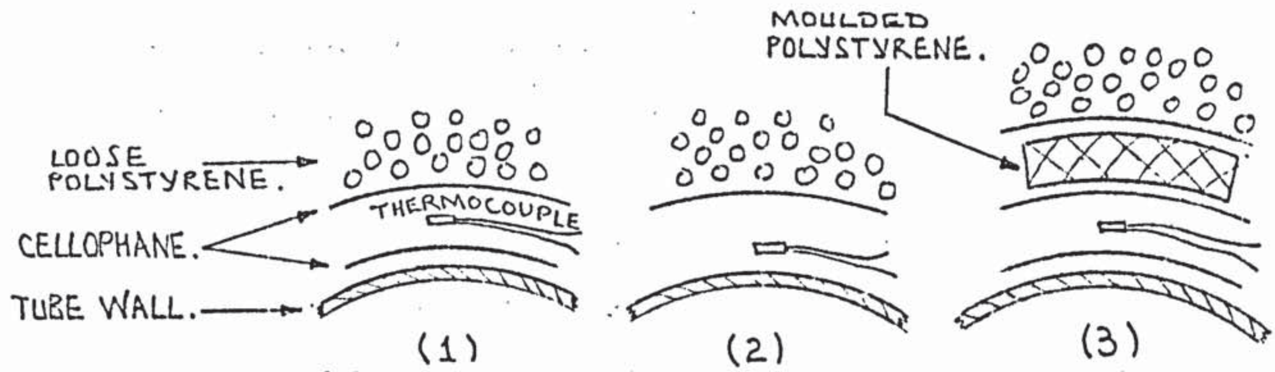

With no applied voltage, fluid at 30°C was circulated around the system and the three thermocouple readings were found to be identical, thus supporting the selection of method (1) for affixing the hot junctions.

The 2.616 cm. bore tube was positioned so that 103 diameters of unheated length preceded 93 diameters of heated length. Thermocouples were distributed axially along the tube to investigate the possibility of the heavy copper lead, at the start of heating, distorting the local heat-flux. Fugure 5.9. shows how during a test at zero applied voltage, with the heat-transfer fluid hotter than ambient, an axial temperature gradient occurred along the tube wall near to the start of heating. This problem was alleviated by fitting a 0 to 50 W electrical heater to the lead at the point of departure from the insulated box. The best operating condition was found to be when the heater was adjusted to give zero temperature gradient in the copper lead, as recorded by two spaced thermocouples. Figure 5.9. shows the distinct improvement which ensued.

Further functional testing was carried out including the continuous reading of flow rate, which was found to vary with time within 1%. The frequency meter was calibrated against a signal generator over 0 to 1000 c/s, and the two turbine-type-flowmeters were calibrated (by the manufacturer) with fluids having kinematic viscosities of 1, 25 and 50 cSt. This type of meter is very reliable, and can be used to measure flow rates with an accuracy of about ±½% (for further details of turbine flow-meters, see the papers in Refs: (K9, K10, K11, K12, K13.)

The continuous reading of potential difference at the test-section was carried out with an 'ultra-violet recorder'. The voltage varied by approximately ± 1% due to fluctuations in the grid-supply, and at certain peak consumption periods the fluctuations became rapid, so it was considered inadvisable to conduct tests at such times.

A simple functional test was carried out on the thermocouple selector switch to reveal any spurious e.m.f.'s; though the probability of these occurring was small. The switch was actuated quickly and repeatedly, whilst a fan heated the contacts to approximately 40°C. The thermocouple readings were found to be unaffected by the action taken.

As a further check on the reliability of the tube-thermocouple readings, a comparison was made between the mixing box and test-section temperatures during an 'isothermal' test. With 12 thermocouples distributed axially along the 5.715 cm. diameter tube, and with a 75% glycol solution recirculating at a high rate of flow, the mixing box and test-section temperatures were recorded. Since zero voltage was applied to the tube, the inlet and outlet temperatures were equal (any difference was immeasureable). The temperature at the tube-exterior was slightly less than the fluid temperature, due in part to conduction through the wall, and in part to imperfect contact of the thermocouples or conduction in the leads. The former was readily assessed, but the latter was estimated from the stated readings. The depression of the thermocouple readings was found to increase with temperature in the following way:-

Fluid temperature ($^{\circ}$C)	28	37	69
Error in thermocouple readings (K)	-0.02	-0.04	-0.06

(Ambient temperature 23°C)

These deviations were tolerated because they represented a small limitation on the accuracy of the measured coefficients of heat transfer - typically $<0.5\%$. The method of applying the thermocouples to the test-section was kept simple in view of the large number of locations which were found necessary; approximately 700 applications were used in the experiments.

5.6. THE HEAT BALANCE.

Generally, in heat-transfer experiments it is advisable to attempt an assessment of the distribution of energy around a boundary which encloses the system. The outcome may not be particularly useful in itself, but an indication of experimental reliability is usually given which helps to justify conclusions based on the results; furthermore it is often possible to assess limiting operational conditions for the apparatus. An example might be when the heat flux in an experiment is limited by the heat loss through the insulation. It is clearly undesirable to rely heavily upon an estimate for conduction losses when determining the forced-convection coefficient of heat transfer. The heat input to the system should be sufficiently high to limit the insulation losses to say 5%.

When aqueous propylene-glycol was used as the heat-transfer fluid, it was found that the increase in temperature between the inlet and outlet of the test-section was very small; in most of the experiments carried out the magnitude was less than 0.5 K. Such small temperature differences were difficult to determine reliably, so it was decided that heat balances would be carried out only when the temperature rise was greater than 0.5 K; the probably accuracy of these temeprature measurements being 0.02 K, or a maximum of 4% of the temperature rise.

The following calculations relate to the initial experiments carried out where the rise in bulk temperature was greater than 0.5 K. Out of the first 39 tests only 10 met this requirement.

With high Prandtl numbers the axial temperature gradient in the fluid is small, even when the tube to fluid temperature difference is comparatively large. This means that the local bulk temperature of the fluid is well approximated by the inlet temperature. It can be reasoned therefore that large errors in the heat balance do not necessarily reflect limitations upon the accuracy of the measured coefficients of heat transfer.

The distribution of heat around the system is as follows:-

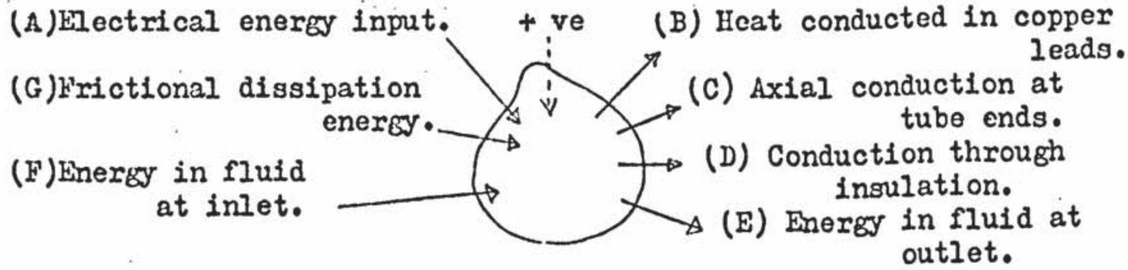

$\sum$ (A),(B),(C),(D),(E),(F),(G) = 0 for equilibrium.

Overleaf (Figure 5.2.) is given a table of the estimated distribution of energy for the cases just mentioned. The experiments were concerned with the heat transfer in a short, uniform diameter tube, and the tests selected included Reynolds numbers in the range 268 to 9,076, with Prandtl numbers in the range 184 to 595. The average temperature difference from tube to fluid varied between 8 and 22 K.

A specimen calculation is now detailed.

Data for test 6S. Fluid - 94.6% aqueous propylene-glycol.

Voltage $V = 10.015$ v. Current $I = 544.0$ A.

Heated length of tube $L_H = 93$ diameters. Unheated length, upstream $L_U = 103$ dia. Thermal conductivities: Insulation $K_{ins} = 0.033 \frac{W}{mK}$, copper $K_c = 384 \frac{W}{mK}$. Radii: Tube exterior $R_A = 1.429$ cm., interior $R_i = 1.308$ cm., outer insulation $R_B \simeq 15$ cm.

Temperature gradient in copper leads: Inlet $g_i = +0.042 \frac{K}{cm}$, outlet $g_o = -0.180 \frac{K}{cm}$.

Temperatures: Average over heated length $T_p = 48.0$ °C, ambient $T_A = 21.8$ °C, fluid inlet $T_i = 24.54$ °C, fluid outlet $T_o =$ 25.30 °C.

Volume flow rate $F = 2.67\ 10^{-3} \frac{m^3}{s}$. Cross section of lead $A = 2.5 \times 2.5 cm^2$.

(A) Electrical power $= 10.015 \times 544.0 = 5448$ W

(B) Total heat loss by lead conduction $Q_{cond} = K_c\, A\, (g_i + g_o)$

$$Q_{cond} = 384 \quad 0.025^2\ (-0.042 + 0.180)\ 10^2$$

$$Q_{cond} = 3.31 \text{ W}$$

(C) Axial conduction from ends of tube $\simeq 0$ W.

Axial conduction of heat must be considerably less than radial conduction.

(D) Conduction through insulation, $Q_{ins} = \dfrac{2\pi K_{ins} \cdot \Delta T}{\log \left(\frac{R_B}{R_A}\right)}$

Figure 5.2

THE HEAT BALANCE (test series 1s. to 39s.)

	TEST NO.	6s.	10s.	14s.	17s.	18s.	22s.	31s.	32s.	33s.	37s.
INPUT	Electrical(W)	5448	4375	7530	4155	7520	5185	422.7	231.2	821.0	959.0
	(A) %	100	100	100	100	100	100	100	100	100	100
	Frictional(W) (G) %		The heat addition by viscous dissipation is assumed to be small								
	Total (W)	5448	4375	7530	4155	7520	5185	422.7	231.2	821.0	959.0
OUTPUT	Copper leads(W)	3.3	3.8	6.6	6.3	5.5	6.0	6.4	7.5	6.7	4.8
	(B) %	0.06	0.07	0.09	0.15	0.07	0.12	1.51	3.26	0.80	0.48
	Tube ends(W) (C) %		The heat loss from the tube ends is assumed to be small								
	Insulation(W)	6.2	6.0	10.9	9.5	11.1	9.7	6.6	8.5	11.6	2.4
	(D) %	0.11	0.13	0.14	0.22	0.14	0.19	1.55	3.69	1.38	0.24
	Fluid(W)	5522	4375	7670	4270	7715	5140	411.5	214.2	821.0	990.0
	(E)-(F) %	99.83	99.80	99.77	99.63	99.79	99.69	96.94	93.05	97.82	99.28
	Total (W)	5531	4385	7688	4286	7732	5156	424.6	230.2	839.0	997.0
	Balance (W)	+83	+10	+158	+131	+212	-29	+1.9	-1.0	+18	+38
	%	1.5	0.2	2.1	3.0	2.8	-0.6	0.4	-0.4	2.2	3.9

where $\Delta T = \left[L_H (T_p - T_A) + L_u (T_i - T_A)\right]$

$Q_{ins} = \frac{2\pi \ 0.033}{\log (10.5)} \left[2.433 \ (26.2) + 2.694 \ (2.7)\right]$

$\underline{Q_{ins} = 6.2 \text{ W}}$

(E) and (F). Enthalpy gain of fluid, $Q_{fluid} = \rho.F.C. \ (T_o - T_i)$

$C \Big]^{94.6\%}_{24.9°C} = 2.63 \ 10^3 \frac{kJ}{kg \ °C}$, $\rho \Big]^{94.6\%}_{24.5°C} = 1.035 \ 10^3 \ \frac{kg}{m^3}$.

$Q_{fluid} = 1.035 \ \ 2.67 \ 2.63 \ 10^3 \ (\ 0.76 \ )$,

$\underline{Q_{fluid} = 5,522 \text{ W}}$

(G). The frictional dissipation-energy can be considered negligible for the present purposes. The design calculations in 5.2.(iii) indicate that this is not unreasonable.

In conclusion, a satisfactory heat balance was obtained under favourable operating conditions. Of the power input to the system, no more than 20 W was dispersed to the surroundings, so that care was taken when operating with less than 400 W heating rate to ensure that insulation losses were less than 5%. In only one test did they exceed 3%.

5.7. MEASUREMENT OF GLYCOL COMPOSITION, AND PROPERTIES.

The percentage by weight of water in the glycol solutions was measured by two methods. The first, direct procedure was to carry out a titration with Karl Fischer reagent. This technique isdescribed in B.S.2511:1954. Whereas the results were accurate - the glycol content being determined within ¼% - the process was a slow one since the apparatus had to be cleaned and dried before use. A day to day check was kept by an indirect method, which consisted of measuring the density of the solution and consulting a chart of density, composition and temperature. To ensure a high degree of precision, the density of 10 known solutions was measured over a range of temperature, with B.S. 718 hydrometers. Comparative densities were used to estimate composition and excellent agreement with the titration results was obtained, the repeatability being expressible as ± ½% of the glycol content.

The major source of property data was the book "Glycols" by Curme and Johnson (Ref. K15). Other references consulted were K16, K17 and K18.
The actual data utilised in this thesis is tabulated in figures 5.10a to 5.10d.

To substantiate the selection of the property values some random checks were made on 70% and 100% glycol solutions at temperatures in the range 20 to 30°C. The density was measured as described above for an extended range of dilutions and temperatures and the data of Curme agreed within 0.05% of these results. The specific heat capacity was measured by comparison with water using a Dewar flask as a calorimeter and determining the 'final' temperature of heated copper and glycol mixture. Values within 1.6% of the reference were recorded. The viscosity was determined with U-tube viscometers in a recirculating water bath; a comparison was made with the viscosity of water. Maximum variations from the reference values of 2% were measured. It was concluded that viscosity, density and specific heat capacity, as recorded in figure 5.10 represented the 'true' properties with a sufficient accuracy. The thermal conductivity could not be readily determined and the results of Bates (Ref. K18.) were referred to, as recommended by Curme(Ref. K15) and Gallant (Ref. K16). An alternative source of data was the work of Riedel (Ref. K19.) which showed a disparity with Bates'. For the range of compositions and

and temperatures considered herein, the Riedel data averaged $3\frac{1}{2}\%$ lower with a maximum of 9%. A discrepency of this magnitude would affect correlations for the coefficient of heat transfer in this thesis by an average of 2%. In 1968 a critical survey by Jamieson (Ref. K17.) suggested that the work of Riedel was probably more reliable than that of Bates.

FIGURE-5.3. THE APPARATUS

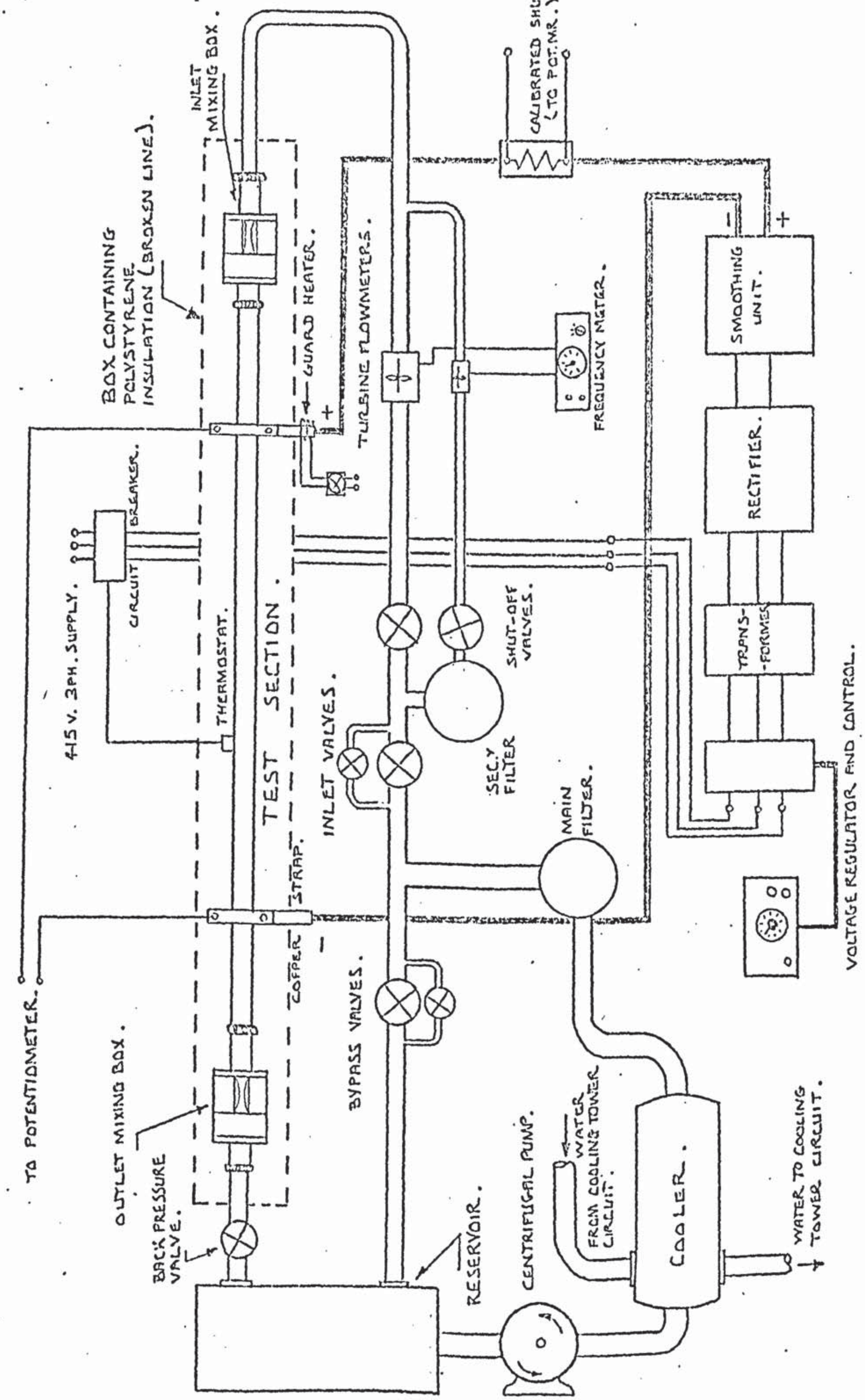

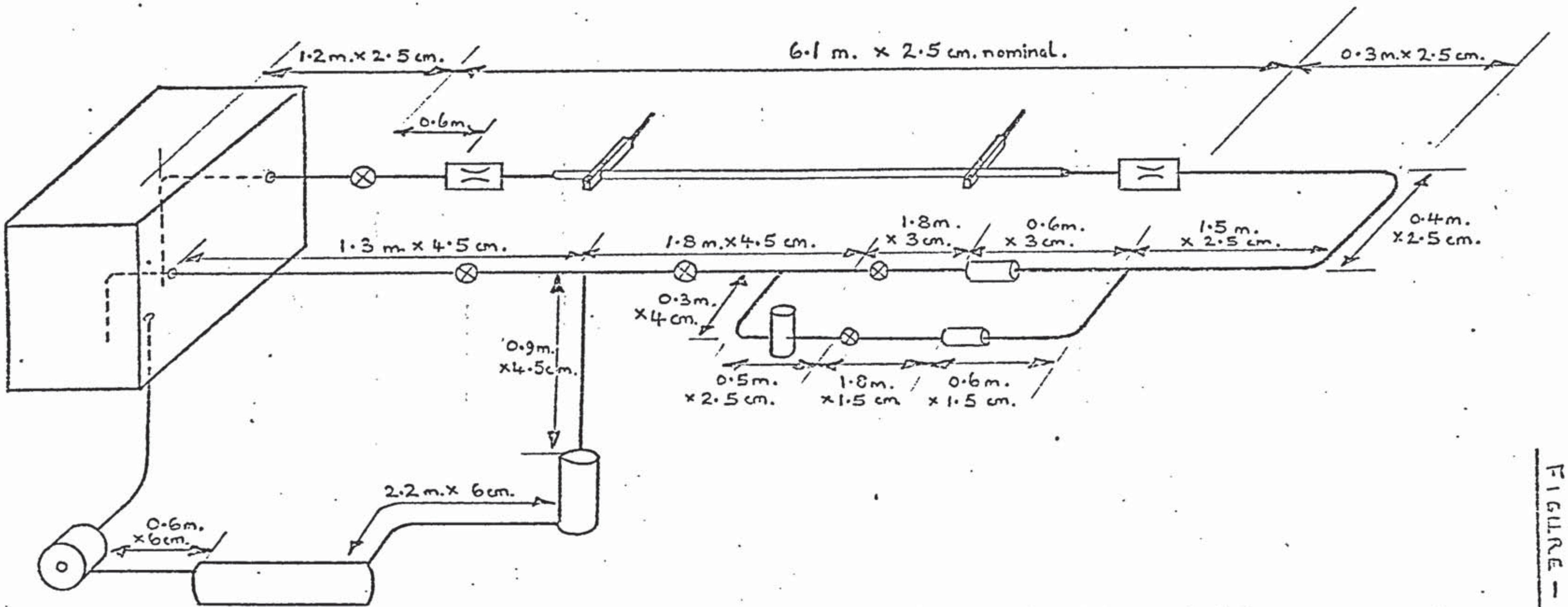

FIGURE – 5.4.

OVERALL DIMENSIONS OF THE APPARATUS, AND SIZES OF CONNECTING PIPEWORK.

FIGURE 5.5.

THE FLANGES REQUIRED FOR JOINING THE THREE LARGER TUBES WITH THE MIXING BOXES.

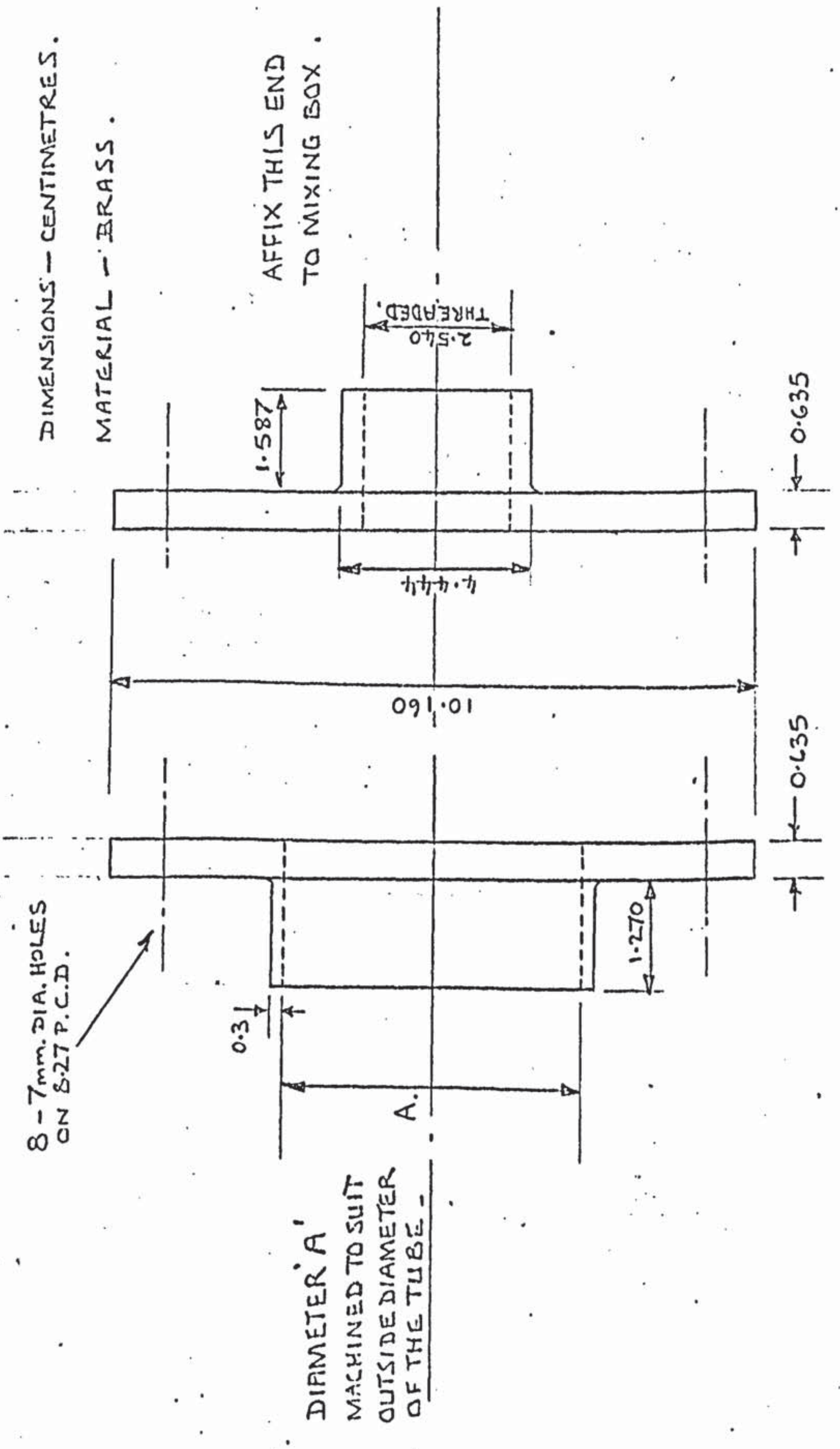

FIGURE 5.6.

THE FITTINGS FOR JOINING TUBES OF DIFFERENT DIAMETER.

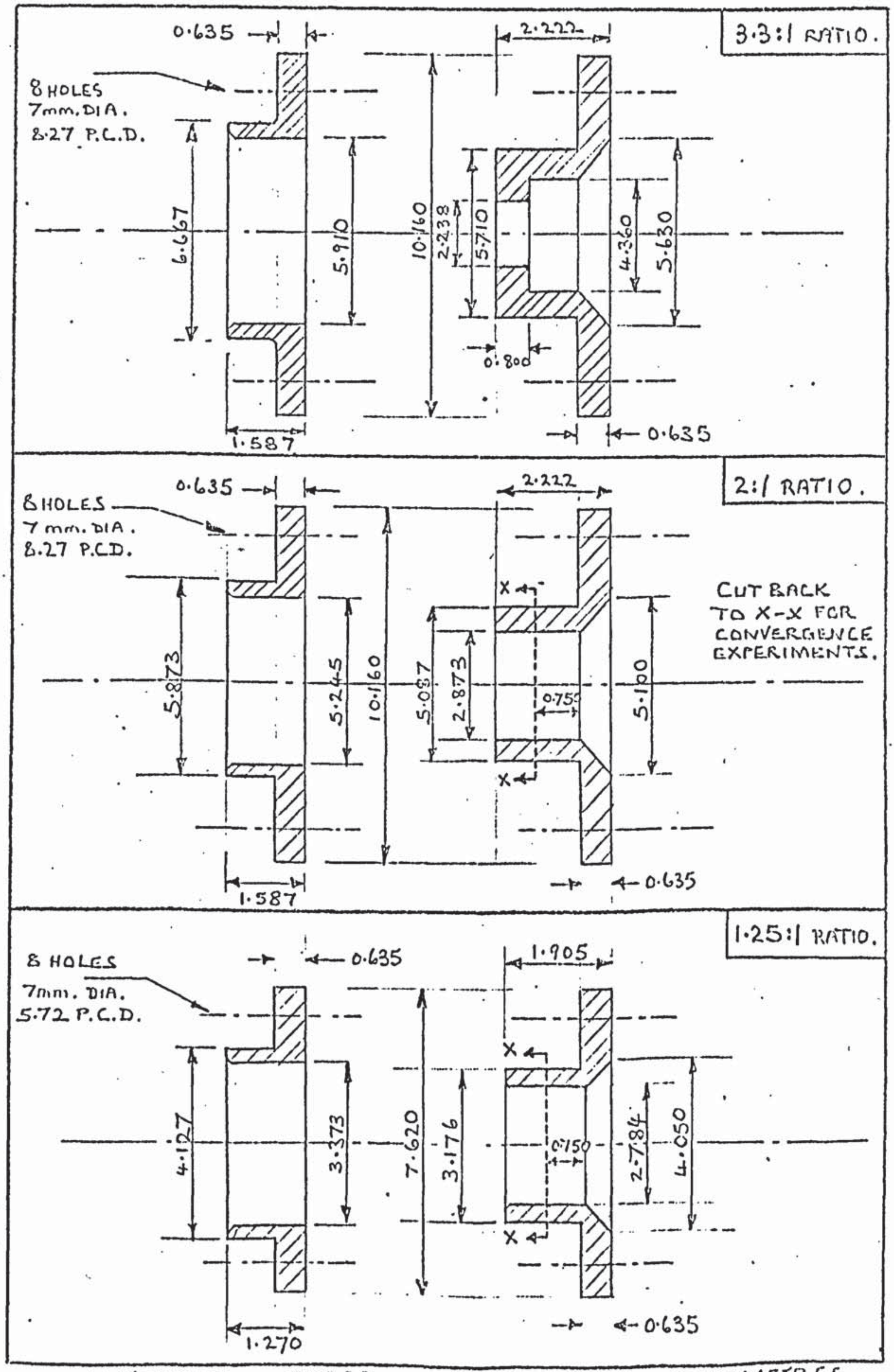

MATERIAL — BRASS. DIMENSIONS — CENTIMETRES.

FIGURE 5.7.

THE FITTINGS FOR ATTACHING THE ELECTRIC-SUPPLY LEADS TO THE TEST SECTION.

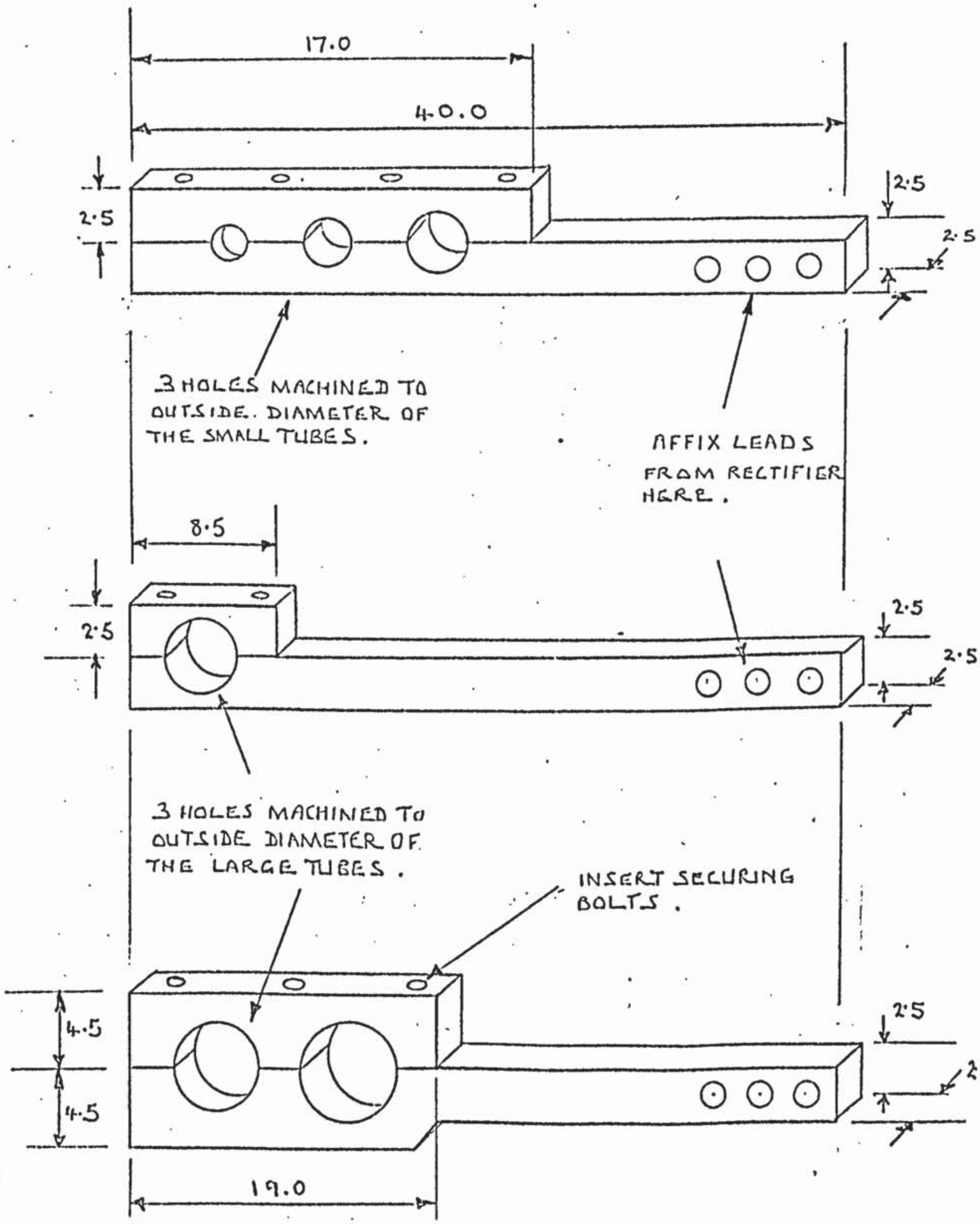

MATERIAL - COPPER. DIMENSIONS - CENTIMETRES.

FIGURE 5.8.

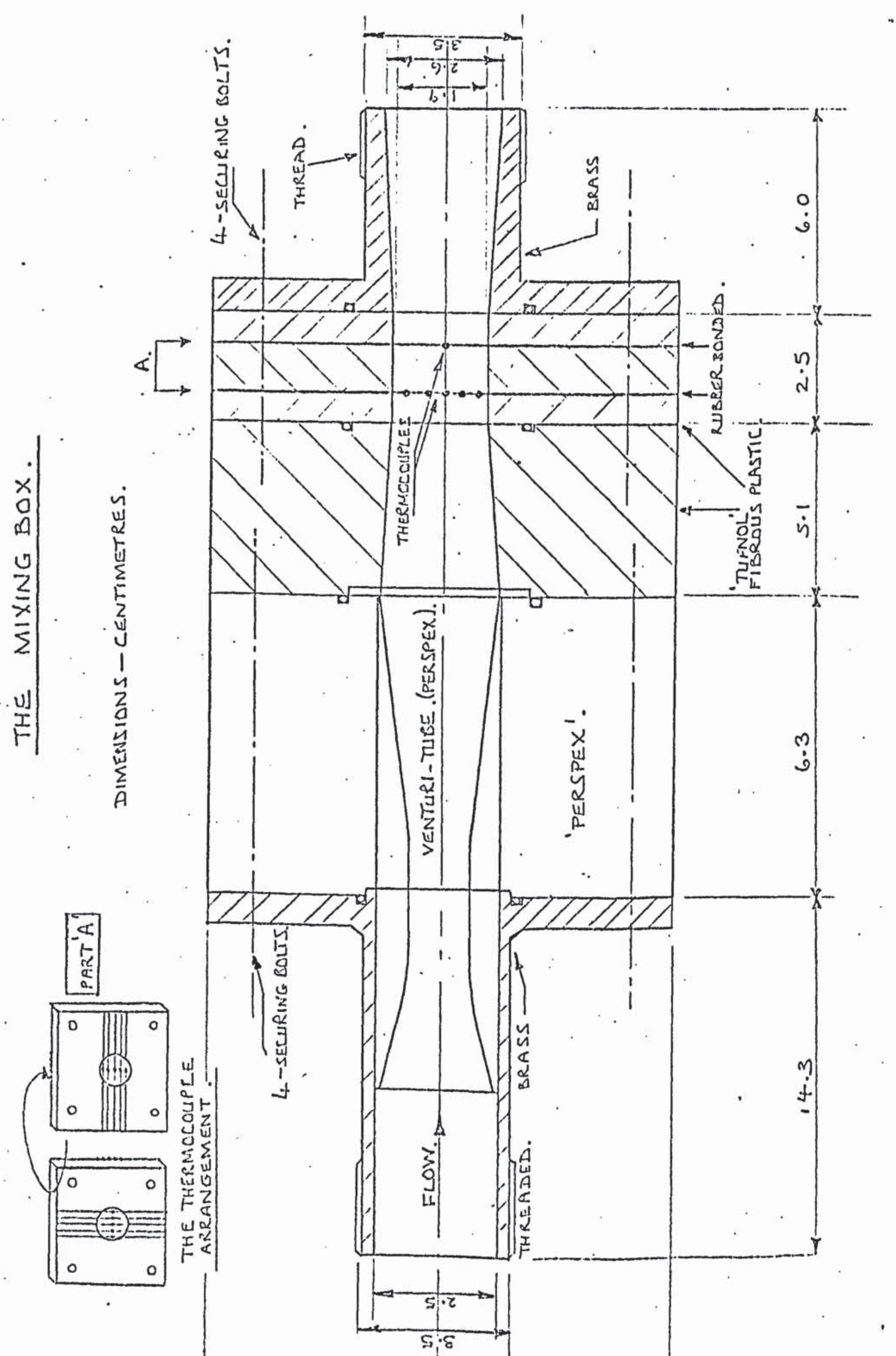
THE MIXING BOX.
DIMENSIONS — CENTIMETRES.
4-SECURING BOLTS.
THREAD.
BRASS
A.
THERMOCOUPLES
RUBBER BONDED.
'TUFNOL' FIBROUS PLASTIC.
VENTURI-TUBE. (PERSPEX).
'PERSPEX'.
4-SECURING BOLTS.
BRASS
FLOW.
THREADED.
PART 'A'
THE THERMOCOUPLE ARRANGEMENT.
3.5
2.6
1.9
6.0
2.5
5.1
6.3
14.3
2.5
3.5
10.0 (SQUARE).

FIGURE – 5.9.

THE TEMPERATURE DISTRIBUTION ALONG AN UNHEATED TUBE, SHOWING HOW THE CONDUCTION OF HEAT IN THE INLET-END LEAD AFFECTS LOCAL TEMPERATURE MEASUREMENTS, AND THE IMPROVEMENT AFTER FITTING A GUARD HEATER.

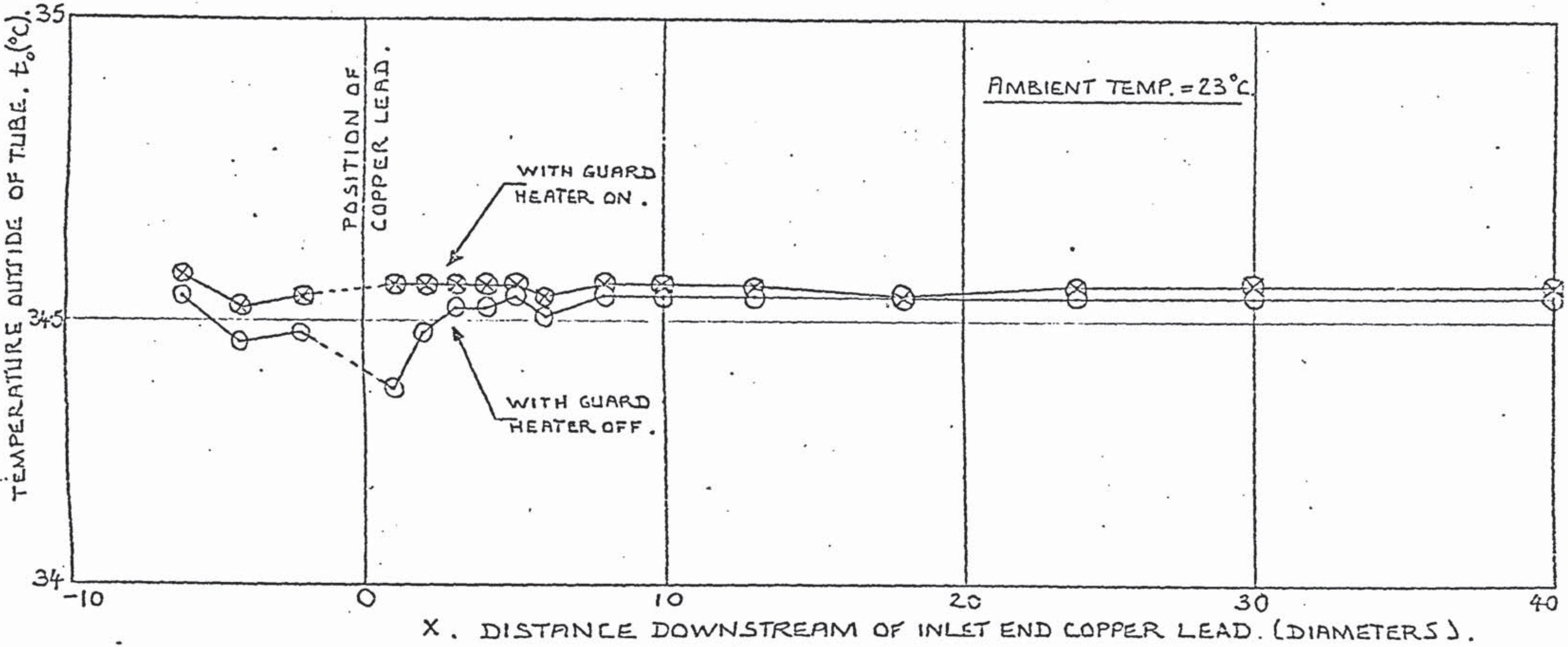

FIGURE 5.10

(a) Thermal Conductivity of Propylene Glycol and its Aqueous Solutions.

Temp °C	Propylene Glycol, % by wt.					
	0	20	40	60	80	100
	Thermal Conductivity, (cal)/(cm.s.°C)					
0	0.00139	0.00117	0.00100	0.00083	0.00068	0.00054
10	142	119	100	82	67	53
20	145	121	100	82	66	52
30	148	123	101	81	65	51
40	0.00151	0.00125	0.00101	0.00080	0.00064	0.00050
50	154	127	101	80	63	49
60	157	129	102	79	62	48
70	160	.131	102	78	61	47

Figure:-

(b) Viscosity of Aqueous Solutions of Propylene Glycol.

Temp °C	Propylene Glycol, % by wt.										
	0	10	20	30	40	50	60	70	80	90	100
	Absolute Viscosity, centipoises										
0	1.79	2.6	4.2	7.1	12.5	18.0	29.0	47.0	72.0	135.0	243.0
10	1.31	1.8	2.9	4.0	7.2	9.3	16.0	22.0	34.0	59.0	111.0
20	1.01	1.35	2.1	3.0	4.4	6.4	9.3	14.0	20.0	33.0	56.0
30	0.80	1.10	1.6	2.9	2.9	4.0	5.6	7.8	12.5	19.0	30.3
40	0.65	0.88	1.2	1.6	2.2	2.9	3.9	5.4	7.4	12.0	18.0
50	0.55	0.73	0.98	1.3	1.7	2.5	2.9	3.9	5.3	7.9	11.3
60	0.47	0.61	0.79	1.0	1.3	1.7	2.2	2.8	3.9	5.4	7.7
70	0.41	0.53	0.68	0.84	1.1	1.3	1.7	2.2	2.9	3.9	5.5

Figure:-

Footnote: Figures a, b and d are as given by reference (K.15.). The units therefore do not conform to the S.I. system.

(c) Density of Aqueous Solutions of Propylene Glycol.

Propylene Glycol, % by wt.	Temperature °C							
	0	10	20	30	40	50	60	70
	True Density, ($10^3 kg/m^3$)							
0	0.9999	0.9997	0.9982	0.9957	0.9923	0.9881	0.9832	0.9778
10	1.0092	1.0082	1.0061	1.0030	0.9993	0.9946	0.9895	0.9837
20	1.0196	1.0178	1.0152	1.0111	1.0069	1.0015	0.9960	0.9898
30	1.0327	1.0282	1.0238	1.0187	1.0134	1.0076	1.0015	0.9950
40	1.0442	1.0376	1.0314	1.0256	1.0199	1.0133	1.0066	0.9997
50	1.0520	1.0445	1.0380	1.0316	1.0250	1.0178	1.0104	1.0028
60	1.0559	1.0490	1.0426	1.0353	1.0279	1.0208	1.0128	1.0046
70	1.0593	1.0517	1.0440	1.0364	1.0290	1.0216	1.0136	1.0055
80	1.0585	1.0510	1.0435	1.0360	1.0284	1.0208	1.0127	1.0045
90	1.0563	1.0488	1.0412	1.0337	1.0258	1.0183	1.0104	1.0024
100	1.0508	1.0435	1.0363	1.0288	1.0213	1.0137	1.0056	0.9977

(d) Specific Heat of Aqueous Propylene Glycol

Propylene Glycol, % by wt.	Temperature °C						
	0	10	20	30	40	50	60
	Specific Heat, (cal)/(g°C)						
0	1.009	1.002	0.999	0.997	0.998	0.998	0.999
10	0.994	0.990	0.989	0.989	0.989	0.990	0.992
20	0.968	0.965	0.963	0.963	0.965	0.968	0.973
30	0.934	0.934	0.935	0.937	0.940	0.944	0.949
40	0.890	0.893	0.897	0.902	0.907	0.912	0.918
50	0.838	0.845	0.852	0.860	0.868	0.877	0.885
60	0.792	0.799	0.807	0.817	0.827	0.837	0.847
70	0.735	0.745	0.754	0.765	0.777	0.788	0.801
80	0.680	0.692	0.703	0.716	0.728	0.741	0.753
90	0.623	0.636	0.648	0.662	0.675	0.688	0.702
100	0.565	0.579	0.593	0.607	0.622	0.635	0.649

6. EXPERIMENTAL PROCEDURE.

6.1. A TYPICAL TEST CARRIED OUT.

To illustrate the experimental procedure a chronological list of the operations involved in a typical test is now presented. An indication of the time scale is given -

Select suitable mixing-box inserts.... (0h 0min)

With the cooling water running, and the power supply switched on, start the pump, set the maximum flow rate, and bleed off air.....

Take a sample of glycol. Check the ice mixtures.... (0h 10min)

Reduce the flow rate to the required value, manipulating the valves so that the bypass and back pressure gates are not fully open. Check the flow for fouling and air bubbles at the mixing box windows.... (0h 15min)

Set the required voltage approximately. Reduce the cooling water rate, permitting the fluid temperature to rise at the test-section inlet, approaching the required value. Calibrate the potentiometer. Measure the density of the glycol to find its composition.... (0h 45min)

Reset the flow rate, voltage setting, and cooling water rate to steady the inlet temperature of the fluid and the tube temperature as they approach the required values. Set the input to the guard heater at the inlet end, copper lead (1h 0min)

Continuously reset the flow, voltage and cooling water until the inlet and tube temperatures are nearly steady at the required values. Check that the thermocouple positions on the tube are suitable for investigating the temperature distribution. Check that the mixing box thermocouples read the same. Reset the input to the guard heater.... (1h 15min)

Record the thermocouple readings at the inlet mixing box and selected readings on the tube surface at intervals of 5 minutes, until conditions are steady. Finally trim the flow rate and voltage.... (2h 0min)

Recalibrate the potentiometer. Continuously read the tube temperature at several, selected locations to estimate the magnitude of any fluctuations which may occur. Finally check the inlet temperature for constancy.... (2h 15min)

Begin the test -

Calibrate the potentiometer. Check the ice mixtures.

Record the following data and readings:-

The time, room temperature, flow rate, voltages and current, inlet and outlet mixing-box thermocouples (20 off), thermocouples on the tube surface (up to 74 off), thermocouples on the copper leads (4 off), the inlet and outlet mixing-box thermocouples, voltages and current, flow rate, the time... (2h 35min)

Check the ice mixtures. Calibrate the potentiometer.

Record the data and readings once more in reverse sequence.

Record the time.... (3h 0min)

End the test.

Small variations in the inlet temperature of the fluid (of the order 0.05K) were eliminated from the results by taking the average of the two sets of readings, provided the mixing box reading recorded half way through the test was the same as the average of the readings at the beginning and end.

6.2. THE CONTROL OF TEST CONDITIONS.

Some difficulty was encountered in controlling the temperature level at the inlet-end of the test-section. This was a consequence of the considerable time required for the interchange of energy between the apparatus and environment to settle to a steady rate. Ideally, it should have been possible to conduct a series of tests in which the Prandtl number of the glycol solution had a particular value. However, the inlet temperature could only be preset with 2K accuracy, so that Pr was found to vary by up to 10% of the value required (due to the temperature dependence of viscosity). This did not significantly impede the experimental analysis.

By increasing the cooling water rate it was possible to reduce the inlet temperature of the fluid, and by increasing the applied voltage the temperature difference between tube and fluid could be set at a convenient value. Although the boundary condition of uniform heat-flux was imposed, it was found useful to discuss the experimental conditions in terms of temperature differences. This follows because 'heat-flux' is a somewhat abstract concept to visualize, and the limitations on the instrumentation were expressed in 'temperature' terms.

There were two ways of obtaining the desired Prandtl number. First, the glycol could be diluted to reduce its viscosity, and hence Pr. Second, the inlet temperature of the glycol at the test-section could be raised, with a subsequent lowering of the viscosity. Both methods were employed, the choice being a matter of practical convenience.

The quantity of fluid returned through the bypass values was found to affect the operating conditions. If the amount bled off was much greater than the main flow rate, and the desired inlet temperature of the fluid was close to the minimum attainable, then small changes in the bypass-flow caused large variations in the inlet temperature. Conversely, if the bypass-flow was small, then the cooling water rate was low, and the inlet temperature became unsteady. The optimal valve settings were determined by experience.

For a given test-section configuration and glycol composition, only three parameters could be varied in the experiments, apart from the points just mentioned. The aforesaid variables were the inlet temperature of the fluid, the heat-flux at the tube wall, and the rate of flow of fluid. Investigations, into the distribution on the tube surface of the coefficient of heat transfer, were performed by finding the functional relationship between the local coefficient and the local properties, heat-flux, fluid bulk-temperature, and flow rate.

6.3. EXPERIMENTAL ERRORS, AN ASSESSMENT.

The following assessment of experimental errors refers to the maximum possible inaccuracies in the measured parameters, excluding those fluctuations in temperature which could arise, for instance, in the transitional flow regime. Mean errors would normally be approximately half the maximum errors. The individual tolerances have all been previously discussed, and the accumulative effect is now to be estimated.

Tube temperature	$\pm$	0.05 K
Fluid temperature	$\pm$	0.02 K
Flow rate	$\pm$	0.5%
Voltage	$\pm$	1%
Current	$\pm$	1%
Circumferential wall-thickness deviations in tubes		2.5%
Axial wall-thickness deviations in tubes		1%
Variations in radius of tubes		0.2%

The maximum accumulative error in the coefficient of heat transfer, h, is given by the formula -

$$\text{if} \quad f = f(x_o, \ldots\ldots\ldots, x_N),$$

$$\text{then} \quad \frac{df}{f} = \sum_{n=o}^{n=N} \frac{\partial f}{\partial x_n} \frac{\delta x_n}{f}.$$

Hence, from Newton's Law of Cooling the error in the axial distribution of h is 5.5%, whereas the circumferential distribution could vary by 7.0%. These estimates are based on a tube to fluid temperature difference of 3 K. At higher differences the corresponding errors become 3.2% and 4.7%.

In practice the probable error in measuring h was likely to be no more than ± 5%, according to the above analysis, and most results should have been within a 3% tolerance.

7. ACCOUNT OF THE TESTS CARRIED OUT.

7.1. THE SHORT STRAIGHT TUBE.

7.1.(i) FULLY DEVELOPED FLOW.

The first investigations dealt with the short, straight tube, and in these experiments the 2.616 cm. bore tube was arranged so that 93 diameters were heated, and a 'calming length' of 103 diameters preceded the heated section. As a consequence, the flow was devoid of any inertial stresses, apart from the minor ones associated with the viscosity-temperature dependence, and the fluctuating components due to turbulence, which were independent of the axial location.

Thermocouples were located at 1, 2, 3, 4, 6, 8, 11, 15, 20, 30, 50 and 70 diameters downstream from the start of heating (sometimes modifications were made to this list.) Four thermocouples were affixed at each axial position, to enable the mean circumferential temperature to be determined, these were equi-spaced at the top, bottom and sides of the tube. To verify that groups of four thermocouples were adequate, twice the usual number were located at 1, 20 and 70 diameters downstream.

In practice, it was only necessary to apply more than four thermocouples at low Reynolds numbers (100 to 500) when the axial distance was greater than approximately 20 diameters.

The initial testing was fairly extensive since the effects of varying each of the experimental parameters - inlet temperature, heat flux, and flow rate - had to be determined for a wide range of conditions. In these experiments the use of fluids having different Prandtl numbers adds an extra dimension to the problem.

With 94.6% (by weight) glycol, the flow rate was set at a high value, $2\tilde{.}7\ 10^{-3} m^3/s$, and the inlet temprature was adjusted to approximately 23, 26, 30, 34 and 40 °C in turn. Four to six tests were carried out at each temperature, the heat flux being different in each case. The fluxes were chosen so that near to the outlet end of the test-section the temperature difference between the tube and the glycol was a suitable value - typically 4, 8, 12 and 20 K. These tests are denoted 1s to 22s.

A similar procedure was followed with the flow rate set at a low value. Fewer tests were carried out this time, the requirements being more easily assessed following the analysis of the former experimental data. Inlet temperature levels in the glycol of 16, 24, 32, and 40 °C were selected, and tests were carried out at each of these for 'tube to fluid' temperature differences between 6 and 35 K, near to the outlet end. These tests are denoted 23s to 33s.

Some final tests, designed to determine the effect of varying the flow rate, were carried out at inlet temperatures between 16 and 40 °C. The difference in temperature between tube and fluid, near to the outlet end, was varied between 5 and 30 K, and the flow rate was varied between the high and low values chosen in the earlier tests, 1s to 33s. These tests were designated 34s to 57s.

At an axial distance of 70 diameters, the range of values for the main dimensionless groups during tests 1s to 58s were nominally -

Reynolds,	Re	-	100 to 10,000
Prandtl,	Pr	-	180 to 650
Grashof,	Gr	-	300 to 16,000
Viscosity ratio,	M_{wall}	-	1.01 to 6.0

The heat flux was varied from 600 to 38,000 $\frac{W}{m^2}$, and the viscosity of the glycol was varied from 15 to 60 cP.

There was little point in extending the range of Re above 10,000, since the local coefficient of heat transfer, h, reached 95% of its constant, limiting value, h_∞, within the first three diameters of tube.

7.1.(ii) UNDEVELOPED FLOW.

Having investigated the short tube with a developing temperature profile and fully developed flow, the case was considered in which the flow and temperature development were simultaneous. It was expected that the temperature profile in the fluid would be a different function of axial distance in the latter case, since the gradient of velocity at the wall was very much higher near to the start of heating, thereby increasing the axial convection of heat.

A 'bellmouth' entrance was fitted to the tube to produce the desired axial velocity profile at the start of heating. Figure:7.1 shows the construction of the bellmouth. The material was Tufnol fibrous plastic, which is a good thermal and electrical insulator, and the design consisted of a 'slow' diffuser, containing 'flow-straighteners', followed by a smooth contraction to the tube diameter. This shape of entrance leads to minimal, radial velocity components, and a nearly uniform axial velocity at the tube entrance. The ratio of diameters, upstream and downstream of the entrance, was estimated in the following way -

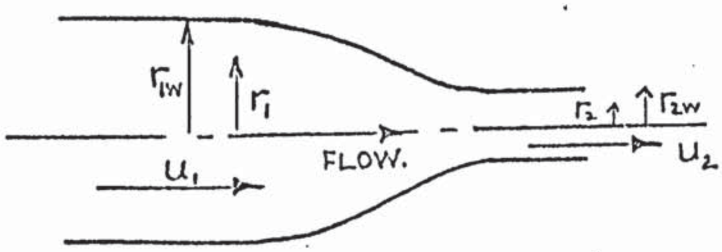

$\bar{u}$ = mean velocity

Assume a parabolic velocity occurs upstream in the tube when conditions are most difficult for producing a uniform velocity downstream.

$$u_1 = 2\,\bar{u}_1\,(1 - r_1^{\,2}/r_{1w}^{\,2}). \qquad (7.1)$$

If the total pressure just inside the downstream section differs little from that in the upstream section, then one is led to assume that (vorticity/radius) is constant, i.e. if the boundary layer equation is rewritten as follows -

$$\frac{d}{dx}\left(p + \frac{2}{r^2}\int_0^r \rho \frac{u^2}{2} r\, dr\right) = 2\frac{\mu}{r}\frac{du}{dr} \qquad (7.2)$$

where radial velocities and pressure gradients are considered to be of second order magnitude then

$$\frac{1}{r}\frac{du}{dr} \simeq \text{constant}$$

thence, $\frac{1}{r_2}\frac{du_2}{dr_2} = \frac{1}{r_1}\frac{du_1}{dr_1} = -4\frac{\bar{u}_1}{r_{1w}^2}$,

and integrating, $$u_2 = -4\frac{\bar{u}_1}{r_{1w}^2}\left(\frac{r_2^2}{2} + C\right). \qquad (7.3)$$

C is obtained with the continuity equation

$$\bar{u}_2 = \frac{2}{r_{2w}^2}\int_0^{r_{2w}} u_2\, r_2\, dr_2 , \qquad (7.4)$$

giving $$C = -r_{2w}^2\left[1 + (r_{1w}/r_{2w})^4\right]/4. \qquad (7.5)$$

The downstream velocity may now be written

$$u_2 = \bar{u}_2\left[1 + (r_{2w}/r_{1w})^4 - 2(r_{2w}/r_{1w})^4 (r_2/r_{2w})^2\right]. \qquad (7.6)$$

The velocity u_2 differs from a constant value by the amount $(r_{2w}/r_{1w})^4$ at the greatest. This represents 1.2% of the mean velocity for a contraction of 3:1. Although the analysis was crude, some idea of the bellmouth's performance was given.

In the tests with undeveloped flow, 187 diameters of the 2.616 cm. tube were heated, there being no calming length. It was considered unnecessary to conduct experiments with such extensive operating conditions as in the previous tests with the calming length, unless the results obtained differed considerably. Glycol with 94.6% composition was used as in the previous experiments, and the thermocouples were located at similar axial distances from the onset of heating, 1, 2, 3, 4, 6, 8, 11, 15, 20, 30 and 70 diameters. These tests were designated 58sB to 72sB.

The ranges of the main dimensionless groups, at an axial distance of 70 **diameters**, were nominally -

Re. - 100 to 10,000,

Pr - 170 to 570,

Gr - 300 to 14,000,

M_{wall} - 1.2 to 4.2 .

The heat flux varied from 550 to 28,000 $\frac{w}{m^2}$, and the viscosity from 15 to 53 cP. Temperature differences between the tube and fluid, at 70 diamesters from the inlet, were in the range 4 to 26 K, and the temperature of the glycol at the inlet varied from 16 to 40 °C.

To permit a direct comparison between the coefficient of heat transfer with undeveloped and developed flow, under similar experimental conditions, i.e. with similar temperatures and flow rates, the tests 74sB to 79sB and 80s to 85s were carried out. Since the difference between the heat-transfer coefficients obtained, in either case, was found to be more pronounced at lower Prandtl numbers, the glycol content was reduced to 69.2% and the inlet temperature raised to 27 °C, thereby producing a low Prandtl number, 91, and a low viscosity, 9 cP. The range of Re was approximately 500 to 15,000.

The values of some important test-parameters are given in part 7.5. for all the experiments carried out with the short tube, 1s to 85s.

7.2. THE SUDDEN CONVERGENCE.

Three ratios of upstream to downstream diameter were investigated in the 'sudden convergence' experiments, these being 3.34:1, 2:1 and 1.25:1. The tube dimensions are given in part 5.3.(i). Long heated lengths of tube were utilised upstream and downstream of the discontinuity in diameter, as follows -

Diameter ratio	Heated length upstream (dia.)	Heated length downstream (dia.)
3.34:1	48	100
2 :1	51	90
1.25:1	90	90

From experience gained with the short, straight tube, it was decided to have four discrete values of Pr for the fluid entering the test-section. This was achieved with two different dilutions of propylene glycol, 91% and 73%, at two different inlet temperature levels. Some practical difficulty was encountered in establishing these conditions, but a reasonable approximation to the objective was attained.

Again, from previous experience, it was found unnecessary to repeat tests for a range of temperature difference from tube to fluid. The differences selected were between 5 and 12 K near to the outlet end of the tube, but only one value was used at a given Reynolds number.

The thermocouple arrangement, downstream of the discontinuity, was similar to the short, straight tube configuration for each of the diameter ratios. Groups of four thermocouples were located at 0.5, 1, 2, 3, 4, 5.5, 7, 8.5, 10, 12, 15, 20, 25, and 40 diameters downstream of the change in section. It was never found necessary to use groups of more than four thermocouples, probably as a consequence of the relatively small tube diameters downstream.

On the larger tube, the measured variation in the local coefficient of heat transfer was found to be slight in the region of the discontinuity. Because results in this region were uninteresting, few thermocuuples were applied, the main locations being at the top and bottom of the tube at 0, 1, and 2 diameters upstream of the discontinuity.

The range of Re was different for each of the four selected Prandtl numbers because of limitations on the available pressure drop. Approximate values of these parameters are now given.

Pr	Maximum Re downstream tube	Minimum Re downstream tube
60	27,000	500
150	10,000	550
200	8,500	450
350	4,700	450

The above applies to all three diameter ratios.

Heat fluxes in the downstream-tube, for each configuration, varied from approximately 1,000 to 25,000 $\frac{w}{m^2}$, the fluxes upstream being less by a factor $\times \frac{(\text{downstream dia.})}{(\text{upstream dia.})}$. The viscosity ranged from 5 to 31 cP.

The values of some important test-parameters are listed in part 7.5. which includes data on all the 'convergence' tests. These tests are designated 1c1 to 18c1 (2:1 ratio), 1c2 to 18c2 (1.25:1 ratio), and 1c3 to 18c3 (3.3:1 ratio).

Having avoided the repetition of tests for a range of heat fluxes, it was considered that some justification for this step should be shown. Tests 1c3, 4c3 and 6c3 were duplicated but with approximately double the heat flux. These tests were numbered 19c3, 20c3, 21c3 respectively.

To evaluate the effects of the heat flux in the upstream tube on the local heat-transfer coefficient in the downstream tube, several tests were carried out with zero voltage applied to the section upstream. This was achieved by moving one copper lead close to the diameter discontinuity. The 'tube to fluid' temperature difference near the outlet, the flow rate, and the inlet temperature were set as close as possible to the values recorded in tests 1c3, 4c3 and 6c3, which included high, medium and low Reynolds numbers. These tests were limited to a Prandtl number of $\tilde{60}$, and the 3.3:1 ratio. The corresponding references are 22c3, 23c3, 24c3.

7.3. THE SUDDEN DIVERGENCE.

The three pairs of tubes in the 'sudden convergence' experiments were reversed to give three divergences in diameter - 1:3.34, 1:2, and 1:1.25. Again, long heated lengths of tube were utilised upstream and downstream of the discontinuity in diamter, as follows -

Diamter ratio.	Heated length upstream.	Heated length downstream.
1: 3.34	100	48
1:2	90	50
1:1.25	90	90

Four discrete Prandtl numbers were selected, as in the 'convergence tests,' and once more it was found that the only significant variations in the local coefficient of heat transfer were those occurring in the downstream tubes. Thermocouples were situated top and bottom at 0, 2, 3 (or 5) diameters upstream of the discontinuity (others situated further upstream were found to give uninteresting information) but the most suitable axial locations on the downstream tube were found to vary with Re. Most of the results were obtained with thermocouples at 0, 0.5, 1, 2, 3, 4, 5.5, 7, 8.5, 10, 11.5, 13, 15, 20, 25 and 40 diameters downstream of the discontinuity. Groups of four thermocouples were positioned, with groups of eight at 1, 15 and 40 diameters to provide a check on the reliability of the mean circumferential temperature, as mentioned in 7.1.(i).

A different range of Re was possible with each fluid and each diameter ratio. The approximate values were -

Diameter Ratio	Pr	Maximum Re Upstream/Downstream	Minimum Re Upstream/Downstream
1:3.34	55	33,000 /11,000	750 /250
1:3.34	150	10,500 / 3,500	750 /250
1:3.34	250	6,000 / 2,000	420 /140
1:3.34	500	3,000 / 1,000	210 / 70
1:2	55	28,000 /14,000	500 /250
1:2	150	10,000 / 5,000	600 /300
1:2	275	7,000 / 3,500	400 /200
1:2	400	3,000 / 1,500	400 /200
1:1.25	60	27,500 /22,000	500 /400
1:1.25	150	10,000 / 8,000	570 /450
1:1.25	225	7,500 / 6,000	375 /300
1:1.25	400	4,375 / 3,500	500 /400

The heat fluxes in the downstream-tubes were 200 to 6,000 $\frac{w}{m^2}$, 500 to 8,500 $\frac{w}{m^2}$ and 700 to 18,000 $\frac{w}{m^2}$, for the ratios 1:3.3, 1:2, and 1:1.25 respectively.

The initial 'sudden divergence' tests concerned the 1:3.3 ratio. First, a series of fifteen tests, 1d1 to 15d1, was carried out with Pr ≃ 55 at the inlet. The flow rate was changed to give a range of Re, but there was no attempt to determine the effects of heat flux on the coefficient of heat transfer. The temperature difference from tube to fluid, at 40 diameters downstream, was in the range 3 to 7 K, the heat fluxes being low in order to minimise 'secondary' effects; such as the dependence of the local coefficient of heat transfer on the functionality between the viscosity and temperature. The next stage was to investigate specifically the effects of varying the heat-flux, and this was done by repeating some of the earlier tests with higher fluxes, as follows -

Test Numbers	Similar to initial tests
16d1 to 18d1	2d1
19d1 to 21d1	3d1
22d1 to 23d1	5d1
24d1	15d1
25d1	12d1
26d1	13d1
27d1	14d1
28d1	2d1

Data on some test-parameters is given in part 7.5 .

Further testing, with different glycol temperatures and compositions, gave evidence as to the effects of Pr on the local heat-transfer coefficient. These were labled -

Test Number	Pr
29d1 to 34d1	150
35d1 to 43d1	500
44d1 to 50d1	250

The 'tube to fluid' temperature differences in the above tests were approximately 10 K at 40 diameters downstream of the discontinuity.

Finally, a few tests were carried out to determine the influence on the downstream-section of the heat flux in the smaller tube by applying zero voltage to that tube in a similar manner to the 'convergence-experiments'. The copper lead upstream was adjusted to a position close to the discontinity in diamter, thus achieving the desired condition. The four tests carried out, 51d1 to 54d1, resembled previous tests in that the flow rate, tube and fluid temperatures were similar to those selected for tests 12d1, 20d1, 9d1 and 7d1. Thereby, a range of Re was covered with a particular Pr ($\tilde{55}$).

In the case of the 1:2 and 1:1.25 divergences far fewer tests were necessary. No investigation into the effects of heat flux values was required, since the main objective was to find the relationship between the diameter ratio and the local coefficients of heat transfer. Moderate heat fluxes were applied giving 'tube to fluid' temperature differences of 5 to 10 K at 40 diameters downstream. Four different Prandtl numbers were used, these were nominally 60, 150, 250 and 400. Further data on these tests is given in part 7.5 , where tests 1d2 to 22d2 refer to the 1:2 diameter ratio, and tests 1d3 to 22d3 to the 1:1.25 ratio.

7.4. FURTHER TESTING

7.4.(i) FLOW VISUALIZATION.

In the course of these experiments some limited investigations were made to help explain certain results obtained with the sudden divergences. The manner in which the local coefficients of heat transfer varied with the axial distance at low values of Re was found to be somewhat erratic and often the measurements were unrepeatable without any obvious cause. An insight into the fluid flow patterns was desirable, and by carrying out the aforesaid investigations, a knowledge of the heat transfer mechanisms was derived, which helped to explain the considerable irregularities in the experimental results. Part of the analysis in 9.7. alludes to the tests described here.

An analagous apparatus was constructed from transparent materials (acrylic plastics) as shown in figure: 7.2 . The discontinuous tube was immersed in a water bath to permit some degree of control of the surrounding temperature, and to minimise refractive parallax. Dye was injected into the flow in the smaller tube upstream, and photographs recorded the traces on entering the larger tube. The fluid passing through the tubes was supplied from a constant head tank and controlled by a gate valve at the exit of the tank. The temperatures were measured with a thermometer. To obtain a sufficiently high Re the viscosity of the fluid had to be fairly low, consequently water was used in most of the tests and a weak dilution of propylene glycol in the remainder.

A series of isothermal tests was tried with a 1:3 divergence ratio, the range of Re being 200 to 2,400 in the large tube. The tests were then repeated with the temperature of the water bath raised above the temperature of the entrained fluid. Whereas the conditions do not even approximate to the 'uniform heat-flux' imposed in the main experiments, it was supposed that a qualitative impression of the flow patterns would be obtained for the case of 'flow with heat transfer'.

The tests just described were carried out once more, but this time with a 1:2 divergence ratio. When the 1:1.25 ratio was investigated, it was found difficult to obtain photographic evidence of the results due to refraction in the tube wall.

With the same apparatus an investigation was carried out into the effects of heating on the flow pattern in a long, uniform tube. This was a brief examination because the observations, whilst providing a description of the flow pattern, did not contribute significantly to the quantitative analysis of the main experimental results. Photographs were obtained for different values of Re and at different bath temperatures.

Part 9.7. contains the continuing discussion of the flow visualization tests, when the significance of these results becomes apparent from the elucidation of the measured coefficients of heat transfer.

7.4.(ii) LARGER DIVERGENCES.

The local coefficient of heat transfer in the larger tube, h, during the 'sudden divergence' experiments, was in general much greater than the corresponding value with no discontinuity present, h_∞. The ratio (h/h_∞) was found to increase with the ratio (larger diameter/small diameter). The question arises, what happens as the diameter ratio tends to a very large value? The ratio (h/h_∞) may or may not increase ad infinitum. Because of this rather speculative argument, and also to support the empirically based hypothesis that the heat-transfer coefficient near to the discontinuity is a function of Re in the smaller rather than the larger tube, some further tests were carried out.

The fittings on the following tubes were modified, (as in figure: 7.3.)

Bore (cm).	Thickness (cm).
5.715	0.0952
2.555	0.159

so that short lengths of small bore-tube could be inserted at the end of the test-section upstream. This had the effect of producing the 'apparent' diameter ratios of 1:14.4, 1:9 and 1:6. This fairly crude expedient enabled evidence to be obtained in support of the hypothesis just stated. The heat generation per unit length was different in each half of the test-section, but the arrangement was such that 92 diameters of the smaller tube were heated and 46 diameters of the larger tube. The sizes of the inserts were as follows - 0.397, 0.635 and 0.953 cm. all being of length 4 cm.

Three tests were carried out in which Re in the smaller tube was approximately 13,000 and Pr at the inlet was $\widetilde{55}$. These extra tests are denoted 1dx, 2dx, 3dx.

7.5. THE RESULTS.

In the 246 tests completed the reduction of the raw experimental data into useable form yielded approximately 50,000 pieces of information, and this was prior to the calculations which were required for the correlation of the results. In view of the large volume of data handled, it was decided to present a detailed account of a few tests, then to list some important test parameters for all cases. The most significant variables not recorded here appear graphically in part 9.

The results referred to are now given.

The definition of symbols used in the computer output is as follows:

RE	Local value of Reynolds number
NU	" " " Nusselt number
PR	" " " Prandtl number
GR	" " " Grashof number
M	" " " (Bulk viscosity)/(Viscosity at wall)
X	" " " Distance from start of heating, or discontinuity (Diameters)
V	Applied voltage to tube (v)
I	Current in tube (A)
R	Radius inside tube (cm)
VISO	Nominal viscosity (cP)
CL	Calming length (dia)
HL	Heated length (dia)
TPO	Outside tube temperature (^{o}C)
TPI	Inside tube temperature (^{o}C)
TX	Bulk temperature (^{o}C)
TIN	Temp. at tube inlet (^{o}C)

In the tests without diameter change, the values of TPO, TPI and TX are listed directly below RE, PR and M.

NOTE: The data following the specimen test results give an indication of the range of the main test parameters.

TEST NO.10.S.

```
V= 8.9550000  I= 488.20000
TIN= 26.040000  R= 1.3080000  VISC= 30.638576
X= 1.0000000  NU= 211.33825
RE= 4409.0585  PR= 350.69272  M= 1.8443130  GR= 1693.0737
 38.450000   37.622704   26.055677DEGC
X= 2.0000000  NU= 184.12198
RE= 4409.8042  PR= 350.63746  M= 2.0330678  GR= 1968.4326
 40.340000   39.502376   26.058686DEGC
X= 3.0000000  NU= 173.00043
RE= 4410.7594  PR= 350.56670  M= 2.1206155  GR= 2097.5486
 41.220000   40.381752   26.062495DEGC
X= 4.0000000  NU= 167.28822
RE= 4411.7545  PR= 350.49302  M= 2.1640358  GR= 2171.1448
 41.720000   40.881395   26.066454DEGC
X= 5.0000000  NU= 162.02130
RE= 4412.7584  PR= 350.41872  M= 2.2067942  GR= 2241.9775
 42.200000   41.361709   26.070446DEGC
X= 6.0000000  NU= 159.92662
RE= 4413.7642  PR= 350.34432  M= 2.2255135  GR= 2273.1832
 42.410000   41.571429   26.074443DEGC
X= 8.0000000  NU= 155.78609
RE= 4415.9140  PR= 350.18539  M= 2.2635647  GR= 2335.8384
 42.830000   41.991476   26.082960DEGC
X= 10.000000  NU= 152.31586
RE= 4417.9567  PR= 350.03451  M= 2.2977296  GR= 2391.2093
 43.200000   42.361528   26.091063DEGC
X= 13.000000  NU= 149.58819
RE= 4421.1246  PR= 349.80078  M= 2.3261235  GR= 2438.4424
 43.510000   42.671519   26.103602DEGC
X= 18.000000  NU= 145.64173
RE= 4426.4770  PR= 349.40659  M= 2.3698329  GR= 2510.6221
 43.980000   43.141570   26.124746DEGC
X= 24.000000  NU= 145.09422
RE= 4432.7480  PR= 348.94591  M= 2.3755198  GR= 2527.4440
 44.070000   43.231559   26.149491DEGC
X= 30.000000  NU= 143.86929
RE= 4438.8730  PR= 348.49713  M= 2.3894284  GR= 2556.1267
 44.240000   43.401579   26.173631DEGC
X= 40.000000  NU= 144.48548
RE= 4449.6041  PR= 347.71369  M= 2.3806273  GR= 2557.8378
 44.210000   43.371572   26.215720DEGC
X= 60.000000  NU= 145.14640
RE= 4471.5662  PR= 346.12140  M= 2.3699420  GR= 2571.9448
 44.220000   43.381573   26.301302DEGC
X= 80.000000  NU= 145.17586
RE= 4492.4810  PR= 344.61873  M= 2.3669488  GR= 2596.0680
 44.300000   43.461573   26.382360DEGC
```

TEST NO. 22 .s.

```
V= 9.8050000  I= 529.00000
TIN= 39.250000  R= 1.3080000  VISC= 15.257071
X= 1.0000000  NU= 281.01421
RE= 9076.3292  PR= 184.17744  M= 1.6095138  GR= 6305.4475
 50.840000   49.857088   39.264811DEGC
X= 2.0000000  NU= 260.63897
RE= 9078.0165  PR= 184.14578  M= 1.6698659  GR= 6876.7667
 51.810000   50.816157   39.268465DEGC
X= 3.0000000  NU= 253.42632
RE= 9080.0254  PR= 184.10810  M= 1.6904029  GR= 7079.5070
 52.150000   51.155633   39.272786DEGC
X= 4.0000000  NU= 249.16126
RE= 9082.0958  PR= 184.06929  M= 1.7030889  GR= 7205.1875
 52.360000   51.365485   39.277233DEGC
X= 5.0000000  NU= 244.54440
RE= 9084.1778  PR= 184.03027  M= 1.7171717  GR= 7343.1305
 52.590000   51.595702   39.281702DEGC
X= 6.0000000  NU= 243.30059
RE= 9086.2625  PR= 183.99122  M= 1.7211948  GR= 7385.5071
 52.660000   51.665520   39.286176DEGC
X= 8.0000000  NU= 240.17741
RE= 9090.7054  PR= 183.90806  M= 1.7311641  GR= 7488.6536
 52.830000   51.835578   39.295685DEGC
X= 10.000000  NU= 239.40751
RE= 9094.9335  PR= 183.82899  M= 1.7335500  GR= 7520.1211
 52.880000   51.885549   39.304743DEGC
X= 13.000000  NU= 238.35115
RE= 9101.4843  PR= 183.70662  M= 1.7367812  GR= 7564.5496
 52.950000   51.955558   39.318749DEGC
X= 18.000000  NU= 237.86468
RE= 9112.5485  PR= 183.50031  M= 1.7378761  GR= 7598.9036
 53.000000   52.005559   39.342359DEGC
X= 24.000000  NU= 237.83227
RE= 9125.5219  PR= 183.25899  M= 1.7373283  GR= 7622.1074
 53.030000   52.035561   39.370007DEGC
X= 30.000000  NU= 237.78730
RE= 9138.2092  PR= 183.02362  M= 1.7368391  GR= 7645.2609
 53.060000   52.065562   39.397007DEGC
X= 40.000000  NU= 237.00190
RE= 9160.3979  PR= 182.61346  M= 1.7384026  GR= 7708.7409
 53.150000   52.155570   39.444015DEGC
X= 60.000000  NU= 237.51876
RE= 9205.7701  PR= 181.78051  M= 1.7343169  GR= 7770.1457
 53.220000   52.225576   39.539528DEGC
X= 80.000000  NU= 238.32051
RE= 9249.0736  PR= 180.99271  M= 1.7293920  GR= 7818.7618
 53.270000   52.275576   39.630143DEGC
```

TEST NO. 26.S.

X= 1.000 NU= 50.97
RE= 110.5 PR= 617.0 M= 2.264 GR= 580.3
TPO= 29.64 TPI= 29.40 TX= 16.00DEGC

X= 2.000 NU= 43.76
RE= 110.7 PR= 616.0 M= 2.581 GR= 694.7
TPO= 32.26 TPI= 32.02 TX= 16.03DEGC

X= 3.000 NU= 38.63
RE= 110.8 PR= 615.1 M= 2.841 GR= 787.8
TPO= 34.37 TPI= 34.13 TX= 16.06DEGC

X= 4.000 NU= 36.41
RE= 111.0 PR= 614.2 M= 3.002 GR= 841.7
TPO= 35.57 TPI= 35.33 TX= 16.08DEGC

X= 6.000 NU= 32.57
RE= 111.4 PR= 612.4 M= 3.352 GR= 946.0
TPO= 37.87 TPI= 37.63 TX= 16.13DEGC

X= 8.000 NU= 30.17
RE= 111.7 PR= 610.5 M= 3.662 GR= 1029
TPO= 39.64 TPI= 39.40 TX= 16.18DEGC

X= 11.00 NU= 27.53
RE= 112.3 PR= 607.8 M= 4.035 GR= 1137
TPO= 41.93 TPI= 41.69 TX= 16.26DEGC

X= 15.00 NU= 25.24
RE= 113.0 PR= 604.2 M= 4.437 GR= 1256
TPO= 44.33 TPI= 44.09 TX= 16.36DEGC

X= 20.00 NU= 23.43
RE= 113.9 PR= 599.6 M= 4.864 GR= 1376
TPO= 46.60 TPI= 46.36 TX= 16.48DEGC

X= 30.00 NU= 21.24
RE= 115.7 PR= 591.0 M= 5.600 GR= 1565
TPO= 49.91 TPI= 49.67 TX= 16.72DEGC

X= 50.00 NU= 20.02
RE= 119.4 PR= 573.8 M= 5.977 GR= 1771
TPO= 52.43 TPI= 52.19 TX= 17.20DEGC

X= 70.00 NU= 19.84
RE= 123.6 PR= 555.4 M= 5.964 GR= 1918
TPO= 53.30 TPI= 53.06 TX= 17.72DEGC

V= 4.828 I= 261.2
R= 1.308 CL= 103.0 HL= 93.00

VISC= 56.15

TEST NO. 33.s.

X= 1.000 NU= 50.77
RE= 383.6 PR= 174.6 M= 1.478 GR= 5949.21
TPO= 49.08 TPI= 48.93 TX= 39.98DEGC

X= 2.000 NU= 42.90
RE= 384.0 PR= 174.4 M= 1.611 GR= 7296.79
TPO= 51.11 TPI= 50.95 TX= 39.99DEGC

X= 3.000 NU= 37.45
RE= 384.3 PR= 174.3 M= 1.707 GR= 8357.19
TPO= 52.70 TPI= 52.55 TX= 40.01DEGC

X= 4.000 NU= 34.97
RE= 384.5 PR= 174.2 M= 1.768 GR= 8998.07
TPO= 53.66 TPI= 53.50 TX= 40.03DEGC

X= 6.000 NU= 30.80
RE= 385.0 PR= 174.0 M= 1.893 GR= 10232.2
TPO= 55.50 TPI= 55.34 TX= 40.06DEGC

X= 8.000 NU= 28.39
RE= 385.6 PR= 173.8 M= 1.992 GR= 11137.7
TPO= 56.84 TPI= 56.68 TX= 40.10DEGC

X= 11.00 NU= 25.59
RE= 386.4 PR= 173.4 M= 2.141 GR= 12396.5
TPO= 58.69 TPI= 58.54 TX= 40.14DEGC

X= 15.00 NU= 23.52
RE= 387.4 PR= 173.0 M= 2.284 GR= 13558.1
TPO= 60.37 TPI= 60.22 TX= 40.21DEGC

X= 20.00 NU= 22.58
RE= 388.7 PR= 172.5 M= 2.344 GR= 14222.3
TPO= 61.29 TPI= 61.14 TX= 40.29DEGC

X= 30.00 NU= 21.52
RE= 391.3 PR= 171.5 M= 2.420 GR= 15122.0
TPO= 62.48 TPI= 62.33 TX= 40.45DEGC

X= 50.00 NU= 20.88
RE= 396.4 PR= 169.5 M= 2.467 GR= 16008.1
TPO= 63.48 TPI= 63.33 TX= 40.77DEGC

X= 70.00 NU= 20.70
RE= 402.1 PR= 167.3 M= 2.476 GR= 16630.7
TPO= 64.04 TPI= 63.89 TX= 41.12DEGC

V= 3.916 I= 209.4
R= 1.308 CL= 103.0 HL= 93.00

VISC= 14.44

TEST NO. 58.SB.

X= 1.000 NU= 102.6
RE= 1615 PR= 199.8 M= 1.346 GR= 3185.18
TPO= 43.61 TPI= 43.39 TX= 36.93DEGC

X= 2.000 NU= 83.25
RE= 1615 PR= 199.8 M= 1.437 GR= 3934.46
TPO= 45.13 TPI= 44.91 TX= 36.94DEGC

X= 3.000 NU= 75.49
RE= 1616 PR= 199.7 M= 1.491 GR= 4353.49
TPO= 45.98 TPI= 45.76 TX= 36.94DEGC

X= 4.000 NU= 69.46
RE= 1616 PR= 199.7 M= 1.543 GR= 4733.70
TPO= 46.75 TPI= 46.53 TX= 36.95DEGC

X= 6.000 NU= 60.68
RE= 1617 PR= 199.6 M= 1.643 GR= 5421.05
TPO= 48.14 TPI= 47.92 TX= 36.96DEGC

X= 8.000 NU= 55.67
RE= 1618 PR= 199.5 M= 1.722 GR= 5916.59
TPO= 49.14 TPI= 48.92 TX= 36.97DEGC

X= 11.00 NU= 49.83
RE= 1619 PR= 199.4 M= 1.837 GR= 6617.00
TPO= 50.55 TPI= 50.33 TX= 36.98DEGC

X= 15.00 NU= 44.60
RE= 1620 PR= 199.2 M= 1.944 GR= 7405.01
TPO= 52.13 TPI= 51.91 TX= 37.00DEGC

X= 20.00 NU= 39.68
E= 1622 PR= 199.0 M= 2.082 GR= 8342.00
TPO= 54.00 TPI= 53.78 TX= 37.03DEGC

X= 30.00 NU= 33.85
RE= 1626 PR= 198.6 M= 2.323 GR= 9817.71
TPO= 56.92 TPI= 56.70 TX= 37.07DEGC

X= 50.00 NU= 28.37
E= 1633 PR= 197.8 M= 2.694 GR= 11815.1
TPO= 60.79 TPI= 60.57 TX= 37.16DEGC

X= 70.00 NU= 25.25
RE= 1642 PR= 196.8 M= 2.952 GR= 13413.6
TPO= 63.79 TPI= 63.57 TX= 37.26DEGC

V= 9.375 I= 250.0
R= 1.308 CL= .00000 HL= 187.20

VISC= 16.741

TEST NO. 68SB.

X= 1.000 NU= 202.4
RE= 6255 PR= 190.8 M= 1.300 GR= 3167.06
TPO= 44.13 TPI= 43.74 TX= 37.93DEGC

X= 2.000 NU= 170.5
RE= 6256 PR= 190.8 M= 1.362 GR= 3761.08
TPO= 45.22 TPI= 44.83 TX= 37.93DEGC

X= 3.000 NU= 160.8
RE= 6256 PR= 190.8 M= 1.388 GR= 3995.01
TPO= 45.65 TPI= 45.26 TX= 37.94DEGC

X= 4.000 NU= 154.4
RE= 6257 PR= 190.8 M= 1.407 GR= 4163.80
TPO= 45.95 TPI= 45.57 TX= 37.94DEGC

X= 6.000 NU= 144.0
RE= 6258 PR= 190.7 M= 1.441 GR= 4463.58
TPO= 46.51 TPI= 46.12 TX= 37.94DEGC

X= 8.000 NU= 139.4
RE= 6260 PR= 190.7 M= 1.459 GR= 4616.02
TPO= 46.79 TPI= 46.40 TX= 37.95DEGC

X= 11.00 NU= 137.0
RE= 6262 PR= 190.6 M= 1.468 GR= 4697.38
TPO= 46.94 TPI= 46.55 TX= 37.96DEGC

X= 15.00 NU= 136.9
RE= 6265 PR= 190.6 M= 1.469 GR= 4707.51
TPO= 46.96 TPI= 46.57 TX= 37.97DEGC

X= 20.00 NU= 140.9
RE= 6269 PR= 190.5 M= 1.453 GR= 4580.48
TPO= 46.73 TPI= 46.34 TX= 37.98DEGC

X= 30.00 NU= 152.6
RE= 6276 PR= 190.3 M= 1.412 GR= 4237.78
TPO= 46.11 TPI= 45.72 TX= 38.00DEGC

X= 50.00 NU= 154.5
RE= 6290 PR= 189.9 M= 1.405 GR= 4204.12
TPO= 46.06 TPI= 45.67 TX= 38.05DEGC

X= 70.00 NU= 154.6
RE= 6305 PR= 189.4 M= 1.405 GR= 4224.91
TPO= 46.11 TPI= 45.72 TX= 38.10DEGC

V= 12.36 I= 334.0
R= 1.308 CL= .00000 HL= 187.20

VISC= 15.926

TEST NO: 74.SB.

X= 1.0000   NU= 348.68
RE= 15014   PR= 92.389   M= 1.2273   GR= 6218.64
TPO= 31.92   TPI= 31.35   TX= 27.76DEGC

X= 2.0000   NU= 324.78
RE= 15016   PR= 92.375   M= 1.2394   GR= 6683.28
TPO= 32.19   TPI= 31.62   TX= 27.77DEGC

X= 3.0000   NU= 319.31
RE= 15018   PR= 92.360   M= 1.2424   GR= 6802.00
TPO= 32.26   TPI= 31.69   TX= 27.77DEGC

X= 4.0000   NU= 317.93
RE= 15021   PR= 92.346   M= 1.2431   GR= 6834.29
TPO= 32.28   TPI= 31.71   TX= 27.77DEGC

X= 6.0000   NU= 315.14
RE= 15026   PR= 92.318   M= 1.2445   GR= 6899.21
TPO= 32.32   TPI= 31.75   TX= 27.78DEGC

X= 8.0000   NU= 313.19
RE= 15031   PR= 92.290   M= 1.2455   GR= 6946.77
TPO= 32.35   TPI= 31.78   TX= 27.78DEGC

X= 11.000   NU= 313.81
RE= 15038   PR= 92.247   M= 1.2449   GR= 6940.08
TPO= 32.35   TPI= 31.78   TX= 27.79DEGC

X= 15.000   NU= 314.63
RE= 15047   PR= 92.191   M= 1.2441   GR= 6931.12
TPO= 32.35   TPI= 31.78   TX= 27.80DEGC

X= 20.000   NU= 315.66
RE= 15060   PR= 92.120   M= 1.2431   GR= 6919.86
TPO= 32.35   TPI= 31.78   TX= 27.81DEGC

X= 30.000   NU= 317.72
RE= 15084   PR= 91.981   M= 1.2411   GR= 6897.45
TPO= 32.35   TPI= 31.78   TX= 27.84DEGC

X= 50.000   NU= 317.04
RE= 15132   PR= 91.701   M= 1.2398   GR= 6957.64
TPO= 32.41   TPI= 31.84   TX= 27.89DEGC

X= 70.000   NU= 317.24
RE= 15182   PR= 91.416   M= 1.2381   GR= 6999.90
TPO= 32.46   TPI= 31.89   TX= 27.94DEGC

V= 14.77   I= 403.0
R= 1.308   CL= .00000   HL= 187.20

VISC= 8.8852

TEST NO. 85.s.

X= 1.0000 NU= 336.85
RE= 14886 PR= 93.152 M= 1.2352 GR= 6233.99
TPO= 31.85 TPI= 31.29 TX= 27.63DEGC

X= 2.0000 NU= 323.52
RE= 14888 PR= 93.137 M= 1.2422 GR= 6502.46
TPO= 32.01 TPI= 31.45 TX= 27.63DEGC

X= 3.0000 NU= 316.29
RE= 14891 PR= 93.123 M= 1.2462 GR= 6653.43
TPO= 32.10 TPI= 31.54 TX= 27.63DEGC

X= 4.0000 NU= 312.52
RE= 14893 PR= 93.109 M= 1.2482 GR= 6736.33
TPO= 32.15 TPI= 31.59 TX= 27.64DEGC

X= 6.0000 NU= 308.23
RE= 14898 PR= 93.081 M= 1.2506 GR= 6834.27
TPO= 32.21 TPI= 31.65 TX= 27.64DEGC

X= 8.0000 NU= 310.20
RE= 14902 PR= 93.053 M= 1.2493 GR= 6795.70
TPO= 32.19 TPI= 31.63 TX= 27.65DEGC

X= 11.000 NU= 310.80
RE= 14909 PR= 93.011 M= 1.2487 GR= 6789.14
TPO= 32.19 TPI= 31.63 TX= 27.65DEGC

X= 15.000 NU= 306.19
RE= 14919 PR= 92.955 M= 1.2511 GR= 6900.05
TPO= 32.26 TPI= 31.70 TX= 27.66DEGC

X= 20.000 NU= 307.17
RE= 14931 PR= 92.885 M= 1.2501 GR= 6889.18
TPO= 32.26 TPI= 31.70 TX= 27.68DEGC

X= 30.000 NU= 306.06
RE= 14954 PR= 92.748 M= 1.2500 GR= 6936.28
TPO= 32.30 TPI= 31.74 TX= 27.70DEGC

X= 50.000 NU= 306.13
RE= 15001 PR= 92.472 M= 1.2484 GR= 6979.36
TPO= 32.35 TPI= 31.79 TX= 27.75DEGC

X= 70.000 NU= 307.03
RE= 15049 PR= 92.190 M= 1.2462 GR= 7004.63
TPO= 32.39 TPI= 31.83 TX= 27.80DEGC

V= 8.025 I= 402.4
R= 1.308 CL= 88.000 HL= 103.00

VISC= 8.9659

TEST NO. 1.c1.

```
X=   0.0     NU= 955.61
RE= 13068    PR=  61.3     M= 1.08     GR=  75155
TPO= 43.87    TPI= 43.55    TX= 41.28  DEGC          Q=  12506    QL=  18.41
X=  10.0     NU= 260.73
RE= 13114    PR=  61.1     M= 1.32     GR= 277422
TPO= 50.04    TPI= 49.73    TX= 41.39  DEGC          Q=  12506    QL=  18.41
X=  30.0     NU= 244.08
RE= 13205    PR=  60.7     M= 1.34     GR= 300569
TPO= 50.83    TPI= 50.51    TX= 41.60  DEGC          Q=  12506    QL=  18.99
X=  49.0     NU= 245.12
RE= 13292    PR=  60.3     M= 1.34     GR= 303367
TPO= 51.00    TPI= 50.68    TX= 41.81  DEGC          Q=  12506    QL=  19.12
X=  50.0     NU= 244.71
RE= 13297    PR=  60.3     M= 1.34     GR= 303941
TPO= 51.02    TPI= 50.71    TX= 41.82  DEGC          Q=  12500    QL=  19.13
X=  51.0     NU= 283.05
RE= 13301    PR=  60.3     M= 1.29     GR= 262960
TPO= 49.83    TPI= 49.51    TX= 41.83  DEGC          Q=  12500    QL=  19.13
X=   0.5     NU= 1088.55
RE= 26488    PR=  60.3     M= 1.06     GR=   7753
TPO= 44.74    TPI= 43.62    TX= 41.83  DEGC          Q=  22288    QL=  22.22
X=   1.0     NU= 770.95
RE= 26490    PR=  60.3     M= 1.08     GR=  10948
TPO= 45.48    TPI= 44.36    TX= 41.83  DEGC          Q=  22288    QL=  22.22
X=   2.0     NU= 554.14
RE= 26494    PR=  60.3     M= 1.12     GR=  15235
TPO= 46.47    TPI= 45.35    TX= 41.84  DEGC          Q=  22286    QL=  23.31
X=   3.0     NU= 509.19
RE= 26498    PR=  60.2     M= 1.13     GR=  16605
TPO= 46.79    TPI= 45.67    TX= 41.84  DEGC          Q=  22312    QL=  23.67
X=   4.0     NU= 470.16
RE= 26502    PR=  60.2     M= 1.14     GR=  17983
TPO= 47.11    TPI= 45.99    TX= 41.85  DEGC          Q=  22305    QL=  24.02
X=   5.5     NU= 454.71
RE= 26508    PR=  60.2     M= 1.15     GR=  18609
TPO= 47.26    TPI= 46.14    TX= 41.86  DEGC          Q=  22311    QL=  24.19
X=   7.0     NU= 442.13
RE= 26515    PR=  60.2     M= 1.15     GR=  19144
TPO= 47.39    TPI= 46.27    TX= 41.86  DEGC          Q=  22308    QL=  24.33
X=   8.5     NU= 451.85
RE= 26521    PR=  60.2     M= 1.15     GR=  18748
TPO= 47.30    TPI= 46.19    TX= 41.87  DEGC          Q=  22316    QL=  24.23
X=  10.0     NU= 439.38
RE= 26527    PR=  60.2     M= 1.15     GR=  19284
TPO= 47.43    TPI= 46.31    TX= 41.88  DEGC          Q=  22310    QL=  24.37
X=  12.0     NU= 440.41
RE= 26535    PR=  60.2     M= 1.15     GR=  19253
TPO= 47.43    TPI= 46.31    TX= 41.89  DEGC          Q=  22312    QL=  24.37
X=  15.0     NU= 435.53
RE= 26548    PR=  60.1     M= 1.16     GR=  19487
TPO= 47.50    TPI= 46.38    TX= 41.90  DEGC          Q=  22312    QL=  24.45
X=  20.0     NU= 429.66
RE= 26568    PR=  60.1     M= 1.16     GR=  19785
TPO= 47.58    TPI= 46.46    TX= 41.93  DEGC          Q=  22311    QL=  24.54
X=  25.0     NU= 434.06
RE= 26589    PR=  60.1     M= 1.16     GR=  19616
TPO= 47.56    TPI= 46.44    TX= 41.95  DEGC          Q=  22311    QL=  24.52
X=  40.0     NU= 439.15
RE= 26651    PR=  59.9     M= 1.15     GR=  19481
TPO= 47.58    TPI= 46.46    TX= 42.03  DEGC          Q=  22311    QL=  24.54
X=  87.0     NU= 460.84
RE= 26848    PR=  59.5     M= 1.15     GR=  18846
TPO= 47.60    TPI= 46.48    TX= 42.25  DEGC          Q=  22312    QL=  24.56
X=  89.0     NU= 445.97
RE= 26856    PR=  59.5     M= 1.15     GR=  19483
TPO= 47.75    TPI= 46.63    TX= 42.26  DEGC          Q=  22307    QL=  24.73
X=  90.0     NU= 455.40
RE= 26860    PR=  59.5     M= 1.15     GR=  19086
TPO= 47.67    TPI= 46.55    TX= 42.27  DEGC          Q=  22307    QL=  24.73
```

TEST NO. 3.c1.

X= 0.0	NU= 377.05				
RE= 3662	PR= 61.3	M= 1.07	GR= 67445		
TPO= 43.41	TPI= 43.30	TX= 41.26	DEGC	Q= 4435	QL= 17.90
X= 10.0	NU= 83.26				
RE= 3678	PR= 61.1	M= 1.36	GR= 308185		
TPO= 50.77	TPI= 50.65	TX= 41.39	DEGC	Q= 4435	QL= 17.90
X= 30.0	NU= 53.04				
RE= 3711	PR= 60.6	M= 1.60	GR= 492104		
TPO= 56.31	TPI= 56.20	TX= 41.67	DEGC	Q= 4431	QL= 22.03
X= 49.0	NU= 61.94				
RE= 3742	PR= 60.1	M= 1.50	GR= 428771		
TPO= 54.49	TPI= 54.38	TX= 41.93	DEGC	Q= 4432	QL= 20.67
X= 50.0	NU= 61.00				
RE= 3743	PR= 60.1	M= 1.51	GR= 434528		
TPO= 54.66	TPI= 54.54	TX= 41.94	DEGC	Q= 4419	QL= 20.80
X= 51.0	NU= 76.41				
RE= 3745	PR= 60.0	M= 1.39	GR= 347181		
TPO= 52.13	TPI= 52.02	TX= 41.96	DEGC	Q= 4419	QL= 20.80
X= 0.5	NU= 453.03				
RE= 7457	PR= 60.0	M= 1.05	GR= 6636		
TPO= 43.87	TPI= 43.47	TX= 41.96	DEGC	Q= 7875	QL= 19.77
X= 1.0	NU= 299.34				
RE= 7458	PR= 60.0	M= 1.08	GR= 10044		
TPO= 44.65	TPI= 44.26	TX= 41.96	DEGC	Q= 7875	QL= 19.77
X= 2.0	NU= 203.71				
RE= 7460	PR= 60.0	M= 1.12	GR= 14774		
TPO= 45.74	TPI= 45.34	TX= 41.97	DEGC	Q= 7879	QL= 20.97
X= 3.0	NU= 174.48				
RE= 7461	PR= 60.0	M= 1.14	GR= 17294		
TPO= 46.32	TPI= 45.93	TX= 41.97	DEGC	Q= 7897	QL= 21.61
X= 4.0	NU= 153.79				
RE= 7463	PR= 60.0	M= 1.16	GR= 19615		
TPO= 46.86	TPI= 46.46	TX= 41.98	DEGC	Q= 7891	QL= 22.20
X= 5.5	NU= 138.88				
RE= 7465	PR= 60.0	M= 1.18	GR= 21740		
TPO= 47.35	TPI= 46.95	TX= 41.99	DEGC	Q= 7893	QL= 22.74
X= 7.0	NU= 132.28				
RE= 7467	PR= 60.0	M= 1.18	GR= 22838		
TPO= 47.60	TPI= 47.21	TX= 42.00	DEGC	Q= 7893	QL= 23.02
X= 8.5	NU= 132.09				
RE= 7469	PP= 60.0	M= 1.19	GR= 22903		
TPO= 47.63	TPI= 47.23	TX= 42.01	DEGC	Q= 7900	QL= 23.04
X= 10.0	NU= 128.03				
RE= 7471	PR= 59.9	M= 1.19	GR= 23628		
TPO= 47.80	TPI= 47.40	TX= 42.02	DEGC	Q= 7895	QL= 23.23
X= 12.0	NU= 127.86				
RE= 7474	PR= 59.9	M= 1.19	GR= 23686		
TPO= 47.82	TPI= 47.42	TX= 42.03	DEGC	Q= 7897	QL= 23.26
X= 15.0	NU= 126.79				
RE= 7479	PR= 59.9	M= 1.19	GR= 23915		
TPO= 47.88	TPI= 47.49	TX= 42.05	DEGC	Q= 7897	QL= 23.33
X= 20.0	NU= 126.51				
RE= 7486	PR= 59.8	M= 1.19	GR= 24016		
TPO= 47.93	TPI= 47.53	TX= 42.08	DEGC	Q= 7897	QL= 23.37
X= 25.0	NU= 127.23				
RE= 7493	PR= 59.8	M= 1.19	GR= 23928		
TPO= 47.93	TPI= 47.53	TX= 42.11	DEGC	Q= 7897	QL= 23.37
X= 40.0	NU= 129.45				
RE= 7516	PR= 59.6	M= 1.19	GR= 23661		
TPO= 47.93	TPI= 47.53	TX= 42.20	DEGC	Q= 7897	QL= 23.37
X= 87.0	NU= 135.20				
RE= 7586	PR= 59.1	M= 1.18	GR= 23089		
TPO= 47.99	TPI= 47.59	TX= 42.49	DEGC	Q= 7897	QL= 23.45
X= 89.0	NU= 131.96				
RE= 7589	PR= 59.1	M= 1.19	GR= 23636		
TPO= 48.12	TPI= 47.72	TX= 42.50	DEGC	Q= 7884	QL= 23.59
X= 90.0	NU= 143.29				
RE= 7590	PR= 59.1	M= 1.17	GR= 21777		
TPO= 47.71	TPI= 47.32	TX= 42.51	DEGC	Q= 7884	QL= 23.59

TEST NO. 6.c1.

```
X=   0.0   NU=  33.67
RE=   236   PR=  62.4   M= 1.10   GR= 93019
TPO= 43.61   TPI= 43.59   TX= 40.67  DEGC   Q=   568   QL=  23.66
X=  10.0   NU=   6.03
RE=   238   PR=  61.9   M= 1.70   GR= 528349
TPO= 57.30   TPI= 57.29   TX= 40.93  DEGC   Q=   568   QL=  23.66
X=  30.0   NU=   6.02
RE=   242   PR=  60.9   M= 1.71   GR= 548122
TPO= 57.87   TPI= 57.86   TX= 41.47  DEGC   Q=   568   QL=  24.08
X=  49.0   NU=   7.39
RE=   246   PR=  60.0   M= 1.55   GR= 463268
TPO= 55.40   TPI= 55.38   TX= 41.98  DEGC   Q=   569   QL=  22.24
X=  50.0   NU=   8.07
RE=   246   PR=  60.0   M= 1.49   GR= 427970
TPO= 54.38   TPI= 54.37   TX= 42.00  DEGC   Q=   574   QL=  21.49
X=  51.0   NU=   8.32
RE=   247   PR=  59.9   M= 1.48   GR= 416038
TPO= 54.04   TPI= 54.03   TX= 42.03  DEGC   Q=   574   QL=  21.49
X=   0.5   NU=  44.88
RE=   491   PR=  59.9   M= 1.06   GR=   8524
TPO= 44.02   TPI= 43.97   TX= 42.03  DEGC   Q=   997   QL=  21.16
X=   1.0   NU=  33.12
RE=   491   PR=  59.9   M= 1.09   GR=  11557
TPO= 44.72   TPI= 44.67   TX= 42.04  DEGC   Q=   997   QL=  21.16
X=   2.0   NU=  27.57
RE=   491   PR=  59.9   M= 1.11   GR=  14279
TPO= 45.35   TPI= 45.30   TX= 42.05  DEGC   Q=  1025   QL=  21.86
X=   3.0   NU=  25.31
RE=   492   PR=  59.9   M= 1.12   GR=  15670
TPO= 45.57   TPI= 45.62   TX= 42.06  DEGC   Q=  1032   QL=  22.22
X=   4.0   NU=  24.18
RE=   492   PR=  59.8   M= 1.13   GR=  16489
TPO= 45.87   TPI= 45.82   TX= 42.07  DEGC   Q=  1036   QL=  22.43
X=   5.5   NU=  22.62
RE=   492   PR=  59.8   M= 1.14   GR=  17662
TPO= 46.15   TPI= 46.10   TX= 42.09  DEGC   Q=  1037   QL=  22.74
X=   7.0   NU=  20.90
RE=   492   PR=  59.8   M= 1.15   GR=  19019
TPO= 46.47   TPI= 46.42   TX= 42.11  DEGC   Q=  1031   QL=  23.09
X=   8.5   NU=  20.93
RE=   493   PR=  59.7   M= 1.15   GR=  19148
TPO= 46.51   TPI= 46.46   TX= 42.13  DEGC   Q=  1038   QL=  23.14
X=  10.0   NU=  20.17
RE=   493   PR=  59.7   M= 1.16   GR=  19847
TPO= 46.68   TPI= 46.63   TX= 42.15  DEGC   Q=  1036   QL=  23.33
X=  12.0   NU=  19.25
RE=   493   PR=  59.7   M= 1.16   GR=  20813
TPO= 46.92   TPI= 46.87   TX= 42.17  DEGC   Q=  1035   QL=  23.59
X=  15.0   NU=  18.64
RE=   494   PR=  59.6   M= 1.17   GR=  21554
TPO= 47.11   TPI= 47.06   TX= 42.21  DEGC   Q=  1035   QL=  23.80
X=  20.0   NU=  18.07
RE=   495   PR=  59.5   M= 1.18   GR=  22319
TPO= 47.33   TPI= 47.28   TX= 42.27  DEGC   Q=  1035   QL=  24.04
X=  25.0   NU=  17.91
RE=   496   PR=  59.4   M= 1.18   GR=  22612
TPO= 47.43   TPI= 47.38   TX= 42.33  DEGC   Q=  1035   QL=  24.15
X=  40.0   NU=  18.11
RE=   499   PR=  59.1   M= 1.18   GR=  22630
TPO= 47.56   TPI= 47.51   TX= 42.52  DEGC   Q=  1035   QL=  24.30
X=  87.0   NU=  17.50
RE=   508   PR=  58.1   M= 1.19   GR=  24301
TPO= 48.31   TPI= 48.26   TX= 43.09  DEGC   Q=  1034   QL=  25.12
X=  89.0   NU=  16.38
RE=   508   PR=  58.0   M= 1.19   GR=  24443
TPO= 48.35   TPI= 48.31   TX= 43.12  DEGC   Q=   972   QL=  25.17
X=  90.0   NU=  29.43
RE=   509   PR=  58.0   M= 1.10   GR=  13616
TPO= 46.06   TPI= 46.02   TX= 43.13  DEGC   Q=   972   QL=  25.17
```

TEST NO. 11.C1.

```
X=   0.0      NU= 628.55
RE=  4011      PR= 204.5      M= 1.19    GR=  12327
TPO= 38.31      TPI= 38.04     TX= 34.35  DEGC        Q=  10661    QL=  20.76
X=  10.0      NU= 139.03
RE=  4032      PR= 203.5      M= 2.10    GR=  56324
TPO= 51.40      TPI= 51.14     TX= 34.46  DEGC        Q=  10661    QL=  20.76
X=  30.0      NU= 101.44
RE=  4074      PR= 201.6      M= 2.65    GR=  78032
TPO= 57.81      TPI= 57.54     TX= 34.69  DEGC        Q=  10657    QL=  25.52
X=  49.0      NU= 113.26
RE=  4114      PR= 199.8      M= 2.41    GR=  72067
TPO= 55.65      TPI= 55.38     TX= 34.90  DEGC        Q=  10659    QL=  23.92
X=  50.0      NU= 109.59
RE=  4117      PR= 199.7      M= 2.47    GR=  74416
TPO= 56.31      TPI= 56.04     TX= 34.91  DEGC        Q=  10639    QL=  24.41
X=  51.0      NU= 130.48
RE=  4119      PR= 199.6      M= 2.18    GR=  62568
TPO= 52.94      TPI= 52.67     TX= 34.93  DEGC        Q=  10639    QL=  24.41
X=   0.5      NU= 835.78
RE=  8202      PR= 199.6      M= 1.12    GR=   1105
TPO= 38.35      TPI= 37.40     TX= 34.93  DEGC        Q=  18925    QL=  17.65
X=   1.0      NU= 566.25
RE=  8203      PR= 199.6      M= 1.19    GR=   1631
TPO= 39.53      TPI= 38.58     TX= 34.93  DEGC        Q=  18925    QL=  17.65
X=   2.0      NU= 344.41
RE=  8205      PR= 199.5      M= 1.33    GR=   2676
TPO= 41.87      TPI= 40.92     TX= 34.93  DEGC        Q=  18875    QL=  20.23
X=   3.0      NU= 291.52
RE=  8207      PR= 199.5      M= 1.39    GR=   3170
TPO= 42.98      TPI= 42.03     TX= 34.94  DEGC        Q=  18917    QL=  21.45
X=   4.0      NU= 256.91
RE=  8209      PR= 199.4      M= 1.45    GR=   3597
TPO= 43.93      TPI= 42.99     TX= 34.94  DEGC        Q=  18909    QL=  22.50
X=   5.5      NU= 233.28
RE=  8212      PR= 199.4      M= 1.49    GR=   3966
TPO= 44.76      TPI= 43.81     TX= 34.95  DEGC        Q=  18916    QL=  23.41
X=   7.0      NU= 219.92
RE=  8214      PR= 199.3      M= 1.53    GR=   4209
TPO= 45.30      TPI= 44.36     TX= 34.96  DEGC        Q=  18912    QL=  24.01
X=   8.5      NU= 218.72
RE=  8217      PR= 199.2      M= 1.53    GR=   4238
TPO= 45.37      TPI= 44.42     TX= 34.97  DEGC        Q=  18922    QL=  24.08
X=  10.0      NU= 214.90
RE=  8220      PR= 199.2      M= 1.54    GR=   4315
TPO= 45.54      TPI= 44.59     TX= 34.97  DEGC        Q=  18919    QL=  24.28
X=  12.0      NU= 212.24
RE=  8224      PR= 199.1      M= 1.55    GR=   4374
TPO= 45.67      TPI= 44.72     TX= 34.98  DEGC        Q=  18919    QL=  24.42
X=  15.0      NU= 213.56
RE=  8230      PR= 199.0      M= 1.55    GR=   4353
TPO= 45.63      TPI= 44.68     TX= 35.00  DEGC        Q=  18920    QL=  24.37
X=  20.0      NU= 211.73
RE=  8239      PR= 198.8      M= 1.55    GR=   4401
TPO= 45.74      TPI= 44.79     TX= 35.02  DEGC        Q=  18920    QL=  24.49
X=  25.0      NU= 212.29
RE=  8249      PR= 198.5      M= 1.55    GR=   4400
TPO= 45.74      TPI= 44.79     TX= 35.05  DEGC        Q=  18920    QL=  24.49
X=  40.0      NU= 213.99
RE=  8278      PR= 197.9      M= 1.55    GR=   4397
TPO= 45.74      TPI= 44.79     TX= 35.13  DEGC        Q=  18920    QL=  24.49
X=  87.0      NU= 221.51
RE=  8370      PR= 195.9      M= 1.52    GR=   4345
TPO= 45.65      TPI= 44.70     TX= 35.36  DEGC        Q=  18920    QL=  24.40
X=  89.0      NU= 219.08
RE=  8374      PR= 195.8      M= 1.53    GR=   4395
TPO= 45.76      TPI= 44.81     TX= 35.37  DEGC        Q=  18911    QL=  24.51
X=  90.0      NU= 225.97
RE=  8376      PR= 195.8      M= 1.51    GR=   4263
TPO= 45.48      TPI= 44.53     TX= 35.38  DEGC        Q=  18911    QL=  24.51
```

TEST NO. 15.c1.

```
X=   0.0      NU= 115.96
RE=   233     PR= 351.5    M= 1.10    GR=  1829
TPO= 25.26    TPI= 25.23   TX= 23.46  DEGC       Q=   964    QL=  5.72
X=  10.0      NU=  27.80
RE=   234     PR= 349.7    M= 1.53    GR=  7714
TPO= 30.98    TPI= 30.96   TX= 23.56  DEGC       Q=   964    QL=  5.72
X=  30.0      NU=  19.27
RE=   237     PR= 346.2    M= 1.77    GR= 11350
TPO= 34.44    TPI= 34.41   TX= 23.76  DEGC       Q=   962    QL=  8.29
X=  49.0      NU=  17.89
RE=   239     PR= 342.9    M= 1.84    GR= 12475
TPO= 35.44    TPI= 35.42   TX= 23.95  DEGC       Q=   961    QL=  9.03
X=  50.0      NU=  17.69
RE=   239     PR= 342.8    M= 1.84    GR= 12502
TPO= 35.46    TPI= 35.44   TX= 23.96  DEGC       Q=   951    QL=  9.05
X=  51.0      NU=  21.59
RE=   240     PR= 342.6    M= 1.67    GR= 10250
TPO= 33.40    TPI= 33.37   TX= 23.97  DEGC       Q=   951    QL=  9.05
X=   0.5      NU=  24.26
RE=   477     PR= 342.6    M= 1.54    GR=  1046
TPO= 31.63    TPI= 31.55   TX= 23.97  DEGC       Q=  1715    QL=  9.47
X=   1.0      NU=  23.44
RE=   477     PR= 342.6    M= 1.56    GR=  1083
TPO= 31.90    TPI= 31.81   TX= 23.97  DEGC       Q=  1715    QL=  9.47
X=   2.0      NU=  22.91
RE=   477     PR= 342.5    M= 1.57    GR=  1116
TPO= 32.15    TPI= 32.06   TX= 23.98  DEGC       Q=  1727    QL=  9.74
X=   3.0      NU=  22.43
RE=   477     PR= 342.4    M= 1.59    GR=  1141
TPO= 32.32    TPI= 32.24   TX= 23.98  DEGC       Q=  1728    QL=  9.94
X=   4.0      NU=  22.13
RE=   478     PR= 342.3    M= 1.59    GR=  1160
TPO= 32.46    TPI= 32.37   TX= 23.99  DEGC       Q=  1731    QL= 10.09
X=   5.5      NU=  21.38
RE=   478     PR= 342.2    M= 1.61    GR=  1200
TPO= 32.75    TPI= 32.66   TX= 23.99  DEGC       Q=  1729    QL= 10.41
X=   7.0      NU=  20.74
RE=   478     PR= 342.1    M= 1.63    GR=  1237
TPO= 33.02    TPI= 32.93   TX= 24.00  DEGC       Q=  1728    QL= 10.70
X=   8.5      NU=  20.30
RE=   478     PR= 342.0    M= 1.65    GR=  1265
TPO= 33.22    TPI= 33.13   TX= 24.01  DEGC       Q=  1728    QL= 10.92
X=  10.0      NU=  19.93
RE=   478     PR= 341.9    M= 1.66    GR=  1289
TPO= 33.40    TPI= 33.31   TX= 24.01  DEGC       Q=  1729    QL= 11.12
X=  12.0      NU=  19.43
RE=   478     PR= 341.7    M= 1.68    GR=  1324
TPO= 33.64    TPI= 33.56   TX= 24.02  DEGC       Q=  1728    QL= 11.39
X=  15.0      NU=  18.92
RE=   479     PR= 341.5    M= 1.70    GR=  1361
TPO= 33.91    TPI= 33.82   TX= 24.04  DEGC       Q=  1728    QL= 11.69
X=  20.0      NU=  18.15
RE=   479     PR= 341.1    M= 1.73    GR=  1422
TPO= 34.35    TPI= 34.26   TX= 24.06  DEGC       Q=  1727    QL= 12.17
X=  25.0      NU=  17.62
RE=   480     PR= 340.7    M= 1.75    GR=  1469
TPO= 34.68    TPI= 34.59   TX= 24.08  DEGC       Q=  1727    QL= 12.53
X=  40.0      NU=  16.61
RE=   482     PR= 339.5    M= 1.80    GR=  1569
TPO= 35.38    TPI= 35.29   TX= 24.15  DEGC       Q=  1726    QL= 13.30
X=  87.0      NU=  14.67
RE=   487     PR= 335.9    M= 1.93    GR=  1818
TPO= 37.06    TPI= 36.97   TX= 24.36  DEGC       Q=  1724    QL= 15.15
X=  89.0      NU=  14.38
RE=   488     PR= 335.7    M= 1.94    GR=  1825
TPO= 37.10    TPI= 37.02   TX= 24.37  DEGC       Q=  1695    QL= 15.20
X=  90.0      NU=  15.71
RE=   488     PR= 335.7    M= 1.84    GR=  1670
TPO= 36.03    TPI= 35.95   TX= 24.38  DEGC       Q=  1695    QL= 15.20
```

TEST NO. 1.22.

```
X=   0.0     NU= 557.54
RE=  6620     PR= 199.7     M= 1.18    GR=   3058
TPO= 38.57     TPI= 38.09     TX= 34.55  DEGC          Q=  14553    QL=  24.39
X=  10.0     NU= 181.42
RE=  6639     PR= 199.2     M= 1.63    GR=   9449
TPO= 45.98     TPI= 45.50     TX= 34.61  DEGC          Q=  14553    QL=  24.39
X=  30.0     NU= 176.13
RE=  6675     PR= 198.2     M= 1.65    GR=   9844
TPO= 46.43     TPI= 45.95     TX= 34.73  DEGC          Q=  14554    QL=  24.82
X=  88.0     NU= 177.66
RE=  6783     PR= 195.4     M= 1.64    GR=  10084
TPO= 46.68     TPI= 46.21     TX= 35.07  DEGC          Q=  14554    QL=  25.06
X=  89.0     NU= 176.09
RE=  6784     PR= 195.3     M= 1.65    GR=  10163
TPO= 46.77     TPI= 46.29     TX= 35.08  DEGC          Q=  14529    QL=  25.14
X=  90.0     NU= 201.34
RE=  6786     PR= 195.3     M= 1.55    GR=   8893
TPO= 45.37     TPI= 44.89     TX= 35.08  DEGC          Q=  14529    QL=  25.14
X=   0.5     NU= 677.28
RE=  8464     PR= 195.3     M= 1.15    GR=   1388
TPO= 38.74     TPI= 38.06     TX= 35.08  DEGC          Q=  18465    QL=  22.26
X=   1.0     NU= 402.34
RE=  8465     PR= 195.2     M= 1.28    GR=   2338
TPO= 40.78     TPI= 40.09     TX= 35.09  DEGC          Q=  18465    QL=  22.26
X=   2.0     NU= 281.96
RE=  8467     PR= 195.2     M= 1.39    GR=   3345
TPO= 42.93     TPI= 42.25     TX= 35.09  DEGC          Q=  18508    QL=  24.61
X=   3.0     NU= 241.92
RE=  8469     PR= 195.2     M= 1.46    GR=   3903
TPO= 44.13     TPI= 43.44     TX= 35.10  DEGC          Q=  18523    QL=  25.91
X=   4.0     NU= 221.86
RE=  8471     PR= 195.1     M= 1.51    GR=   4259
TPO= 44.89     TPI= 44.20     TX= 35.10  DEGC          Q=  18525    QL=  26.73
X=   5.5     NU= 210.05
RE=  8474     PR= 195.1     M= 1.54    GR=   4503
TPO= 45.41     TPI= 44.72     TX= 35.11  DEGC          Q=  18530    QL=  27.30
X=   7.0     NU= 205.57
RE=  8477     PR= 195.0     M= 1.55    GR=   4604
TPO= 45.63     TPI= 44.94     TX= 35.12  DEGC          Q=  18530    QL=  27.54
X=   8.5     NU= 206.21
RE=  8480     PR= 194.9     M= 1.55    GR=   4594
TPO= 45.61     TPI= 44.92     TX= 35.12  DEGC          Q=  18533    QL=  27.51
X=  10.0     NU= 208.21
RE=  8483     PR= 194.9     M= 1.55    GR=   4552
TPO= 45.52     TPI= 44.83     TX= 35.13  DEGC          Q=  18532    QL=  27.42
X=  12.0     NU= 215.72
RE=  8486     PR= 194.8     M= 1.52    GR=   4409
TPO= 45.22     TPI= 44.53     TX= 35.14  DEGC          Q=  18536    QL=  27.09
X=  15.0     NU= 216.05
RE=  8492     PR= 194.7     M= 1.52    GR=   4398
TPO= 45.20     TPI= 44.51     TX= 35.16  DEGC          Q=  18534    QL=  27.06
X=  20.0     NU= 219.70
RE=  8502     PR= 194.5     M= 1.51    GR=   4335
TPO= 45.07     TPI= 44.37     TX= 35.18  DEGC          Q=  18534    QL=  26.92
X=  25.0     NU= 219.25
RE=  8511     PR= 194.3     M= 1.51    GR=   4354
TPO= 45.11     TPI= 44.42     TX= 35.20  DEGC          Q=  18534    QL=  26.97
X=  40.0     NU= 217.93
RE=  8540     PR= 193.7     M= 1.52    GR=   4411
TPO= 45.24     TPI= 44.55     TX= 35.28  DEGC          Q=  18534    QL=  27.11
X=  87.0     NU= 220.90
RE=  8632     PR= 191.8     M= 1.51    GR=   4448
TPO= 45.35     TPI= 44.66     TX= 35.51  DEGC          Q=  18534    QL=  27.23
X=  89.0     NU= 224.69
RE=  8636     PR= 191.7     M= 1.50    GR=   4374
TPO= 45.20     TPI= 44.51     TX= 35.52  DEGC          Q=  18519    QL=  27.06
X=  90.0     NU= 248.24
RE=  8638     PR= 191.6     M= 1.44    GR=   3961
TPO= 44.35     TPI= 43.66     TX= 35.52  DEGC          Q=  18519    QL=  27.06
```

TEST NO. 3.02.

```
X=   0.0     NU= 1682.88
RE=   972     PR= 201.0    M= 1.01    GR=     92
TPO= 34.44    TPI= 34.39    TX= 34.28  DEGC          Q=   1354    QL=  16.81
X=  10.0     NU=  45.65
RE=   974     PR= 201.6    M= 1.21    GR=   3403
TPO= 38.39    TPI= 38.35    TX= 34.32  DEGC          Q=   1354    QL=  16.81
X=  30.0     NU=  26.67
RE=   977     PR= 201.0    M= 1.38    GR=   5855
TPO= 41.32    TPI= 41.28    TX= 34.40  DEGC          Q=   1352    QL=  19.59
X=  88.0     NU=  17.86
RE=   987     PR= 199.2    M= 1.59    GR=   8901
TPO= 44.91    TPI= 44.87    TX= 34.61  DEGC          Q=   1349    QL=  23.00
X=  89.0     NU=  17.61
RE=   987     PR= 199.2    M= 1.59    GR=   8958
TPO= 44.98    TPI= 44.94    TX= 34.62  DEGC          Q=   1338    QL=  23.06
X=  90.0     NU=  18.68
RE=   988     PR= 199.1    M= 1.55    GR=   8448
TPO= 44.39    TPI= 44.35    TX= 34.62  DEGC          Q=   1338    QL=  23.06
X=   0.5     NU=  22.21
RE=  1232     PR= 199.1    M= 1.47    GR=   3752
TPO= 43.07    TPI= 43.00    TX= 34.62  DEGC          Q=   1709    QL=  24.76
X=   1.0     NU=  21.17
RE=  1232     PR= 199.1    M= 1.49    GR=   3936
TPO= 43.48    TPI= 43.42    TX= 34.62  DEGC          Q=   1709    QL=  24.76
X=   2.0     NU=  20.93
RE=  1232     PR= 199.1    M= 1.50    GR=   4033
TPO= 43.70    TPI= 43.63    TX= 34.62  DEGC          Q=   1731    QL=  25.00
X=   3.0     NU=  20.54
RE=  1232     PR= 199.1    M= 1.51    GR=   4111
TPO= 43.87    TPI= 43.81    TX= 34.63  DEGC          Q=   1731    QL=  25.19
X=   4.0     NU=  20.21
RE=  1232     PR= 199.0    M= 1.52    GR=   4169
TPO= 44.00    TPI= 43.94    TX= 34.63  DEGC          Q=   1727    QL=  25.33
X=   5.5     NU=  20.64
RE=  1233     PR= 199.0    M= 1.51    GR=   4110
TPO= 43.87    TPI= 43.81    TX= 34.64  DEGC          Q=   1738    QL=  25.19
X=   7.0     NU=  19.89
RE=  1233     PR= 199.0    M= 1.53    GR=   4246
TPO= 44.17    TPI= 44.11    TX= 34.64  DEGC          Q=   1730    QL=  25.52
X=   8.5     NU=  19.64
RE=  1233     PR= 198.9    M= 1.54    GR=   4305
TPO= 44.30    TPI= 44.24    TX= 34.64  DEGC          Q=   1731    QL=  25.66
X=  10.0     NU=  19.58
RE=  1233     PR= 198.9    M= 1.54    GR=   4324
TPO= 44.35    TPI= 44.28    TX= 34.65  DEGC          Q=   1732    QL=  25.71
X=  12.0     NU=  19.46
RE=  1234     PR= 198.8    M= 1.55    GR=   4353
TPO= 44.41    TPI= 44.35    TX= 34.66  DEGC          Q=   1732    QL=  25.78
X=  15.0     NU=  19.04
RE=  1234     PR= 198.7    M= 1.56    GR=   4450
TPO= 44.63    TPI= 44.57    TX= 34.66  DEGC          Q=   1732    QL=  26.02
X=  20.0     NU=  18.62
RE=  1235     PR= 198.6    M= 1.58    GR=   4557
TPO= 44.87    TPI= 44.81    TX= 34.68  DEGC          Q=   1731    QL=  26.27
X=  25.0     NU=  18.33
RE=  1236     PR= 198.5    M= 1.59    GR=   4635
TPO= 45.04    TPI= 44.98    TX= 34.70  DEGC          Q=   1731    QL=  26.46
X=  40.0     NU=  17.85
RE=  1239     PR= 198.1    M= 1.61    GR=   4782
TPO= 45.37    TPI= 45.31    TX= 34.74  DEGC          Q=   1731    QL=  26.82
X=  87.0     NU=  16.51
RE=  1247     PR= 196.9    M= 1.66    GR=   5236
TPO= 46.36    TPI= 46.30    TX= 34.89  DEGC          Q=   1730    QL=  27.90
X=  89.0     NU=  16.25
RE=  1247     PR= 196.9    M= 1.66    GR=   5237
TPO= 46.36    TPI= 46.30    TX= 34.89  DEGC          Q=   1702    QL=  27.90
X=  90.0     NU=  18.50
RE=  1247     PR= 196.8    M= 1.56    GR=   4581
TPO= 44.93    TPI= 44.87    TX= 34.89  DEGC          Q=   1702    QL=  27.90
```

TEST NO. 6.c2.

```
X=   0.0    NU= 241.97
RE=  1100    PR= 341.2    M= 1.05    GR=   229
TPO= 24.61    TPI= 24.56    TX= 23.71  DEGC     Q=  1541   QL=  5.31
X=  10.0    NU=  47.65
RE=  1101    PR= 340.9    M= 1.28    GR=  1164
TPO= 28.09    TPI= 28.04    TX= 23.73  DEGC     Q=  1541   QL=  5.31
X=  30.0    NU=  30.86
RE=  1103    PR= 340.1    M= 1.48    GR=  1804
TPO= 30.47    TPI= 30.42    TX= 23.77  DEGC     Q=  1539   QL=  7.57
X=  88.0    NU=  20.93
RE=  1111    PR= 338.0    M= 1.70    GR=  2692
TPO= 33.73    TPI= 33.68    TX= 23.90  DEGC     Q=  1536   QL= 10.67
X=  89.0    NU=  20.68
RE=  1111    PR= 337.9    M= 1.70    GR=  2711
TPO= 33.80    TPI= 33.75    TX= 23.90  DEGC     Q=  1528   QL= 10.73
X=  90.0    NU=  21.62
RE=  1111    PR= 337.9    M= 1.67    GR=  2594
TPO= 33.37    TPI= 33.32    TX= 23.90  DEGC     Q=  1528   QL= 10.73
X=   0.5    NU=  24.54
RE=  1386    PR= 337.9    M= 1.60    GR=  1210
TPO= 32.50    TPI= 32.43    TX= 23.90  DEGC     Q=  1958   QL= 11.19
X=   1.0    NU=  23.74
RE=  1386    PR= 337.9    M= 1.62    GR=  1251
TPO= 32.79    TPI= 32.72    TX= 23.91  DEGC     Q=  1958   QL= 11.19
X=   2.0    NU=  23.36
RE=  1386    PR= 337.9    M= 1.64    GR=  1280
TPO= 32.99    TPI= 32.92    TX= 23.91  DEGC     Q=  1971   QL= 11.41
X=   3.0    NU=  23.04
RE=  1386    PR= 337.8    M= 1.65    GR=  1299
TPO= 33.13    TPI= 33.06    TX= 23.91  DEGC     Q=  1972   QL= 11.55
X=   4.0    NU=  22.75
RE=  1387    PR= 337.8    M= 1.66    GR=  1315
TPO= 33.24    TPI= 33.17    TX= 23.91  DEGC     Q=  1970   QL= 11.68
X=   5.5    NU=  22.75
RE=  1387    PR= 337.7    M= 1.66    GR=  1318
TPO= 33.26    TPI= 33.19    TX= 23.91  DEGC     Q=  1975   QL= 11.70
X=   7.0    NU=  22.29
RE=  1387    PR= 337.7    M= 1.67    GR=  1343
TPO= 33.44    TPI= 33.37    TX= 23.92  DEGC     Q=  1971   QL= 11.89
X=   8.5    NU=  22.04
RE=  1387    PR= 337.7    M= 1.68    GR=  1359
TPO= 33.55    TPI= 33.48    TX= 23.92  DEGC     Q=  1972   QL= 12.02
X=  10.0    NU=  21.84
RE=  1387    PR= 337.6    M= 1.69    GR=  1372
TPO= 33.64    TPI= 33.57    TX= 23.92  DEGC     Q=  1972   QL= 12.11
X=  12.0    NU=  21.60
RE=  1388    PR= 337.5    M= 1.69    GR=  1388
TPO= 33.75    TPI= 33.68    TX= 23.93  DEGC     Q=  1972   QL= 12.23
X=  15.0    NU=  21.27
RE=  1388    PR= 337.5    M= 1.70    GR=  1410
TPO= 33.91    TPI= 33.84    TX= 23.93  DEGC     Q=  1972   QL= 12.40
X=  20.0    NU=  20.82
RE=  1389    PR= 337.3    M= 1.72    GR=  1441
TPO= 34.13    TPI= 34.06    TX= 23.94  DEGC     Q=  1972   QL= 12.64
X=  25.0    NU=  20.44
RE=  1389    PR= 337.2    M= 1.74    GR=  1470
TPO= 34.33    TPI= 34.25    TX= 23.95  DEGC     Q=  1971   QL= 12.86
X=  40.0    NU=  19.57
RE=  1391    PR= 336.7    M= 1.77    GR=  1539
TPO= 34.81    TPI= 34.74    TX= 23.98  DEGC     Q=  1971   QL= 13.38
X=  87.0    NU=  17.92
RE=  1398    PR= 335.3    M= 1.85    GR=  1696
TPO= 35.88    TPI= 35.81    TX= 24.06  DEGC     Q=  1970   QL= 14.55
X=  89.0    NU=  17.74
RE=  1398    PR= 335.2    M= 1.86    GR=  1702
TPO= 35.92    TPI= 35.85    TX= 24.06  DEGC     Q=  1956   QL= 14.59
X=  90.0    NU=  18.79
RE=  1398    PR= 335.2    M= 1.80    GR=  1607
TPO= 35.27    TPI= 35.20    TX= 24.07  DEGC     Q=  1956   QL= 14.59
```

TEST NO. 802.

X=	NU=	RE=	PR=	M=	GR=	TPO=	TPI=	TX= (DEGC)	Q=	QL=
0.0	414.09	3674	334.8	1.13	617	26.51	26.29	24.09	6825	7.80
10.0	115.64	3680	334.3	1.55	2218	32.21	31.99	24.12	6825	7.80
30.0	98.48	3692	333.3	1.65	2622	33.64	33.42	24.18	6824	9.16
88.0	103.43	3727	330.4	1.62	2544	33.37	33.15	24.35	6824	8.90
89.0	105.38	3727	330.3	1.60	2493	33.20	32.97	24.35	6809	8.73
90.0	121.12	3728	330.3	1.52	2169	32.08	31.85	24.36	6809	8.73
0.5	350.16	4650	330.3	1.16	396	27.33	27.01	24.36	8688	4.66
1.0	257.53	4650	330.3	1.23	538	28.29	27.97	24.36	8688	4.66
2.0	190.99	4651	330.2	1.33	727	29.56	29.23	24.36	8700	6.04
3.0	162.24	4651	330.2	1.41	856	30.42	30.10	24.36	8705	6.98
4.0	145.35	4652	330.2	1.45	956	31.09	30.77	24.36	8707	7.71
5.5	129.60	4653	330.1	1.50	1073	31.88	31.55	24.37	8706	8.56
7.0	120.31	4654	330.0	1.54	1156	32.44	32.11	24.37	8707	9.17
8.5	114.41	4655	330.0	1.57	1216	32.84	32.51	24.38	8706	9.61
10.0	111.10	4656	329.9	1.59	1253	33.08	32.76	24.38	8706	9.88
12.0	109.71	4657	329.8	1.59	1269	33.20	32.87	24.38	8707	10.00
15.0	111.88	4659	329.7	1.58	1246	33.04	32.71	24.39	8707	9.83
20.0	123.34	4662	329.5	1.53	1132	32.28	31.95	24.40	8709	9.00
25.0	133.44	4665	329.3	1.49	1048	31.72	31.40	24.42	8710	8.39
40.0	135.90	4674	328.7	1.48	1033	31.63	31.31	24.45	8710	8.30
87.0	135.52	4703	326.8	1.48	1049	31.77	31.44	24.57	8709	8.44
89.0	137.24	4705	326.7	1.47	1035	31.68	31.35	24.57	8699	8.34
90.0	150.16	4705	326.7	1.44	946	31.09	30.77	24.57	8699	8.34

TEST NO. II:C2.

```
X=   0.0    NU= 433.25
RE=  6003    PR=  59.9    M= 1.05    GR=  13184
TPO= 42.91    TPI= 42.71    TX= 41.15  DEGC      Q=  6256   QL=  21.02
X=  10.0    NU= 109.11
RE=  6017    PR=  59.8    M= 1.22    GR=  52606
TPO= 47.63    TPI= 47.42    TX= 41.22  DEGC      Q=  6256   QL=  21.02
X=  30.0    NU= 105.50
RE=  6046    PR=  59.5    M= 1.23    GR=  54943
TPO= 47.99    TPI= 47.78    TX= 41.37  DEGC      Q=  6256   QL=  21.36
X=  88.0    NU= 104.27
RE=  6130    PR=  58.7    M= 1.24    GR=  57183
TPO= 48.50    TPI= 48.30    TX= 41.81  DEGC      Q=  6255   QL=  21.85
X=  89.0    NU= 105.19
RE=  6132    PR=  58.7    M= 1.23    GR=  56583
TPO= 48.44    TPI= 48.23    TX= 41.82  DEGC      Q=  6242   QL=  21.79
X=  90.0    NU= 122.96
RE=  6133    PR=  58.7    M= 1.19    GR=  48430
TPO= 47.52    TPI= 47.31    TX= 41.82  DEGC      Q=  6242   QL=  21.79
X=   0.5    NU= 410.00
RE=  7650    PR=  58.7    M= 1.06    GR=   7656
TPO= 43.80    TPI= 43.51    TX= 41.82  DEGC      Q=  7962   QL=  21.10
X=   1.0    NU= 247.51
RE=  7650    PR=  58.7    M= 1.09    GR=  12685
TPO= 44.91    TPI= 44.62    TX= 41.83  DEGC      Q=  7962   QL=  21.10
X=   2.0    NU= 172.22
RE=  7652    PR=  58.7    M= 1.14    GR=  18284
TPO= 46.15    TPI= 45.85    TX= 41.83  DEGC      Q=  7983   QL=  22.45
X=   3.0    NU= 147.55
RE=  7653    PR=  58.7    M= 1.16    GR=  21377
TPO= 46.83    TPI= 46.54    TX= 41.84  DEGC      Q=  7993   QL=  23.19
X=   4.0    NU= 133.69
RE=  7655    PR=  58.7    M= 1.18    GR=  23597
TPO= 47.33    TPI= 47.03    TX= 41.85  DEGC      Q=  7991   QL=  23.73
X=   5.5    NU= 126.69
RE=  7657    PR=  58.7    M= 1.19    GR=  24932
TPO= 47.63    TPI= 47.33    TX= 41.85  DEGC      Q=  7996   QL=  24.05
X=   7.0    NU= 122.57
RE=  7659    PR=  58.6    M= 1.20    GR=  25783
TPO= 47.82    TPI= 47.52    TX= 41.86  DEGC      Q=  7995   QL=  24.26
X=   8.5    NU= 122.31
RE=  7662    PR=  58.6    M= 1.20    GR=  25853
TPO= 47.84    TPI= 47.54    TX= 41.87  DEGC      Q=  7995   QL=  24.29
X=  10.0    NU= 124.90
RE=  7664    PR=  58.6    M= 1.20    GR=  25338
TPO= 47.73    TPI= 47.44    TX= 41.88  DEGC      Q=  7997   QL=  24.17
X=  12.0    NU= 129.19
RE=  7667    PR=  58.6    M= 1.19    GR=  24520
TPO= 47.56    TPI= 47.26    TX= 41.90  DEGC      Q=  7998   QL=  23.98
X=  15.0    NU= 130.67
RE=  7671    PR=  58.6    M= 1.19    GR=  24269
TPO= 47.52    TPI= 47.22    TX= 41.91  DEGC      Q=  7997   QL=  23.94
X=  20.0    NU= 133.61
RE=  7679    PR=  58.5    M= 1.18    GR=  23784
TPO= 47.43    TPI= 47.14    TX= 41.94  DEGC      Q=  7998   QL=  23.84
X=  25.0    NU= 132.76
RE=  7686    PR=  58.5    M= 1.18    GR=  23984
TPO= 47.50    TPI= 47.20    TX= 41.98  DEGC      Q=  7997   QL=  23.91
X=  40.0    NU= 131.86
RE=  7709    PR=  58.3    M= 1.19    GR=  24292
TPO= 47.63    TPI= 47.33    TX= 42.07  DEGC      Q=  7997   QL=  24.05
X=  87.0    NU= 133.28
RE=  7781    PR=  57.8    M= 1.18    GR=  24492
TPO= 47.86    TPI= 47.56    TX= 42.36  DEGC      Q=  7997   QL=  24.31
X=  89.0    NU= 136.21
RE=  7784    PR=  57.8    M= 1.18    GR=  23951
TPO= 47.75    TPI= 47.46    TX= 42.37  DEGC      Q=  7986   QL=  24.19
X=  90.0    NU= 155.34
RE=  7785    PR=  57.8    M= 1.16    GR=  21010
TPO= 47.13    TPI= 46.84    TX= 42.38  DEGC      Q=  7986   QL=  24.19
```

TEST NO. 1c3.

```
X=   0.0    NU= 740.40
 RE= 10205    PR=  58.4    M= 1.07    GR= 114135
 TPO= 44.50    TPI= 44.24    TX= 42.02  DEGC        Q=  8478    QL=  20.63
X=  10.0    NU= 212.44
 RE= 10241    PR=  58.2    M= 1.29    GR= 400658
 TPO= 50.13    TPI= 49.87    TX= 42.13  DEGC        Q=  8478    QL=  20.63
X=  30.0    NU= 181.66
 RE= 10313    PR=  57.8    M= 1.34    GR= 475262
 TPO= 51.66    TPI= 51.40    TX= 42.35  DEGC        Q=  8477    QL=  21.71
X=  46.2    NU= 187.60
 RE= 10372    PR=  57.5    M= 1.33    GR= 465615
 TPO= 51.55    TPI= 51.29    TX= 42.53  DEGC        Q=  8477    QL=  21.64
X=  47.2    NU= 186.07
 RE= 10375    PR=  57.5    M= 1.33    GR= 468784
 TPO= 51.62    TPI= 51.36    TX= 42.54  DEGC        Q=  8459    QL=  21.68
X=  48.2    NU= 331.91
 RE= 10379    PR=  57.5    M= 1.17    GR= 262990
 TPO= 47.75    TPI= 47.50    TX= 42.55  DEGC        Q=  8459    QL=  21.68
X=   0.5    NU= 2178.27
 RE= 34699    PR=  57.5    M= 1.02    GR=   1075
 TPO= 45.61    TPI= 43.31    TX= 42.55  DEGC        Q= 28362    QL=  38.26
X=   1.0    NU= 840.38
 RE= 34701    PR=  57.5    M= 1.06    GR=   2788
 TPO= 46.81    TPI= 44.51    TX= 42.56  DEGC        Q= 28362    QL=  38.26
X=   2.0    NU= 619.81
 RE= 34705    PR=  57.5    M= 1.09    GR=   3818
 TPO= 47.56    TPI= 45.24    TX= 42.56  DEGC        Q= 28641    QL=  39.38
X=   3.0    NU= 568.49
 RE= 34709    PR=  57.5    M= 1.10    GR=   4173
 TPO= 47.82    TPI= 45.49    TX= 42.56  DEGC        Q= 28703    QL=  39.76
X=   4.0    NU= 541.84
 RE= 34712    PR=  57.4    M= 1.10    GR=   4381
 TPO= 47.97    TPI= 45.64    TX= 42.56  DEGC        Q= 28716    QL=  39.98
X=   5.5    NU= 513.87
 RE= 34718    PR=  57.4    M= 1.11    GR=   4620
 TPO= 48.14    TPI= 45.81    TX= 42.57  DEGC        Q= 28709    QL=  40.23
X=   7.0    NU= 511.52
 RE= 34723    PR=  57.4    M= 1.11    GR=   4643
 TPO= 48.16    TPI= 45.83    TX= 42.58  DEGC        Q= 28717    QL=  40.27
X=   8.5    NU= 515.85
 RE= 34729    PR=  57.4    M= 1.11    GR=   4607
 TPO= 48.14    TPI= 45.81    TX= 42.58  DEGC        Q= 28721    QL=  40.23
X=  10.0    NU= 516.64
 RE= 34735    PR=  57.4    M= 1.11    GR=   4601
 TPO= 48.14    TPI= 45.81    TX= 42.59  DEGC        Q= 28721    QL=  40.23
X=  12.0    NU= 514.27
 RE= 34742    PR=  57.4    M= 1.11    GR=   4624
 TPO= 48.16    TPI= 45.83    TX= 42.59  DEGC        Q= 28720    QL=  40.27
X=  15.0    NU= 509.11
 RE= 34753    PR=  57.4    M= 1.11    GR=   4674
 TPO= 48.20    TPI= 45.87    TX= 42.60  DEGC        Q= 28720    QL=  40.33
X=  20.0    NU= 505.09
 RE= 34772    PR=  57.4    M= 1.11    GR=   4716
 TPO= 48.25    TPI= 45.92    TX= 42.62  DEGC        Q= 28719    QL=  40.39
X=  25.0    NU= 507.68
 RE= 34790    PR=  57.3    M= 1.11    GR=   4698
 TPO= 48.25    TPI= 45.92    TX= 42.64  DEGC        Q= 28720    QL=  40.39
X=  40.0    NU= 505.53
 RE= 34846    PR=  57.2    M= 1.11    GR=   4733
 TPO= 48.31    TPI= 45.98    TX= 42.69  DEGC        Q= 28720    QL=  40.49
X=  97.0    NU= 502.02
 RE= 35058    PR=  56.9    M= 1.11    GR=   4826
 TPO= 48.52    TPI= 46.20    TX= 42.88  DEGC        Q= 28719    QL=  40.81
X=  99.0    NU= 499.44
 RE= 35065    PR=  56.9    M= 1.11    GR=   4832
 TPO= 48.52    TPI= 46.21    TX= 42.88  DEGC        Q= 28599    QL=  40.81
X= 100.0    NU= 751.91
 RE= 35069    PR=  56.9    M= 1.07    GR=   3210
 TPO= 47.41    TPI= 45.09    TX= 42.89  DEGC        Q= 28599    QL=  40.81
```

TEST NO; 3c3.

```
X=   0,0     NU= 406,71
RE=  3444    PR=  58,3     M= 1,06    GR= 101012
TPO= 44,13   TPI= 44,01    TX= 42,04  DEGC        Q=  4116   QL= 19,79
X=  10,0     NU=  84,74
RE=  3461    PR=  58,1     M= 1,36    GR= 489870
TPO= 51,74   TPI= 51,62    TX= 42,20  DEGC        Q=  4116   QL= 19,79
X=  30,0     NU=  46,69
RE=  3497    PR=  57,5     M= 1,76    GR= 906427
TPO= 59,72   TPI= 59,59    TX= 42,52  DEGC        Q=  4110   QL= 25,45
X=  46,2     NU=  50,50
RE=  3525    PR=  57,1     M= 1,68    GR= 852299
TPO= 58,69   TPI= 58,57    TX= 42,78  DEGC        Q=  4111   QL= 24,72
X=  47,2     NU=  50,85
RE=  3527    PR=  57,1     M= 1,67    GR= 841049
TPO= 58,48   TPI= 58,36    TX= 42,79  DEGC        Q=  4080   QL= 24,57
X=  48,2     NU=  92,03
RE=  3529    PR=  57,0     M= 1,33    GR= 465156
TPO= 51,53   TPI= 51,41    TX= 42,81  DEGC        Q=  4080   QL= 24,57
X=   0,5     NU= 806,38
RE= 11798    PR=  57,0     M= 1,03    GR=   1418
TPO= 44,89   TPI= 43,79    TX= 42,81  DEGC        Q= 13619   QL= 32,92
X=   1,0     NU= 374,92
RE= 11799    PR=  57,0     M= 1,07    GR=   3051
TPO= 46,02   TPI= 44,92    TX= 42,81  DEGC        Q= 13619   QL= 32,92
X=   2,0     NU= 267,02
RE= 11801    PR=  57,0     M= 1,10    GR=   4352
TPO= 46,94   TPI= 45,82    TX= 42,81  DEGC        Q= 13832   QL= 34,29
X=   3,0     NU= 233,77
RE= 11802    PR=  57,0     M= 1,12    GR=   4991
TPO= 47,39   TPI= 46,27    TX= 42,82  DEGC        Q= 13883   QL= 34,95
X=   4,0     NU= 215,50
RE= 11804    PR=  57,0     M= 1,13    GR=   5419
TPO= 47,69   TPI= 46,56    TX= 42,82  DEGC        Q= 13891   QL= 35,40
X=   5,5     NU= 202,16
RE= 11807    PR=  57,0     M= 1,14    GR=   5782
TPO= 47,95   TPI= 46,82    TX= 42,83  DEGC        Q= 13898   QL= 35,78
X=   7,0     NU= 196,31
RE= 11810    PR=  57,0     M= 1,14    GR=   5960
TPO= 48,07   TPI= 46,95    TX= 42,84  DEGC        Q= 13904   QL= 35,97
X=   8,5     NU= 192,60
RE= 11812    PR=  57,0     M= 1,15    GR=   6077
TPO= 48,16   TPI= 47,03    TX= 42,85  DEGC        Q= 13902   QL= 36,10
X=  10,0     NU= 191,99
RE= 11815    PR=  57,0     M= 1,15    GR=   6100
TPO= 48,18   TPI= 47,06    TX= 42,85  DEGC        Q= 13904   QL= 36,13
X=  12,0     NU= 193,48
RE= 11819    PR=  56,9     M= 1,15    GR=   6058
TPO= 48,16   TPI= 47,03    TX= 42,86  DEGC        Q= 13908   QL= 36,10
X=  15,0     NU= 193,14
RE= 11824    PR=  56,9     M= 1,15    GR=   6074
TPO= 48,18   TPI= 47,06    TX= 42,88  DEGC        Q= 13907   QL= 36,13
X=  20,0     NU= 192,28
RE= 11833    PR=  56,9     M= 1,15    GR=   6111
TPO= 48,22   TPI= 47,10    TX= 42,90  DEGC        Q= 13907   QL= 36,20
X=  25,0     NU= 191,42
RE= 11842    PR=  56,8     M= 1,15    GR=   6148
TPO= 48,27   TPI= 47,14    TX= 42,93  DEGC        Q= 13906   QL= 36,26
X=  40,0     NU= 193,76
RE= 11870    PR=  56,7     M= 1,15    GR=   6103
TPO= 48,29   TPI= 47,16    TX= 43,00  DEGC        Q= 13906   QL= 36,29
X=  97,0     NU= 195,57
RE= 11974    PR=  56,3     M= 1,14    GR=   6155
TPO= 48,52   TPI= 47,40    TX= 43,27  DEGC        Q= 13906   QL= 36,64
X=  99,0     NU= 192,52
RE= 11977    PR=  56,2     M= 1,15    GR=   6193
TPO= 48,55   TPI= 47,43    TX= 43,28  DEGC        Q= 13766   QL= 36,67
X= 100,0     NU= 279,16
RE= 11979    PR=  56,2     M= 1,10    GR=   4272
TPO= 47,26   TPI= 46,15    TX= 43,28  DEGC        Q= 13766   QL= 36,67
```

TEST NO, 6c3.

```
X=   0,0     NU= 7405,95
RE=  228     PR=  58,0     M= 1,00     GR=    552
TPO= 42,28   TPI= 42,27    TX= 42,26  DEGC      Q=  404    QL= 18,51
X=  10,0     NU=    9,39
RE=  230     PR=  57,6     M= 1,32     GR= 442259
TPO= 50,85   TPI= 50,84    TX= 42,50  DEGC      Q=  404    QL= 18,51
X=  30,0     NU=   10,08
RE=  233     PR=  56,8     M= 1,29     GR= 425428
TPO= 50,77   TPI= 50,75    TX= 42,97  DEGC      Q=  404    QL= 18,45
X=  46,2     NU=    8,97
RE=  236     PR=  56,1     M= 1,33     GR= 488547
TPO= 52,09   TPI= 52,07    TX= 43,35  DEGC      Q=  403    QL= 19,39
X=  47,2     NU=    8,85
RE=  236     PR=  56,1     M= 1,31     GR= 466537
TPO= 51,70   TPI= 51,69    TX= 43,38  DEGC      Q=  379    QL= 19,12
X=  48,2     NU=   28,42
RE=  237     PR=  56,0     M= 1,09     GR= 145530
TPO= 46,00   TPI= 45,99    TX= 43,40  DEGC      Q=  379    QL= 19,12
X=   0,5     NU=   64,08
RE=  791     PR=  56,0     M= 1,04     GR=   1732
TPO= 44,65   TPI= 44,55    TX= 43,40  DEGC      Q= 1271    QL= 30,35
X=   1,0     NU=   43,62
RE=  791     PR=  56,0     M= 1,06     GR=   2545
TPO= 45,20   TPI= 45,09    TX= 43,40  DEGC      Q= 1271    QL= 30,35
X=   2,0     NU=   37,53
RE=  791     PR=  56,0     M= 1,07     GR=   3209
TPO= 45,65   TPI= 45,54    TX= 43,41  DEGC      Q= 1379    QL= 31,03
X=   3,0     NU=   33,76
RE=  791     PR=  56,0     M= 1,08     GR=   3623
TPO= 45,93   TPI= 45,82    TX= 43,42  DEGC      Q= 1399    QL= 31,45
X=   4,0     NU=   30,96
RE=  792     PR=  56,0     M= 1,09     GR=   3969
TPO= 46,17   TPI= 46,06    TX= 43,42  DEGC      Q= 1405    QL= 31,80
X=   5,5     NU=   27,42
RE=  792     PR=  56,0     M= 1,10     GR=   4471
TPO= 46,51   TPI= 46,40    TX= 43,44  DEGC      Q= 1401    QL= 32,31
X=   7,0     NU=   25,18
RE=  792     PR=  56,0     M= 1,11     GR=   4877
TPO= 46,79   TPI= 46,68    TX= 43,45  DEGC      Q= 1403    QL= 32,72
X=   8,5     NU=   23,51
RE=  792     PR=  55,9     M= 1,12     GR=   5220
TPO= 47,03   TPI= 46,92    TX= 43,46  DEGC      Q= 1401    QL= 33,07
X=  10,0     NU=   22,53
RE=  793     PR=  55,9     M= 1,13     GR=   5465
TPO= 47,20   TPI= 47,09    TX= 43,47  DEGC      Q= 1404    QL= 33,33
X=  12,0     NU=   21,39
RE=  793     PR=  55,9     M= 1,13     GR=   5771
TPO= 47,41   TPI= 47,30    TX= 43,48  DEGC      Q= 1407    QL= 33,65
X=  15,0     NU=   19,38
RE=  794     PR=  55,9     M= 1,15     GR=   6362
TPO= 47,82   TPI= 47,71    TX= 43,51  DEGC      Q= 1403    QL= 34,25
X=  20,0     NU=   17,31
RE=  795     PR=  55,8     M= 1,17     GR=   7133
TPO= 48,35   TPI= 48,24    TX= 43,54  DEGC      Q= 1402    QL= 35,05
X=  25,0     NU=   16,55
RE=  795     PR=  55,7     M= 1,18     GR=   7484
TPO= 48,61   TPI= 48,50    TX= 43,58  DEGC      Q= 1403    QL= 35,43
X=  40,0     NU=   14,93
RE=  798     PR=  55,6     M= 1,20     GR=   8353
TPO= 49,25   TPI= 49,14    TX= 43,69  DEGC      Q= 1402    QL= 36,38
X=  97,0     NU=   13,61
RE=  809     PR=  54,9     M= 1,22     GR=   9405
TPO= 50,19   TPI= 50,08    TX= 44,11  DEGC      Q= 1400    QL= 37,78
X=  99,0     NU=    9,95
RE=  809     PR=  54,8     M= 1,21     GR=   9044
TPO= 49,94   TPI= 49,86    TX= 44,12  DEGC      Q=  984    QL= 37,40
X= 100,0     NU=   32,56
RE=  810     PR=  54,8     M= 1,06     GR=   2766
TPO= 45,96   TPI= 45,88    TX= 44,12  DEGC      Q=  984    QL= 37,40
```

TEST NO. 11.C3.

```
X=   0.0     NU=  15.24
RE=   209    PR= 343.3    M= 1.91   GR=  18463
TPO= 34.46    TPI= 34.43   TX= 22.13  DEGC      Q=   799   QL=  10.05
X=  10.0     NU=  14.66
RE=   210    PR= 341.6    M= 1.95   GR=  19400
TPO= 35.05    TPI= 35.03   TX= 22.24  DEGC      Q=   799   QL=  10.05
X=  30.0     NU=  14.26
RE=   212    PR= 338.7    M= 1.98   GR=  20381
TPO= 35.62    TPI= 35.59   TX= 22.45  DEGC      Q=   798   QL=  10.46
X=  46.2     NU=  15.10
RE=   214    PR= 335.5    M= 1.91   GR=  19612
TPO= 35.07    TPI= 35.05   TX= 22.62  DEGC      Q=   799   QL=  10.07
X=  47.2     NU=  14.71
RE=   214    PR= 335.3    M= 1.91   GR=  19618
TPO= 35.07    TPI= 35.05   TX= 22.63  DEGC      Q=   778   QL=  10.07
X=  48.2     NU=  23.21
RE=   214    PR= 335.2    M= 1.56   GR=  12452
TPO= 30.54    TPI= 30.51   TX= 22.64  DEGC      Q=   778   QL=  10.07
X=   0.5     NU=  30.52
RE=   716    PR= 335.2    M= 1.40   GR=    255
TPO= 28.87    TPI= 28.66   TX= 22.64  DEGC      Q=  2614   QL=  12.55
X=   1.0     NU=  28.33
RE=   716    PR= 335.1    M= 1.44   GR=    274
TPO= 29.33    TPI= 29.12   TX= 22.64  DEGC      Q=  2614   QL=  12.55
X=   2.0     NU=  27.64
RE=   716    PR= 335.1    M= 1.48   GR=    291
TPO= 29.73    TPI= 29.51   TX= 22.64  DEGC      Q=  2703   QL=  13.14
X=   3.0     NU=  27.00
RE=   716    PR= 335.0    M= 1.50   GR=    301
TPO= 29.98    TPI= 29.76   TX= 22.65  DEGC      Q=  2732   QL=  13.51
X=   4.0     NU=  25.85
RE=   716    PR= 335.0    M= 1.53   GR=    313
TPO= 30.25    TPI= 30.03   TX= 22.65  DEGC      Q=  2714   QL=  13.91
X=   5.5     NU=  25.19
RE=   717    PR= 334.9    M= 1.55   GR=    323
TPO= 30.49    TPI= 30.27   TX= 22.65  DEGC      Q=  2731   QL=  14.27
X=   7.0     NU=  24.17
RE=   717    PR= 334.8    M= 1.57   GR=    335
TPO= 30.78    TPI= 30.56   TX= 22.66  DEGC      Q=  2719   QL=  14.70
X=   8.5     NU=  23.75
RE=   717    PR= 334.8    M= 1.58   GR=    343
TPO= 30.96    TPI= 30.74   TX= 22.66  DEGC      Q=  2730   QL=  14.97
X=  10.0     NU=  23.05
RE=   717    PR= 334.7    M= 1.59   GR=    352
TPO= 31.18    TPI= 30.96   TX= 22.67  DEGC      Q=  2722   QL=  15.30
X=  12.0     NU=  22.58
RE=   717    PR= 334.6    M= 1.61   GR=    361
TPO= 31.39    TPI= 31.17   TX= 22.68  DEGC      Q=  2728   QL=  15.60
X=  15.0     NU=  21.55
RE=   718    PR= 334.4    M= 1.63   GR=    378
TPO= 31.79    TPI= 31.57   TX= 22.68  DEGC      Q=  2724   QL=  16.20
X=  20.0     NU=  20.45
RE=   718    PR= 334.2    M= 1.67   GR=    399
TPO= 32.28    TPI= 32.06   TX= 22.70  DEGC      Q=  2723   QL=  16.93
X=  25.0     NU=  19.97
RE=   719    PR= 333.9    M= 1.68   GR=    409
TPO= 32.53    TPI= 32.31   TX= 22.72  DEGC      Q=  2725   QL=  17.30
X=  40.0     NU=  18.38
RE=   721    PR= 333.2    M= 1.75   GR=    446
TPO= 33.40    TPI= 33.18   TX= 22.76  DEGC      Q=  2723   QL=  18.60
X=  97.0     NU=  15.57
RE=   727    PR= 330.3    M= 1.90   GR=    536
TPO= 35.44    TPI= 35.22   TX= 22.95  DEGC      Q=  2720   QL=  21.64
X=  99.0     NU=  14.34
RE=   728    PR= 330.2    M= 1.89   GR=    535
TPO= 35.40    TPI= 35.20   TX= 22.95  DEGC      Q=  2498   QL=  21.57
X= 100.0     NU=  17.26
RE=   728    PR= 330.1    M= 1.72   GR=    445
TPO= 33.33    TPI= 33.13   TX= 22.96  DEGC      Q=  2498   QL=  21.57
```

TEST NO. 15.C3.

```
X=   0.0    NU= 533.88
RE=  2921   PR= 197.6   M= 1.18   GR=  17998
TPO= 37.17  TPI= 36.92  TX= 33.31  DEGC   Q=  8068   QL= 19.28
X=  10.0    NU= 121.89
RE=  2939   PR= 196.5   M= 2.01   GR=  79802
TPO= 49.53  TPI= 49.28  TX= 33.44  DEGC   Q=  8068   QL= 19.28
X=  30.0    NU=  74.37
RE=  2974   PR= 194.4   M= 2.97   GR= 133905
TPO= 59.91  TPI= 59.66  TX= 33.71  DEGC   Q=  8061   QL= 26.65
X=  46.2    NU=  75.03
RE=  3003   PR= 192.7   M= 2.95   GR= 135405
TPO= 59.91  TPI= 59.66  TX= 33.92  DEGC   Q=  8061   QL= 26.65
X=  47.2    NU=  74.67
RE=  3005   PR= 192.6   M= 2.94   GR= 135505
TPO= 59.91  TPI= 59.66  TX= 33.94  DEGC   Q=  8019   QL= 26.65
X=  48.2    NU= 116.22
RE=  3007   PR= 192.5   M= 2.07   GR=  87169
TPO= 50.72  TPI= 50.48  TX= 33.95  DEGC   Q=  8019.  QL= 26.65
X=   0.5    NU= 945.33
RE= 10052   PR= 192.5   M= 1.10   GR=    288
TPO= 38.17  TPI= 35.99  TX= 33.95  DEGC   Q= 26917   QL= 25.00
X=   1.0    NU= 629.14
RE= 10053   PR= 192.4   M= 1.15   GR=    433
TPO= 39.20  TPI= 37.02  TX= 33.95  DEGC   Q= 26917   QL= 25.00
X=   2.0    NU= 384.24
RE= 10054   PR= 192.4   M= 1.27   GR=    705
TPO= 41.13  TPI= 38.95  TX= 33.96  DEGC   Q= 26789   QL= 27.86
X=   3.0    NU= 322.70
RE= 10056   PR= 192.4   M= 1.33   GR=    843
TPO= 42.11  TPI= 39.93  TX= 33.96  DEGC   Q= 26876   QL= 29.33
X=   4.0    NU= 294.67
RE= 10058   PR= 192.3   M= 1.36   GR=    925
TPO= 42.70  TPI= 40.51  TX= 33.97  DEGC   Q= 26924   QL= 30.20
X=   5.5    NU= 266.44
RE= 10061   PR= 192.3   M= 1.40   GR=   1023
TPO= 43.39  TPI= 41.21  TX= 33.97  DEGC   Q= 26912   QL= 31.24
X=   7.0    NU= 255.30
RE= 10063   PR= 192.3   M= 1.42   GR=   1069
TPO= 43.72  TPI= 41.53  TX= 33.98  DEGC   Q= 26924   QL= 31.72
X=   8.5    NU= 251.30
RE= 10066   PR= 192.2   M= 1.42   GR=   1087
TPO= 43.85  TPI= 41.66  TX= 33.98  DEGC   Q= 26935   QL= 31.91
X=  10.0    NU= 248.65
RE= 10069   PR= 192.2   M= 1.43   GR=   1099
TPO= 43.93  TPI= 41.75  TX= 33.99  DEGC   Q= 26933   QL= 32.04
X=  12.0    NU= 248.98
RE= 10072   PR= 192.1   M= 1.43   GR=   1099
TPO= 43.93  TPI= 41.75  TX= 34.00  DEGC   Q= 26938   QL= 32.04
X=  15.0    NU= 248.66
RE= 10078   PR= 192.0   M= 1.43   GR=   1101
TPO= 43.96  TPI= 41.77  TX= 34.01  DEGC   Q= 26938   QL= 32.08
X=  20.0    NU= 248.62
RE= 10087   PR= 191.8   M= 1.43   GR=   1104
TPO= 43.98  TPI= 41.79  TX= 34.03  DEGC   Q= 26938   QL= 32.11
X=  25.0    NU= 248.57
RE= 10096   PR= 191.7   M= 1.43   GR=   1106
TPO= 44.00  TPI= 41.82  TX= 34.05  DEGC   Q= 26938   QL= 32.14
X=  40.0    NU= 249.12
RE= 10123   PR= 191.2   M= 1.43   GR=   1109
TPO= 44.04  TPI= 41.86  TX= 34.11  DEGC   Q= 26938   QL= 32.21
X=  97.0    NU= 250.23
RE= 10227   PR= 189.4   M= 1.42   GR=   1128
TPO= 44.24  TPI= 42.05  TX= 34.34  DEGC   Q= 26937   QL= 32.50
X=  99.0    NU= 247.62
RE= 10231   PR= 189.4   M= 1.42   GR=   1126
TPO= 44.20  TPI= 42.04  TX= 34.34  DEGC   Q= 26379   QL= 32.43
X= 100.0    NU= 437.11
RE= 10233   PR= 189.3   M= 1.23   GR=    638
TPO= 40.86  TPI= 38.71  TX= 34.35  DEGC   Q= 26379   QL= 32.43
```

TEST NO. 1.D1.

```
X=   0     NU= 886.25
RE= 35624     PR=  55.3     M= 1.05     GR=   2076
TPO= 44.13    TPI= 42.34    TA= 40.93   DEGC        Q= 22103     QL= 38.32
X=  10     NU= 594.16
RE= 35652     PR=  55.3     M= 1.07     GR=   3101
TPO= 44.85    TPI= 43.05    TA= 40.95   DEGC        Q= 22103     QL= 38.32
X=  50     NU= 557.59
RE= 35765     PR=  55.1     M= 1.07     GR=   3326
TPO= 45.09    TPI= 43.29    TA= 41.06   DEGC        Q= 22103     QL= 38.68
X=  95     NU= 553.78
RE= 35894     PR=  54.9     M= 1.07     GR=   3374
TPO= 45.22    TPI= 43.42    TA= 41.17   DEGC        Q= 22103     QL= 38.87
X=  98     NU= 549.86
RE= 35903     PR=  54.9     M= 1.07     GR=   3398
TPO= 45.24    TPI= 43.45    TA= 41.18   DEGC        Q= 22092     QL= 38.91
X= 100     NU= 636.71
RE= 35909     PR=  54.9     M= 1.06     GR=   2936
TPO= 44.93    TPI= 43.14    TA= 41.18   DEGC        Q= 22092     QL= 38.91
X=   0     NU= 740.24
RE= 10738     PR=  54.9     M= 1.05     GR=  92050
TPO= 43.02    TPI= 42.83    TA= 41.18   DEGC        Q=  6440     QL= 16.94
X=   1     NU= 785.79
RE= 10741     PR=  54.9     M= 1.05     GR=  86760
TPO= 42.93    TPI= 42.74    TA= 41.19   DEGC        Q=  6440     QL= 16.94
X=   2     NU= 1249.78
RE= 10744     PR=  54.9     M= 1.03     GR=  54624
TPO= 42.37    TPI= 42.17    TA= 41.20   DEGC        Q=  6446     QL= 16.53
X=   3     NU= 1232.45
RE= 10746     PR=  54.9     M= 1.03     GR=  55412
TPO= 42.39    TPI= 42.19    TA= 41.21   DEGC        Q=  6444     QL= 16.55
X=   4     NU= 902.16
RE= 10749     PR=  54.9     M= 1.04     GR=  75733
TPO= 42.76    TPI= 42.56    TA= 41.22   DEGC        Q=  6444     QL= 16.81
X=   5     NU= 603.69
RE= 10752     PR=  54.9     M= 1.07     GR= 113179
TPO= 43.43    TPI= 43.24    TA= 41.22   DEGC        Q=  6443     QL= 17.29
X=   6     NU= 429.37
RE= 10755     PR=  54.8     M= 1.09     GR= 159221
TPO= 44.26    TPI= 44.06    TA= 41.23   DEGC        Q=  6441     QL= 17.88
X=  10     NU= 244.82
RE= 10766     PR=  54.8     M= 1.17     GR= 279781
TPO= 46.43    TPI= 46.23    TA= 41.27   DEGC        Q=  6440     QL= 19.42
X= 16.7    NU= 193.81
RE= 10780     PR=  54.7     M= 1.22     GR= 354310
TPO= 47.78    TPI= 47.58    TA= 41.31   DEGC        Q=  6439     QL= 20.38
X=  25     NU= 188.58
RE= 10808     PR=  54.6     M= 1.23     GR= 366070
TPO= 48.03    TPI= 47.84    TA= 41.39   DEGC        Q=  6439     QL= 20.56
X=  40     NU= 190.99
RE= 10850     PR=  54.4     M= 1.23     GR= 364338
TPO= 48.07    TPI= 47.88    TA= 41.51   DEGC        Q=  6439     QL= 20.59
X=  46     NU= 202.81
RE= 10866     PR=  54.3     M= 1.21     GR= 344227
TPO= 47.75    TPI= 47.56    TA= 41.56   DEGC        Q=  6440     QL= 20.36
X=  47     NU= 192.61
RE= 10869     PR=  54.3     M= 1.23     GR= 362375
TPO= 48.07    TPI= 47.88    TA= 41.57   DEGC        Q=  6435     QL= 20.59
X=  48     NU= 218.06
RE= 10872     PR=  54.3     M= 1.20     GR= 320263
TPO= 47.35    TPI= 47.15    TA= 41.58   DEGC        Q=  6435     QL= 20.59
```

TEST NO. 8D1.

```
X=   0    NU= 560,06
RE= 12817     PR=  54,9     M= 1,02    GR=   1105
TPO= 42,50    TPI= 41,91    TX= 41,17  DEGC          Q=   7320    QL=  30,38
X=  10    NU= 226,67
RE= 12826     PR=  54,9     M= 1,06    GR=   2734
TPO= 43,61    TPI= 43,02    TX= 41,19  DEGC          Q=   7320    QL=  30,38
X=  50    NU= 224,88
RE= 12864     PR=  54,8     M= 1,06    GR=   2772
TPO= 43,72    TPI= 43,12    TX= 41,29  DEGC          Q=   7320    QL=  30,54
X=  95    NU= 219,44
RE= 12907     PR=  54,6     M= 1,06    GR=   2861
TPO= 43,87    TPI= 43,28    TX= 41,39  DEGC          Q=   7320    QL=  30,76
X=  98    NU= 215,27
RE= 12910     PR=  54,6     M= 1,06    GR=   2917
TPO= 43,91    TPI= 43,32    TX= 41,40  DEGC          Q=   7320    QL=  30,83
X=  10    NU= 218,96
RE= 12827     PR=  54,9     M= 1,06    GR=   2830
TPO= 43,67    TPI= 43,08    TX= 41,19  DEGC          Q=   7320    QL=  30,83
X=   0    NU= 330,18
RE=  3836     PR=  54,9     M= 1,04    GR=  68405
TPO= 42,48    TPI= 42,41    TX= 41,19  DEGC          Q=   2133    QL=  13,76
X=   1    NU= 310,03
RE=  3837     PR=  54,9     M= 1,04    GR=  72888
TPO= 42,57    TPI= 42,50    TX= 41,20  DEGC          Q=   2133    QL=  13,76
X=   2    NU= 459,58
RE=  3837     PR=  54,9     M= 1,03    GR=  49299
TPO= 42,15    TPI= 42,09    TX= 41,21  DEGC          Q=   2138    QL=  13,47
X=   3    NU= 452,17
RE=  3838     PR=  54,9     M= 1,03    GR=  50115
TPO= 42,17    TPI= 42,11    TX= 41,22  DEGC          Q=   2137    QL=  13,48
X=   4    NU= 339,22
RE=  3839     PR=  54,9     M= 1,04    GR=  66812
TPO= 42,48    TPI= 42,41    TX= 41,22  DEGC          Q=   2136    QL=  13,70
X=   5    NU= 242,97
RE=  3840     PR=  54,8     M= 1,05    GR=  93301
TPO= 42,96    TPI= 42,89    TX= 41,23  DEGC          Q=   2136    QL=  14,04
X=   6    NU= 178,27
RE=  3841     PR=  54,8     M= 1,07    GR= 127155
TPO= 43,57    TPI= 43,50    TX= 41,24  DEGC          Q=   2135    QL=  14,47
X=  10    NU=  96,20
RE=  3845     PR=  54,8     M= 1,14    GR= 235941
TPO= 45,52    TPI= 45,46    TX= 41,27  DEGC          Q=   2133    QL=  15,86
X= 167    NU=  67,86
RE=  3849     PR=  54,7     M= 1,21    GR= 335089
TPO= 47,30    TPI= 47,24    TX= 41,31  DEGC          Q=   2132    QL=  17,13
X=  25    NU=  58,30
RE=  3859     PR=  54,6     M= 1,25    GR= 391887
TPO= 48,35    TPI= 48,29    TX= 41,38  DEGC          Q=   2131    QL=  17,87
X=  40    NU=  61,22
RE=  3873     PR=  54,4     M= 1,24    GR= 375974
TPO= 48,14    TPI= 48,07    TX= 41,50  DEGC          Q=   2132    QL=  17,72
X=  46    NU=  64,19
RE=  3878     PR=  54,3     M= 1,23    GR= 359723
TPO= 47,88    TPI= 47,82    TX= 41,55  DEGC          Q=   2132    QL=  17,54
X=  47    NU=  63,09
RE=  3879     PR=  54,3     M= 1,23    GR= 365603
TPO= 47,99    TPI= 47,92    TX= 41,55  DEGC          Q=   2129    QL=  17,61
X=  48    NU=  70,26
RE=  3880     PR=  54,3     M= 1,20    GR= 328477
TPO= 47,35    TPI= 47,28    TX= 41,56  DEGC          Q=   2129    QL=  17,61
```

TEST NO. 16D1.

```
X=   0    NU= -16.35
 RE=   821     PR=  55.0     M= 0.93     GR=  -3372
 TPO= 38.92     TPI= 38.87     TX= 41.12  DEGC         Q=     654     QL=  26.84
 X=  10     NU=  40.08
 RE=   822     PR=  55.0     M= 1.03     GR=   1379
 TPO= 42.13     TPI= 42.08     TX= 41.16  DEGC         Q=     654     QL=  26.84
 X=  50     NU=  14.97
 RE=   825     PR=  54.8     M= 1.08     GR=   3719
 TPO= 43.80     TPI= 43.75     TX= 41.29  DEGC         Q=     653     QL=  29.33
 X=  95     NU=  12.60
 RE=   829     PR=  54.5     M= 1.10     GR=   4455
 TPO= 44.41     TPI= 44.36     TX= 41.44  DEGC         Q=     653     QL=  30.23
 X=  98     NU=  12.13
 RE=   829     PR=  54.5     M= 1.10     GR=   4544
 TPO= 44.48     TPI= 44.43     TX= 41.45  DEGC         Q=     641     QL=  30.33
 X= 100     NU=  13.65
 RE=   829     PR=  54.5     M= 1.09     GR=   4039
 TPO= 44.15     TPI= 44.10     TX= 41.45  DEGC         Q=     641     QL=  30.33
 X=   0     NU=  15.55
 RE=   248     PR=  54.5     M= 1.07     GR= 115216
 TPO= 43.48     TPI= 43.47     TX= 41.45  DEGC         Q=     166     QL=  15.44
 X=   1     NU=   7.21
 RE=   248     PR=  54.5     M= 1.15     GR= 248689
 TPO= 45.83     TPI= 45.82     TX= 41.46  DEGC         Q=     166     QL=  15.44
 X=   2     NU=  12.34
 RE=   248     PR=  54.5     M= 1.10     GR= 165096
 TPO= 44.37     TPI= 44.36     TX= 41.47  DEGC         Q=     189     QL=  14.40
 X=   3     NU=  15.66
 RE=   248     PR=  54.4     M= 1.08     GR= 131072
 TPO= 43.78     TPI= 43.78     TX= 41.48  DEGC         Q=     190     QL=  13.99
 X=   4     NU=  12.62
 RE=   248     PR=  54.4     M= 1.09     GR= 157908
 TPO= 44.26     TPI= 44.26     TX= 41.49  DEGC         Q=     185     QL=  14.33
 X=   5     NU=  11.09
 RE=   248     PR=  54.4     M= 1.11     GR= 179804
 TPO= 44.65     TPI= 44.65     TX= 41.50  DEGC         Q=     185     QL=  14.60
 X=   6     NU=   9.95
 RE=   248     PR=  54.4     M= 1.12     GR= 199243
 TPO= 45.00     TPI= 44.99     TX= 41.51  DEGC         Q=     183     QL=  14.85
 X=   7     NU=   9.73
 RE=   248     PR=  54.4     M= 1.12     GR= 206250
 TPO= 45.13     TPI= 45.13     TX= 41.52  DEGC         Q=     185     QL=  14.94
 X=   8     NU=   8.67
 RE=   249     PR=  54.4     M= 1.13     GR= 226983
 TPO= 45.50     TPI= 45.49     TX= 41.53  DEGC         Q=     182     QL=  15.21
 X=   9     NU=   9.10
 RE=   249     PR=  54.3     M= 1.13     GR= 220304
 TPO= 45.39     TPI= 45.39     TX= 41.54  DEGC         Q=     185     QL=  15.13
 X=  10     NU=   8.82
 RE=   249     PR=  54.3     M= 1.13     GR= 226097
 TPO= 45.50     TPI= 45.49     TX= 41.55  DEGC         Q=     184     QL=  15.21
 X= 167     NU=   8.65
 RE=   249     PR=  54.3     M= 1.14     GR= 231389
 TPO= 45.63     TPI= 45.63     TX= 41.61  DEGC         Q=     184     QL=  15.30
 X=  25     NU=   9.88
 RE=   250     PR=  54.1     M= 1.12     GR= 204270
 TPO= 45.24     TPI= 45.23     TX= 41.71  DEGC         Q=     184     QL=  15.02
 X=  40     NU=  10.34
 RE=   251     PR=  53.8     M= 1.11     GR= 197250
 TPO= 45.24     TPI= 45.23     TX= 41.86  DEGC         Q=     184     QL=  15.02
 X=  46     NU=   6.42
 RE=   252     PR=  53.7     M= 1.19     GR= 314540
 TPO= 47.28     TPI= 47.28     TX= 41.93  DEGC         Q=     182     QL=  16.47
 X=  47     NU=   6.01
 RE=   252     PR=  53.7     M= 1.18     GR= 297857
 TPO= 47.01     TPI= 47.00     TX= 41.93  DEGC         Q=     161     QL=  16.28
 X=  48     NU= -39.02
 RE=   252     PR=  53.7     M= 0.98     GR= -45867
 TPO= 41.17     TPI= 41.16     TX= 41.94  DEGC         Q=     161     QL=  16.28
```

TEST NO. 26D1.

```
X=   0    NU=-157,16
RE=  1212    PR=  54,9    M= 0,97    GR=  -1392
TPO= 40,47    TPI= 40,26    TA= 41,19  DEGC    Q=  2584    QL=  36,49
X=  10    NU=  30,86
RE=  1215    PR=  54,8    M= 1,16    GR=   7129
TPO= 46,21    TPI= 46,01    TA= 41,28  DEGC    Q=  2584    QL=  36,49
X=  50    NU=  16,55
RE=  1228    PR=  54,2    M= 1,33    GR=  13572
TPO= 50,64    TPI= 50,43    TA= 41,63  DEGC    Q=  2580    QL=  43,07
X=  95    NU=  16,00
RE=  1244    PR=  53,6    M= 1,35    GR=  14403
TPO= 51,34    TPI= 51,13    TA= 42,03  DEGC    Q=  2580    QL=  44,12
X=  98    NU=  15,44
RE=  1245    PR=  53,5    M= 1,35    GR=  14728
TPO= 51,55    TPI= 51,35    TA= 42,05  DEGC    Q=  2542    QL=  44,43
X= 100    NU=  17,34
RE=  1245    PR=  53,5    M= 1,31    GR=  13131
TPO= 50,55    TPI= 50,35    TX= 42,07  DEGC    Q=  2542    QL=  44,43
X=   0    NU=  23,91
RE=   372    PR=  53,5    M= 1,21    GR= 345955
TPO= 47,93    TPI= 47,90    TA= 42,07  DEGC    Q=   738    QL=  19,35
X=   1    NU=  20,48
RE=   373    PR=  53,5    M= 1,25    GR= 404637
TPO= 48,93    TPI= 48,91    TA= 42,10  DEGC    Q=   738    QL=  19,35
X=   2    NU=  20,78
RE=   373    PR=  53,4    M= 1,25    GR= 399875
TPO= 48,87    TPI= 48,84    TA= 42,13  DEGC    Q=   739    QL=  19,30
X=   3    NU=  24,64
RE=   373    PR=  53,4    M= 1,20    GR= 340244
TPO= 47,88    TPI= 47,86    TA= 42,15  DEGC    Q=   744    QL=  18,60
X=   4    NU=  29,59
RE=   374    PR=  53,3    M= 1,16    GR= 281694
TPO= 46,92    TPI= 46,90    TA= 42,18  DEGC    Q=   739    QL=  17,92
X=   5    NU=  59,17
RE=   374    PR=  53,3    M= 1,08    GR= 143502
TPO= 44,63    TPI= 44,61    TA= 42,21  DEGC    Q=   751    QL=  16,29
X=   6    NU= 128,37
RE=   374    PR=  53,3    M= 1,04    GR=  66466
TPO= 43,37    TPI= 43,35    TA= 42,24  DEGC    Q=   753    QL=  15,40
X=   7    NU= 123,64
RE=   375    PR=  53,2    M= 1,04    GR=  68800
TPO= 43,43    TPI= 43,41    TA= 42,27  DEGC    Q=   750    QL=  15,44
X=   8    NU=  81,84
RE=   375    PR=  53,2    M= 1,06    GR= 103845
TPO= 44,04    TPI= 44,02    TA= 42,30  DEGC    Q=   748    QL=  15,88
X=   9    NU=  56,94
RE=   375    PR=  53,1    M= 1,08    GR= 149498
TPO= 44,83    TPI= 44,80    TA= 42,32  DEGC    Q=   747    QL=  16,43
X=  10    NU=  40,23
RE=   376    PR=  53,1    M= 1,12    GR= 211077
TPO= 45,87    TPI= 45,85    TA= 42,35  DEGC    Q=   744    QL=  17,17
X= 167    NU=  30,32
RE=   377    PR=  52,9    M= 1,16    GR= 282731
TPO= 47,16    TPI= 47,15    TA= 42,49  DEGC    Q=   745    QL=  18,09
X=  25    NU=  26,97
RE=   381    PR=  52,4    M= 1,19    GR= 323492
TPO= 48,01    TPI= 47,99    TA= 42,77  DEGC    Q=   744    QL=  18,70
X=  40    NU=  27,74
RE=   386    PR=  51,8    M= 1,18    GR= 323207
TPO= 48,29    TPI= 48,27    TA= 43,20  DEGC    Q=   744    QL=  18,89
X=  46    NU=  18,90
RE=   388    PR=  51,5    M= 1,28    GR= 478288
TPO= 50,81    TPI= 50,79    TA= 43,37  DEGC    Q=   742    QL=  20,68
X=  47    NU=  18,13
RE=   388    PR=  51,5    M= 1,28    GR= 489747
TPO= 51,00    TPI= 50,98    TA= 43,39  DEGC    Q=   727    QL=  20,82
X=  48    NU=  33,75
RE=   389    PR=  51,4    M= 1,14    GR= 263523
TPO= 47,52    TPI= 47,50    TA= 43,42  DEGC    Q=   727    QL=  20,82
```

TEST NO, 38.D1.

```
X=   0   NU= 198.92
RE=  2076   PR= 499.3   M= 1.09   GR=   30
TPO= 24.99   TPI= 24.68   TX= 23.21  DEGC   Q=  3776   QL= 10.85
X=  10   NU=  64.12
RE=  2077   PR= 499.0   M= 1.32   GR=   92
TPO= 28.09   TPI= 27.78   TX= 23.22  DEGC   Q=  3776   QL= 10.85
X=  50   NU=  36.65
RE=  2082   PR= 497.8   M= 1.62   GR=  161
TPO= 31.54   TPI= 31.24   TX= 23.27  DEGC   Q=  3772   QL= 15.99
X=  95   NU=  29.13
RE=  2088   PR= 496.5   M= 1.79   GR=  204
TPO= 33.64   TPI= 33.34   TX= 23.32  DEGC   Q=  3769   QL= 19.11
X=  98   NU=  28.80
RE=  2089   PR= 496.4   M= 1.80   GR=  205
TPO= 33.71   TPI= 33.41   TX= 23.32  DEGC   Q=  3751   QL= 19.21
X= 100   NU=  30.35
RE=  2089   PR= 496.4   M= 1.75   GR=  195
TPO= 33.20   TPI= 32.89   TX= 23.33  DEGC   Q=  3751   QL= 19.21
X=   0   NU=  29.89
RE=   625   PR= 496.4   M= 1.75   GR= 7260
TPO= 32.88   TPI= 32.85   TX= 23.33  DEGC   Q=  1100   QL=  7.19
X=   1   NU=  37.68
RE=   625   PR= 496.3   M= 1.59   GR= 5760
TPO= 30.92   TPI= 30.88   TX= 23.33  DEGC   Q=  1100   QL=  7.19
X=   2   NU=  49.11
RE=   625   PR= 496.2   M= 1.44   GR= 4433
TPO= 29.18   TPI= 29.14   TX= 23.33  DEGC   Q=  1102   QL=  5.95
X=   3   NU=  61.51
RE=   625   PR= 496.1   M= 1.33   GR= 3534
TPO= 28.00   TPI= 27.97   TX= 23.34  DEGC   Q=  1100   QL=  5.12
X=   4   NU=  86.15
RE=   625   PR= 496.0   M= 1.22   GR= 2531
TPO= 26.69   TPI= 26.66   TX= 23.34  DEGC   Q=  1103   QL=  4.18
X=   5   NU= 123.77
RE=   625   PR= 495.9   M= 1.14   GR= 1762
TPO= 25.69   TPI= 25.65   TX= 23.34  DEGC   Q=  1103   QL=  3.47
X=   6   NU= 194.07
RE=   625   PR= 495.8   M= 1.09   GR= 1125
TPO= 24.85   TPI= 24.82   TX= 23.35  DEGC   Q=  1103   QL=  2.88
X=   7   NU= 382.83
RE=   626   PR= 495.7   M= 1.04   GR=  573
TPO= 24.13   TPI= 24.10   TX= 23.35  DEGC   Q=  1107   QL=  2.37
X=   8   NU= 317.02
RE=   626   PR= 495.6   M= 1.05   GR=  690
TPO= 24.29   TPI= 24.26   TX= 23.36  DEGC   Q=  1105   QL=  2.48
X=   9   NU= 192.61
RE=   626   PR= 495.5   M= 1.09   GR= 1135
TPO= 24.88   TPI= 24.84   TX= 23.36  DEGC   Q=  1104   QL=  2.90
X=  10   NU= 128.44
RE=   626   PR= 495.4   M= 1.14   GR= 1700
TPO= 25.62   TPI= 25.58   TX= 23.36  DEGC   Q=  1102   QL=  3.42
X=  17   NU=  51.24
RE=   627   PR= 494.8   M= 1.41   GR= 4266
TPO= 28.98   TPI= 28.94   TX= 23.39  DEGC   Q=  1100   QL=  5.81
X=  25   NU=  37.09
RE=   628   PR= 494.0   M= 1.60   GR= 5906
TPO= 31.12   TPI= 31.08   TX= 23.42  DEGC   Q=  1098   QL=  7.33
X=  40   NU=  29.38
RE=   630   PR= 492.5   M= 1.76   GR= 7495
TPO= 33.17   TPI= 33.14   TX= 23.47  DEGC   Q=  1097   QL=  8.79
X=  46   NU=  27.05
RE=   631   PR= 492.0   M= 1.83   GR= 8156
TPO= 34.02   TPI= 33.99   TX= 23.50  DEGC   Q=  1096   QL=  9.39
X=  47   NU=  26.86
RE=   631   PR= 491.9   M= 1.84   GR= 8208
TPO= 34.09   TPI= 34.05   TX= 23.50  DEGC   Q=  1095   QL=  9.44
X=  48   NU=  27.62
RE=   631   PR= 491.8   M= 1.81   GR= 7984
TPO= 33.80   TPI= 33.77   TX= 23.50  DEGC   Q=  1095   QL=  9.44
```

TEST NO. 41.D/.

```
X=   0    NU= 177.16
RE=   883    PR= 498.1    M= 1.04    GR=    12
TPO= 23.98    TPI= 23.87    TX= 23.26  DEGC    Q=  1389    QL=   6.56
X=  10    NU=  46.18
RE=   884    PR= 497.9    M= 1.15    GR=    47
TPO= 25.71    TPI= 25.60    TX= 23.27  DEGC    Q=  1389    QL=   6.56
X=  50    NU=  26.52
RE=   885    PR= 496.9    M= 1.28    GR=    82
TPO= 27.47    TPI= 27.35    TX= 23.31  DEGC    Q=  1387    QL=   9.18
X=  95    NU=  21.34
RE=   888    PR= 495.7    M= 1.36    GR=   103
TPO= 28.49    TPI= 28.38    TX= 23.35  DEGC    Q=  1385    QL=  10.70
X=  98    NU=  20.96
RE=   888    PR= 495.6    M= 1.37    GR=   104
TPO= 28.53    TPI= 28.42    TX= 23.35  DEGC    Q=  1372    QL=  10.77
X= 100    NU=  22.65
RE=   888    PR= 495.6    M= 1.33    GR=    96
TPO= 28.16    TPI= 28.04    TX= 23.36  DEGC    Q=  1372    QL=  10.77
X=   0    NU=  23.61
RE=   266    PR= 495.6    M= 1.30    GR=  3339
TPO= 27.73    TPI= 27.72    TX= 23.36  DEGC    Q=   398    QL=   4.81
X=   1    NU=  21.95
RE=   266    PR= 495.5    M= 1.33    GR=  3593
TPO= 28.07    TPI= 28.05    TX= 23.36  DEGC    Q=   398    QL=   4.81
X=   2    NU=  25.21
RE=   266    PR= 495.4    M= 1.28    GR=  3150
TPO= 27.49    TPI= 27.48    TX= 23.36  DEGC    Q=   401    QL=   4.40
X=   3    NU=  33.78
RE=   266    PR= 495.3    M= 1.20    GR=  2365
TPO= 26.47    TPI= 26.45    TX= 23.37  DEGC    Q=   403    QL=   3.67
X=   4    NU=  53.40
RE=   266    PR= 495.2    M= 1.12    GR=  1507
TPO= 25.35    TPI= 25.34    TX= 23.37  DEGC    Q=   406    QL=   2.88
X=   5    NU=  89.28
RE=   266    PR= 495.2    M= 1.07    GR=   902
TPO= 24.56    TPI= 24.55    TX= 23.37  DEGC    Q=   406    QL=   2.32
X=   6    NU= 160.24
RE=   266    PR= 495.1    M= 1.04    GR=   504
TPO= 24.04    TPI= 24.03    TX= 23.38  DEGC    Q=   407    QL=   1.95
X=   7    NU= 212.03
RE=   266    PR= 495.0    M= 1.03    GR=   381
TPO= 23.89    TPI= 23.88    TX= 23.38  DEGC    Q=   407    QL=   1.84
X=   8    NU= 156.17
RE=   266    PR= 494.9    M= 1.04    GR=   517
TPO= 24.07    TPI= 24.06    TX= 23.38  DEGC    Q=   406    QL=   1.97
X=   9    NU=  97.58
RE=   266    PR= 494.8    M= 1.06    GR=   825
TPO= 24.47    TPI= 24.46    TX= 23.38  DEGC    Q=   405    QL=   2.25
X=  10    NU=  68.81
RE=   266    PR= 494.7    M= 1.09    GR=  1168
TPO= 24.92    TPI= 24.91    TX= 23.39  DEGC    Q=   404    QL=   2.57
X=  17    NU=  33.80
RE=   266    PR= 494.2    M= 1.20    GR=  2378
TPO= 26.51    TPI= 26.50    TX= 23.41  DEGC    Q=   403    QL=   3.70
X=  25    NU=  26.09
RF=   267    PR= 493.5    M= 1.27    GR=  3085
TPO= 27.44    TPI= 27.43    TX= 23.44  DEGC    Q=   403    QL=   4.37
X=  40    NU=  18.67
RE=   267    PR= 492.3    M= 1.42    GR=  4324
TPO= 29.07    TPI= 29.05    TX= 23.48  DEGC    Q=   402    QL=   5.52
X=  46    NU=  11.77
RE=   268    PR= 491.8    M= 1.68    GR=  6818
TPO= 32.28    TPI= 32.27    TX= 23.50  DEGC    Q=   399    QL=   7.80
X=  47    NU=  11.56
RE=   268    PR= 491.7    M= 1.68    GR=  6801
TPO= 32.26    TPI= 32.25    TX= 23.51  DEGC    Q=   390    QL=   7.79
X=  48    NU=  15.75
RE=   268    PR= 491.6    M= 1.50    GR=  4992
TPO= 29.93    TPI= 29.92    TX= 23.51  DEGC    Q=   390    QL=   7.79
```

TEST NO. 1.D2.

```
X=   0.0   NU= 578.42
RE= 27852   PR=  57.6   M= 1.08   GR=  11013
TPO= 44.11   TPI= 43.30   TX= 40.93  DEGC   Q= 16073   QL= 27.60
X=  10.0   NU= 458.96
RE= 27882   PR=  57.5   M= 1.10   GR=  13910
TPO= 44.76   TPI= 43.95   TX= 40.96  DEGC   Q= 16073   QL= 27.60
X=  50.0   NU= 450.16
RE= 28002   PR=  57.3   M= 1.10   GR=  14306
TPO= 44.96   TPI= 44.15   TX= 41.10  DEGC   Q= 16073   QL= 27.81
X=  87.0   NU= 449.64
RE= 28113   PR=  57.1   M= 1.10   GR=  14439
TPO= 45.09   TPI= 44.28   TX= 41.23  DEGC   Q= 16073   QL= 27.96
X=  89.0   NU= 450.41
RE= 28119   PR=  57.1   M= 1.10   GR=  14415
TPO= 45.09   TPI= 44.28   TX= 41.23  DEGC   Q= 16066   QL= 27.96
X=  90.0   NU= 493.18
RE= 28122   PR=  57.1   M= 1.09   GR=  13168
TPO= 44.83   TPI= 44.02   TX= 41.24  DEGC   Q= 16066   QL= 27.96
X=   0.0   NU= 588.15
RE= 14122   PR=  57.1   M= 1.08   GR=  95688
TPO= 44.02   TPI= 43.80   TX= 41.24  DEGC   Q=  8853   QL= 17.53
X=   1.0   NU= 840.21
RE= 14125   PR=  57.1   M= 1.06   GR=  67015
TPO= 43.26   TPI= 43.04   TX= 41.24  DEGC   Q=  8853   QL= 17.53
X=   2.0   NU= 922.20
RE= 14128   PR=  57.0   M= 1.05   GR=  61077
TPO= 43.11   TPI= 42.89   TX= 41.25  DEGC   Q=  8852   QL= 17.41
X=   3.0   NU= 836.88
RE= 14132   PR=  57.0   M= 1.06   GR=  67334
TPO= 43.28   TPI= 43.06   TX= 41.26  DEGC   Q=  8852   QL= 17.54
X=   4.0   NU= 669.67
RE= 14135   PR=  57.0   M= 1.07   GR=  84175
TPO= 43.74   TPI= 43.52   TX= 41.27  DEGC   Q=  8851   QL= 17.88
X=   5.5   NU= 488.03
RE= 14140   PR=  57.0   M= 1.10   GR= 115574
TPO= 44.59   TPI= 44.36   TX= 41.28  DEGC   Q=  8850   QL= 18.51
X=   7.0   NU= 377.60
RE= 14145   PR=  57.0   M= 1.14   GR= 149462
TPO= 45.50   TPI= 45.28   TX= 41.29  DEGC   Q=  8848   QL= 19.19
X=   8.5   NU= 318.10
RE= 14150   PR=  57.0   M= 1.16   GR= 177533
TPO= 46.26   TPI= 46.03   TX= 41.30  DEGC   Q=  8848   QL= 19.76
X=  10.0   NU= 286.77
RE= 14155   PR=  56.9   M= 1.18   GR= 195706
TPO= 46.75   TPI= 46.53   TX= 41.31  DEGC   Q=  8848   QL= 20.12
X=  11.5   NU= 268.41
RE= 14160   PR=  56.9   M= 1.20   GR= 210692
TPO= 47.16   TPI= 46.93   TX= 41.32  DEGC   Q=  8847   QL= 20.42
X=  13.0   NU= 256.21
RE= 14165   PR=  56.9   M= 1.21   GR= 220873
TPO= 47.43   TPI= 47.21   TX= 41.33  DEGC   Q=  8847   QL= 20.63
X=  15.0   NU= 248.70
RE= 14172   PR=  56.9   M= 1.22   GR= 227764
TPO= 47.63   TPI= 47.40   TX= 41.35  DEGC   Q=  8847   QL= 20.77
X=  20.0   NU= 244.17
RE= 14188   PR=  56.8   M= 1.22   GR= 232543
TPO= 47.78   TPI= 47.55   TX= 41.39  DEGC   Q=  8847   QL= 20.89
X=  25.0   NU= 242.28
RE= 14205   PR=  56.8   M= 1.22   GR= 234917
TPO= 47.86   TPI= 47.64   TX= 41.42  DEGC   Q=  8847   QL= 20.95
X=  40.0   NU= 249.38
RE= 14255   PR=  56.6   M= 1.22   GR= 229883
TPO= 47.80   TPI= 47.57   TX= 41.54  DEGC   Q=  8847   QL= 20.90
X=  48.0   NU= 255.54
RE= 14282   PR=  56.5   M= 1.21   GR= 225203
TPO= 47.71   TPI= 47.49   TX= 41.60  DEGC   Q=  8847   QL= 20.84
X=  49.0   NU= 252.21
RE= 14285   PR=  56.5   M= 1.21   GR= 228296
TPO= 47.80   TPI= 47.57   TX= 41.60  DEGC   Q=  8847   QL= 20.90
X=  50.0   NU= 245.40
RE= 14288   PR=  56.5   M= 1.22   GR= 234664
TPO= 47.97   TPI= 47.74   TX= 41.61  DEGC   Q=  8847   QL= 20.90
```

TEST NO. 6.D2.

```
X=    0,0    NU=-2277,92
RE=  4104     PR=  57,4     M= 1,00    GR=   -320
TPO= 41,06     TPI= 40,97     TX= 41,04  DEGC        Q=   1826     QL=  25,26
X=   10,0    NU=  74,87
RE=  4108     PR=  57,4     M= 1,07    GR=   9752
TPO= 43,24     TPI= 43,15     TX= 41,06  DEGC        Q=   1826     QL=  25,26
X=   50,0    NU=  75,58
RE=  4122     PR=  57,2     M= 1,07    GR=   9728
TPO= 43,33     TPI= 43,24     TX= 41,17  DEGC        Q=   1827     QL=  25,36
X=   87,0    NU=  74,41
RE=  4134     PR=  57,0     M= 1,07    GR=   9943
TPO= 43,46     TPI= 43,37     TX= 41,27  DEGC        Q=   1827     QL=  25,50
X=   89,0    NU=  74,37
RE=  4135     PR=  57,0     M= 1,07    GR=   9922
TPO= 43,46     TPI= 43,37     TX= 41,27  DEGC        Q=   1821     QL=  25,50
X=   90,0    NU=  82,16
RE=  4135     PR=  57,0     M= 1,06    GR=   8983
TPO= 43,26     TPI= 43,17     TX= 41,28  DEGC        Q=   1821     QL=  25,50
X=    0,0    NU= 109,76
RE=  2077     PR=  57,0     M= 1,05    GR=  58725
TPO= 42,87     TPI= 42,84     TX= 41,28  DEGC        Q=   1011     QL=  16,01
X=    1,0    NU= 332,41
RE=  2077     PR=  57,0     M= 1,02    GR=  19398
TPO= 41,83     TPI= 41,80     TX= 41,28  DEGC        Q=   1011     QL=  16,01
X=    2,0    NU= 296,55
RE=  2077     PR=  57,0     M= 1,02    GR=  21650
TPO= 41,89     TPI= 41,87     TX= 41,29  DEGC        Q=   1007     QL=  16,06
X=    3,0    NU= 222,93
RE=  2078     PR=  57,0     M= 1,02    GR=  28799
TPO= 42,09     TPI= 42,06     TX= 41,29  DEGC        Q=   1006     QL=  16,21
X=    4,0    NU= 163,78
RE=  2078     PR=  57,0     M= 1,03    GR=  39194
TPO= 42,37     TPI= 42,34     TX= 41,30  DEGC        Q=   1006     QL=  16,42
X=    5,5    NU= 114,61
RE=  2079     PR=  57,0     M= 1,05    GR=  56023
TPO= 42,83     TPI= 42,80     TX= 41,31  DEGC        Q=   1005     QL=  16,76
X=    7,0    NU=  86,17
RE=  2079     PR=  56,9     M= 1,06    GR=  74504
TPO= 43,33     TPI= 43,30     TX= 41,32  DEGC        Q=   1005     QL=  17,13
X=    8,5    NU=  70,92
RE=  2080     PR=  56,9     M= 1,08    GR=  90555
TPO= 43,76     TPI= 43,74     TX= 41,33  DEGC        Q=   1005     QL=  17,45
X=   10,0    NU=  61,68
RE=  2080     PR=  56,9     M= 1,09    GR= 104172
TPO= 44,13     TPI= 44,11     TX= 41,33  DEGC        Q=   1005     QL=  17,73
X=   11,5    NU=  53,42
RE=  2081     PR=  56,9     M= 1,11    GR= 120257
TPO= 44,57     TPI= 44,54     TX= 41,34  DEGC        Q=   1004     QL=  18,05
X=   13,0    NU=  49,21
RE=  2081     PR=  56,9     M= 1,12    GR= 130632
TPO= 44,85     TPI= 44,82     TX= 41,35  DEGC        Q=   1004     QL=  18,26
X=   15,0    NU=  44,34
RE=  2082     PR=  56,9     M= 1,13    GR= 145030
TPO= 45,24     TPI= 45,21     TX= 41,36  DEGC        Q=   1004     QL=  18,55
X=   20,0    NU=  36,55
RE=  2084     PR=  56,8     M= 1,16    GR= 176144
TPO= 46,09     TPI= 46,06     TX= 41,39  DEGC        Q=   1003     QL=  19,18
X=   25,0    NU=  32,30
RE=  2086     PR=  56,8     M= 1,18    GR= 199632
TPO= 46,73     TPI= 46,70     TX= 41,42  DEGC        Q=   1002     QL=  19,66
X=   40,0    NU=  29,88
RE=  2092     PR=  56,6     M= 1,20    GR= 216957
TPO= 47,24     TPI= 47,22     TX= 41,51  DEGC        Q=   1002     QL=  20,04
X=   48,0    NU=  23,37
RE=  2095     PR=  56,5     M= 1,27    GR= 277803
TPO= 48,87     TPI= 48,84     TX= 41,55  DEGC        Q=   1001     QL=  21,25
X=   49,0    NU=  22,65
RE=  2095     PR=  56,5     M= 1,28    GR= 285032
TPO= 49,06     TPI= 49,03     TX= 41,56  DEGC        Q=    995     QL=  21,39
X=   50,0    NU=  26,45
RE=  2095     PR=  56,5     M= 1,23    GR= 244122
TPO= 47,99     TPI= 47,96     TX= 41,56  DEGC        Q=    995     QL=  21,39
```

TEST NO. 18.D2.

```
X=   0.0    NU=-125.31
RE=   368    PR= 234.5    M= 0.96    GR=   -277
TPO= 33.62    TPI= 33.57    TX= 34.41  DEGC      Q=  931   QL= 19.29
X=  10.0    NU=  28.40
RE=   369    PR= 234.0    M= 1.20    GR=   1226
TPO= 38.22    TPI= 38.17    TX= 34.46  DEGC      Q=  931   QL= 19.29
X=  50.0    NU=  13.69
RE=   372    PR= 232.0    M= 1.44    GR=   2582
TPO= 42.37    TPI= 42.32    TX= 34.66  DEGC      Q=  927   QL= 23.86
X=  87.0    NU=  14.10
RE=   375    PR= 230.2    M= 1.43    GR=   2550
TPO= 42.33    TPI= 42.28    TX= 34.84  DEGC      Q=  928   QL= 23.82
X=  89.0    NU=  13.92
RE=   376    PR= 230.1    M= 1.43    GR=   2564
TPO= 42.37    TPI= 42.32    TX= 34.85  DEGC      Q=  920   QL= 23.86
X=  90.0    NU=  14.44
RE=   376    PR= 230.1    M= 1.41    GR=   2474
TPO= 42.11    TPI= 42.06    TX= 34.85  DEGC      Q=  920   QL= 23.86
X=   0.0    NU=  15.78
RE=   189    PR= 230.1    M= 1.42    GR=  19628
TPO= 42.11    TPI= 42.10    TX= 34.85  DEGC      Q=  507   QL= 16.10
X=   1.0    NU=  15.30
RE=   189    PR= 230.0    M= 1.43    GR=  20268
TPO= 42.35    TPI= 42.34    TX= 34.86  DEGC      Q=  507   QL= 16.10
X=   2.0    NU=  15.37
RE=   189    PR= 229.9    M= 1.43    GR=  20201
TPO= 42.33    TPI= 42.31    TX= 34.87  DEGC      Q=  507   QL= 16.09
X=   3.0    NU=  15.96
RE=   189    PR= 229.8    M= 1.41    GR=  19543
TPO= 42.09    TPI= 42.07    TX= 34.88  DEGC      Q=  509   QL= 15.91
X=   4.0    NU=  16.33
RE=   189    PR= 229.6    M= 1.40    GR=  19119
TPO= 41.93    TPI= 41.92    TX= 34.89  DEGC      Q=  509   QL= 15.80
X=   5.5    NU=  16.75
RE=   189    PR= 229.5    M= 1.39    GR=  18688
TPO= 41.78    TPI= 41.77    TX= 34.91  DEGC      Q=  510   QL= 15.68
X=   7.0    NU=  16.38
RE=   189    PR= 229.3    M= 1.40    GR=  19091
TPO= 41.93    TPI= 41.92    TX= 34.93  DEGC      Q=  508   QL= 15.80
X=   8.5    NU=  16.44
RE=   190    PR= 229.2    M= 1.40    GR=  19077
TPO= 41.93    TPI= 41.92    TX= 34.94  DEGC      Q=  509   QL= 15.80
X=  10.0    NU=  16.37
RE=   190    PR= 229.0    M= 1.40    GR=  19182
TPO= 41.98    TPI= 41.97    TX= 34.96  DEGC      Q=  509   QL= 15.83
X=  11.5    NU=  16.19
RE=   190    PR= 228.8    M= 1.41    GR=  19407
TPO= 42.07    TPI= 42.05    TX= 34.97  DEGC      Q=  509   QL= 15.89
X=  13.0    NU=  16.21
RE=   190    PR= 228.7    M= 1.40    GR=  19393
TPO= 42.07    TPI= 42.05    TX= 34.99  DEGC      Q=  508   QL= 15.89
X=  15.0    NU=  17.69
RE=   190    PR= 228.5    M= 1.37    GR=  17872
TPO= 41.52    TPI= 41.51    TX= 35.01  DEGC      Q=  510   QL= 15.49
X=  20.0    NU=  16.31
RE=   191    PR= 227.9    M= 1.40    GR=  19448
TPO= 42.11    TPI= 42.10    TX= 35.06  DEGC      Q=  509   QL= 15.93
X=  25.0    NU=  16.13
RE=   191    PR= 227.4    M= 1.41    GR=  19763
TPO= 42.24    TPI= 42.23    TX= 35.12  DEGC      Q=  509   QL= 16.02
X=  40.0    NU=  15.81
RE=   193    PR= 225.8    M= 1.41    GR=  20481
TPO= 42.54    TPI= 42.53    TX= 35.27  DEGC      Q=  509   QL= 16.25
X=  48.0    NU=  10.57
RE=   193    PR= 225.0    M= 1.65    GR=  30673
TPO= 46.15    TPI= 46.14    TX= 35.36  DEGC      Q=  505   QL= 18.93
X=  49.0    NU=   9.99
RE=   193    PR= 224.9    M= 1.64    GR=  30311
TPO= 46.02    TPI= 46.01    TX= 35.37  DEGC      Q=  471   QL= 18.84
X=  50.0    NU=  32.76
RE=   194    PR= 224.8    M= 1.18    GR=   9248
TPO= 38.63    TPI= 38.62    TX= 35.38  DEGC      Q=  471   QL= 18.84
```

TEST NO. 20.D2.

```
X=    0.0    NU= 208.70
RE=  2235    PR= 415.2    M= 1.10    GR=   162
TPO= 25.15   TPI= 24.99   TX= 23.28  DEGC   Q= 3210   QL=  9.04
X=   10.0    NU=  76.43
RE=  2237    PR= 414.9    M= 1.32    GR=   444
TPO= 28.11   TPI= 27.95   TX= 23.30  DEGC   Q= 3210   QL=  9.04
X=   30.0    NU=  43.44
RE=  2244    PR= 413.6    M= 1.61    GR=   785
TPO= 31.70   TPI= 31.54   TX= 23.36  DEGC   Q= 3206   QL= 12.99
X=   87.0    NU=  40.82
RE=  2251    PR= 412.4    M= 1.65    GR=   841
TPO= 32.28   TPI= 32.12   TX= 23.41  DEGC   Q= 3206   QL= 13.63
X=   89.0    NU=  41.45
RE=  2251    PR= 412.3    M= 1.64    GR=   825
TPO= 32.12   TPI= 31.96   TX= 23.42  DEGC   Q= 3196   QL= 13.46
X=   90.0    NU=  43.75
RE=  2252    PR= 412.3    M= 1.61    GR=   782
TPO= 31.68   TPI= 31.52   TX= 23.42  DEGC   Q= 3196   QL= 13.46
X=    0.0    NU=  58.10
RE=  1131    PR= 412.3    M= 1.51    GR=  5158
TPO= 30.22   TPI= 30.18   TX= 23.42  DEGC   Q= 1779   QL=  5.35
X=    1.0    NU= 108.43
RE=  1131    PR= 412.2    M= 1.23    GR=  2764
TPO= 27.09   TPI= 27.04   TX= 23.42  DEGC   Q= 1779   QL=  5.35
X=    2.0    NU= 163.59
RE=  1131    PR= 412.1    M= 1.15    GR=  1829
TPO= 25.87   TPI= 25.82   TX= 23.42  DEGC   Q= 1775   QL=  4.44
X=    3.0    NU= 196.82
RE=  1131    PR= 412.1    M= 1.12    GR=  1518
TPO= 25.46   TPI= 25.42   TX= 23.43  DEGC   Q= 1772   QL=  4.14
X=    4.0    NU= 231.26
RE=  1132    PR= 412.0    M= 1.10    GR=  1293
TPO= 25.17   TPI= 25.12   TX= 23.43  DEGC   Q= 1772   QL=  3.92
X=    5.5    NU= 255.82
RE=  1132    PR= 411.9    M= 1.09    GR=  1169
TPO= 25.01   TPI= 24.97   TX= 23.44  DEGC   Q= 1772   QL=  3.80
X=    7.0    NU= 232.73
RE=  1132    PR= 411.8    M= 1.10    GR=  1286
TPO= 25.17   TPI= 25.12   TX= 23.44  DEGC   Q= 1773   QL=  3.92
X=    8.5    NU= 158.76
RE=  1132    PR= 411.7    M= 1.15    GR=  1885
TPO= 25.96   TPI= 25.91   TX= 23.45  DEGC   Q= 1772   QL=  4.50
X=   10.0    NU= 112.23
RE=  1133    PR= 411.6    M= 1.22    GR=  2666
TPO= 26.98   TPI= 26.93   TX= 23.45  DEGC   Q= 1770   QL=  5.27
X=   11.5    NU=  91.83
RE=  1133    PR= 411.5    M= 1.28    GR=  3259
TPO= 27.76   TPI= 27.71   TX= 23.46  DEGC   Q= 1770   QL=  5.84
X=   13.0    NU=  79.09
RE=  1133    PR= 411.4    M= 1.34    GR=  3785
TPO= 28.44   TPI= 28.40   TX= 23.46  DEGC   Q= 1769   QL=  6.36
X=   15.0    NU=  67.07
RE=  1134    PR= 411.2    M= 1.42    GR=  4465
TPO= 29.33   TPI= 29.29   TX= 23.47  DEGC   Q= 1768   QL=  7.02
X=   20.0    NU=  52.50
RE=  1135    PR= 410.9    M= 1.56    GR=  5712
TPO= 30.96   TPI= 30.92   TX= 23.49  DEGC   Q= 1767   QL=  8.23
X=   25.0    NU=  44.88
RE=  1136    PR= 410.5    M= 1.65    GR=  6691
TPO= 32.23   TPI= 32.19   TX= 23.50  DEGC   Q= 1766   QL=  9.18
X=   40.0    NU=  34.95
RE=  1139    PR= 409.5    M= 1.85    GR=  8632
TPO= 34.74   TPI= 34.70   TX= 23.55  DEGC   Q= 1765   QL= 11.04
X=   48.0    NU=  32.29
RE=  1141    PR= 408.9    M= 1.93    GR=  9367
TPO= 35.68   TPI= 35.64   TX= 23.58  DEGC   Q= 1764   QL= 11.74
X=   49.0    NU=  31.86
RE=  1141    PR= 408.8    M= 1.95    GR=  9487
TPO= 35.84   TPI= 35.79   TX= 23.58  DEGC   Q= 1762   QL= 11.86
X=   50.0    NU=  32.45
RE=  1141    PR= 408.8    M= 1.93    GR=  9318
TPO= 35.62   TPI= 35.57   TX= 23.59  DEGC   Q= 1762   QL= 11.86
```

TEST NO.7.D3.

```
X=   0.0       NU= 176.46
RE=  1219       PR= 386.1      M= 1.07      GR=     126
TPO= 24.94      TPI= 24.88      TX= 23.73  DEGC           Q=   1841    QL=   6.60
X=  10.0       NU=  49.88
RE=  1221       PR= 385.7      M= 1.27      GR=     447
TPO= 27.87      TPI= 27.80      TX= 23.75  DEGC           Q=   1841    QL=   6.60
X=  50.0       NU=  27.55
RE=  1225       PR= 384.4      M= 1.54      GR=     814
TPO= 31.21      TPI= 31.14      TX= 23.82  DEGC           Q=   1838    QL=  10.23
X=  87.0       NU=  23.02
RE=  1229       PR= 383.1      M= 1.64      GR=     980
TPO= 32.70      TPI= 32.64      TX= 23.88  DEGC           Q=   1836    QL=  11.85
X=  89.0       NU=  23.10
RE=  1230       PR= 383.1      M= 1.64      GR=     978
TPO= 32.68      TPI= 32.61      TX= 23.88  DEGC           Q=   1837    QL=  11.83
X=  90.0       NU=  22.90
RE=  1230       PR= 383.0      M= 1.64      GR=     983
TPO= 32.73      TPI= 32.66      TX= 23.88  DEGC           Q=   1837    QL=  11.83
X=   0.0       NU=  19.80
RE=   986       PR= 383.0      M= 1.71      GR=    2091
TPO= 33.55      TPI= 33.51      TX= 23.88  DEGC           Q=   1392    QL=  11.44
X=   0.5       NU=  19.22
RE=   986       PR= 383.0      M= 1.73      GR=    2154
TPO= 33.84      TPI= 33.80      TX= 23.89  DEGC           Q=   1392    QL=  11.44
X=   1.0       NU=  20.14
RE=   986       PR= 383.0      M= 1.72      GR=    2115
TPO= 33.66      TPI= 33.62      TX= 23.89  DEGC           Q=   1431    QL=  11.27
X=   2.0       NU=  19.88
RE=   986       PR= 383.0      M= 1.72      GR=    2130
TPO= 33.73      TPI= 33.69      TX= 23.89  DEGC           Q=   1422    QL=  11.33
X=   3.0       NU=  19.75
RE=   986       PR= 382.9      M= 1.73      GR=    2145
TPO= 33.80      TPI= 33.75      TX= 23.89  DEGC           Q=   1423    QL=  11.40
X=   4.0       NU=  19.55
RE=   986       PR= 382.9      M= 1.73      GR=    2164
TPO= 33.89      TPI= 33.84      TX= 23.89  DEGC           Q=   1421    QL=  11.48
X=   5.5       NU=  19.57
RE=   987       PR= 382.8      M= 1.73      GR=    2164
TPO= 33.89      TPI= 33.84      TX= 23.90  DEGC           Q=   1422    QL=  11.48
X=   7.0       NU=  19.68
RE=   987       PR= 382.8      M= 1.73      GR=    2154
TPO= 33.84      TPI= 33.80      TX= 23.90  DEGC           Q=   1422    QL=  11.44
X=   8.5       NU=  19.67
RE=   987       PR= 382.7      M= 1.73      GR=    2155
TPO= 33.84      TPI= 33.80      TX= 23.90  DEGC           Q=   1421    QL=  11.44
X=  10.0       NU=  19.86
RE=   987       PR= 382.6      M= 1.72      GR=    2135
TPO= 33.75      TPI= 33.71      TX= 23.91  DEGC           Q=   1422    QL=  11.35
X=  11.5       NU=  20.12
RE=   987       PR= 382.6      M= 1.71      GR=    2111
TPO= 33.64      TPI= 33.60      TX= 23.91  DEGC           Q=   1423    QL=  11.25
X=  13.0       NU=  20.06
RE=   987       PR= 382.5      M= 1.71      GR=    2116
TPO= 33.66      TPI= 33.62      TX= 23.91  DEGC           Q=   1422    QL=  11.27
X=  15.0       NU=  20.21
RE=   988       PR= 382.4      M= 1.71      GR=    2101
TPO= 33.60      TPI= 33.55      TX= 23.92  DEGC           Q=   1423    QL=  11.21
X=  20.0       NU=  20.19
RE=   988       PR= 382.2      M= 1.71      GR=    2106
TPO= 33.62      TPI= 33.57      TX= 23.93  DEGC           Q=   1422    QL=  11.23
X=  25.0       NU=  19.98
RE=   989       PR= 382.0      M= 1.72      GR=    2131
TPO= 33.73      TPI= 33.69      TX= 23.94  DEGC           Q=   1422    QL=  11.33
X=  40.0       NU=  19.68
RE=   991       PR= 381.4      M= 1.73      GR=    2171
TPO= 33.91      TPI= 33.86      TX= 23.97  DEGC           Q=   1422    QL=  11.50
X=  88.0       NU=  17.90
RE=   996       PR= 379.5      M= 1.81      GR=    2411
TPO= 34.98      TPI= 34.04      TX= 24.07  DEGC           Q=   1421    QL=  12.52
X=  89.0       NU=  17.88
RE=   996       PR= 379.4      M= 1.80      GR=    2406
TPO= 34.96      TPI= 34.02      TX= 24.07  DEGC           Q=   1416    QL=  12.50
X=  90.0       NU=  18.44
RE=   996       PR= 379.4      M= 1.78      GR=    2333
TPO= 34.63      TPI= 34.59      TX= 24.07  DEGC           Q=   1416    QL=  12.50
```

TEST NO. 10.D3.

```
X=   0.0     NU= 597.27
RE= 26466    PR=  60.7    M= 1.12    GR= 14592
TPO= 45.50    TPI= 44.62    TX= 41.19  DEGC      Q= 23543    QL= 26.06
X=  10.0     NU= 440.74
RE= 26509    PR=  60.6    M= 1.16    GR= 19840
TPO= 46.77    TPI= 45.89    TX= 41.24  DEGC      Q= 23543    QL= 26.06
X=  50.0     NU= 430.01
RE= 26681    PR=  60.3    M= 1.17    GR= 20607
TPO= 47.09    TPI= 46.21    TX= 41.45  DEGC      Q= 23543    QL= 26.41
X=  87.0     NU= 431.66
RE= 26842    PR=  59.9    M= 1.17    GR= 20783
TPO= 47.26    TPI= 46.39    TX= 41.63  DEGC      Q= 23542    QL= 26.59
X=  89.0     NU= 444.54
RE= 26851    PR=  59.9    M= 1.16    GR= 20190
TPO= 47.13    TPI= 46.26    TX= 41.65  DEGC      Q= 23538    QL= 26.45
X=  90.0     NU= 473.62
RE= 26855    PR=  59.9    M= 1.15    GR= 18957
TPO= 46.86    TPI= 45.08    TX= 41.65  DEGC      Q= 23538    QL= 26.45
X=   0.0     NU= 555.94
RF= 21531    PR=  59.9    M= 1.12    GR= 30384
TPO= 45.83    TPI= 45.23    TX= 41.65  DEGC      O= 18299    QL= 20.57
X=   0.5     NU= 902.33
RE= 21533    PR=  59.9    M= 1.07    GR= 18724
TPO= 44.46    TPI= 43.86    TX= 41.65  DEGC      O= 18299    QL= 20.57
X=   1.0     NU= 748.72
RE= 21535    PR=  59.0    M= 1.09    GR= 22430
TPO= 44.89    TPI= 44.29    TX= 41.66  DEGC      O= 18185    QL= 20.98
X=   2.0     NU= 540.15
RF= 21540    PR=  59.9    M= 1.12    GR= 31079
TPO= 45.91    TPI= 45.32    TX= 41.66  DEGC      Q= 18172    QL= 21.95
X=   3.0     NU= 481.80
RE= 21544    PR=  59.0    M= 1.14    GR= 34871
TPO= 46.36    TPI= 45.77    TX= 41.67  DEGC      Q= 18179    QL= 22.30
X=   4.0     NU= 445.26
RE= 21548    PR=  59.9    M= 1.15    GR= 37746
TPO= 46.71    TPI= 46.11    TX= 41.67  DEGC      Q= 18178    QL= 22.71
X=   5.5     NU= 423.70
RE= 21554    PR=  59.9    M= 1.16    GR= 39694
TPO= 46.94    TPI= 46.34    TX= 41.68  DEGC      Q= 18179    QL= 22.93
X=   7.0     NU= 413.16
RE= 21561    PR=  59.8    M= 1.17    GR= 40732
TPO= 47.07    TPI= 46.47    TX= 41.69  DEGC      Q= 18180    QL= 23.05
X=   8.5     NU= 401.35
RE= 21567    PR=  59.8    M= 1.17    GR= 41955
TPO= 47.22    TPI= 46.62    TX= 41.70  DEGC      Q= 18179    QL= 23.19
X=  10.0     NU= 391.84
RE= 21573    PR=  59.8    M= 1.18    GR= 42997
TPO= 47.35    TPI= 46.75    TX= 41.71  DEGC      Q= 18178    QL= 23.32
X=  11.5     NU= 395.99
RE= 21579    PR=  59.8    M= 1.18    GR= 42578
TPO= 47.30    TPI= 46.71    TX= 41.72  DEGC      Q= 18181    QL= 23.28
X=  13.0     NU= 381.91
RE= 21586    PR=  59.8    M= 1.18    GR= 44169
TPO= 47.50    TPI= 46.90    TX= 41.73  DEGC      Q= 18179    QL= 23.46
X=  15.0     NU= 369.04
RE= 21594    PR=  59.8    M= 1.19    GR= 45745
TPO= 47.69    TPI= 47.09    TX= 41.74  DEGC      Q= 18179    QL= 23.64
X=  20.0     NU= 359.61
RE= 21615    PR=  59.7    M= 1.20    GR= 47039
TPO= 47.86    TPI= 47.26    TX= 41.77  DEGC      O= 18179    QL= 23.80
X=  25.0     NU= 353.33
RE= 21636    PR=  59.6    M= 1.20    GR= 47970
TPO= 47.99    TPI= 47.39    TX= 41.80  DEGC      Q= 18179    QL= 23.93
X=  40.0     NU= 357.87
RE= 21700    PR=  59.5    M= 1.20    GR= 47647
TPO= 48.01    TPI= 47.41    TX= 41.90  DEGC      Q= 18179    QL= 23.95
X=  88.0     NU= 352.12
RE= 21904    PR=  59.0    M= 1.20    GR= 49361
TPO= 48.40    TPI= 47.80    TX= 42.19  DEGC      Q= 18178    QL= 24.31
X=  89.0     NU= 366.48
RE= 21908    PR=  59.0    M= 1.19    GR= 47444
TPO= 48.18    TPI= 47.59    TX= 42.19  DEGC      Q= 18178    QL= 24.11
X=  90.0     NU= 386.88
RE= 21912    PR=  58.9    M= 1.18    GR= 44961
TPO= 47.90    TPI= 47.31    TX= 42.20  DEGC      O= 18178    QL= 24.11
```

TEST NO. 14.D3.

```
X=   0.0    NU= 278.15
RE=  7450    PR=  61.1    M= 1.07    GR=  9145
TPO= 43.41    TPI= 43.15    TX= 40.97  DEGC     Q=  6970    QL=  23.76
X=  10.0    NU= 122.05
RE=  7463    PR=  61.0    M= 1.17    GR= 20916
TPO= 46.26    TPI= 46.00    TX= 41.03  DEGC     Q=  6970    QL=  23.76
X=  50.0    NU= 124.74
RE=  7513    PR=  60.6    M= 1.17    GR= 20752
TPO= 46.36    TPI= 46.10    TX= 41.24  DEGC     Q=  6971    QL=  23.88
X=  87.0    NU= 127.68
RE=  7561    PR=  60.3    M= 1.17    GR= 20535
TPO= 46.45    TPI= 46.19    TX= 41.44  DEGC     Q=  6971    QL=  23.97
X=  89.0    NU= 129.67
RE=  7563    PR=  60.3    M= 1.16    GR= 20226
TPO= 46.39    TPI= 46.13    TX= 41.45  DEGC     Q=  6968    QL=  23.90
X=  90.0    NU= 134.76
RE=  7565    PR=  60.3    M= 1.16    GR= 19470
TPO= 46.21    TPI= 45.95    TX= 41.45  DEGC     Q=  6968    QL=  23.90
X=   0.0    NU= 159.46
RE=  6065    PR=  60.3    M= 1.13    GR= 31534
TPO= 45.39    TPI= 45.21    TX= 41.45  DEGC     Q=  5518    QL=  18.06
X=   0.5    NU= 337.27
RE=  6066    PR=  60.3    M= 1.06    GR= 14912
TPO= 43.41    TPI= 43.23    TX= 41.46  DEGC     Q=  5518    QL=  18.06
X=   1.0    NU= 334.74
RE=  6066    PR=  60.3    M= 1.06    GR= 14735
TPO= 43.39    TPI= 43.21    TX= 41.46  DEGC     Q=  5411    QL=  18.04
X=   2.0    NU= 225.12
RE=  6067    PR=  60.2    M= 1.09    GR= 21814
TPO= 44.24    TPI= 44.06    TX= 41.47  DEGC     Q=  5384    QL=  18.84
X=   3.0    NU= 190.67
RE=  6069    PR=  60.2    M= 1.10    GR= 25785
TPO= 44.72    TPI= 44.54    TX= 41.47  DEGC     Q=  5389    QL=  19.30
X=   4.0    NU= 169.40
RE=  6070    PR=  60.2    M= 1.12    GR= 29031
TPO= 45.11    TPI= 44.93    TX= 41.48  DEGC     Q=  5388    QL=  19.67
X=   5.5    NU= 153.45
RE=  6072    PR=  60.2    M= 1.13    GR= 32076
TPO= 45.48    TPI= 45.30    TX= 41.49  DEGC     Q=  5389    QL=  20.02
X=   7.0    NU= 141.70
RE=  6074    PR=  60.2    M= 1.14    GR= 34758
TPO= 45.80    TPI= 45.63    TX= 41.50  DEGC     Q=  5389    QL=  20.33
X=   8.5    NU= 130.41
RE=  6075    PR=  60.2    M= 1.16    GR= 37787
TPO= 46.17    TPI= 45.09    TX= 41.51  DEGC     Q=  5388    QL=  20.68
X=  10.0    NU= 121.38
RE=  6077    PR=  60.2    M= 1.17    GR= 40613
TPO= 46.51    TPI= 46.34    TX= 41.52  DEGC     Q=  5387    QL=  21.00
X=  11.5    NU= 117.50
RE=  6079    PR=  60.1    M= 1.17    GR= 42000
TPO= 46.68    TPI= 46.51    TX= 41.53  DEGC     Q=  5389    QL=  21.17
X=  13.0    NU= 110.11
RE=  6081    PR=  60.1    M= 1.19    GR= 44832
TPO= 47.03    TPI= 46.85    TX= 41.54  DEGC     Q=  5388    QL=  21.49
X=  15.0    NU= 102.50
RE=  6084    PR=  60.1    M= 1.20    GR= 48192
TPO= 47.43    TPI= 47.26    TX= 41.55  DEGC     Q=  5387    QL=  21.88
X=  20.0    NU=  96.19
RE=  6090    PR=  60.0    M= 1.22    GR= 51459
TPO= 47.84    TPI= 47.66    TX= 41.58  DEGC     Q=  5387    QL=  22.26
X=  25.0    NU=  96.71
RE=  6096    PR=  60.0    M= 1.22    GR= 51294
TPO= 47.84    TPI= 47.66    TX= 41.61  DEGC     Q=  5387    QL=  22.26
X=  40.0    NU= 100.81
RE=  6115    PR=  59.8    M= 1.21    GR= 49515
TPO= 47.69    TPI= 47.51    TX= 41.71  DEGC     Q=  5387    QL=  22.12
X=  88.0    NU= 100.60
RE=  6175    PR=  59.3    M= 1.21    GR= 50624
TPO= 48.01    TPI= 47.83    TX= 42.02  DEGC     Q=  5387    QL=  22.43
X=  89.0    NU= 102.12
RE=  6176    PR=  59.3    M= 1.21    GR= 49846
TPO= 47.93    TPI= 47.75    TX= 42.02  DEGC     Q=  5382    QL=  22.35
X=  90.0    NU= 109.61
RE=  6177    PR=  59.2    M= 1.19    GR= 46459
TPO= 47.54    TPI= 47.36    TX= 42.03  DEGC     Q=  5382    QL=  22.35
```

TEST NO. 16.D3.

```
X=   0.0     NU=-408.05
RE=  1942     PR=  61.2     M= 0.99     GR=  -1434
TPO= 40.64     TPI= 40.59     TX= 40.93  DEGC     Q=  1608     QL=  23.37
X=  10.0     NU=  56.77
RE=  1945     PR=  61.1     M= 1.08     GR=  10337
TPO= 43.50     TPI= 43.44     TX= 40.98  DEGC     Q=  1608     QL=  23.37
X=  50.0     NU=  19.60
RE=  1957     PR=  60.8     M= 1.26     GR=  30083
TPO= 48.31     TPI= 48.25     TX= 41.16  DEGC     Q=  1603     QL=  28.60
X=  87.0     NU=  17.14
RE=  1968     PR=  60.5     M= 1.31     GR=  34910
TPO= 49.53     TPI= 49.47     TX= 41.34  DEGC     Q=  1601     QL=  29.93
X=  89.0     NU=  17.18
RE=  1968     PR=  60.5     M= 1.30     GR=  34799
TPO= 49.51     TPI= 49.45     TX= 41.35  DEGC     Q=  1599     QL=  29.90
X=  90.0     NU=  17.47
RE=  1969     PR=  60.4     M= 1.30     GR=  34238
TPO= 49.38     TPI= 49.32     TX= 41.35  DEGC     Q=  1599     QL=  29.90
X=   0.0     NU=  13.10
RE=  1578     PR=  60.4     M= 1.36     GR=  78174
TPO= 50.77     TPI= 50.73     TX= 41.35  DEGC     Q=  1131     QL=  28.58
X=   0.5     NU=  11.49
RE=  1579     PR=  60.4     M= 1.42     GR=  89163
TPO= 52.09     TPI= 52.05     TX= 41.35  DEGC     Q=  1131     QL=  28.58
X=   1.0     NU=  12.69
RE=  1579     PR=  60.4     M= 1.41     GR=  87003
TPO= 51.83     TPI= 51.79     TX= 41.36  DEGC     Q=  1220     QL=  28.33
X=   2.0     NU=  14.55
RE=  1579     PR=  60.4     M= 1.36     GR=  77398
TPO= 50.68     TPI= 50.64     TX= 41.36  DEGC     Q=  1243     QL=  27.24
X=   3.0     NU=  15.53
RE=  1579     PR=  60.4     M= 1.33     GR=  72055
TPO= 50.04     TPI= 50.00     TX= 41.37  DEGC     Q=  1234     QL=  26.64
X=   4.0     NU=  16.76
RE=  1580     PR=  60.4     M= 1.30     GR=  66324
TPO= 49.36     TPI= 49.32     TX= 41.37  DEGC     Q=  1226     QL=  25.99
X=   5.5     NU=  23.27
RE=  1580     PR=  60.4     M= 1.21     GR=  48419
TPO= 47.22     TPI= 47.18     TX= 41.38  DEGC     Q=  1242     QL=  23.95
X=   7.0     NU=  31.43
RE=  1580     PR=  60.4     M= 1.15     GR=  35825
TPO= 45.72     TPI= 45.68     TX= 41.39  DEGC     Q=  1241     QL=  22.53
X=   8.5     NU=  45.40
RE=  1581     PR=  60.4     M= 1.10     GR=  24867
TPO= 44.41     TPI= 44.37     TX= 41.40  DEGC     Q=  1243     QL=  21.29
X=  10.0     NU=  65.86
RE=  1581     PR=  60.3     M= 1.07     GR=  17170
TPO= 43.50     TPI= 43.46     TX= 41.41  DEGC     Q=  1245     QL=  20.42
X=  11.5     NU=  85.24
RE=  1582     PR=  60.3     M= 1.05     GR=  13287
TPO= 43.04     TPI= 43.00     TX= 41.42  DEGC     Q=  1246     QL=  19.99
X=  13.0     NU=  79.99
RE=  1582     PR=  60.3     M= 1.06     GR=  14134
TPO= 43.15     TPI= 43.11     TX= 41.42  DEGC     Q=  1243     QL=  20.09
X=  15.0     NU=  64.53
RE=  1583     PR=  60.3     M= 1.07     GR=  17512
TPO= 43.57     TPI= 43.53     TX= 41.44  DEGC     Q=  1241     QL=  20.48
X=  20.0     NU=  42.20
RE=  1584     PR=  60.2     M= 1.11     GR=  26799
TPO= 44.70     TPI= 44.66     TX= 41.46  DEGC     Q=  1240     QL=  21.56
X=  25.0     NU=  32.16
RE=  1586     PR=  60.2     M= 1.14     GR=  35205
TPO= 45.72     TPI= 45.68     TX= 41.49  DEGC     Q=  1239     QL=  22.53
X=  40.0     NU=  23.46
RE=  1590     PR=  60.0     M= 1.20     GR=  48470
TPO= 47.35     TPI= 47.31     TX= 41.58  DEGC     Q=  1238     QL=  24.08
X=  88.0     NU=  18.29
RE=  1604     PR=  59.6     M= 1.27     GR=  63196
TPO= 49.23     TPI= 49.19     TX= 41.85  DEGC     Q=  1236     QL=  25.86
X=  89.0     NU=  18.15
RE=  1604     PR=  59.6     M= 1.27     GR=  62807
TPO= 49.19     TPI= 49.15     TX= 41.85  DEGC     Q=  1219     QL=  25.82
X=  90.0     NU=  21.36
RE=  1604     PR=  59.5     M= 1.22     GR=  53387
TPO= 48.10     TPI= 48.06     TX= 41.86  DEGC     Q=  1219     QL=  25.82
```

TEST NO. 21.D3.

```
X=   0.0    NU= 230.68
RE=  4572   PR= 153.6    M= 1.23   GR=  2336
TPO= 24.67   TPI= 24.26   TX= 20.22 DEGC   Q= 11052   QL= 7.66
X=  10.0    NU= 108.99
RE=  4584   PR= 153.2    M= 1.61   GR=  4969
TPO= 29.24   TPI= 28.83   TX= 20.27 DEGC   Q= 11052   QL= 7.66
X=  50.0    NU= 111.20
RE=  4630   PR= 151.7    M= 1.60   GR=  4971
TPO= 29.29   TPI= 28.88   TX= 20.48 DEGC   Q= 11052   QL= 7.71
X=  87.0    NU= 111.18
RE=  4674   PR= 150.4    M= 1.60   GR=  5068
TPO= 29.49   TPI= 29.08   TX= 20.68 DEGC   Q= 11052   QL= 7.92
X=  89.0    NU= 112.47
RE=  4676   PR= 150.3    M= 1.59   GR=  5013
TPO= 29.40   TPI= 28.99   TX= 20.69 DEGC   Q= 11047   QL= 7.83
X=  90.0    NU= 116.60
RE=  4677   PR= 150.3    M= 1.56   GR=  4838
TPO= 29.11   TPI= 28.70   TX= 20.70 DEGC   Q= 11047   QL= 7.83
X=   0.0    NU= 132.78
RE=  3750   PR= 150.3    M= 1.46   GR=  8151
TPO= 27.93   TPI= 27.65   TX= 20.70 DEGC   Q=  8758   QL= 2.14
X=   0.5    NU= 266.49
RE=  3751   PR= 150.3    M= 1.19   GR=  4063
TPO= 24.45   TPI= 24.16   TX= 20.70 DEGC   Q=  8758   QL= 2.14
X=   1.0    NU= 325.84
RE=  3751   PR= 150.3    M= 1.15   GR=  3274
TPO= 23.78   TPI= 23.49   TX= 20.70 DEGC   Q=  8627   QL= 1.50
X=   2.0    NU= 239.37
RE=  3752   PR= 150.2    M= 1.21   GR=  4432
TPO= 24.76   TPI= 24.48   TX= 20.71 DEGC   Q=  8574   QL= 2.44
X=   3.0    NU= 196.38
RE=  3754   PR= 150.2    M= 1.27   GR=  5404
TPO= 25.60   TPI= 25.31   TX= 20.71 DEGC   Q=  8571   QL= 3.23
X=   4.0    NU= 174.58
RE=  3755   PR= 150.1    M= 1.31   GR=  6084
TPO= 26.18   TPI= 25.90   TX= 20.72 DEGC   Q=  8574   QL= 3.78
X=   5.5    NU= 152.57
RE=  3756   PR= 150.1    M= 1.37   GR=  6968
TPO= 26.93   TPI= 26.65   TX= 20.73 DEGC   Q=  8573   QL= 4.50
X=   7.0    NU= 138.76
RE=  3758   PR= 150.0    M= 1.42   GR=  7670
TPO= 27.53   TPI= 27.25   TX= 20.74 DEGC   Q=  8574   QL= 5.07
X=   8.5    NU= 125.62
RE=  3760   PR= 149.9    M= 1.48   GR=  8478
TPO= 28.22   TPI= 27.94   TX= 20.75 DEGC   Q=  8572   QL= 5.72
X=  10.0    NU= 116.77
RE=  3762   PR= 149.9    M= 1.54   GR=  9130
TPO= 28.78   TPI= 28.50   TX= 20.76 DEGC   Q=  8573   QL= 6.25
X=  11.5    NU= 108.48
RE=  3763   PR= 149.8    M= 1.60   GR=  9836
TPO= 29.38   TPI= 29.10   TX= 20.77 DEGC   Q=  8572   QL= 6.82
X=  13.0    NU= 101.03
RE=  3765   PR= 149.7    M= 1.67   GR= 10569
TPO= 30.00   TPI= 29.72   TX= 20.78 DEGC   Q=  8571   QL= 7.41
X=  15.0    NU=  93.67
RE=  3767   PR= 149.7    M= 1.73   GR= 11413
TPO= 30.72   TPI= 30.43   TX= 20.79 DEGC   Q=  8570   QL= 8.09
X=  20.0    NU=  84.01
RE=  3773   PR= 149.4    M= 1.81   GR= 12764
TPO= 31.85   TPI= 31.57   TX= 20.82 DEGC   Q=  8569   QL= 9.17
X=  25.0    NU=  81.71
RE=  3779   PR= 149.2    M= 1.83   GR= 13165
TPO= 32.19   TPI= 31.91   TX= 20.86 DEGC   Q=  8569   QL= 9.49
X=  40.0    NU=  87.62
RE=  3797   PR= 148.6    M= 1.77   GR= 12393
TPO= 31.54   TPI= 31.26   TX= 20.95 DEGC   Q=  8570   QL= 8.87
X=  88.0    NU=  88.96
RE=  3853   PR= 146.5    M= 1.76   GR= 12583
TPO= 31.70   TPI= 31.42   TX= 21.26 DEGC   Q=  8569   QL= 9.02
X=  89.0    NU=  90.14
RE=  3855   PR= 146.5    M= 1.75   GR= 12417
TPO= 31.56   TPI= 31.28   TX= 21.27 DEGC   Q=  8563   QL= 8.89
X=  90.0    NU=  95.08
RE=  3856   PR= 146.4    M= 1.71   GR= 11780
TPO= 31.05   TPI= 30.77   TX= 21.27 DEGC   Q=  8563   QL= 8.89
```

SOME TEST PARAMETERS.

TEST REF.	Reynolds Number		Pr	Gr	Flux (W/m²)
	At start of heating, or just upstream and downstream of discontinuity			at 30-40 dia.	[illegible] downstream
1 S	TESTS	3744	401	352	3040
2 S	DENOTED	3682	409	640	5809
3 S	"S"	3693	409	792	7366
4 S	UNHEATED	3747	403	1221	11495
5 S	UPSTREAM	3790	400	1666	16019
6 S	Re SAME	4031	380	2773	27030
7 S	AS NEXT	4455	347	651	4928
8 S	COLUMN.	4435	349	1228	9673
9 S		4394	352	1713	13236
10 S		4409	351	2557	21727
11 S		5766	275	813	4488
12 S		5784	274	1884	10626
13 S		5812	274	2280	12970
14 S		6032	266	6227	37417
15 S		7473	219	1623	6975
16 S		7253	225	2211	9567
17 S		7346	222	[illegible]	20622
18 S		7403	222	8047	37437
19 S		9234	181	1579	5090
20 S		9259	180	2716	8437
21 S		9016	186	4999	16542
22 S		9076	184	7708	25806
23 S		114	594	212	607
24 S		114	600	529	1695
25 S		114	600	901	3096
26 S		110	617	1565	6273
27 S		166	406	811	1094
28 S		167	402	2496	3709
29 S		169	397	2045	2267
30 S		272	246	1461	675
31 S		267	251	4021	2039
32 S		365	183	4585	1130
33 S		384	175	15122	4059
34 S		205	594	182	660
35 S		536	355	1204	179
36 S		871	360	1577	2911
37 S		417	595	868	4771

38 S		507	607	536	2097
39 S		659	650	315	2252
40 S		969	614	981	8112
41 S		1139	623	218	1608
42 S		2265	257	3207	3522
43 S		3268	253	6831	18240
44 S		3480	197	4239	5813
45 S		4216	193	10270	19550
46 S		1901	203	3835	2162
47 S		1311	632	505	4545
48 S		1477	638	937	10075
49 S		2561	355	1387	5623
50 S		2876	356	813	3935
51 S		1690	626	218	1903
52 S		1905	618	845	2830
53 S		8534	194	4539	16195
54 S		3568	369	1123	7985
55 S		4968	260	3386	14730
56 S		6156	193	4296	10825
57 S		7702	187	2967	8642
58 SB	ALL TESTS	1615	200	9818	5778
59 SB	DENOTED	6474	215	7530	27914
60 SB	"SB"	116	574	207	555
61 SB	BELLMOUTH	173	388	2979	4742
62 SB	ENTRY.	425	577	905	4596
63 SB	Re = 0	1035	574	1038	7627
64 SB	UPSTREAM	2190	254	2999	3435
65 SB	EFFECTIVELY	2570	351	1228	3547
66 SB		2920	350	892	2853
67 SB		3291	250	7959	16200
68 SB		6255	191	4238	10233
69 SB		3780	394	815	6469
70 SB		3986	373	3021	26017
71 SB		4927	260	2424	14313
72 SB		9507	175	2211	2395
73 SB		Results	not	analysed.	
74 SB		15014	92.4	6897	14782
75 SB		7464	92.9	7020	7586
76 SB		3610	92.5	7395	3616
77 SB		1807	92.9	9202	1174
78 SB		911	93.1	10643	1177
79 SB		464	93.2	9909	969

80 s		470	92.8	9527	968
81 s		918	92.4	9575	1191
82 s		1801	93.2	9158	1669
83 s		3596	92.9	7105	3130
84 s		7474	92.8	7153	7152
85 s		14886	93.1	7004	14578
1 c1	13301	26468	60.3	19481	22336
2 c1	7472	14879	60.2	20820	13643
3 c1	3745	7457	60.0	23661	7920
4 c1	1725	3434	60.4	22848	3796
5 c1	740	1474	60.7	27516	1378
6 c1	247	491	59.9	22630	1059
7 c1	287	572	154	7030	2180
8 c1	742	1478	156	6646	3150
9 c1	2273	4478	153	[illegible]	12234
10 c1	5002	[illegible]	148	3597	16301
11 c1	4119	8202	200	4397	18944
12 c1	1593	3172	200	3773	4364
13 c1	625	1244	198	5066	2175
14 c1	218	433	198	4741	1494
15 c1	240	477	342	1569	1739
16 c1	675	1343	346	1186	1698
17 c1	1331	2651	346	1077	3275
18 c1	2274	4529	340	1268	11869
1 c2	6786	8464	195	4411	18561
2 c2	2564	3197	197	4654	2695
3 c2	988	1232	199	4782	1757
4 c2	354	441	194	5157	1536
5 c2	388	484	336	1546	1487
6 c2	1111	1386	337	1539	1984
7 c2	2147	2677	342	1429	2485
8 c2	3728	4650	330	1033	8717
9 c2	20919	26071	58.9	23281	24897
10 c2	12180	15196	58.7	23133	14766
11 c2	6133	7650	58.7	21292	8021
12 c2	8097	10097	144	5772	25480
13 c2	3669	4576	147	6167	15601
14 c2	1211	1510	152	6662	2419
15 c2	472	589	149	6575	2078
16 c2	431	537	57.5	24030	1030
17 c2	1208	1507	59.2	23564	1350
18 c2	2787	3477	59.4	25990	3356

1 c3	10379	34679	57.5	4733	33760
2 c3	6967	23293	57.2	5390	22741
3 c3	3529	11798	57.0	6103	13943
4 c3	1624	5431	56.6	7050	8145
5 c3	679	2336	57.2	8885	2402
6 c3	237	791	56.0	8353	1439
7 c3	288	963	137	2342	3423
8 c3	758	2533	138	2163	7301
9 c3	2205	7372	138	1556	20718
10 c3	3870	12939	139	1569	26096
11 c3	214	716	335	446	2741
12 c3	613	2049	339	437	4146
13 c3	1188	3971	338	384	15424
14 c3	1573	5260	335	386	20128
15 c3	3007	10052	192	1109	26970
16 c3	1456	4866	192	1276	15052
17 c3	563	1881	194	1397	3828
18 c3	193	644	192	1521	2467
19 c3	9137	30547	62.8	8886	53657
20 c3	1542	5156	61.1	12222	14014
21 c3	223	747	60.4	14557	2942
22 c3	UNHEATED	29325	64.9	4379	27587
23 c3	UNHEATED	4745	64.9	6485	7872
24 c3	UNHEATED	694	64.6	7457	1618
1 d1	35909.	10738	54.9	364338	6459
2 d1	836	250	54.1	155828	184.8
3 d1	1609	481	54.6	193009	439
4 d1	2395	716	54.5	208935	502
5 d1	3167	947	54.9	203647	506
6 d1	4817	1440	54.4	230463	606
7 d1	6311	1887	54.3	242485	678
8 d1	12827	3836	54.9	375974	2149
9 d1	19258	5759	55.2	386729	3629
10 d1	25642	7668	55.1	376749	4721
11 d1	32160	9617	54.7	388965	6096
12 d1	645	193	54.2	155938	183.6
13 d1	1217	364	54.7	152657	190.0
14 d1	2004	599	54.8	163083	231.1
15 d1	2772	829	55.0	156941	335
16 d1	829	248	54.5	197250	199.3
17 d1	832	249	54.3	235927	237.3
18 d1	834	249	54.2	281776	275.9
19 d1	1587	475	54.8	222804	538

20 d1	1618	482	54.5	297748	[illegible]
21 d1	1633	488	53.9	377095	[illegible]
22 d1	3202	958	54.6	294555	[illegible]
23 d1	3212	960	54.5	39[illegible]71	10[illegible]
24 d1	2789	834	54.7	336322	[illegible]
25 d1	698	209	53.2	26[illegible]19	[illegible]
26 d1	1245	372	53.5	323257	[illegible]
27 d1	2023	605	54.3	353594	[illegible]
28 d1	807	241	54.7	152053	359
29 d1	826	247	137	41237	611
30 d1	1837	549	139	44376	763
31 d1	3658	1094	138	54155	949
32 d1	7445	2226	139	61163	1637
33 d1	10284	3075	137	71579	2427
34 d1	11981	3583	138	74571	4597
35 d1	3594	1075	502	7363	1324
36 d1	3004	898	497	7641	1244
37 d1	2551	763	497	7628	1192
38 d1	2029	625	496	7495	1105
39 d1	1725	516	493	7244	979
40 d1	1346	403	497	6756	845
41 d1	888	266	496	4324	457
42 d1	443	132	495	4379	378
43 d1	238	71	488	4292	374
44 d1	3850	1151	277	23024	970
45 d1	2842	850	274	22728	840
46 d1	1663	497	272	20953	697
47 d1	5223	1562	277	24913	1196
48 d1	809	242	274	15612	429
49 d1	7078	2116	274	26419	1497
50 d1	420	126	272	14330	273
51 d1	UNHEATED	187	57.2	179924	414
52 d1	UNHEATED	415	56.8	292924	731
53 d1	UNHEATED	5578	57.1	397292	3620
54 d1	UNHEATED	1829	57.3	263106	722
1 d2	28122	14122	57.1	229883	8868
2 d2	25362	11731	56.8	229145	7233
3 d2	18319	9199	56.8	219762	5446
4 d2	13023	6540	56.8	227577	3920
5 d2	7845	3940	57.0	236[illegible]	2287
6 d2	4135	2077	57.0	216957	1022
7 d2	2061	1035	57.0	199307	828
8 d2	1049	526	56.3	174363	623

9 d2	533	268	55.9	132640	·492
10 d2	10281	5163	143	56412	8412
11 d2	4828	2424	144	54942	2447
12 d2	1589	798	144	52592	1577
13 d2	604	304	142	49547	1127
14 d2	7111	3571	232	28484	4546
15 d2	3436	1725	232	16828	1647
16 d2	1408	707	231	26751	1182
17 d2	651	327	231	26293	961
18 d2	376	189	230	20481	524
19 d2	3117	1565	416	8527	2055
20 d2	2252	1131	412	8632	1775
21 d2	1050	527	408	7972	1238
22 d2	403	202	408	7704	89.5
1 d3	7520	6029	270	7292	12034
2 d3	3571	2863	221	7516	4070
3 d3	1499	1202	217	8460	2373
4 d3	655	525	220	7574	1502
5 d3	388	311	213	7320	1127
6 d3	423	339	387	2141	1113
7 d3	1230	986	383	2171	1433
8 d3	2411	1933	386	2460	5767
9 d3	3998	3206	385	2342	7005
10 d3	26855	21531	59.9	47647	18202
11 d3	22233	17825	60.1	47100	15124
12 d3	17207	13796	60.0	47753	12007
13 d3	12323	9880	60.1	48362	8829
14 d3	7565	6065	60.3	49515	5409
15 d3	3920	3143	59.8	63724	3329
16 d3	1969	1578	60.4	48470	1261
17 d3	904	797	59.5	45283	863
18 d3	521	418	58.8	36131	690
19 d3	567	454	151	10625	1443
20 d3	1524	1222	151	12148	2001
21 d3	4677	3750	150	12328	2578
22 d3	9955	7982	149	11894	18212
1 dx	12238	850	62.4	426640	1134
2 dx	12075	1241	62.9	495929	1253
3 dx	12370	2061	63.4	386251	1281

FIGURE 7.1.

THE BELLMOUTH-ENTRANCE.

NOT TO SCALE

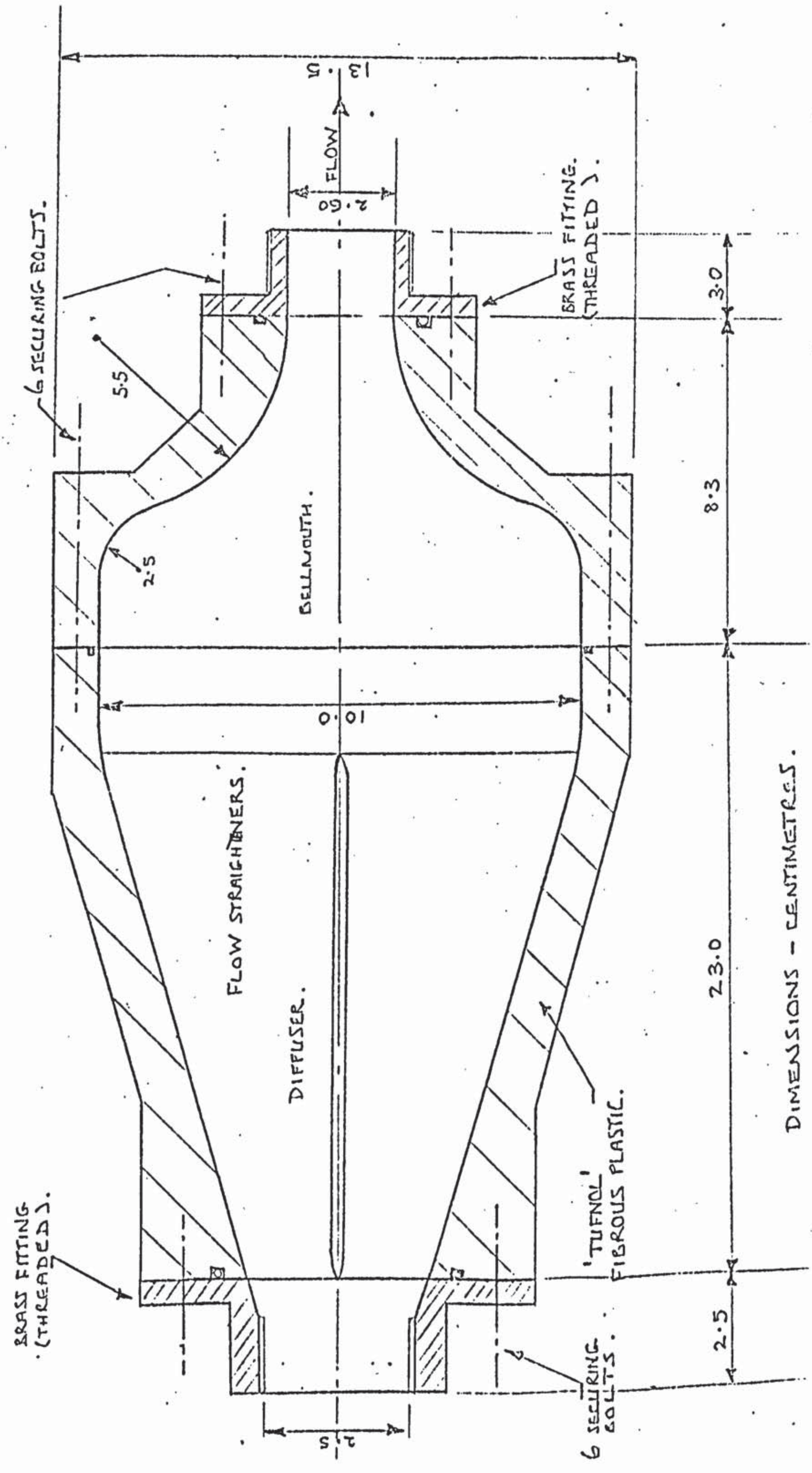

FIGURE 7.2

FLOW VISUALISATION APPARATUS.

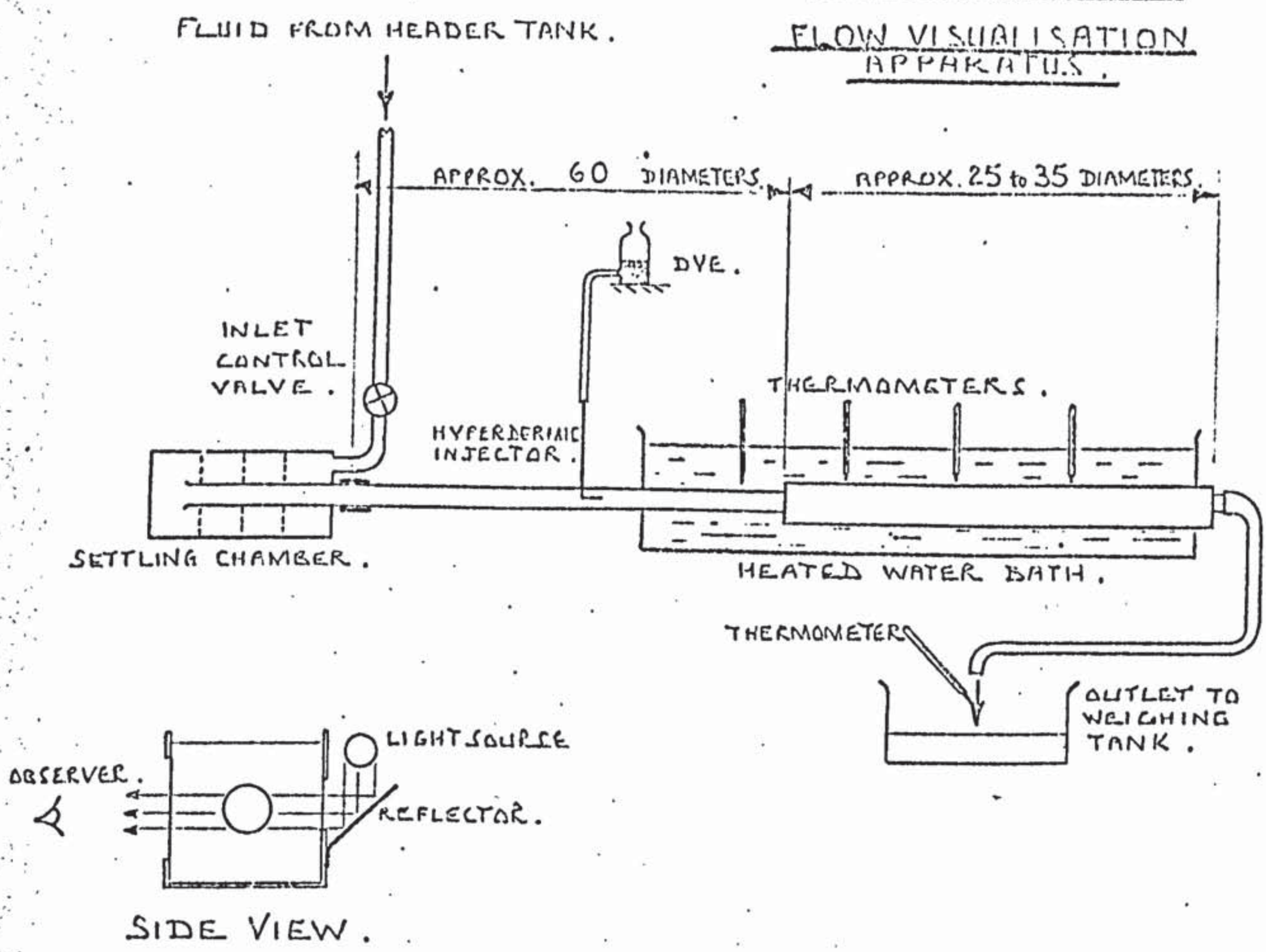

FIGURE 7.3

THE INSERTS USED TO PRODUCE LARGE, SUDDEN DIVERGENCES IN DIAMETER.

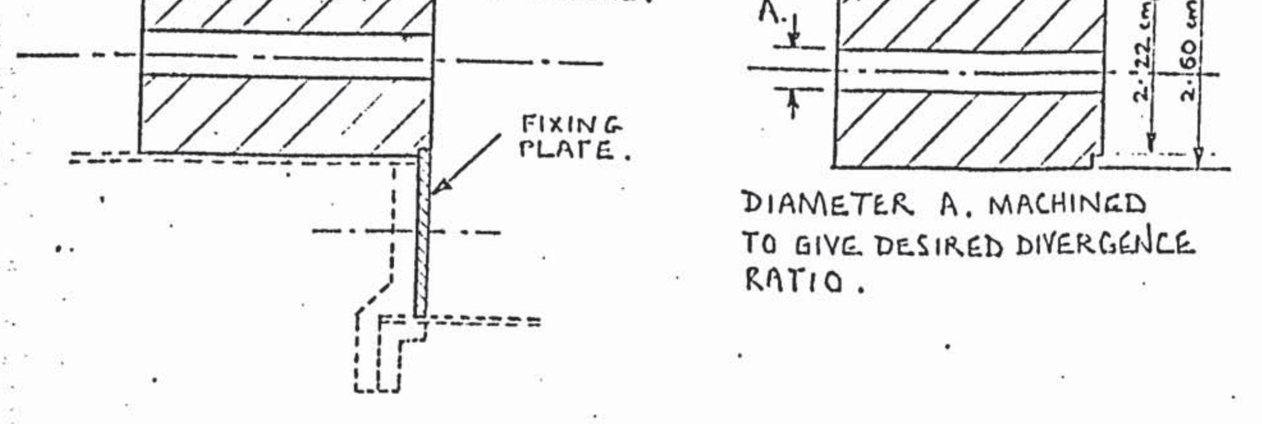

8. THE REDUCTION OF RAW EXPERIMENTAL DATA, AND ASSOCIATED CALCULATIONS

8.1. INTRODUCTION.

The reduction of experimental results into a useful form was initially carried out on a desk calculator, with a number of graphical aids and much tabulated data. This procedure was tedious and time consuming, but it did provide a logical sequence of calculations which could be easily arranged as a computer programme.

The numerical data which could be extracted from each test may be generalised as follows: ambient temperature; flowmeter reading; voltages and current in experimental tubes; thermocouple readings in the heat-transfer fluid at entry and exit of the tubes; the composition of the fluid; the dimensions of the tubes; and finally the thermocouple readings at various locations on the outer surface of the tubes with their corresponding positions. These were supplemented by a flowmeter calibration, thermocouple calibration and physical property data for the fluid and other materials utilised.

From the data above the following variables had to be determined - the circumferential, mean coefficient of heat transfer at each axial position on the tubes, the bulk temperature of the fluid and the temperature at the inner surface of the tube for each location, the heat flux, and various dimensionless groups dependent on the local properties of the fluid, such as the local values of the Nusselt, Reynolds, Prandtl and Grashof numbers. Further information was added to this list in some cases, but the essential components are as stated.

The calculations which were carried out in the reduction of the experimental data are described in the next section, and a typical computer programme incorporating these will be given. For simplicity, the explanation of the calculations follows a similar sequence to the 'programme'.

At the end of this section a discussion concerning the heat balance will be presented.

8.2. THE CALCULATIONS.

8.2.(a) Flowmeter and thermocouple calibrations.

The frequency reading from the flowmeter was converted into volume flow-rate by using Figure 8.2 which is referred to in part 5. This step was not included in the computer programme. The thermocouple readings could be converted into temperature simply using a graph of the calibration data (Figure: 8.3.). This technique was used when the peripheral temperature distribution was being investigated, but a numerical method was found to be more satisfactory for the majority of the calculations. The most useful results, in general, were those appertaining to axial, but not peripheral, tube locations. Hence the data input for the computer programme included mean thermocouple readings for given axial positions, and these were converted into temperatures with an interpolation 'procedure'.

The numerical interpolation was based on discrete temperature increments and the corresponding thermocouple voltages. These values were determined graphically from basic calibration results, and the temperature increment was chosen at 4K so that linear interpolation sufficed.

8.2.(b) The interpolation of property data.

The propylene glycol-water mixtures had to be specified in terms of composition and temperature for the purpose of determining by reference the density, thermal conductivity, specific heat capacity, and viscosity. The values referred to are tabulated in figures 5.10a to 5.10d.

A unified approach was required for the interpolation of intermediate property values for use in the programme (the properties being stored in the computer at discrete 'temperature' and 'percentage glycol in water by weight' values, as shown in the tables). Upon inspection of the property data it was noted that density, conductivity, and specific heat capacity could be interpolated linearly over a large 'temperature' or 'per cent' range (i.e. less than 1% difference was estimated between interpolated property values and graphically presented reference data for 10K or 10% increments). The viscosity, however, could not be interpolated linearly unless very small increments were chosen (i.e. approximately 1% maximum departure from reference values occurred for 3K or 3% increments).

Rather than increase the computer data required to store the viscosity functions by a factor of about 10 times, it was decided to improve the interpolation formula. Instead of assuming linearity between any two adjacent, tabulated values, an exponential relation was proposed to fit any three adjacent values, as follows:

Interpolated viscosity $\mu = A + B.x^n$,

where, at a given coposition x = (temperature - reference temperature), or, at constant temperature x = (per cent glycol - reference per cent). A, B and n may be determined from the three knownconditions,

Hence, $$\mu = \mu_1 + (\mu_3 - \mu_1)\left(\frac{t - t_1}{t_3 - t_1}\right)^{\log\left(\frac{\mu_2-\mu_1}{\mu_3-\mu_1}\right)\Big/\log\left(\frac{t_2-t_1}{t_3-t_1}\right)}$$

where t = temperature or per cent glycol in water.

Since viscosity was know to reduce exponentially with increasing temperature or water content, a considerable improvement was expected over the linear analysis. Further, this exponential form could be utilised for the other properties since linearity was permissible as a special case.

Using the above technique, it was found possible to choose increments in temperature and per cent glycol of 10K and 10%. The interpolation error was assessed by plotting graphs of viscosity versus temperature for given mixtures, the most severe test on the method being the case of 100% glycol at 'middle of increment' temperature values. A maximum interpolation error of 2% could occur at 25 °C (graphical estimates are shown in Figure 8.4) but the mean error over the full temperature range (0 to 70 °C) was approximately 0.7%. With 90% glycol the maximum possible errors were much reduced, the corresponding figures being 0.9% and 0.4%. For lower glycol content the error estimates were small and unrealistic. The estimated errors were very small for the other properties over the entire range of tabulated values.

In applying the interpolation procedure for a given composition, and temperature, nine values of viscosity (the closest to the region of interest) were utilised in four applications of the formula.

It could be argued that a more reliable interpolation would have been a polynomial curve fit using as many reference points as were available, however, the present method was adopted as being sufficiently reliable, whilst combining mathematical simplicity with ease of application. Two dimensional arrays of different size and grid spacing could be handled without difficulty.

8.2.(c) Conduction in the tube wall.

In part 5. some calculations were carried out on the effects of axial conduction in the tube wall very close to fittings which could distort the temperature distribution. It was concluded that this effect was likely to be very localised for the test conditions anticipated. Assuming this to be so (though not at this stage entirely dismissing it as a possible source of discrepancy) an investigation of conduction in a tube of infinite length may be carried out advantageously; the purpose of this analysis being to produce formulae for the local temperature difference across the tube wall and the local heat flux.

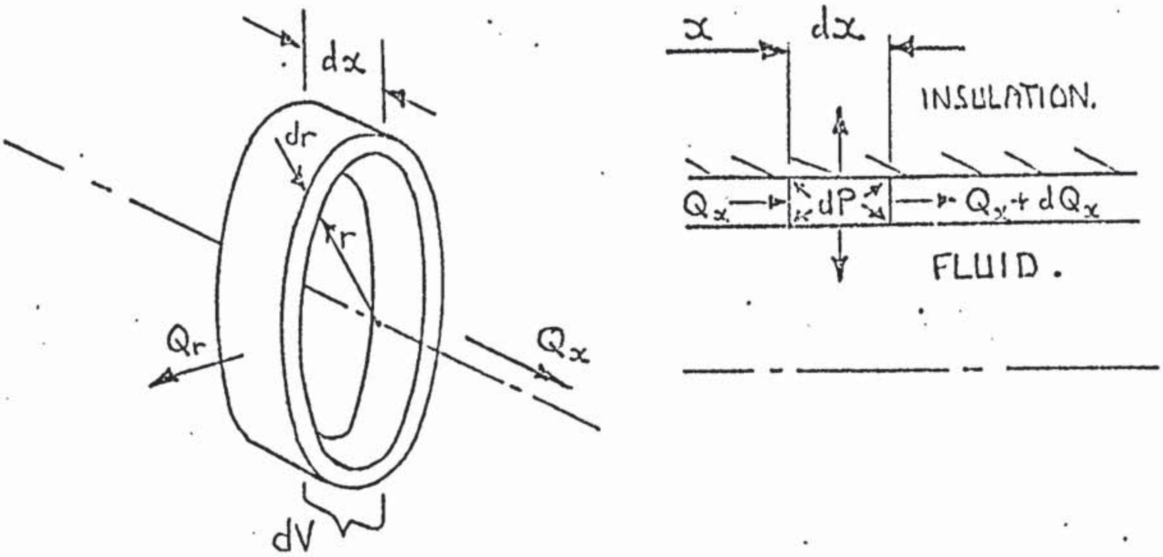

Figure: 8.1

Consider figure 8.1. The diagram shows the coordinates used to describe an elemental ring of the tube having axially symmetric temperature.

At the inside surface (i) heat is transferred to the fluid.

At the outside surface (o) a small quantity of heat is conducted through an imperfect insulator.

Assume: (i) Thermal and electrical properties vary little with temperature. (For stainless steel, as used in the experiments, electrical and thermal conductivities vary by a nominal 0.02 per cent per Kelvin).

(ii) The tube wall is thin compared with its radius. This cannot be defined any more specifically, but constitutes a necessary condition if the experimental method of measuring outside wall temperatures is considered valid, and this is likely to be the case when the overall temperature correction is much smaller than the temperature difference used in calculating heat transfer. (i.e. temperature drop across the tube wall is much less than the temperature difference between the inner tube surface and the entrained fluid.)

The conduction equation is

$$\frac{\partial^2 t}{\partial r^2} + \frac{1}{r}\frac{\partial t}{\partial r} + \frac{\partial^2 t}{\partial x^2} + \frac{1}{K_p e}\left(\frac{dV}{dx}\right)^2 = 0. \quad (8.1.)$$

From assumption (i) the fourth term becomes a constant (λ say). A solution may be obtained by separation of the variables, but the result would be in a fairly complex form and would be difficult to apply in practice, particularly since the two axial boundary conditions are not clearly defined.

An integral form of the equation was used in conjunction with certain assumptions based on (ii) (above) to give a more promising approach to the problem. This method, though not mathematically rigorous, yields an approximate solution containing a first order estimate for the effects of axial conduction in the tube wall (the third term in the equation).

Integrating the equation with 'x' constant,

$$r\frac{\partial t}{\partial r} + \int \frac{\partial^2 t}{\partial x^2} r\,dr + \frac{\lambda r^2}{2} + f(x) = 0. \quad (8.2)$$

the first boundary condition is $\frac{\partial t}{\partial r} = \frac{\partial t}{\partial r_o}(x, r_o)$, $r = r_o$,

giving

$$\frac{\partial t}{\partial r} + \frac{1}{r}\int \frac{\partial^2 t}{\partial x^2} r\,dr + \frac{\lambda r}{2} - \frac{1}{r}\left(\frac{\lambda r_o^2}{2} + r_o\frac{\partial t}{\partial r_o}\right) = 0 \quad (8.3).$$

A second integration with the condition $t = t_o(x, r_o)$, $r = r_o$, is written -

$$t - t_o + \int_{r_o}^{r}\frac{1}{r}\int_{r_o}^{r}\frac{\partial^2 t}{\partial x^2} r\,dr\,dr + \frac{\lambda}{4}\left(r^2 - r_o^2\right) - \left(\frac{\lambda r_o^2}{2} + r_o\frac{\partial t}{\partial r_o}\right)\log\left(\frac{r}{r_o}\right) = 0 \quad (8.4)$$

Now the second term may be evaluated approximately by making a plausible assumption regarding the magnitude of $\frac{\partial^2 t}{\partial x^2}$.

From (ii) it is implied that the form of $t_o(x)$ is similar to $t_i(x)$

so that
$$\left.\frac{\partial^2 t}{\partial x^2}\right|_o \simeq \left.\frac{\partial^2 t}{\partial x^2}\right|_i$$
It seems reasonable therefore to make $\frac{\partial^2 t}{\partial x^2}$ approximately $\left.\frac{\partial^2 t}{\partial x^2}\right|_o$, at least this will indicate how the second term affects the resulting temperature difference $(t_o - t_i)$, and a measure of reliability is achieved in practice when applying the resulting formula to particular experimental conditions.

Now the equation is

$$(t - t_o) = \left(\lambda + \frac{\partial^2 t}{\partial x_o^2}\right)\left(\frac{r_o^2 - r^2}{4}\right) + \left(r_o\frac{\partial t}{\partial r_o} + \frac{r_o^2}{2}\left[\lambda + \frac{\partial^2 t}{\partial x_o^2}\right]\right)\log\left(\frac{r}{r_o}\right) \quad (8.5)$$

Putting $\phi \equiv \left(\frac{\partial t}{\partial r}\right)$ and $S \equiv \left(\frac{r_i}{r_o}\right)$,

and replacing $\left(\lambda + \frac{\partial^2 t}{\partial x_o^2}\right)$ by $\frac{(S\phi_i - \phi_o)}{(1 - S^2)}\cdot\frac{1}{r_o}$ for convenience, the overall temperature difference is

$$(t_i - t_o) \doteq \frac{(\phi_i - S\phi_o)}{(1 - S^2)}\left[r_i \log(S) + S(1 - S^2)\frac{r_o}{2}\right] - (1 - S^2)\frac{r_o}{2}\cdot\phi_o \quad ; \quad (8.6)$$

where the ratio of axial to radial conduction of heat out of an element is approximately -

$$\text{RATIO} = K_p e.\frac{\partial^2 t}{\partial x_o^2}\Bigg/\left(\frac{dV}{dx}\right)^2 , \quad (8.7)$$

when radial conduction predominates.

The integration of the axial derivative could be improved by using a better approximation for the temperature profile, but this was considered unnecessary since it was required only to estimate the possible effects of axial conduction on the experimental results.

Equation (8.6) is the main result of the analysis, now the gradients ϕ_i and ϕ_o must be stated. Figure 8.1. shows how the heat is distributed in a short length of tube. The assumptions made already in deriving (8.6) apply here also. The equation describing this situation is:

$$\frac{dQ_i}{dx} = I\frac{dV}{dx} + \pi K_p(r_o^2 - r_i^2)\frac{\partial^2 t}{\partial x_o^2} - 2\pi K_{ins}(t_o - t_A)\Big/\log(r_A/r_o) \quad \ldots\ldots (8.8)$$

where t_A = ambient temp., r_A = mean outer radius insulation,

also $Q_i' = V.I/L + \pi K p.r_o^2.(1 - S^2)\frac{\partial^2 t}{\partial x_o^2} - Q_{ins}'$, (8.9)

and $Q_{ins}' = 2\pi K_{ins}(t_o - t_n) / \log(r_A/r_o)$ (8.10) with Q' - heating rate per unit length

Subscript ins - insulation.

V, L - Total applied voltage and length over which applied.

Note that ϕ_o and ϕ_i may be easily obtained using (8.9) and (8.10), as follows:

$$\phi_i = Q_i' / (2\pi K_P r_i) , \qquad (8.11)$$

and

$$\phi_o = Q_{ins}' / (2\pi K_P r_o). \qquad (8.12)$$

The preceding analysis results in equations (8.6), (8.9) and (8.10) which permit a first order approximation for axial conduction effects. If these are set at zero, the result is similar to that obtained by Ede (Ref: H.2). Although no great accuracy is claimed by using this form of solution, a clarification of assumptions has been made, and an order of magnitude for axial conduction terms is permitted; this will be discussed quantitatively in part 9.

The term $\frac{\partial^2 t}{\partial x^2}_o$ can be found in practice by using three, adjacent, local temperatures, the accuracy improves as the gap between thermocouples reduces. The result is like a parabolic interpolation on the axial temperature profile,

i.e.
$$\frac{\partial^2 t}{\partial x^2}_o = \left\{ \frac{(t_3 - t_2)}{(x_3 - x_2)} - \frac{(t_2 - t_1)}{(x_2 - x_1)} \right\} . \frac{2}{(x_3 - x_1)} \qquad (8.13)$$

The values for the thermal conductivities of type 321 AISI stainless steel, and moulded polystyrene insulation are taken to be 15.5 $\frac{W}{mK}$ and 0.033 $\frac{W}{mK}$. The values are assumed to be constant.

8.2.(d) The bulk fluid temperature.

To calculate the bulk fluid temperature at each axial location, a summation must be made of the heat addition to the fluid between the tube entrance and the section of interest. In general, the configuration consisted of an unheated length of tube with conduction through the insulation, which preceded an upstream-tube with a given power input and heat conduction through the insulation, then a downstream-tube having a different power input. The calculation for temperature rise in the fluid is a simple one which can be applied over short lengths of the tubes, the total temperature rise being the summation of all such lengths.

Q_i' = local heating rate per unit length

H = specific enthalpy of fluid.

If $(x_2 - x_1)\,\bar{Q}_i' = (H_2 - H_1).\,\rho.\,F.$,

then $(t_2 - t_1) = \dfrac{\bar{Q}_i'\,(x_2 - x_1)}{\rho.\ \bar{C}\ .\ F.}$ (8.14)

where ρ = Density at inlet to tube,

F = Volume flow rate at inlet,

$\bar{C}$ = Mean specific heat capacity.

Note that $\bar{C} = \dfrac{1}{(t_2 - t_1)} \displaystyle\int_{t_1}^{t_2} C \; dt \; \triangleq \dfrac{(C_1 + C_2)}{2}$

and $\bar{Q}_i' = \dfrac{1}{(x_2 - x_1)} \displaystyle\int_{x_1}^{x_2} Q_i' \; dx \; \triangleq \dfrac{(Q_{i1}' + Q_{i2}')}{2}$.

Since '$\bar{C}$' is a function of temperature, the fluid temperature rise is calculated using two iterations of the formula stated, updating '$\bar{C}$' at each stage.

8.2(c) Dimensionless groups and heat-transfer coefficients.

The local dimensionless groups Reynolds, Prandtl and Grashof numbers together with the viscosity ratio (μ_{bulk}/μ_{wall}), were calculated at each axial location in the tube. Little explanation is required for these straightforward computations, it should be mentioned however that all properties were obtained by a simple call on the interpolation 'procedure', and that the reference temperature utilised was the bulk temperature of the fluid. (This was the most convenient reference, and conforms with the generally established practice in tube flow problems, as discussed in part 2.3.(iii)). One obvious exception is the viscosity ratio (μ_{bulk}/μ_{wall}) which requires viscosity at the local wall temperature. Some further notes follow which give details of formulae used in the programme:

(i) $$Re = \left(\frac{2\ \rho_o\ F_o}{\pi\ \mu_b\ r_i}\right) \qquad Pr = \left(\frac{\mu_b\ C_b}{K_b}\right)$$

Viscosity Ratio, $M_{wall} = \left(\frac{\mu_b}{\mu_w}\right)$

$$Gr = \left(\frac{(2r_i)^3\ (\rho_b)^2\ \beta(t_w - t_b)\ g}{(\mu_b)^2}\right)$$

Where ρ_o, F_o - Density, Volume flow rate at inlet.

μ_b - Local viscosity at bulk temperature.

μ_w - Local viscosity at wall temperature.

r_i - Local, inner tube radius

C_b - Local, bulk specific heat capacity.

K_b - Local, bulk thermal conductivity.

P - Per cent glycol in water by weight.

h - Local heat transfer coefficient.

t_w - Local, inner wall temperature.

t_b - Local bulk fluid temperature.

β - Local bulk coeffient of thermal expansion.

(ii) In deriving the Grasho f group, it was necessary to know the local coefficient of thermal expansion at the bulk temperature. This property was obtained from the density reference data, and a graph of the values was plotted (Figure: 8.5). These coefficients werebased on density difference over a 20K temperature variation in order to establish reasonable accuracy (density differences being small). The results were found to be linear in temperature, and hence expressible in a single formula for a given glycol mixture. The numerical constants, however were highly dependent on the composition of the liquid, and were expressed as second order polynomials in 'per cent glycol by weight (P)'. The following numerical formulae were derived:

$$\text{for } 30 < P < 70, \beta\left(\frac{10^{-6}}{K}\right) = (6.065 - 0.0615.P)\ t(^{\circ}C) - 7.050 + 15.27.P - 0.07875.P^2, \qquad (8.15)$$

$$\text{and } 70 < P < 100, \beta\left(\frac{10^{-6}}{K}\right) = (0.6880 + 0.0016.t(^{\circ}C)).10^3 . \qquad (8.16)$$

The formulae well represented the experimentally derived β values, the average scatter being approximately 1% with a maximum of 2½% in the range 20°C to 70°C. (Figure: 8.5).

8.3. A DATA REDUCTION COMPUTER PROGRAMME FOR TUBES HAVING A DIAMETER DISCONTINUITY.

The computor programme given here (see Figure: 8.6) was based on the calculations shown in 8.2. It was used to reduce the data obtained from the experiments on two straight tubes connected in line, having different heat generations and with different diameters. It will be obvious after inspecting it that few modifications would be necessary to permit its application to other similar experimental configurations. The cases of no diameter change, and of heating only one tube were dealt with using nearly identical programmes. A flow chart (Figure: 8.6.) shows the simplicity of the programme construction.

The programming language Algol 60 was used, and the computor was an ICL 1905. Early calculations were carried out on an Elliot 805 with the Elliot Algol language, but the programmes were substantially the same. A typical computing time for one set of test data would be about 20 to 30 seconds, but this depended on the total volume of data input. It should be noted that a large section of the programme deals with the output of results, and the requirements here could vary considerably. In the case shown various combinations of dimensionless groups were computed, the details are unimportant since they illustrate merely the kind of output which was found to be useful in a particular analysis of experimental results.

A list of programming symbols (and units) follows:—

Subscript H = 1 for upstream tube, 2 for downstream tube.

Subscript G = Number of axial thermocouple locations from start of heating.

XX[H]	Number of thermocouple locations (axial) less one.
TIN, TOUT	Bulk fluid temperature at inlet and outlet ($^{\circ}$ C)
FLO	Volume flow rate at inlet (10^{-3} m^3/s)
V[H]	Voltage applied to tube (Volts).
I	Current through tube walls (Amperes).
L[H]	Length of heated section (m)
RI, RO[H]	Inner and outer tube radii (cm).
LU	Unheated length of tube upstream of heated section (m).
TAMB	Ambient temperature ($^{\circ}$C).
KP	Tube thermal conductivity (W/mK).
KINS	Insulation thermal conductivity (W/mK).
RA	Outer radius of insulation (cm).
S[H]	Ratio inner/outer tube radii.
COMP	Percentage of glycol in water by weight.
K	Thermal conductivity (cal/cm.s$^{\circ}$C)*
VC	Viscosity (centipoise).
CP	Specific heat capacity(cal/g.$^{\circ}$C).*
DS	Density (10^3kg/m^3).

(K, VC, CP, DS:) Tabulated properties of propylene glycol-water mixtures. Double subscript used i.e. [W,H] where W and H denote number of temperature and % glycol increments up to position in the table.

X[H]	Axial distance from start of heating (tube diameters).
TIT, TPC [H,G]	Local inner and outer surface tube temperatures ($^{\circ}$C, or calibration V).
QI[H,G]	Local heating rate per unit length, to fluid (W/m).

QINS [H,G]	Local heating rate per unit lenght, through insulation (W/m)
TX [H,G]	Local bulk fluid temperature (^{o}C)
KX, DSX, CPX, VCX [H,G]	Interpolated values of DS, CP, VC and K for given mixture and temperature.
RE [H,G]	Local tube Reynolds number
GRX [H,G]	Local tube Grashoff number
PRX [H,G]	Local, bulk fluid Prandtl number
NUX [H,G]	Nusselt number at given axial location
M [H,G]	Viscosity ratio, bulk fluid/tube surface
B [H,G]	Local, bulk coefficient of thermal expansion of fluid (K^{-1})
CALT, CALV	Thermocouple calibration temperatures (^{o}C) and corresponding potentials (μV).
TI, PI	The size of temperature and per cent increments in property arrays (K, %).
II, JJ	The number of temperature and per cent increments stored for a given property.

All other symbols used are dummy variables used to facilitate programme contruction. The following titles are given to function-procedures:

INT	Interpolation procedure used to derive intermediate properties from the reference data supplied
CAL	Conversion of thermocouple readings (μV) to temperature (^{o}C)

* Note that the use of 'caloric' does not conform with the SI system of units (BSI publication PD5686), and is included here simply because the relevant property data was obtained by direct reference to Curme (Ref: K.8) who preferred this unit.

8.4. THE HEAT BALANCE.

In part 5.6. there is a description of the calculations carried out to determine the distribution of energy over a closed boundary which surronds the system. It was found that the temperature rise obtained in propylene glycol solutions passing through the test-section was very small; usually less than 1 K, and often less than 0.5 K. This is a consequence of the high Prandtl numbers encountered in the experiments, because for a given temperature difference between tube and fluid, and for a given Re the rise in the bulk temperature of the fluid, Δt_{bulk}, is related to Pr in the following way:

$$\Delta t_{bulk} \propto Pr^{-\frac{2}{3}} \quad .$$

Initially, a heat balance was attempted for each experiment carried out, and the calculations were incorporated into the computer programme (8.3.) This practice was abandoned because of limitations on the reliability of the results; for example; for a rise in bulk temperature of 0.25 K, the confidence limits on the thermocouple readings gave rise to at least $\pm$ 20 % uncertainty in the calculated enthalpy rise of the fluid.

Heat balances were obtained for several tests on the uniform diameter tube where favourable conditions prevailed (a bulk temperature rise greater than 0.5 K). These were discussed earlier in part 5.6.

Figure 8.2.

Flowmeter calibration.

Frequency (c/s)	Flowrate Small meter ($10^{-3}m^3/S$)			Flowrate Large meter ($10^{-3}m^3/S$)		
	Kinematic Viscosity			Kinematic Viscosity		
	1 c St	25 c St	50 c St	1 c St	25 cSt	50 cSt
150	0.15608	0.16888	0.17563	1.6054	1.5712	1.5865
250	0.26018	0.27572	0.28277	2.6890	2.6091	2.6278
500	0.51866	0.54356	0.55212	5.3780	5.2229	5.2217
600	-	-	-	8.6253	6.2965	6.3009
800	0.82541	0.86716	0.88095			
1,000	1.03060	1.07673	1.09363			

Figure 8.3.

Thermocouple calibration.

Temperature(°C)	10	14	18	22	26	30
Microvolts	431	599	773	948	1126	1306
Temperature(°C)	34	38	42	46	50	54
Microvolts	1485	1668	1851	2035	2222	2410
Temperature(°C)	58	62	66	70	74	78
Microvolts	2599	2790	2982	3173	3367	3565
Temperature(°C)	82	86	90	95		
Microvolts	3761	3961	4161	4360		

FIGURE 8.4.

VISCOSITY OF PROPYLENE GLYCOL MIXTURES—INTERPOLATION.

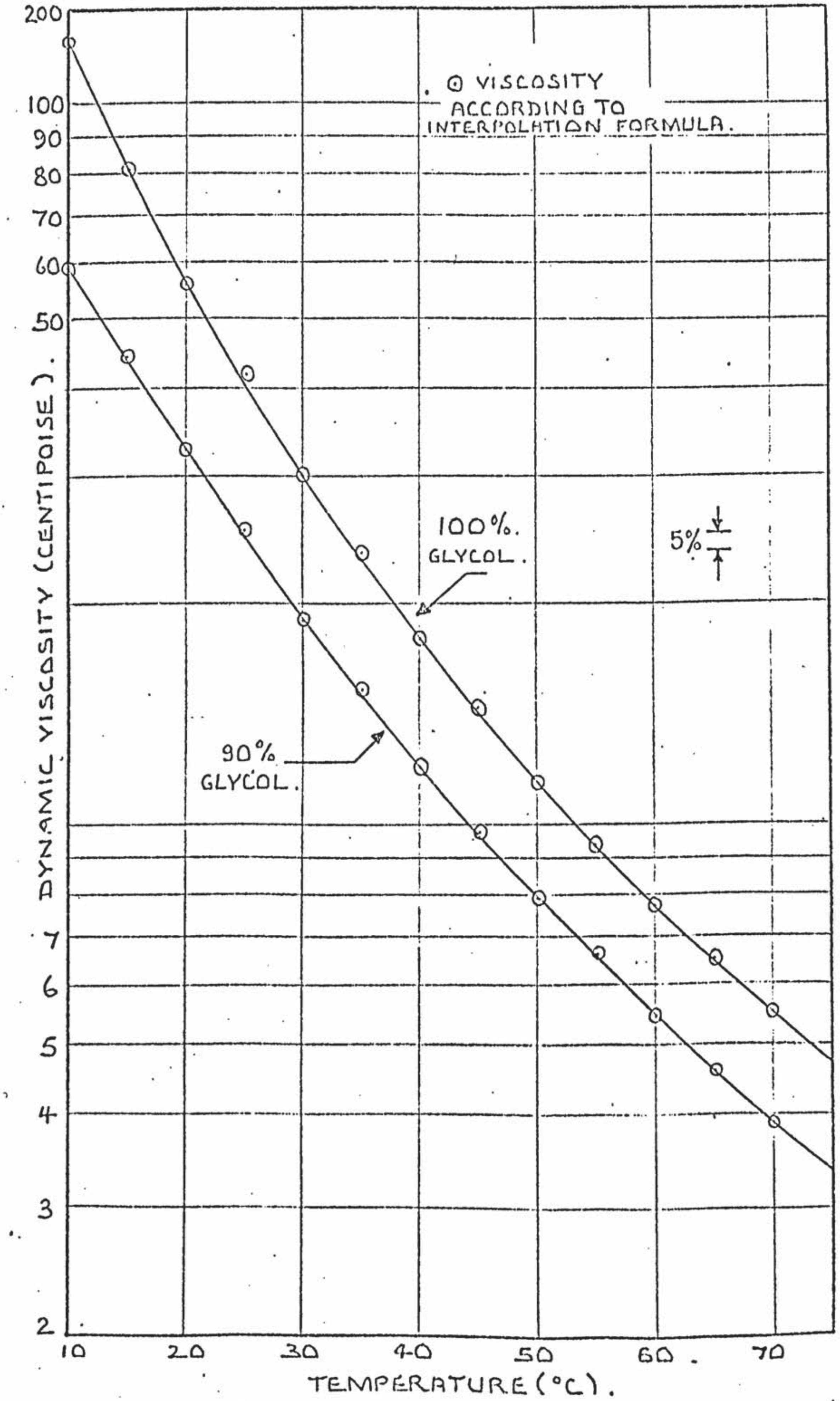

FIGURE 8.5.

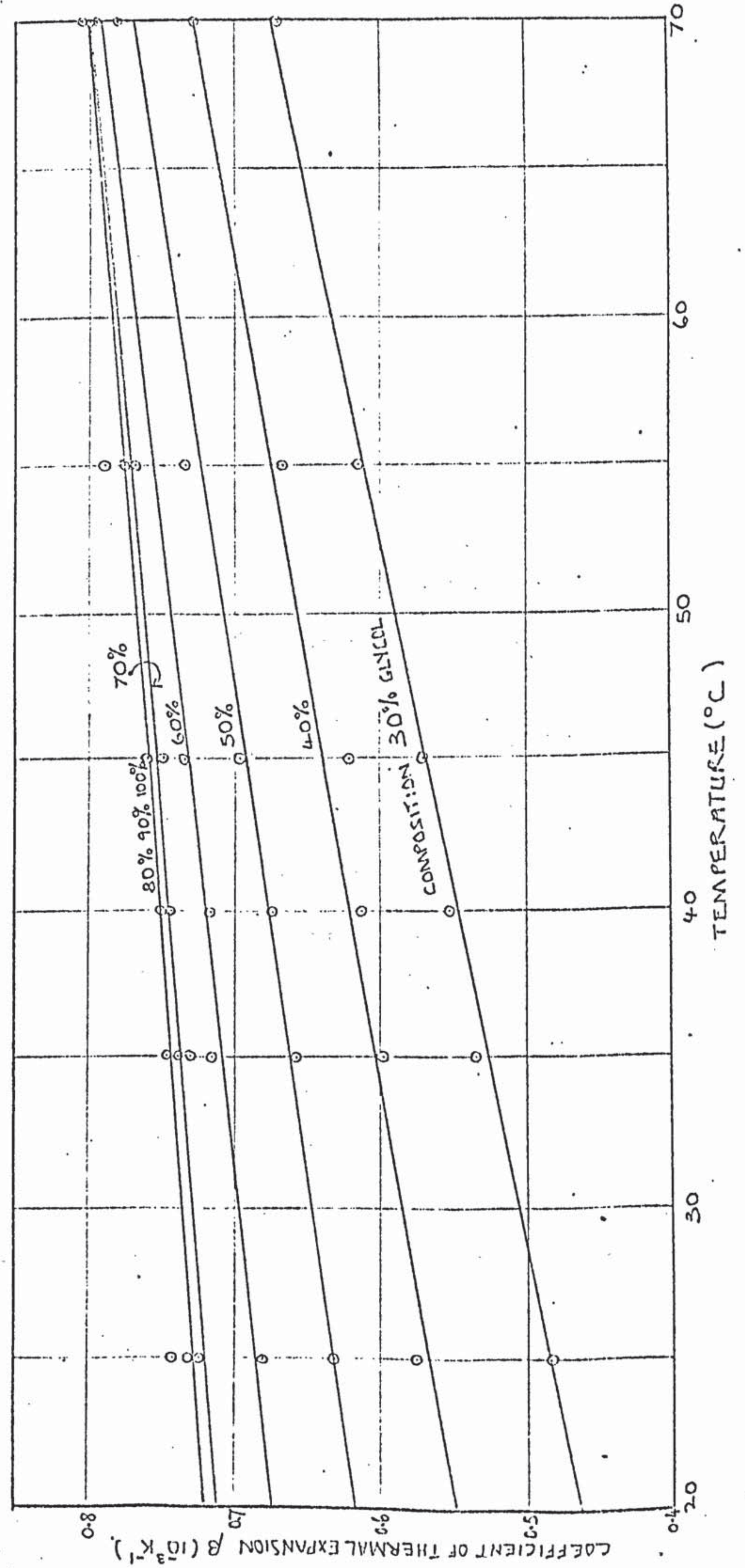

THE COEFFICIENT OF THERMAL EXPANSION FOR AQUEOUS PROPYLENE GLYCOL MIXTURES.

FIGURE 8.6.

COMPUTOR - PROGRAMME FLOW-CHART FOR REDUCTION OF RAW DATA.

'SECTCHANGE'

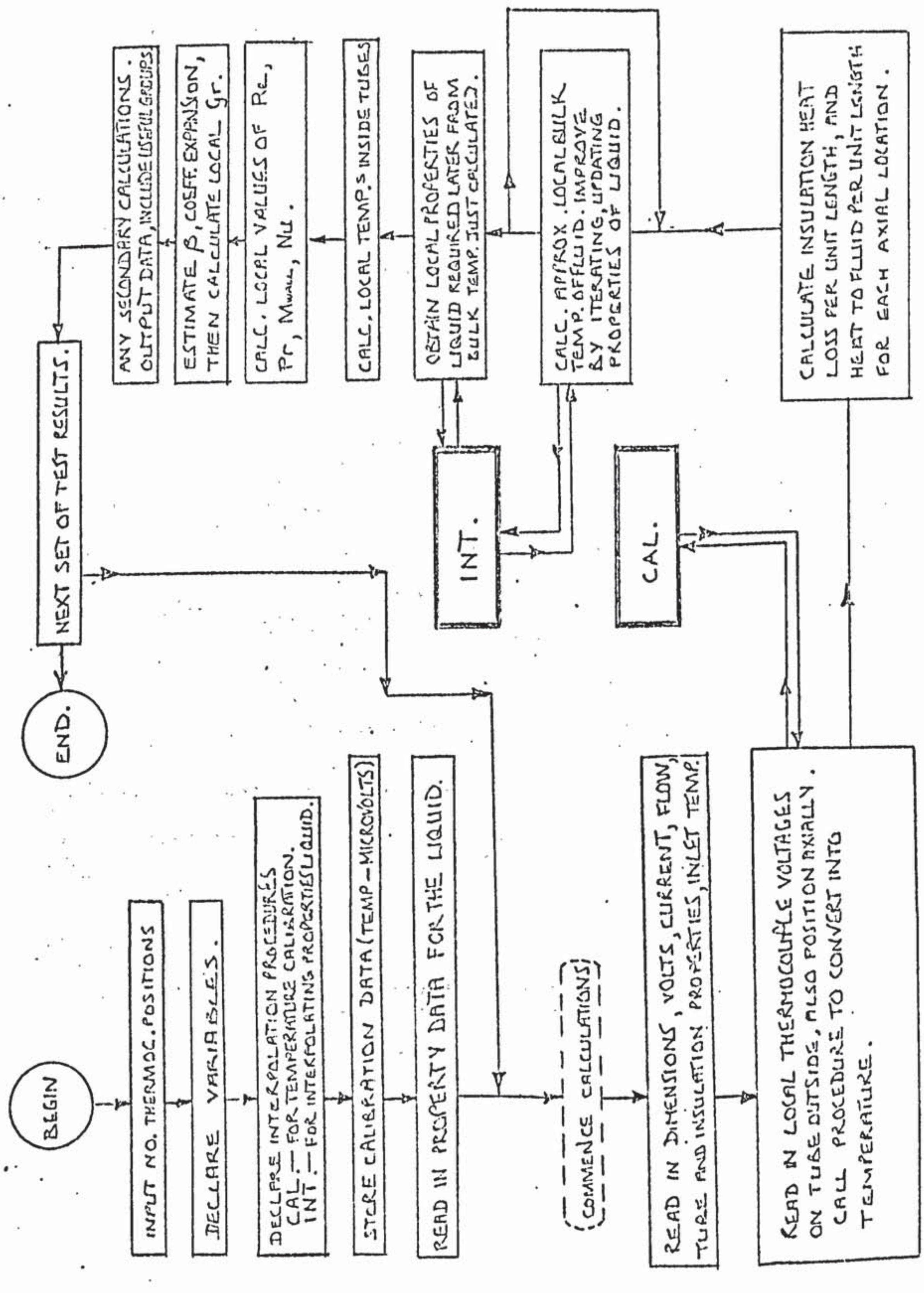

```
'BEGIN' 'COMMENT' MESTF116    SECTCHANGE;

'COMMENT' READ IN NO. THERMO. LOCATIONS;

'INTEGER' 'ARRAY' XX[1:2];    XX[1]:=READ; XX[2]:=READ;

'COMMENT' DECLARE VARIABLES;

'BEGIN' 'REAL' TIN,TOUT,FIO,I,TAMB,KP,KINS,RA,COMP,LU;
'INTEGER' G,E,H,W;   'REAL' 'ARRAY' K[0:7,0:5],VC,CP,DS[0:7,0:10],TPO,
TPI,X,QINS,QI,TX,DSX,CPX,VCX,KX,RE,PRX,M,NUX,B,GRX[1:2,0:XX[2]],CALV,
CALT[0:21],V,I,RO,RI,S[1:2];

'COMMENT' DECLARE SUB ROUTINES;

'COMMENT' INTERPOLATION SUB ROUTINE;

'REAL' 'PROCEDURE' INT(TW,PX,PI,TI,II,JJ,A);
'VALUE' TW,PX,PI,TI,II,JJ;   'REAL' TW,PX;' 'REAL' 'ARRAY' A;
'INTEGER' PI,TI,II,JJ;
'BEGIN' 'REAL' 'ARRAY' AA[1:3],T[0:7],P[0:10];   'INTEGER' Y,N,M;
'FOR' N:=0 'STEP' 1 'UNTIL' II 'DO'  T[N]:=N*TI;
'FOR' M:=0 'STEP' 1 'UNTIL' JJ 'DO'  P[M]:=M*PI;     N:=0; M:=0;
FF: 'IF' TW>T[N] 'THEN' 'BEGIN' N:=N+1; 'GOTO' FF; 'END';
BB: 'IF'   PX>P[M] 'THEN'   'BEGIN' M:=M+1; 'GOTO' BB 'END';
         Y:=1; N:=N-2;  M:=M-1;
CC: 'IF' A[N,M]=A[N,M-1] 'OR' A[N,M-1]=A[N,M+1] 'THEN'
'BEGIN' AA[Y]:=A[N,M];  'GOTO' DD; 'END';
AA[Y]:=A[N,M-1]+(A[N,M+1]-A[N,M-1])*((PX-P[M-1])/(P[M+1]-P[M-1]))'**'
(LN((
A[N,M]-A[N,M-1])/(A[N,M+1]-A[N,M-1]))/LN((P[M]-P[M-1])/(P[M+1]-P[M-1])))
; DD: 'IF' Y<3 'THEN' 'BEGIN' Y:=Y+1; N:=N+1; 'GOTO' CC; 'END'; N:=N-1;
'IF' AA[1]=AA[2] 'OR'  AA[2]=AA[3] 'OR' AA[3]=AA[1] 'THEN'
'BEGIN' INT:=AA[2]; 'GOTO' EE; 'END';
INT:=AA[1]+(AA[3]-AA[1])*((TW-T[N-1])/(T[N+1]-T[N-1]))'**'(LN((AA[2]-
AA[1])
/(AA[3]-AA[1]))/LN((T[N]-T[N-1])/(T[N+1]-T[N-1])));
EE: 'END' INT;

'COMMENT' THERMOC. CALIBRATION SUB ROUTINE;

'REAL' 'PROCEDURE' CAL(AV,CV,CT); 'VALUE' AV; 'REAL' AV; 'REAL' 'ARRAY'
CV,CT;     'BEGIN' 'INTEGER' U; U:=0;     LL: 'IF' AV>CV[U] 'THEN'
'BEGIN' U:=U+1; 'GOTO' LL; 'END';     CAL:=CT[U-1]+(AV-CV[U-1])*
(CT[U]-CT[U-1])/(CV[U]-CV[U-1]);   'END' CAL;

'COMMENT' CALIB. DATA;

CALT[0]:=10; 'FOR' H:=1 'STEP' 1 'UNTIL' 21 'DO' CALT[H]:=CALT[H-1]+4;
CALV[0]:=431;  CALV[1]:=599; CALV[2]:=773; CALV[3]:=948; CALV[4]:=1126;
CALV[5]:=1306; CALV[6]:=1485; CALV[7]:=1668; CALV[8]:=1851;
CALV[9]:=2035; CALV[10]:=2222; CALV[11]:=2410; CALV[12]:=2599;
CALV[13]:=2790; CALV[14]:=2982; CALV[15]:=3173; CALV[16]:=3367;
CALV[17]:=3565; CALV[18]:=3761; CALV[19]:=3961; CALV[20]:=4161;
CALV[21]:=4360;
```

```
'COMMENT' READ IN PROPERTY DATA;

'FOR' H:=0 'STEP' 1 'UNTIL' 5 'DO' 'FOR' W:=0 'STEP' 1 'UNTIL' 7 'DO'
  K[W,H]:=READ;
'FOR' H:=0 'STEP' 1 'UNTIL' 10 'DO' 'FOR' W:=0 'STEP' 1 'UNTIL' 7 'DO'
  VC[W,H]:=READ;
'FOR' H:=0 'STEP' 1 'UNTIL' 10 'DO' 'FOR' W:=0 'STEP' 1 'UNTIL' 6 'DO'
  CP[W,H]:=READ;
'FOR' H:=0 'STEP' 1 'UNTIL' 10 'DO' 'FOR' W:=0 'STEP' 1 'UNTIL' 7 'DO'
  DS[W,H]:=READ;

'COMMENT' START CALCS.                    *********** ;

'COMMENT' READ IN EXPERIMENTAL DATA;

AGAIN: TIN:=READ; TOUT:=READ; FLO:=READ; I:=READ; TAMB:=READ; KP:=READ;
KINS:=READ; RA:=READ; COMP:=READ; LU:=READ; 'FOR' G:=1,2 'DO' 'BEGIN'
V[G]:=READ; L[G]:=READ; RO[G]:=READ; RI[G]:=READ;              'END';
TIN:=CAL(TIN,CALV,CALT); 'IF' TOUT>100 'THEN' TOUT:=CAL(TOUT,CALV,CALT);

'COMMENT' READ TUBE TEMPS AND LOCATIONS;

'FOR' H:=1,2 'DO' 'BEGIN' S[H]:=RI[H]/RO[H];
'FOR' G:=0 'STEP' 1 'UNTIL' XX[H] 'DO' 'BEGIN' X[H,G]:=READ;
TPO[H,G]:=READ; TPO[H,G]:=CAL(TPO[H,G],CALV,CALT); 'END';

'COMMENT' CALC. LOSS THRO. INSULATION THEN LOCAL HEAT FLUX;

'FOR' G:=1 'STEP' 1 'UNTIL' (XX[H]-1) 'DO' 'BEGIN'
QINS[H,G]:=2*3.1416*KINS*(TPO[H,G]-TAMB)/LN(RA/RO[H]);
QI[H,G]:=V[H]*I/L[H]+3.1416*KP*(RO[H]'**'2)*(1-S[H]'**'2)*((TPO[H,(G+1)
]-
TPO[H,G])/(X[H,(G+1)]-X[H,G])-(TPO[H,G]-TPO[H,(G-1)])/(X[H,G]-X[H,(G-1)]
))/((X[H,(G+1)]-X[H,(G-1)])*0.5*(2*RI[H])'**'2)-QINS[H,G];    'END';
QINS[H,0]:=QINS[H,1];    QINS[H,XX[H]]:=QINS[H,(XX[H]-1)];
QI[H,0]:=QI[H,1]; QI[H,XX[H]]:=QI[H,(XX[H]-1)]; 'END';

'COMMENT' CALC. LOCAL FLUID TEMPS;

DSX[1,0]:=INT(TIN,COMP,10,10,7,10,DS);     CPX[1,0]:=INT(TIN,COMP,10,10,6
,10,CP);  TX[1,0]:=TIN-(2*3.1416*KINS*LU*(TIN-TAMB)/LN(RA/RO[1]))/(DSX[1
,0]*FLO*CPX[1,0]*4.185&3);    CPX[1,0]:=INT(TX[1,0],COMP,10,10,6,10,CP)
;'FOR' H:=1,2 'DO' 'BEGIN' 'FOR' G:=1 'STEP' 1 'UNTIL' XX[H] 'DO'
'BEGIN'
'IF' H=2 'AND' G=1 'THEN' 'BEGIN' TX[2,0]:=TX[1,XX[1]]; CPX[2,0]:=CPX[1,
XX[1]]; 'END';
'BEGIN' TX[H,G]:=(X[H,G]-X[H,(G-1)])*RI[H]*(QI[H,G]+QI[H,(G-1)])/((CPX[H
,(G-1)]*FLO*DSX[1,0])*(4.185&5))+TX[H,(G-1)];       E:=0;
CYCLE: CPX[H,G]:=INT(TX[H,G],COMP,10,10,6,10,CP);
TX[H,G]:=(X[H,G]-X[H,(G-1)])*RI[H]*(QI[H,G]+QI[H,(G-1)])/((0.5*(
CPX[H,(G-1)]+CPX[H,G])*FLO*DSX[1,0])*(4.185&5))+TX[H,(G-1)];
'IF' E<1 'THEN' 'BEGIN' E:=E+1; 'GOTO' CYCLE 'END'; 'END'; 'END';
'END';

'COMMENT' OBTAIN LOCAL PROPERTIES AND CALC. INSIDE TUBE TEMPS. ;

'FOR' H:=1,2 'DO' 'BEGIN' 'FOR' G:=0 'STEP' 1 'UNTIL' XX[H] 'DO' 'BEGIN'
  DSX[H,G]:=INT(TX[H,G],COMP,10,10,7,10,DS);  KX[H,G]:=INT(TX[H,G],
COMP, 20,10,7,5,K);    VCX[H,G]:=INT(TX[H,G],COMP,10,10,7,10,VC);
```

```
TPI[H,G]:=TPO[H,G]+((QI[H,G]+(S[H]'**'2)*QINS[H,G])/(4*3.1416*KP))*(
1-2*(
LN(1/S[H]))/(1-S[H]'**'2))+(1-S[H]'**'2)*QINS[H,G]/(4*3.1416*KP);

'COMMENT' CALC. RE,VISC.RATIO,PR,NU LOCALLY;

RE[H,G]:=2*DSX[1,0]*FLO/(3.1416*VCX[H,G]*RI[H]*(1&-5));
M[H,G]:=VCX[H,G]/(INT(TPI[H,G],COMP,10,10,7,10,VC));
PRX[H,G]:=VCX[H,G]*CPX[H,G]/(KX[H,G]*100);
NUX[H,G]:=QI[H,G]/(3.1416*KX[H,G]*(TPI[H,G]-TX[H,G])*418.5);

'COMMENT' OBTAIN LOCAL COEFF.EXPANSION AND CALC. GR;

'IF' COMP'LE'70 'THEN' B[H,G]:=((6.06-.0615*COMP)*TX[H,G]-7.05+15.27*
COMP-
.07875*(COMP'**'2))*(1&-6);    'IF' COMP>70 'THEN'
B[H,G]:=(.688+.0016*TX[H,G])*(1&-3);GRX[H,G]:=((2*RI[H])'**'3)*(DSX[H,G
]'**'2)*B[H,G]*(TPI[H,G]-TX[H,G])/(VCX[H,G]'**'2)*(9.80686); 'END';
'END';

'COMMENT' END OF MAIN CALCS.                  **********
          NOW OUTPUT DATA. THIS SECTION INCLUDES ANY USEFUL MINOR CALCS.
          REQUIRED OUTPUT MAY VARY BETWEEN TESTS;

WRITETEXT('(''('P4C')'TEST%NO.')');
NEWLINE(2);
'FOR' H:=1,2 'DO' 'BEGIN' 'FOR' G:=0 'STEP' 1 'UNTIL' XX[H] 'DO'
'BEGIN' WRITETEXT('(''('1C')'X=')');      PRINT(X[H,G],3,1);
WRITETEXT('(''('2S')'NU=')'); PRINT(NUX[H,G],3,2); WRITETEXT('(''('1C')'
RE=')'); PRINT(RE[H,G],5,0); WRITETEXT('(''('2S')'PR=')'); PRINT(PRX[H,G
],3,1); WRITETEXT('(''('2S')'M=')'); PRINT(M[H,G],1,2); WRITETEXT('(''('
2S')'GR=')'); PRINT(GRX[H,G],6,0);  WRITETEXT('(''('1C')'TPO=')');
PRINT(TPO[H,G],2,2);  WRITETEXT('(''('2S')'TPI=')'); PRINT(TPI[H,G]
,2,2);
WRITETEXT('(''('2S')'TX=')'); PRINT(TX[H,G],2,2); WRITETEXT('('DEGC')');
WRITETEXT('(''('8S')'Q=')'); PRINT(QI[H,G]/(.06283*RI[H]),6,0);
WRITETEXT('(''('2S')'QL=')'); PRINT(QINS[H,G]/(.06283*RI[H]),3,2);
'END'; 'END'; WRITETEXT('(''('P4C')'TEST%NO.')');
WRITETEXT('(''('2C')'V1=')'); PRINT(V[1],2,3); WRITETEXT('(''('2S')'V2='
)'); PRINT(V[2],2,3); WRITETEXT('(''('2S')'I=')'); PRINT(I,3,1);
WRITETEXT('(''('2C')'TIN=')'); PRINT(TIN,2,2); WRITETEXT('(''('2S')'TOUT
=')');
PRINT(TOUT,2,2); WRITETEXT('(''('2C')'TOTH=')'); PRINT(TX[2,XX[2]],2,2);
WRITETEXT('(''('2C')'R1=')'); PRINT(RI[1],1,3); WRITETEXT('(''('2S')'R2=
')'); PRINT(RI[2],1,3); WRITETEXT('(''('2S')'L1=')'); PRINT(L[1],1,3);
WRITETEXT('(''('2S')'L2=')'); PRINT(L[2],1,3); WRITETEXT('(''('2C')'FLUX
1=')'); PRINT(V[1]*I/(L[1]*.06283*RI[1]),6,1); WRITETEXT('(''('2S')'FLUX
2=')'); PRINT(V[2]*I/(L[2]*.06283*RI[2]),6,1);
WRITETEXT('(''('2S')'VISC=')'); PRINT(VCX[2,0],2,2);
WRITETEXT('(''('C4S')'X'('11S')'M14'('9S')'GP'('10S')'GP4'('9S')'N/P3'('
8S')'N/P3M14'('5S')'RP'('10S')'GP4/RP3'('6S')'N/RP3'('6S')'N/RP3M14')');
'FOR' H:=1,2 'DO' 'BEGIN' 'FOR' G:=0 'STEP' 1 'UNTIL' XX[H] 'DO' 'BEGIN'
'IF' GRX[H,G]>1 'THEN' 'BEGIN'
NEWLINE(1); PRINT(X[H,G],0,3); PRINT((M[H,G]'**'.14),0,3); PRINT((GRX[H,
G]*
PRX[H,G]),0,3); PRINT(((GRX[H,G]*PRX[H,G])'**'.25),0,3); PRINT((NUX[H,G]
/(
PRX[H,G]'**'.333)),0,3); PRINT(NUX[H,G]/((PRX[H,G]'**'.333)*(M[H,G]'**'
.14)),0,3
); PRINT((RE[H,G]*PRX[H,G]),0,3); PRINT(((GRX[H,G]*PRX[H,G])'**'.25)/((
```

```
RE[H
,G]*PRX[H,G])'**'.333),0,3); PRINT((NUX[H,G]/((RE[H,G]*PRX[H,G])'**'.333
)),0,3
); PRINT((NUX[H,G]/((RE[H,G]*PRX[H,G])'**'.333)/(M[H,G]'**',14)),0,3);
'END';
'END'; NEWLINE(2); 'IF' TOUT>10 'THEN' 'BEGIN' PRINT(CPX[1,0],0,3);
PRINT((INT(TOUT,COMP,10,10,6,10,CP)),0,3); 'END';
'END';
'GOTO' AGAIN; 'END'; 'END';
```

9. ANALYSIS OF THE RESULTS.

9.1. THE RELIABILITY AND SIGNIFICANCE OF TEMPERATURE MEASUREMENTS.

The local coefficients of heat transfer, which are referred to throughout this thesis, are measured or calculated from the mixed, mean temperature of the fluid, and the circumferential mean temperature at the inner surface of the tube. This is not to say that the temperature distribution within the fluid was axi-symmetrical, indeed vertical symmetry and asymmetry were both encountered. Although the relavence of such phenomena will be considered in part 9, the greater portion of this discussion concerns the axial distributions of Nu.

The local temperature and heat flux were susceptible to errors induced through inaccurate measurements, variations in the wall thickness, the conduction of heat in the tube-wall and changes with time in the fluid flow pattern. A critical appraisal of the thermocouple measurements has already been carried out, (5.3., 5.4., 6.3.) so the first source of error mentioned may be disregarded in this discussion. The local heat flux was proportional to the wall thickness and must have had a similar fractional variation from the mean value. Since the cross-sectional area of a cold drawn, seamless tube can be considered constant, the circumferential mean temperature at any axial position must have been independent of small, dimensional variations. The second source of error can therefore be disregarded for practical reasons. Parts 9.2. and 9.3. include an appreciation of the 'conduction' and 'time dependent' aspects of tube temperature measurement. These possible sources of error bear closer examination since the magnitudes involved were difficult to determine.

9.2. THE EFFECTS OF TUBE WALL CONDUCTION.

In calculating the local temperature and heat flux at the inner surface of the tube an estimate was made for the amount of heat conducted axially, radially and circumferentially in the wall. The temperature difference across the wall and the heat flux were assessed for the case of no circumferential conduction and a small amount of axial conduction.

It was discovered during the experimental work however that at low values of Re ($<$ 2000) and for large axial distances ($>$ 20 diameters) the top of the tube was considerably hotter than the bottom. This gave rise to a distortion of the circumferential temperature distribution, and the corresponding 'point' value for the coefficient of heat transfer, h_s, (this parameter is defined below, and has relevance only within the present discussion.) The extent to which circumferential conduction affected the measured values of h_s was determined as follows:-

Consider the coordinate system below and the assumptions stated. The model proposed takes a rather crude view of the convection process, since conduction in the tube is the main concern.

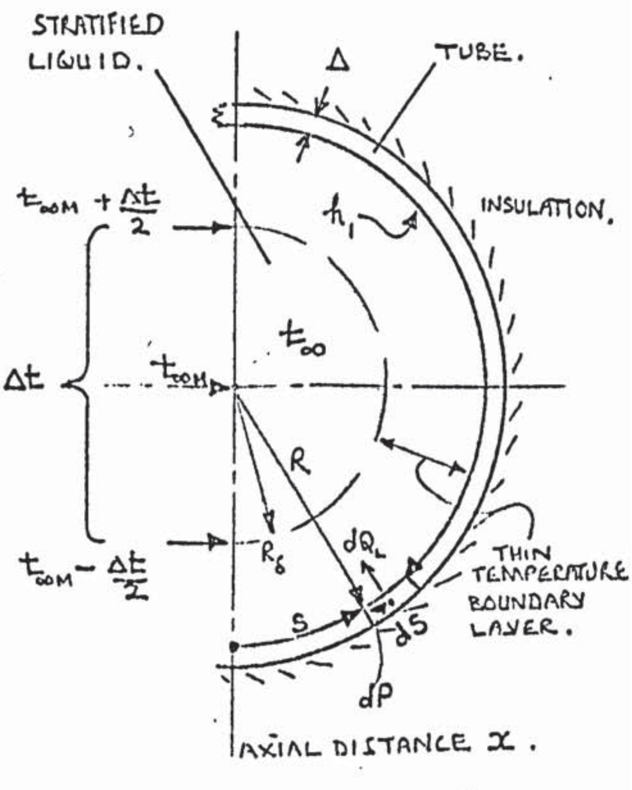

Assume -

(i) The wall is thin and ideally insulated.

(ii) Axial temperature gradients are small at large axial distances

(iii) The circumferential variation in h_1 (not h_s) is not great when h_1 is defined $h_1 = q/(t_w - t_\infty)$

Compare this with $h_s = q/(t_w - t_{\infty m})$.

(iv) In the cental core the fluid is stratified so that t_∞ varies linearly in the vertical direction, to a first approximation.

(v) An axial voltage gradient is applied to the tube.

The governing equation is

$$\frac{I}{2\pi R K_p \Delta} \cdot \frac{dV}{dx} = \frac{h_1}{K_p \Delta} \cdot (t_w - t_\infty) - \frac{\partial^2 t_w}{\partial s^2} , \qquad (9.1)$$

where $$t_\infty = t_{\infty m} - \frac{\Delta t}{2} \cdot \cos\left(\frac{s}{R}\right) \qquad (9.2)$$

putting $\phi = (t_w - t_{\infty m})$,

gives $$\phi'' - \left(\frac{h_1}{K_p \Delta}\right) \phi + \left(\frac{I \frac{dV}{dx}}{2\pi R K_p \Delta}\right) = \left(\frac{h_1 \Delta t}{2 K_p \Delta}\right) \cdot \cos\left(\frac{s}{R}\right) \qquad (9.3)$$

Since the boundary conditions are $\phi'(0) = 0 = \phi'(\pi R)$,

then $$\phi = \frac{I \frac{dV}{dx}}{2 R h_1} - \frac{\Delta t}{2\left(1 + \frac{K_p \Delta}{h_1 R^2}\right)} \cdot \cos \frac{s}{R} \qquad (9.4)$$

In the absence of circumferential conduction

$$\phi = \phi_o = \frac{I \cdot \frac{dV}{dx}}{2 R h_1} - \frac{\Delta t}{2} \cdot \cos\left(\frac{s}{R}\right) \qquad (9.5)$$

so that $$(\phi - \phi_o) = \frac{\left[\left(\frac{K_p \Delta}{h_1 R^2}\right) \cdot \frac{\Delta t}{2} \cdot \cos\left(\frac{s}{R}\right)\right]}{\left[1 + \frac{K_p \Delta}{h_1 R^2}\right]} \qquad (9.6)$$

The maximum error which would be incurred through neglecting circumferential conduction in the measurement of h_s is given approximately by -

error $$\epsilon \simeq 0.5 \gamma \left[\frac{\frac{K_p \Delta}{h_s R^2}}{1 + \frac{K_p \Delta}{h_1 R^2}}\right] \qquad (9.7)$$

---

where γ = $\dfrac{\text{(Temperature difference from top to bottom)}}{\text{(temperature difference used to calculate } h_s)}$.

The greatest degree of temperature stratification (Δt) occured in tubes having a large diameter, so for a typical case put

$K_p = 15.5 \frac{W}{mK}$, $\Delta = 0.075$ cm, $R = 2.8$ cm, $h_s = 100 \frac{W}{m^2K}$

Now $\dfrac{K_p \Delta}{h_s R^2} = 0.148,$

Therefore $\underline{\theta = 0.0645\,\gamma}$

As the degree of stratification reaches the same order of magnitude as the circumferential mean temperature difference used in calculating Nu, it is evident that $\theta = 6\frac{1}{2}\%$ maximum.

The measured value of h_s was likely to be much less than 6% inaccurate during the most severe experimental conditions, and it was probable that the accuracy of measured values of Nu - a function of axial position only - was independent of the degree of temperature stratification. From the preceding argument it was proposed that any further investigation into the effects of circumferential conduction would have a small relevance to this work.

The dependence of the local heat flux and temperature drop across the tube wall on the amount of axial conduction was evaluated in the analyses 5.3(iii) and 8.2(c). These effects were found to be most severe at small axial distances were rapid changes occurred in the axial temperature distribution. The local heat flux was calculated and compared with the mean value for the entire tube, at each thermocouple station. This comparison yielded the percentage of heat generated which was dispersed by axial conduction in an elemental length.

In the experiments on the short, straight tube, measurements showed this percentage to be always $< 1.1\%$. The greatest estimate for axial conduction occurred at one diameter from the start of heating, with the lowest value of the (Re x Pr) product - 43,000 (as in test 79sB) - and with the bellmouth fitted. The amount of axial conduction calculated would probably have increased considerably at smaller distances had these been investigated.

To substantiate the order of magnitude obtained it was assumed that the axial distribution of Nu was similar to the theoretical solution of Sellars for laminar flow (Ref: C.13)

viz - $$Nu = 1.30 \left(\frac{RePr}{X_1}\right)^{\frac{1}{3}}$$

The ratio of axial to radial conduction from a small length of tube is given (part 8.2(c)) by

$$\text{Ratio} = K_P \ e \ \frac{\partial^2 t}{\partial x^2} \Big/ \left(\frac{dV}{dx}\right)^2$$

or rewriting another way

$$\text{Ratio} = \frac{K_P}{K_L} \ \frac{\delta}{D} \ \frac{\partial^2}{\partial X_1^2} \left(Nu^{-1}\right), \text{ where}$$

P = tube subscript
L = liquid subscript
δ = wall thickness
D = tube diameter
$X_1 = x/D$

hence $$\text{Ratio} = 0.171 \ \frac{K_P}{K_L} \ \frac{\delta}{D} \left(RePrX_1^5\right)^{-\frac{1}{3}}$$

Now $\frac{\delta}{D} = 0.0466$, $\frac{K_P}{K_L} \simeq 64$, $(RePr)_{minimum} = 43,000$,

So that $$\underline{\text{Ratio} = 0.015 \ X_1^{-5/3}} \quad \text{maximum.}$$

In the turbulent flow regime the effects of axial conduction on measured values of Nu were less important than in laminar flow. This result can be justified by substituting a different expression for Nu in the above analysis. A theoretical investigation of turbulent heat-transfer (in part 11.2.(iv)) showed that for very small axial distances

$$Nu = 0.1855 \left(\frac{Pr^{\frac{1}{3}} \, Re^{0.6}}{X_1^{\frac{1}{3}}} \right).$$

For a low Re = 4,000, and a low Pr = 100, the following equation applies - Ratio = $0.0053\ X_1^{-5/3}$. It is clear that radial conduction exceeds axial conduction considerably when $X_1 > 1$.

In the experiments with the sudden convergence in tube diameter, the axial distribution of Nu was similar to that in the 'bellmouth' tests, the configurations being qualitatively similar. But since the section of tube downstream generally had a greater thickness to diameter ratio, since equally low (RePr) products were recorded, and because smaller axial distances were considered - it was probable that axial conduction would have a more significant effect on the measured coefficients of heat transfer in the 'convergence' experiments. The local heat flux was corrected for axial conduction by a maximum of 9½% in test 6c3, where the (RePr) product was small at 44,300; the convergence ratio was greatest at 3.34:1, and the axial distance was 0.5 to 1.0 diameters from the discontinuity. The correction reduced to 2% at 2 diameters. With turbulent flow and low values of Re ($\sim$ 4,000), it was found that a large correction to the heat flux of 10% was necessary. This was the case in tests 13c3 and 14c3, where Pr was greatest at $\widetilde{340}$, and the axial distance was 0.5 to 1.0 diameters. The correction reduced rapidly to $\ll 1\%$ at 2 diameters. At higher values of Re the conduction effects became negligible.

In the experiments with the 'sudden divergences' the second derivative of temperature, $\frac{\partial^2 t}{\partial x^2}$, was greatest near to the positions of maximum and minimum tube temperature which occurred a short distance downstream of the discontinuity. Once again it was found that axial conduction had little effect on the local heat flux, except where low values of Re (200-400) were encountered and Pr was low ($\widetilde{50}$). The maximum correction to the local heat flux was $\widetilde{10}$% (occurring in tests 18d3 and 16d1) and the magnitude of the corrections was similar for the three diameter ratios utilised.

9.3. MEASURED VARIATIONS IN TIME FOR TUBE TEMPERATURES.

In part 6.1. it was described how continuous readings of the tube temperature were carried out. The only experimental configuration for which such an investigation was not implemented was the short tube with a calming length. Variations in the instantaneous temperatures occurred, under certain experimental conditions, which could only be attributed to changes in the flow pattern. These were generally slow, cyclic fluctuations which were continuous but irregular, having a typical periodicity of 10 to 100 sec. More rapid fluctuations were undetectable because of transient conduction in the tube wall.

The changing electrical supply may well have contributed slightly to the measured variations, but such changes were easily determined and were found to be small.

For the short tube with a bellmouth-entrance, there was some evidence that the tube temperature was unstable during the transition from laminar to turbulent flow,,that is in the range Re = 2,000 to 10,000. In figure 9.5 the points plotted represent measured variations in the tube temperature, over a period of 1 to 2 min., expressed as a percentage of the local temperature difference from tube to fluid ($t_w - t_b$). This criterion occurs frequently throughout the following discussion.) The measurements were taken at axial distances of 1, 3, 4, 11, 20 and 70 diameters, but the magnitude of the variations did not depend simply on the axial location. Maximum variations of approximately 7% occurred at Re ~ 3000, and for very large or very small Re the variations were less than 1%. Ede (Ref: A.1.) made similar observations in experiments with water and air, but variations of 20% at Re = 3,000 were recorded which reduced to zero at Re = 9,000.

The experiments on the convergences were in general agreement with the bellmouth tests, with respect to the temperature fluctuations. Typical data for the 1.25:1 and 3.34:1 convergences are plotted (Fig: 9.6) for distances of 1, 5.5, 15 and 40 diameters, in a similar manner to that already described. The magnitudes of the variations measured at one diameter downstreamt of the discontinuity were very large for the 3.34:1 convergence: a maximum of 35% of $(t_w - t_b)$ occurred at Re = 5,400. The measurements otherwise were comparable in magnitude and distribution with the bellmouth results.

In the case of the 'sudden divergence' experiments a more complicated description of the unsteadiness in the tube temperature is necessary. Considering the 1:3.34 divergence, the fluctuations were greatest in the approximate range Re ≃ 200/668 (Downstream/Upstream) to 800/2,672 and the maximum variations measured were in the range 0% to 30%, with the exception of a few results taken when the flow was highly unstable. Figure 9.7 shows how the magnitude of the fluctuations varied with axial distance in a typical test. It is apparent that the maximum fluctuations occurred near to the position of minimum tube temperature (or maximum Nu). The probable reason for this became apparent after measuring the maximum and minimum tube temperatures for a particular flow rate and heat flux, then comparing these results with the corresponding 'instantaneous' temperatures measured during a short time interval. This procedure was followed in a test where the fluctuations were particularly severe. The comparison of the axial temperature distributions thus obtained is given in figure 9.8 . It is clear that small axial movements in the disposition of flow could cause severe variations in the local, instantaneous temperature by virtue of the high axial temperature gradients near to the location of the minimum tube temperature. The minimum temperature recorded was found to be almost identical for the readings taken with and without a time dwell. The way in which the fluctuations varied with Re is shown in figure 9.9. which includes typical experimental data measured at 5 and 40 diameters downstream, and a diagram giving an idealised picture of the distribution of the maximum variations. Below Re $\simeq$ 200/668 the fluctuations were negligibly small. Between Re $\simeq$ 200/668 and 800/2,672 the fluctuations were either negligible (0%) or large (mostly 8% to 30%). Between Re $\simeq$ 800/2,672 and 2,500/8,350 the maximum fluctuations were typically 4% to 15%. From Re $\simeq$ 2,500/8350 to 10,000/33,400 the fluctuations were approximately 4% to 7%.

The alternative condition proposed in the range Re $\simeq$ 200/668 to 800/2,672 was indicative of a bi-stable flow system, which could be described loosely as being either 'laminar' or 'turbulent' (the latter term implies a disturbed, laminar flow and not a sustained turbulence as in the usual sense of the term). The existence of the two flow conditions was established beyond doubt in a particular test (48d1) when the tube temperature oscillated between characteristically high and low values near to the diameter discontinuity. The three tests with extreme fluctuations in figure 9.9 had flows of this nature. By manipulating the flow-control valves it was possible to sustain the lower temperature, which corresponded to turbulent flow. When the higher tube temperature prevailed, the fluctuations were always immeasurably small.

Figure 9.9 also illustrates the magnitude of the maximum fluctuations at a considerable distance (40 dia.) from the divergence These variations became large in the Re range 2,000/6,680 to 10,000/33,400 when their magnitude decreased from 20% to 4% with increasing Re.

Further discussion on the relationship between heat transfer and the flow regime will be contained in part 9.7, but a recapitulation of the foregoing argument will be stated here.

Transitional flow in a divergence is more complex than in a uniform tube. Near to the discontinuity the laminar regime persists with increasing flow rate until a lower, critical Reynolds number is reached, which is considerablyless than the 2,500 usually quoted for a uniform tube. At higher Re values, laminar flow may persist or turbulence may develop, large fluctuations in the tube temperature being associated with the latter. When Re > 2,500 upstream, laminar flow can no longer exist downstream, except at considerable distances from the discontinuity. Smaller temperature fluctuations persist in this region, of the same order of magnitude as were obtained with transitional flow in the 'bellmouth' tests. The fluctuations diminished and became negligible as Re tended to 10,000 downstream, when turbulence pervaded throughout.

Up to now just the 1:3.34 divergence has been considered and the results appertaining to the 1:1.25 and 1:2 ratios should be mentioned. As the ratio of diameters tended to unity the abovementioned 'lower critical Re' increased, reducing the size of the first part of the transition range, (Re $<$ 2,500 upstream). Further, the tube temperatures associated with laminar and turbulent flow approached each other, thereby making it more difficult to demonstrate the distinction between the different flow regimes. The magnitudes of the fluctuations recorded during transitional flow were generally similar for each of the three divergence ratios investigated; most of the variations being of the order 5% to 30% of $(t_w - t_b)$ the maximum being close to the position of minimum temperature.

9.4. THE SHORT STRAIGHT TUBE; LOCAL TUBE TEMPERATURES.

A brief description will now be given of the kind of temperature distributions obtained with the short, straight tube having a calming length. Because the results obtained with the bellmouth entrance were qualitatively similar, these results are omitted from the discussion.

Figure 9.1 shows the axial temperature profile for the top and bottom of the tube as measured in test 32s; the circumferential, mean tube temperature is also indicated, together with the bulk temperatue of the fluid. In this test Re was low, increasing from 366 at the inlet to 372 at the outlet due to the temperature dependence of the physical properties. The value of Pr reduced from 183 to 181 for the same reason. (For ease of discussion, these small changes will be ignored henceforth, and the value at the position 'x = 0' will be quoted). The tube temperature continues to rise with increasing distance from the onset of heating, but the gradient decreases. The top of the tube becomes progressively hotter than the bottom as the distance increases, the maximum difference being equivalent to 42% of $(t_w - t_b)$, which is the difference used to calculate the local coefficient of heat transfer. The peripheral distribution of the tube temperature is given at axial distances of 1, 20 and 70 diameters downstream, and these diagrams show an almost vertical symmetry. The slight asymmetry could not be positively identified as being related to perturbations in the tubes geometry or uneveness of heating, but in other tests the 'right-handed' tendency was reversed (see for example Fig: 9.3). No effort was made to ensure a truly symmetrical temperature profile, since it was clear that a relatively minor disturbance would change the temperature distribution and create major, practical difficulties, whereas; there could be no significant benefits from having such an idealised system. The only other pertinent feature of this diagram is that the axial temperature gradient on the bottom of the tube quickly reaches the same rate of increase as bulk temperature of the fluid.

The temperature stratification in the fluid appears to follow the proposals of part 3.5 in which a vertical, secondary motion of the fluid near to the tube wall is supposed to carry the less dense, heated fluid to the upper surfaces of the tube. Some photographic evidence of these effects was obtained in the flow visualization tests (described in 7.4.(i)). Figure 9.41 A. shows water heated in a long tube with Re = 550. The fast moving central core travels slowly downward, and the slow moving elements near to the wall climb almost vertically to the top of the tube. Figures 9.41 B and C show how increasing Re suppresses the secondary flow, and how increasing the rate of heat transfer enhances this motion.

The temperature distributions in test 33s were obtained with similar values of Re and Pr to test 32s already mentioned. In this case however the heat flux was increased by 3½ times.

The same general observations apply to the temperature profiles of both tests (see figure 9.2) but in 33s the stratification develops more rapidly with distance. The greatest temperature difference from top to bottom was equivalent to 59% of $(t_w - t_b)$. This is not such a dramatic increase over the previous 42%, considering that the heat flux was almost quadrupled.

From figure 9.3 , the results of test 42s exhibit far less stratification than in the previous cases. The value of Re was 2,265 and Pr was 257. Re was high, although still in the laminar range, and it was evident that this caused the stratificationto develop at a slow rate, as was indicated previously in the photographic study. The maximum degree of temperature stratification in this test was only 16% of $(t_w - t_b)$.

Increasing the Reynolds number even further caused the onset of turbulence and, as might be expected, the stratification was entirely suppressed by the random motions of the fluid. It may well be that free convection could have occurred at extremely high heat fluxes, but the subject was outside the scope of this work.

Figure 9.4 gives the temperature profiles for Re= 4,216 and Pr = 194 (test 45s). The temperature curves for the top and bottom of the tube are coincident, and these become parallel with the bulk temperature line after approximately 20 diameters from the start of heating.

9.5. THE SHORT STRAIGHT TUBE; HEAT TRANSFER COEFFICIENTS.

9.5.(i) THE TUBE WITH A CALMING LENGTH.

Considering first the short, straight tube with a calming length, and restricting the discussion to transitional and turbulent flows, the initial objective was to determine unique correlations between the local Nu and the various dimensionless parameters already discussed. Empirical and analytical techniques were utilised to this end. Suppose that

$Nu = f$ (Re, Pr, Gr, X, P, Q), where P and Q are variables which take account of the 'viscosity - temperature' dependence, and 'dissipation' dependence of Nu, (The parameter X is $(x/2r_w)$).

In part 9.4. the free convectional contribution to heat transfer was shown to be small during turbulent flow from observation of the experimental temperature profiles. Gr can therefore be eliminated from the expression above.

An analytical investigation of dissipation in forced convection (part 11.1.(v)) indicated that the value of Nu was likely to be dependent on the parameter $E = (\mu \bar{u}^2/qr_w)$ - which corresponds to the variable Q. However, the neglect of this parameter was likely to cause errors of $<\frac{1}{2}\%$ when estimating Nu, so the value of Q can be set at zero in the expression above.

A suitable variable P was postulated in the analysis of 'variable viscosity' convection (11.2.(iii) and (iv)) - the viscosity ratio M_{wall} $(=\mu_{bulk}/\mu_{wall})$. Some justification for the use of this parameter at small axial distances was given, but the present knowledge of turbulence precludes anything other than a tentative argument regarding its general applicability.

The conclusion at this juncture is that

$$Nu = F(Re, Pr, X, M_{wall}).$$

Another result of the theoretical investigations, 11.2.(iv), was that for high Prandtl number fluids Nu is proportional to Pr^n, where n is probably $\frac{1}{3}$, but could be as low as $\frac{1}{4}$. The preceding expression can be modified accordingly, and with only a small loss of generality the following is obtained -

for constant X, $Nu = F_1(M_{wall}) . Pr^{\frac{1}{3}} F_2(Re)$,

where $F_1 \rightarrow 1$ for a 'constant viscosity' fluid.

The functions F_1 and F_2 are to be determined empirically.

The exponent of Pr selected was $\frac{1}{3}$, which was to be justified experimentally. The advantage of using this value initially was that it was known to be valid for the laminar regime (as described in the theory 11.2(i)) and thus the correlation of the experimental parameters was simplified. Despite the substantial range of Pr utilised in these experiments (approximately 90 to 400 for turbulent flow) the difference between the exponents $\frac{1}{3}$ and $\frac{1}{4}$ was equivalent to only 12% of the Nusselt number for the purposes of correlation. Whereas such a discrepancy should have been detectable, it was unlikely that the exponent could be resolved to better then 10%.

In correlating the measured parameters it was noted that M_{wall} varied considerably at large axial distances, so the function $F_1(M_{wall})$ was investigated initially at 70 diameters downstream of the onset of heating.

Figure 9.10 shows how the group $(Nu/Pr^{\frac{1}{3}})$ was plotted with Re as the abscissa. The correlation was poor because $F_1(M_{wall})$ was ignored; deviations of 20% in $(Nu/Pr^{\frac{1}{3}})$ were observed. During tests 1s to 57s the heat flux was varied keeping Re almost constant (described in 7.1.(i)) so that after making corrections for the small Re variations, it was possible to eliminate the heat flux, and therefore M_{wall}, dependence from the correlation by graphical procedure. The latter is illustrated in Figure 9.11. where graphs of $(Nu/Pr^{\frac{1}{3}})$ versus the temperature difference $(t_w - t_b)$ are shown, for particular Re values. The magnitude of $(Nu/Pr^{\frac{1}{3}})$ for the 'zero heat-flux' condition could be obtained by extrapolation. Returning now to figure 9.10, the line representing the function $F_2(Re)$ could be drawn for $F_1(M_{wall})$ equal to unity. This was necessarily a first approximation to be refined in due course. Having obtained this function it was possible to determine the Nu dependence on the viscosity variation, or $F_1(M_{wall})$. This was achieved by plotting (Nu/Nu_o) versus (M_{wall}) - where Nu_o is the value of Nu corresponding to $M_{wall} = 1$. The latter is given in figure 9.12 for the axial position of 70 diameters. The function F_1 was found to be well approximated by putting $F_1 = M_{wall}^{a}$. From a 'least squares' regression, the most suitable value of 0.16 was calculated for 'a'. In the theoretical analyses 11.2(iii) and 11.2(vi) values in the range 0.14 to 0.17 were postulated for laminar flow, near to the start of heating, and it is proposed (in 11.2.(vii)) that a similar value be utilised in the turbulent regime.

Sieder and Tate (Ref: D.I.) showed that for large axial distances a suitable value for 'a' would be 0.14. From the graph (Nu/Nu_o) versus M_{wall} it can be seen that $M_{wall}^{0.14}$ differs only slightly from $M_{wall}^{0.16}$ in these experiments; the maximum extent of the scatter in the results being +4%, -2½% when $F_1 = M_{wall}^{0.16}$, and +4½%, -2½% when $F_1 = M_{wall}^{0.14}$.

To verify that the function $F_1(M_{wall})$ was independent of axial position, the entire procedure, for obtaining F_1 and F_2, was repeated at one diameter axial distance. The lower temperature differences obtained near to the inlet yielded smaller values for M_{wall}. Figure 9.12 gives the resulting dependence of Nu on M_{wall}, and it is apparent once more that, whereas '$F_1 = M_{wall}^{0.16}$' gives the best fit to the experimental data, the relationship '$F_1 = M_{wall}^{0.14}$' adequately describes the results.

The group $\left(\frac{Nu}{Pr^{\frac{1}{3}} M_{wall}^{0.14}}\right)$ was chosen to be a function of Re and X for the purpose of correlating the experimental results in the turbulent regime. The exponent 0.14 being selected in keeping with the widely used Seider-Tate correction. Figure 9.13 shows such a relationship, in which graphs of $\left(\frac{Nu}{Pr^{\frac{1}{3}} M_{wall}^{0.14}}\right)$ versus Re are drawn at constant, axial distances of 1, 3, 6, 11, 20 and 70 diameters. The lines indicate the interpolation necessary to give a minimum deviation from the mean on the vertical axis; this is not necessarily the 'smoothest' curve through the experimental points. Although most data falls within 2% of the interpolated values, approximately 8% of the points plotted lie between 2% and 5%. These errors are not a simple function of the Reynolds number.

To ensure that the 'scatter' in the above mentioned correlation was not due to the wrongful selection of the Pr exponent, a graph of $\left(\frac{Nu}{F_2(Re) M_{wall}^{0.14}}\right)$ versus Pr was plotted (see figure 9.14), for a distance of 70 diameters, where $F_2(Re)$ was obtained graphically from figure 9.10 . The data plotted applies to tests 1s to 57s, which encompassed the approximate range of Prandtl number 180 to 400. The errors are seen to be independent of Pr. A comparison between the hypothesis "$Nu \sim Pr^{\frac{1}{3}}$" and "$Nu \sim Pr^{\frac{1}{4}}$" shows that the exponent $\frac{1}{3}$ is to be preferred; the maximum deviation from the mean being 6% in the latter case and 5% when $\frac{1}{3}$ is chosen.

Specific data from tests 1s, 12s and 22s are given in figure 9.15, which states graphically the measured values of the Nusselt number obtained at particular axial locations. Due to the effect of temperature on the viscosity, the Reynolds number increased with axial distance and the Prandtl number decreased. For this reason, and to a lesser extent because the ratio M_{wall} increased with axial distance, the value of Nu was expected to increase gradually after approximately 40 diameters. Any such increase was found to be immeasurably small, but this would not have been the case had $(Nu/Pr^{\frac{1}{3}})$ been plotted instead of Nu. In these experiments the axial temperature gradient in the fluid was very small because high Prandtl numbers were encountered, and consequently the effects just mentioned were minimised.

The general shape of the Nu functions described is such that a rapid diminution occurs with increasing distance, from a high initial value to an almost constant, limiting value. The limiting value is reached at approximately 40 diameters when Re $\simeq$ 3,750, and this reduces with increasing Re, so that the limit occurs at approximately 15 diameters when Re $\simeq$ 9,200. The way in which the Nusselt number varies, in the entrance region of a heated tube, can be expressed in a more practical form by plotting curves of $\dfrac{Nu}{Pr^{\frac{1}{3}}\, M_{wall}^{0.14}}$ versus the dimensionless, axial distance, $X = (x/2r_w)$, for constant values of the Reynolds number. This information is recorded in figure 9.16. The effects of axial variations in the fluid properties have been eliminated from these results.

In the laminar regime the selection of the significant groups of parameters, required for correlating the experimental results, was backed by a considerable amount of theory. Starting once again with the premise

$$Nu = \phi\,(Re, Pr, Gr, X, P, \omega),$$

and considering the results obtained with a calming length upstream. The theoretical analyses 11.2.(ii) and (vii) indicated that dissipation could be neglected, its effect on the coefficient of heat transfer being $\ll 1\%$. The theoretical investigations to determine the dependence of Nu on the variation in viscosity with temperature (11.2.(iii)) have already been mentioned. A complete solution to the energy and momentum equations was obtained which led to $\dfrac{Nu}{Pr^{\frac{1}{3}}} = \phi_1\,(M_{wall}).\,1.647\,.\,Re^{\frac{1}{3}}.\left(\dfrac{x}{r_w}\right)^{-\frac{1}{3}}$,

where $\phi_1\,(M_{wall}) = M_{wall}^{0.14}$ was found to be a good approximation. The most significant omission from this solution is the dependence of Nu on free convective heat transfer. Guided by the result stated, a correlation was attempted of the form $\left(\dfrac{Nu}{Pr^{\frac{1}{3}} M_{wall}^{0.14}}\right) = \phi_2(Re, X)$,

where $X = (x/2r_w)$.

This relationship is shown graphically for X = 1,3,6,11,20 and 70 diameters, in the test series 1s to 57s, (see figure 9.17)
A maximum scatter of 50% occurred in the correlation and it was evident that the greatest errors occurred, in general, at 70 diameters, when Re was low and Gr was high. Clearly free convection could not be ignored.

Before proceeding with this analysis, a discussion concerning combined forced and free convection is in order, to help establish the important dimensionless groups which can be used to define the problem symbolically.

To give some insight into the process of combined free and forced convection in the entrance region of a horizontal tube, a simplified model of the system is to be proposed. By inspection of the governing equations, significant groups of variables can be obtained for application in the empirical analysis.

The axial velocity in the tube is assumed to be fully developed near to the entrance, and fluid with a high Prandtl number is considered. Free convection arises as a small perturbation in the flow pattern, and the uniform heat flux condition is imposed. Additional simplifications are expressed 'in loco'.

For the coordinate system shown below, the following parameters are defined.

$t_w(x,\zeta)$ = wall temperature, t_∞ = temperature at inlet,

u, $\bar{u}$ = axial, mean axial velocity, w = circumferential velocity,

v = velocity towards axis, $\theta = (t - t_\infty)/(qr_w/K)$,

$U = (u/4\bar{u})$, $V = (vRePr)/(2\bar{u})$, $W = (wRePr)/(2\bar{u})$, $Y = (y/r_w)$

$\bar{X} = (x/2r_w)/(RePr)$, $Z = (\zeta/r_w)$, $Nu_{FC} = \dfrac{2h(x,\zeta)\, r_w}{K} = \dfrac{2}{\theta(x,0,\zeta)}$,

$$Gr_{FC} = \frac{8g\rho^2\beta(t_w - t_\infty)\, r_w^3}{\mu^2}$$

$$Nu = \frac{1}{\pi}\int_{-\pi/2}^{\pi/2} Nu_{FC}\, dZ$$

$$Gr = \frac{1}{\pi}\int_{-\pi/2}^{\pi/2} Gr_{FC}\, dZ$$

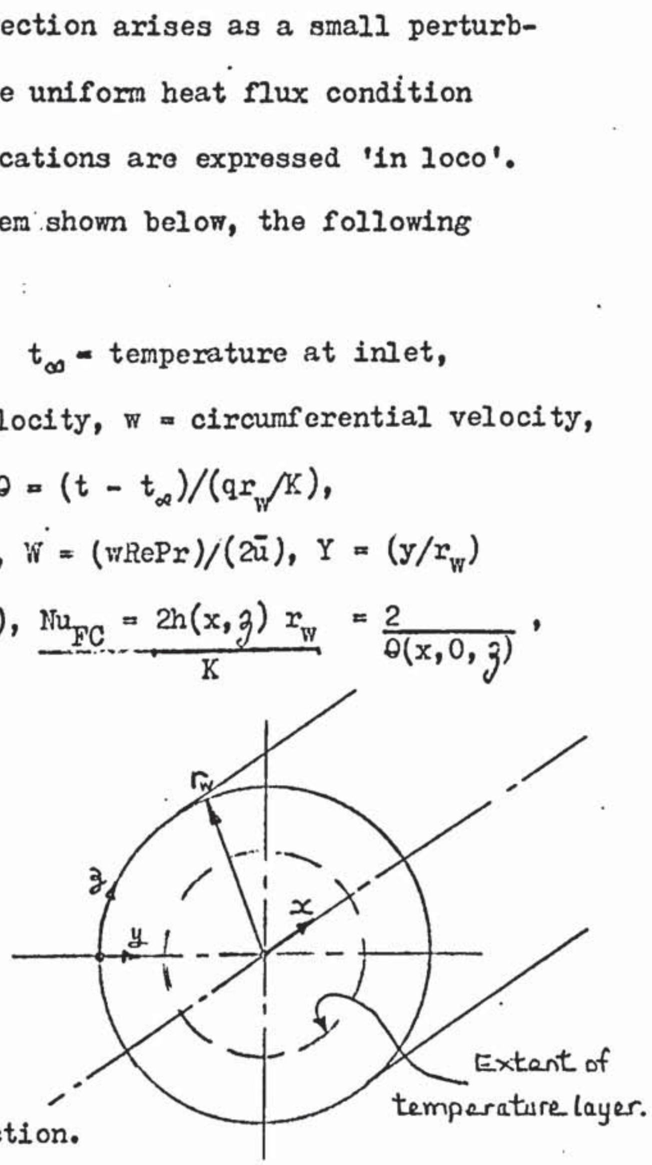

Suffix - 0 - without free convection.

The energy equation can be simplified if circumferential and axial conduction are neglected -

$$U\frac{\partial\theta}{\partial\bar{X}} + W\frac{\partial\theta}{\partial Z} + V\frac{\partial\theta}{\partial Y} = \frac{\partial^2\theta}{\partial Y^2} \qquad (9.8)$$

The axial velocity distribution close to the wall can be linearised, and for a thin temperature layer will remain virtually unaffected by free convection. Hence $U \simeq Y$.

If radial pressure gardients are considered small and viscous forces predominate, the circumferential velocity is given approximately by -

$$\frac{\partial^2 W}{\partial Y^2} = -\frac{(NuGrPr)}{16} \cdot \Theta \cdot \cos Z. \qquad (9.9)$$

The radial velocity is assumed to be given by the continuity equation $\frac{\partial W}{\partial Z} + \frac{\partial V}{\partial Y} = 0$, so that (9.10)

$$\frac{\partial^3 V}{\partial Y^2} = \frac{(NuGrPr)}{16}\left(\frac{\partial \Theta}{\partial Z} \cos Z - \Theta \operatorname{Sin} Z\right) \qquad (9.11)$$

Proceeding with the analysis as though the forced convection solution were required, a similarity variable is derived from inspection of the energy equation and consideration of the temperature boundary conditions.

$$\Theta = \bar{X}^{\frac{1}{3}} f(\bar{X}, \eta, Z) \text{ where } \eta = \bar{X}^{-\frac{1}{3}} Y. \qquad (9.12)$$

Substitution into the energy equation yields -

$$\eta \bar{X} \frac{\partial f}{\partial \bar{X}} + \frac{\eta}{3} f - \frac{\eta^2}{3} \frac{\partial f}{\partial \eta} - \frac{(NuGrPr)}{16} \bar{X}^{5/3}\left(\frac{P\partial f}{\partial z} - \frac{Q\partial f}{\partial \eta}\right) = \frac{\partial^2 f}{\partial \eta^2}, \qquad (9.13)$$

where $\frac{\partial^2 P}{\partial \eta^2} = f \cos Z$, and $\frac{\partial^3 Q}{\partial \eta^3} = \left(\frac{\partial f}{\partial Z} \cos Z - f \sin Z\right)$.

Without attompting to solve the equations for f, it can be appreciated that the group of parameters $(NuGrPr)\bar{X}^{5/3}$ plays a significant role in the convection process. With $Gr = 0$, the resulting value of f at the wall can be shown to be $f_0(\bar{X}, 0, Z) = A$, a constant. The corresponding result for the case $Gr \neq 0$ can be stated·

$$f(\bar{X}, 0, Z) = A \cdot \phi_1\left((NuGrPr)\bar{X}^{5/3}, Z\right) \qquad (9.14)$$

The circumferential mean temperature $\bar{\Theta}$ becomes

$$\bar{\Theta} = A\, \bar{X}^{\frac{1}{3}} \cdot \phi_2 (NuGrPr\, \bar{X}^{5/3}) \equiv \bar{\Theta}_0 \phi_2 . \qquad (9.15)$$

The Nusselt number is written

$$\frac{Nu}{Nu_o} = \frac{\bar{\theta}_o}{\theta}$$

$$= f_3\left(\frac{Nu}{Nu_o} . Gr.Pr.\bar{X}^{4/3}\right) . \qquad (9.16)$$

Making the assumption that

$$f_3 \simeq \bar{M}\left(\frac{Nu}{Nu_o} Gr\ Pr\ \bar{X}^{4/3}\right)^m \qquad . (9.17)$$

for a limited range of the independent variable, the final expression is determined

$$\frac{Nu}{Nu_o} = \bar{M}\left(\frac{(GrPr)^{\frac{1}{4}}}{(RePr)^{\frac{1}{3}}} \left(\frac{x}{2r_w}\right)^{\frac{1}{3}}\right)^{\frac{4m}{1-m}} \qquad (9.18)$$

where $\bar{M}$ and m are weak functions of the independent variable, such that $\bar{M} \rightarrow 1$ and $m \rightarrow 0$ as $\left[\frac{(GrPr)^{\frac{1}{4}}}{(RePr)^{\frac{1}{3}}}\left(\frac{x}{2r_w}\right)^{\frac{1}{3}}\right] \longrightarrow 0$

It will be shown that suitable values are $\bar{M} = 0.48$ to 1.0, and $m = 1/6$ to 0.

From the argument just stated, a plausible method for correlating the laminar heat transfer coefficients ensued. Plotting the graph of $\left(\frac{Nu}{Pr^{\frac{1}{3}}M_{wall}^{0.14}}\right)$ versus Re for particular axial locations (as described previously. Fig: 9.17) a line was drawn through those points corresponding to low Grashof numbers. The Nusselt number given by this function (Nu_o) was compared with that (Nu) obtained for all the tests in the range 1s to 57s. A graph of (Nu/Nu_o) versus $(GrPr)^{\frac{1}{4}}$ / $(RePr)^{\frac{1}{3}}$ was drawn and the whole procedure was repeated to improve the initial $\left(\frac{Nu_o}{Pr^{\frac{1}{3}}M_{wall}^{0.14}}\right)$ function.

Figure 9.18 shows that the free convectional contribution to Nu was small at distances of less than 20 diameters. At 70 diameters, up to 50% increase in Nu was apparent when $(GrPr)^{\frac{1}{4}}/(RePr)^{\frac{1}{3}}$ approached unity. When this value was less than 0.6, free convection did not cause Nu to increase above Nu_o.

At 70 diameters downstream Nu could be expressed

$$(Nu/Nu_o) = 0.28 + 1.2\ (GrPr)^{\frac{1}{4}}/(RePr)^{\frac{1}{3}} \text{ for } Nu > Nu_o.$$

In keeping with the derivation of the dimensionless groups (above) an alternative equation of the following type is obtained:

$$(Nu/Nu_o) \equiv \Phi = 0.48 \left[\frac{(GrPr)^{\frac{1}{4}}}{(RePr)^{\frac{1}{3}}} \left(\frac{x}{2r_w}\right)^{\frac{1}{3}}\right]^{0.8} \quad \text{for } Nu > Nu_o,$$

$$\text{and} \quad \Phi = 1 \text{ for } (GrPr)^{\frac{1}{4}}(x/2r_w)^{\frac{1}{3}}/(RePr)^{\frac{1}{3}} < 2.5$$

Where the latter proposal applies to any axial position, and gives the critical condition below which free convection can be ignored altogether It is worth noting the theoretical result, equation (11.17), gives $Nu_0 = 1.642\ (RePrr_w/x)^{\frac{1}{3}}$ (neglecting dissipation). Now suppose at large values of Φ (outside the experimental range) the above exponent 0.8 tended to unity, this would lead to the e expression $Nu = 0.623\ (GrPr)^{\frac{1}{4}}$ after substituting for Nu_o. There is a remarkable similarity between this and other well known expressions proposed for pure free convection processes. (See for example Ref: K2)

The improved correlation was attempted -

$\left(\frac{Nu}{\Phi\ Pr^{\frac{1}{3}} M_{wall}^{0.14}}\right)$ versus (Re), at constant axial distance.

Figure: 9.19 shows the result for X = 3, 20 and 70 diameters. The experimental points fall within 10% of the mean lines, most data being within 5%. The exceptions to this statement were tests 23s and 34s which were 22% and 15% lower than the mean at 3 diameters, downstream. No explanation could be found for these low measurements but it is probable that some uncertainty attaches to the results obtained with very low heat fluxes, and the lowest heat fluxes used throughout the experiments occurred in these tests, that is 600 W/m^2.

Figure 9.20 shows the interpolated Nusselt numbers plotted in a more useful form, viz:

$\left(\dfrac{Nu}{\frac{1}{\Phi} Pr^{\frac{1}{3}} M_{wall}^{0.14}}\right)$ versus (Axial distance), at constant Re.

The value of Nu is seen to reduce with increasing axial distance from a high initial value. The magnitude of Nu does not tend towards a limiting value at large axial distances ($<$70 dia.), as was the case with the turbulent results (Fig: 9.16).

The use of the viscosity correction factor $M_{wall}^{0.14}$ is justified empirically in figure 9.21 where the group $\left(\dfrac{Nu}{\frac{1}{\Phi} Nu_o}\right)$ is plotted against M_{wall}. (Here, Nu_o is the Nusselt number without viscosity variation or free convection.) The data shown relates to an axial distance of 70 diameters.

With the bellmouth entrance fitted, higher Nusselt numbers were obtained in the laminar region, and lower values were obtained in the turbulent region. The analysis of these results proceeded on those lines already described, and a direct comparison was made with the 'calming length' results. Figure 9.22 shows the Nu variation with axial distance for tests 74sB to 85s. With Pr = 91, a comparison is made between the two configurations at particular Re values.

In the transitional and turbulent regimes unique graphs of $\left(\dfrac{Nu}{Pr^{\frac{1}{3}} M_{wall}^{0.14}}\right)$ versus Re were obtained for particular axial locations. (Figure 9.23). The results included a range of Pr from 170 to 570 (as in tests 58sB to 72sB) and the dependent variable stated was found to be adequate in describing the Pr dependence of Nu. The shape of these functions differed markedly from those obtained with a 'calming length' upstream, and the difference is clearly indicated when graphs of $\left(\frac{Nu}{Pr^{\frac{1}{3}}M_{wall}^{0.14}}\right)$ versus (axial distance) are compared for both configurations (Fig: 9.24) at particular Re values. Significant reductions in Nu arise when flow development is present in the system. The maximum reduction is approximately 30% at Re = 3,000, but becomes 10% at Re = 10,000.

A comparison between 'calming length' and 'bellmouth' results was carried out for the laminar regime. The analysis of 'bellmouth' data followed the method used for the 'calming length' data. A graph of $\left(\frac{Nu}{\Phi Pr^{\frac{1}{3}}M_{wall}^{0.14}}\right)$ versus (Re) for the particular axial positions, 3, 11, 20, and 70 diameters (Fig: 9.25) indicated that unique functions could only be plotted for specific Prandtl numbers. Figure 9.25 shows that in general Nu was greater for the case of developing velocity. This increase was greatest at small axial distances, and the magnitude was minimised at small Re. The values of Nu were highest when low Prandtl numbers were utilised, so that at 3 diameters downstream with Pr = 91, the 'bellmouth' results were 19% to 35% higher. At 20 diameters, the corresponding increases were 7% to 16%. For very high Prandtl numbers, say 500, velocity development caused an increase in Nu for Re = 0 (1,000) but its influence was not so marked as in the case Pr = 91.

Figure 9.26 shows the axial distribution of $\left(\frac{Nu}{\Phi Pr^{\frac{1}{3}}M_{wall}^{0.14}}\right)$ for given Reynolds numbers, and with Pr $\simeq$ 91. The 'calming length' results are given for comparison. In general, the effect of velocity development was to increase Nu significantly at small axial distances even when the fluid was highly viscous. This phenomenon is discussed theoretically in some detail in reference J.14 where the rate of velocity development is shown to depend on both the initial velocity profile and the variation in viscosity with temperature.

9.6. HEAT TRANSFER IN A CONVERGENCE.

Insofaras the convergence in diameter is qualitatively similar to the bellmouth entrance, it was assumed at the outset that it would be possible to correlate the experimental results in a similar way, i.e. graphs of $(Nu/Pr^{\frac{1}{3}})$ versus (axial distance) were plotted for each test (therefore particular values of Re and Pr). The variation of $(Nu/Pr^{\frac{1}{3}})$ with Pr was expected to be of second order magnitude. However, such a dependence was not precluded from the correlations because it was possible to classify the experimental results into groups having particular values of Pr.

Moderate temperature differences were utilised in these experiments in order to minimise the effects of viscosity variation with temperature and free convectinn. Any increase in Nu due to these secondary considerations was neglected as insignificant from experience gained in the short tube experiments.

Figure 9.27 shows the axial distribution of $(Nu/Pr^{\frac{1}{3}})$ downstream of a 3.34:1 contraction with $Pr \simeq 57$. Comparing these results with figures 9.24 and 9.26, indicates a general agreement with the functions derived for the bellmouth tests. But at the higher Reynolds numbers downstream (Re_2), the sudden contraction exhibited appreciably higher values for $(Nu/Pr^{\frac{1}{3}})$ close to the change in section, whereas with the lower values of Re_2 (<2336) marginally smaller values were obtained. (NB. The Reynolds numbers at $x = 0$ quoted on the graphs are actually the values at thermocouple locations just upstream and downstream of of the discontinuity).

Some substantiation of the assumption that the secondary effects due to viscosity variations and free convection can be neglected in these experiments is shown in figure 9.28. A large increase in heat flux was found to cause a comparatively small increase in $(Nu/Pr^{\frac{1}{3}})$ at distances of the order 1 diameter when turbulent flow prevailed ($Re_2 = 30,550$). In the laminar regime ($Re_2 = 747$) a small reduction ensued which diminished with increasing distance up to approximately 30 diameters. In the transition region ($Re_2 = 5,156$) the value of $(Nu/Pr^{\frac{1}{3}})$ was initially suppressed at $\tilde{1}$ diameter, but increased in the range 2 to 6 diameters, exhibiting some of both the laminar and turbulent tendencies. The results obtained at less than 1 diameter were shown to be sensitive to 'tube-wall conduction' (see part 9.2.) so some uncertainty attaches to the reliability of measurements taken in this region, with this in mind it was considered reasonable to suppose that heat-flux dependence was of second order magnitude.

The effects of reducing the heat flux to zero in the section of tube upstream are demonstrated for the 3.34:1 convergence in figure 9.29. The value of $(Nu/Pr^{\frac{1}{3}})$ was increased at small distances downstream. At 1 diameter the increase was $\tilde{15}\%$ with $Re_2 = 29,325$ rising to $1\tilde{00}\%$ with $Re_2 = 694$. These differences reduced rapidly in the downstream direction, the corresponding values at 3 diameters being $\tilde{2}\%$ and $\tilde{25}\%$ respectively. Once again it should be noted that 'tube-wall conduction' could tend to distort the measurements at small axial distances (approximately <2 diameters), (see parts 9.2. and 5.3.(iii)).

Figures 9.30, 9.31 and 9.32 give comparable results to the $Pr \simeq 57$ case, but with $Pr \simeq 140$, 190 and 340. In general, the effect of increasing Pr was to reduce ($Nu/Pr^{\frac{1}{3}}$) in the laminar regime (($Re_2 < 2,500$) but no significant effect was observed in the turbulent regime ($Re_2 > 10,000$). With $Re_2 \simeq 700$ and at 1 diameter downstream, ($Nu/Pr^{\frac{1}{3}}$) varied by a factor of three. The effect of Pr on ($Nu/Pr^{\frac{1}{3}}$) reduced with increasing axial distance. For transitional Reynolds numbers (2,500 to 10,000) a peak occurred in ($Nu/Pr^{\frac{1}{3}}$) at approximately 1 diameter downstream. This was particularly well defined at high Prandtl numbers, and was probably a function of the heat transfer mechanism in the short, separated-flow region which must occur just downstream of the sharp discontinuity - In separated regions the relationship between Nu and Pr may differ from that in a region where the boundary layer is attached (for example see part 11.3.(vii)). It is also possible that the breakdown of the laminar boundary layer into turbulent flow which occurs close to a discontinuity could be dependent on the viscosity of the fluid and hence (indirectly) on the Prandtl number. It was not considered to be of sufficient significance to warrant a detailed investigation of the underlying mechanisms, but there was no reason to doubt the existence of maximum in the ($Nu/Pr^{\frac{1}{3}}$) function.

In figures 9.33 to 9.38 data is presented for 2:1 and 1.25:1 convergences, for a similar range of Prandtl numbers. Although there is close qualitative similarity with the results already described, the following differences were noted with reducing diameter ratio. At all values of Pr, ($Nu/Pr^{\frac{1}{3}}$) close to the discontinuity was reduced by a factor of $1\frac{1}{2}$ to 2, with laminar Reynolds numbers, as the diameter ratio reduced from 3.34:1 to 1.25:1. The most part of this reduction occurred as the ratio was changed from 1:2 to 1:1.25, and the effect was less pronounced at high Prandtl numbers ($\tilde{3}50$). The reduction in ($Nu/Pr^{\frac{1}{3}}$) with increasing diameter ratio was small when $Re_2 > \tilde{2},500$ except at distances downstream of the order $\frac{1}{2}$ diameter when a variation similar in magnitude to the low Re_2 results was observed.

The differences between $(Nu/Pr^{\frac{1}{3}})$ at the various diameter ratios, as discussed above, where not so marked at distances downstream greater than approximately 10 diameters.

9.7. HEAT TRANSFER IN A DIVERGENCE.

9.7.(i) The mechanisms of heat transfer and fluid flow through a sudden divergence were found to be extremely complex, particularly at low Reynolds numbers. Extensive testing was required initially with the 1:3.34 diameter ratio, and some of the results obtained have been omitted from the graphical data presented for the sake of clarity. Such omissions have been made only where inexperience led to unnecessary elaboration of phenomena observed throughout testing.

9.7.(ii) FLOW VISUALIZATION TESTS.

It became apparent from preliminary experimentation that an investigation of the flow patterns through a divergence would be essential to the understanding of the heat transfer phenomena observed in the main experiments. The results of this investigation will now be presented in the form of a commentary on photographic data with a summary of some important results in graphical form. Brief notes are given on each of the photographs in figures 9.39 and 9.40 .

Re_2 = Reynolds number downstream of step.

X = Distance (diameters) downstream of step.

ΔT = Temperature water bath - temperature within tube (approximate).

All initial tests with water Pr = 8 to 9.5

<u>Figure 9.39 . The 1:3 Divergence.</u>

A) $Re_2 = 199$ $\Delta T = 0$. Thin dye trace travels through centre of tube undisturbed.

B) $Re_2 = 457$ $\Delta T = 0$. Thin dye trace gives poor photograph of flow. Flood upstream leg with dye. Instability or localised turbulence occurs in flow at $X \simeq 6$. Heat transfer in turbulent region will probably be much higher than if flow were undisturbed.

C) $Re_2 = 700$ $\Delta T = 0$
D) $Re_2 = 925$ $\Delta T = 0$
E) $Re_2 = 1450$ $\Delta T = 0$

Increasing Re_2 causes instability to move upstream, until at onset of turbulence in upstream leg flow develops as a conical, turbulent jet issuing from upstream leg.

F),G),H) $Re_2 = 490$ $\Delta T = 0$. Shows development of flow entering downstream leg. G) and H) are 10 and 30 seconds after F). H) indicates diffusion of dye does not affect stability of flow.

I) $Re_2 = 148$ $\Delta T = 0.4\ ^{\circ}C$
J) $Re_2 = 148$ $\Delta T = 0.6\ ^{\circ}C$
K) $Re_2 = 148$ $\Delta T = 0.6\ ^{\circ}C$
L) $Re_2 = 148$ $\Delta T = 1.0\ ^{\circ}C$
M) $Re_2 = 148$ $\Delta T = 2.0\ ^{\circ}C$

I) through M) show effect of increasing heat transfer with Re_2 constant, when flow is laminar-stable. (N.B. It is assumed that phenomena with constant temperature bath will resemble uniform heat flux imposed in main experiments.) J) and K) differ only in type of dye trace used. Cold fluid from upstream drops to bottom of downstream leg due to bouyancy, possibly causing a small local peak in heat transfer coefficient versus distance. Rises up wall of tube. J) shows tendency to recirculate upstream at top of tube. Distance to 'bottoming' point reduces with increasing temperature difference.

N) $Re_2 = 333$ $\Delta T = 2.4^{\circ}C$
O) $Re_2 = 333$ $\Delta T = \underline{6}^{\circ}C$
P) $Re_2 = 333$ $\Delta T = 14^{\circ}C$

Shows effect of free convection (increasing ΔT) at higher value of Re_2. Instability is present in flow.

Instability tends to occur at bottom of tube where cold fluid from upstream leg 'bottoms' downstream, and hence probable location of peak heat transfer coefficient moves upstream as heat transfer rate increases. This will be a fairly prominent peak due to local turbulence.

Q) $Re_2 = 190$ $\Delta T = 14$. At a reduced Re_2 the free convection causes cold fluid from upstream leg to drop probably causing a small peak in local heat transfer coefficient at $X = 1\frac{1}{2}$ to 2. Then downstream, at $X = 3$ to 5, the flow becomes unstable which probably leads to a second, higher peak in the heat transfer coefficient versus distance.

Figure 9.40. The 1:2 Divergence.

A) $Re_2 = 379$ $\Delta T = 0$ Flood upstream leg with dye. Travels undisturbed through downstream leg. Flow stable. Slight fall in core due to buoyancy effect.

B) $Re_2 = 703$ $\Delta T = 0$ Instability starts at $X \simeq 11$. This is much further downstream than for same Re_2 with 1:3 divergence.

C) $Re_2 = 1092$ $\Delta T = 0$. Shows how instability moves upstream with increasing Re_2.

D) $Re_2 = 452$ $\Delta T = 4.3^\circ C$
E) $Re_2 = 452$ $\Delta T = 4.3^\circ C$
Heat transfer causes core to fall with distance increasing. E) is 1 minute after D). Effects of recirculation are evident. Instability caused when core from upstream leg touches bottom downstream.

F) $Re_2 = 422$ $\Delta T = 18.7^\circ C$. No severe instability when Re_2 is reduced slightly. Cold core entering downstream leg. Photograph taken 40 seconds after dye enteres downstream leg. Recirculation evident.

G) $Re_2 = 650$ $\Delta T = 18.6^\circ C$
H) $Re_2 = 904$ $\Delta T = 17.8^\circ C$
I) $Re_2 = 1890$ $\Delta T = 20.1^\circ C$
Including F), shows effect of increasing flow-rate with ΔT approximately constant. Buoyancy effects suppressed with increasing Re_2. Position of local turbulence first at $X \simeq 4.5$ because core drops quickly to bottom (G). In H) the instability moves downstream with increasing flow as buoyancy effects are suppressed. Further increase in flow rate causes instability to move back

upstream, probably due to increased rate of shear (I).

Three characteristic flow patterns emerged from the visualization tests, first an undisturbed laminar flow, normally associated with characteristically low Nusselt numbers, second a disturbed laminar flow with localised turbulence which is associated with high Nusselt numbers, and third a fully turbulent flow where high Nusselt numbers are likely.

The position of the turbulent instability was a function of the heat-transfer rate and the Reynolds number. Figures 9.42 and 9.43 show how the position of the instability varied with Re_2 for the divergence ratios 1:3 and 1:2, with zero heat transfer. In the case of the 1:3 divergence a series of tests was carried out using a weak mixture of glycol and water, the purpose being to demonstrate that increasing the viscosity of the fluid did not significantly modify the onset of instability in the flow. The glycol mixture had a Prandtl number three times that of water.

As Re_2 was increased the instability moved rapidly upstream until a limiting position was reached, corresponding approximately to the onset of turbulence upstream.

It is proposed that a Critical Reynolds Number can be derived which will specify the location of the instability uniquely, for all Reynolds numbers below 2,500 upstream, and valid for all divergence ratios. This Reynolds number is defined by:-

$$Re_{crit} = \left(\frac{\rho . \bar{u}_1 . (D_2/D_1) . x_1}{\mu} \right)$$

(Where the parameters are defined in figure 9.44).

The actual value of Re_{crit} was found to be approximately 64,000, and experimental corroboration of this is demonstrated in figure 9.44 .

Figures 9.45 and 9.46 give a comparison between the location of the turbulent flow instability during flow visualization, and the location of the maximum value of Nusselt number downstream of the two divergences (from the main heat transfer experiments, discussed in part 9.7.(iii)). It is evident that the main effect of free convection, when the heat transfer rate is above zero, is to cause the instability, or peak Nusselt number, to move upstream. The effect was pronounced at the lower Reynolds numbers.

In an attempt to correlate the positions of the peak Nusselt numbers in a useful way, the following argument was derived.

It is assumed that the maximum Nusselt number occurs where the cold core of fluid from the tube upstream drops until it touches the bottom of the tube downstream. The approximate distance downstream can be determined as follows:

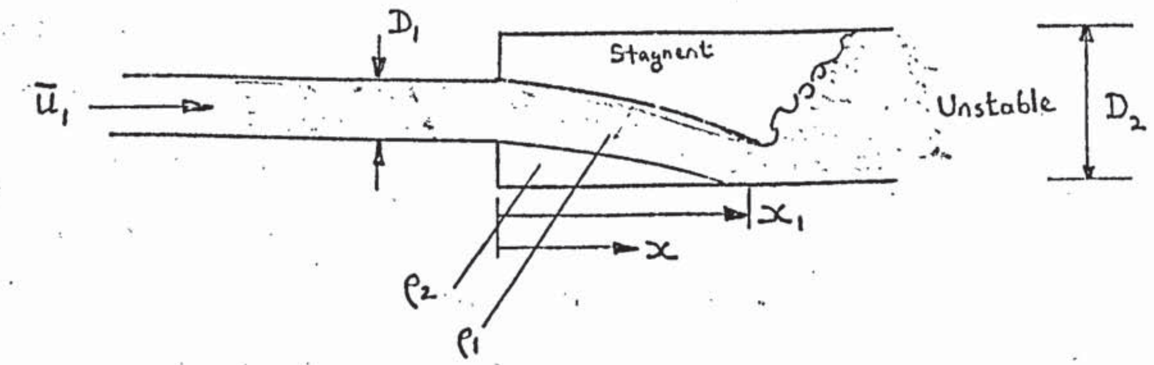

Assume core diameter $\simeq D_1$, and viscous effects are negligible. From simple buoyancy considerations

$$x_1 \simeq \left(\frac{\bar{u}_1^{\,2}\ \rho\ D_2}{g\ \Delta\rho}\right)^{\frac{1}{2}} \qquad \text{where} \begin{cases} \rho_2 \simeq \rho \simeq \rho_1 \\ (\rho_1 - \rho_2) = \Delta\rho \end{cases}$$

or

$$\left(\frac{x_1}{D_2}\right) \simeq \left(\frac{D_2}{D_1}\right)^2 \frac{Re_2}{Gr^{\frac{1}{2}}} \quad .$$

From the preceding, crude analysis an attempt was made at correlating the distance to the peak Nusselt number for low Reynolds number tests. Figure 9.47 shows that the location of the peak Nusselt number is dependent on the local value of the group (Gr/Re_2^2). Although the results were inconclusive, the trend was as anticipated. A more detailed analysis would be required to establish a reliable method of correlating the different parameters involved. (The detailed discussion of the experimental results is given in part 9.7.(iii)).

9.7.(iii) HEAT TRANSFER COEFFICIENT DOWNSTREAM OF A SUDDEN DIVERGENCE.

Figures 9.48 and 9.49 show the distribution of $(Nu/Pr^{\frac{1}{3}})$ in the downstream section of tube for the 1:3.34 divergence with $Pr \simeq 55$. The results were plotted as described in order to eliminate most of the effect of Prandtl number, for comparison purposes, and the only justification for selecting the exponent $\frac{1}{3}$ was that Nu was known to be proportional to $Pr^{\frac{1}{3}}$ at large distances (from the tests on other configurations). Deviations for particular tests from the values of Pr quoted throughout part 9.7.(iii) were of the order 5% and can be ignored for all practical purposes. The tests were grouped into several values of Prandtl number so that any secondary effects of Pr on Nu could be readily determined. Someuncertainty attaches to the experimental measurements made at distances of approximately 0.5 diameters or less downstream because of the 'end effects' already discussed (5.3.(iii)).

The results obtained with turbulent flow upstream and turbulent or transitional flow downstream (i.e. Reynolds numbers > 2,500) are presented in figure 9.48. The Nusselt number quickly reaches a peak at $2\tilde{5}$ diameters, then falls to a constant value at 15 - 25 diameters downstream. The shape of this function is almost the same at all Reynolds numbers, the peak value being 5 to 8 times the limiting value.

With lower Reynolds numbers the distribution of $(Nu/Pr^{\frac{1}{3}})$ becomes more complex, as shown in figure 9.49. Initially, as the Reynolds number downstream (Re_2) is reduced - so that laminar flow must occur at very large axial distances - the trend is for the large peak in the function, which is still present, to move downstream. However, it is evident that for a particular Reynolds number the maximum value of $(Nu/Pr^{\frac{1}{3}})$ can be one of two values, which differ by a factor of $\tilde{5}$, and that subsequent values of the function, at distances of the order 40 diameters, differ by a factor of 2 to 3. This phenomenan is explained in part 9.7.(ii) as being caused by a localised region of turbulence which may or may not arise at low Reynolds numbers when the laminar flow pattern tends to be unstable.

The axial disposition of the peak Nusselt number appears to be dependent on the heat flux at the very low Reynolds numbers, which is in keeping with the arguments proposed in part 9.7.(ii), where the location of the peak was shown to be dependent on $(Re/Gr^{\frac{1}{3}})$. To highlight the complexity of the heat transfer mechanisms at low values of Re_2, a graph was plotted showing $(Nu/Pr^{\frac{1}{3}})$ versus (axial distance) with $Re_2 \simeq 250$ for five independent tests. (figure 9.51).

It is clear that for low Reynolds numbers it is impossible to provide a unique relationship between heat transfer coefficient and distance, but it is probable that Nu, for a given Re_2 and Pr, can be either characteristically laminar or turbulent, will be a function of the critical length derived from Re_{crit} (see part 9.7.(ii)), and will depend on $(Re/Gr^{\frac{1}{3}})$. Figures 9.42, 9.45 and 9.47 should be used in conjunction with the basic data for $(Nu/Pr^{\frac{1}{3}})$, discussed above, when it is necessary to interpolate from these experimental results to heat transfer coefficients at other operating conditions.

Figure 9.50 demonstrates how the Nusselt number downstream is affected by varying the rate of heat transfer in the section of tube upstream. The condition mormally imposed, of uniform heat transfer per unit length in each section, is compared with the case of zero heat flux upstream. It was impracticable to conduct two tests with different boundary conditions at exactly the same Reynolds number, but similar values of Re_2 were possible, and in comparing $(Nu/Pr^{\frac{1}{3}})$ an allowance for the small differences in Re_2 could be made by assuming $Nu \propto Re^n$. Whence, (% change in Nu) = n (% change in Re) where n can be estimated (as discussed later in this section). Bearing this in mind, it was shown that for fully turbulent flow ($Re_2 > 10{,}000$) $(Nu/Pr^{\frac{1}{3}})$ was within 2% with the upstream leg either heated or unheated.

It is to be expected that Nu will be unaffected by conditions upstream, since the very thin temperature layers close to the wall, which are normally associated with high values of Pr, are unlikely to be physically carried to the region of the wall downstream. It is more likely that the temperature boundary layers will become diffuse shortly after the discontinuity. With low values of Pr this might not be the case, Ede (Ref: H.1.), for example, showed that an increase in Nu of the order 20% could occur when the heat source was removed from upstream. The fluid utilised was water $Pr \simeq 8$ and the configuration was similar to the present apparatus.

At low values of Re_2 a comparison was more difficult because of instability in the flow and the secondary effects of free convection. The maximum value of $(Nu/Pr^{\frac{1}{3}})$ was once again within 2% for the heated and unheated case. When the heat source upstream was removed, there was a tendency for the location of the peak to move downstream slightly, this was particularly pronounced with low Reynolds numbers, but in view of the foregoing arguments it is apparent that slight variations in a number of parameters could easily lead to such phenomena.

Figures 9.52, 9.53 and 9.54 give the axial distribution of $(Nu/Pr^{\frac{1}{3}})$ for Prandtl numbers 140, 275 and 500. In general the shape and magnitude of the functions obtained with various values of Pr, when Re_2 was above approximately 2,000, was independent of the Prandtl number. At much lower Reynolds numbers the trend was for the peak value of

$(Nu/Pr^{\frac{1}{3}})$ to increase significantly with increasing Pr, although substantial changes were not apparent 40 diameters downstream.

A theoretical analysis of stable laminar motion through a 1:2 divergence (see part 11.3.) indicated that $Nu \propto Pr^n$ varied between 1/5 and $\frac{1}{3}$ depending on axial position. This means the peak value of $(Nu/Pr^{\frac{1}{3}})$ should reduce marginally with increasing Pr, but the experimental results were inconclusive in this repsect, because the secondary effects of flow instability and free convection tended to distort the $(Nu/Pr^{\frac{1}{3}})$ functions. The theory also indicated that close to the discontinuity the value of $(Nu/Pr^{\frac{1}{3}})$ might reduce with increasing Reynolds number. Figure 9.49 (with $Pr \approx 55$) shows that $(Nu/Pr^{\frac{1}{3}})$ could indeed reduce with increasing Re_2 ($\gtrsim 1,000$).

The figures 9.55 to 9.58 show comparable data on $(Nu/Pr^{\frac{1}{3}})$ versus (axial distance), but with the divergence ratio 1:2. The same general observations made for the 1:3.34 divergence were applicable but the following differences were noted. The shape of the functions in the region of the peak value was such that the 1:2 curves exhibited a smaller maximum, whilst the length of this region was approximately the same as the 1:3.34 case - the basis of the comparison being particular values of Re_2 downstream. The ratio (Nu at peak)/(Nu at 40 diameters) was 3 to 6 (compared with 5 to 8) for $Re_2 \lesssim 2,500$. $(Nu/Pr^{\frac{1}{3}})$ at the lower Reynolds numbers was lower than the 1:3.34 case for particular values of Re_2. At high values of Re_2 the location of the peak was $\tilde{2}.0$ diameters downstream (compared with $\tilde{2}.5$).

For the 1:1.25 divergence the peak in the $(Nu/Pr^{\frac{1}{3}})$ functions at $Re_2 \lesssim 2,500$, was sharply defined and occurred at $\tilde{0}.5$ diameters downstream; the value of the ratio (Nu at peak)/(Nu at 40 diameters) was 2 to 4. The results are given in figures 9.59 to 9.62. There was a clear distinction between the magnitude of the apparently 'turbulent' and 'laminar' Nusselt numbers, and with lower values of Re_2, large variations in Re_2 were necessary to cause substantial changes in the magnitude of $(Nu/Pr^{\frac{1}{3}})$. In this region the functions tended to be almost a constant downstream of approximately 5 diameters.

To demonstrate the effects of diameter ratio, on Nu in the region of the discontinuity, over a wide range of ratios, a graph was plotted (Fig: 9.63) of $(Nu/Pr^{\frac{1}{3}})$ versus (axial distance) for particular Reynolds numbers and $Pr \simeq 60$. From the theoretical findings of part 11.3., and from the conclusions of the flow visualization tests, it was decided that the peak value of $(Nu/Pr^{\frac{1}{3}})$, with either 'localised' or 'full' turbulence present in the downstream leg, was likely to be a function of Re_1 (The Reynolds number in the upstream leg). Consideration was given to the results of tests carried out with an extended range of diameter ratios (see part 7.4.(ii).

$(Nu/Pr^{\frac{1}{3}})$ is given (Fig: 9.63) for $Re_1 = 12{,}500$ ($\pm$ 4%). It is apparent from this graph that Nu is substantially a function of Re_1 for the first 4 diameters downstream, then largely a function of Re_2 downstream of $\stackrel{\sim}{}25$ diameters. The range of diameter ratios considered was 1:1.25 to 1:14.4. Figure 9.64 gives a more detailed expression of how the peak value of $(Nu/Pr^{\frac{1}{3}})$, and the location of the peak, depends on the divergence ratio, at high Reynolds numbers. With low 'ratios', such that the flow close to the divergence is turbulent upstream and downstream ($Re_1 \gtrsim 2{,}500$), $(Nu/Pr^{\frac{1}{3}})_{max}$ reduces by $\sim$10% with increasing divergence ratio. This could be because the distance between the exit of the upstream leg, and tube wall downstream, increases with the divergence ratio. The turbulence energy (or eddying) in the flow will probably decay with the increasing distance, which would cause a reduction in rate of transport of heat from the tube wall downstream.

At higher divergence ratios ($Re_1 < 2{,}500$) the Nusselt number suddenly starts to increase with 'ratio', until $(Nu/Pr^{\frac{1}{3}})_{max}$ is approximately 50% higher (with the 1:14.4 divergence). The rate of increase in Nu with 'ratio' reduces as the divergence ratio increases. Although it was not demonstrated experimentally, the peak value of $(Nu/Pr^{\frac{1}{3}})$ will eventually reduce with increasing diameter ratio because, as 'ratio' tends to infinity the turbulence energy transported from upstream will probably be damped by viscous action, before reaching the tube wall downstream. Such phenomena could only be observed with 'ratios' much greater than 1:14.4. In the range of 'ratios' considered, however, the effect of reducing the velocity downstream to a sub-turbulent level by increasing the ratio was to increase $(Nu/Pr^{\frac{1}{3}})_{max}$, the mechanisms being too complex for an elementary explanation to be propounded. The relative rates at which turbulence energy is generated, diffused and damped in the laminar-unstable region downstream could lead to a complex relationship between divergence ratio and Nusselt number.

The axial position at which the peak value of $(Nu/Pr^{\frac{1}{3}})$ occurs depends on the divergence ratio as follows. With the low 'ratios'(so that $Re_2 \gtrsim 2{,}500$) the efflux from the upstream leg expanded downstream in a similar fashion to a submerged, round, turbulent jet (e.g. Ref: K.1). As indicated by the flow visualization tests the initial mixing downstream occurred at a full angle of approximately 30° (see figure 9.39E) which is characteristic of turbulent jets and wakes in general. If it is assumed that the maximum value of Nu arises where the conical mixing region fills the downstream leg, then the distance to this point must be given approximately by

$$(x/D_2)_{max} = (1 - D_1/D_2) \cot\alpha$$

where α = half angle of conical mixing region.

or $\quad (x/D_2)_{max} = 3.73\ (S - 1)/S$

where $\quad S$ = diameter ratio.

This formula is shown plotted in figure 9.64 and is denoted "THEORY". Good agreement is demonstrated with experiment.

At the higher ratios the distance to the peak value of $(Nu/Pr^{\frac{1}{3}})$ varies only marginally with diameter ratio, the position is nearer to the discontinuity than the above theory would indicate. Once, more, the mechanisms of unstable laminar flow are too complex to permit a simple explanation of the phenomena.

Since the maximum value of $(Nu/Pr^{\frac{1}{3}})$ was seen to be largely dependent upon the Reynolds number upstream Re_1, graphs of the peak value $(Nu/Pr^{\frac{1}{3}})_{max}$ versus Re_1 were plotted for each individual diameter ratio. These are given in figures 9.65 to 9.67, and different values of Pr are specified. When Re_1 exceeds approximately 2,900 unique functions can be defined which represent the experimental results with a maximum deviation of 40%. For two of the configurations these functions could be conveniently expressed; thus -

For 1:3.34 ratio, $\quad Nu_{max} = 0.292.\ Re_1^{\frac{2}{3}} . Pr^{\frac{1}{3}}$.

For 1:2.00 ratio, $\quad Nu_{max} = 0.255.\ Re_1^{\frac{2}{3}} . Pr^{\frac{1}{3}}$.

In the case of the 1:1.25 divergence a similar expression was found to be equally reliable when $Re_1 > 3,000$, viz:

For 1:1.25 ratio, $\quad Nu_{max} = 0.255.\ Re_1^{\frac{2}{3}} . Pr^{\frac{1}{3}}$.

However, it is apparent from figure 9.67 that the above equation will consistently overestimate Nu_{max} until Re_1 exceeds 8,000.

Since the peak value of $(Nu/Pr^{\frac{1}{3}})$ appeared to be a function of the Reynolds number upstream to a first approximation, a graph of $(Nu/Pr^{\frac{1}{3}})_{max}$ versus Re_1 was plotted with the experimental results derived from all three divergences. Figure 9.68 shows that in the range $Re_1 \simeq 700$ to 35,000 the following equation can be used to represent the peak Nusselt number for flows which are characteristically turbulent or unstable-laminar:

$$Nu_{max} = 0.28 \; Re_1^{\frac{2}{3}} \; Pr^{\frac{1}{3}} \; .$$

The experimental deviations from the above function were as follows. With fully turbulent flow upstream, i.e. $Re_1 \gtrsim 10^4$, variations of 20% were observed. With lower values of Re_1, 90% of the data was within 50% of the equation given. In a few tests the flow was 'transitional', that is neither characteristically laminar nor turbulent. In these tests deviations from the above expression led to values of Nu_{max} which were of the order 40 to 50% of the proposed turbulent function.

When the Reynolds number upstream was in the laminar range ($Re_1 \lesssim 2{,}500$) the Nusselt numbers derived for stable-laminar motion were typically a factor of 1/5 to 1/7 of the turbulent, or unstable-laminar, values. The values of $(Nu/Pr^{\frac{1}{3}})_{max}$ were scattered within 0.45 and 1.9 times the mean function when the results for all divergence ratios were compared (see figure 9.68). When particular divergence ratios were considered the results were more meaningful, (Figs: 9.65 to 9.67). For the 1:3.34 ratio a transition range of Re_1 was evident between $\tilde{7}00$ and $2,\tilde{8}00$, in which the flow was either characteristically laminar or turbulent (as indicated by the magnitude of Nu_{max}). Below $Re_1 \simeq 700$ the flow was never turbulent in character, and above $Re_1 \simeq 2{,}800$ the flow was never laminar. For the 1:2.00 and 1:1.25 ratios, the transition region was not so clearly defined, At the lower end of the region it was found that characteristically turbulent flow could not be sustained below values of Re_1 of $1,\tilde{0}00$ and $1,\tilde{5}00$ respectively. Hence, the length of the transition region. increased with divergence ratio (the upper limit of Re_1 can be considered invariant at approximately 2,500, the onset of normal turbulence upstream.) The phenomenon described is consistent with the idea that the onset of the flow-instability depends on the shearing action arising from the difference between the velocities of the liquid upstream and downstream of the step. This difference in velocity, and therefore shearing rate, must be a function of the divergence ratio.

The 'laminar' values of $(Nu/Pr^{\frac{1}{3}})_{max}$ for the 1:3.34 divergence are reasonably well defined by a unique function, as shown in figure 9.65 the experimental deviations did not exceed ± 40%. With the 1:2.00 and 1:1.25 ratios, the results were scattered and did not correlate well. In view of the previous argument on transitional regions, and considering that free convectional contributions to Nu_{max} have been excluded from the correlation, it is understandable that a unique function representing these results could not be obtained using the methods described.

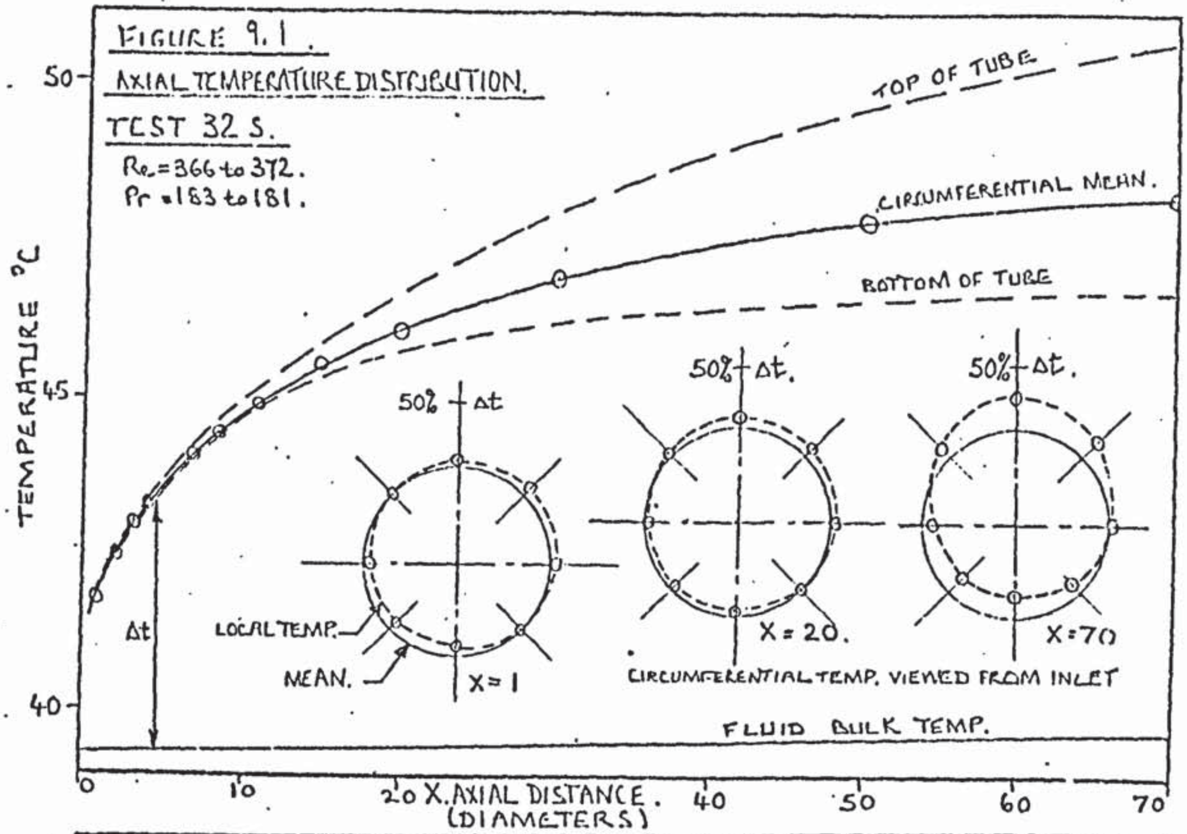
FIGURE 9.1.
AXIAL TEMPERATURE DISTRIBUTION.
TEST 32 S.
Re = 366 to 372.
Pr = 183 to 181.
TOP OF TUBE
CIRCUMFERENTIAL MEAN.
BOTTOM OF TUBE
50% Δt
50% Δt.
50% Δt.
LOCAL TEMP.
MEAN.
X = 1
X = 20.
X = 70
CIRCUMFERENTIAL TEMP. VIEWED FROM INLET
FLUID BULK TEMP.
Δt
TEMPERATURE °C
50
45
40
0
10
20
40
50
60
70
X. AXIAL DISTANCE. (DIAMETERS)

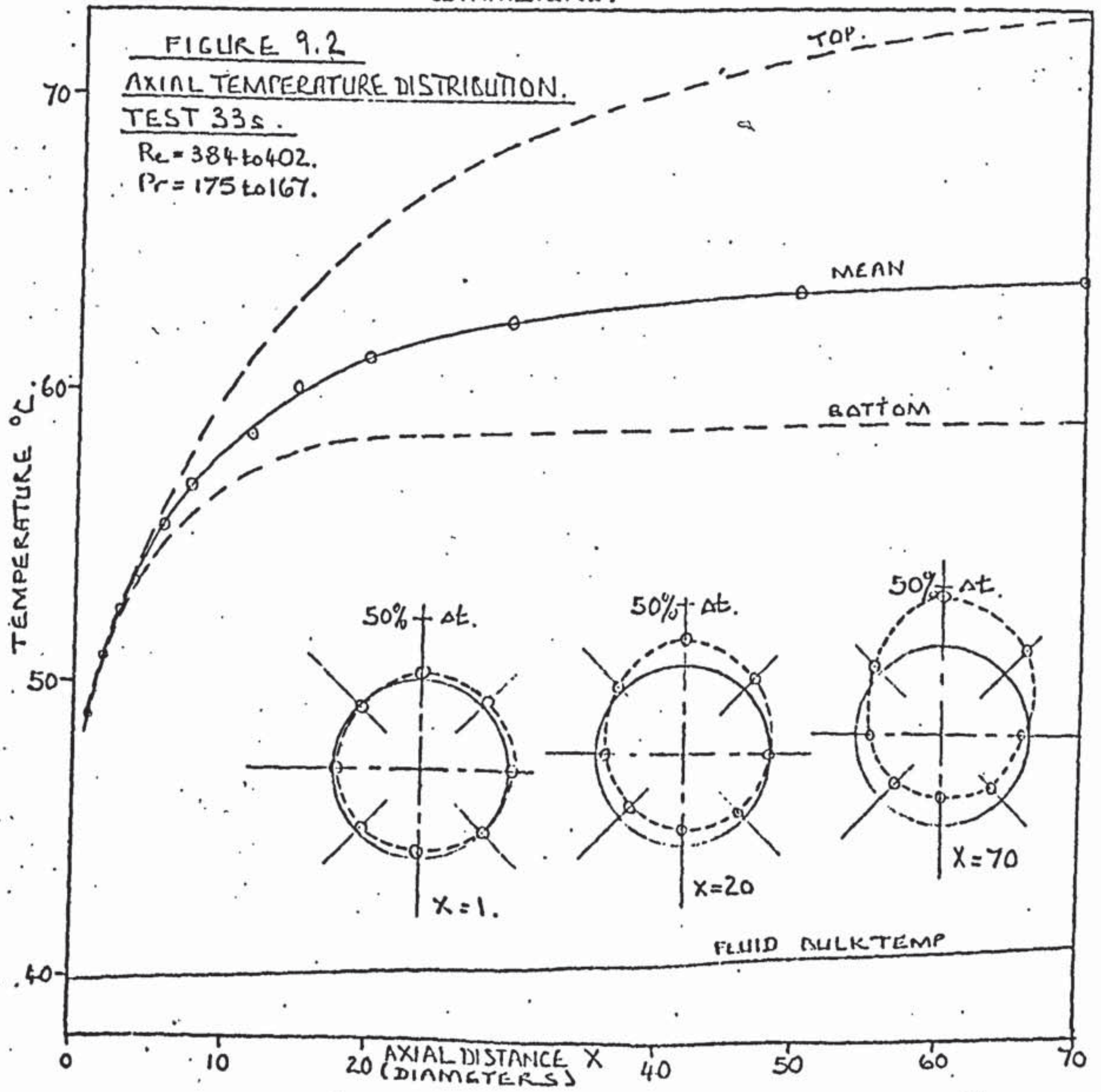
FIGURE 9.2
AXIAL TEMPERATURE DISTRIBUTION.
TEST 33s.
Re = 384 to 402.
Pr = 175 to 167.
TOP.
MEAN
BOTTOM
50% Δt.
50% Δt.
50% Δt.
X = 1.
X = 20
X = 70
FLUID BULK TEMP
TEMPERATURE °C
70
60
50
40
0
10
20
40
50
60
70
AXIAL DISTANCE X (DIAMETERS)

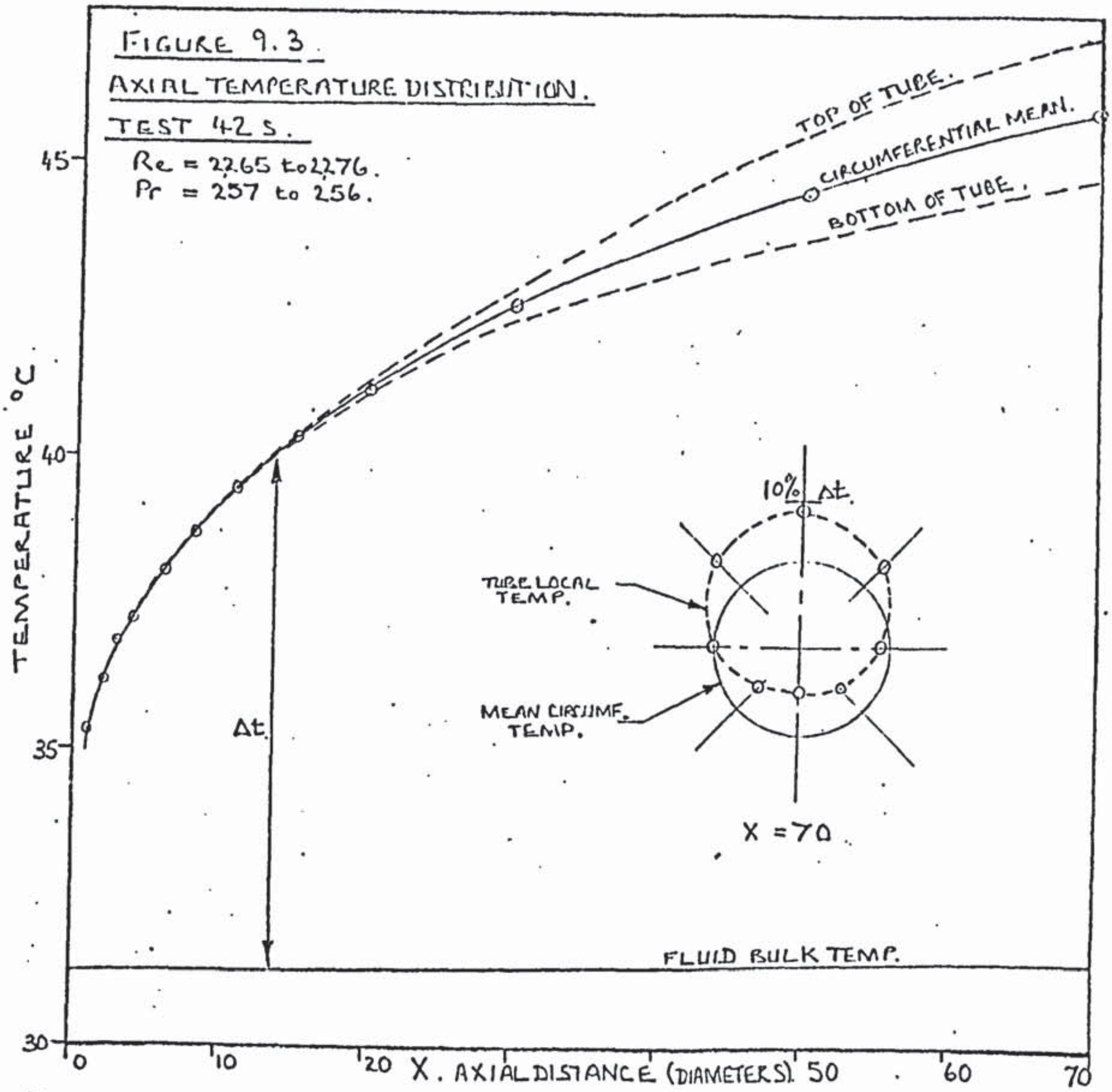

FIGURE 9.3.

AXIAL TEMPERATURE DISTRIBUTION.

TEST 42 S.

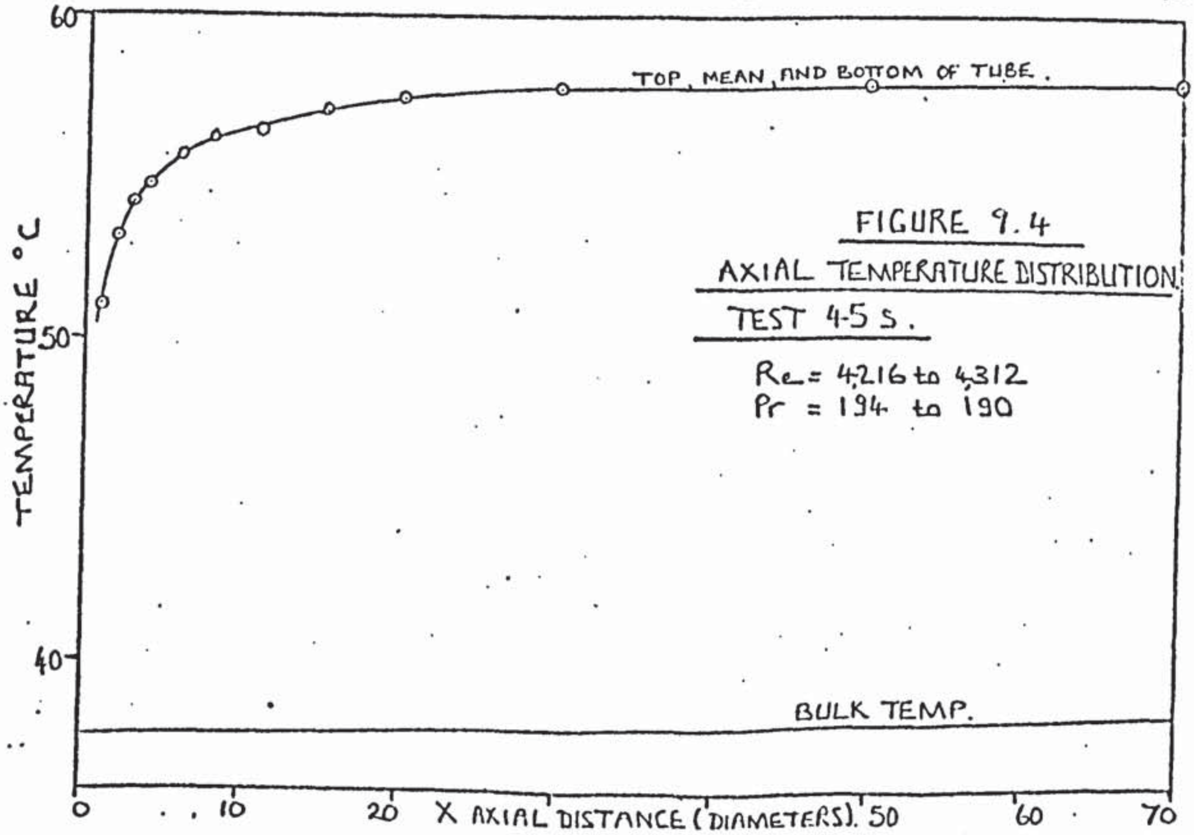

FIGURE 9.4

AXIAL TEMPERATURE DISTRIBUTION

TEST 45 S.

FIGURE 9.5.

TUBE TEMPERATURE FLUCTUATIONS WITH TIME AT 1,3,4,11,20,70 DIAMETERS DOWNSTREAM, FOR BELLMOUTH ENTRANCE — DERIVED FROM CRUDE MEASUREMENTS.

(TESTS 60SB TO 72SB).

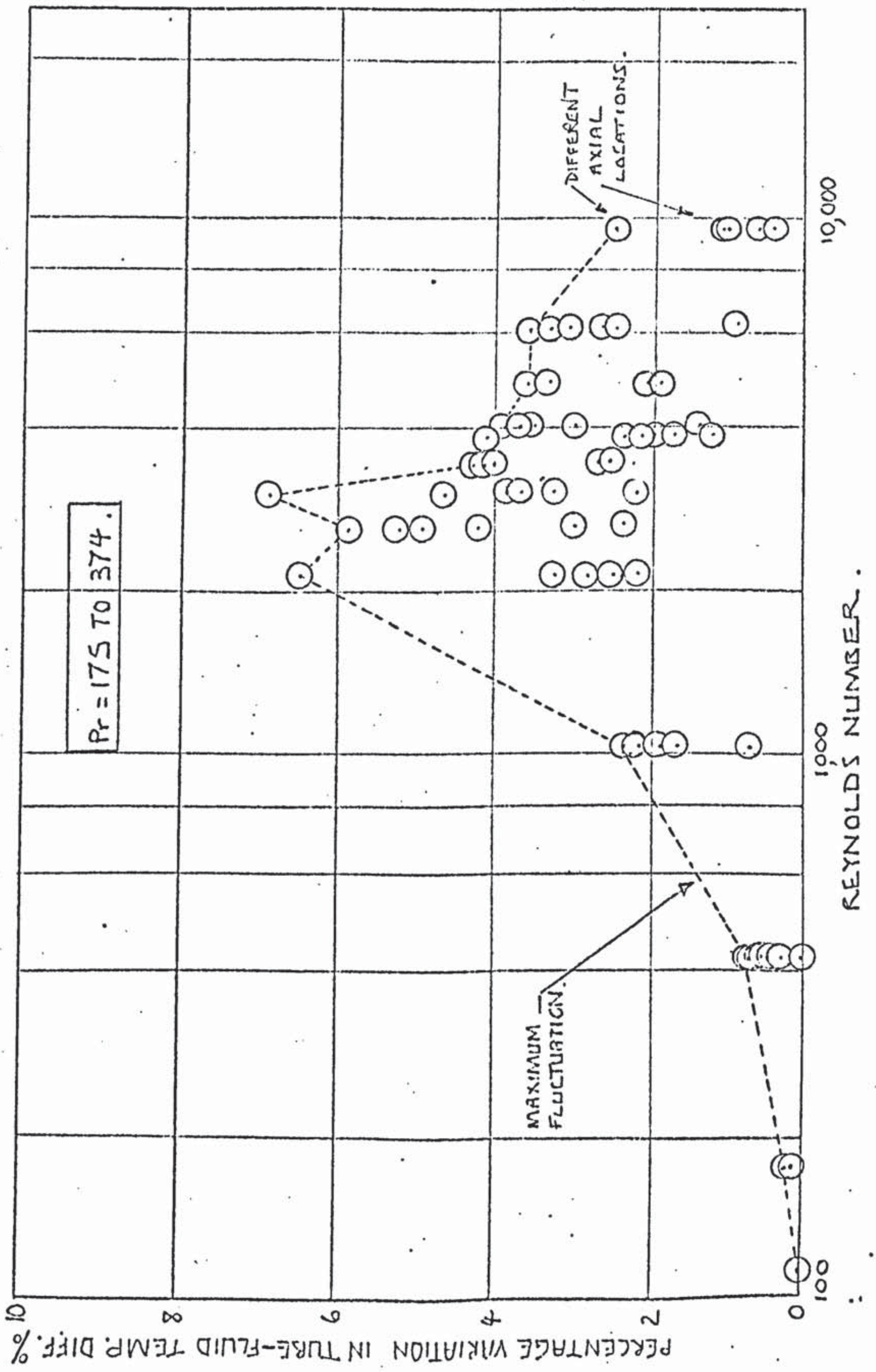

FIGURE 9.6.

TUBE TEMPERATURE FLUCTUATIONS WITH TIME AT 1, 5·5, 15, 40 DIAMETERS DOWNSTREAM, FOR SUDDEN CONVERGENCE EXPERIMENTS. — DERIVED FROM CRUDE MEASUREMENTS.

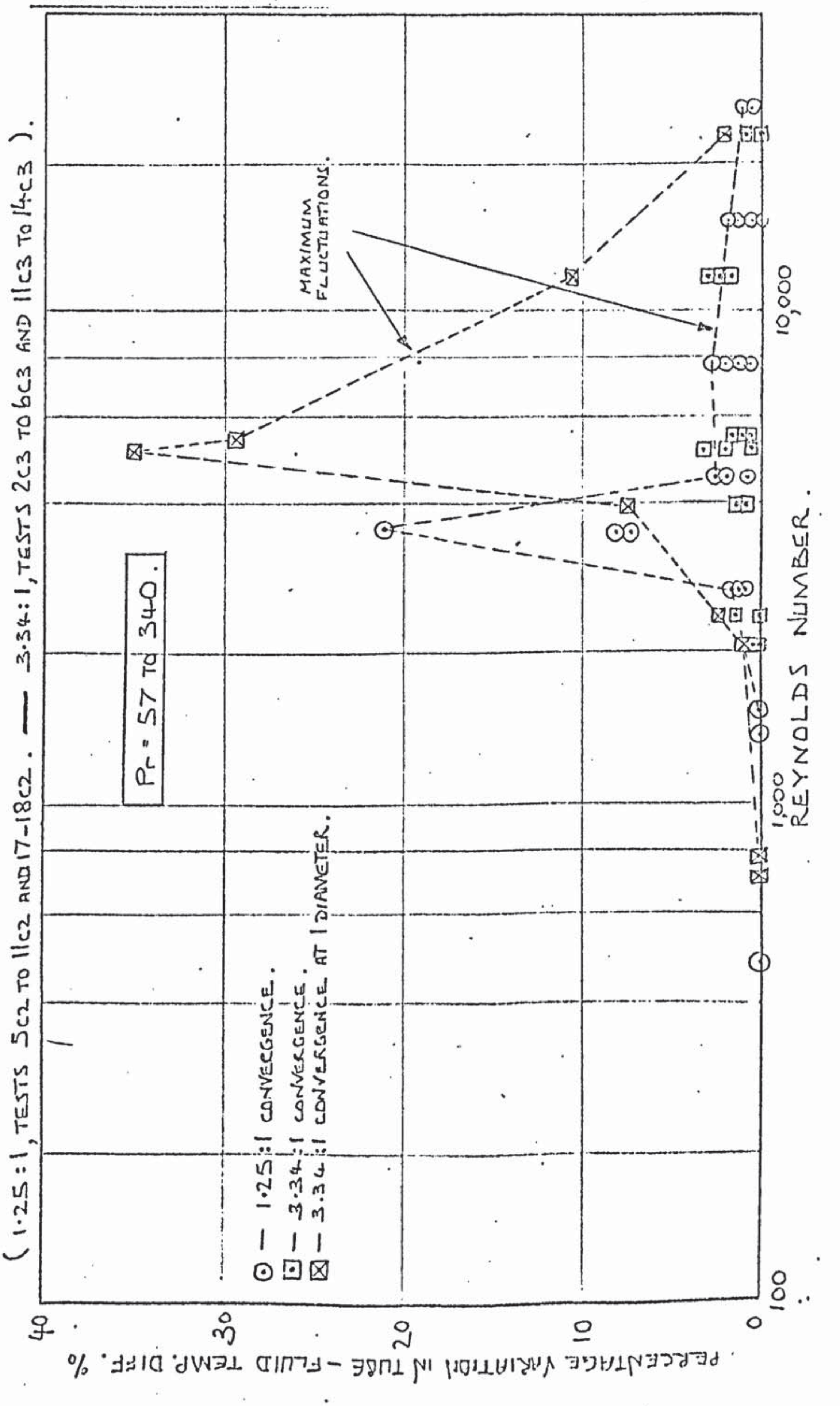

FIGURE 9.7 .

VARIATIONS IN TIME FOR TUBE TEMPERATURE IN TEST 46D1.

DIVERGENCE RATIO = 1:3.34 . Re = 497/1663 . Pr = 271 .

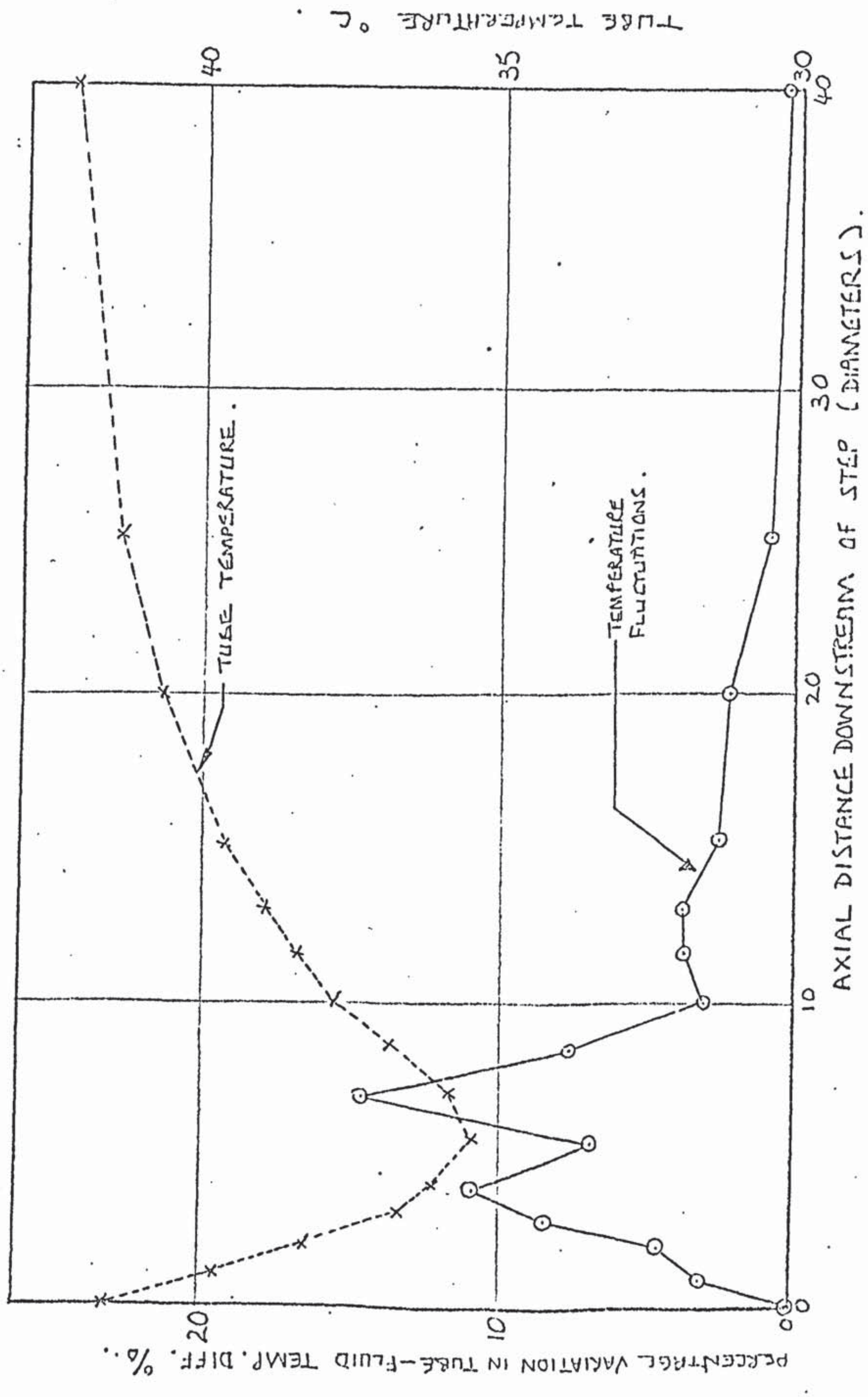

FIGURE 9.8.

AXIAL TEMPERATURE PROFILE MEASURED IN TEST 48D1.

DIVERGENCE RATIO = 1:3.34. Re = 242/809. Pr = 275.

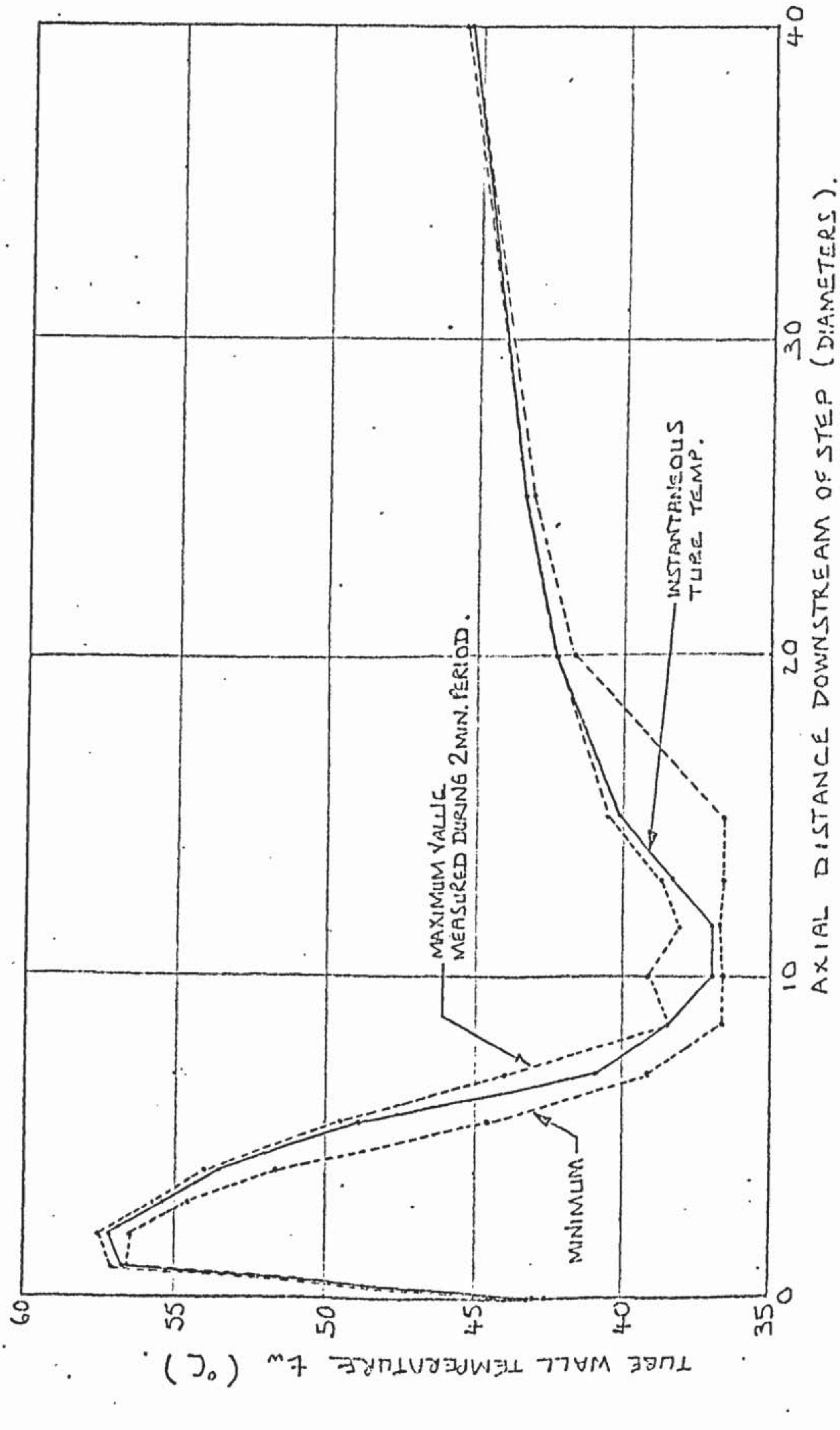

FIGURE 9.9.

MEASURED VARIATIONS IN TUBE WALL TEMPERATURE WITH TIME. 1:3·34 DIVERGENCE. 5 AND 40 DIAMETERS DOWNSTREAM.

(TESTS 1 DI. TO 51 DI.).

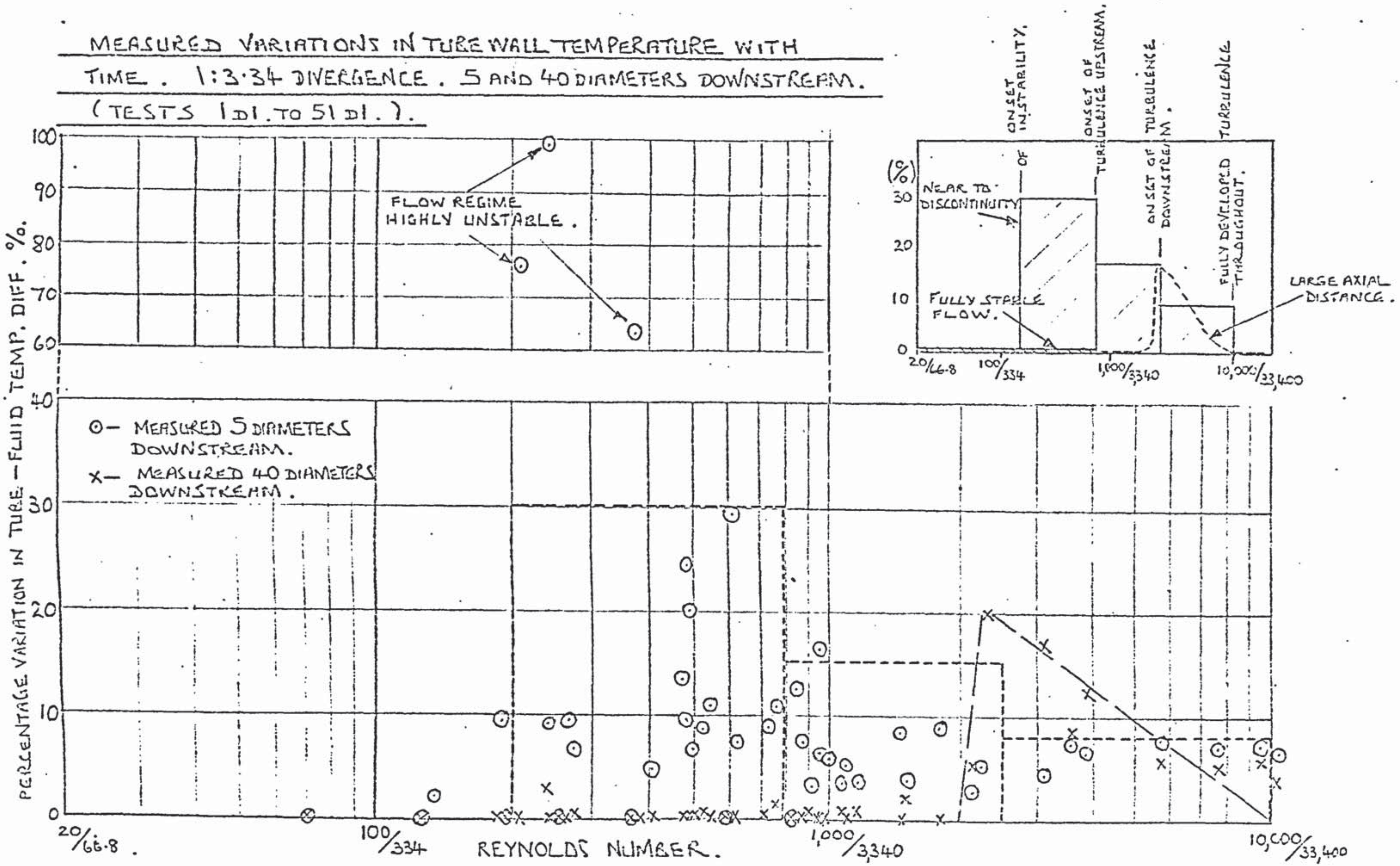

FIGURE 9.10

THE DIMENSIONLESS COEFFICIENT OF HEAT TRANSFER 70 DIAMETERS DOWNSTREAM. WITH CALMING LENGTH. WITHOUT VISCOSITY CORRECTION.

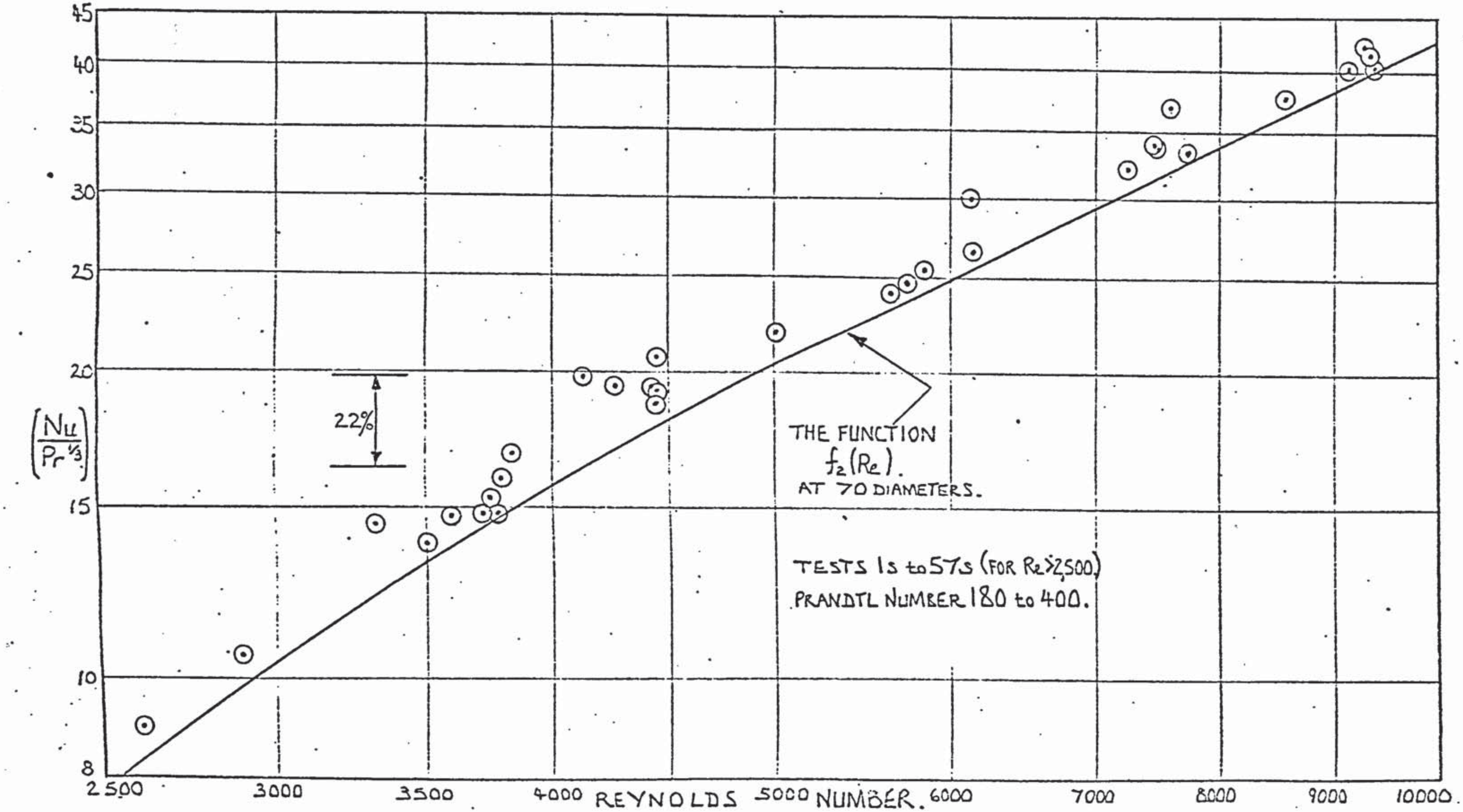

FIGURE 9.11.

EXTRAPOLATION OF NUSSELT NUMBER TO THE ZERO HEAT FLUX CONDITION ELIMINATING THE PROPERTY VARIATION WITH TEMPERATURE.

(CALMING LENGTH FITTED. MEASURMENTS AT 70 DIA.)

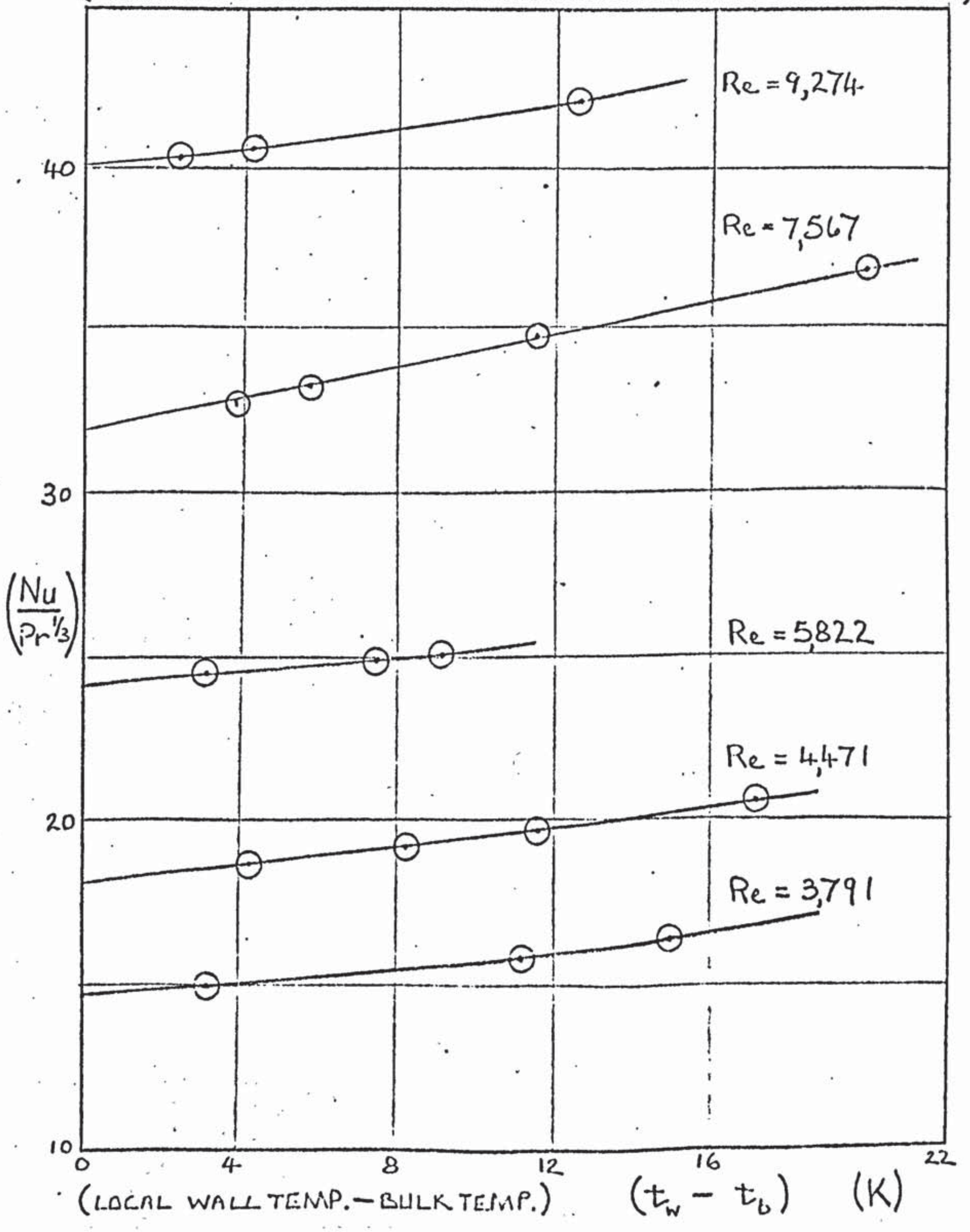

FIGURE 9.12.

THE DEPENDENCE OF NUSSELT NUMBER ON THE RATIO (VISCOSITY AT BULK TEMP.)/(VISCOSITY AT WALL TEMP.) — TESTS 1s to 57s.

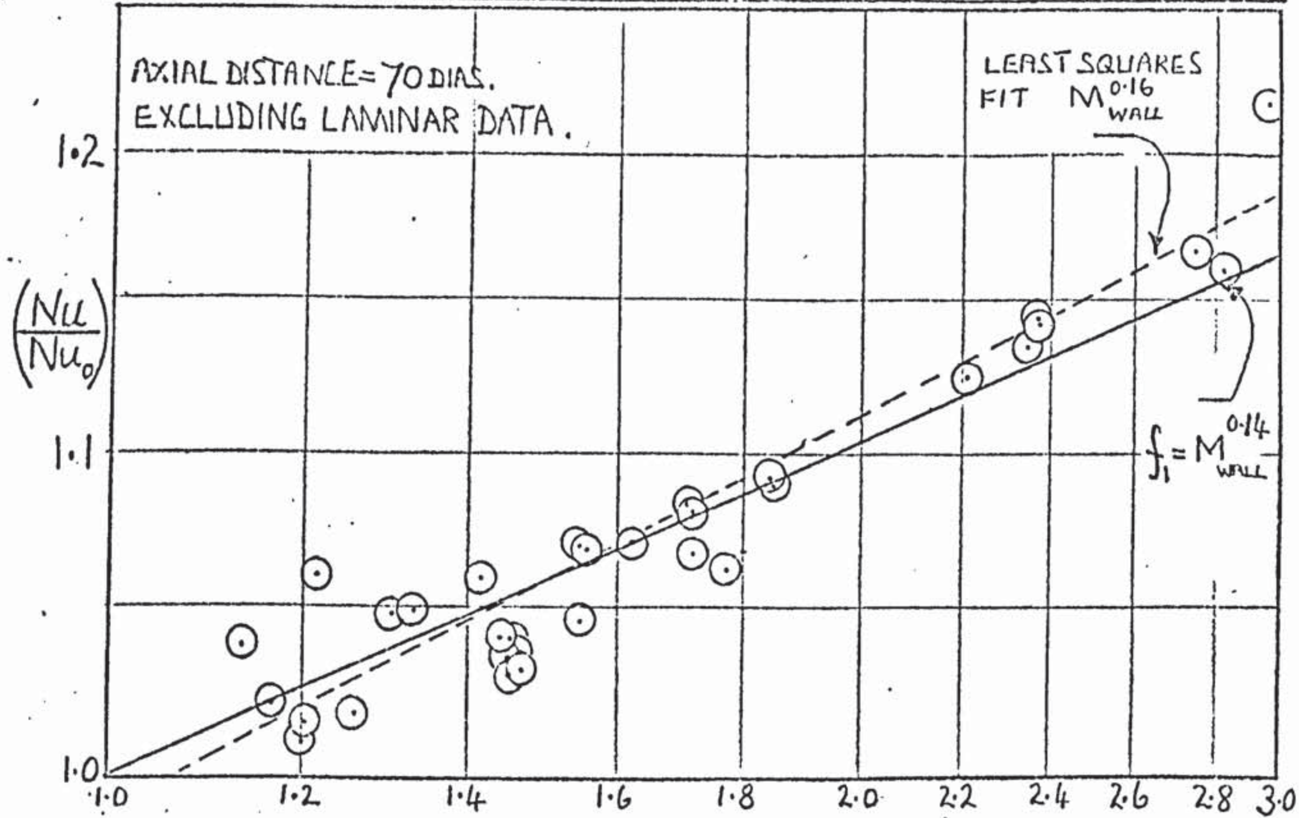

(Nu_o = NUSSELT NUMBER WHEN VISCOSITY IS INDEPENDENT OF TEMPERATURE.)

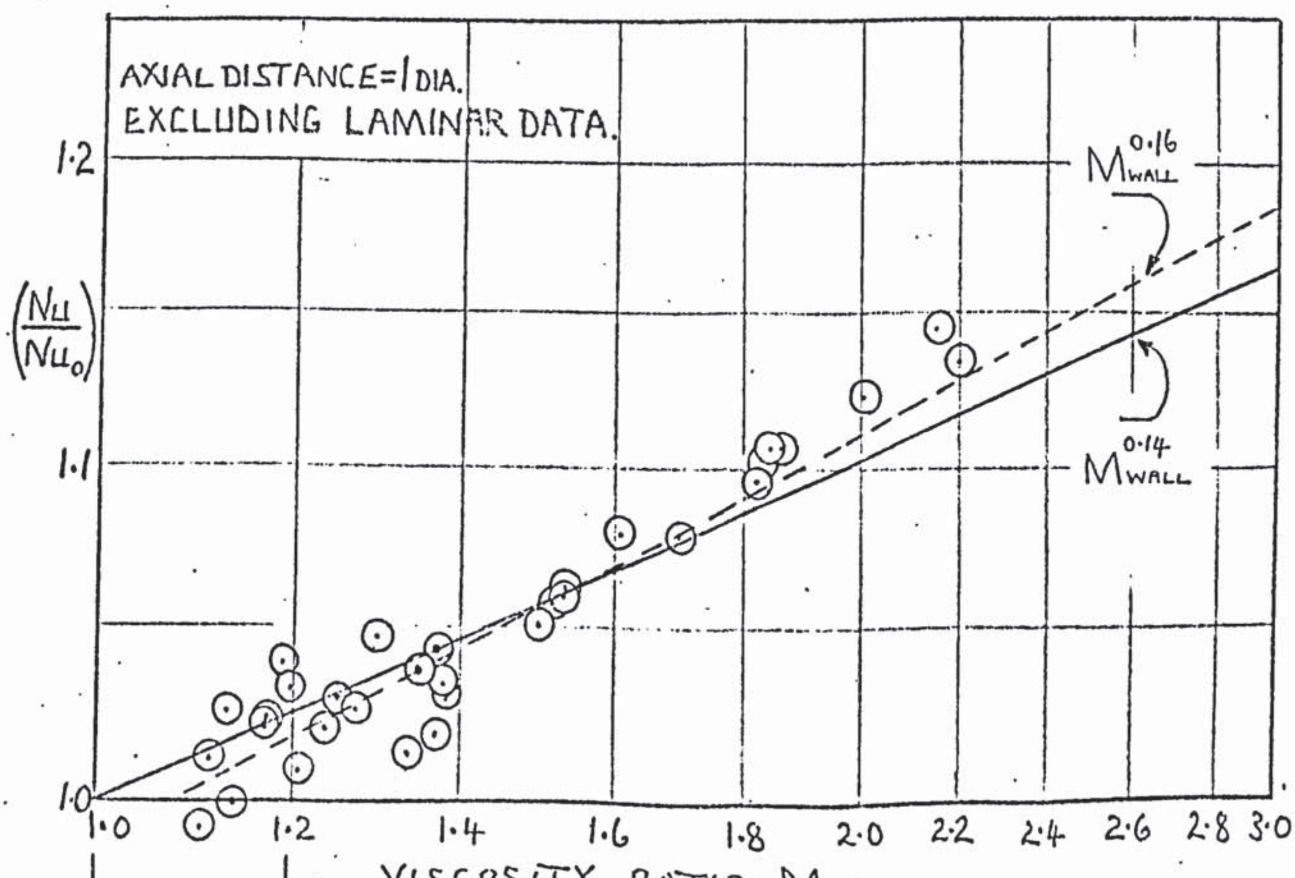

FIGURE 9.13

THE DEPENDENCE OF NUSSELT NUMBER ON REYNOLDS NUMBER FOR PARTICULAR AXIAL POSITIONS. CALMING LENGTH FITTED. Re = 2500 to 10,000.

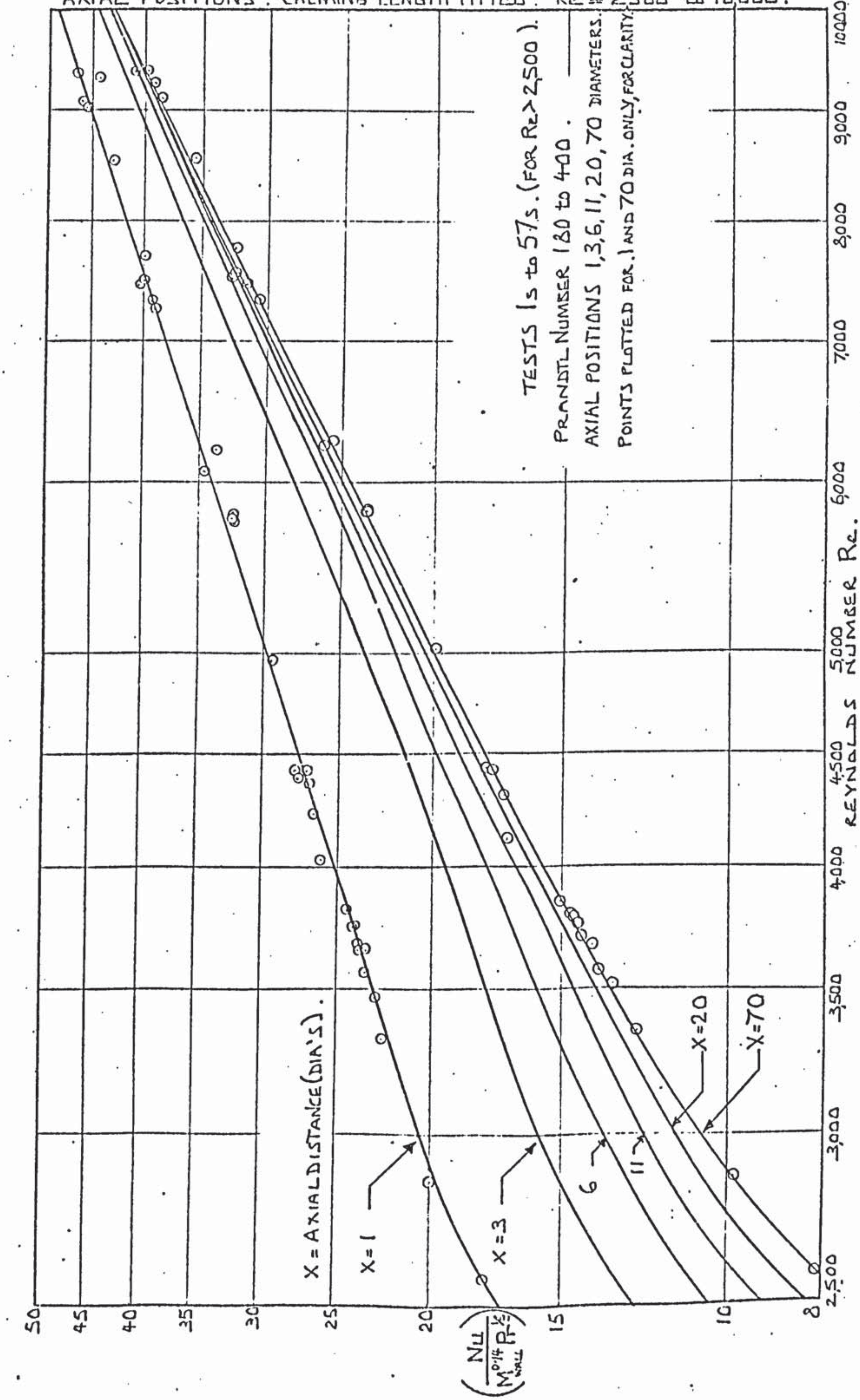

FIGURE 9.14.

THE DEPENDENCE OF NUSSELT NUMBER ON PRANDTL NUMBER.

$\left(\frac{Nu}{M_{WALL}^{0.14} \cdot f_2(Re)}\right)$ VERSUS (Pr) FOR TESTS 1s to 57s

EXCLUDING LAMINAR FLOW DATA. CALMING LENGTH FITTED.

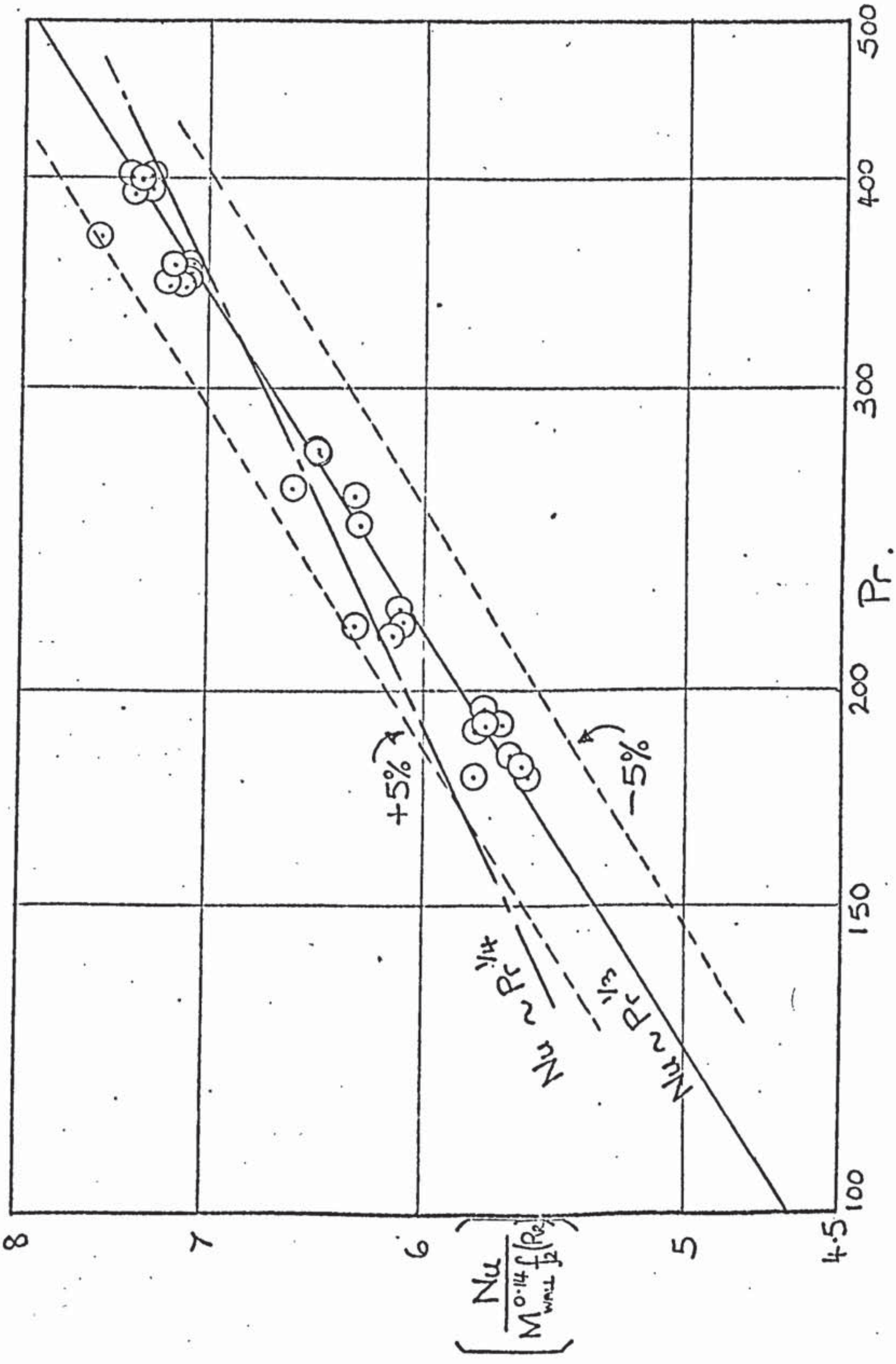

FIGURE 9.15.

THE VARIATION IN NUSSELT NUMBER WITH AXIAL POSITION. CALMING LENGTH FITTED — TESTS 1S, 12S, 22S. — Re > 2,500.

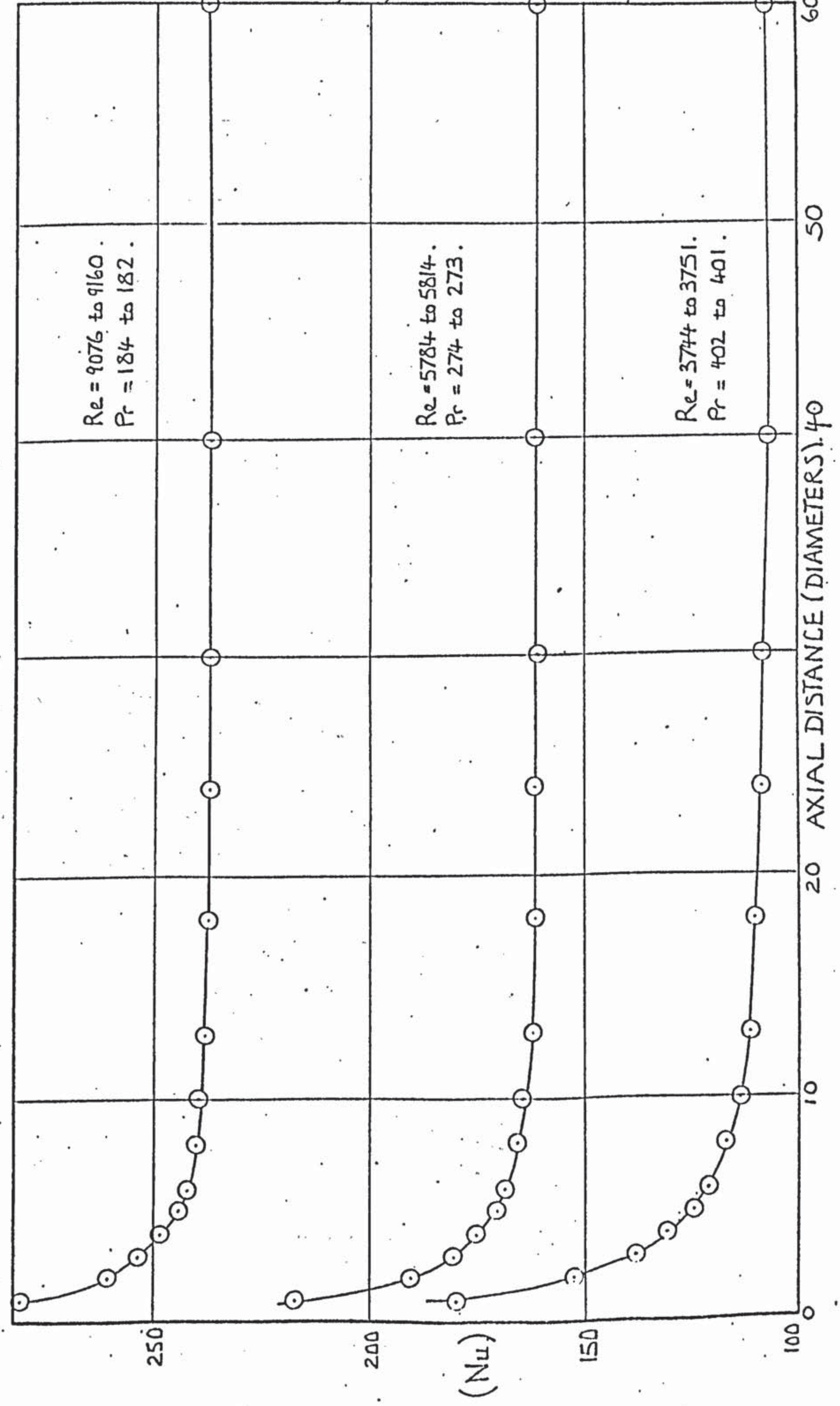

FIGURE 9.16.

NUSSELT NUMBER IN THE ENTRANCE REGION. CALMING LENGTH FITTED. Re>2,500.

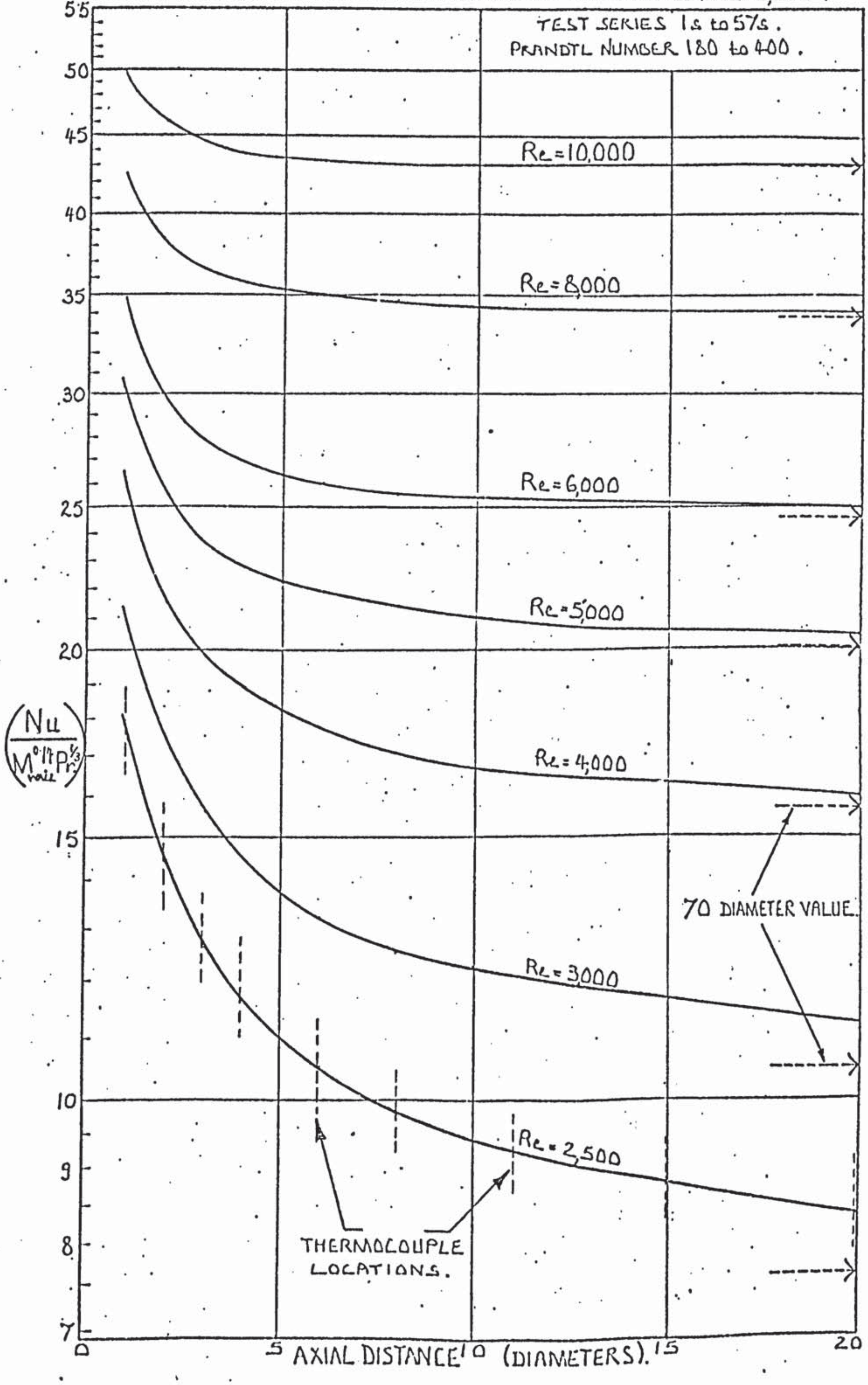

FIGURE. 9.17.

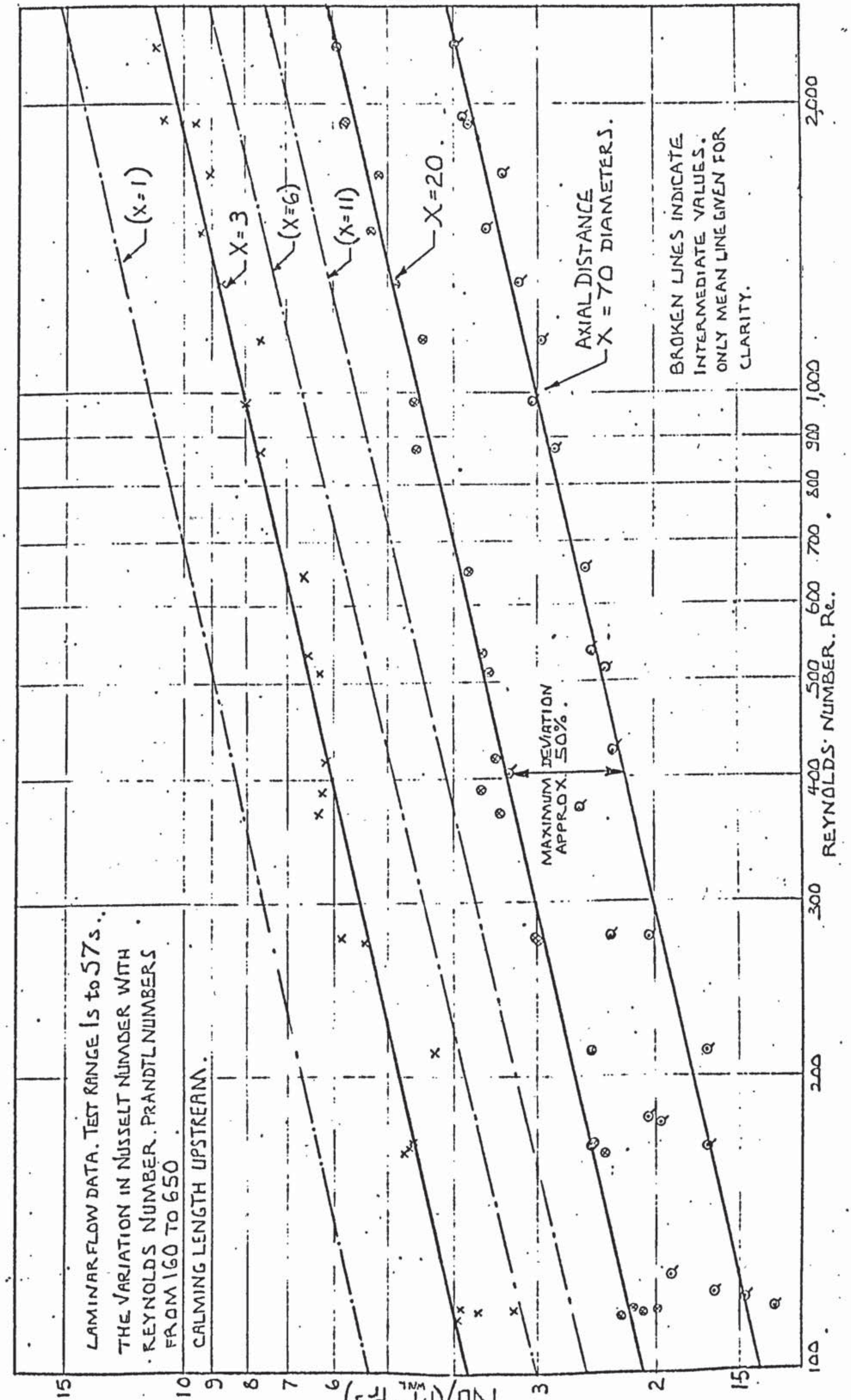
LAMINAR FLOW DATA. TEST RANGE 1s to 57s.
THE VARIATION IN NUSSELT NUMBER WITH REYNOLDS NUMBER. PRANDTL NUMBERS FROM 160 TO 650
CALMING LENGTH UPSTREAM.
(X=1)
X=3
(X=6)
(X=11)
X=20
AXIAL DISTANCE X = 70 DIAMETERS.
BROKEN LINES INDICATE INTERMEDIATE VALUES. ONLY MEAN LINE GIVEN FOR CLARITY.
MAXIMUM DEVIATION APPROX. 50%.
REYNOLDS NUMBER. Re.
100
200
300
400
500
600
700
800
900
1,000
2,000
15
10
9
8
7
6
3
2
1.5

FIGURE 9.18.

THE INCREASE IN NUSSELT NUMBER BY FREE CONVECTION AS INDICATED BY THE GROUP $(Gr\,Pr)^{1/4}/(Re\,Pr)^{1/3}$. LAMINAR FLOW DATA FOR TESTS IN THE RANGE 1s. to 82s. ON THE SHORT TUBE. REYNOLDS NUMBER ≃ 100 – 2000. PRANDTL NUMBER ≃ 90 — 650

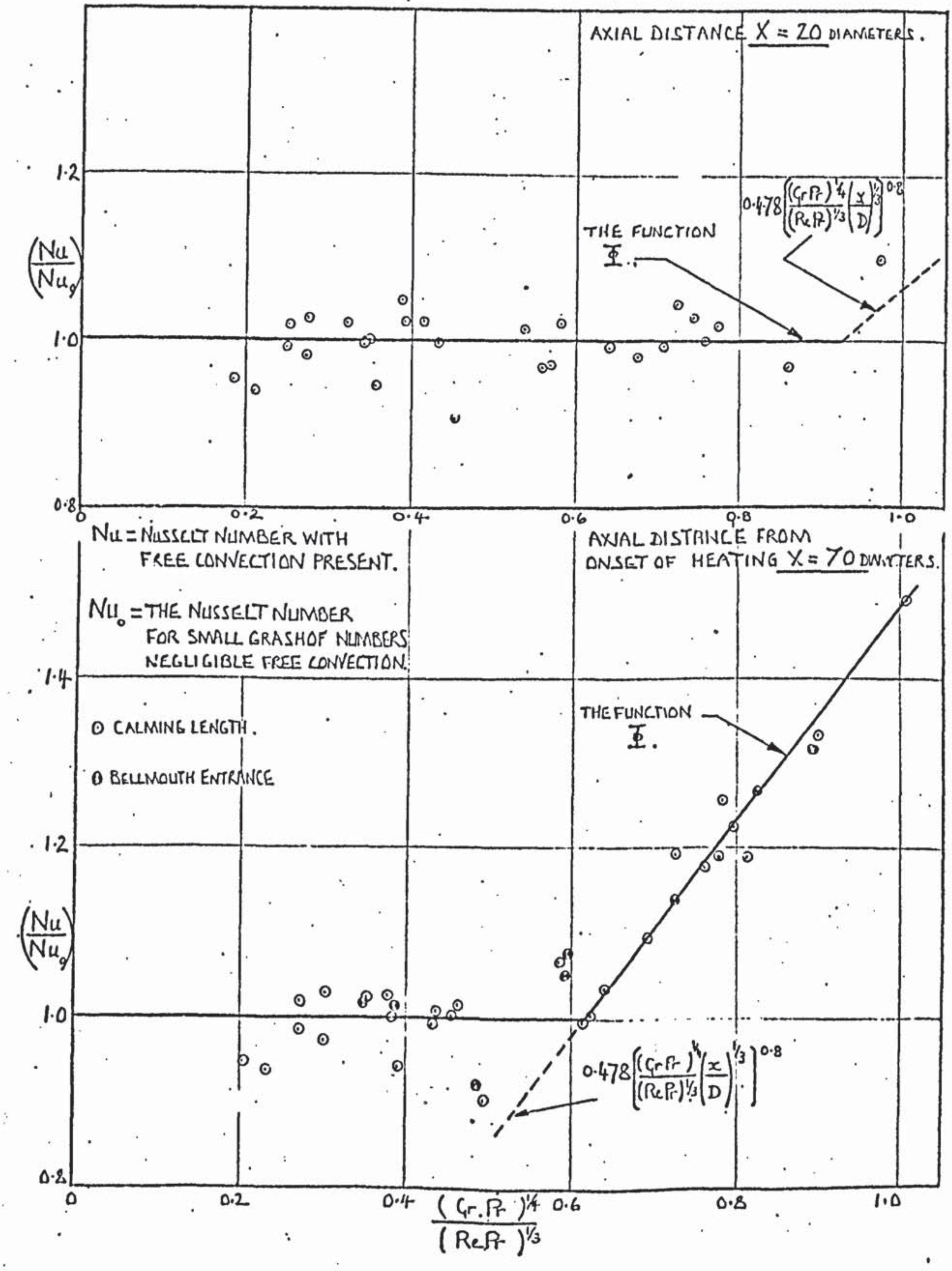

FIGURE 9.19.

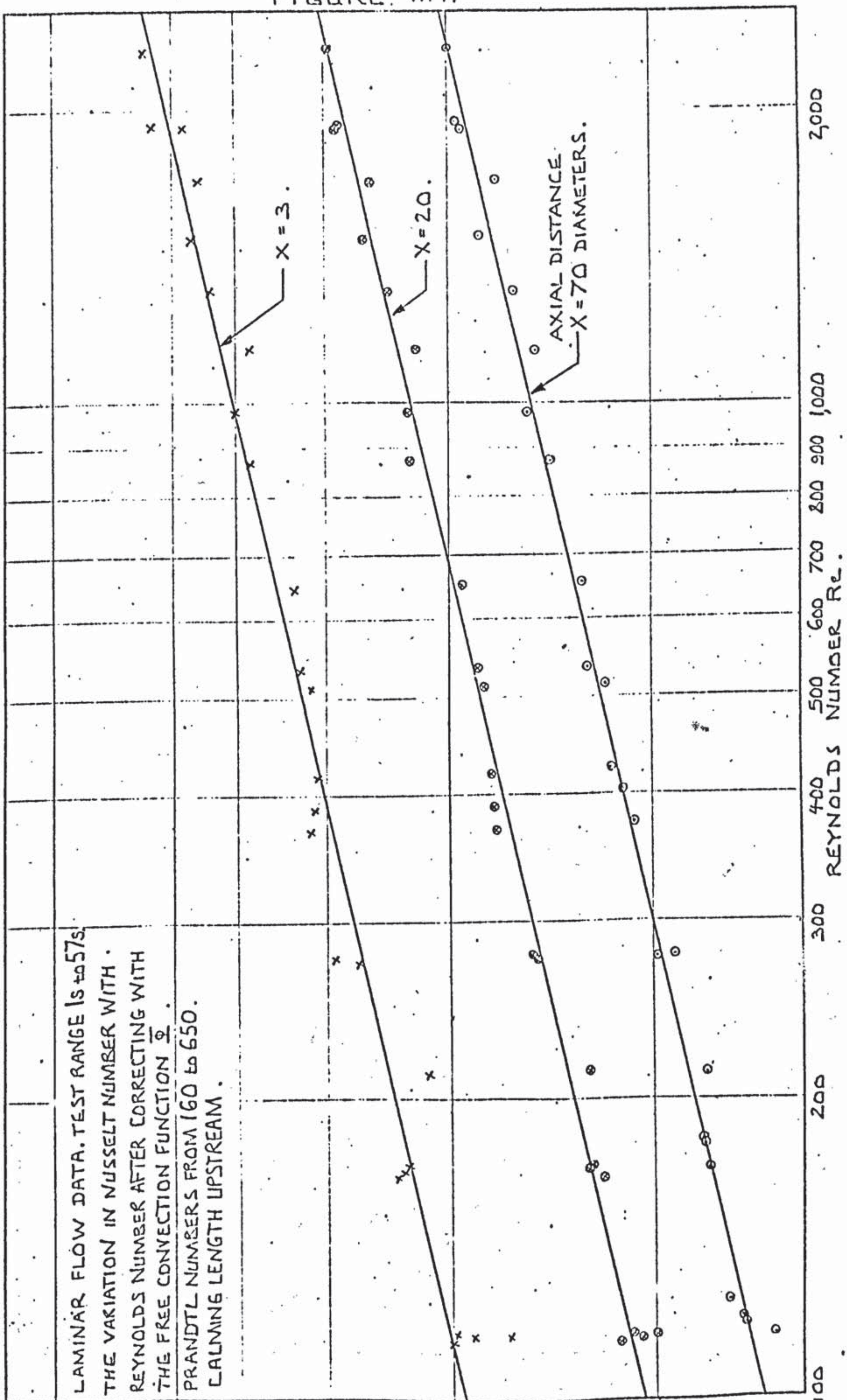

LAMINAR FLOW DATA. TEST RANGE 1s to 57s.
THE VARIATION IN NUSSELT NUMBER WITH
REYNOLDS NUMBER AFTER CORRECTING WITH
THE FREE CONVECTION FUNCTION Φ.
PRANDTL NUMBERS FROM 160 to 650.
CALMING LENGTH UPSTREAM.
X = 3.
X = 20.
AXIAL DISTANCE
X = 70 DIAMETERS.
$Nu\,(M^{0.14}_{WALL}\,Pr^{1/3}\,\Phi)^{-1}$
15
10
8
6
4
2
100
200
300
400
500
600
700
800
900
1,000
2,000
REYNOLDS NUMBER Re.

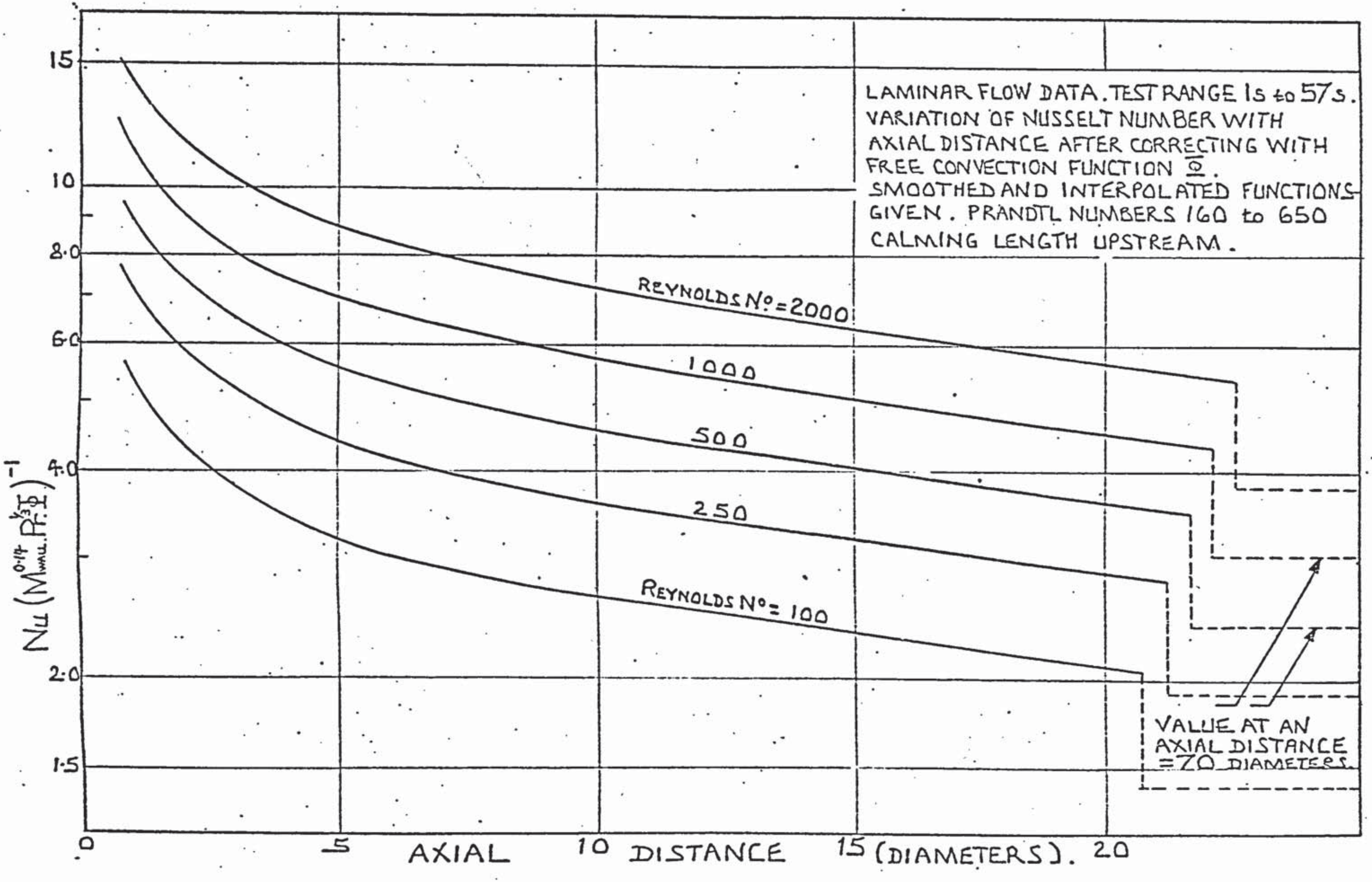

LAMINAR FLOW DATA. TEST RANGE 1s to 57s.
VARIATION OF NUSSELT NUMBER WITH AXIAL DISTANCE AFTER CORRECTING WITH FREE CONVECTION FUNCTION Φ.
SMOOTHED AND INTERPOLATED FUNCTIONS GIVEN. PRANDTL NUMBERS 160 to 650
CALMING LENGTH UPSTREAM.
REYNOLDS No = 2000
1000
500
250
REYNOLDS No = 100
VALUE AT AN AXIAL DISTANCE = 70 DIAMETERS.
$Nu\,(M_{wall}^{0.14}\,Pr^{1/3}\,\Phi)^{-1}$
15
10
8.0
6.0
4.0
2.0
1.5
0
5
10
15
20
AXIAL DISTANCE (DIAMETERS).

FIGURE 9.20

FIGURE 9.21.

THE RATIO OF NUSSELT NUMBER WITH VARIABLE VISCOSITY TO NUSSELT NUMBER WITH CONSTANT VISCOSITY (AFTER ELIMINATING THE CONTRIBUTION OF FREE CONVECTION USING THE FUNCTION Φ) — THE DEPENDENCE ON VISCOSITY RATIO M_{WALL} FOR LAMINAR FLOW. TEST RANGE 1s to 57s.

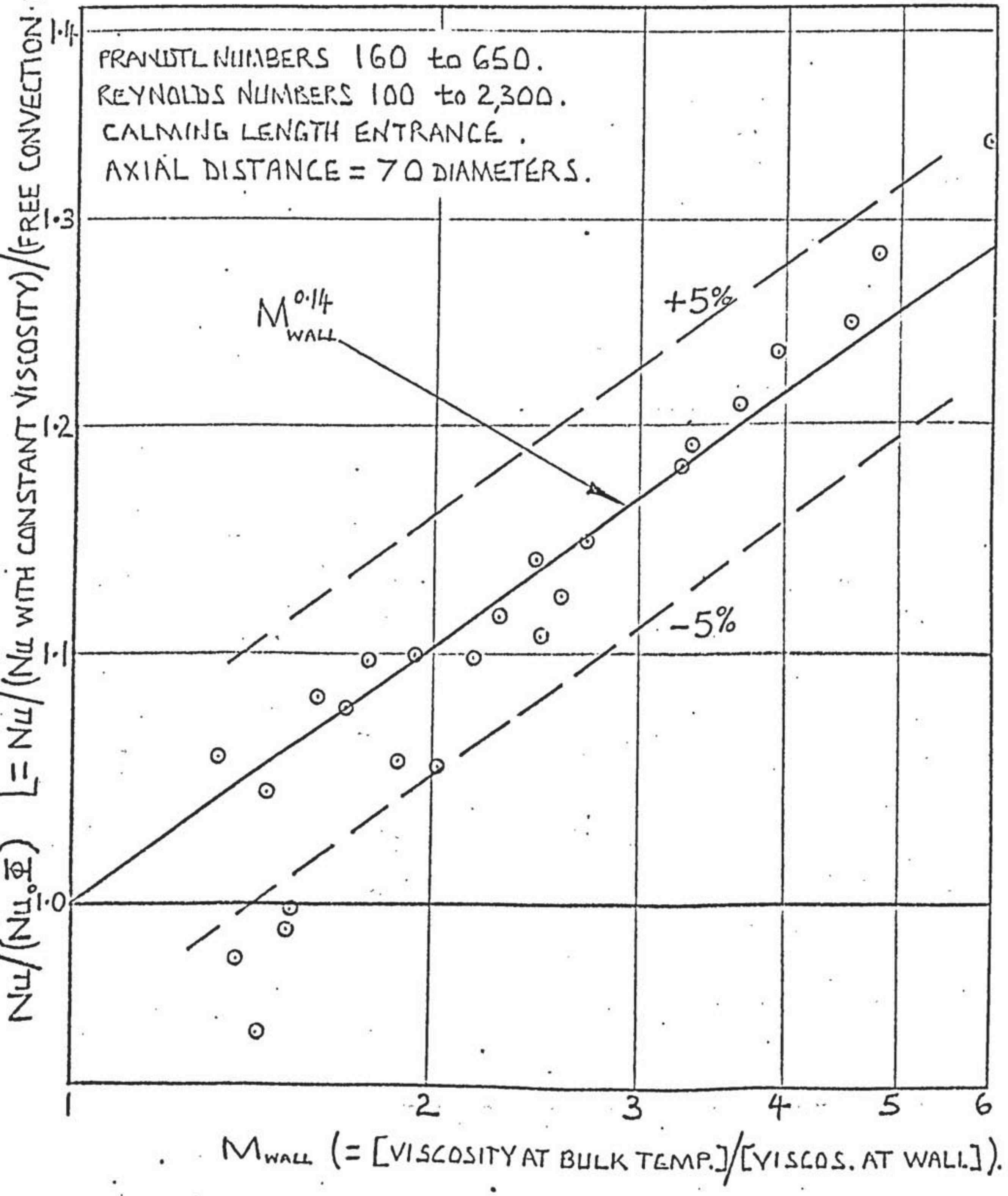

FIGURE 9.22.

NUSSELT NUMBER DISTRIBUTION IN THE ENTRANCE REGION OF A SHORT TUBE. A COMPARISON BETWEEN DEVELOPED AND UNDEVELOPED FLOW CONDITIONS. Tests 74SB to 85S.

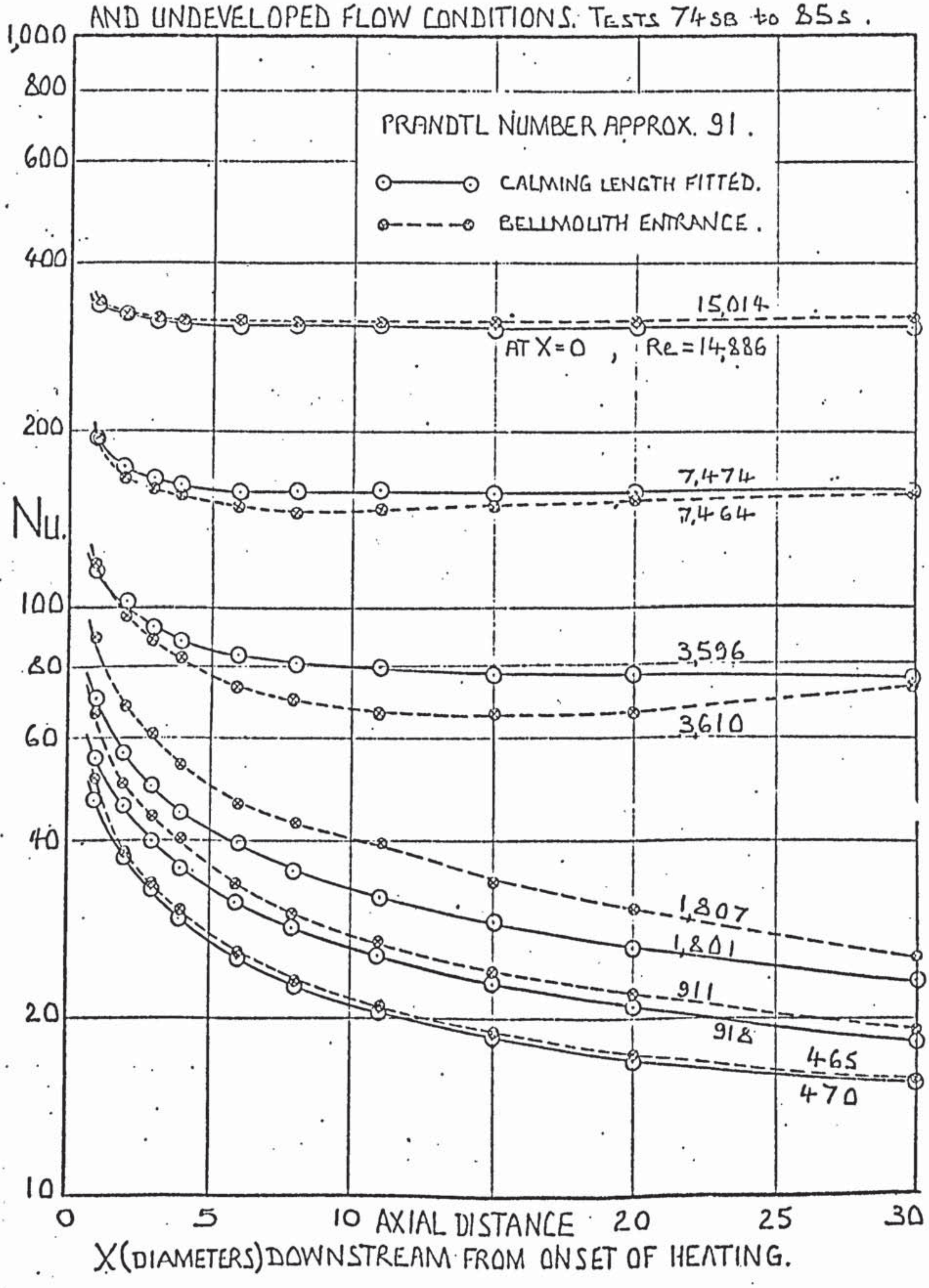

FIGURE 9.23.

THE DEPENDENCE OF NUSSELT NUMBER ON REYNOLDS NUMBER FOR PARTICULAR AXIAL POSITIONS. BELLMOUTH FITTED AT INLET. Re =2,500 to 10,000.

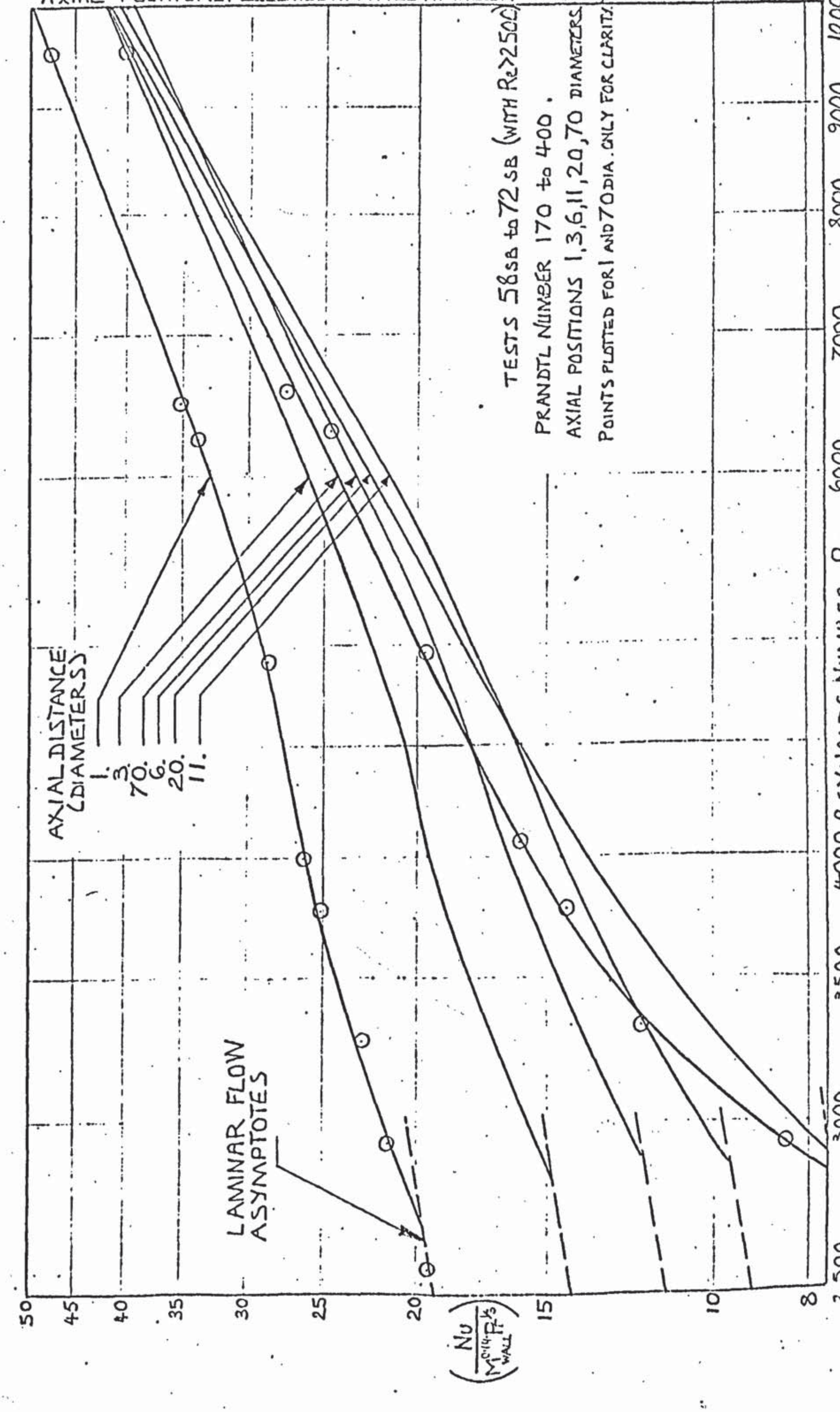

FIGURE 9.24.

NUSSELT NUMBER IN THE ENTRANCE REGION. BELLMOUTH ENTRY FITTED. Re > 2,500

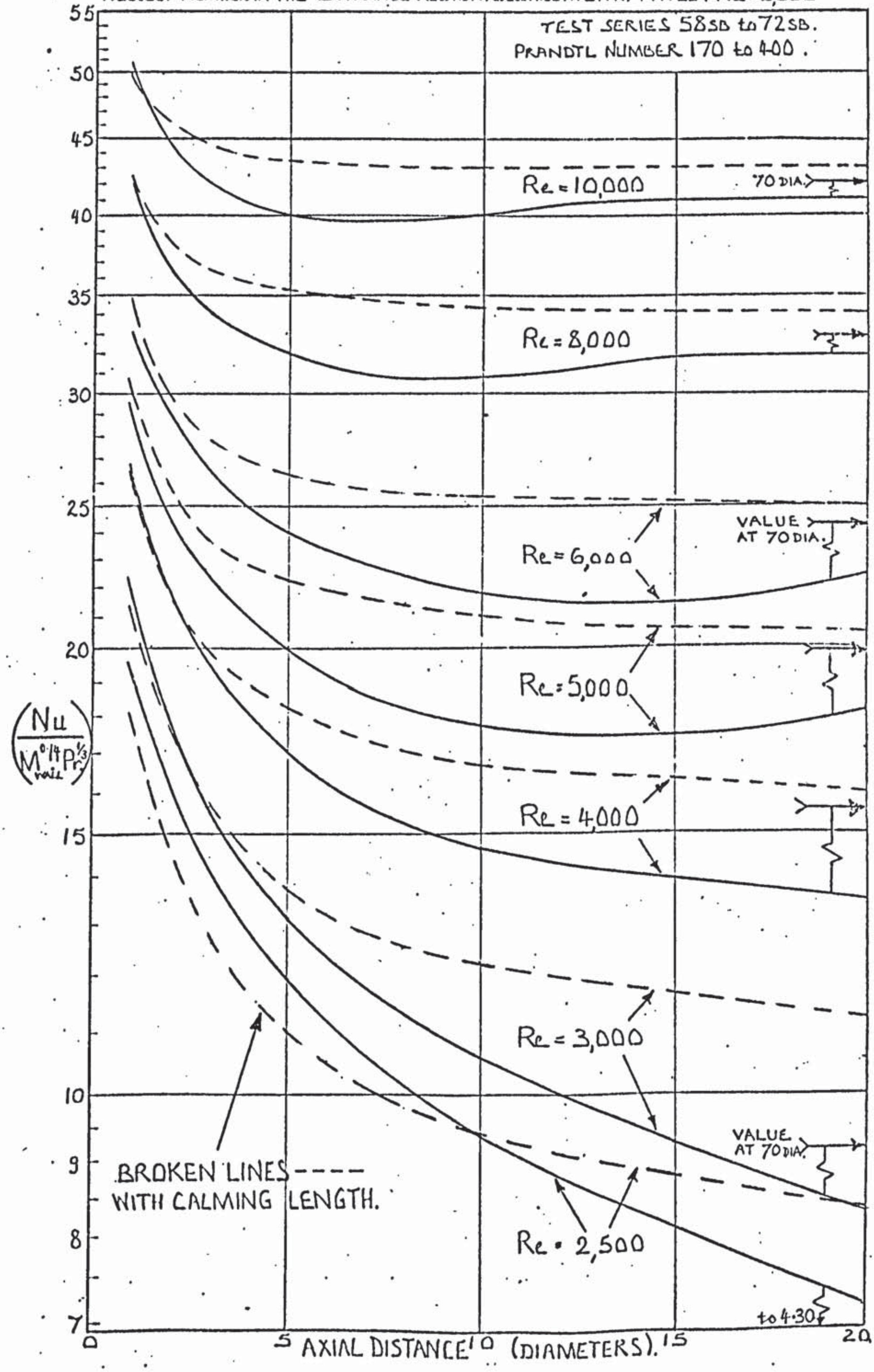

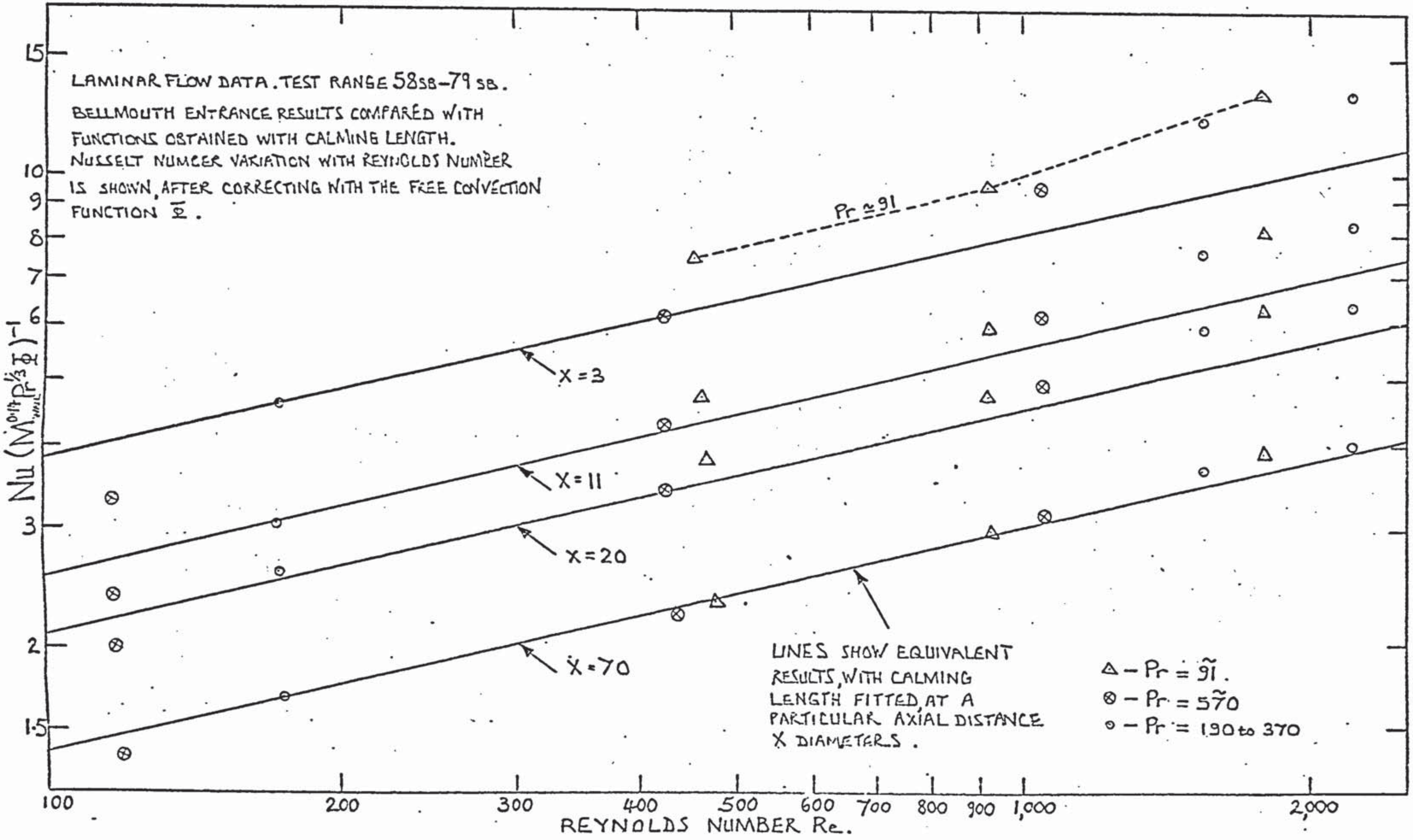
LAMINAR FLOW DATA. TEST RANGE 58SB–79SB.
BELLMOUTH ENTRANCE RESULTS COMPARED WITH FUNCTIONS OBTAINED WITH CALMING LENGTH.
NUSSELT NUMBER VARIATION WITH REYNOLDS NUMBER IS SHOWN, AFTER CORRECTING WITH THE FREE CONVECTION FUNCTION Φ.
$Pr \simeq 91$
X = 3
X = 11
X = 20
X = 70
LINES SHOW EQUIVALENT RESULTS, WITH CALMING LENGTH FITTED AT A PARTICULAR AXIAL DISTANCE X DIAMETERS.
△ – $Pr = \tilde{91}$.
⊗ – $Pr = \tilde{570}$
○ – Pr = 190 to 370
$Nu\,(M_{wall}^{0.17} Pr^{1/3} \Phi)^{-1}$
15
10
9
8
7
6
3
2
1.5
100
200
300
400
500
600
700
800
900
1,000
2,000
REYNOLDS NUMBER Re.

FIGURE 9.25.

FIGURE 9.26.

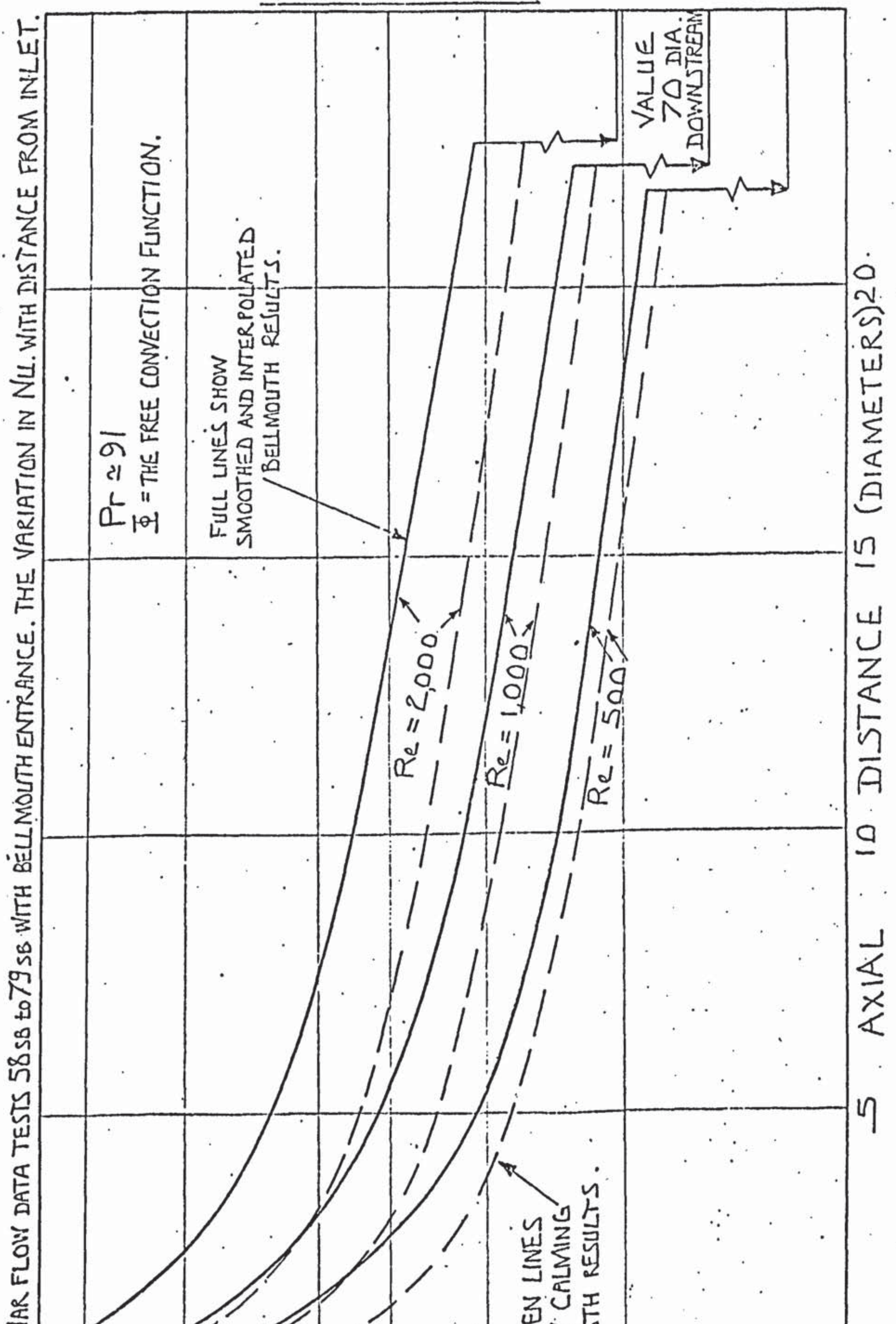
LAMINAR FLOW DATA TESTS 58SB to 79SB WITH BELLMOUTH ENTRANCE. THE VARIATION IN Nu. WITH DISTANCE FROM INLET.
Pr ≃ 91
Φ = THE FREE CONVECTION FUNCTION.
FULL LINES SHOW SMOOTHED AND INTERPOLATED BELLMOUTH RESULTS.
Re = 2,000
Re = 1,000
Re = 500
VALUE 70 DIA. DOWNSTREAM
BROKEN LINES SHOW CALMING LENGTH RESULTS.
0
5
10
15
20
AXIAL DISTANCE (DIAMETERS)
2
4
8
10
15
20
Nu

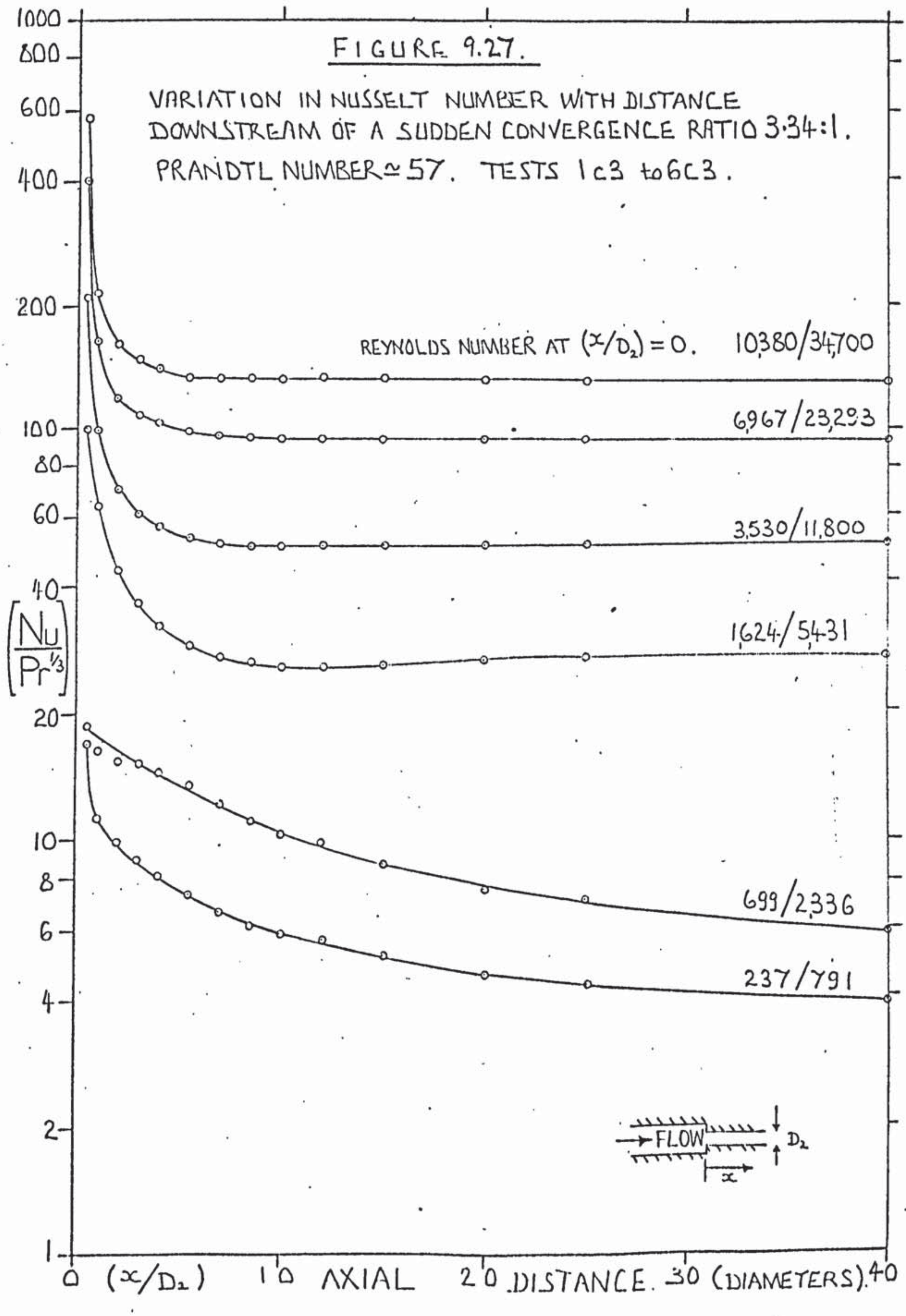
FIGURE 9.27.
VARIATION IN NUSSELT NUMBER WITH DISTANCE
DOWNSTREAM OF A SUDDEN CONVERGENCE RATIO 3·34:1.
PRANDTL NUMBER ≃ 57. TESTS 1c3 to 6C3.
REYNOLDS NUMBER AT (x/D₂) = 0.
10,380/34,700
6,967/23,293
3,530/11,800
1,624/5,431
699/2,336
237/791
FLOW
D₂
x
[Nu/Pr^1/3]
1000
800
600
400
200
100
80
60
40
20
10
8
6
4
2
1
0 (x/D₂) 10 AXIAL 20 DISTANCE 30 (DIAMETERS) 40

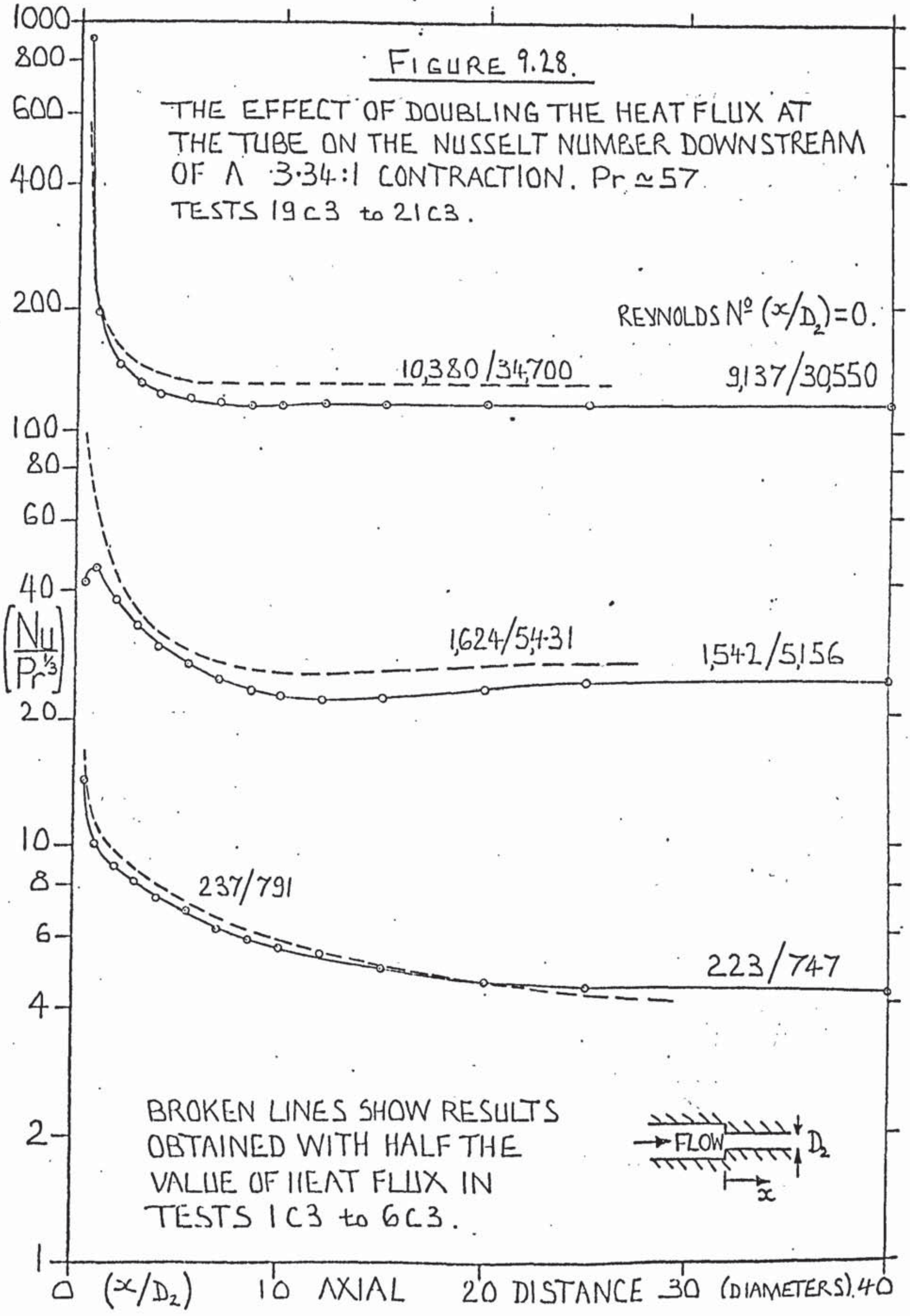
FIGURE 9.28.
THE EFFECT OF DOUBLING THE HEAT FLUX AT THE TUBE ON THE NUSSELT NUMBER DOWNSTREAM OF A 3·34:1 CONTRACTION. Pr ≃ 57
TESTS 19c3 to 21c3.
REYNOLDS Nº (x/D2)=0.
10,380/34,700
9,137/30,550
1,624/54·31
1,542/5,156
237/791
223/747
BROKEN LINES SHOW RESULTS OBTAINED WITH HALF THE VALUE OF HEAT FLUX IN TESTS 1C3 to 6C3.
FLOW
D2
x
1000
800
600
400
200
100
80
60
40
(Nu/Pr⅓)
20
10
8
6
4
2
1
0 (x/D2) 10 AXIAL 20 DISTANCE 30 (DIAMETERS). 40

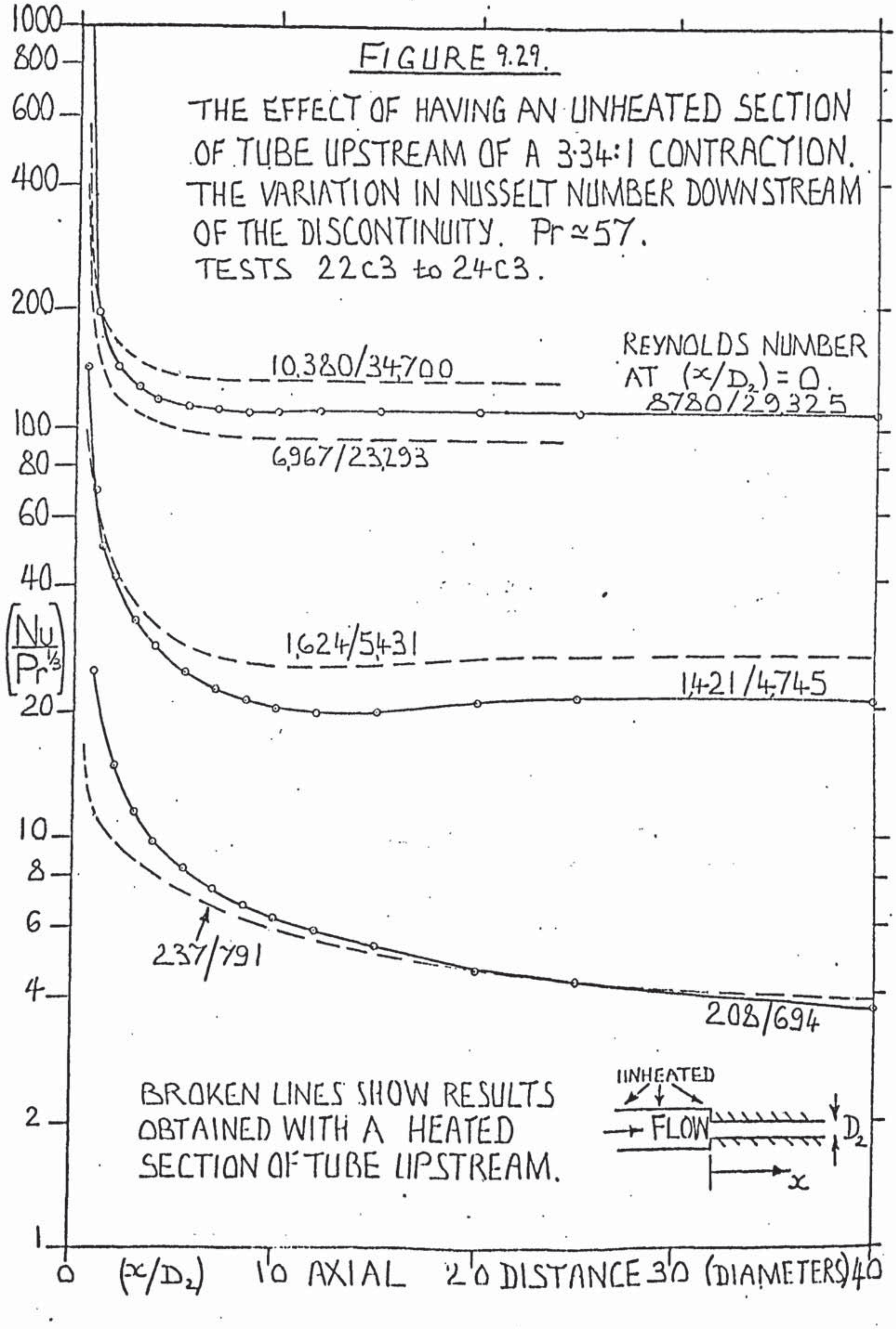

FIGURE 9.29.
THE EFFECT OF HAVING AN UNHEATED SECTION OF TUBE UPSTREAM OF A 3·34:1 CONTRACTION. THE VARIATION IN NUSSELT NUMBER DOWNSTREAM OF THE DISCONTINUITY. Pr ≃ 57.
TESTS 22C3 to 24C3.
REYNOLDS NUMBER AT (x/D2) = 0.
10,380/34,700
8780/29325
6,967/23,293
1,624/5431
1,421/4,745
237/791
208/694
BROKEN LINES SHOW RESULTS OBTAINED WITH A HEATED SECTION OF TUBE UPSTREAM.
UNHEATED
FLOW
D2
x
Nu/Pr^1/3
1000
800
600
400
200
100
80
60
40
20
10
8
6
4
2
1
0
(x/D2)
10 AXIAL
20 DISTANCE
30 (DIAMETERS)
40

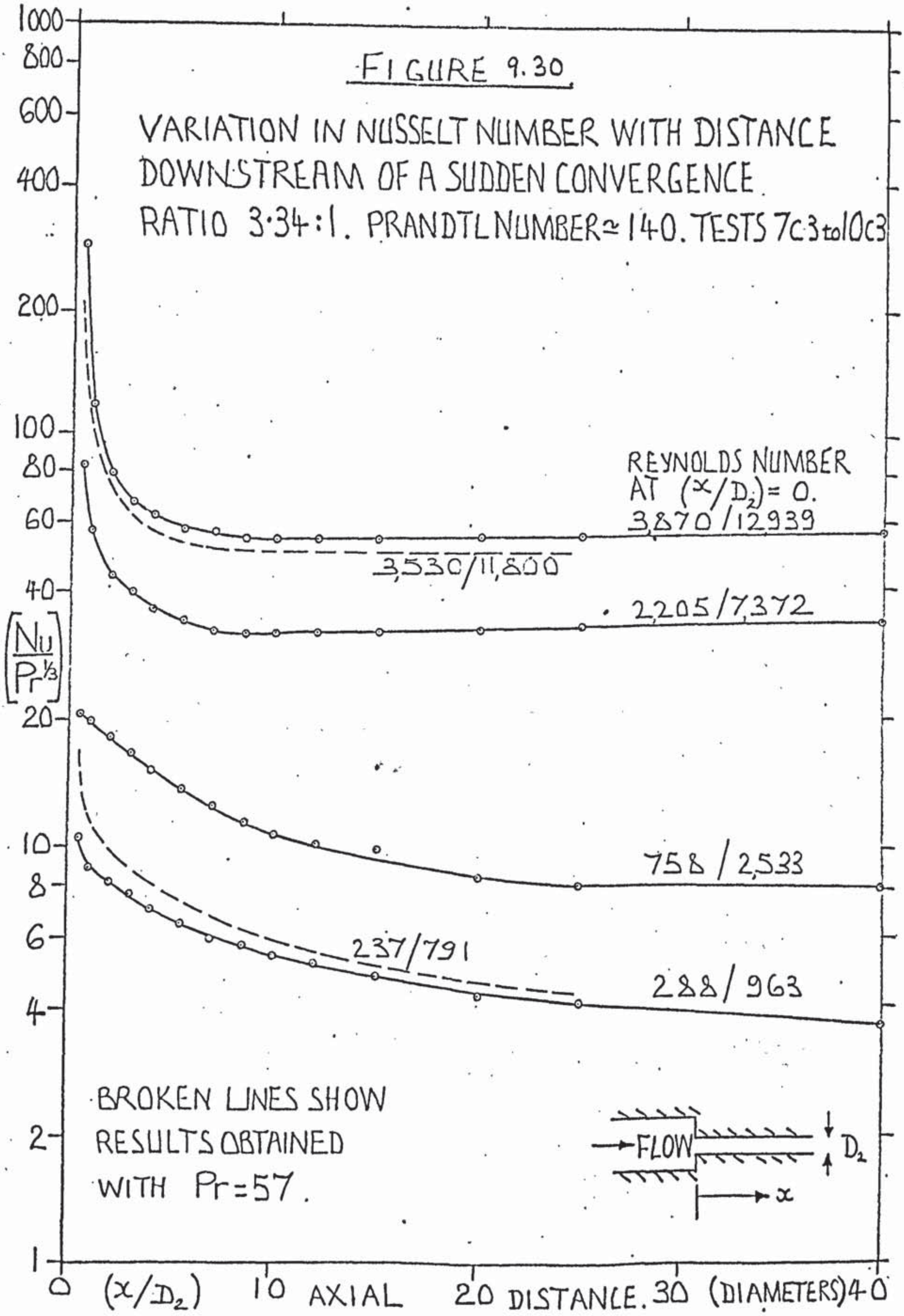
FIGURE 9.30
VARIATION IN NUSSELT NUMBER WITH DISTANCE DOWNSTREAM OF A SUDDEN CONVERGENCE RATIO 3·34:1. PRANDTL NUMBER ≃ 140. TESTS 7C3 to 10C3
1000
800
600
400
200
100
80
60
40
20
10
8
6
4
2
1
[Nu/Pr^1/3]
REYNOLDS NUMBER AT (x/D2) = 0.
3,870/12939
3,530/11,800
2,205/7,372
758/2,533
237/791
288/963
BROKEN LINES SHOW RESULTS OBTAINED WITH Pr=57.
FLOW
D2
x
0 (x/D2) 10 AXIAL 20 DISTANCE. 30 (DIAMETERS) 40

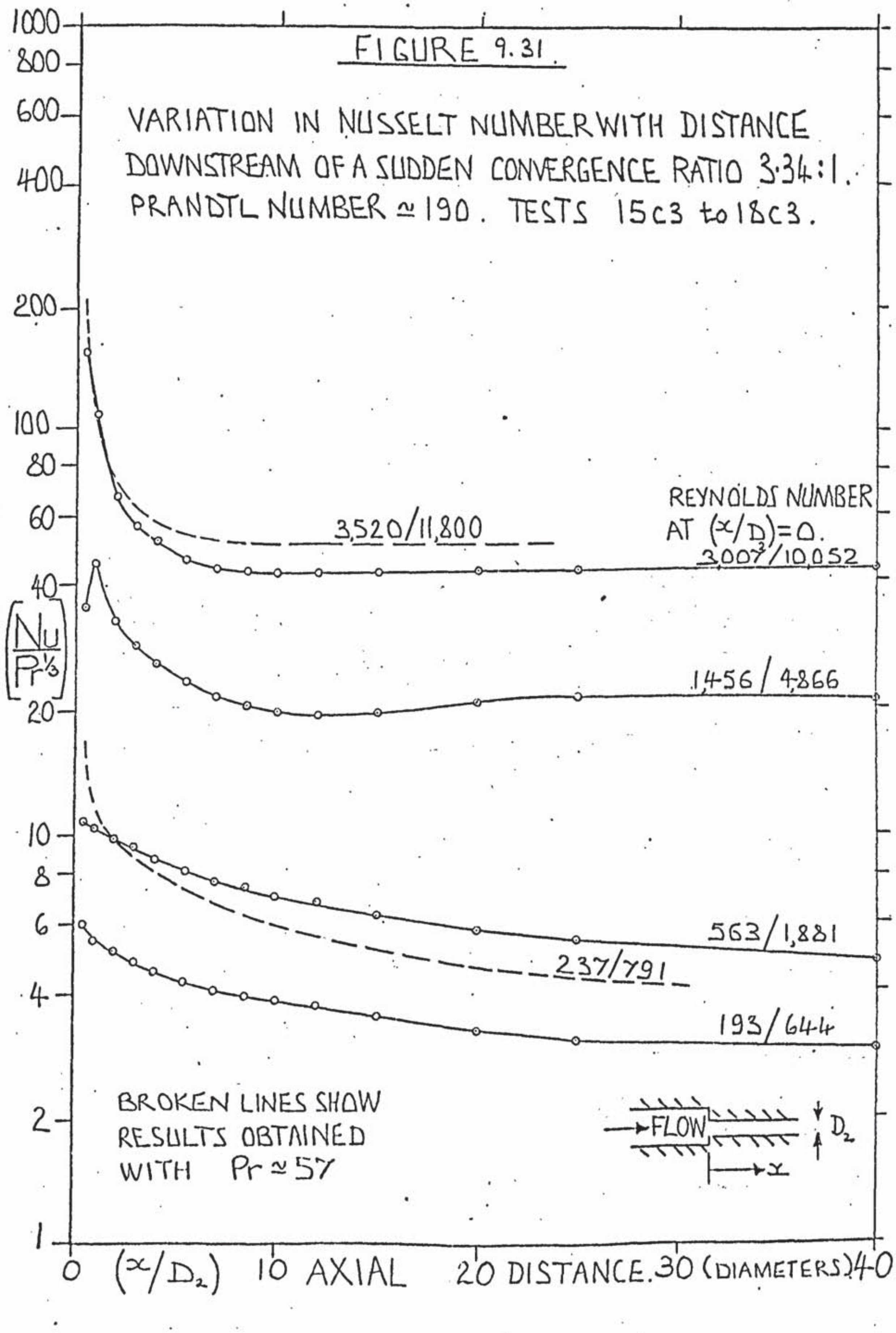

FIGURE 9.31.
VARIATION IN NUSSELT NUMBER WITH DISTANCE DOWNSTREAM OF A SUDDEN CONVERGENCE RATIO 3·34:1. PRANDTL NUMBER ≃ 190. TESTS 15c3 to 18c3.
1000
800
600
400
200
100
80
60
40
20
10
8
6
4
2
1
Nu/Pr⅓
REYNOLDS NUMBER AT (x/D)=0.
3,520/11,800
3007/10,052
1,456/4,866
563/1,881
237/791
193/644
BROKEN LINES SHOW RESULTS OBTAINED WITH Pr ≃ 57
FLOW
D₂
x
0
(x/D₂)
10
AXIAL
20
DISTANCE.
30
(DIAMETERS)
40

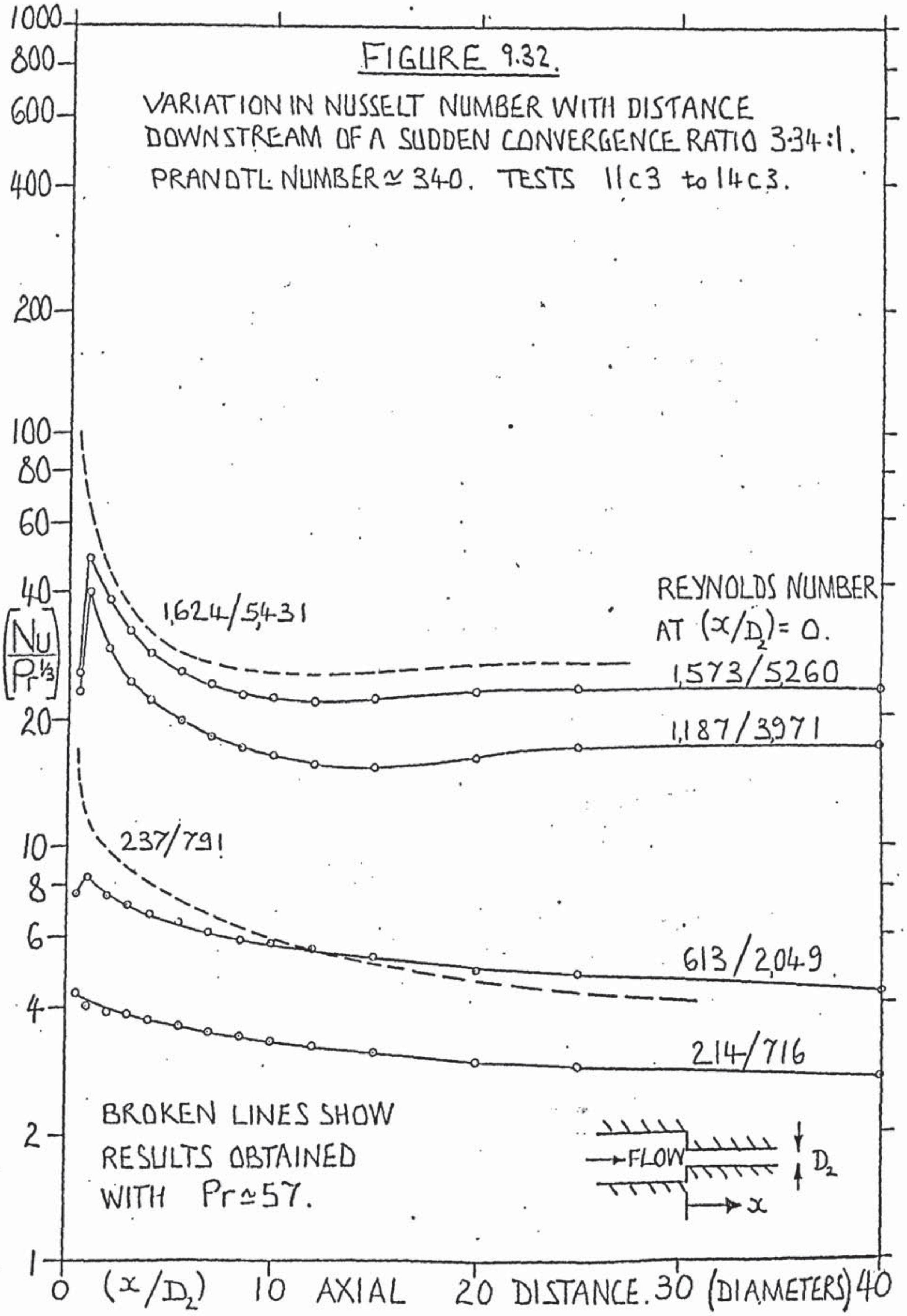

FIGURE 9.32.
VARIATION IN NUSSELT NUMBER WITH DISTANCE DOWNSTREAM OF A SUDDEN CONVERGENCE RATIO 3.34:1.
PRANDTL NUMBER ≃ 340. TESTS 11c3 to 14c3.
1000
800
600
400
200
100
80
60
40
20
10
8
6
4
2
1
$\left[\frac{Nu}{Pr^{1/3}}\right]$
1,624/5,431
REYNOLDS NUMBER AT (x/D_2) = 0.
1,573/5260
1,187/3,971
237/791
613/2,049
214/716
BROKEN LINES SHOW RESULTS OBTAINED WITH Pr≃57.
FLOW
D_2
x
0 (x/D_2) 10 AXIAL 20 DISTANCE. 30 (DIAMETERS) 40

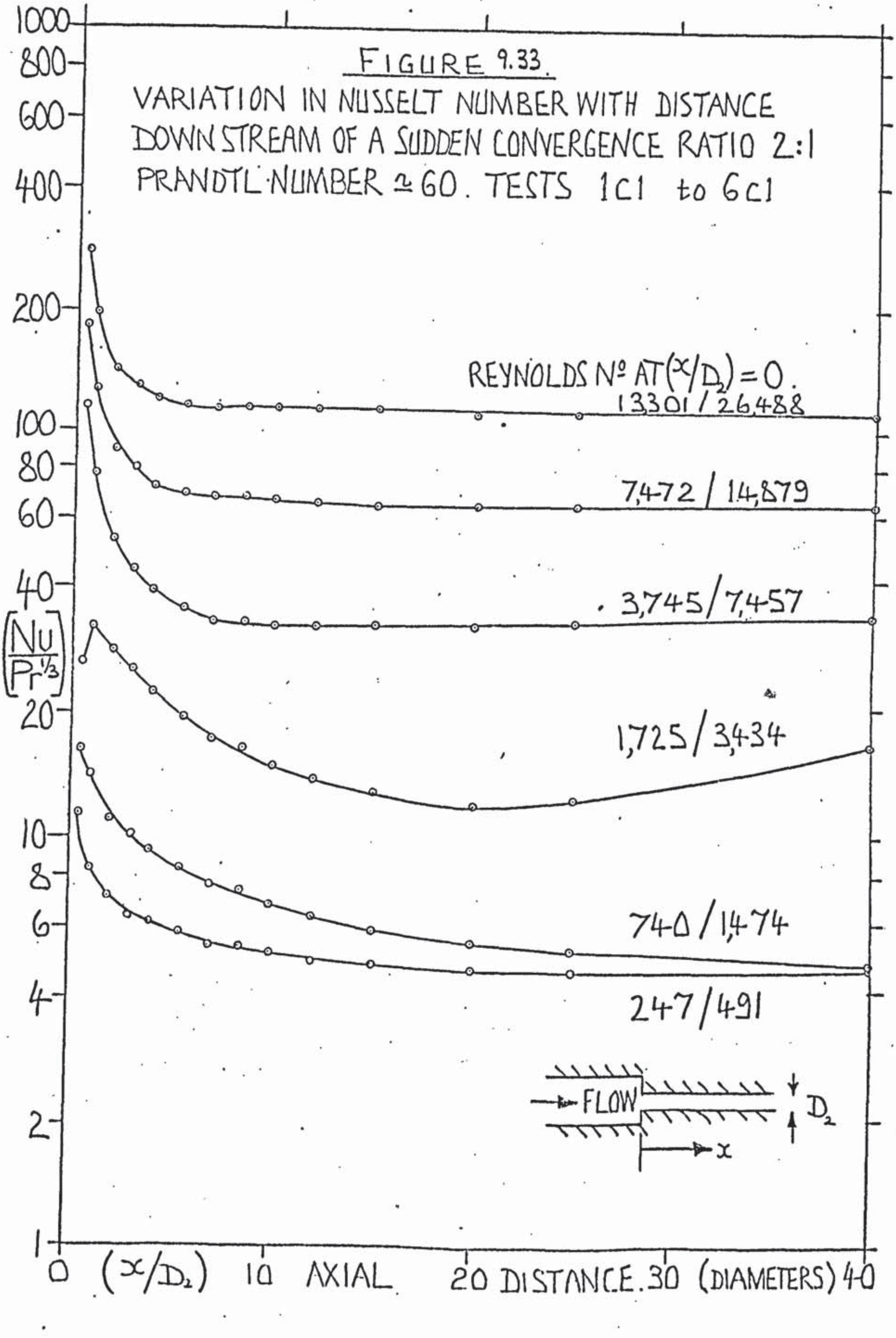
FIGURE 9.33.
VARIATION IN NUSSELT NUMBER WITH DISTANCE DOWNSTREAM OF A SUDDEN CONVERGENCE RATIO 2:1
PRANDTL NUMBER ≃ 60. TESTS 1C1 to 6C1
REYNOLDS Nº AT (x/D2) = 0.
13301 / 26,488
7,472 / 14,879
3,745 / 7,457
1,725 / 3,434
740 / 1,474
247 / 491
FLOW
D2
x
[Nu/Pr^1/3]
1000
800
600
400
200
100
80
60
40
20
10
8
6
4
2
1
0 (x/D2) 10 AXIAL 20 DISTANCE 30 (DIAMETERS) 40

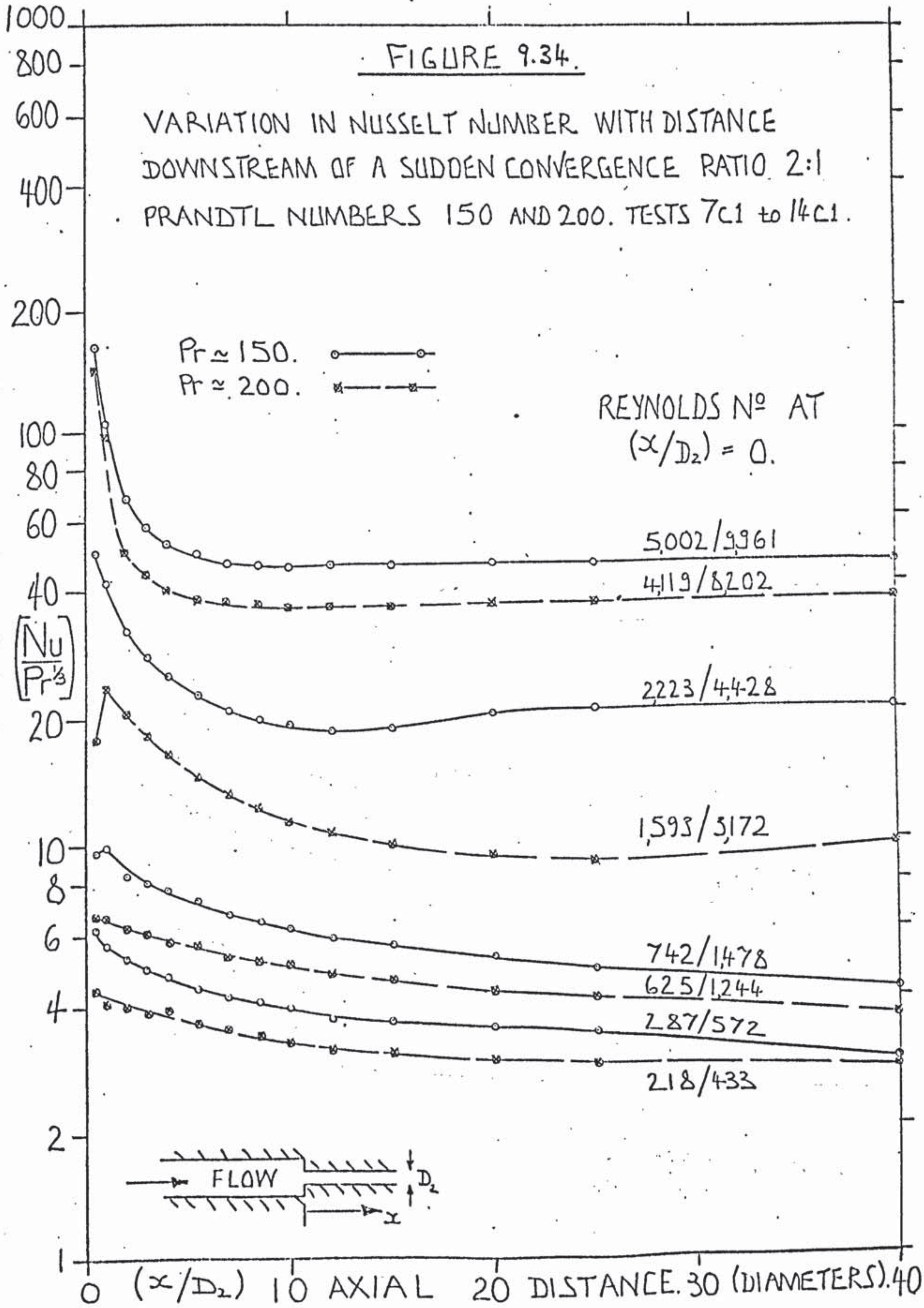

FIGURE 9.34.
VARIATION IN NUSSELT NUMBER WITH DISTANCE DOWNSTREAM OF A SUDDEN CONVERGENCE RATIO 2:1 PRANDTL NUMBERS 150 AND 200. TESTS 7C1 to 14C1.
Pr ≃ 150.
Pr ≃ 200.
REYNOLDS Nº AT (x/D2) = 0.
5,002/9,961
4,119/8,202
2223/4,428
1,593/3,172
742/1,478
625/1,244
287/572
218/433
FLOW
D2
x
[Nu/Pr^1/3]
1000
800
600
400
200
100
80
60
40
20
10
8
6
4
2
1
0 (x/D2) 10 AXIAL 20 DISTANCE. 30 (DIAMETERS). 40

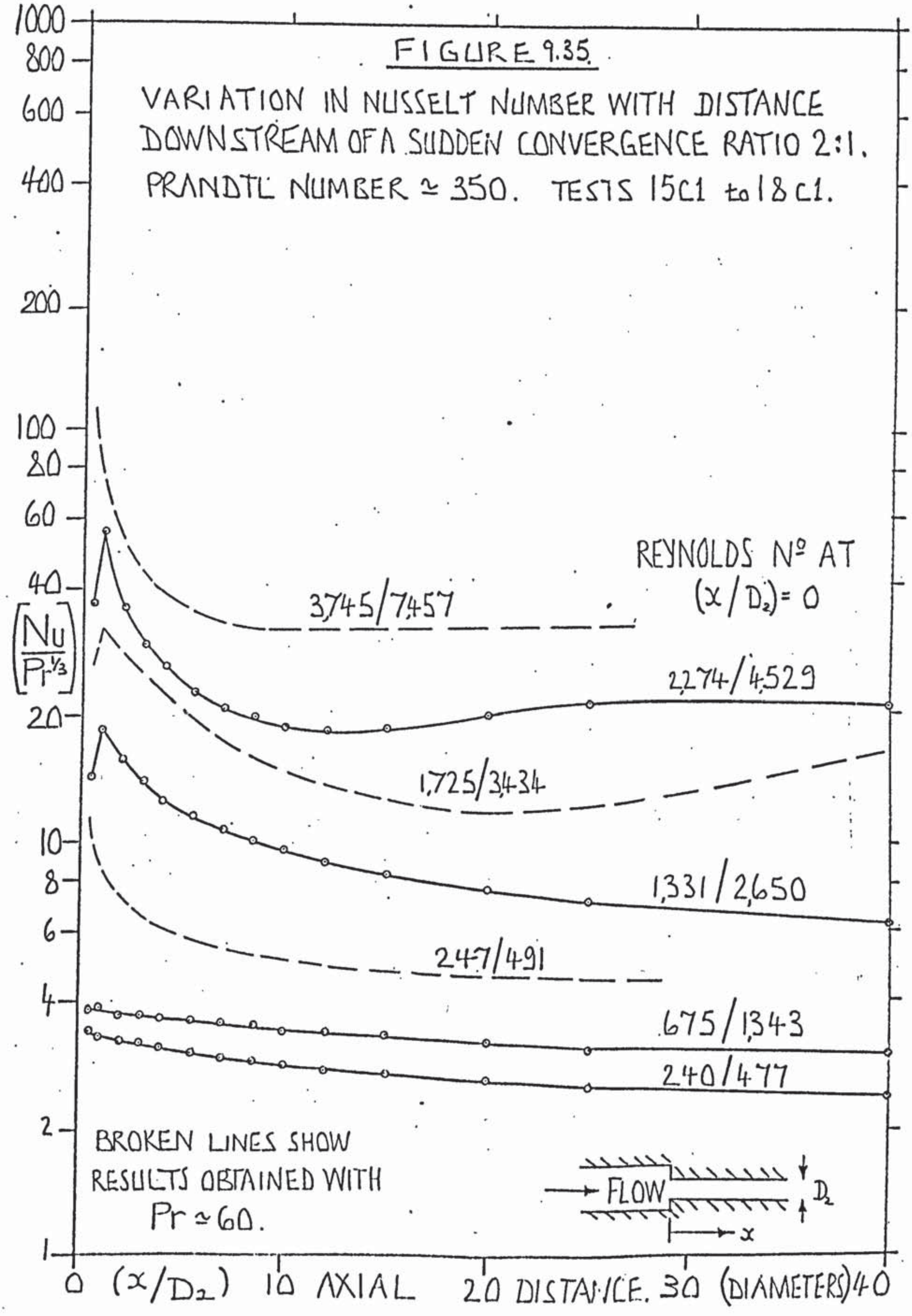

FIGURE 9.35.
VARIATION IN NUSSELT NUMBER WITH DISTANCE DOWNSTREAM OF A SUDDEN CONVERGENCE RATIO 2:1.
PRANDTL NUMBER ≃ 350. TESTS 15C1 to 18C1.
1000
800
600
400
200
100
80
60
40
20
10
8
6
4
2
1
$\left[\frac{Nu}{Pr^{1/3}}\right]$
REYNOLDS Nº AT $(x/D_2) = 0$
3745/7457
2,274/4,529
1,725/3,434
1,331/2,650
247/491
675/1,343
240/477
BROKEN LINES SHOW RESULTS OBTAINED WITH $Pr \simeq 60$.
FLOW
D_2
x
0 (x/D_2) 10 AXIAL 20 DISTANCE. 30 (DIAMETERS) 40

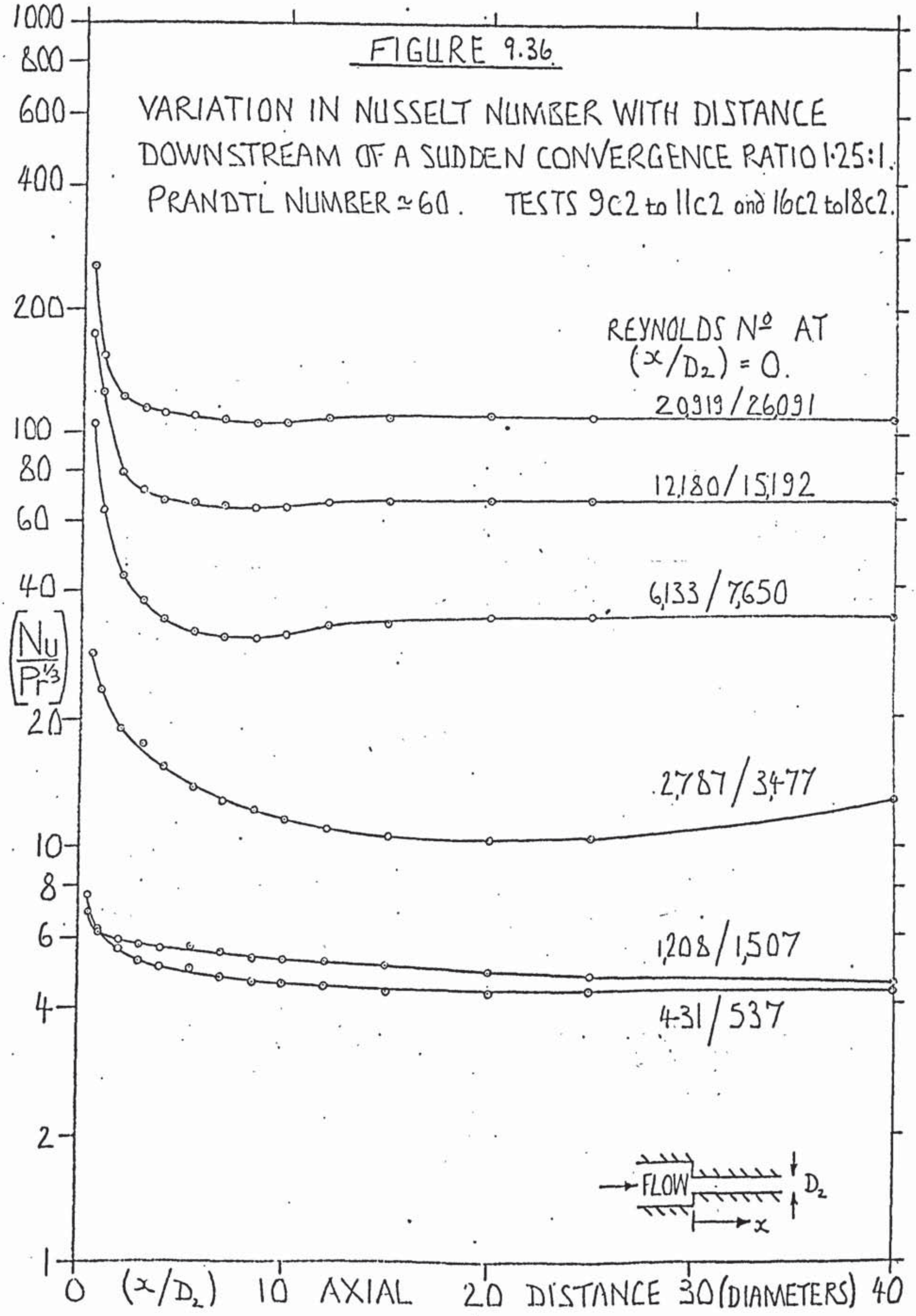
FIGURE 9.36
VARIATION IN NUSSELT NUMBER WITH DISTANCE DOWNSTREAM OF A SUDDEN CONVERGENCE RATIO 1·25:1.
PRANDTL NUMBER ≃ 60. TESTS 9C2 to 11C2 and 16C2 to 18C2.
REYNOLDS Nº AT (x/D2) = 0.
20,919/26,091
12,180/15,192
6,133/7,650
2,787/3,477
1,208/1,507
431/537
1000
800
600
400
200
100
80
60
40
[Nu/Pr^1/3]
20
10
8
6
4
2
1
FLOW
D2
x
0 (x/D2) 10 AXIAL 20 DISTANCE 30 (DIAMETERS) 40

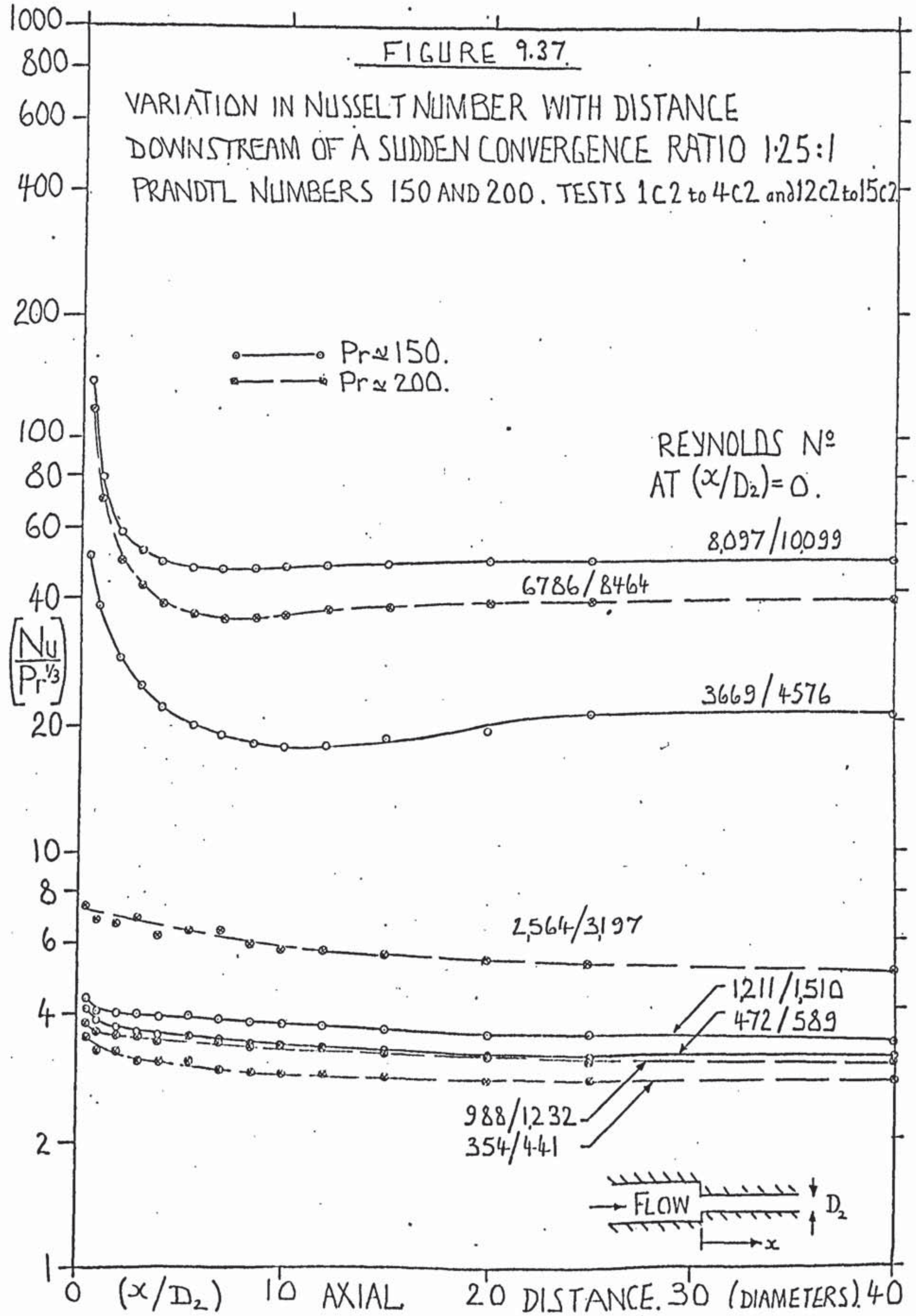
FIGURE 9.37.
VARIATION IN NUSSELT NUMBER WITH DISTANCE
DOWNSTREAM OF A SUDDEN CONVERGENCE RATIO 1·25:1
PRANDTL NUMBERS 150 AND 200. TESTS 1C2 to 4C2 and 12C2 to 15C2
Pr ≃ 150.
Pr ≃ 200.
REYNOLDS Nº
AT (x/D2) = 0.
8,097/10,099
6786/8464
3669/4576
2,564/3,197
1211/1,510
472/589
988/1,232
354/441
FLOW
D2
x
1000
800
600
400
200
100
80
60
40
20
10
8
6
4
2
1
[Nu/Pr^1/3]
0
10
20
30
40
(x/D2) AXIAL DISTANCE. (DIAMETERS).

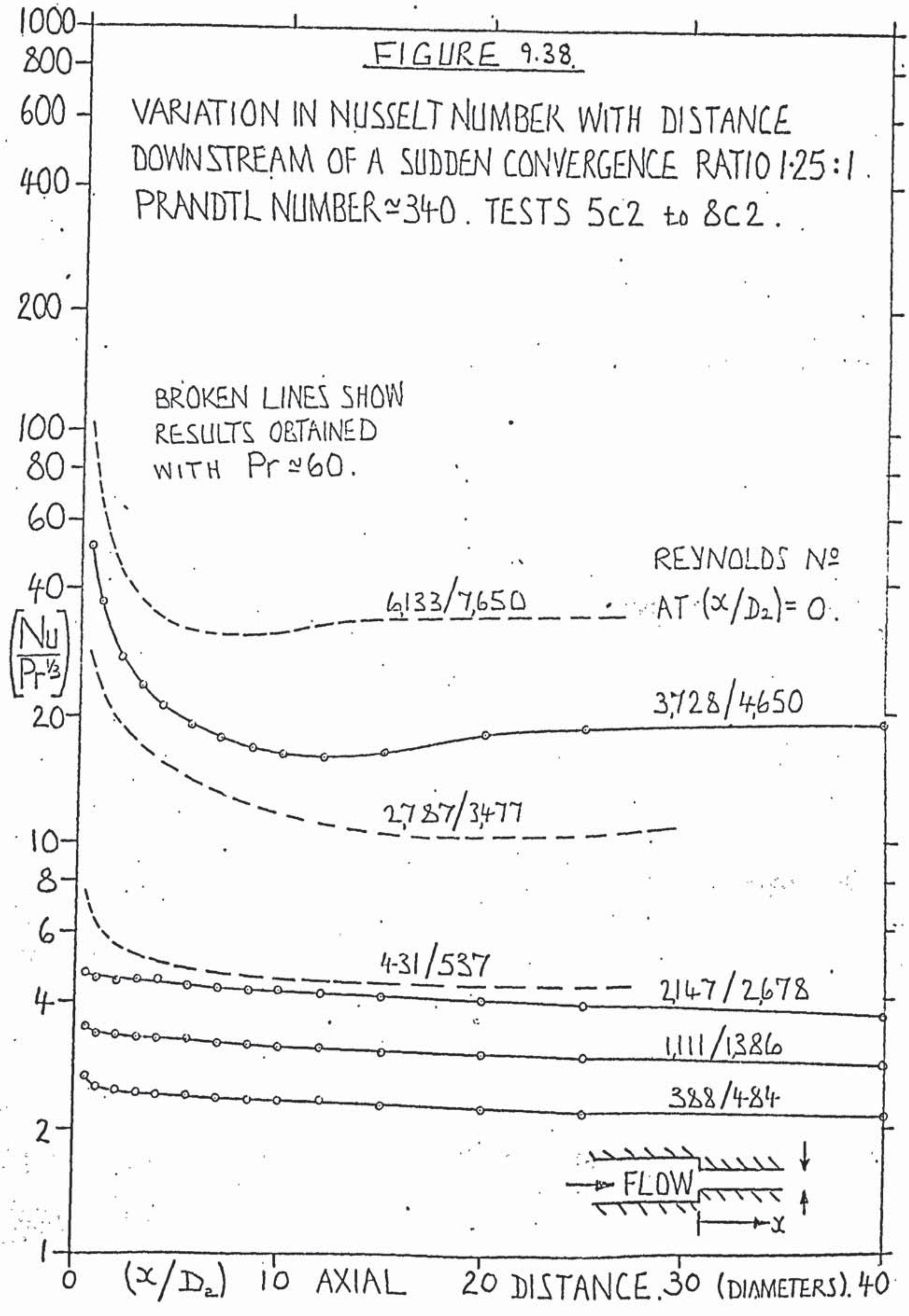

FIGURE 9.38.
VARIATION IN NUSSELT NUMBER WITH DISTANCE DOWNSTREAM OF A SUDDEN CONVERGENCE RATIO 1·25:1. PRANDTL NUMBER≃340. TESTS 5c2 to 8c2.
BROKEN LINES SHOW RESULTS OBTAINED WITH Pr≃60.
REYNOLDS No AT (x/D2) = 0.
6,133/7,650
3,728/4,650
2,787/3,477
431/537
2,147/2,678
1,111/1,386
388/484
[Nu/Pr1/3]
1000
800
600
400
200
100
80
60
40
20
10
8
6
4
2
1
0
(x/D2) 10 AXIAL 20 DISTANCE. 30 (DIAMETERS). 40
FLOW
x

FIGURE 9.39.

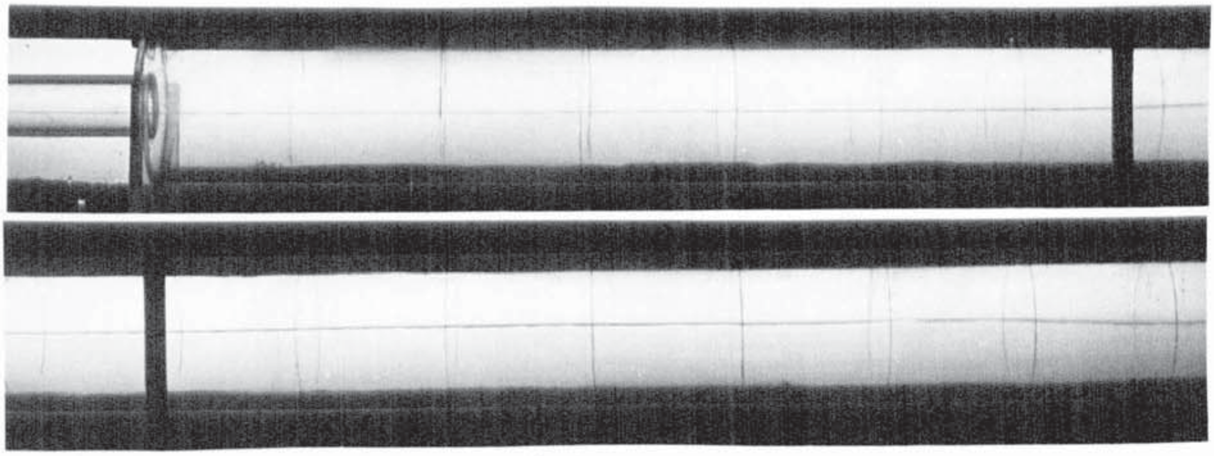

A.

B.

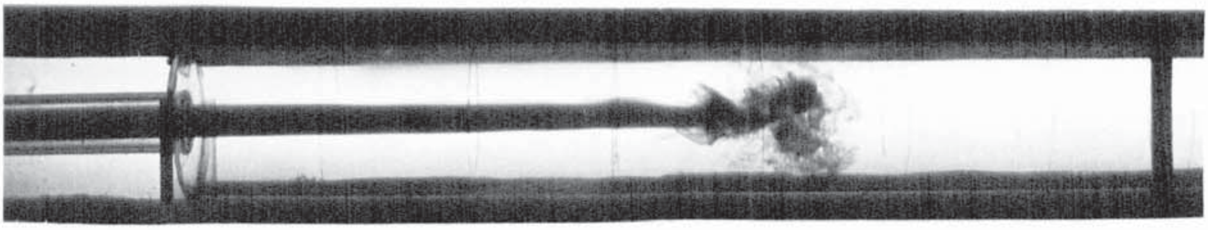

C.

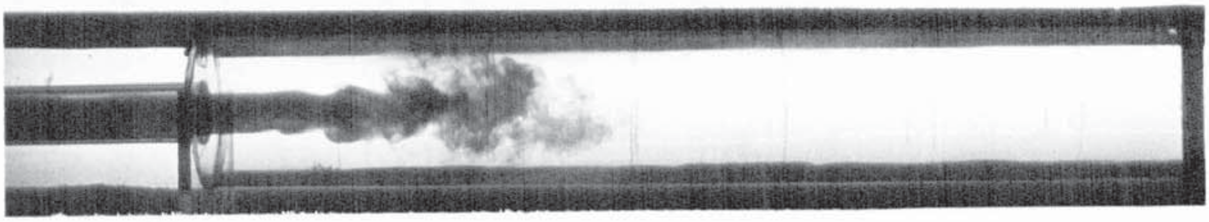

D.

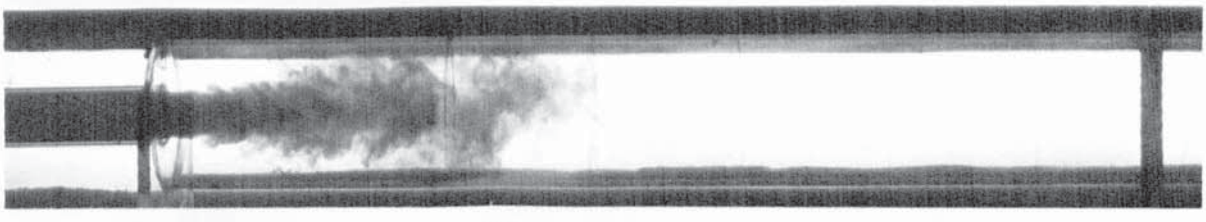

E.

FIGURE 9.39 ..... cont...

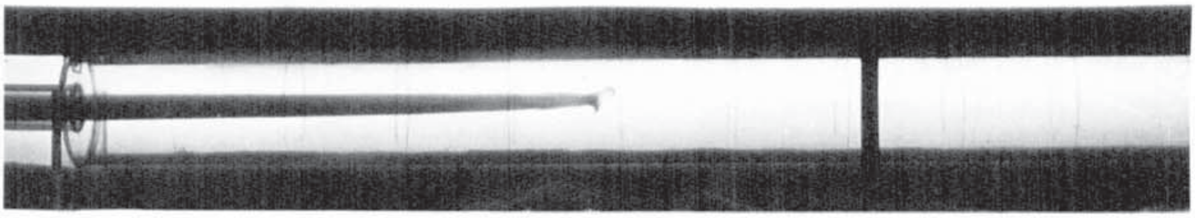

F.

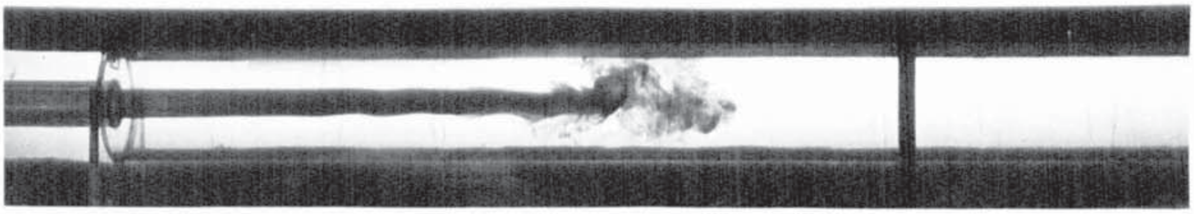

G.

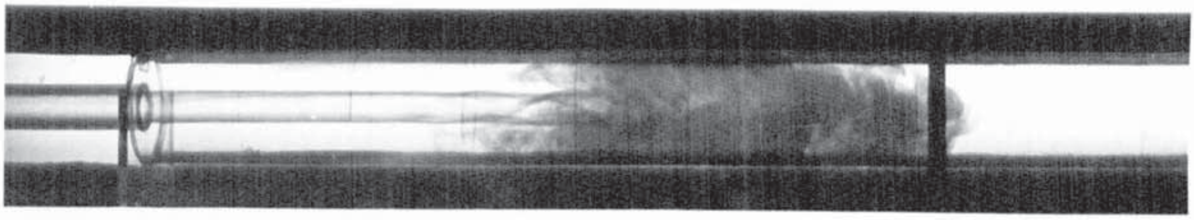

H.

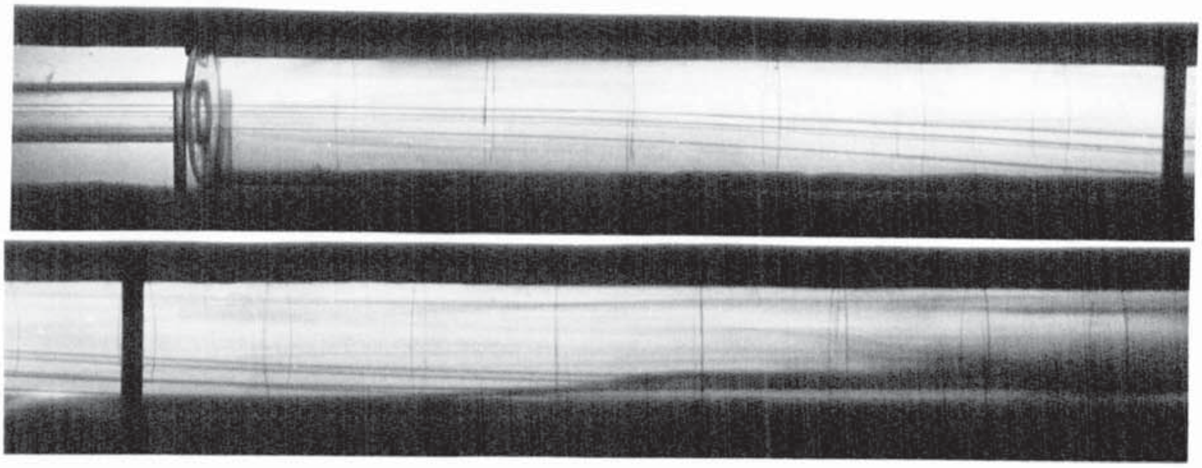

I.

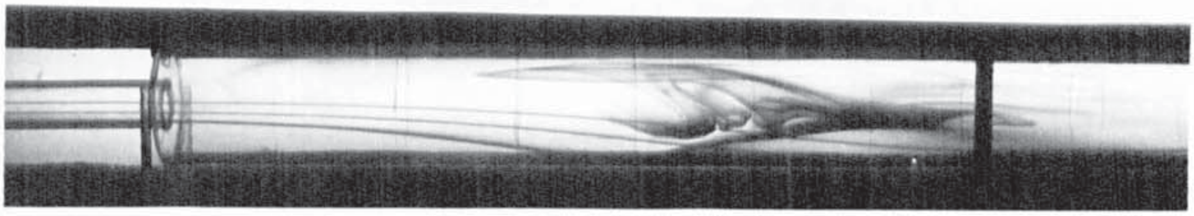

J.

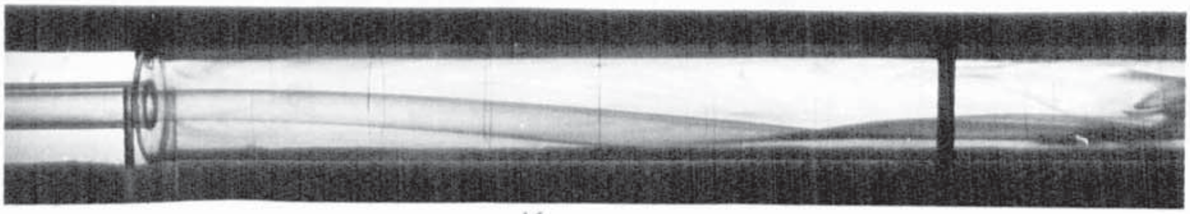

K.

FIGURE 9.39......cont....

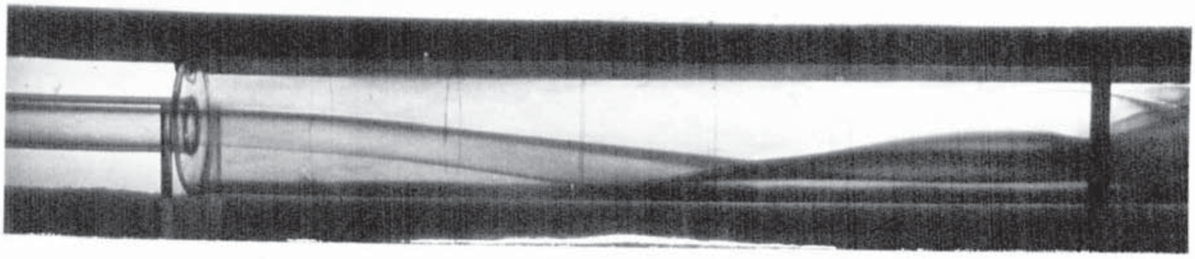

L.

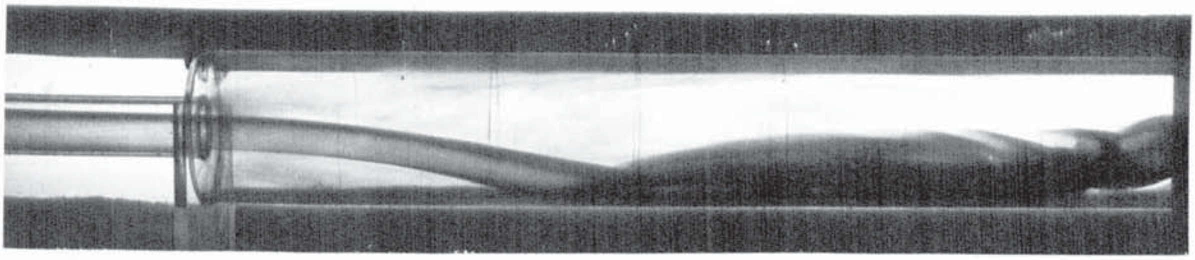

M.

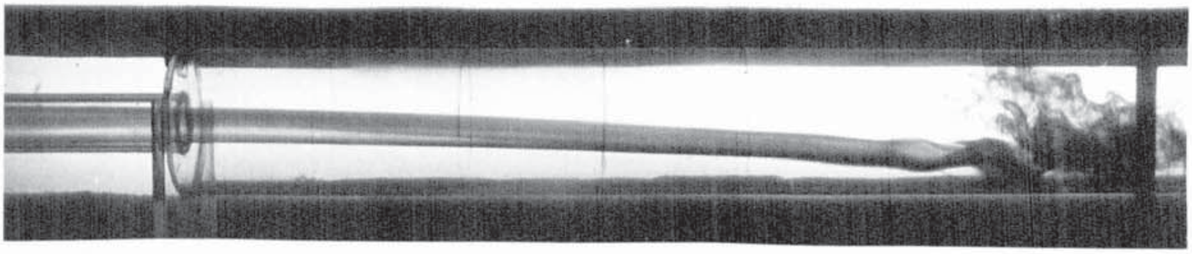

N.

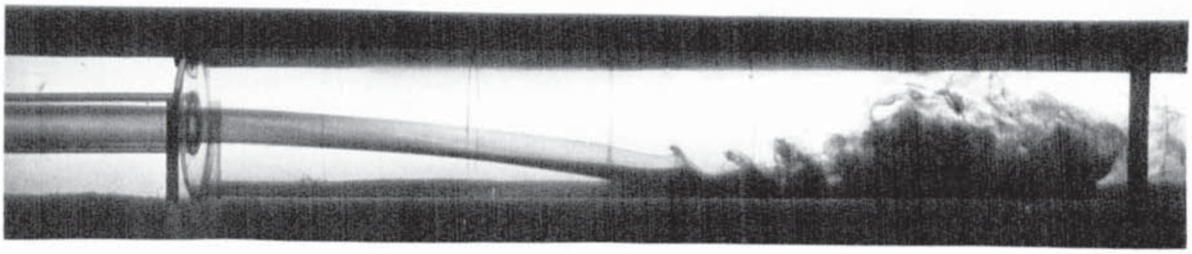

O.

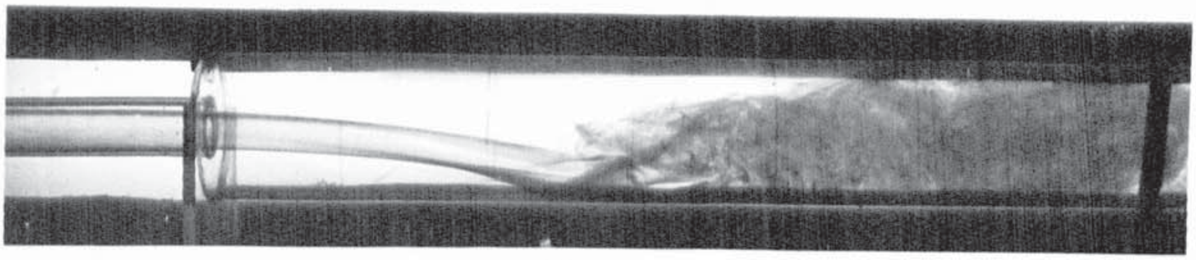

P.

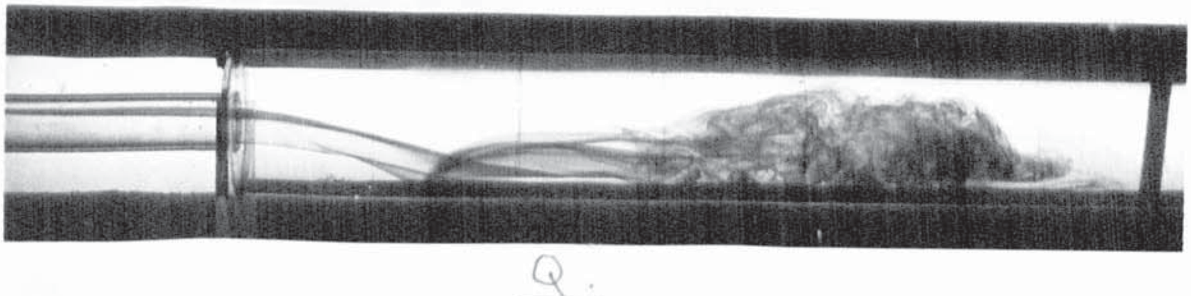

Q.

FIGURE 9.40.

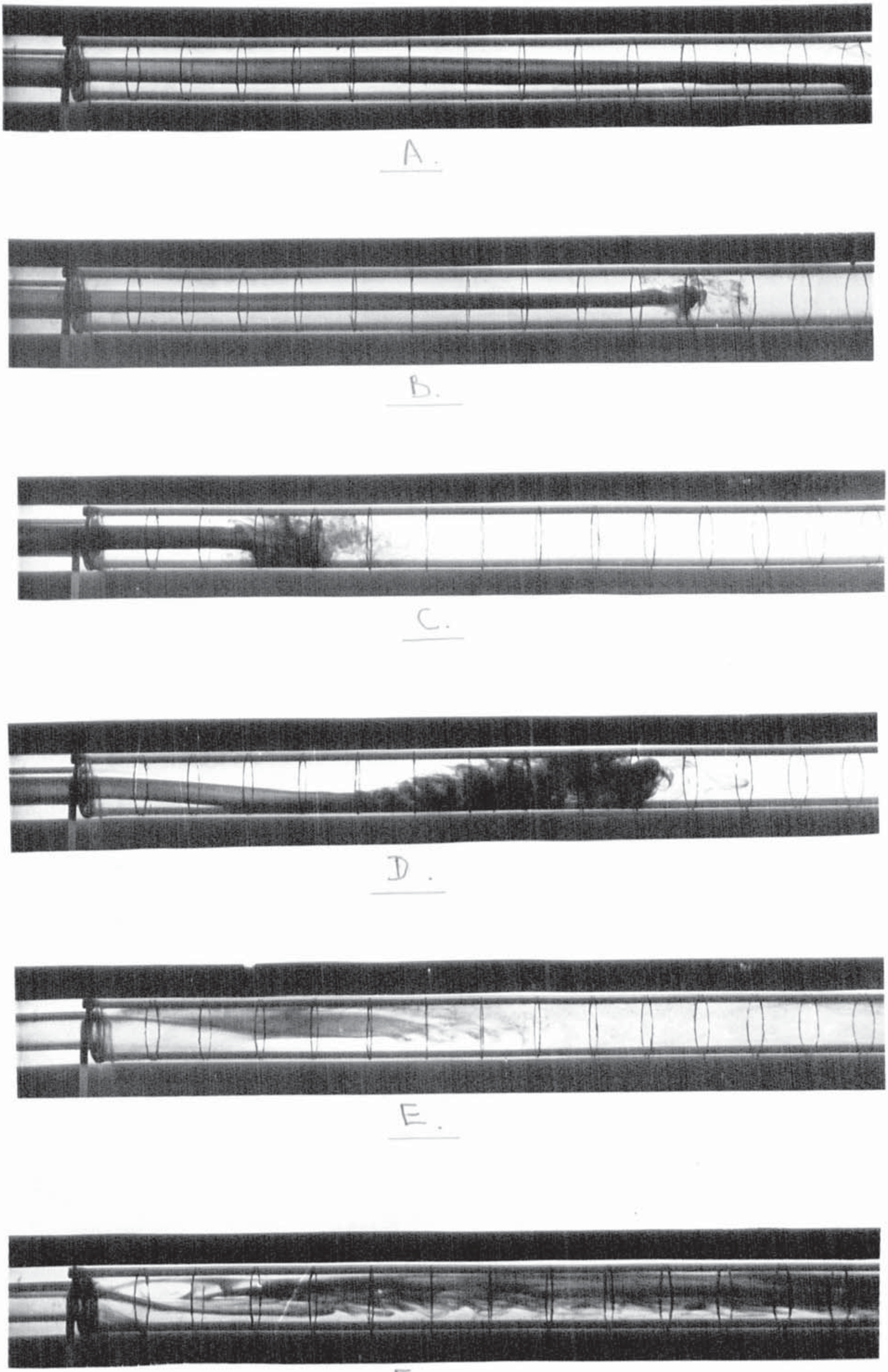

FIGURE 9.40 ..... cont ...

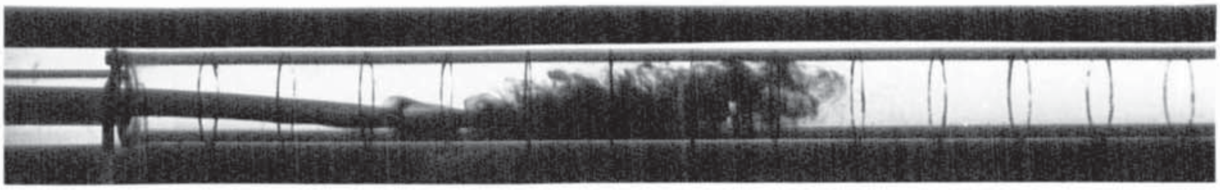

G.

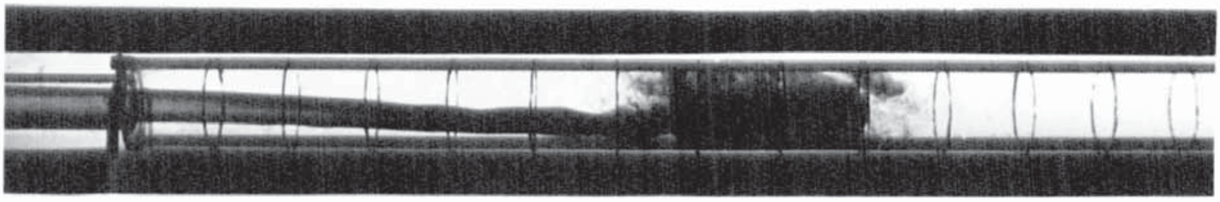

H.

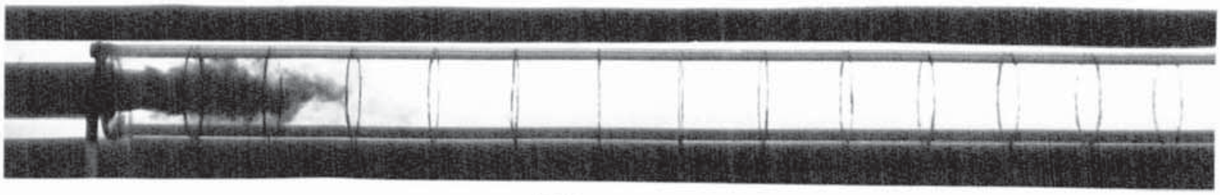

I.

FIGURE 9.41.

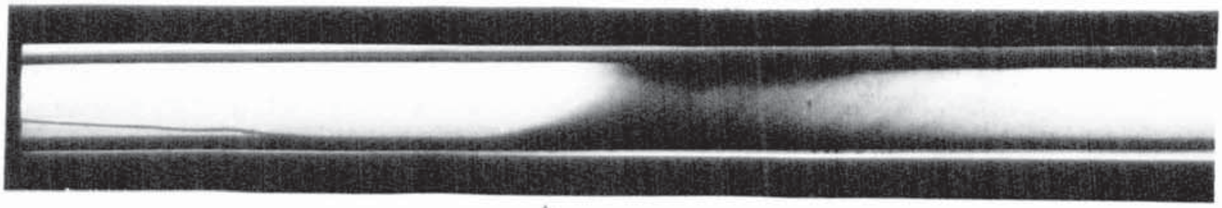

Re = 550.
Δt = 14 °C.

A.

(bath temp - bulk temp. inside tube) = Δt.

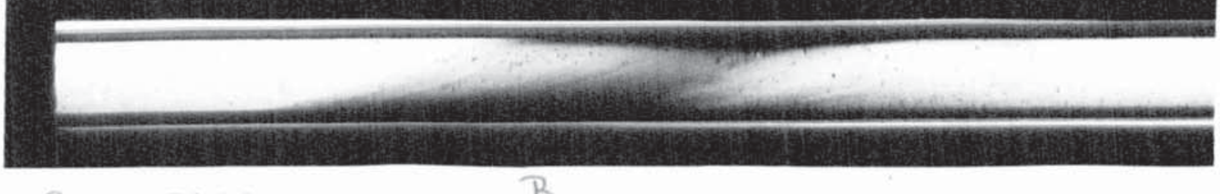

Re = 1370.
Δt = 14 °C.

B.

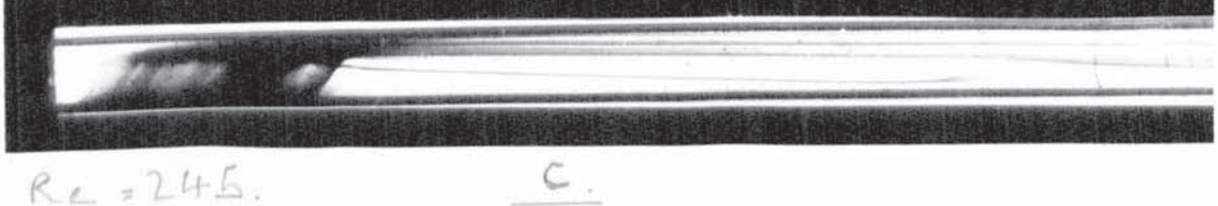

Re = 245.
Δt = 9 °C.

C.

FIGURE 9.42.

THE POSITION OF THE ONSET OF UNSTABLE FLOW DOWSTREAM OF A SUDDEN EXPANSION RATIO 1:3.

UTILISING WATER $Pr = 9.2$ AND GLYCOL-WATER MIXTURE $Pr = 24.1$.

X_1 = DISTANCE TO THE ONSET OF UNSTABLE FLOW AT THE TUBE WALL. X_2 = DISTANCE TO ONSET OF INSTABILITY AT TUBE AXIS.

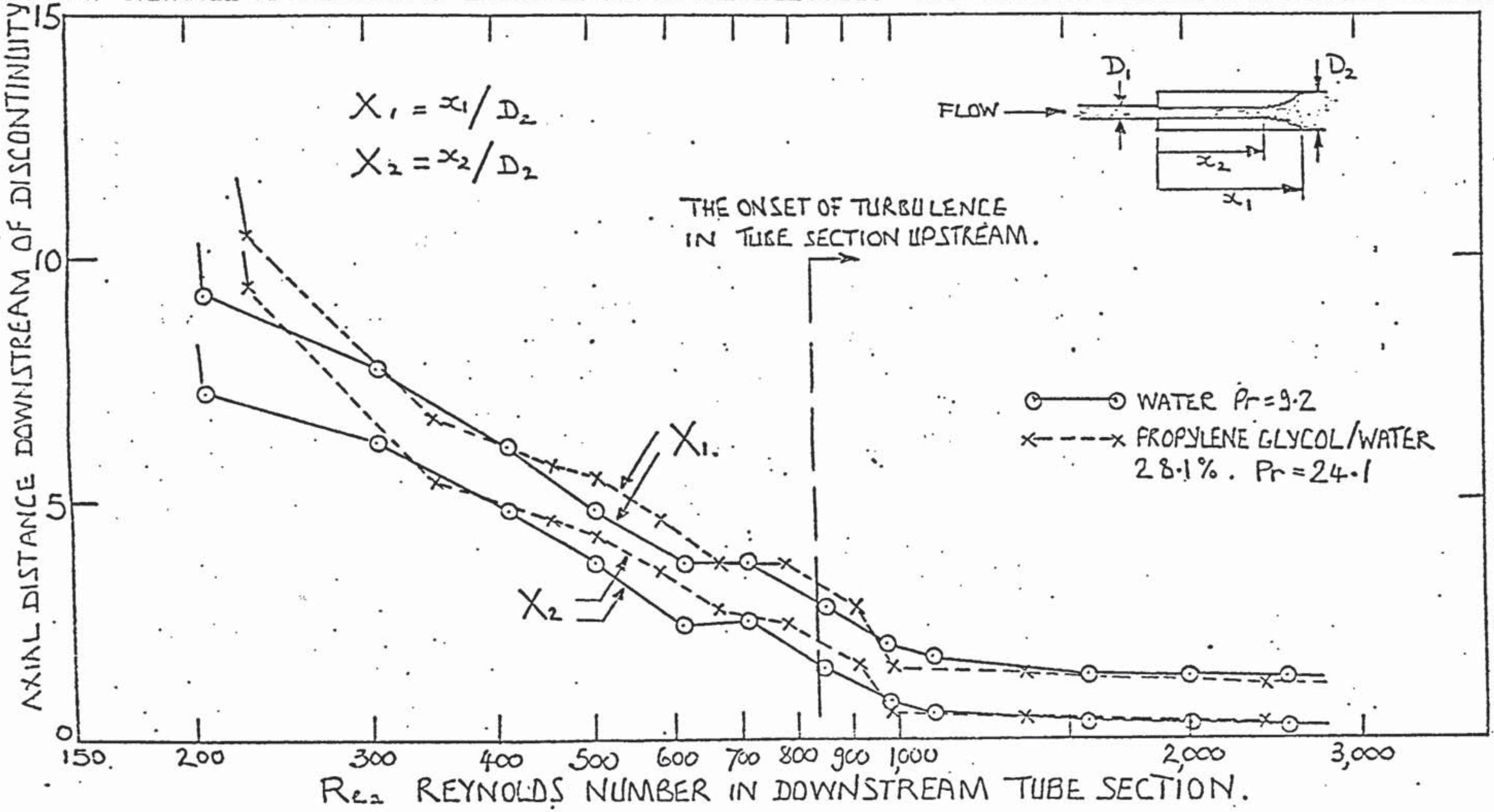

FIGURE 9.43.

THE POSITION OF THE ONSET OF UNSTABLE FLOW, DOWNSTREAM OF A SUDDEN EXPANSION RATIO 1:2, UTILISING WATER $Pr = 9.2$.

X_1 = DISTANCE TO THE ONSET OF UNSTABLE FLOW AT THE TUBE WALL.

X_2 = DISTANCE TO THE ONSET OF INSTABILITY AT TUBE AXIS.

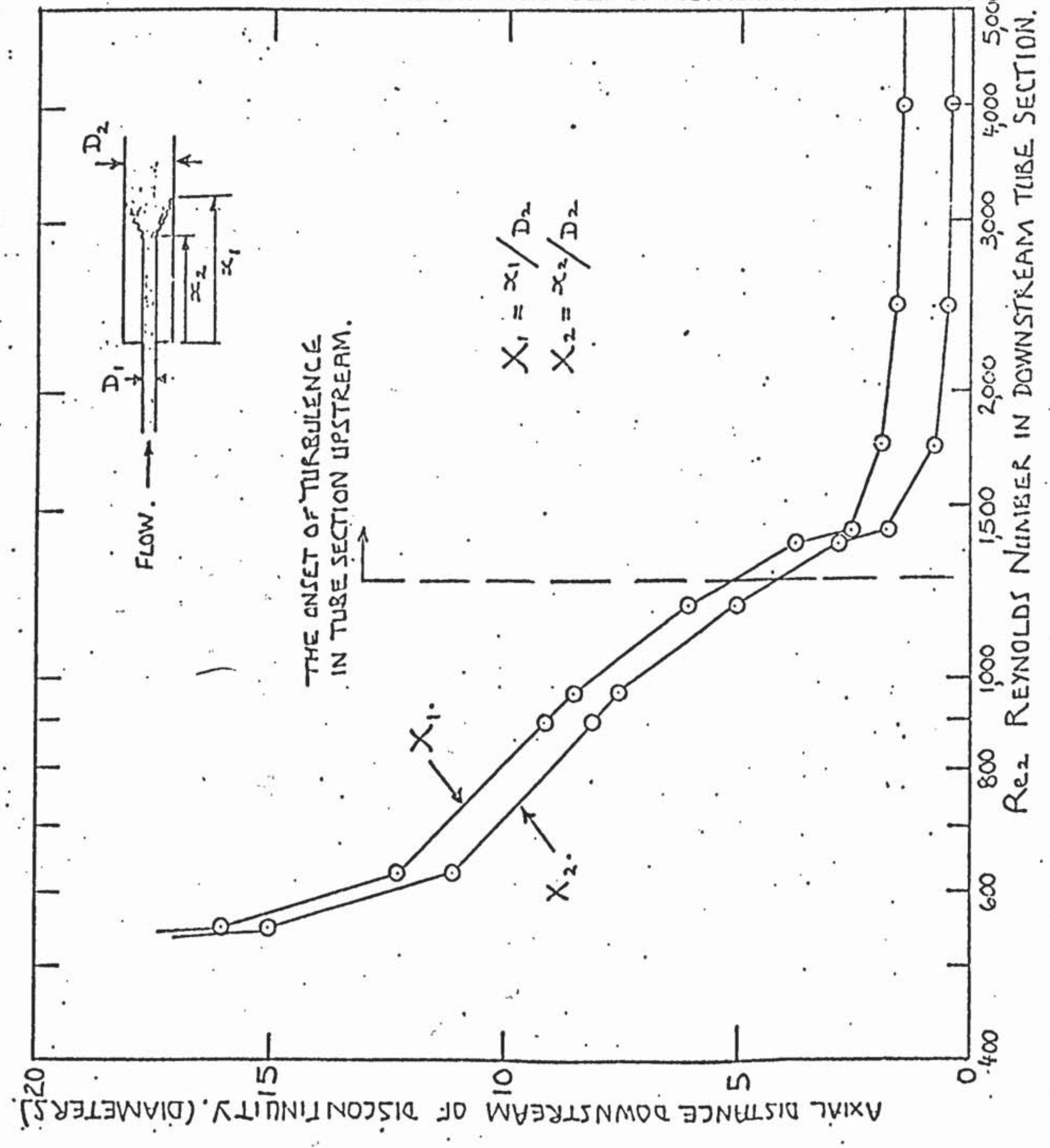

THE POSITION OF THE ONSET OF UNSTABLE FLOW DOWNSTREAM OF A SUDDEN EXPANSION — RATIOS 1:2 AND 1:3 — AS A FUNCTION OF REYNOLDS NUMBER UPSTREAM. $Pr = 9.2$ (WATER).

CRITICAL REYNOLDS NUMBER $Re_{CRIT} = \left(\frac{\rho \bar{U}_1 (D_2/D_1) x_1}{\mu} \right) \simeq 64{,}000$.

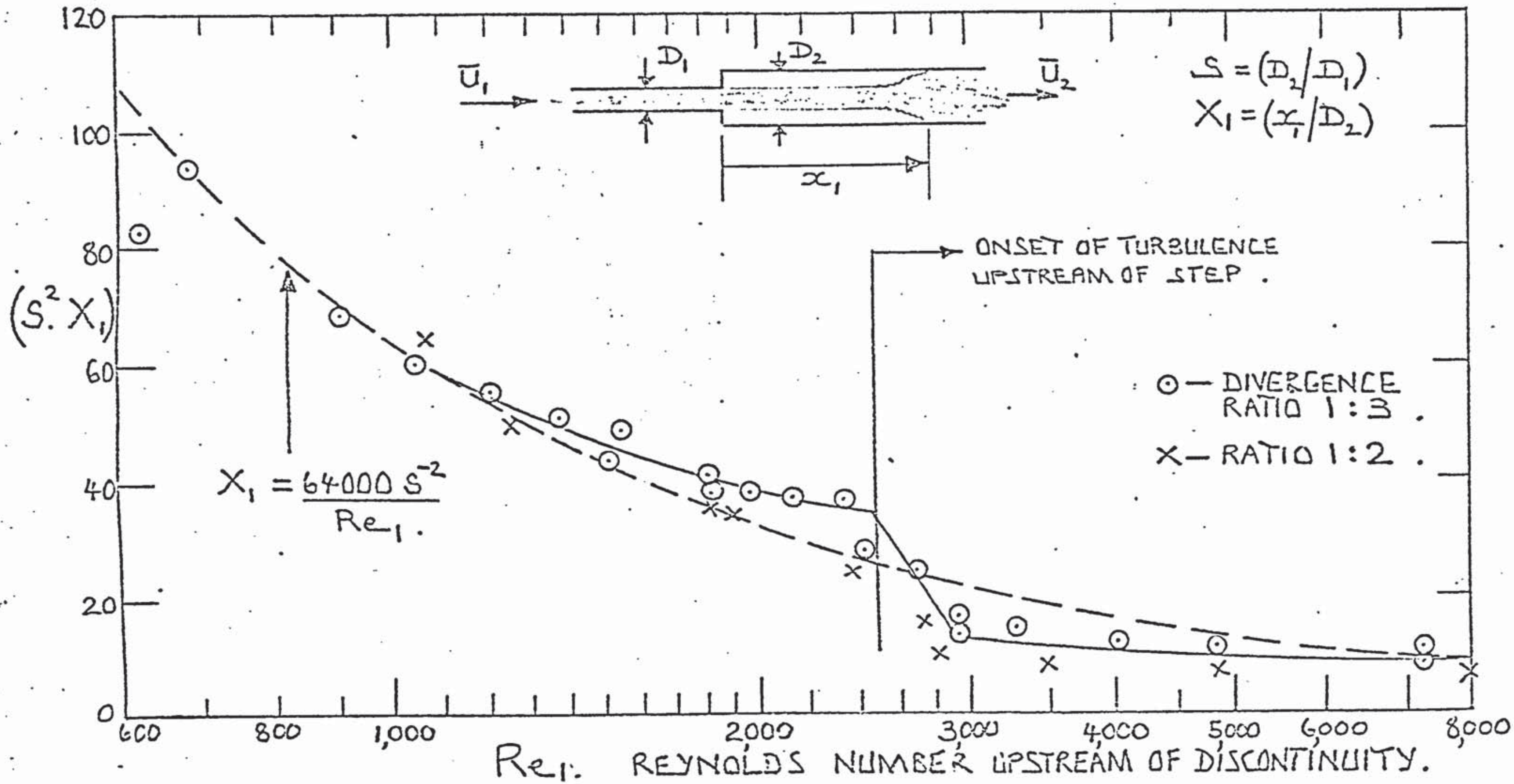

FIGURE 9.44.

THE AXIAL DISTANCE (DOWNSTREAM OF A 1:3·34 SUDDEN INCREASE IN DIAMETER) TO THE LOCATION OF THE MAXIMUM NUSSELT NUMBER. MEASUREMENTS FROM TESTS 1D1 to 50D1. PRANDTL NUMBERS 55, 140, 275, 500 (APPROX.) THE DEPENDENCE ON REYNOLDS NUMBER IS SHOWN AND A COMPARISON IS MADE WITH FLOW VISUALISATION DATA.

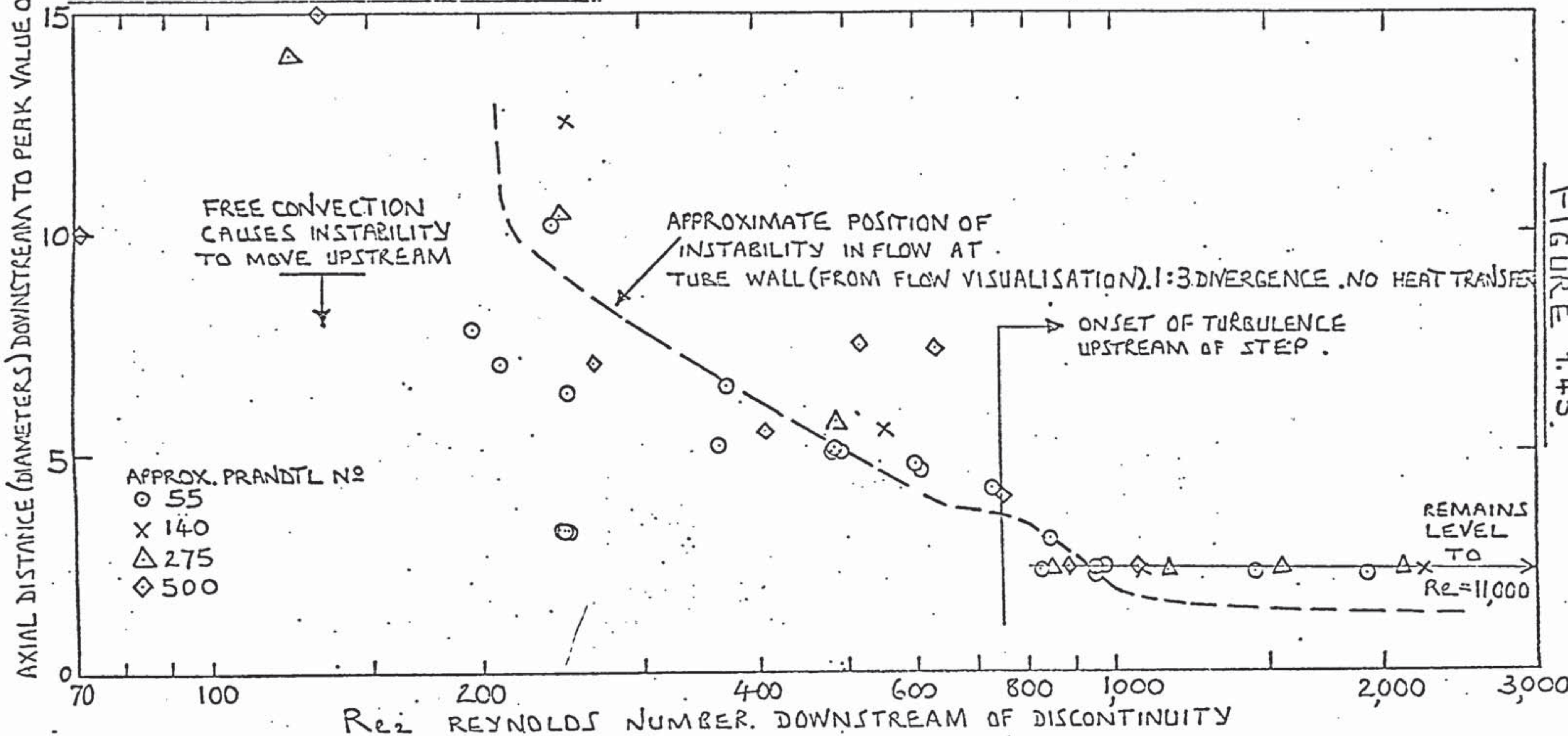

FIGURE 9.45.

THE AXIAL DISTANCE (DOWNSTREAM OF A 1:2 SUDDEN INCREASE IN DIAMETER) TO THE LOCATION OF THE MAXIMUM NUSSELT NUMBER. MEASUREMENTS FROM TESTS 1D2 to 22D2. PRANDTL NUMBERS 55, 150, 275, 400 (APPROX) THE DEPENDENCE ON REYNOLDS NUMBER IS SHOWN AND A COMPARISON IS MADE WITH FLOW VISUALISATION DATA.

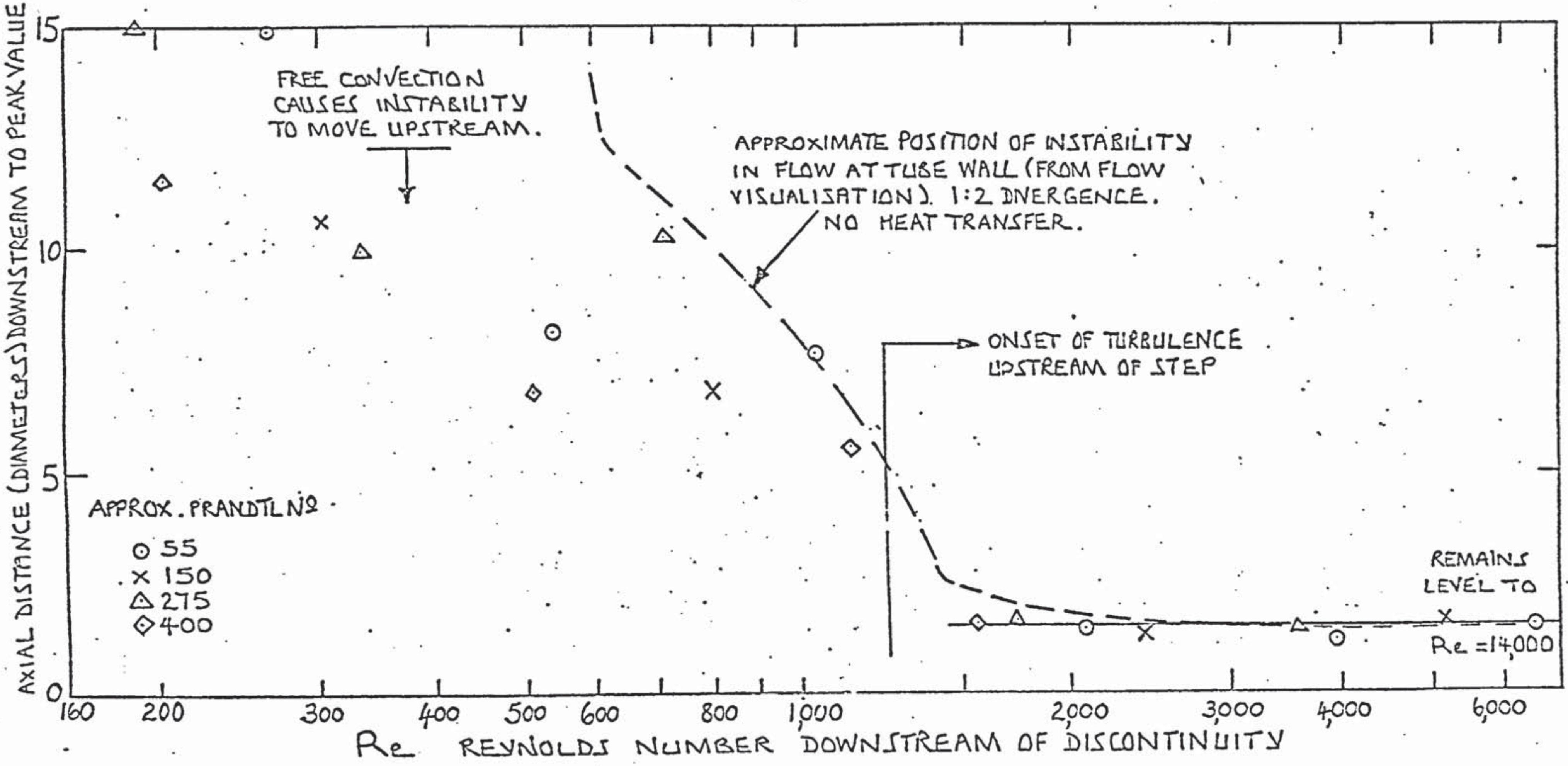

FIGURE 9.46.

DISTANCE TO PEAK VALUE OF NUSSELT NUMBER DOWNSTREAM OF A SUDDEN DIVERGENCE. THE VARIATION IN LENGTH DUE TO FREE CONVECTIONAL EFFECTS AT LOW REYNOLDS NUMBERS.

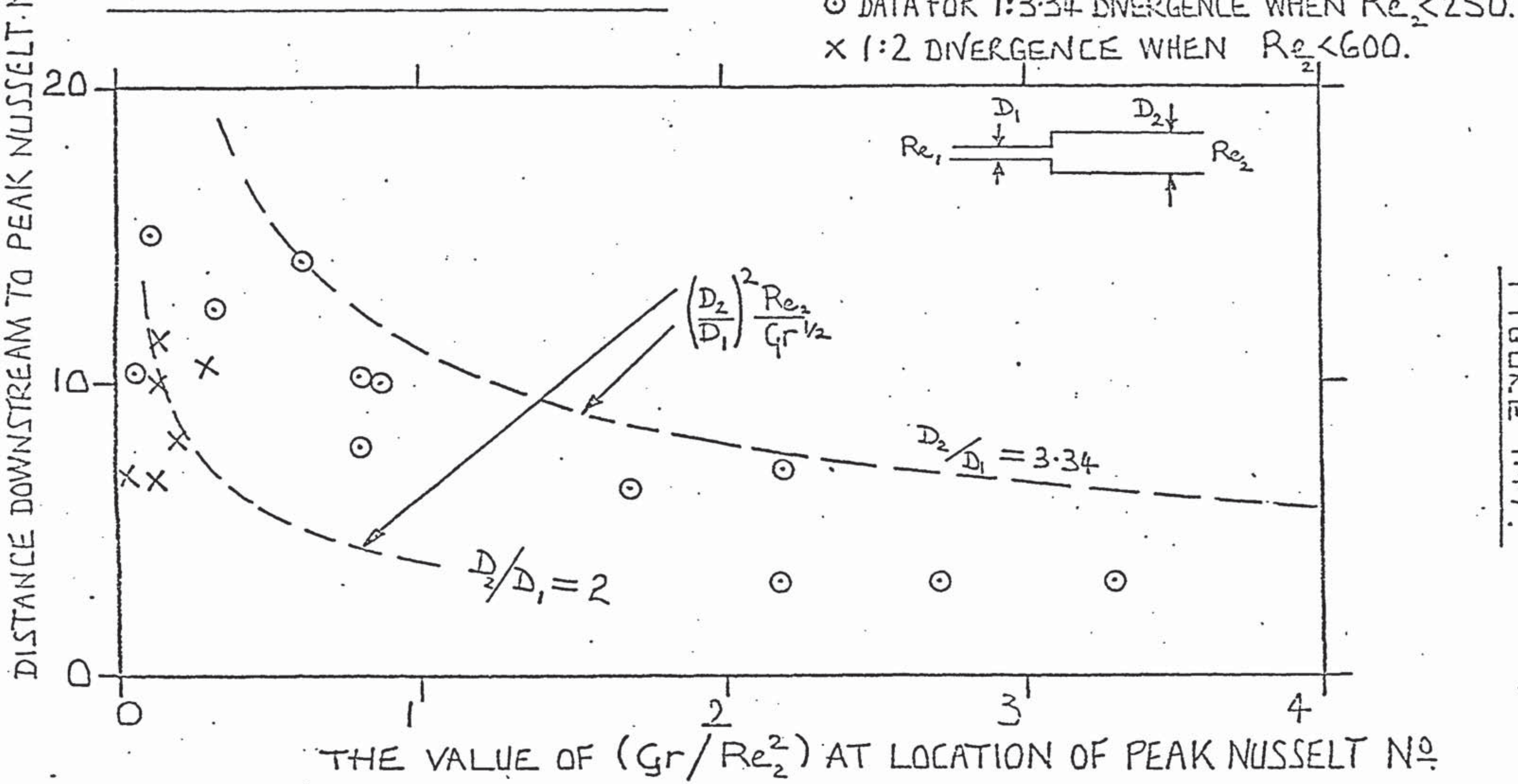

FIGURE 9.47.

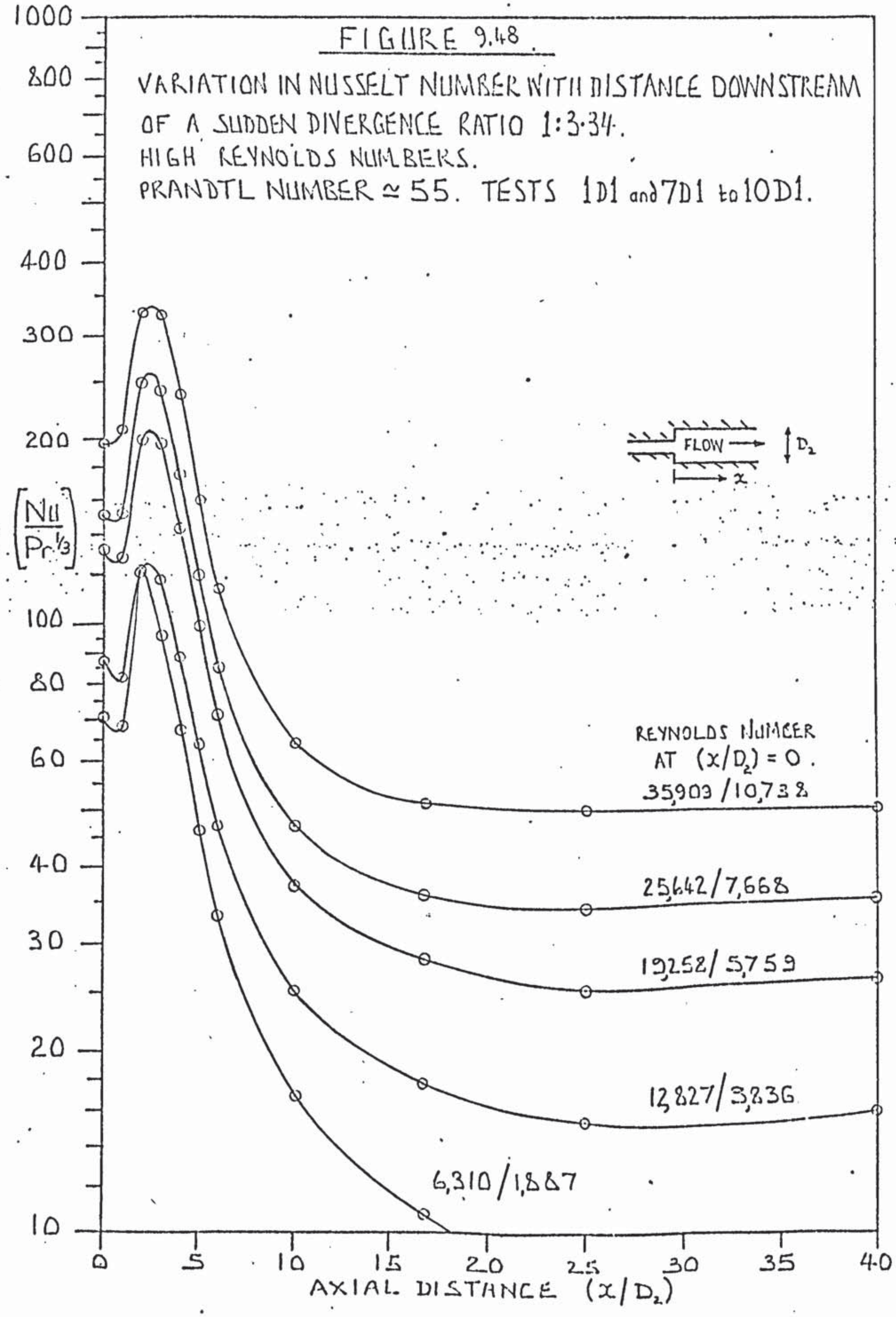

FIGURE 9.48.
VARIATION IN NUSSELT NUMBER WITH DISTANCE DOWNSTREAM OF A SUDDEN DIVERGENCE RATIO 1:3·34.
HIGH REYNOLDS NUMBERS.
PRANDTL NUMBER ≃ 55. TESTS 1D1 and 7D1 to 10D1.
FLOW
D_2
x
$\left[\frac{Nu}{Pr^{1/3}}\right]$
REYNOLDS NUMBER AT $(x/D_2) = 0$.
35,903 / 10,738
25,642 / 7,668
19,252 / 5,759
12,827 / 3,836
6,310 / 1,887
AXIAL DISTANCE (x/D_2)
1000
800
600
400
300
200
100
80
60
40
30
20
10
0
5
10
15
20
25
30
35
40

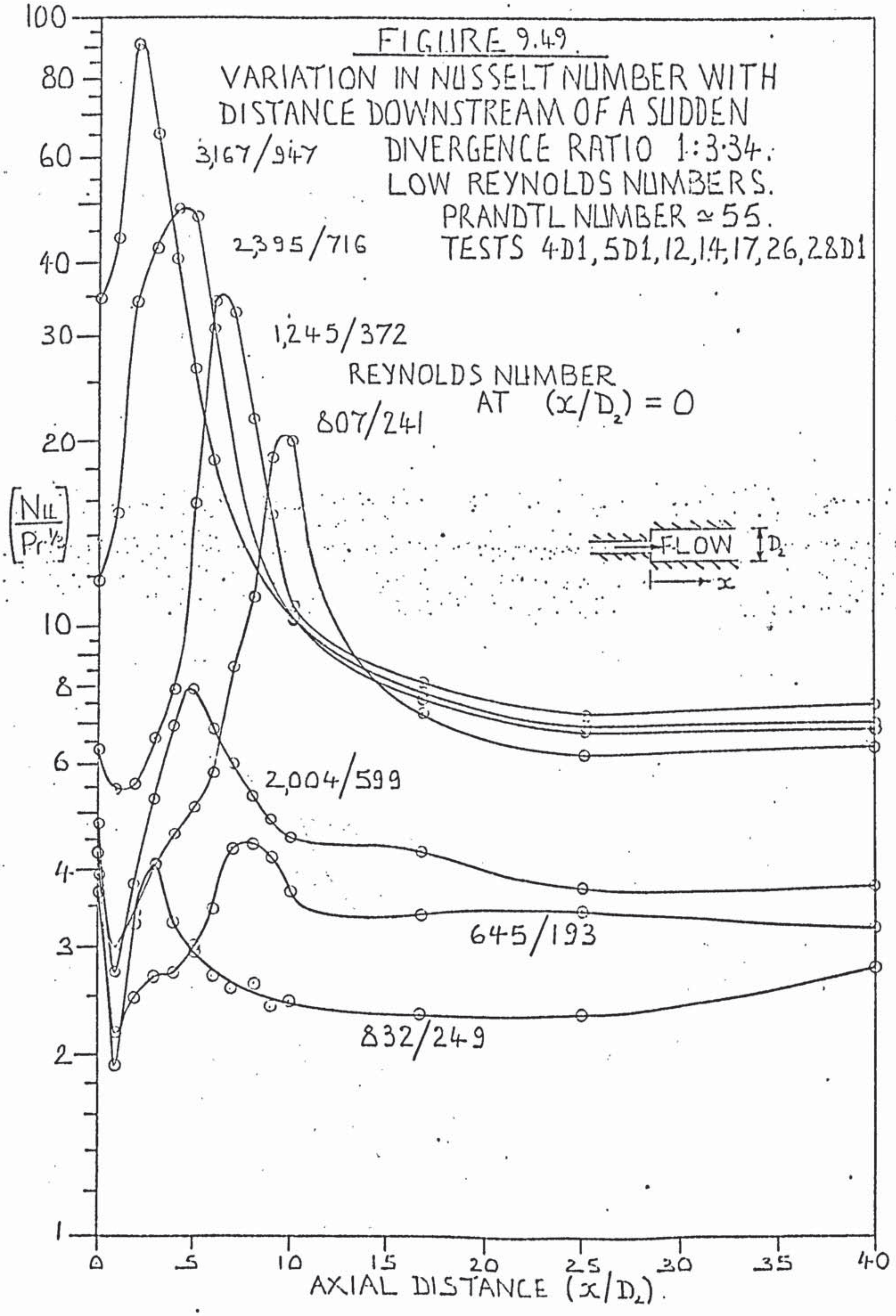

FIGURE 9.49.
VARIATION IN NUSSELT NUMBER WITH DISTANCE DOWNSTREAM OF A SUDDEN DIVERGENCE RATIO 1:3·34.
LOW REYNOLDS NUMBERS.
PRANDTL NUMBER ≃ 55.
TESTS 4D1, 5D1, 12, 14, 17, 26, 28D1
3,167/947
2,395/716
1,245/372
REYNOLDS NUMBER AT (x/D2) = 0
807/241
2,004/599
645/193
832/249
FLOW
D2
x
[Nu/Pr½]
AXIAL DISTANCE (x/D2)
100
80
60
40
30
20
10
8
6
4
3
2
1
0
5
10
15
20
25
30
35
40

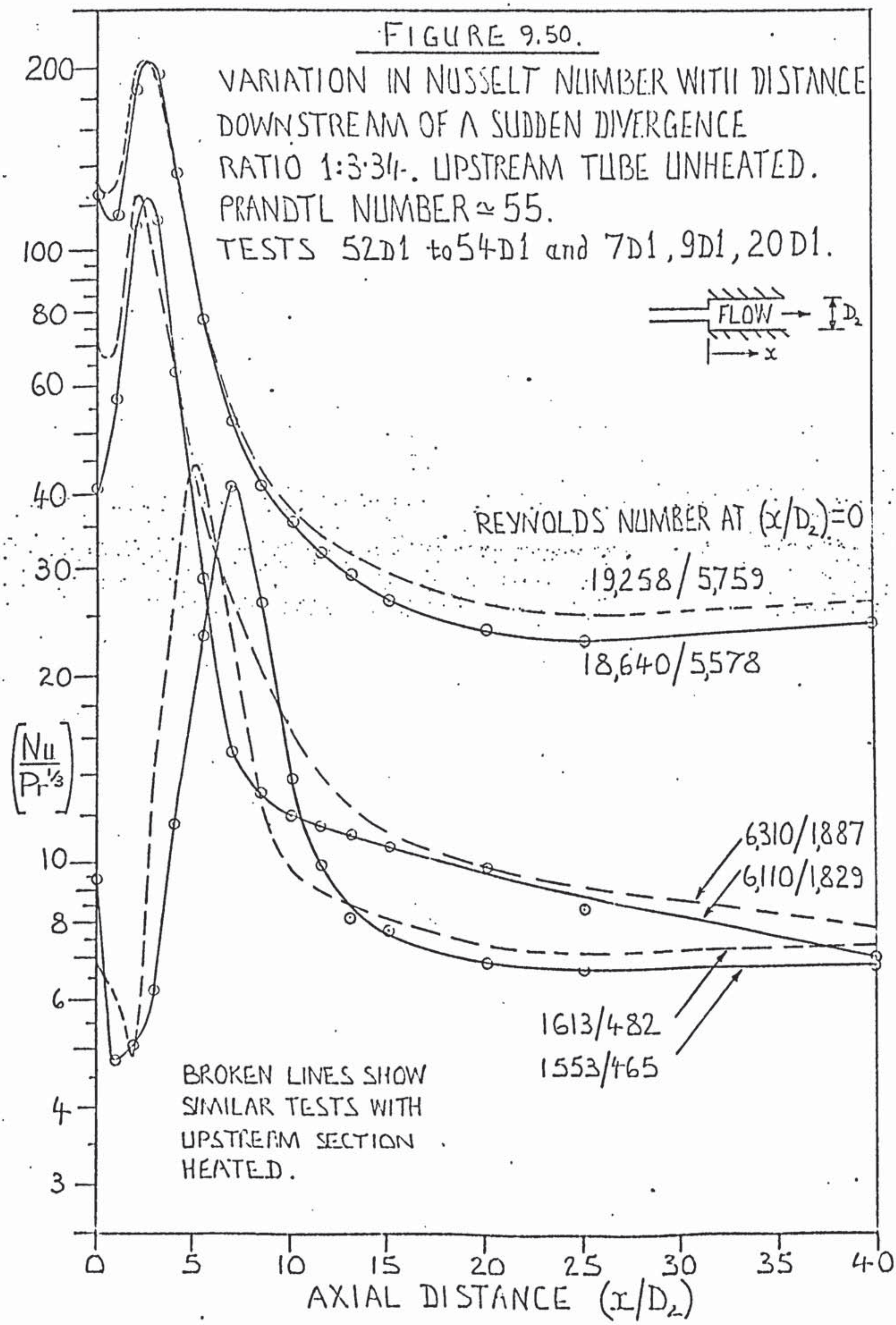

FIGURE 9.50.
VARIATION IN NUSSELT NUMBER WITH DISTANCE DOWNSTREAM OF A SUDDEN DIVERGENCE RATIO 1:3·34. UPSTREAM TUBE UNHEATED. PRANDTL NUMBER ≃ 55.
TESTS 52D1 to 54D1 and 7D1, 9D1, 20D1.
FLOW
D_2
x
REYNOLDS NUMBER AT $(x/D_2)=0$
19,258/5,759
18,640/5,578
6,310/1,887
6,110/1,829
1613/482
1553/465
BROKEN LINES SHOW SIMILAR TESTS WITH UPSTREAM SECTION HEATED.
$\left[\frac{Nu}{Pr^{1/3}}\right]$
200
100
80
60
40
30
20
10
8
6
4
3
0
5
10
15
20
25
30
35
40
AXIAL DISTANCE (x/D_2)

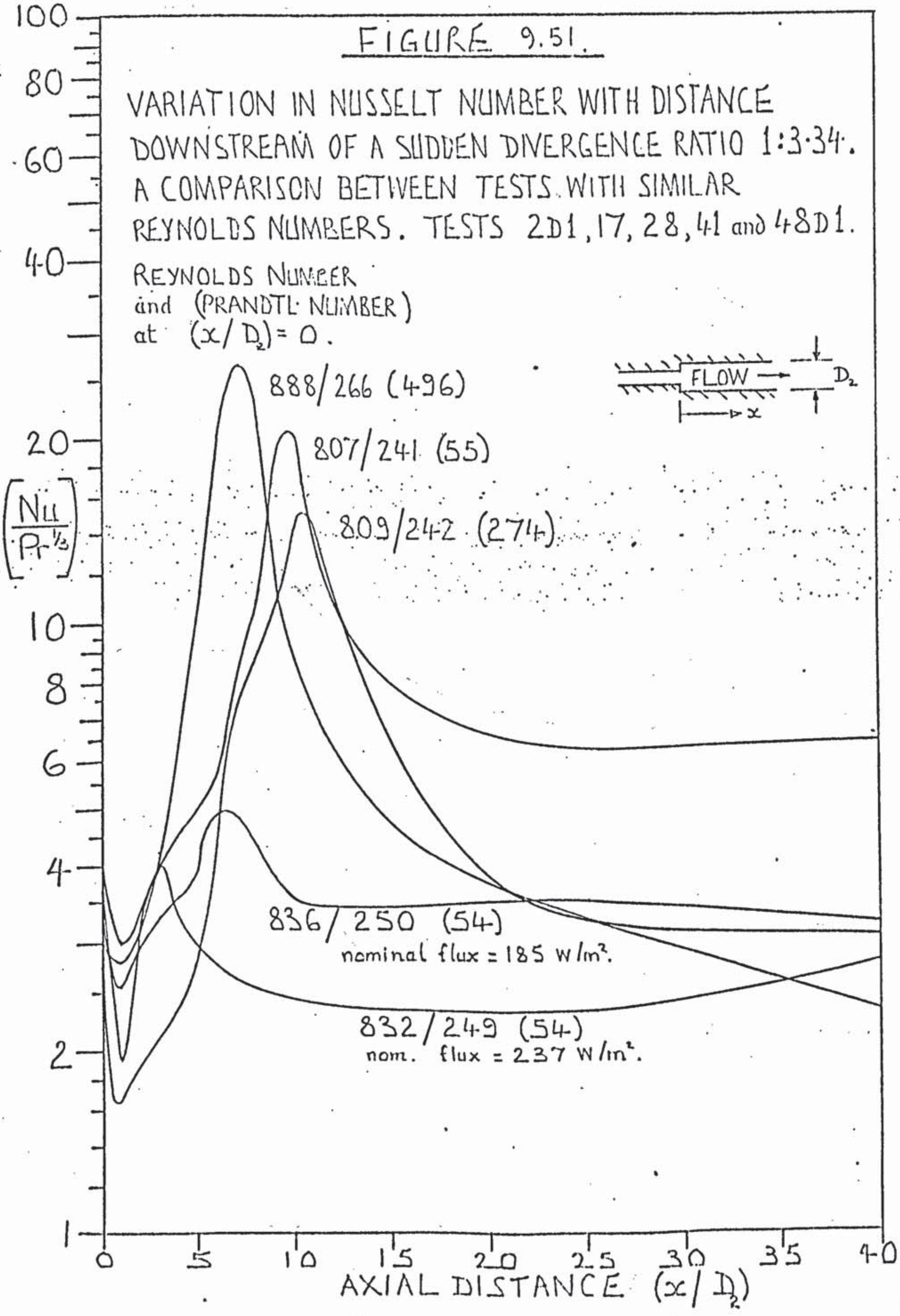

FIGURE 9.51.

VARIATION IN NUSSELT NUMBER WITH DISTANCE DOWNSTREAM OF A SUDDEN DIVERGENCE RATIO 1:3·34. A COMPARISON BETWEEN TESTS WITH SIMILAR REYNOLDS NUMBERS. TESTS 2D1, 17, 28, 41 and 48D1.

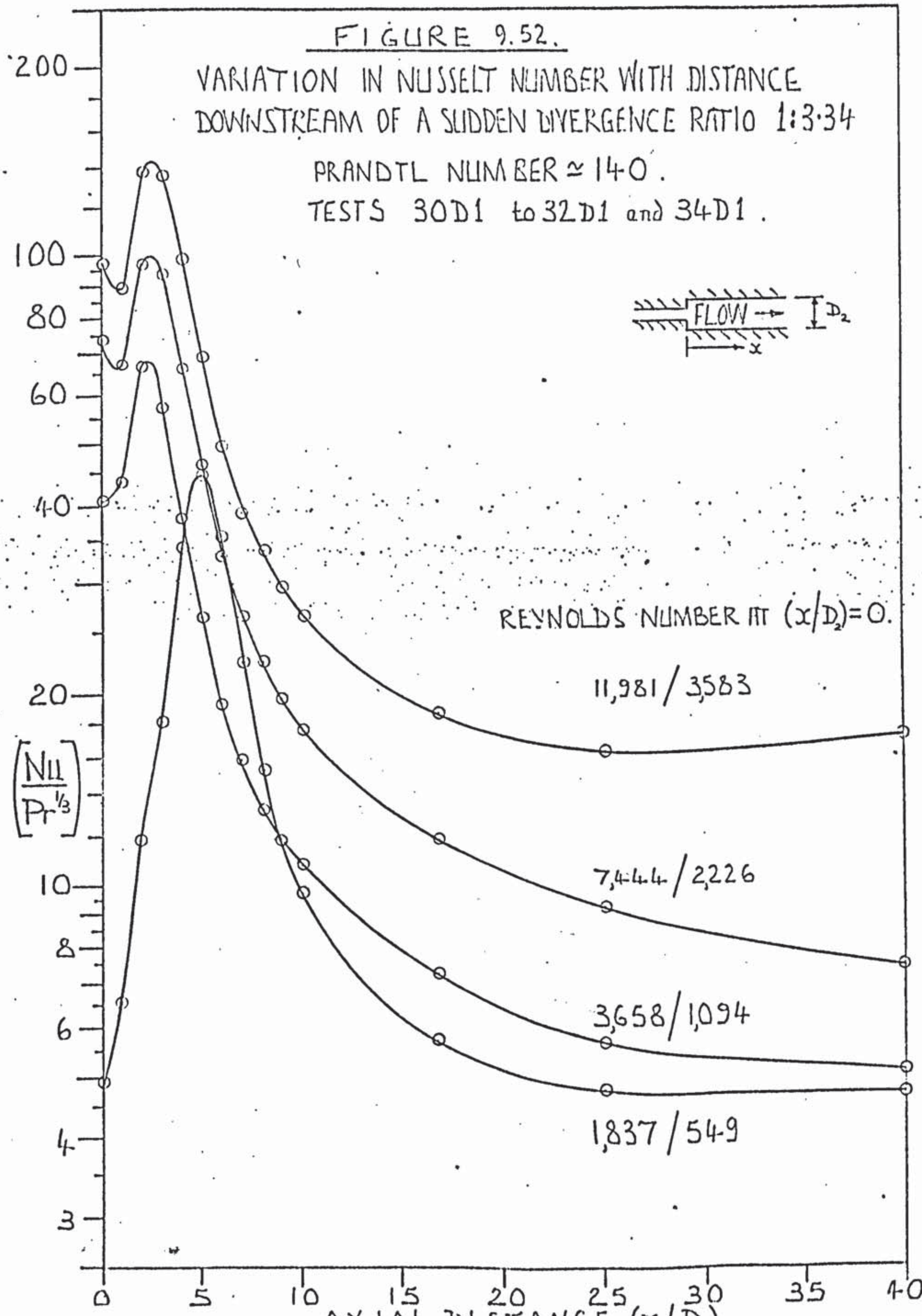
FIGURE 9.52.
VARIATION IN NUSSELT NUMBER WITH DISTANCE DOWNSTREAM OF A SUDDEN DIVERGENCE RATIO 1:3·34
PRANDTL NUMBER ≃ 14·0.
TESTS 30D1 to 32D1 and 34D1.
FLOW
D_2
x
REYNOLDS NUMBER AT $(x/D_2)=0$.
11,981/3,583
7,444/2,226
3,658/1,094
1,837/549
$\left[\frac{Nu}{Pr^{1/3}}\right]$
200
100
80
60
40
20
10
8
6
4
3
0
5
10
15
20
25
30
35
40
AXIAL DISTANCE (x/D_2)

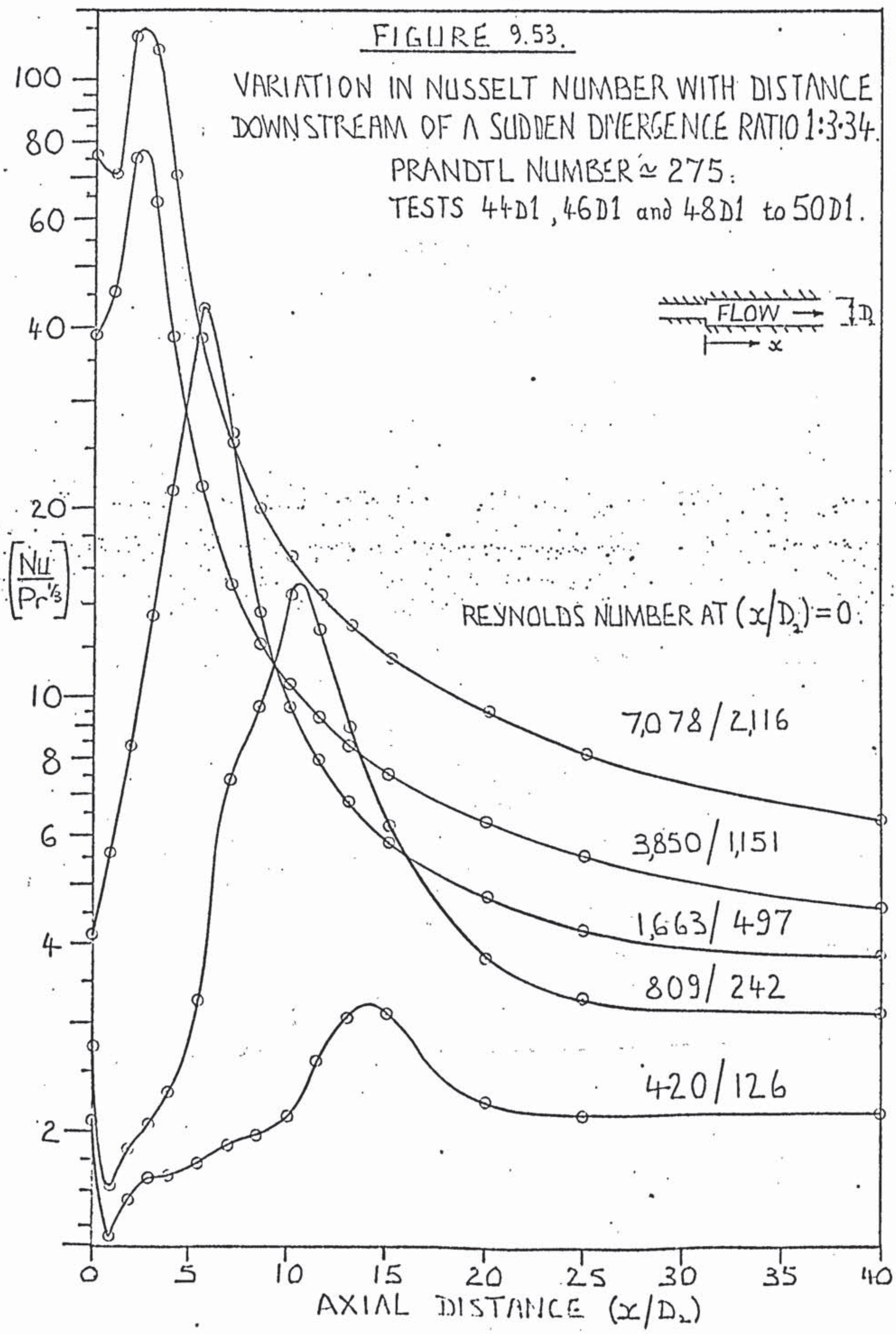
FIGURE 9.53.
VARIATION IN NUSSELT NUMBER WITH DISTANCE DOWNSTREAM OF A SUDDEN DIVERGENCE RATIO 1:3·34.
PRANDTL NUMBER ≃ 275.
TESTS 44D1, 46D1 and 48D1 to 50D1.
FLOW
D_2
x
REYNOLDS NUMBER AT $(x/D_2)=0$:
7,078/2,116
3,850/1,151
1,663/497
809/242
420/126
$\left[\frac{Nu}{Pr^{1/3}}\right]$
100
80
60
40
20
10
8
6
4
2
0
5
10
15
20
25
30
35
40
AXIAL DISTANCE (x/D_2)

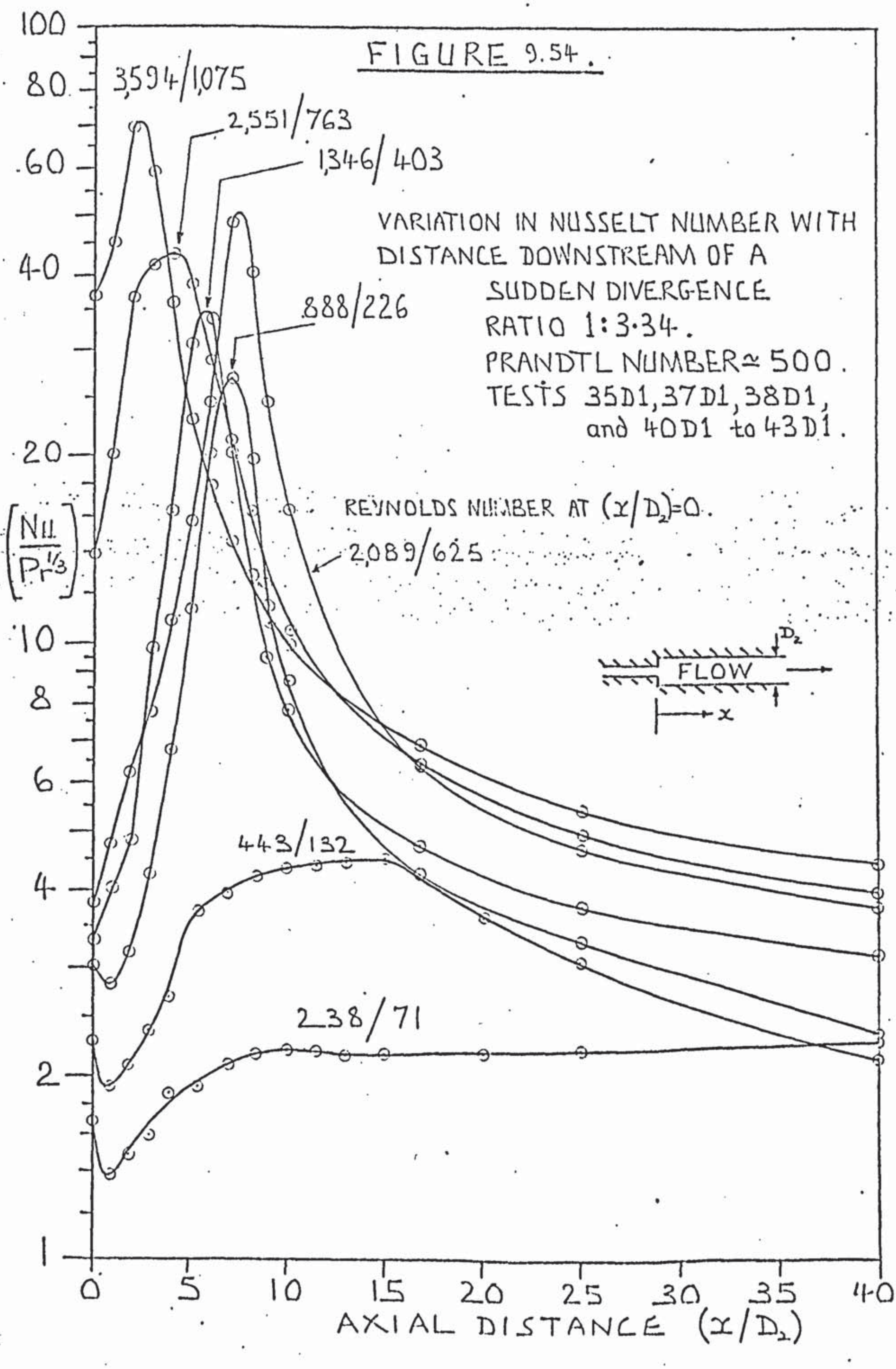

FIGURE 9.54.
VARIATION IN NUSSELT NUMBER WITH DISTANCE DOWNSTREAM OF A SUDDEN DIVERGENCE
RATIO 1:3·34.
PRANDTL NUMBER ≃ 500.
TESTS 35D1, 37D1, 38D1, and 40D1 to 43D1.
REYNOLDS NUMBER AT $(x/D_2)=0$.
3,594/1,075
2,551/763
1,346/403
888/226
2,089/625
443/132
238/71
FLOW
D_2
x
$\left[\frac{Nu}{Pr^{1/3}}\right]$
AXIAL DISTANCE (x/D_2)
100
80
60
40
20
10
8
6
4
2
1
0
5
10
15
20
25
30
35
40

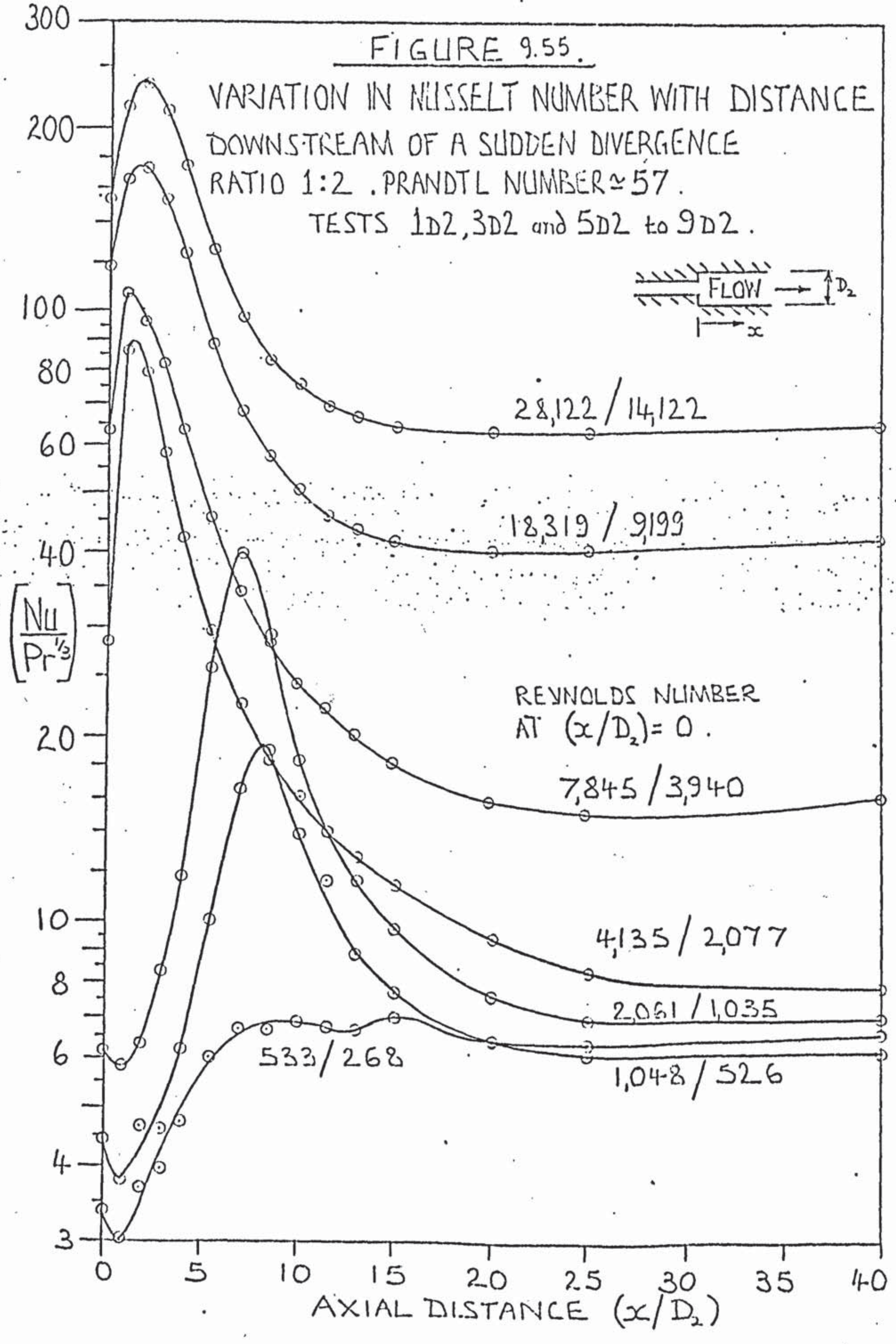

FIGURE 9.55.
VARIATION IN NUSSELT NUMBER WITH DISTANCE
DOWNSTREAM OF A SUDDEN DIVERGENCE
RATIO 1:2 . PRANDTL NUMBER ≃ 57.
TESTS 1D2, 3D2 and 5D2 to 9D2.
FLOW
D_2
x
28,122 / 14,122
18,319 / 9,199
REYNOLDS NUMBER
AT $(x/D_2) = 0$.
7,845 / 3,940
4,135 / 2,077
2,061 / 1,035
533 / 268
1,048 / 526
$\left[\frac{Nu}{Pr^{1/3}}\right]$
300
200
100
80
60
40
20
10
8
6
4
3
0
5
10
15
20
25
30
35
40
AXIAL DISTANCE (x/D_2)

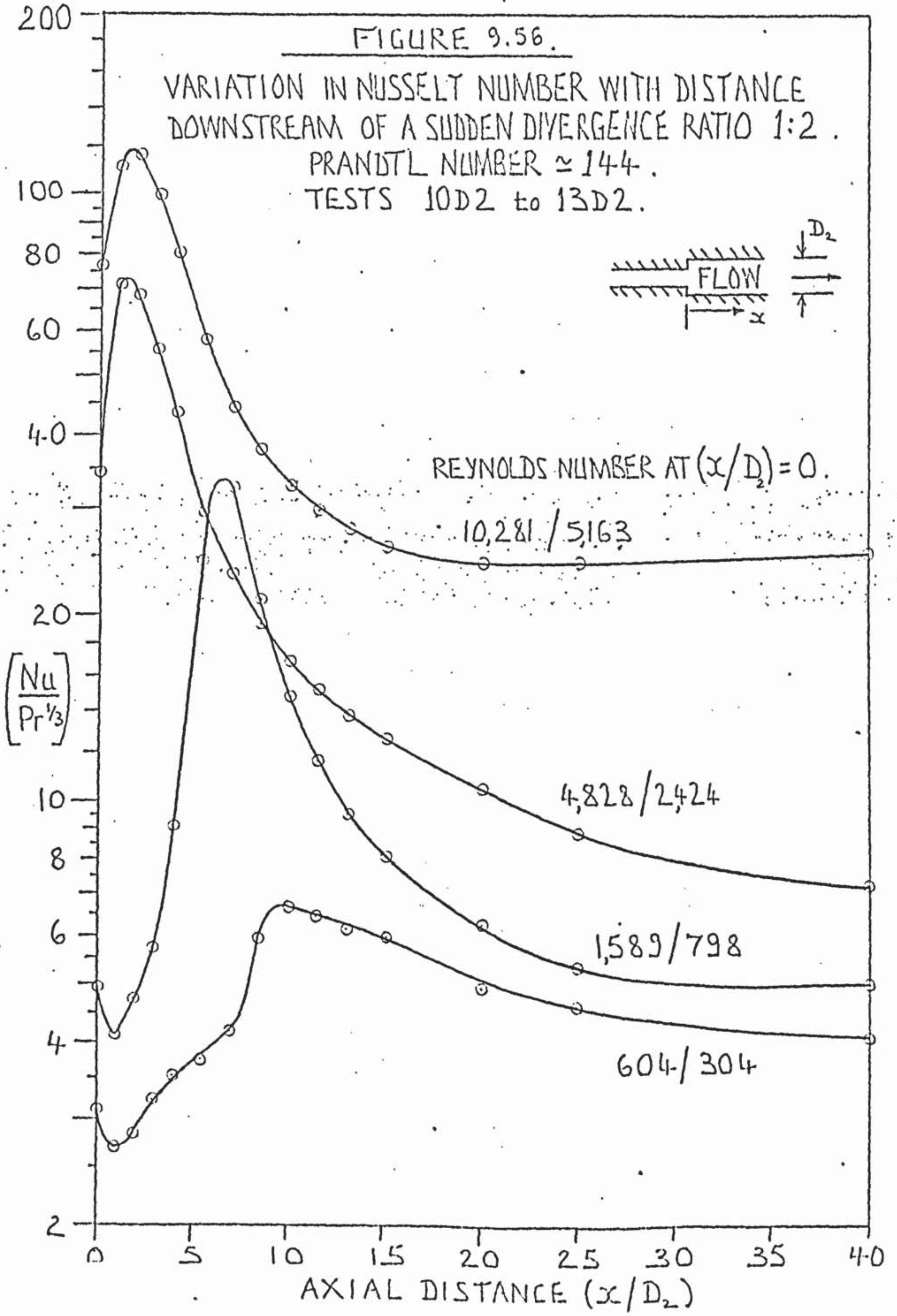

FIGURE 9.56.
VARIATION IN NUSSELT NUMBER WITH DISTANCE
DOWNSTREAM OF A SUDDEN DIVERGENCE RATIO 1:2.
PRANDTL NUMBER ≃ 144.
TESTS 10D2 to 13D2.
FLOW
D_2
x
REYNOLDS NUMBER AT $(x/D_2) = 0$.
10,281 / 5,163
4,828 / 2,424
1,589 / 798
604 / 304
$\left[\frac{Nu}{Pr^{1/3}}\right]$
AXIAL DISTANCE (x/D_2)
200
100
80
60
40
20
10
8
6
4
2
0
5
10
15
20
25
30
35
40

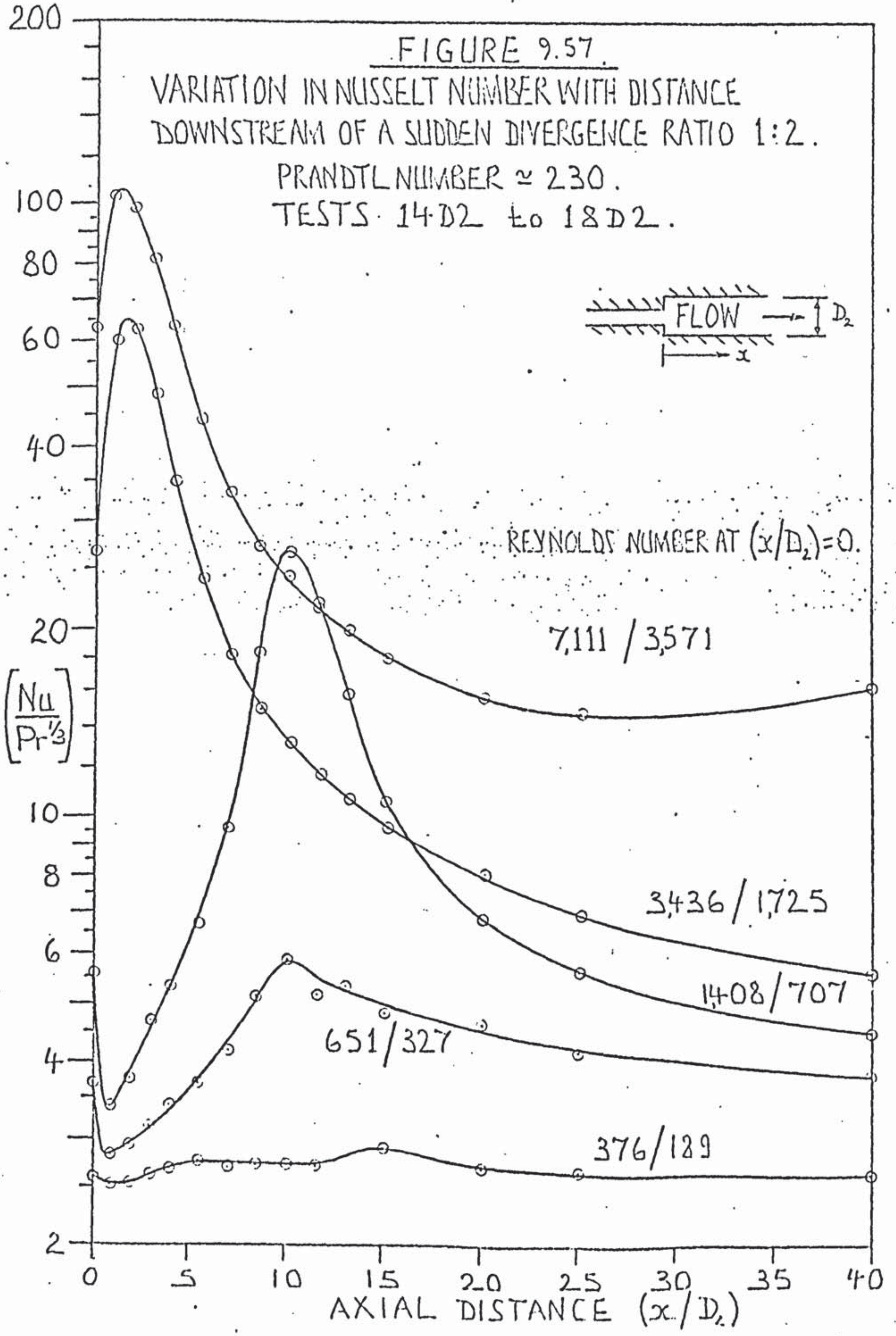

FIGURE 9.57.
VARIATION IN NUSSELT NUMBER WITH DISTANCE DOWNSTREAM OF A SUDDEN DIVERGENCE RATIO 1:2.
PRANDTL NUMBER ≃ 230.
TESTS 14D2 to 18D2.
FLOW
D_2
x
REYNOLDS NUMBER AT $(x/D_2)=0$.
7,111 / 3,571
3,436 / 1,725
1,408 / 707
651 / 327
376 / 189
$\left[\frac{Nu}{Pr^{1/3}}\right]$
200
100
80
60
40
20
10
8
6
4
2
0
5
10
15
20
25
30
35
40
AXIAL DISTANCE (x/D_2)

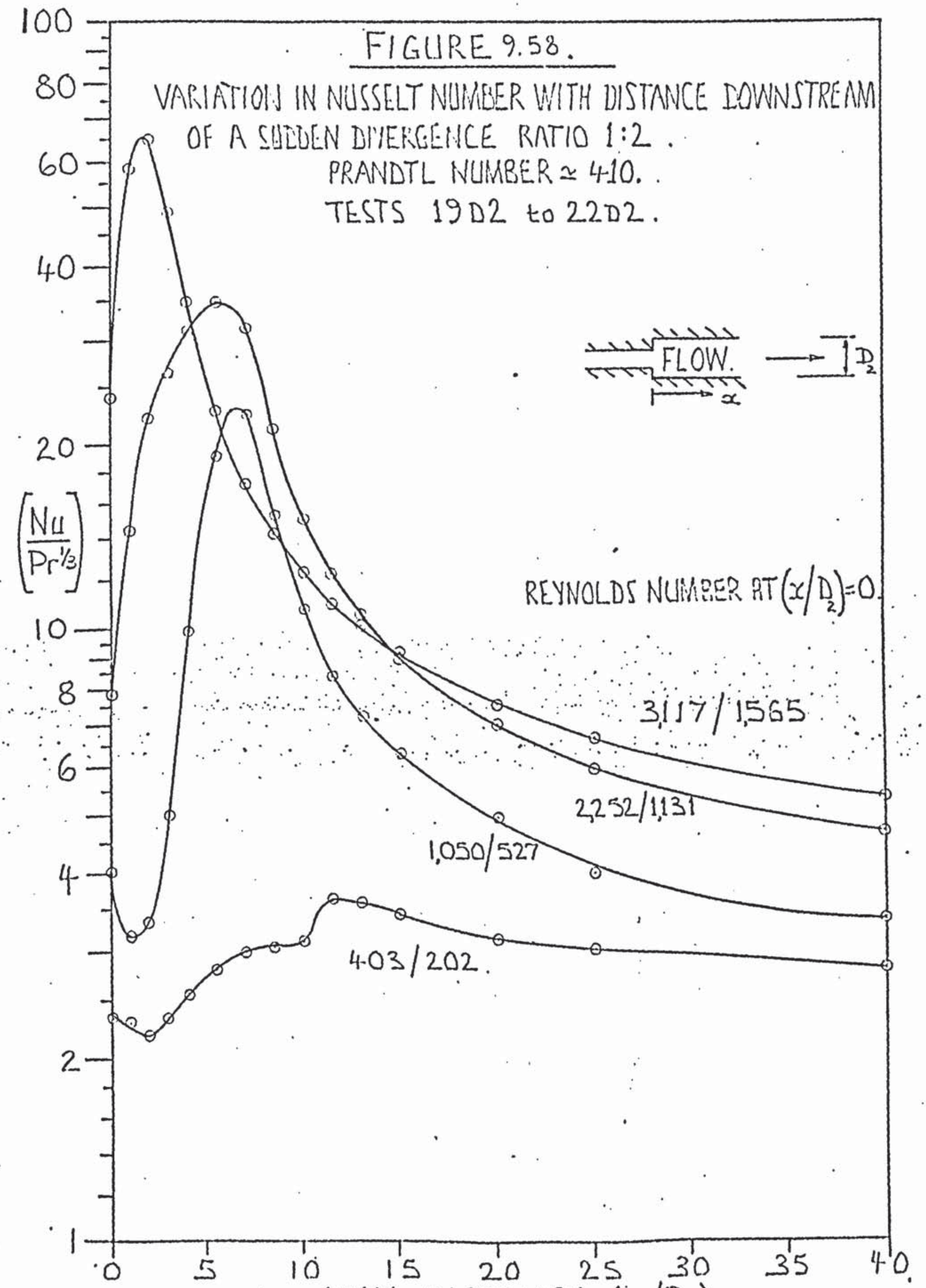

FIGURE 9.58.
VARIATION IN NUSSELT NUMBER WITH DISTANCE DOWNSTREAM OF A SUDDEN DIVERGENCE RATIO 1:2.
PRANDTL NUMBER ≃ 410.
TESTS 19D2 to 22D2.
FLOW.
REYNOLDS NUMBER AT (x/D2)=0.
3,117/1,565
2,252/1,131
1,050/527
403/202.
100
80
60
40
20
10
8
6
4
2
1
(Nu/Pr^1/3)
0
5
10
15
20
25
30
35
40
AXIAL DISTANCE (x/D2)

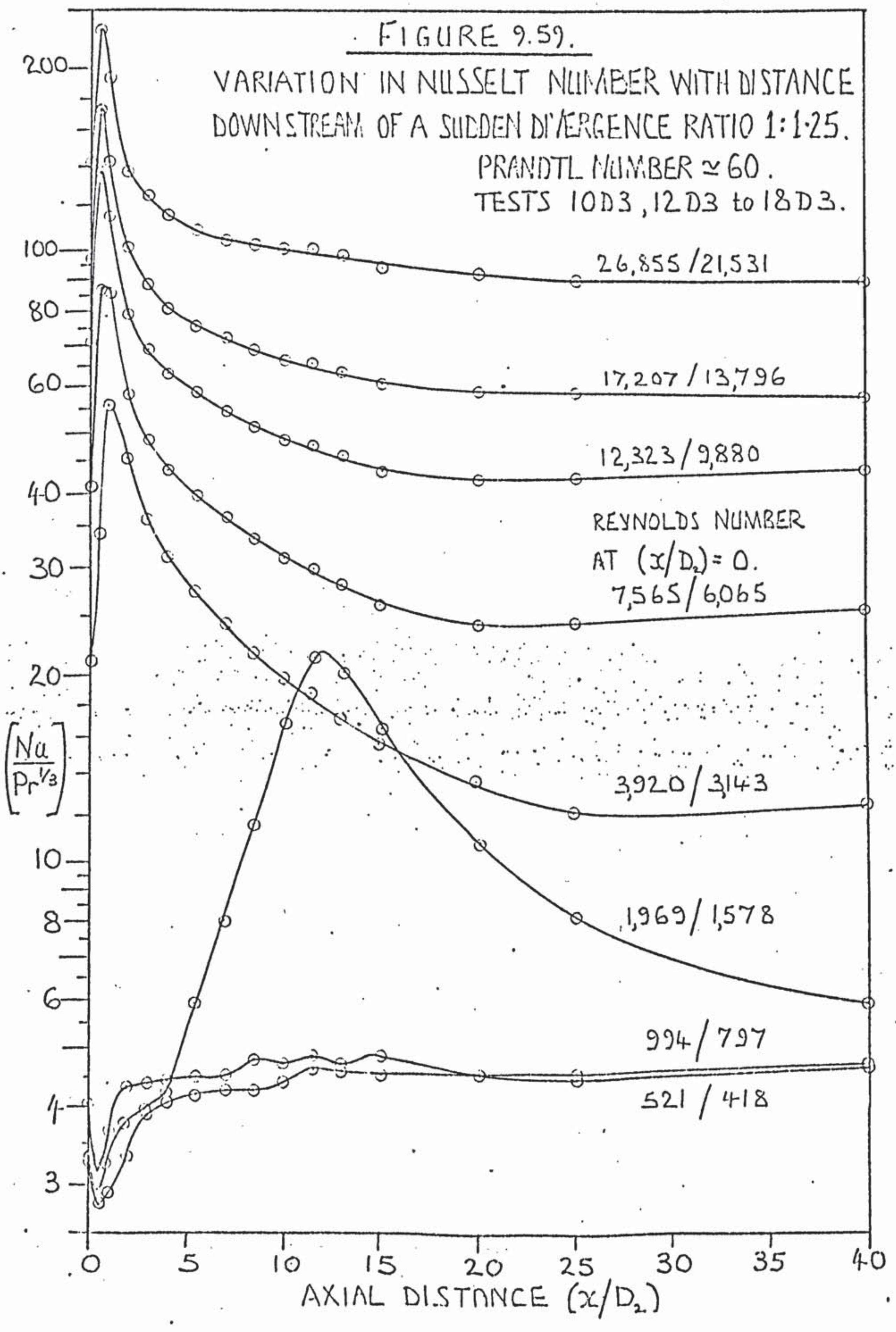

FIGURE 9.59.
VARIATION IN NUSSELT NUMBER WITH DISTANCE DOWNSTREAM OF A SUDDEN DIVERGENCE RATIO 1:1·25.
PRANDTL NUMBER ≃ 60.
TESTS 10D3, 12D3 to 18D3.
26,855/21,531
17,207/13,796
12,323/9,880
REYNOLDS NUMBER AT (x/D₂) = 0.
7,565/6,065
3,920/3,143
1,969/1,578
994/797
521/418
200
100
80
60
40
30
20
10
8
6
4
3
[Nu/Pr^1/3]
0
5
10
15
20
25
30
35
40
AXIAL DISTANCE (x/D₂)

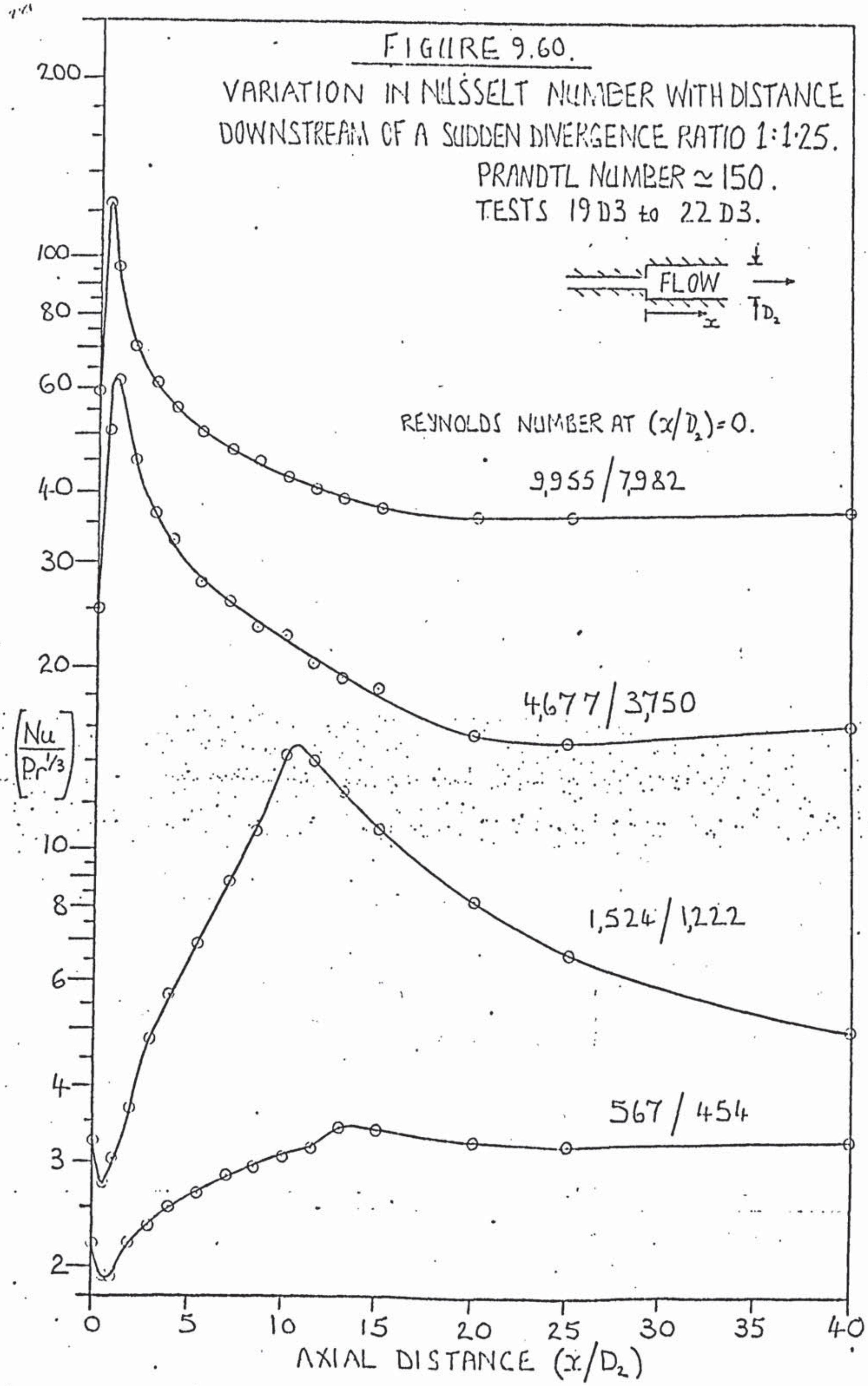

FIGURE 9.60.

VARIATION IN NUSSELT NUMBER WITH DISTANCE DOWNSTREAM OF A SUDDEN DIVERGENCE RATIO 1:1·25.

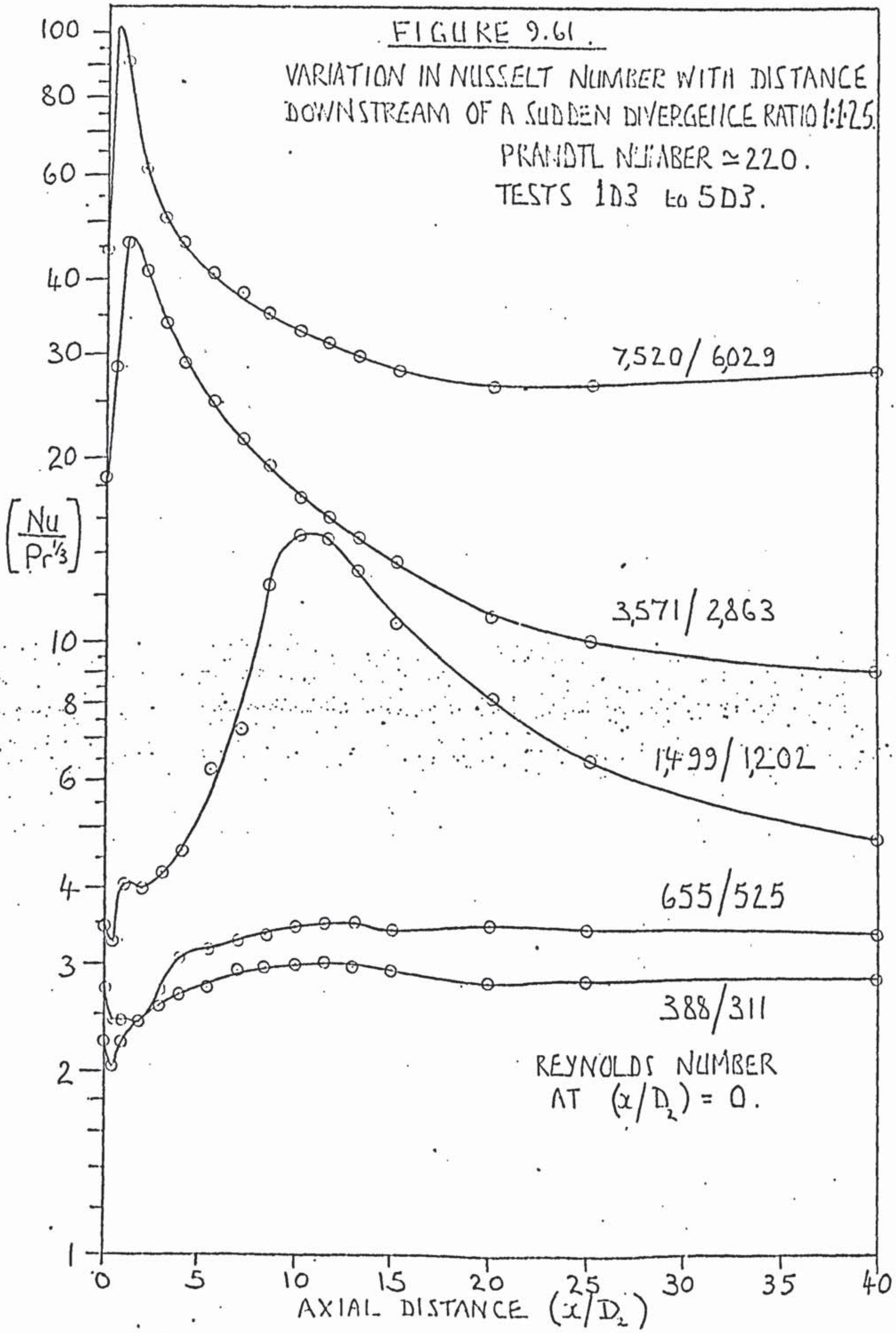

FIGURE 9.61.
VARIATION IN NUSSELT NUMBER WITH DISTANCE DOWNSTREAM OF A SUDDEN DIVERGENCE RATIO 1:1·25.
PRANDTL NUMBER ≃ 220.
TESTS 1D3 to 5D3.
7,520/6,029
3,571/2,863
1,499/1,202
655/525
388/311
REYNOLDS NUMBER AT (x/D2) = 0.
[Nu/Pr^1/3]
100
80
60
40
30
20
10
8
6
4
3
2
1
0
5
10
15
20
25
30
35
40
AXIAL DISTANCE (x/D2)

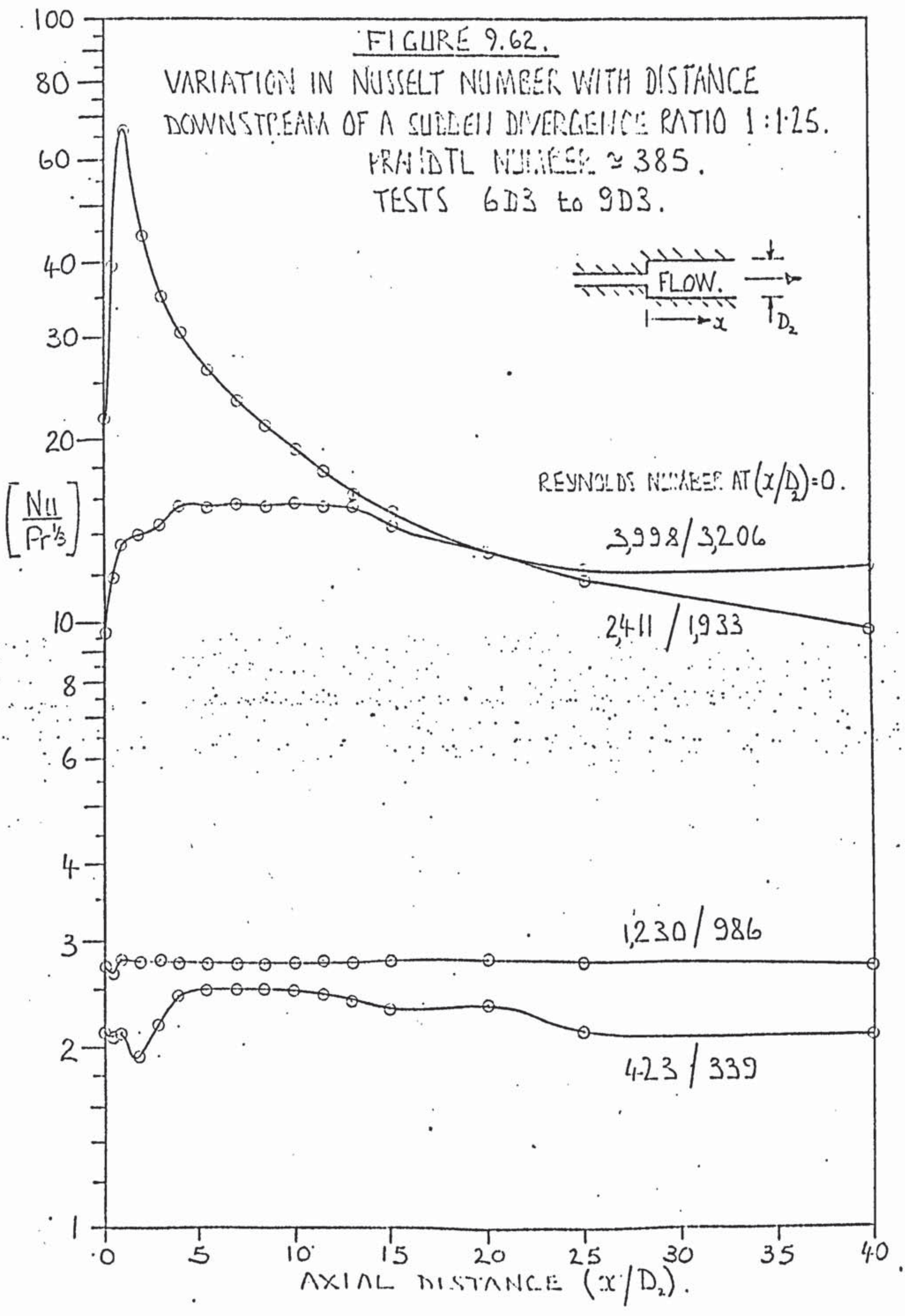

FIGURE 9.62.
VARIATION IN NUSSELT NUMBER WITH DISTANCE DOWNSTREAM OF A SUDDEN DIVERGENCE RATIO 1:1·25.
PRANDTL NUMBER ≃ 385.
TESTS 6D3 to 9D3.
FLOW.
x
D_2
REYNOLDS NUMBER AT $(x/D_2)=0$.
3,998/3,206
2,411/1,933
1,230/986
423/339
$\left[\frac{Nu}{Pr^{1/3}}\right]$
100
80
60
40
30
20
10
8
6
4
3
2
1
0
5
10
15
20
25
30
35
40
AXIAL DISTANCE (x/D_2).

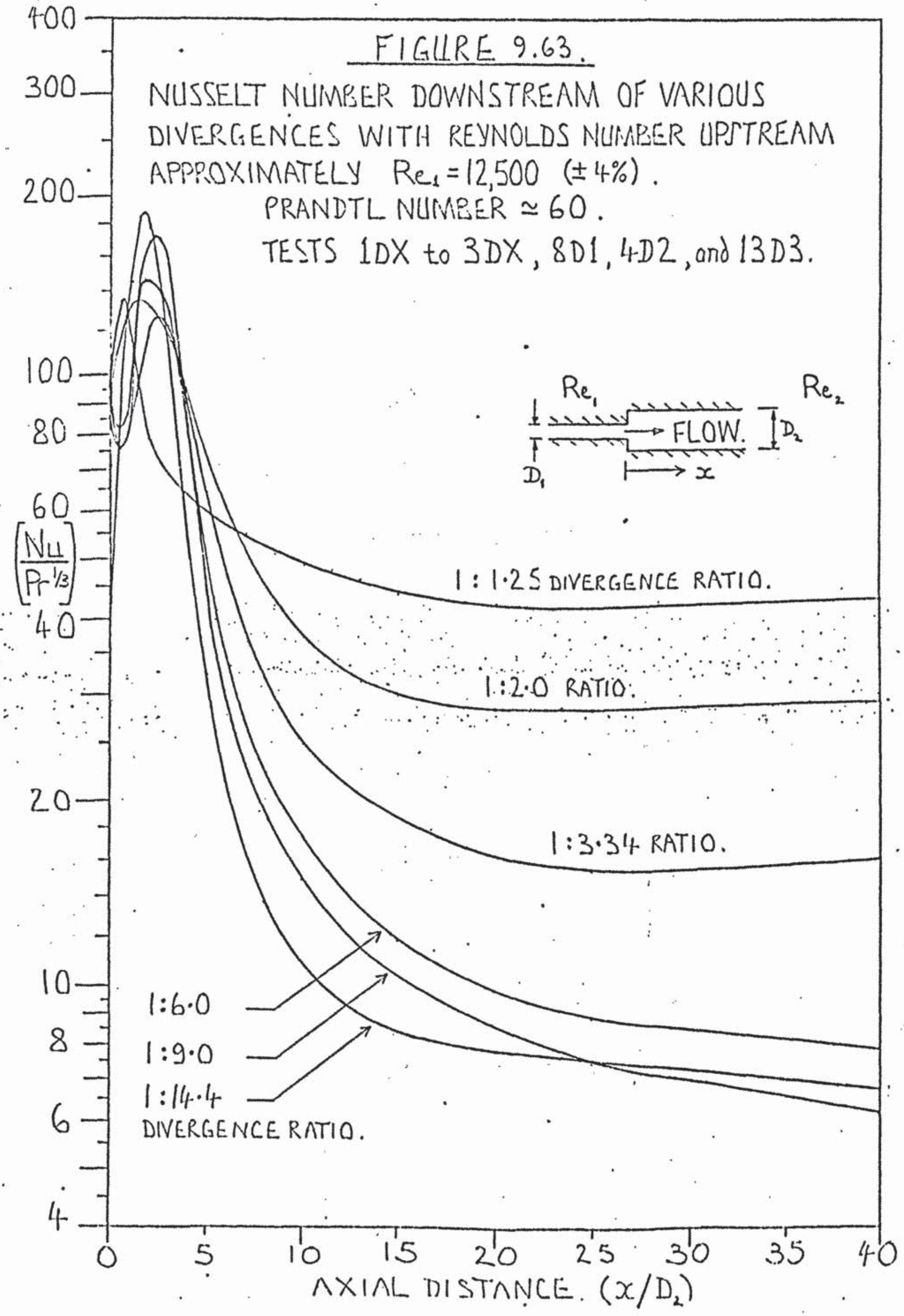
FIGURE 9.63.
NUSSELT NUMBER DOWNSTREAM OF VARIOUS DIVERGENCES WITH REYNOLDS NUMBER UPSTREAM APPROXIMATELY Re₁ = 12,500 (± 4%).
PRANDTL NUMBER ≃ 60.
TESTS 1DX to 3DX, 8D1, 4D2, and 13D3.
Re₁
Re₂
FLOW.
D₁
D₂
x
1:1·25 DIVERGENCE RATIO.
1:2·0 RATIO.
1:3·34 RATIO.
1:6·0
1:9·0
1:14·4
DIVERGENCE RATIO.
[Nu/Pr^1/3]
400
300
200
100
80
60
40
20
10
8
6
4
0
5
10
15
20
25
30
35
40
AXIAL DISTANCE. (x/D₂)

FIGURE 9.64.

MAXIMUM LOCAL VALUE OF $(Nu/Pr^{1/3})$ VERSUS DIAMETER RATIO OF DIVERGENCE. REYNOLDS NUMBER UPSTREAM APPROXIMATELY 12,500. PRANDTL NUMBER ≃ 60.

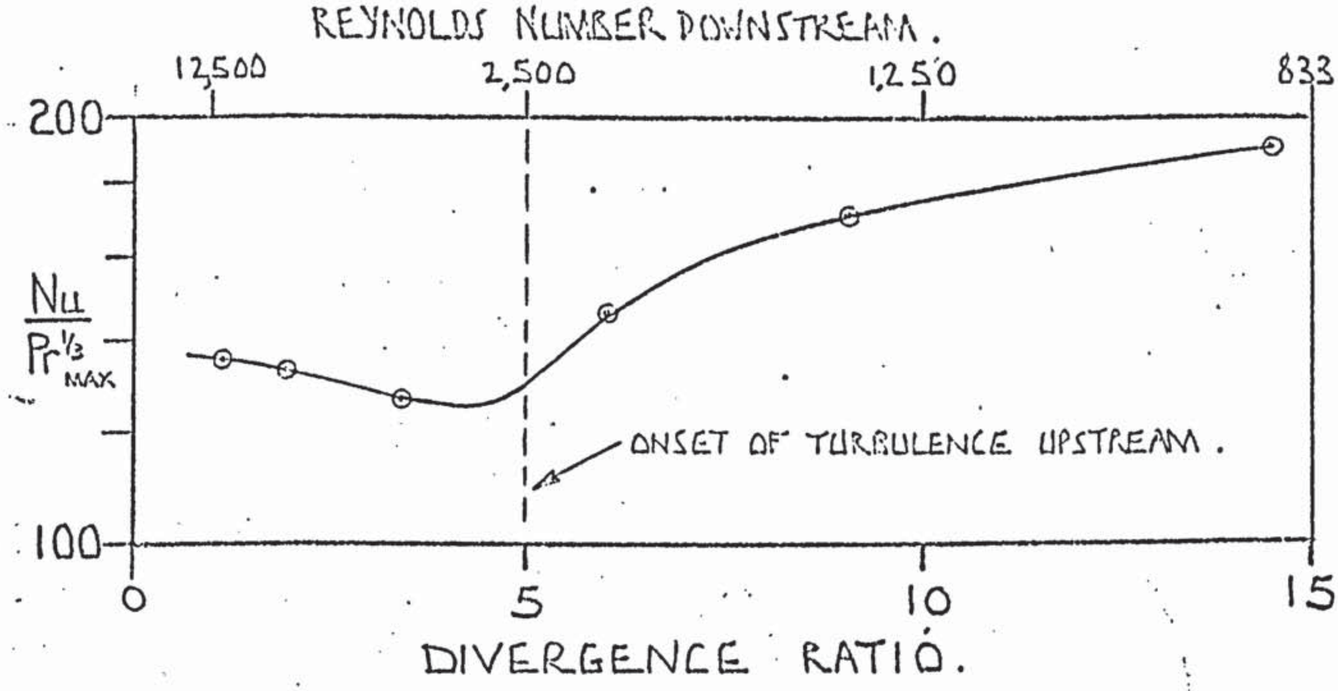

DISTANCE (x/D_2) DOWNSTREAM OF DIVERGENCE TO POSITION OF MAXIMUM VALUE OF $(Nu/Pr^{1/3})$.

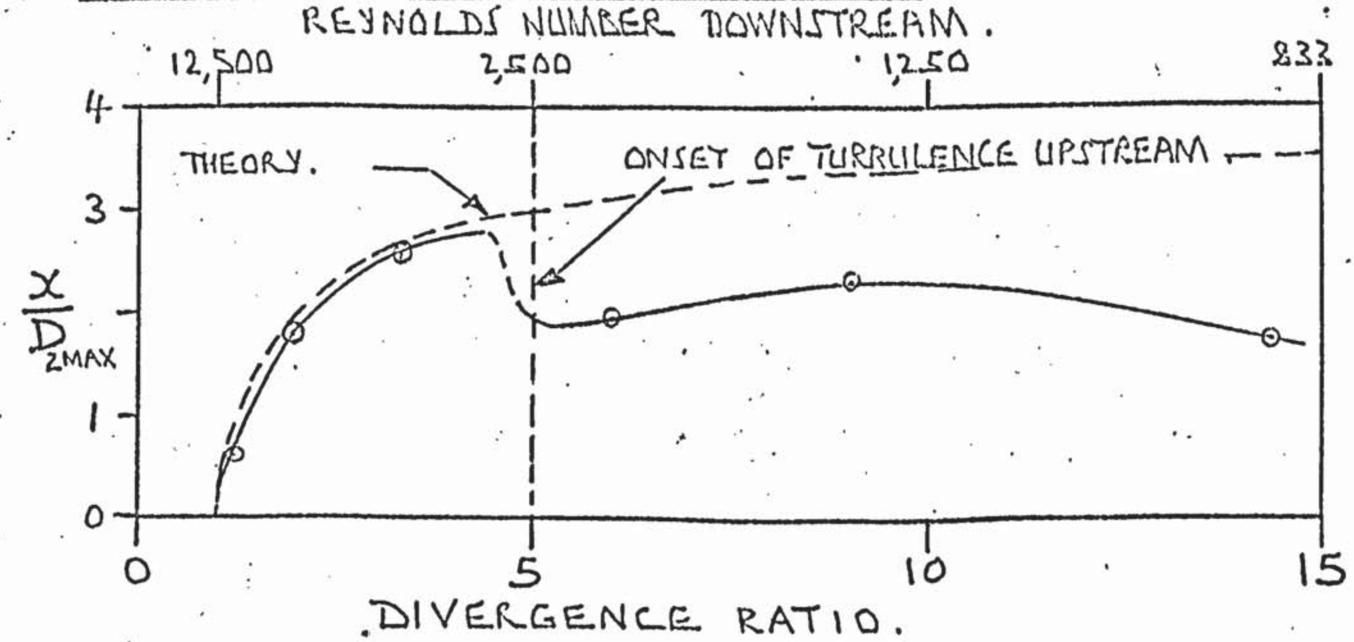

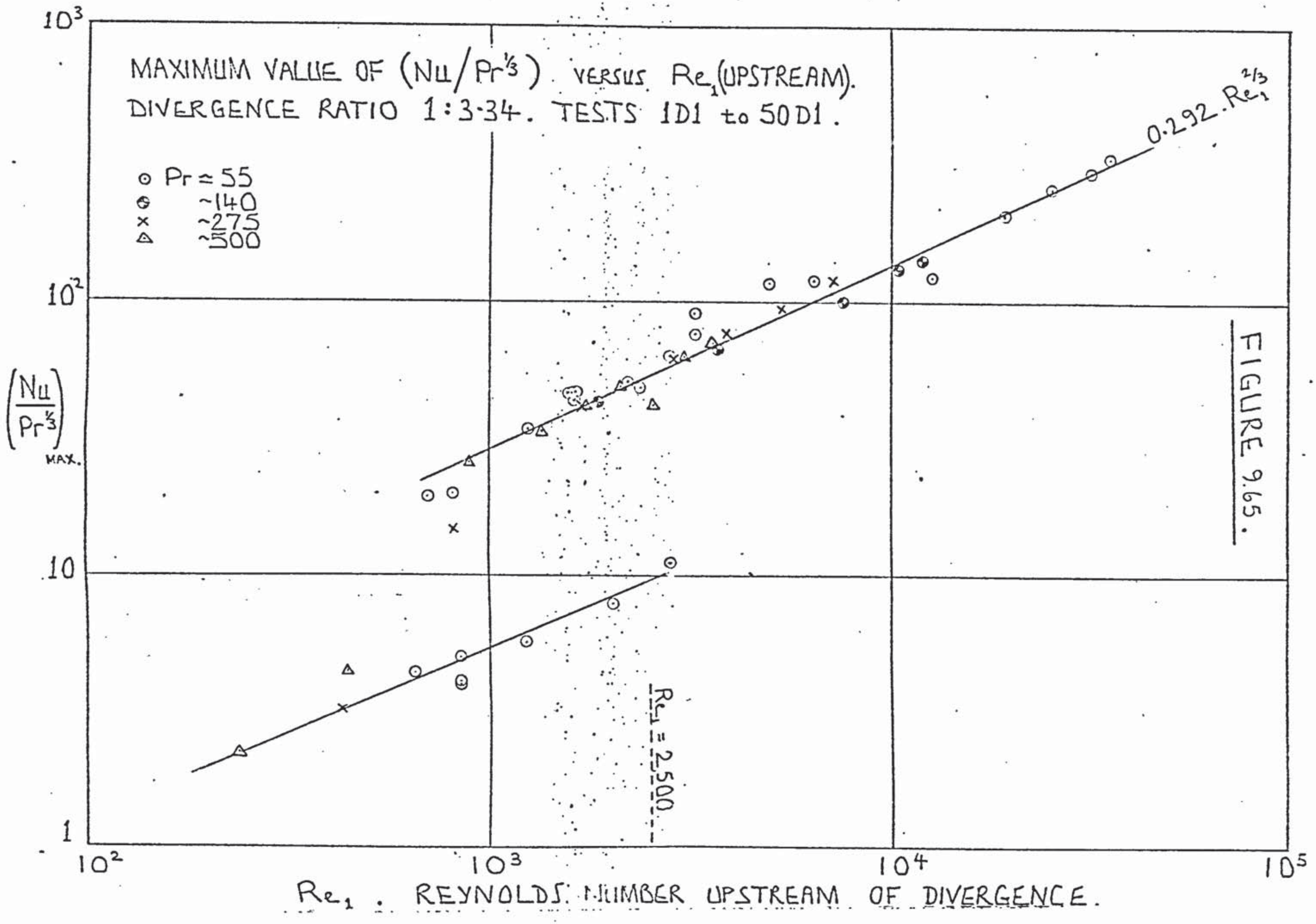
MAXIMUM VALUE OF $(Nu/Pr^{1/3})$ VERSUS Re_1(UPSTREAM).
DIVERGENCE RATIO 1:3·34. TESTS 1D1 to 50D1.
$Pr \simeq 55$
~140
~275
~500
$0.292 . Re_1^{2/3}$
$Re_1 = 2,500$
$\left(\frac{Nu}{Pr^{1/3}}\right)_{MAX.}$
10^3
10^2
10
1
10^2
10^3
10^4
10^5
Re_1 . REYNOLDS NUMBER UPSTREAM OF DIVERGENCE.

FIGURE 9.65.

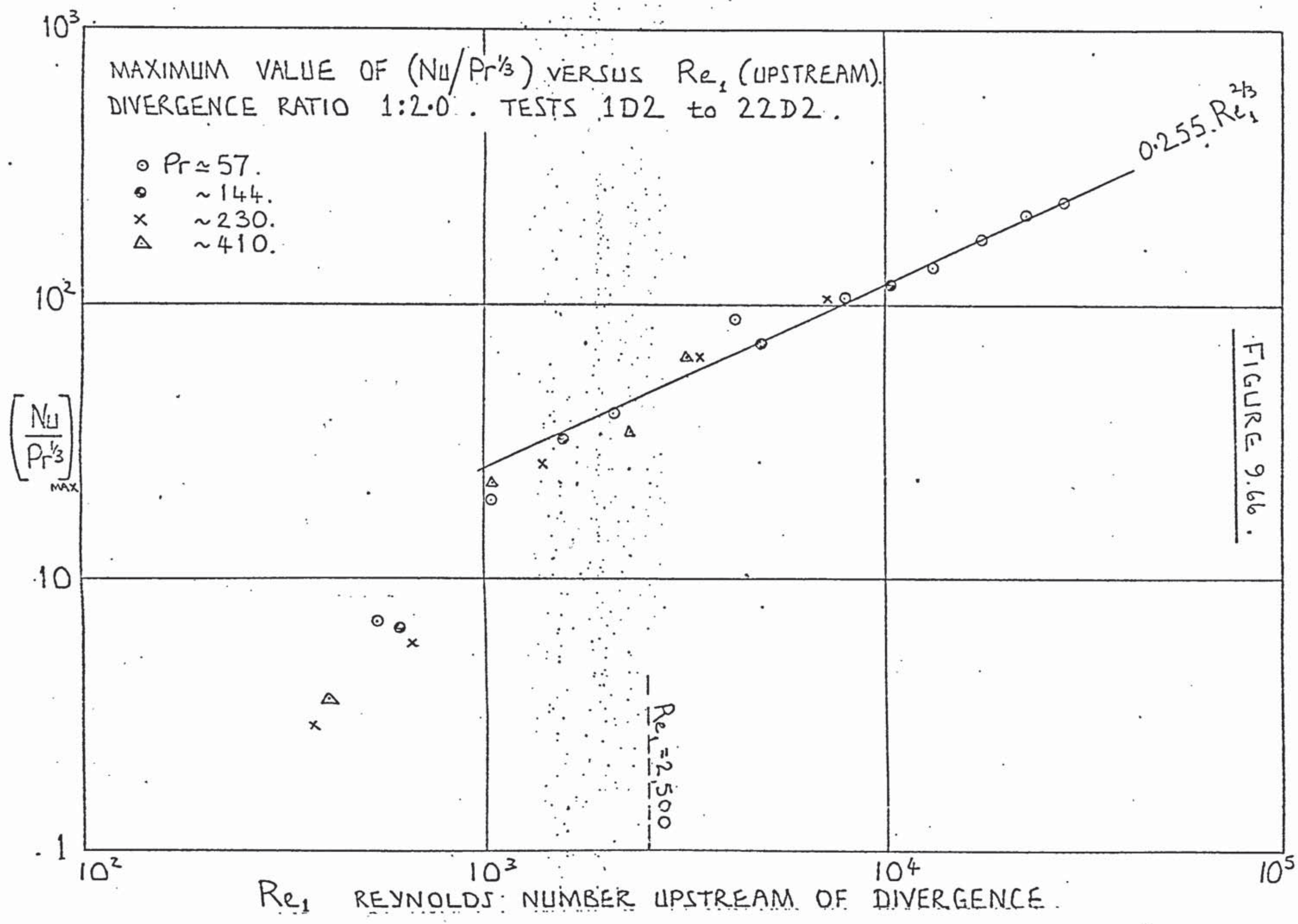

MAXIMUM VALUE OF $(Nu/Pr^{1/3})$ VERSUS Re_1 (UPSTREAM).
DIVERGENCE RATIO 1:2·0 . TESTS 1D2 to 22D2 .
⊙ $Pr \simeq 57$.
~144.
× ~230.
△ ~410.
$0{\cdot}255.Re_1^{2/3}$
$Re_1 = 2{,}500$
$\left[\frac{Nu}{Pr^{1/3}}\right]_{MAX}$
10^3
10^2
10
1
10^2
10^3
10^4
10^5
Re_1 REYNOLDS NUMBER UPSTREAM OF DIVERGENCE

FIGURE 9.66.

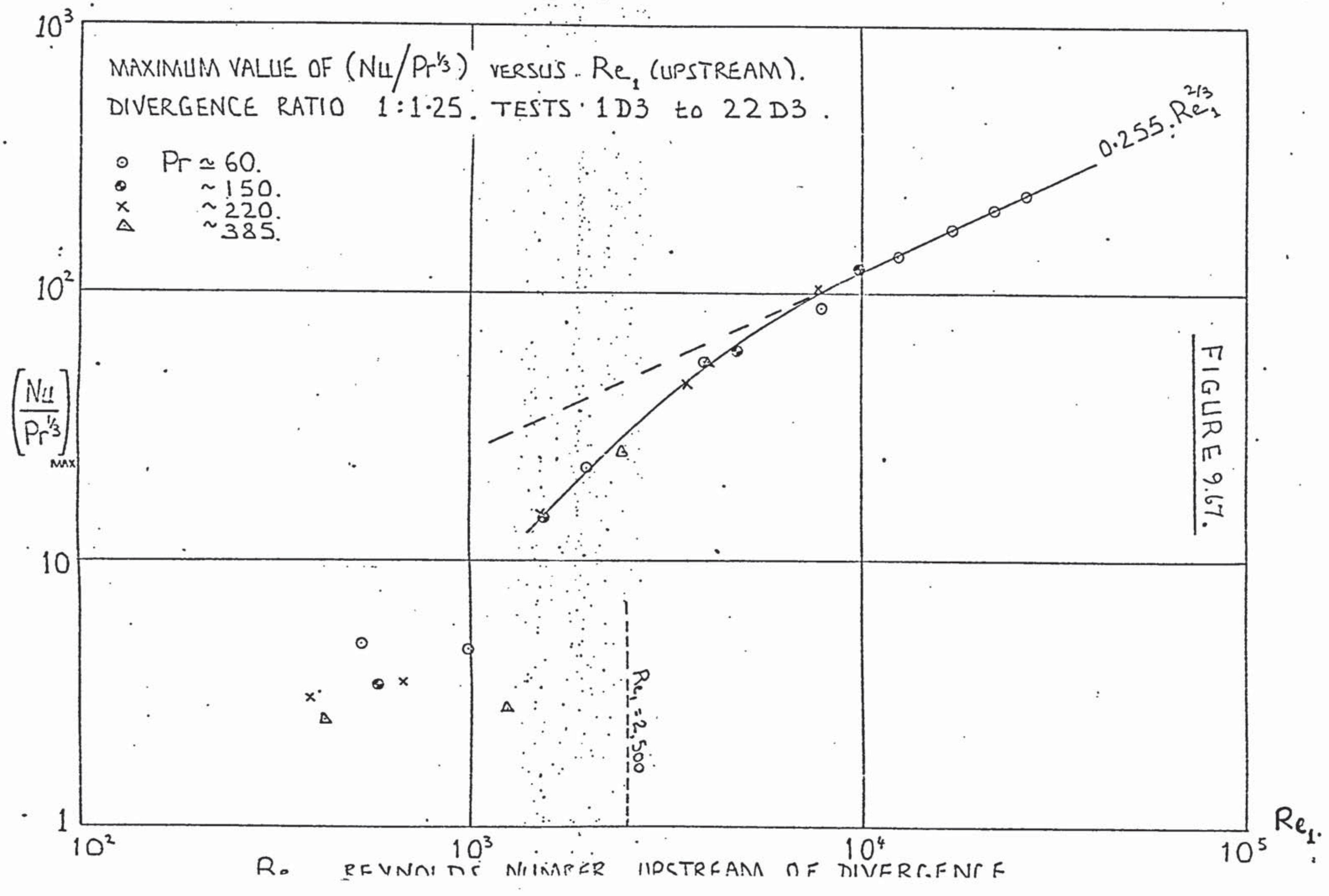
MAXIMUM VALUE OF (Nu/Pr^1/3) VERSUS Re1 (UPSTREAM).
DIVERGENCE RATIO 1:1·25. TESTS 1D3 to 22D3.
Pr ≃ 60.
~150.
~220.
~385.
0·255. Re1^2/3
Re1 = 2,500
(Nu/Pr^1/3)MAX
10^3
10^2
10
1
10^2
10^3
10^4
10^5
Re1.
Re REYNOLDS NUMBER UPSTREAM OF DIVERGENCE

FIGURE 9.67.

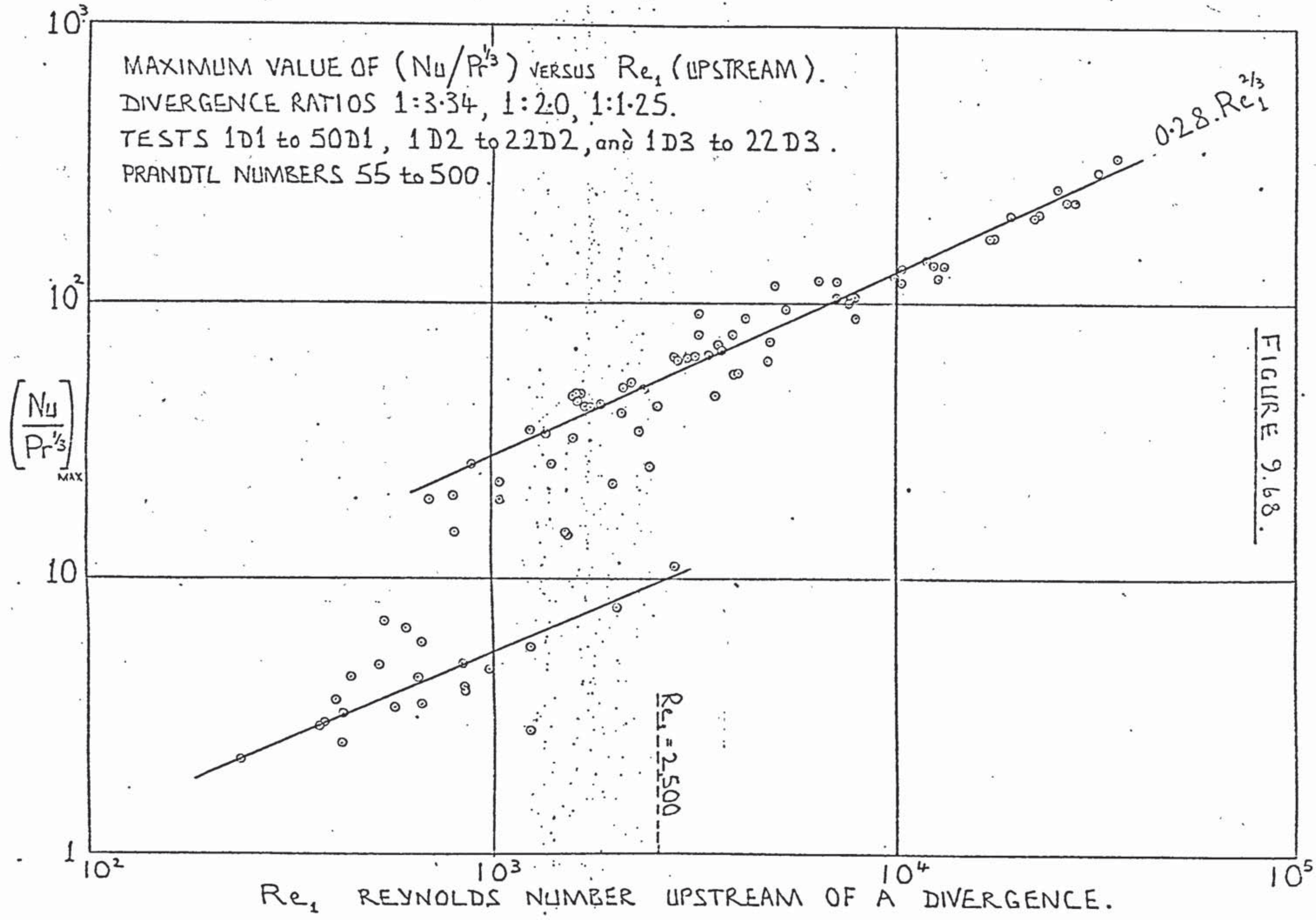
MAXIMUM VALUE OF $(Nu/Pr^{1/3})$ VERSUS Re_1 (UPSTREAM).
DIVERGENCE RATIOS 1:3·34, 1:2·0, 1:1·25.
TESTS 1D1 to 50D1, 1D2 to 22D2, and 1D3 to 22D3.
PRANDTL NUMBERS 55 to 500.
$0{\cdot}28.Re_1^{2/3}$
FIGURE 9.68.
$Re_1 = 2{,}500$
$\left[\frac{Nu}{Pr^{1/3}}\right]_{MAX}$
10^3
10^2
10
1
10^2
10^3
10^4
10^5
Re_1 REYNOLDS NUMBER UPSTREAM OF A DIVERGENCE.

10. COMPARISON OF RESULTS WITH PREVIOUS WORK.

10.1. THE SHORT TUBE.

For the laminar regime, none of the publications discussed in part 3 contained experimental data which could be compared with the results of these investigations. With the fully developed flow arrangement, the theoretical results of Sellars (Ref: C.13) were used for this purpose, and the experimental values of Nu (or Nu') were first corrected for variations in viscosity, and the contribution of free convection as discussed in part 9. The 'smoothed' experimental data was interpolated to suitable values of Re. Figure 10.1 shows this comparison between experiment and theory. The experimental values of Nu' were mostly between 2% and 10% less than the theoretical estimate, but in the first few diameters downstream the experimental data was a maximum of 20% less. The influence of conduction in the tube wall has been demonstrated to have a significant effect on measurements made in the first few diameters, and this could account for the more severe differences between the two cases. It is considered that the agreement is fairly good for the remainder of the data.*

With the bellmouth fitted, the experimental results obtained for $Pr \simeq 91$ can be compared with the theoretical results of Roy (Ref: C.12), who considered the effects of developing flow with $Pr = 100$. Figure 10.2 shows this comparison, and it is evident that the experimental and theoretical values of Nu' were in good agreement. The disparity between the two cases could be expressed as a maximum of $\pm$ 7% deviation in Nu'.+

In the transitional and turbulent flow regimes few data were available for comparison. Figure 10.3 shows the results of Hartnett (Ref: B.2), for an electrically heated tube with a calming length; the fluid was oil. The experimental work discussed in this thesis showed markedly lower heat-transfer coefficients near to the start of heating. No satisfactory explanation of this could be found. The theoretical work described in part 11 (see figure 11.18) and the analysis of Diessler (Ref: C.2) - summarised in figure 10.4 - tends to confirm the findings of this work in preference to those of Hartnett, and indicates that the substantially higher values of h reported by Hartnett for the entrance region are probably misleading.

With undeveloped transitional or turbulent flow at the inlet, no alternative source of Nu for the entrance-region could be found in which the worker had used a viscous liquid. Mills provided some data for Reynolds numbers in excess of 10,000 where the fluid considered was air. Figure 3.6 shows the distribution of h near the inlet of the tube. Comparing the case of Re - 10,000 it was evident, from figure 9.24, that the location of the minimum in the 'dip' region was different. The minimum value of h for air occurred much further downstream than with viscous liquid. No reasonable basis for comparison was possible.

* The results of a recent paper by Martin (Ref: J.14), incorporating both experimental and analytical work (on similar short-tube configurations to those discussed herein) compare more favourably with the results of this author than do the previous comparisons made with data from Sellars and Roy (See Figs: 10.1 & 10.2.)

10.2. THE CONVERGENCE.

A direct comparison was possible between the experimental coefficients of heat-transfer and those of Ede (Ref: H.1) for the convergence system. The fluid used by Ede was water, and it was to be expected that some differences might occur between the results as a consequence of the higher Prandtl numbers covered in these tests.

A comparison for the 2:1 convergence ratio is shown in figures 10.5 to 10.7. At the higher Reynolds numbers good agreement was evident when (h/h_{∞}) was plotted versus axial distance (fig: 10.5), this was generally the case for fully turbulent flow downstream ($Re_2 > 10,000$). As Re_2 was reduced to the laminar level ($Re_2 \precsim 2,500$) considerable disagreement between the two sets of data occurred. Severe differences were apparent when Re_2 was laminar rather than transitional (Re_2 = 2,500 to 10,000). The discussion in part 9 indicated that the shape of the $(Nu/Pr^{\frac{1}{3}})$ - distance functions was strongly dependent on Pr at low Reynolds numbers, for the tests carried out. This was not unexpected since the theoretical analysis in part 11 (which discusses separation and divergence systems) showed that in flows embodying a region of boundary-layer separation, the distribution of temperature in the fluid can vary considerably with changes in Pr.

10.3. THE DIVERGENCE.

The measured distribution of h in the region of a sudden divergence was compared directly with the data presented by Ede (Ref: H.1), for heat-transfer to water. Figures 10.8 to 10.10 show the axial variation in (h/h_o). With fully turbulent flow ($Re_2 > 10,000$) the results for water compared favourably with those for glycol. Figures 10.8 and 10.9 give data for the 1:3.3 and 1:1.25 diameter ratios. It was concluded generally from the analysis of the test results (part 9) that the shape of the $(Nu/Pr^{\frac{1}{3}})$ - distance functions was invariant with Pr. This is consistent with the preceding comparisón.

Figure 10.10 shows that, for the 1:2 divergence, substantial differences between the results of Ede and the present test data were apparent at low Reynolds numbers (of the order 1,000 downstream). It was extremely difficult to make any reasonable comparison between the values of h obtained from different sources where Re was small. The complex nature of the flow pattern and its dependence on the heat-flux (as discussed in part 9.) make it virtually impossible at this moment in time, to arrive at a unique function which can be used to define h. All that can be said is that the shape of both graphs in figure 10.10 are in qualitative agreement.

FIGURE 10.1.

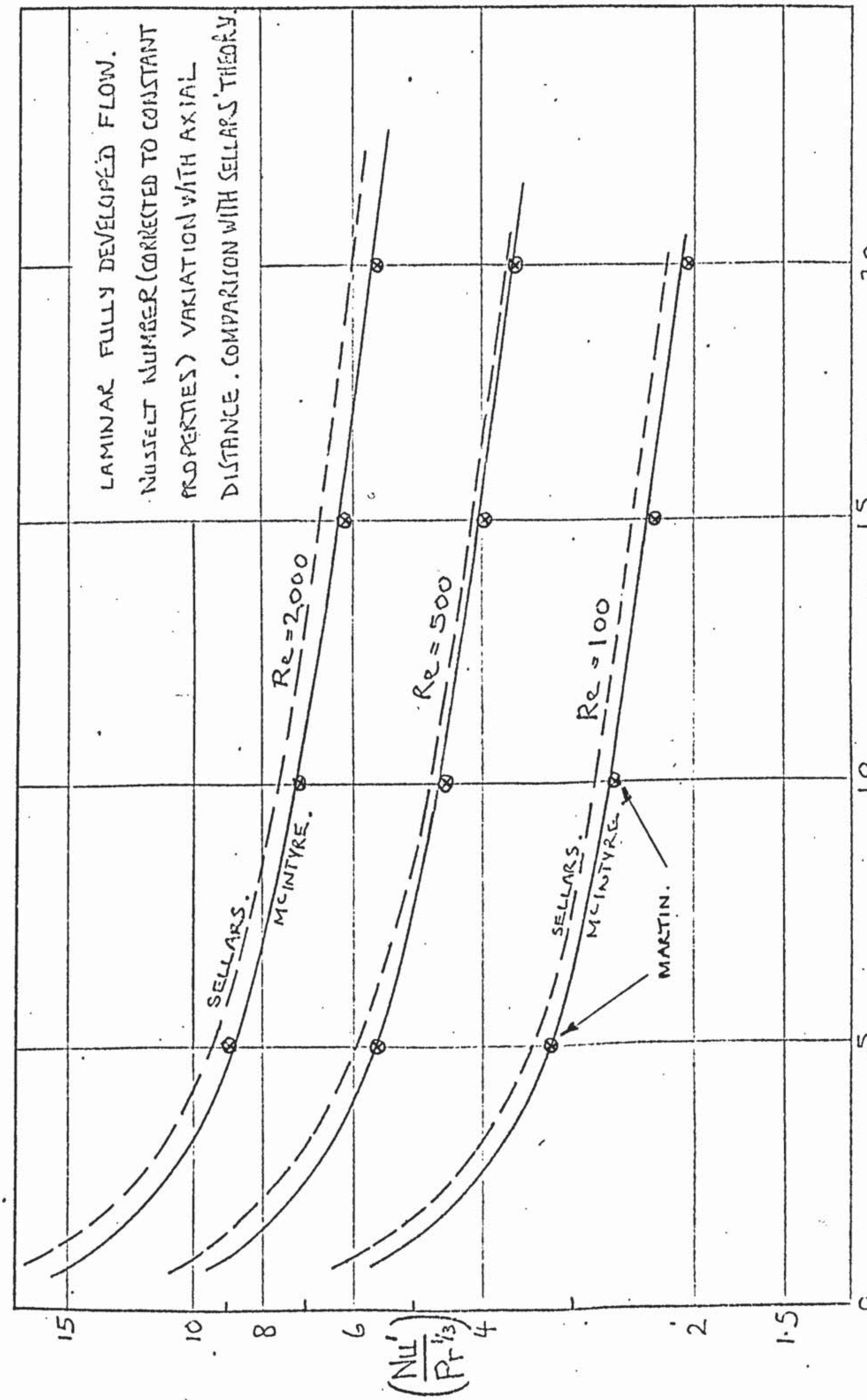
LAMINAR FULLY DEVELOPED FLOW.
NUSSELT NUMBER (CORRECTED TO CONSTANT PROPERTIES) VARIATION WITH AXIAL DISTANCE. COMPARISON WITH SELLARS' THEORY.
Re = 2,000
Re = 500
Re = 100
SELLARS.
McINTYRE.
SELLARS.
McINTYRE.
MARTIN.
0
5
10
15
20
AXIAL DISTANCE (DIAMETERS).
15
10
8
6
4
2
1.5
$\left(\frac{Nu'}{Pr^{1/3}}\right)$

FIGURE 10.2.

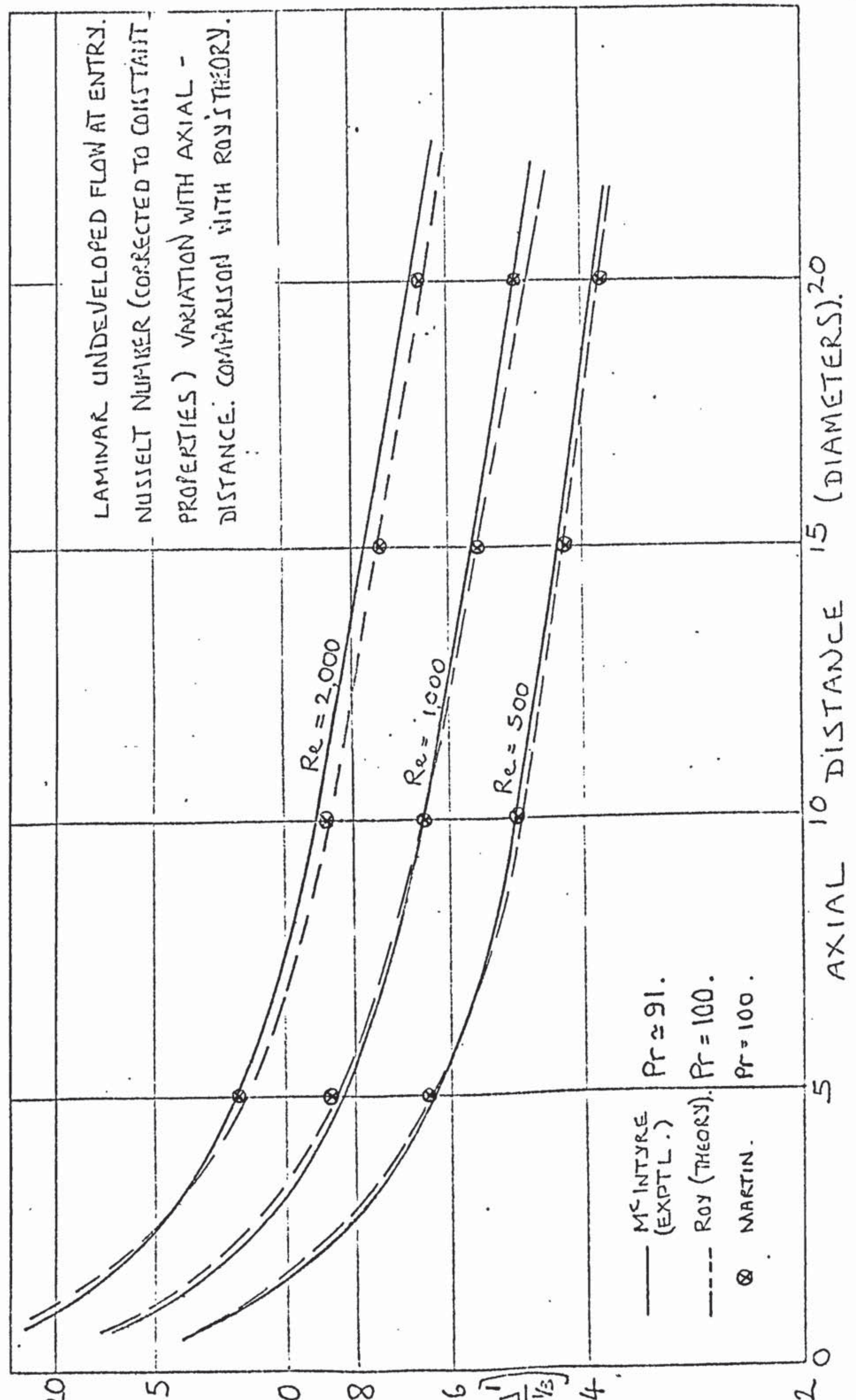
LAMINAR UNDEVELOPED FLOW AT ENTRY. NUSSELT NUMBER (CORRECTED TO CONSTANT PROPERTIES) VARIATION WITH AXIAL - DISTANCE. COMPARISON WITH ROY'S THEORY.
Re = 2,000
Re = 1,000
Re = 500
AXIAL DISTANCE (DIAMETERS).
0
5
10
15
20
20
15
10
8
6
4
2
$\left[\frac{Nu'}{Pr^{1/3}}\right]$
Mc INTYRE (EXPTL.) Pr ≃ 91.
ROY (THEORY). Pr = 100.
MARTIN. Pr = 100.

FIGURE 10.3.

COMPARISON WITH THE RESULTS OF HARTNETT. (h/h_∞) VERSUS AXIAL DISTANCE.

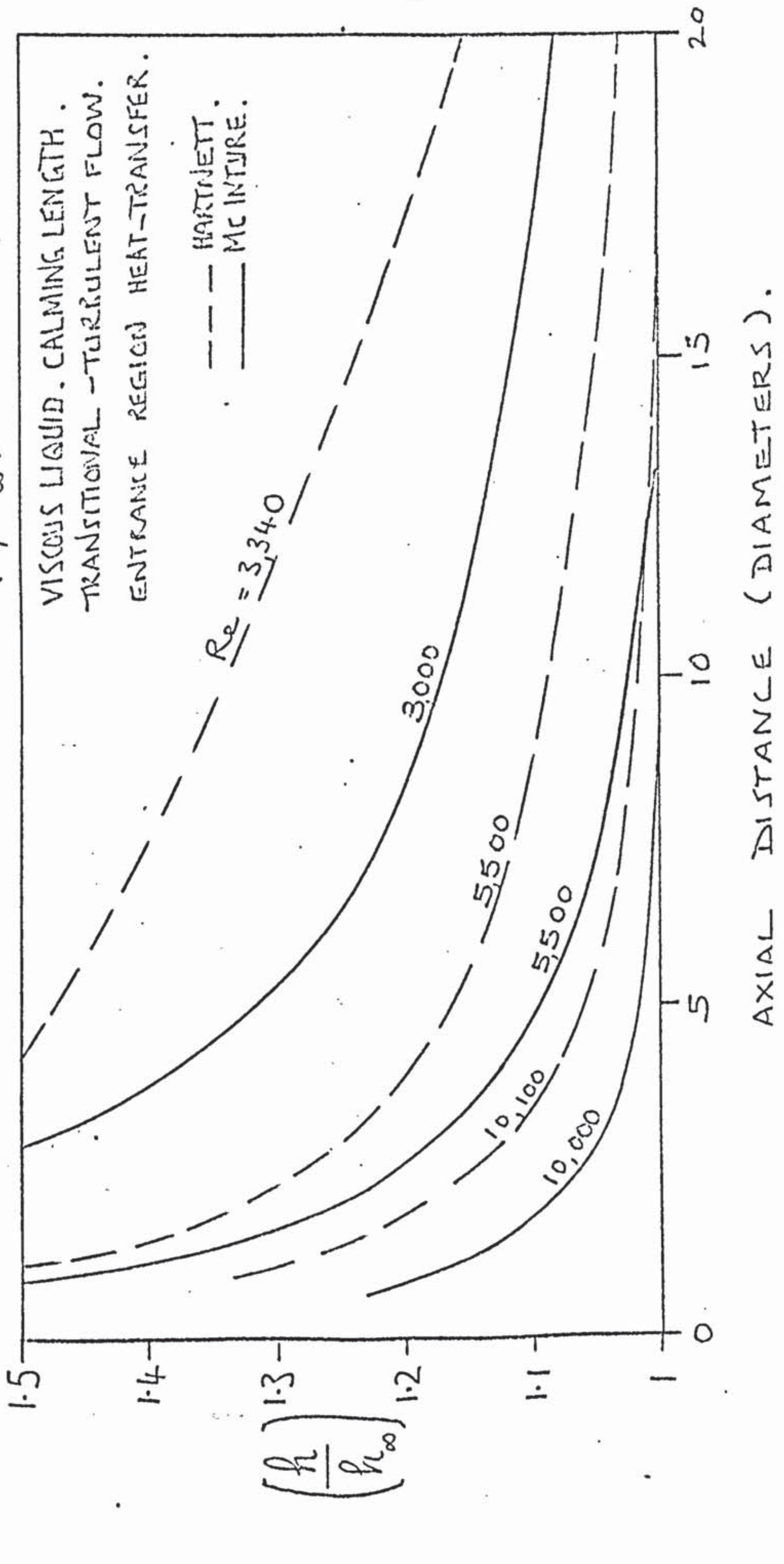

FIGURE 10.4.

THE ANALYTICAL RESULTS OF DEISSLER FOR ENTRANCE-REGION HEAT TRANSFER, TURBULENT FLOW.

Nu_d = FULLY DEVELOPED VALUE OF Nu.

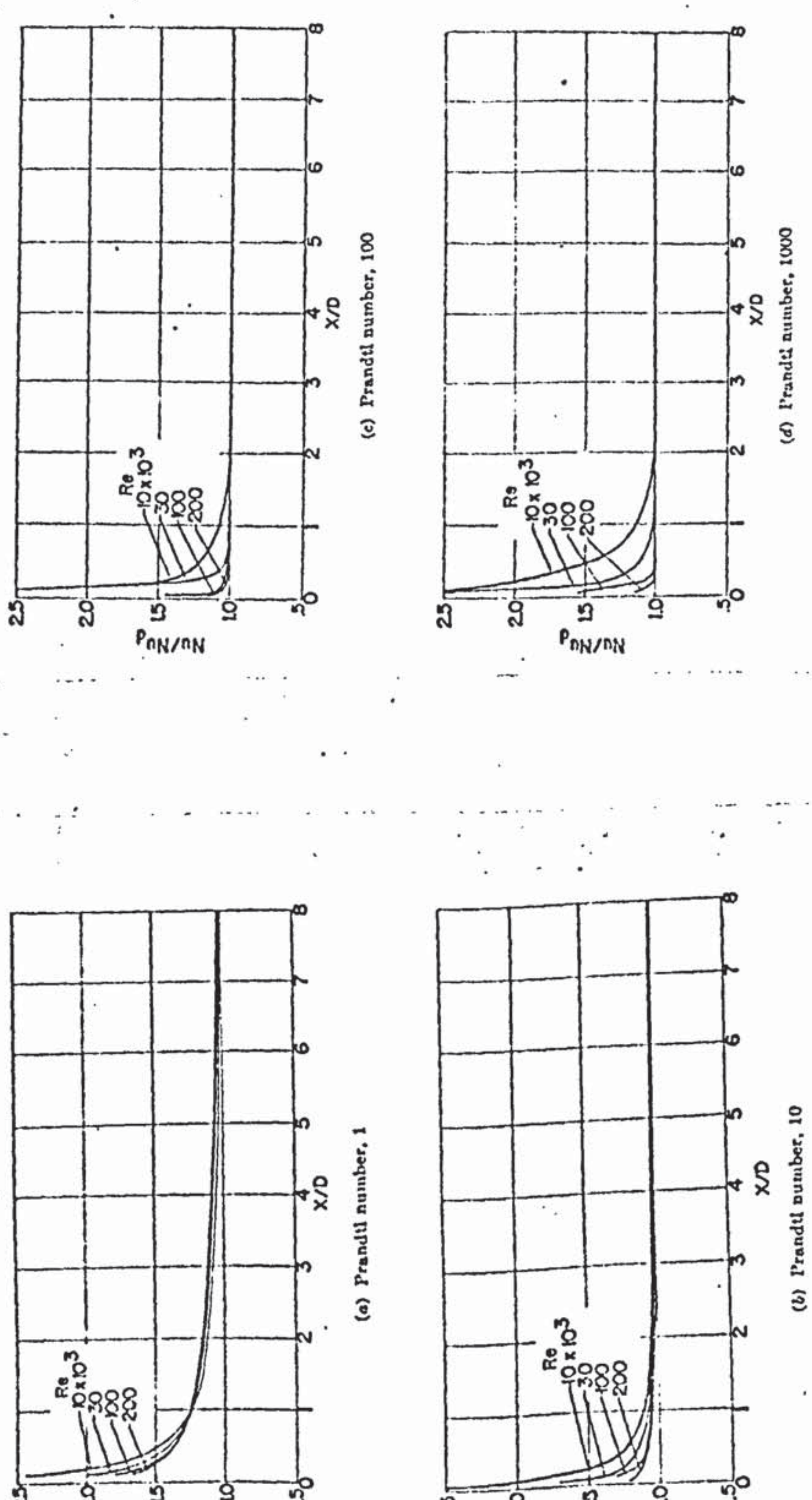

CURVES SHOWING EFFECT OF PRANDTL NUMBER ON HEAT TRANSFER IN THERMAL ENTRANCE REGION OF TUBE

(Uniform wall heat flux, uniform initial temperature distribution, fully developed velocity distribution, and constant properties.)

FIGURE 10.5

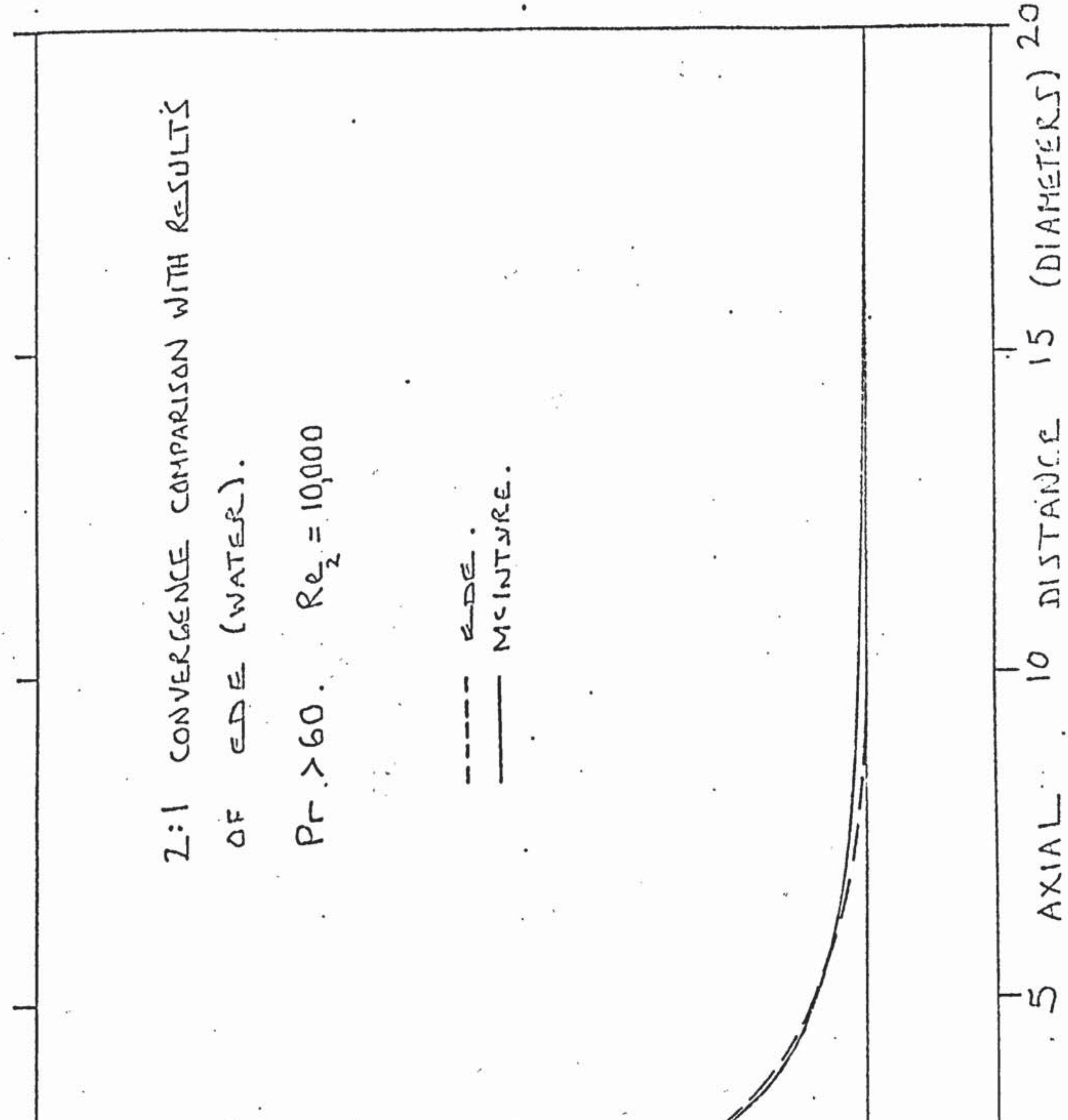
2:1 CONVERGENCE COMPARISON WITH RESULTS OF EDE (WATER).
Pr > 60. Re2 = 10,000
EDE.
McINTYRE.
AXIAL DISTANCE (DIAMETERS)
0
5
10
15
20
(h/h∞)
2
1.5
1.0
0.9
0.8

FIGURE 10.6.

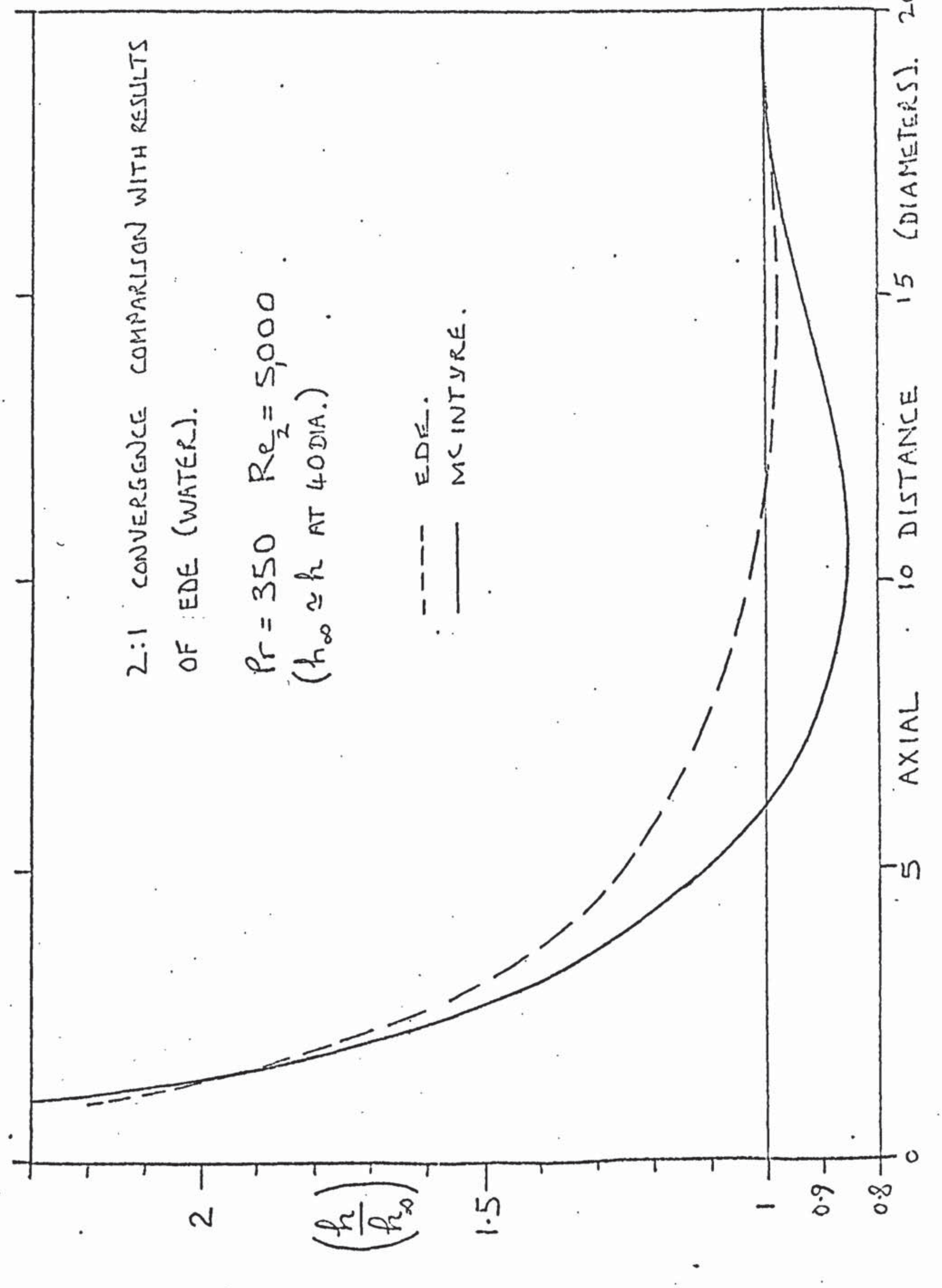
2:1 CONVERGENCE COMPARISON WITH RESULTS
OF EDE (WATER).
$Pr = 350$ $Re_2 = 5,000$
($h_\infty \simeq h$ AT 40 DIA.)
EDE.
McINTYRE.
AXIAL DISTANCE (DIAMETERS).
0
5
10
15
20
$\left(\frac{h}{h_\infty}\right)$
2
1·5
1
0·9
0·8

FIGURE 10.7.

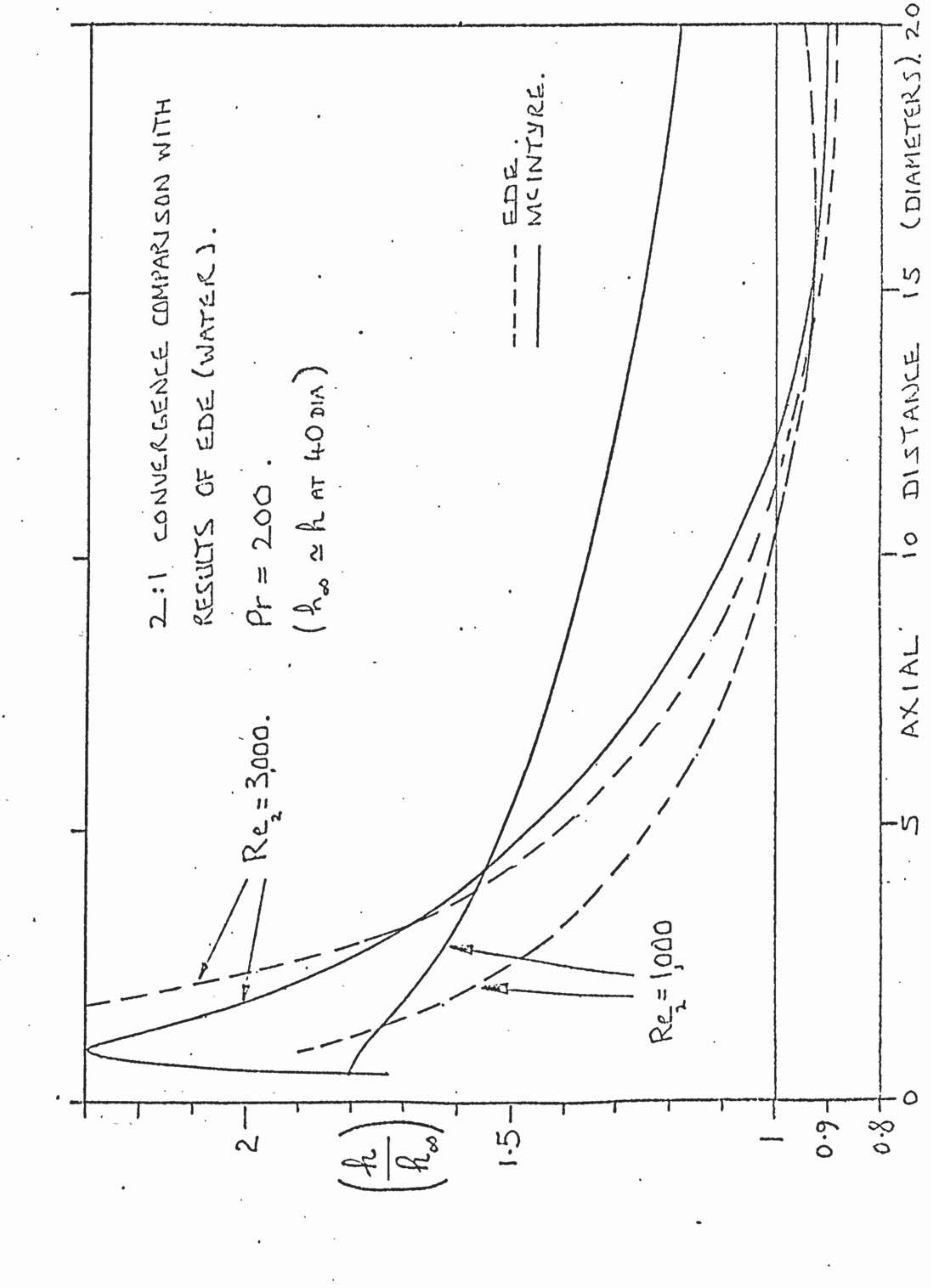

2:1 CONVERGENCE COMPARISON WITH
RESULTS OF EDE (WATER).
$Pr = 200$.
($h_\infty \simeq h$ AT 40 DIA)
EDE.
McINTYRE.
$Re_2 = 3,000$.
$Re_2 = 1,000$
AXIAL DISTANCE (DIAMETERS)
0
5
10
15
20
$\left(\frac{h}{h_\infty}\right)$
2
1.5
1
0.9
0.8

FIGURE 10.8.

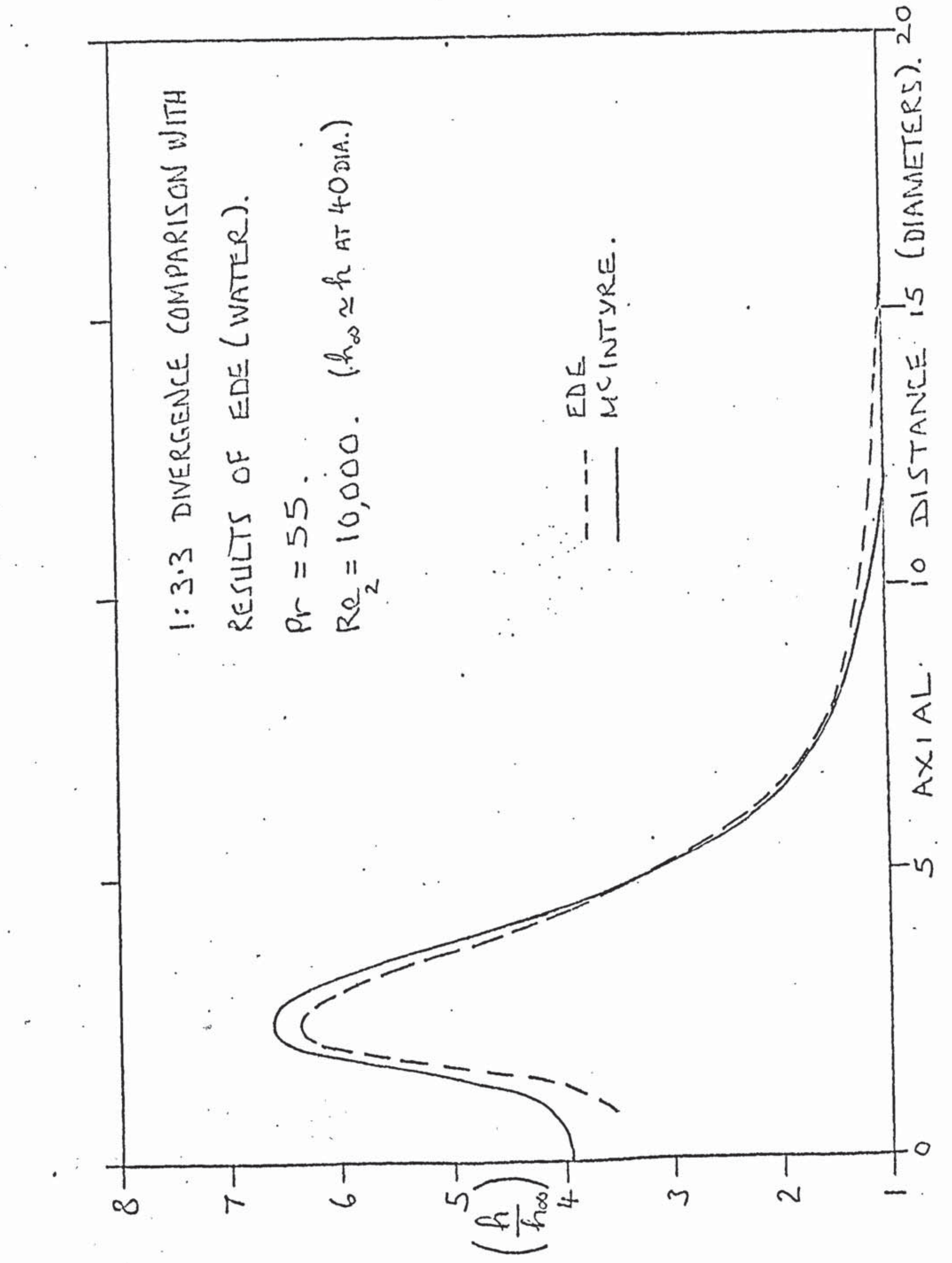

1:3·3 DIVERGENCE COMPARISON WITH
RESULTS OF EDE (WATER).
Pr = 55.
Re₂ = 10,000. ($h_\infty \simeq h$ AT 40 DIA.)
EDE
McINTYRE.
AXIAL DISTANCE (DIAMETERS).
0
5
10
15
20
$\left(\frac{h}{h_\infty}\right)$
1
2
3
4
5
6
7
8

FIGURE 10.9.

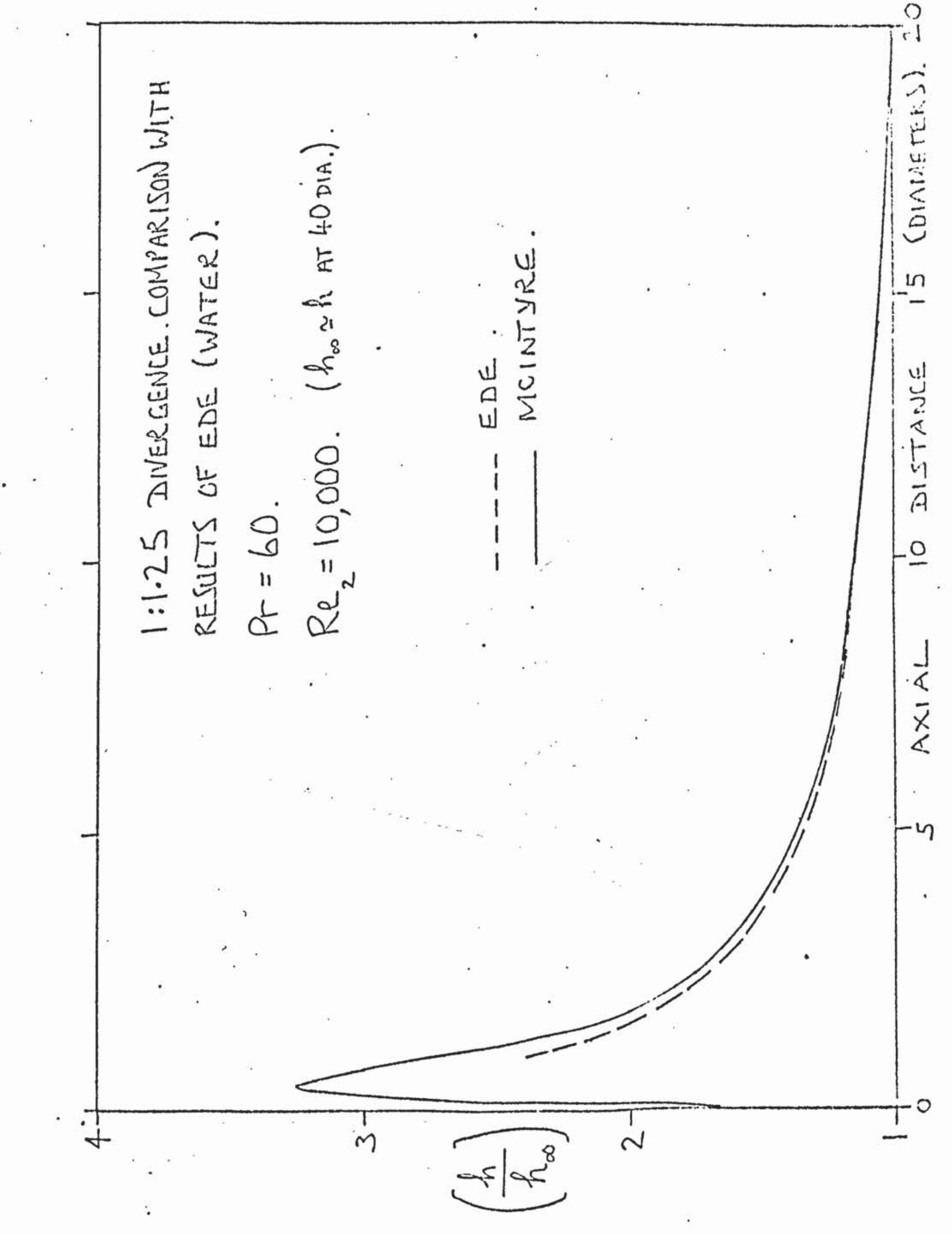

1:1·25 DIVERGENCE. COMPARISON WITH RESULTS OF EDE (WATER).
Pr = 60.
$Re_2 = 10,000$. ($h_\infty \simeq h$ AT 40 DIA.)
EDE
MCINTYRE.
AXIAL DISTANCE (DIAMETERS).
0
5
10
15
20
$\left(\frac{h}{h_\infty}\right)$
1
2
3
4

FIGURE 10.10.

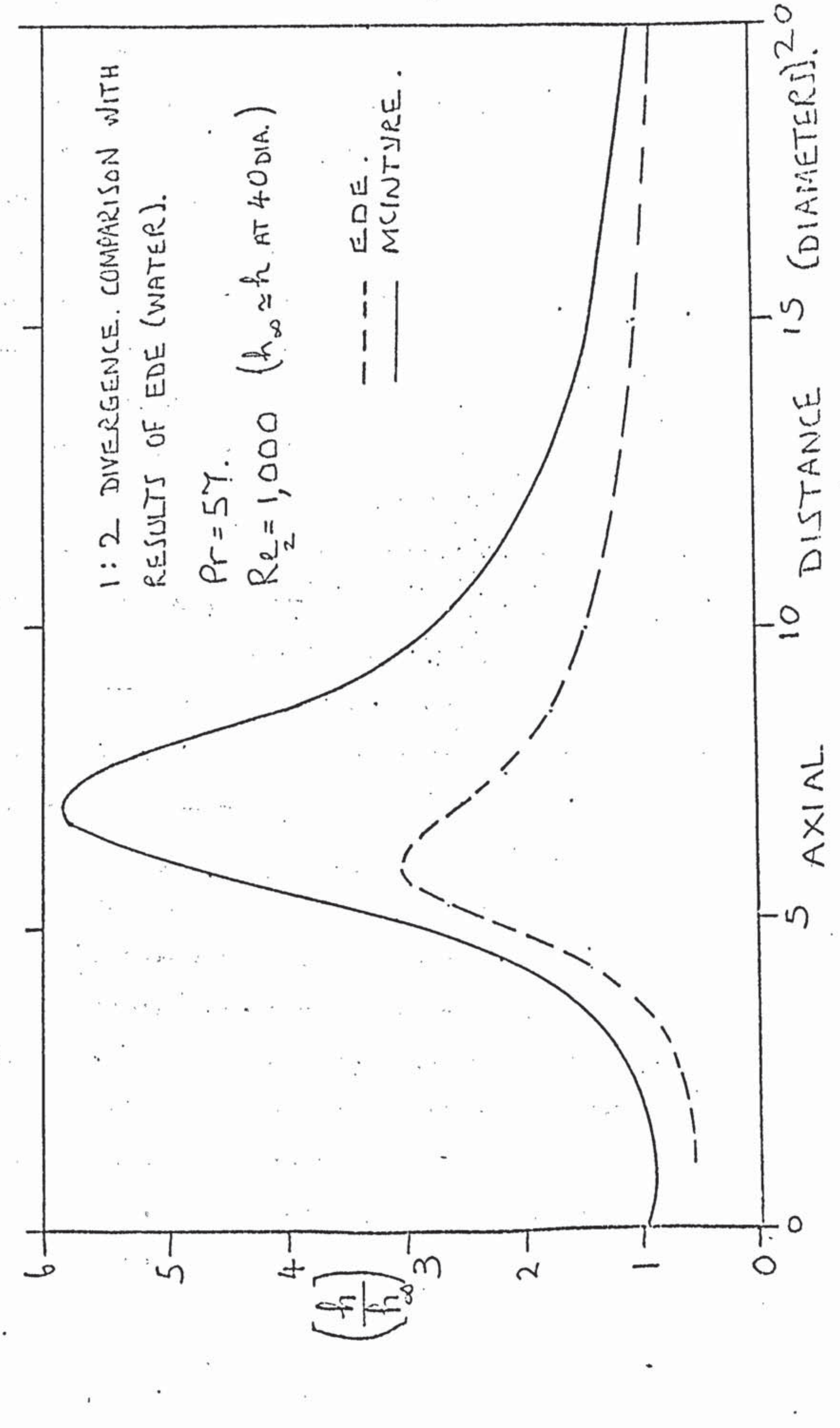

1 : 2 DIVERGENCE. COMPARISON WITH
RESULTS OF EDE (WATER).
Pr = 57.
Re_z = 1,000 (h∞ ≃ h AT 40 DIA.)
EDE.
MCINTYRE.
AXIAL DISTANCE (DIAMETERS).
0
5
10
15
20
(h/h∞)
0
1
2
3
4
5
6

11 THEORETICAL ANALYSES AND COMPARISON WITH EXPERIMENTS.

11.1 INTRODUCTION.

The reasons for carrying out the theoretical investigations discussed in part 11 can be summarised as follows: to permit a fuller appreciation of the mechanisms of heat transfer in the experimental systems, to justify the selection of certain significant variables used in correlating experimental data, to support the empirically derived coefficients of heat transfer, to help realise inherent limitations in certain results which are presented for practical use, and to derive simple formulae where possible to explain experimental behaviour.

The analyses have been combined into a single section (part 11) because the different problems considered bear close relationship to one another. In practice however the theoretical and experimental work progressed simultaneously, and reference to the theoretical findings is made throughout the thesis whenever appropriate, (as mentioned in the Preface).

Initially, heat transfer in a short tube is considered, after which some calculations appertaining to a sudden divergence in diameter are described.

11,2 THE SHORT, STRAIGHT TUBE.

The local coefficient of heat transfer in a short tube may well be dependent on the dissipation of mechanical energy into heat if the heat-transfer fluid is highly viscous. Such effects may be significant even at low Reynolds numbers.

It is characteristic of highly viscous fluids that the viscosity varies considerably with temperature, and the dependence of 'h' on the viscosity variation may be significant.

A detailed investigation of these phenomena is now given.

11.2(i) NON-DISSIPATIVE LAMINAR FLOW WITH CONSTANT VISCOSITY.

It is well known that for a fluid having a high Prandtl number, the rate of increase in thickness (in the flow direction) of a thermal boundary layer is very much less than the rate at which the associated velocity layer thickens. This means that the axial velocity profile near the entrance of a tube develops much more rapidly than the temperature profile (see for example ref: K.5). It can be assumed therefore that fully developed flow conditions prevail at the entrance of a tube for the purposes of this analysis, but that the coefficients of heat transfer calculated provide a reasonably good approximation for any other entry conditions.

Leveque further approximated the form of the axial velocity profile for the case of a short tube at constant temperature (as discussed in part 2.4(ii)), and calculated local Nusselt numbers for high values of Pr. The simplifying assumption used was the the distribution of axial velocity near to the tube-wall was a linear function of radial distance. Morgan (Ref: I.1) shows this to be a good approximation with high Prandtl numbers because the temperature layer is much thinner than the velocity layer.

Sellars (Ref: C.13) modified the result of Leveque for the 'uniform heat-flux' boundary condition. The value of the local Nusselt number was given by -

$$Nu = \frac{2^{1/3}\, 9^{2/3}\, \Gamma(5/3)}{3} \cdot (x/r_w Re Pr)^{-1/3}$$

or
$$Nu = 1.639 \left[\frac{x}{r_w Re Pr} \right]^{-1/3} \qquad (11.1)$$

In appendix (B) a similar problem is solved by means of the Sellars technique, which arises elsewhere (11.2(vii)).

11.2(ii) DISSIPATIVE LAMINAR FLOW WITH CONSTANT VISCOSITY.

A solution to the problem of dissipation in laminar high speed gas flows, with heat transfer from a constant temperature plate, can be found in many of the standard text books (e.g. Ref: K.5, K.6). A solution to the apparently similar problem, of forced convection with dissipation in tubes, cannot be obtained using the same sort of mathematical procedure. Kudryashev (Ref: F.1, F.2), investigated a tube at constant temperature, by modifying the solution of Graetz (described in part 2.4(ii)). The result contained the sum of two eigenvalue series, which were slowly convergent at high Prandtl numbers.

The following analysis relates to the 'uniform heat-flux' tube, with a 'high Prandtl number' fluid, the flow is 'fully developed' and 'viscous dissipation' is considered. The approach to the problem embodies the simplifications made by Leveque.

11.2(ii)a.

Consider first the limiting behaviour for large axial distances x.

The momentum and energy equations (as in Part 2.2(ii)) can be written -

$$\frac{\mu}{r}\frac{\partial}{\partial r}\left(r\frac{\partial u}{\partial r}\right) = \frac{dp}{dx} \qquad (11.2)$$

and

$$c\rho\, u\frac{dt}{dx} = \frac{K}{r}\frac{\partial}{\partial r}\left(r\frac{\partial t}{\partial r}\right) + \mu\left(\frac{\partial u}{\partial r}\right)^2 \qquad (11.3)$$

where $$\frac{\partial t}{\partial x} \rightarrow \frac{dt}{dx} = \frac{dt_b}{dx} \text{ as } x \rightarrow \infty, \qquad (11.4)$$

with the boundary conditions -

$$\frac{\partial u}{\partial r} = 0 = \frac{\partial t}{\partial r} \text{ at } r = 0,$$

and $u = 0$, $t = t_w$ at $r = r_w$.

The integrations are straightforward.

$$u = 2\bar{u}\,(1 - (r/r_w)^2) \qquad (11.4)$$

and
$$t - t_w = \frac{\bar{C}}{4}\left(\frac{r}{r_w}\right)^2 - \left(\bar{C} + 16\frac{\mu\bar{u}^2}{K}\right)\left(\frac{r}{2r_w}\right)^4 - \left(\frac{3\bar{C}}{16} - \frac{\mu\bar{u}^2}{K}\right) \qquad (11.5)$$

where $\bar{C} = r_w \text{ Re Pr } \frac{dt_b}{dx}$.

From the definition of bulk temperature

$$(t_b - t_w) = -\left(\frac{11}{96}\frac{dt_b}{dx} r_w \text{ Re Pr} - \frac{5}{6}\frac{\mu\bar{u}^2}{K}\right) . \qquad (11.6)$$

Since
$$\left(2\frac{hr_w}{K}\right) = \left(2\, r_w \left.\frac{\partial t}{\partial r}\right|_w\right) \Big/ \left(t_w - t_b\right) ,$$

the limiting Nusselt number Nu_∞ becomes

$$Nu_\infty = \frac{48}{11}\left(\frac{dt_b}{dx} - \frac{8\mu\bar{u}}{r_w^2\rho c}\right) \Big/ \left(\frac{dt_b}{dx} - \frac{40}{11}\frac{\mu\bar{u}}{r_w^2\rho c}\right) ,$$

which reduces to

$$Nu_\infty = \frac{48}{11} \Big/ \left(1 + \frac{24}{11}\frac{\mu\bar{u}^2}{qr_w}\right) \qquad (11.7)$$

Kudryashev pointed out that $Nu_\infty = 9.6$ with the 'constant temperature' constraint. However, it is apparent here that for 'uniform heat-flux,' Nu_∞ tends to 48/11 with high heat fluxes, and zero at low heat fluxes. This indicates that tube temperature can easily be underestimated when small heating rates are encountered in practice provided the fluid is highly viscous and the Reynolds number large. At small negative fluxes (when cooling the fluid) Nu_∞ becomes large and negative (or $Nu_\infty \to -\infty$, as $q \to -(24/11)(\mu\bar{u}^2/r_w)$). This implies that heat flows out of the system whilst the wall temperature is greater than the bulk temperature of the fluid. The phenomenon is easily explained by the fact that a point of inflection occurs in the radial temperature distribution, in the region of high shear stress close to the tube wall. At higher cooling rates the effect is insignificant and $Nu_\infty = 48/11$.

11.2.(ii)b Consider now the effects of dissipation at small axial distances x. The energy equation (see part 2.2(ii)) is now written

$$u \frac{\partial t}{\partial x} + v \frac{\partial t}{\partial r} = \frac{K}{\rho c} \frac{1}{r} \frac{\partial}{\partial r} \left(r \frac{\partial t}{\partial r} \right) + \frac{\mu}{\rho c} \left(\frac{\partial u}{\partial r} \right)^2$$

If Pr is high, and the thickness of the temperature layer is consequently much less than the radius of the tube, a simplification can be made:

$$\frac{1}{r} \frac{\partial}{\partial r} \left(r \frac{\partial t}{\partial r} \right) \simeq \frac{\partial^2 t}{\partial r^2}$$

With the following substitutions,

$$X = \frac{\text{[illegible]}\, x}{r_w Re Pr} , \quad Y = \frac{r_w - r}{r_w} , \quad \theta = (t - t_\infty) \Big/ \frac{q r_w}{K} , \quad V = \frac{u}{\bar{u}} ,$$

where t_∞ = the temperature of the fluid at the start of heating $(x = 0)$, the energy equation for fully developed flow becomes

$$\frac{V}{2} \frac{\partial \theta}{\partial X} = \frac{\partial^2 \theta}{\partial Y^2} + 16 \left(\frac{\mu \bar{u}^2}{q r_w} \right) \left(\frac{1}{4} \frac{\partial V}{\partial Y} \right)^2 . \qquad (11.8)$$

The velocity is $V = 4 (Y - Y^2)$ for fully developed flow, and from the Leveque approximation, $Y^2 \ll Y$, hence,

$$V \simeq 4 Y. \qquad (11.9)$$

The final form of the energy equation is therefore

$$2 Y \frac{\partial \theta}{\partial X} = \frac{\partial^2 \theta}{\partial Y^2} + \phi \qquad (11.10)$$

where $\phi = 16 (\mu \bar{u}^2)/(q r_w)$.

Equation 11.10 is to be solved with the boundary conditions

$\frac{\partial \theta}{\partial Y} = -1$, $Y = 0$, all X, $\theta = 0$, $Y = Y_\infty$(the limit of the temp. layer), All X.

$\theta = 0$, all Y, $X = 0$.

The first condition specifies uniform heat-flux, the second implies the existence of a temperature boundary layer, such that the temperature outside this layer is equal to the inlet temperature, and the third condition states that the temperature at the start of heating ($x = 0$) is uniform. The latter may not be achieved in practice because dissipative heating could occur upstream of $x = 0$. The condition imposed however is the only reasonable one.

A similarity solution is sought, putting

$$f = X^m . \theta \quad \text{and} \quad \eta = X^n . Y.$$

By transforming equation (11.10), and considering the boundary conditions, the values of m and n are chosen to be $(-\frac{1}{3})$.

A solution which satisfies the required boundary conditions is
$$f(\eta, X) = g(\eta) + \delta(X) . \gamma(\eta) . \qquad (11.11)$$
Putting equation (11.11) into (11.10) yields

$$\frac{2}{3}\eta(-\eta g' - \eta\delta\gamma' + 3X\delta'\gamma + g + \delta.\gamma) = \phi X^{\frac{1}{3}} + g'' + \delta\gamma'' \qquad (11.12)$$

Whereupon by separating the variables

$$g'' + \tfrac{2}{3}\eta^2 g' - \tfrac{2}{3}\eta g = 0 \qquad (11.13)$$

$$\gamma'' + \tfrac{2}{3}\eta^2\gamma' - \tfrac{4}{3}\eta\gamma + 1 = 0 \qquad (11.14)$$

$$\delta = \phi . X^{\frac{1}{3}} \qquad (11.15)$$

The transformed boundary conditions are

$$g(\infty) = 0, \quad g'(0) = -1,$$

$$\gamma(\infty) = 0, \quad \gamma'(0) = 0.$$

The solution to equations (11.13) and (11.14) were obtained by a finite difference method, and the computer programme used for this purpose is shown in figure 11.2.

The procedure used in the programme was to add the results of two arbitrary, single point boundary-condition solutions in such a way that the final function satisfied the two point boundary-conditions as follows -

Putting L = a linear operator,

the differential equations to be solved can be written

$$L(f) = \psi(\eta).$$

Putting $\quad f = \alpha y_1 + \beta y_2$

it can then be shown that $\alpha L(y_1) + \beta L(y_2) = \psi$.

This means that f can be found from the solutions of

$$L(y_1) = 0, \quad L(y_2) = \beta^{-1}\psi .$$

The starting conditions required for y_1 and y_2 are arbitrary, whence α and β are chosen to satisfy the original boundary conditions.

The functions g and γ are illustrated in figure: 11.3. The wall values were quite insensitive to the selection of $\eta(\infty)$ (the boundary layer limit) and a suitable value was $\eta(\infty) = 3.6$. The dissipation function γ is greatest in the fluid layers close to the heated surface. This provides some justification for the selection of $\theta(Y_\infty) = 0$ in the first place.

The main purpose of the analysis is to determine the local Nusselt number -

$$Nu = 2\left(g(o)\,X^{\frac{1}{3}} + \gamma(o)\,\phi\,X^{\frac{2}{3}}\right)^{-1} \tag{11.16}$$

The bulk temperature is assumed to be similar to t_∞, which is reasonable at high Prandtl numbers, because the axial temperature gradient along the tube wall is always much greater than the axial bulk-temperature gradient.

The final form of the local Nusselt number is

$$Nu = 1.642\,\frac{(r_w\,RePr)^{\frac{1}{3}}}{x}\left[1 + 11.26\left(\frac{\mu\bar{u}^2}{qr_w}\right)\left(\frac{x}{r_w RePr}\right)^{\frac{1}{3}}\right]^{-1} \tag{11.17}$$

Equation (11.17) compares favourably with the result of Sellars (Ref: C.13), $Nu = 1.639\,\frac{(r_w RePr)^{\frac{1}{3}}}{x}$, when the heat flux is large.

Putting $\quad E = \left(\frac{\mu\bar{u}^2}{qr_w}\right)$,

and $\quad Nu_o$ = the theoretical value of Nu if dissipation is neglected, the following relationships are obtained.

$$\frac{Nu}{Nu_o} = \left[1 + 18.51\,\frac{E}{Nu_o}\right]^{-1} \quad \text{at small distances } (X < 0.0072) \qquad (11.18)$$

$$\frac{Nu}{Nu_o} = \left[1 + 2.182\,E\right]^{-1} \quad \text{at large distances } (X > 0.0072) \qquad (11.19)$$

The effects of dissipation on the local Nusselt number are therefore vanishingly small for short tube lengths. An indication of the magnitudes can be gained from the simple equations (11.18) and (11.19). Part 11.2(vii) contains a discussion of how these findings were applied in the experimental work.

11.2(iii) NON-DISSIPATIVE, LAMINAR FLOW WITH VARIABLE VISCOSITY.

Several attempts have been made at solving the problem of laminar heat transfer with temperature dependent viscosity in circular tubes. Particular consideration has been given to the evaluation of Nusselt numbers at large axial distances Nu_∞ (see Ref: D6, D7, D9, D10). Few investigators have been concerned with short tubes. Yang (Ref: D3) used an iterative, integral procedure to solve the equations of momentum and energy, with uniform heat-flux, which yielded a complicated expression for the local Nusselt Number. Nu could be related to the corresponding value for a fluid with constant viscosity Nu_o by an expression of the kind

$$Nu = (\mu_b / \mu_w)^{0.14} \; Nu_o \; . \qquad (11.20)$$

where Nu_o = the local Nusselt number with constant viscosity.

This form of expression was first postulated by Sieder and Tate (Ref: D1) in their empirical analysis (details are given in Part 2.4(ii)) but was based on mean values of Nusselt number (Nu_m) rather than local values (Nu). The equation (11.20) represents the data of Yang approximately, but $\left(\frac{Nu}{Nu_o}\right)$ was not a unique function of $\left(\frac{\mu_b}{\mu_w}\right)$.

Rosenberg (Ref: D8) investigated the tube with uniform wall temperature by a finite difference method. The axial velocity profile was undeveloped at the inlet of thetube, and results were obtained at different Prandtl numbers. The few data given showed reasonable agreement with equation (11.20), but the value of (Nu/Nu_o) was weakly dependent on $(x/r_w)/(Re\ Pr)$ the dimensionless axial distance. Inertial effects were shown to be insignificant at high Prandtl number ($\tilde{1}00$) and Nu was similar to the 'fully developed flow' value.

Test (Ref: D5) found a solution similar to Rosenberg's uniform wall temperature case. Instead of starting with the simplified boundary-layer equations (as in part 2.2.(ii)), the full Navier-Stokes equations were considered. The scope of the results was limited by the increased complexity of the solution, and large spatial differences were necessary in the interests of economy of computer time. Test found that equation (11.20) overestimated Nu considerably during heating.

Shannon (Ref: D10) investigated the uniform heat-flux boundary condition with fully developed flow. Most of the data reported refers to large axial distances, and the equation (11.20) was in good agreement with these. The results appertaining to small axial distances were generally in disagreement with the analysis of Yang and with equation (11.20). Insufficient information was recorded to form any detailed conclusions, but the value of (Nu/Nu_o) was found once more to be a function of the dimensionless axial distance $(x/r_w)/(RePr)$.

The analysis now to be presented was an attempt to fulfil the following -

(a) To prove or otherwise the validity of the expression

$$(Nu/Nu_o) = (\mu_b/\mu_w)^{0.14} .$$

(b) To show that $Nu = Nu_o.f\ (\mu_b/\mu_w)$.

(c) To find the dependence of Nu on (μ_b/μ_w) at very small tube lengths.

(d) To determine the relationship in (b) for the inlet region of a tube with fully developed flow.

The generality of the numerical solution is improved by selecting developed flow at the inlet, then assuming that inertia terms arising from the viscosity-temperature dependence are negligible. These conditions are most likely to be well approximated with highly viscous fluids, but the solution is an asymptotic one and strictly only applies to a hypothetical fluid in which Pr tends to infinity.

The boundary-layer equations of momentum and energy (described in part 2.2.(ii) can be simplified for non-dissipative, fully developed laminar flow in a short tube. The following assumptions are made -

(1) Radial velocity components are small .

(2) The flow is fully developed at x = 0, the start of heating.

(3) Inertia effects due to viscosity variations are negligible.

(4) Radial pressure gradients are negligible.

The equations become (after referring to the notation used in part 11.2.(ii) b) -

$$\frac{\partial}{\partial Y}\left[\frac{(1-Y)}{M}\cdot\frac{\partial V}{\partial Y}\right] = \left[\frac{dp}{dx}\cdot\frac{r_w^2}{\mu_0 \bar{u}}\right](1-Y) \qquad (11.21)$$

where μ_0 = the viscosity at the start of heating x = 0,

and $M = (\mu_0/\mu)$, the viscosity ratio.

$$\frac{V}{2}\cdot\frac{\partial\theta}{\partial X} = \frac{1}{(1-Y)}\cdot\frac{\partial}{\partial Y}\left[(1-Y).\frac{\partial\theta}{\partial Y}\right] \qquad (11.22)$$

Integrating equation (11.21) with (V)/(Y) = 0 at Y = 1,

$$\frac{\partial V}{\partial Y} = \left[-\frac{1}{2}\,\frac{dp}{dx}\cdot\frac{r_w^2}{\mu_0\bar{u}}\right].(1-Y).M \qquad (11.23)$$

and differentiating equation (11.22),

$$V\,\frac{\partial\theta}{\partial X} = 2\left[\frac{\partial^2\theta}{\partial Y^2} - \frac{1}{(1-Y)}\,\frac{\partial\theta}{\partial Y}\right] \qquad (11.24)$$

The equation of continuity is required for a solution to be obtained, and this can be stated $2\int_0^1 V(1-Y)\,dY = 1$. (11.25)

To define the problem fully it is necessary to specify how the viscosity ratio M varies with temperature Θ. An exponential relationship is proposed - $\log(\mu) = (A + Bt)$ - which is reasnnably general, and well represents viscosity in practice for a moderate temperature range. Figure 8.4. shows that $\log(\mu)$ is almost linear in temperature for propylene glycol-water mixtures over a small interval. For 100% glycol the viscosity can be determined within $4\frac{1}{2}$% by such a relationship within the temperature range 20 to 40°C.

The resulting viscosity ratio M is given by $M = \exp\left[\frac{q r_W B \Theta}{K}\right]$, so that the effect of varying the heat flux is the same as varying the viscosity-temperature dependence. A single parameter "ζ" is used in

$$M = \exp(\zeta\,\Theta) \tag{11.26}$$

The momentum equation (11.23) is non-linear, and a finite difference solution was sought, being the most straightforward approach.

Central differences were used in the Y - direction, and forward differences in the X-direction. 'n' is the Y-wise suffix, and 'm' the X-wise suffix. Computations were carried out giving Θ as a function of X, for particular values of the parameter ζ.

Defining the new variable G -

$$G = V \Big/ \left[-\frac{1}{2}\ \frac{dp}{dx}\cdot\frac{r_W^2}{\mu_0 a}\right] \tag{11.27}$$

first, the momentum equation is solved for G at a particular axial position.

$$G[n,m] = G[n-1,m] + \frac{\Delta Y}{4}\,(2-Y[n]+Y[n-1])(M[n,m]+M[n-1,m]) \tag{11.28}$$

with the condition $\quad G[0,m] = 0.$

The values of M are derived by reference to equation (11.26) requiring Θ, which is known because forward differences are used axially in calculating Θ.

Next, the variable G is converted into axial velocity with the continuity equation from

$$V[n,m] = G[n,m]\left(\sum_{Y=0}^{1} G[n,m]\,(1-Y[n])\,\Delta Y\right)^{-1} \qquad (11.29)$$

The energy equation can now be solved giving θ at the next axial increment

$$\theta[n,m+1] = \theta[n,m] + \frac{2\Delta X}{V[n,m]}\left\{\frac{\theta[n+1,m] + \theta[n-1,m] - 2\theta[n,m]}{\Delta Y\,.\,\Delta Y} - \frac{1}{(1-Y[n])}\left(\frac{\theta[n+1,m] - \theta[n-1,m]}{2.\Delta Y}\right)\right\} \qquad (11.30)$$

The condition for uniform heat-flux is $\theta[0,m] = \theta[1,m] + \Delta Y$,

and for symmetry at the axis $\theta[n_{max},m] = \theta[n_{max}-1,m]$,

with the inlet condition $\theta[n,0] = 0$.

Finally, the local Nusselt number is calculated from

$$Nu[m] = 2/(\theta[0,m] - TT) \qquad (11.31)$$

where the local bulk temperature TT is given by

$$TT = 2\sum_{Y=0}^{1} \theta[n,m].V[n,m].(1-Y[n])\ \Delta Y.$$

The choice of radial increment affected the accuracy of the calculated wall temperature at small axial distances X. By definition, $Nu = \infty$ at $X = 0$, but a maximum calculable value of Nu limited the results, the value of which depended on the computation time available and the smallest value of X required. For an increment ΔY at the tube wall, the maximum possible value of Nu was $(2/\Delta Y_\omega)$, and in most of the calculations carried out the maximum value of Nu was 210.

An acceptable computation time was achieved with 20 radial increments ΔY. The size of increment increased linearly with distance from the tube wall, because the temperature changed rapidly in the wall region, but slowly near the axis. Typically, the increments were increased from 0.0095 at the wall to 0.146 at the axis. If smaller axial distances had been investigated, the value 0.0095 would have been too large and the Nusselt numbers underestimated. A suitable grid spacing was determined by trial.

The axial increments ΔX expanded linearly with the distance downstream. The first and smallest step was determined by the shortest axial distance for which Nu was required, and a suitable value was found to be $\Delta X = 6.10^{-9}$. The maximum step size was limited by the stability of the solution, and for distances up to $X = 10^{-3}$ stability was ensured if ΔX was always less than 10^{-6}. A maximum value of $\Delta X = 7.5\ 10^{-7}$ was specified at the maximum dimensionless axial distance of $X = 10^{-3}$.

Nu as a function of X was calculated on an ICL 1905 computer for the values of the viscosity-variation parameter ζ of 0, 10, 20, 50, 100 and 500. The Nusselt numbers calculated were unreliable at dimensionless axial distances X of less than 10^{-6}, because the radial grid spacing was too large. The calculated Nusselt numbers are compared with Sellars' theory (part 11.2.(i)) putting $\zeta = 0$, (see figure 11.4). A good agreement is indicated. The results obtained with $\zeta > 50$ were found to be sensitive to the radial step size, and these Nusselt numbers are presented merely to show the trend with very considerable viscosity variations. With $\zeta < 50$ a reduction of 20% in the step size was found to have negligible effect on the local Nessult number when $X > 2.10^{-6}$.

The results of the preceding analysis are given in figures 11.4 and 11.9 to 11.11 and the theoretical result of Sellars is superimposed on the graphs for comparison. The calculated Nusselt numbers for slug-flow (uniform velocity) based on Sellars method (see appendix (B)) are plotted for reasons described in a later section. The significance of these results is discussed in 11.2(vii).

11.2.(vii). The preceding finite difference analysis 11.2.(vi) will be unreliable when the temperature layer is thin, as occurs when X tends to zero. The following analytical approach was used to enable

Nu to be determined in the limit as $X \to 0$. The method described has the advantage of being able to show that $Nu = Nu_0 . \psi(\mu_b/\mu_w)$ in the region considered.

Starting with the energy equation in the form used in the dissipation analysis, equation (11.8), but neglecting the dissipation term ϕ for the purposes of this analysis -

$$\frac{V}{2}\frac{\partial\theta}{\partial X} = \frac{\partial^2\theta}{\partial Y^2} \tag{11.32}$$

and restating the momentum equation (11.23) already discussed -

$$\frac{\partial V}{\partial Y} = \left(-\frac{1}{2}\frac{dp}{dx}.\frac{r_w^2}{\mu_0 \bar{u}}\right).(1-Y).\exp\left[\zeta.\theta\right] \tag{11.23}$$

These equations are transformed in a similar way to part 11.1.(ii)b,

$f = X^{-\frac{1}{3}}.\theta, \quad S = X^{-\frac{1}{3}}.V \quad$ and $\quad \eta = X^{-\frac{1}{3}}.Y$.

A series solution is attempted which is convergent at small X, as follows -

$$f(\eta,X) = f_0(\eta) + \zeta.X^{\frac{1}{3}}.f_1(\eta) + \zeta^2.X^{\frac{2}{3}}.f_2 ++ \tag{11.33}$$

Substituting equation (11.33) into the energy equation (11.32)

$$\frac{S}{6\eta}\left[\eta.f_0 + 2(\zeta X^{\frac{1}{3}})\eta.f_1 - \eta^2.f_0' - (\zeta X^{\frac{1}{3}}).\eta^2.f_1' +\right] = f_0'' + (\zeta X^{\frac{1}{3}}).f_1'' + \tag{11.34}$$

The velocity is expressed as the series -

$$S(\eta,X) = S_0(\eta) + \zeta.X^{\frac{1}{3}}.S_1(\eta) ++ \tag{11.35}$$

which can be substituted into the momentum equation (11.23)

$$S_0' + \zeta X^{\frac{1}{3}}.S_1' = \left(-\frac{1}{2}\frac{dp}{dx}.\frac{r_w^2}{\mu_0\bar{u}}\right).(1-X^{\frac{1}{3}}\eta)\left[1+\zeta.X^{\frac{1}{3}}(f_0++) + \frac{\zeta^2.X^{\frac{2}{3}}(f_0++)^2}{2}++\right] \tag{11.36}$$

When $X^{\frac{1}{3}}$ is small, terms in $X^{\frac{2}{3}}$ must be negligible, so the series (11.32) and (11.35) can be truncated after two terms.

In (11.36) dp/dx is a weak function of X. By inspection of the continuity equation viz:

$$1 = 2\int_0^1 (1-Y)\int_0^Y (1-Y).M.\left(-\frac{1}{2}\frac{dp}{dx}.\frac{r_w^2}{\mu_0\bar{u}}\right) dY\, dY \tag{11.37}$$

it can be shown that $\left(-\frac{1}{2}\cdot\frac{dp}{dx}\cdot\frac{r_w^2}{\mu_o\bar{u}}\right) = 4$ to the order $(\xi X^{\frac{1}{3}})^2$,

(dp/dx) can therefore be considered constant in generating the first two terms of the series.

Separating the variables in equation (11.36) yields

$$S_o' = 4 \quad \text{and } S_1' = 4f_o,$$

after making the approximation $(1 - X^{\frac{1}{3}}\eta) \simeq 1$, which is the Leveque approximation already discussed.

Integrating with the boundary conditions $S_o(o) = 0$, $S_1(o) = 0$,

$$S_o = 4\eta \quad \text{and } S_1 = 4\int_o^{\eta} f_o \, d\eta \qquad . \quad (11.38)$$

The velocity functions (11.38) can be substituted into the energy equation (11.34), and after separating the variables -

$$f_o'' + \frac{2}{3}\eta^2 . f_o' - \frac{2}{3}\eta . f_o = 0 \quad \text{with } \begin{cases} f_o(\infty) = 0 \\ f_o'(o) = -1 \end{cases} \qquad (11.39)$$

and

$$f_1'' + \frac{2}{3}.\eta^2 . f_1' - \frac{4}{3}.\eta . f_1 = \frac{2}{3}\left(f_o - \eta . f_o'\right).\int_o^{\eta} f_o \, d\eta \qquad (11.40)$$

$$\text{with } \begin{cases} f_1(\infty) = 0 \\ f_1'(o) = 0 \end{cases}$$

Equations (11.39) and (11.40) were solved in a similar way to the dissipation equations of part 11.1.(ii)b. The boundary layer limit was set at $\eta(\infty) = 4$. The function $f_o(o)$ should correspond with the dissipation function g(o) (part 11.2.(ii)b) but a small error is apparent being attributable to the computation error involved in setting $\eta(\infty)$ at a slightly different value.

The functions f_o and f_1 are shown in figure 11.5. The local Nusselt number with viscosity variation at very small axial distances becomes -

$$Nu = 2X^{-\frac{1}{3}} \left[f_o(o) + \xi X^{\frac{1}{3}} . f_1(o) + \right]^{-1}$$

The parameter is eliminated straightforwardly, giving

$$Nu = 2X^{-\frac{1}{3}} \left[f_o(o) + \frac{f_1(o)}{f_o(o)} \quad (M_{wall} - 1) + \right]$$

where $X = (x)/(r_w \text{ Re Pr})$ as usual and $M_{wall} = (\mu_o/\mu_w) \simeq (\mu_b/\mu_w)$

The final result of the calculations is

$$\frac{Nu}{Nu_o} = \left[1 - 0.170 \; (M_{wall} - 1) + \right]^{-1} \tag{11.41}$$

where $Nu_o = 1.647 \; X^{-\frac{1}{3}}$, the theoretical value of local Nusselt number without viscosity variation.

Equation (11.41) can be considered as the first two terms of a binomial expansion of the function

$$\left(\frac{Nu}{Nu_o}\right) = M_{wall}^{0.17} \tag{11.42}$$

Numerical results of the preceding analysis are given in figure 11.12, where a comparison is made with the finite difference solution of part 11.2(iii).

11.2.(iv) NON-DISSIPATIVE TURBULENT FLOW WITH CONSTANT VISCOSITY.

From the literature survey (part 3) it is clear that a considerable amount of research has been done into solving problems of heat transfer with turbulent flow in tubes, theories of turbulence and analytical methods are evolving continually. A detailed study of 'turbulence' is outside the scope of this work, but reference can be made to papers by Wolfshtien (Ref: H.23) and Spalding (Ref:H.22) where some of the most recent advances in this field are discussed.

The following analysis is an attempt to solve the particular problem at hand - that is the investigation of heat transfer with turbulent flow, at high Prandtl numbers, in the entrance region of a tube, at uniform heat-flux - and is based on well established models of turbulent flow.

The hypotheses of Reichardt (Ref: I.10), Deissler (Ref: C.2) and Van Driest (Ref: I.6) have been widely used in analysing internal fluid flows. The second and third of these are simple to apply and have a great deal in common. These will be described in more detail and form the basis of the subsequent analysis.

The difficulty in solving turbulent flow problems is in specifying the 'apparent' transport properties. Prandtl's mixing-length theory states that the turbulent viscosity component is -

$$\mu_t = \rho A^2 . y^2 . \frac{du}{dy}$$

in boundary-layer flow, where

u = velocity parallel to the heated surface,

y = distance from the heated surface,

A = a constant,

suffix t = turbulent component.

Both Deissler and Van Driest propose similar formulae, which can be described as follows -

$$\mu_t = \rho A^2 . y^2 . \frac{du}{dy} . f$$

where f is a damping factor; this is required because, although turbulence has been shown to be present as $y \to 0$ (see Ref: I.4, I.5) the turbulence eddies are dampted by viscous action near to the wall.

According to Deissler, $f = \left(1 - \exp\left[-\left(\rho . B^2 . \frac{y^2}{\mu} . \left(\frac{u}{y}\right)\right)\right]\right)$ (B constant)

where (du/dy) is replaced by (u/y), and from Van Driest

$$f = \left(1 - \exp\left[-\left(\rho . B^2 . \frac{y^2}{\mu} . \frac{du}{dy}\right]^{\frac{1}{2}}\right)^2 .$$

In the limit as $y \to 0$, both hypotheses give

$$\mu_t = C . \frac{\rho^2}{\mu} . \left(\frac{du}{dy_o}\right)^2 . \; y^4 \qquad \text{(C constant)}$$

where the index 4 is a consequence of the arbitrary damping factor.

Other workers (for example Harriott, Ref: I.9) and Hubbard, Ref: I.8) have proposed that the index 4 causes μ_t to vary too rapidly with y, and a value of 3 would be more suitable. Little experimental evidence is available to support either case because velocity cannot be measured easily close to a wall (discussed in Ref: I.4, I.5). The hypotheses discussed above have been used in many of the tube-flow analyses, (Ref: C.2, C.3, C.4, C.10) but there has been comparatively little experimental work done with high Prandtl number fluids where the value of the index described is critical (because thin temperature layers occur when Pr is large.)

Deissler and Sparrow (Ref: C.2, C.4) considered high Prandtl number fluids analytically. The former used an integral procedure depending on an approximate radial temperature profile in the inlet region of the tube. Sparrow found a more satisfactory result to the problem posed by Deissler, by finding an eigenvalue series-solution. The 'exact' result of Sparrow made use of Deissler's model of turbulence, but the range of results was somewhat limited. Reynolds numbers above 50,000 were considered with Prandtl numbers less than 100. The very short thermal entrance lengths predicted were of little practical value in the case of Pr = 100, and results at lower Reynolds numbers would have been valuable.

The energy and momentum equations for fully developed turbulent flow with constant viscosity and no dissipation (from Part 2.2.(iv)) can be stated -

$$\frac{\rho c}{K} . u . \frac{\partial t}{\partial x} = \frac{\partial}{\partial y}\left(\left[1 + \left(\frac{K_t}{K}\right)\right] . \frac{\partial t}{\partial y} \right) \qquad (11.43)$$

$$\frac{1}{\mu} \frac{\partial p}{\partial x} = \frac{\partial}{\partial y}\left(\left[1 + \left(\frac{\mu_t}{\mu}\right)\right] . \frac{\partial u}{\partial y} \right) \qquad (11.44)$$

(subscript t = turbulent component, as usual)

Putting M_t (μ_t/μ), $\sigma \simeq Pr$,

then $(K_t/K) = (\sigma/\sigma_t).M_t \simeq \sigma.M_t$ (Reynolds analogy) .

Introducing the dimensionless parameters -

$V = (u/\bar{u})$, $X = (x/r_w \, Re \, \sigma)$, $Y = (y/r_w)$, $\theta = (t - t_\infty)/(qr_w/K)$

where t_∞ = the inlet temperature of the fluid,

equations (11.43) and (11.44) can be written

$$\frac{V}{2}\cdot\frac{\partial\theta}{\partial X} = \frac{\partial}{\partial Y}\left(\left[1 + \sigma M_t\right]\frac{\partial\theta}{\partial Y}\right) \qquad (11.45)$$

and

$$V = \left(\frac{\partial V}{\partial Y}\right)_0 \int_0^Y \frac{dY}{1 + M_t} \qquad (11.46)$$

where the approximation $\frac{\partial p}{\partial x}.y \simeq \frac{\partial p}{\partial x}.r_w$ is made in (11.46) and

suffix o = wall value.

Now suppose

$$U = V\left(\frac{\partial V}{\partial Y}\right)_0^{-1}, \quad R = \left[\frac{Re}{2}\left(\frac{\partial V}{\partial Y}\right)_0\right]^{1/2}, \quad Z = X\left(\frac{\partial V}{\partial Y}\right)_0^{-1}$$

The turbulent viscosity component is chosen to be

$M_t = a\,R^3\,Y^3$, as $Y \longrightarrow 0$, where a = constant.

This expression permits temperature to be calculated as $Pr \longrightarrow \infty$, but will be inaccurate for the calculation of velocity profiles except within the temperature layer. The limitation is a consequence of the boundary conditions $\theta = 0$ and $U = U_\infty$ at large values of Y.

Equations (11.45) and (11.46) now become

$$\frac{U}{2}\,\frac{\partial\theta}{\partial Z} = \frac{\partial}{\partial Y}\left(\left[1 + a.\sigma.R^3.Y^3\right]\frac{\partial\theta}{\partial Y}\right) \qquad (11.47)$$

$$U = \int_0^Y \frac{dY}{1 + aR^3Y^3} \equiv \sum_{n=0}^{\infty} \frac{(-aR^3)^n\,Y^{3n+1}}{(3n+1)} \qquad (11.48)$$

The series in equation (11.48) converges for $(aR^3y^3) < 1$ only, but the product $U.\frac{\partial\theta}{\partial Z}$ must always converge so this present no problem.

The equations are transformed by introducing

$$\eta = Z^{-\frac{1}{3}}Y \qquad \text{and} \qquad f = Z^{-\frac{1}{3}}\theta.$$

Hence

$$Z^{-\frac{1}{3}}\ \frac{U}{2}\left(\frac{Z\partial f}{\partial Z} + \frac{f}{3} - \frac{\eta}{3}\ \frac{\partial f}{\partial \eta}\right) = \frac{\partial}{\partial \eta}\ \left(\left[1 + \sigma\,(ZaR^3)\,\eta^3\right]\frac{\partial f}{\partial \eta}\right) \qquad (11.49)$$

$$\text{and}\quad Z^{-\frac{1}{3}}U = \eta - \frac{\eta^4}{4}.(ZaR^3) + (ZaR^3)^2\ \frac{\eta^7}{7}\ - \qquad (11.50)$$

The temperature variable is expressed as a series which converges at small Z, $\quad f\ (\eta, Z) = f_o(\eta) + (\sigma aR^3Z).f_1(\eta) + (\sigma aR^3Z)^2.f_2(\eta) +$

and the first two terms are generated by combining equations (11.49) and (11.50).

$$\left(\eta - \frac{\epsilon\,\eta^4}{4\sigma}\right)\left(4\epsilon f_1 + f_o - \eta f_1' - \epsilon\,\eta f_1'\right) = 6\,\frac{\partial}{\partial\eta}\left(\left[1 + \epsilon\eta^3\right]\left[f_o' + \epsilon f_1'\right]\right)$$

where $\epsilon = (\sigma\ aR^3Z)$ (independent of Prandtl number).

This leads to

$$\eta.f_o - \eta^2.f_o' = 6\,f_o'' \qquad \text{where} \begin{cases} f_o\,(\infty) = 0 \\ f_o'\,(o) = -1 \end{cases} \qquad (11.51)$$

$$\text{and} - \frac{1}{24\sigma}\left(\eta^4.f_o - \eta^5.f_o'\right) + \frac{1}{6}\left(4\eta.f_1 - \eta^2.f_1'\right) = f_1'' + \eta^3.f_o'' + 3\eta^2.f_o'$$

$$\text{where} \begin{cases} f_1(\infty) = 0 \\ f_1'(o) = 0 \end{cases} \qquad (11.52)$$

The first term of equation (11.52) is identical to $\frac{-\eta^3}{4\sigma}.\ f_o''$, and is therefore small when $\sigma > 0.25$.

The local Nusselt number is given by -

$$Nu = \frac{2}{f_o(o)}.\left(Re\ \sigma\frac{\partial V}{\partial Y_o}\Big/\frac{x}{r_w}\right)^{\frac{1}{3}}.\left(1 + \frac{f_1(o)}{f_o(o)}\ \left[\frac{a}{2^{3/2}}\cdot\left(\frac{x}{r_w}\right)\left(Re\frac{V}{Y_o}\right)^{\frac{1}{2}}\right]\right)^{-1} \qquad (11.53)$$

The functions f_o and f_1 are shown in figures 11.6, and the computations were carriedout as in part 11.2.(ii).

The effect of function f_1 is to cause a flattening of the radial temperature profile, and this is characteristic of turbulent flows in general. The change in sign of f_1 has no particular significance since at a given axial location the temperature is everywhere less than that based on the f_o term only. The (f_o) term has close similarity to the (g) term in the laminar solution of part 11.1.(ii).

In deriving Nu it is necessary to know $\left(\frac{\partial V}{\partial Y}\right)_o$. For fully turbulent flows a well know expression can be used (as described in Knudson & Katz Ref: K.3) which has been derived from measurements of pressure drop through tubes.

$$\left(\frac{\partial V}{\partial Y}\right)_o = 0.0115 \quad Re^{0.8} \quad .$$

The local Nusselt number becomes

$$Nu = 0.1855\ Pr^{\frac{1}{3}}\ Re^{0.6}(x/2r_w)^{-\frac{1}{3}}\ (1 - 0.0645\ a\ (x/2r_w)\ Re^{0.9})^{-1} \qquad (11.54)$$

A limiting Nusselt number is reached at large axial distances when $(\partial t/\partial x)$ becomes constant. Equation 11.54 must be matched to this solution.

The energy equation 11.45 is simplified at large axial distancesbecause $(\partial\Theta/\partial X)$ becomes samll, and can be set to zero.

$$0 = \frac{\partial}{\partial Y}\left[(1 + a\ \sigma\ R^3Y^3)\ \frac{\partial\theta}{\partial Y}\right] \qquad (11.55)$$

Integrating with the boundary conditions

$\Theta(\infty) = 0$ and $\Theta'(o) = -1$

gives $\Theta(o) = \pi(3\ a^{\frac{1}{3}}\ \sigma^{-\frac{1}{3}}\ R\ \sin(\pi/3))^{-1}$.

From the definition of $\left(\frac{\partial V}{\partial Y}\right)_o$, the parameter R can be stated

$R = 0.07583\ Re^{0.9}$,

and since $Nu_\infty = 2/\Theta(o)$ if $t_b \simeq t_\infty$,

the Nusselt number at large axial distances Nu_∞ is

$$Nu_\infty = 0.1254\ a^{\frac{1}{3}}.Pr^{\frac{1}{3}}.Re^{0.9} \qquad (11.56)$$

This equation must be used in conjunction with 11.54 so that Nu is not underestimated at large axial distances.

A value is required for the constant "a", and this is discussed in part 11.2.(vii).

11.2.(v) TURBULENT FLOW WITH CONSTANT VISCOSITY AND DISSIPATION.

The effect of dissipation on heat transfer in turbulent flow of viscous fluid in tubes has apparently not been investigated theoretically. As in the laminar flow case some work has been done for gases flowing over flat plates (Refs: K.5, K.6) which is of little help in the problem under consideration. The following analysis is a simplified theory for assessing the magnitude of the thermal effect caused by dissipation. There is little point in refining such an analysis since the result can be no more accurate than the turbulence model permits. Most of the dissipative contribution to the temperature profile is concentrated in the laminar sub-layer so it is probable that the solution gives a reasonable indication of the orders of magnitude involved.

Once again the limiting case is discussed first, and the energy equation as formulated in part 11.1.(iv) (see equation 11.55).

$$0 = \frac{\partial}{\partial Y}\left(\left[1 + a\,\sigma\,R^3Y^3\right]\frac{\partial \theta}{\partial Y}\right) + \left(\frac{\mu \bar{u}^2}{q r_w}\right)\left[1 + aR^3Y^3\right]\left(\frac{\partial V}{\partial Y}\right)_o^2 \qquad (11.57)$$

The symbols have the usual definitions.

Putting $E = \left(\frac{\mu \bar{u}^2}{q r_w}\right)$, $\frac{\partial V}{\partial Y} \simeq \left(\frac{\partial V}{\partial Y}\right)_o \left[1 + a\,R^3Y^3\right]^{-1}$

then integrating 11.57 with $\theta'(o) = -1$ and $\theta(\infty) = 0$,

the result is $\theta(o) = I_1 + I_2$ (11.58)

where $I_1 = \int_o^\infty \left[1 + a\,\sigma\,R^3Y^3\right]^{-1} dY$,

and $I_2 = E\left(\frac{\partial V}{\partial Y}\right)_o^2 \int_o^\infty \left[1 + a\,\sigma\,R^3Y^3\right]^{-1} \int_o^Y \left[1 + aR^3Y^3\right]^{-1} dY\, dY$

Now $I_1 = \pi(aR^3\sigma)^{-\frac{1}{3}}/\,3.\sin(\pi/3)$, as in 11.2.(iv).

Integrating

$$I_2 = E.\left(\frac{\partial V}{\partial Y}\right)_0^2 \int_0^\infty [1+a\sigma R^3Y^3]^{-1}.\left(\sum_{n=0}^{\infty} \frac{(-1)^n}{a^{1/3}R}.\frac{(a^{1/3}RY)^{3n+1}}{(3n+1)}\right) dY$$

which becomes

$$I_2 = E\left(\frac{\partial V}{\partial Y}\right)_0^2.\frac{\pi(a\sigma R^3)^{-2/3}}{3\sin(2\pi/3)}.\sum_{n=0}\frac{\sigma^{-n}}{(3n+1)} \qquad (11.59)$$

As σ tends to infinity the result becomes

$$\theta(o) = 1.210\ (aR^3\sigma)^{-\frac{1}{3}}\left[1 + E\left(\frac{\partial V}{\partial Y}\right)_0^2 (aR^3\sigma)^{-\frac{1}{3}}\right] \qquad (11.60)$$

and substituting for $\left(\frac{\partial V}{\partial Y}\right)_0$ as in equation 11.54, with $Nu_\infty = \frac{2}{\theta(o)}$

$$Nu_\infty = 0.1254\ a^{\frac{1}{3}}\ Pr^{\frac{1}{3}}\ Re^{0.9}\ \left[1 + 1.745.10^{-3}.a^{\frac{1}{3}}.E\ Re^{0.7}\ Pr^{-\frac{1}{3}}\right] \qquad (11.61)$$

Another was of expressing 11.61 is as follows

$$\frac{Nu_\infty}{Nu_o} = \left[1 + 2.188.\ 10^{-4}\ \frac{E}{Nu_o}\ Re^{1.6}\right]^{-1} \qquad (11.62)$$

where Nu_o = the Nusselt number at large axial distances without dissipation.

For the entrance region of the tube the energy equation is stated

$$\frac{U}{2}\frac{\partial\theta}{\partial Z} = \frac{\partial}{\partial Y}\left(\left[1 + aR^3Y^3\right]\frac{\partial\theta}{\partial Y}\right) + E\left(\frac{\partial V}{\partial Y}\right)_0^2\left[1 + aR^3Y^3\right]^{-1} \qquad (11.63)$$

where the parameters still have the definitions of part 11.2.(iv).

If a small perturbation solution were sought for small values of Z (dimensionless axial distance), the perturbation parameter would be defined by $\Delta = (a\ \sigma\ R^3)^{\frac{2}{3}}.Z^{\frac{1}{3}}$ (independent of σ) in

$$\theta = Z^{\frac{1}{3}}\left[b_o\ (Y/Z^{\frac{1}{3}}) + \Delta.b_1 + \Delta^2.b_2 +\right]$$

It becomes evident after inserting this expression in 11.63 that the turbulent components of viscosity and conductivity are of order Δ^3, and this implies that the first order solution will be identical to the laminar solution of part 11.2.(ii)b, but the velocity gradient at the wall will be different. The range of axial distance over which this kind of result is applicable will be smaller than for the corresponding laminar flow result because the perturbation parameter selected is different.

Omitting all terms of higher orders than Δ^1, the energy equation becomes
$$\frac{U}{2}\frac{\partial\theta}{\partial Z} = \frac{\partial^2\theta}{\partial Y^2} + E\left(\frac{\partial V}{\partial Y}\right)_o^2 \qquad (11.64)$$

and the integrated momentum equation (order Δ^1) is
$$U = Y \qquad (11.65)$$

Stating $\mathcal{Z} = 4Z$

then
$$2Y\frac{\partial\theta}{\partial \mathcal{Z}} = \frac{\partial^2\theta}{\partial Y^2} + E\left(\frac{\partial V}{\partial Y}\right)_o^2$$

which is solved in part 11.2.(ii), i.e. equation (11.10), for the boundary conditions $\theta(\infty,X) = 0$, $\frac{\partial\theta}{\partial Y}(o,X) = -1$, $\theta(Y,o) = 0$.

Writing the earlier result in terms of $\mathcal{Z}^{\frac{1}{3}}$
$$\theta(o,X) = 1.217 + 0.857\, E\left(\frac{\partial V}{\partial Y}\right)_o^2 \mathcal{Z}^{\frac{1}{3}} \qquad (11.66)$$

The local Nusselt number in the entrance region is therefore
$$Nu = \frac{0.1855\, Pr^{\frac{1}{3}}\, Re^{0.6}\, (x/2r_w)^{-\frac{1}{3}}}{\left[1 + 8.26\ 10^{-4}\, E\, Re(x/2r_w)^{\frac{1}{3}}/Pr^{\frac{1}{3}}\right]}$$

or
$$\frac{Nu}{Nu_o} = \left[1 + 1.532.10^{-4}\, \frac{E}{Nu_o}.Re^{1.6}\right]^{-1}$$

where the usual substitution is made for $\left(\frac{\partial V}{\partial Y}\right)_o$, and Nu_o is the local value of Nu when there is no dissipation.

The equation (11.67) may be compared with the large X solution, equation (11.62). The coefficient $1.532\ 10^{-4}$ in (11.67) is close to the value $2.188\ 10^{-4}$ in (11.62). This indicates that in an equation applicable to allregions, the coefficient would have to be a weak function of axial distance. A constant value would be a reasonable approximation.

Further discussion of the above analysis is included in part 11.2.(vii).

11.2.(vi) TURBULENT FLOW WITH VARIABLE VISCOSITY, AND NO DISSIPATION

The main theoretical work - on variable viscosity with turbulence at high Prandtl number, in tube-flow - has been carried out by Deissler (Ref: C.2). The relationship between Nusselt number at large axial distances and viscosity variation was accounted for by using a weighted reference temperature for determinining the viscosity. If the results are expressed in the exponential form used for the laminar flow cases discussed previously i.e.

$$Nu = Nu\ (\text{constant viscosity}).\ M^{n}_{wall} \ ,$$

then the value of index 'n' increases with Prandtl number. For Pr increasing from 1 to 100, n increases from 0.2 to 0.4. The theory of Deissler was not justified experimentally with high Prandtl number fluids.

Sieder and Tate proposed a value of n of 0.14 (as discussed in part 2.3.(iii)) but this was based on mean Nusselt numbers and a crude experimental technique. Malina (as in part 3.2.(ii)) carried out local measurements with water and oil in long tubes. It was concluded that a satisfactory value of n would be 0.05 for Prandtl numbers up to 75.

Clearly, the effects of viscosity variation must depend strongly on the model of turbulence proposed in a theoretical analysis. Since there is disagreement on the magnitude of these effects (on the Nusselt number) it would be outside the scope of this work to attempt to provide an analytical solution. However, it may be said that for very small axial distances Nu depends on M_{wall} in the same was as in the laminar flow solution. This can be concluded after attempting a perturbation solution of the energy and momentum equations for small axial distances in a similar way to the dissipation solution of part 11.2.(v). It is implied in such an analysis that the only significant variations in viscosity occur in the laminar sublayers, and that for small axial distances the value of exponent n would correspond to the laminar result. Such values were shown in part 11.2.(iii) to be in the range 0.14 to 0.17.

11.2.(vii) DISCUSSION ON THEORETICAL RESULTS AND COMPARISON WITH EXPERIMENT.

The value of the dissipation parameter E ($\equiv \mu \bar{u}^2/qr_w$) was always small in the laminar flow experiments with the short straight tube. The range of E was 3.5×10^{-5} to 2.86×10^{-2}, and the maximum effect was observed at Re = 1,690, Pr = 625. The theoretical reduction in Nu due to dissipation must be maximum at the greatest axial distance (70 diameters) and this was calculated to be 1.7%. Had the tube been of infinite length the result would have been 6.2%. At all other test conditions the reduction was always less than 1%.

It was not possible to justify the theory experimentally because of practical limitations. To increase the value of E suitably it would be necessary to reduce the tube to fluid temperature difference or the cross sectional area of the tube by a factor of approximately 100.

Figure 11.7 shows the theoretical effects of dissipation for constant values of parameter E at large and small values of the (Re x Pr) product. Dissipation is more pronounced at low values of (Re x Pr), and the greatest reduction in Nu occurs at large axial distances.

In the turbulent regime the maximum value of E was 2.8×10^{-3}, and this occurred at Re = 7,750, Pr = 186. Dissipation was shown theoretically, to cause a reduction in Nu of 0.5% at large axial distances. It was impracticable to attempt an empirical study of dissipation during turbulence as explained above in the discussion of laminar flows.

A map of the theoretical results on dissipation is given in figure 11.8. Nusselt numbers greater than 8.48 are considered and both the laminar and turbulent regimes are shown.

The theoretical work on the variable viscosity dependence of Nusselt number was confined to the laminar regime, but it was argued in 11.2.(vi) that the results could be applied to turbulent flow for very short tube lengths. Figure 11.9 records the numerical data of the finite difference solution: values of Nusselt number (≡Nu), the ratio (Nusselt number)/(constant viscosity Nusselt number) (≡ Nu/Nu_o), the ratio (viscosity at local bulk temperature)/(viscosity at local wall temperature) (≡ M_{wall}). The group (Re.Pr) appears in the dimensionless axial distance term (≡ X), and data is shown for specific values of the viscosity variation parameter (≡ ζ) of part 11.2.(iii).

The functions Nu = f(X) are plotted in figure 11.4. The effect of increasing ζ is seen to be an increase in Nu, and this is pronounced at large value of X. When ζ is very large, say 500, there is a limit to the extent to which Nu can be augmented. An inspection of the velocity and temperature profiles (Fig: 11.10) shows that velocity is parabolic in radius when ζ = 0, but tends towards a uniform distribution as ζ becomes large. The temperature profiles corresponding to the two extreme cases give rise to an upper and lower bound on Nu, the former are illustrated in figure 11.4.

The way in which Nu varies with axial distance is demonstrated in figure 11.11 for(Re.Pr) = 10^5 and (Re.Pr) = 10^6. For a particular value of ζ, and at a given location, the ratio ($Nu/Nu_{\zeta=0}$) decreases as (Re.Pr) increases. It is only at considerable axial distances that Nu depends significantly on the parameter ζ. Therefore, in tests designed to investigate viscosity variations, large axial distances must be used (when uniform flux is imposed). It was found (see part 3.5.) that under such circumstances temperature stratification could occur in the fluid due to free convection, and some difficulty was encountered in carrying out the tests.

An attempt at correlating (Nu/Nu_o) with M_{wall} is shown in figure 11.12; the enormous viscosity variations when $\zeta = 500$ are omitted. (Nu/Nu_o) is evidently a very weak function of X, and nearly all the data fall between $(Nu/Nu_o) = M_{wall}^{0.14}$ and $(Nu/Nu_o = M_{wall}^{0.15}$. The exponent 0.14 is identical to that proposed by Sieder and Tate (Ref: D.1) for estimating mean values of Nusselt numbers, Nu_M. A comparison made between $M_{wall}^{0.14}$ and calculated values of (Nu/Nu_o) - figure 11.13 - indicated a maximum difference of approximately $2\frac{1}{2}\%$ at $X \simeq 10^{-4}$. If the exponent 0.15 had been considered, the corresponding difference would have been 0.1%, but this would be combined with a loss of accuracy at larger values of X. For moderate variations in viscosity (say $\zeta < 20$) the errors incurred in using the approximation $M_{wall}^{0.14}$ were much less than 1%.

When $\zeta = 500$, (Nu/Nu_o) was found to be a function of axial distance X. In this region the numerical results became suspect (see part 11.1.(iii)) and merely indicated the trend for very large viscosity variations. Figure 11.14 shows how Nu became asymptotic to the case of uniform velocity heat transfer:

$$Nu = 1.252.X^{-\frac{1}{2}} . \quad \text{(see appendix B).}$$

An alternative expression used is stated

$$(Nu/Nu_o) = 0.895\ (\zeta/\log M_{wall})^{\frac{1}{3}}.$$

It is improbable that, in practice, M_{wall} would be great enough to approach the asymptotic case described above.

The analytical solution obtained for small values of X indicated that $(Nu/Nu_o)_{X \to 0} = M_{wall}^{0.17}$. This was compatible with the finite difference results which showed the exponent to increase from 0.14 to 0.15 with decreasing X. In the analysis it was considered unnecessary to generate more than the linear perturbation terms in the solution, because the main objectives were adequately demonstrated as follows. The dependence of Nu on M_{wall} was substantially the same for large and small values of axial distance, and the assumption $(Nu/Nu_o) = f(M_{wall})$ was valid in the entrance region.

Both the findings of Yang (Ref: D.3) and Shannon (Ref:D.10) are at variance with the above theoretical results. The data of Yang were interpreted and compared graphically in figure 11.12; the data of Shannon could not be extracted in the same form, but it suffices to say that at small values of X the exponent of M_{wall} tended to 0.3 approximately.

The experimental dependence of Nu on M_{wall} could not be derived readily. This was due to the effects of free convection. In part 9.5. of the thesis the empirical findings are discussed.

In analysing heat transfer with turbulent flow in the entrance region, two expressions were derived which enabled Nu to be estimated at small and large values of axial distance. The wall-gradient "$\frac{\partial V}{\partial Y_o}$" and constant "a" appear in both results. The former can be evaluated from the well known empirical relationship $\frac{\partial V}{\partial Y_o} = 0.0115\ Re^{0.8}$ proposed in part 11.1.(iv), but the reliability of this expression comes into question at the lower values of Re in the turbulent regime. Such Reynolds numbers (say 10^4) were encountered in the experiments, so a new expression was sought based on measurements of pressure-drop in tubes. Figure 11.15 shows the function $\frac{\partial V}{\partial Y_o}$ versus Re according to Kays (Ref: K.20). For the range 4,000 < Re < 10,000, the following formula was determined

$$\frac{\partial V}{\partial Y_o} = 3.18 \times 10^{-4}\ Re^{1.2} .$$

Whereas, the existing formulae suffice for Re > 10,000 (i.e. Eq. 11.54 and 11.56) their counterparts, incorporating the new $\frac{\partial V}{\partial Y_o}$, permit a comparison between theory and experiment.

The revised formulae are -

at large X, $$Nu_\infty = 0.02087\ a^{\frac{1}{3}}\ Re^{1.1}\ Pr^{\frac{1}{3}} \qquad (11.68)$$

at small X, $$Nu = \frac{0.05625 Re^{0.733}(x/2r_w)^{-\frac{1}{3}}\ Pr^{\frac{1}{3}}}{1 - 0.01077.\ a.(x/2r_w)\ Re^{1.1}} \qquad (11.69)$$

A suitable value for "a" was derived by comparing equation 11.68 with experiment. Inserting $a = 5.22 \times 10^{-4}$ into equations 11.68 and 11.69, results in -

at large X, $$Nu_\infty = 1.68 \times 10^{-3}\ Re^{1.1}\ Pr^{\frac{1}{3}} \qquad (11.70)$$

at small X, $$Nu = \frac{0.0562\ Re^{0.733}(x/2r_w)^{-\frac{1}{3}}\ Pr^{\frac{1}{3}}}{1 - 5.62 \times 10^{-6}(x/2r_w)\ Re^{1.1}} \qquad (11.71)$$

In figure 11.16 a comparison between experiment and theory is shown for a small distance (1 diameter) and a large distance (70 diameters). Reasonable agreement is demonstrated. The experimental Nusselt numbbrs used were corrected for viscosity variation and the graph shown represents the best fit through the data.

The most important conclusion which can be drawn from the theory is that Nu can be represented by a relationship of the kind

$$Nu = Pr^{\frac{1}{3}}.\ f\ (Re, X)$$

at small and large values of axial distance. This simplifies the analysis of experimental data, as a comparison with initial proposal

$Nu = f\ (Pr, Re, X)$ indicates. Prandtl number is eliminated as an independent variable.

In addition, the asymptotic behaviour of Nu with distance is shown. This helps to justify the experimental findings near the start of heating where heat conduction in the tube wall becomes significant, and may be used in the absence of experimental data for distances of less than one diameter.

The asymptotic behaviour is demonstrated in figure 11.17 where the experimental variation in Nu with distance, Re and Pr is shown. As Re increase from 4,000 to 10,000, the temperature profile develops more rapidly, the fully developed state being reached in 15 and 4 diameters respectively. Since the 'small X' result can only be valid for about 25% of this length, it was not possible to obtain experimental corroboration of the theory at high Reynolds numbers. Nevertheless, a reasonable agreement is shown, even when the 'small X' result is taken to its limit (the function is minimised when the denominator becomes 0.75). The maximum difference between theory and experiment increased from 3% to 12% as Re was increased. The error is consistent with the accuracy of the approximate expression for $\frac{\partial V}{\partial Y_o}$, which overestimated the data of Kays by 10% at Re = 10,000.

Finally, the theory may be used to produce a semi-theoretical expression for Nu valid at all distances along the tube. An interpolation is carried out between small and large distance asymptotes, in the region $4,000 < Re < 10,000$ (similar expressions can easily be determined for any other range of Re).

In the proceding analysis for small values of $\theta\ (x)$

$$f\ (o) = f_o(o) + \theta\ f_1(o).$$

Now suppose for moderate values of θ a better value of $f(o)$ is given by

$$f(o) = f_o(o) + \lambda.\theta.f_1(o)$$

where λ is a correction factor of the order unity. Selecting a suitable value for λ the condition $\frac{\partial \theta}{\delta x} = 0$ at $Nu = Nu_\infty$ can be satisfied. Hence, λ is chosen to be 0.512.

This leads to an expression for enctrance length as follows:

$$\left(\frac{x}{2r_w}\right)_{max} = 8.69 \times 10^4 . \, Re^{-1.1} \quad . \tag{11.72}$$

It is possible that a more accurate result for f(o) could be obtained by generating further terms in the series, though this would make the problem much more complicated, and was not considered to be a suitable approach.

The resulting Nusselt number becomes

$$Nu = \frac{0.0562 \, Re^{0.733} (x/2r_w)^{-\frac{1}{3}} \, Pr^{\frac{1}{3}}}{1 - 2.87 \times 10^{-6} \left(\frac{x}{2r_w}\right) Re^{1.1}} \tag{11.73}$$

This equation is plotted in figure 11.18 together with the experimental results, and resonable agreement is indicated.

11.3. THE DIVERGENCE.

11.3.(i) Introduction.

The measured values of the local heat-transfer coefficient in the region of a sudden divergence in diameter exhibited certain characteristics which could not be readily explained. In an attempt to understand the mechanisms of heat transfer the following theoretical analysis of the system was carried out. Initially, the work was motivated by the fact that very low coefficients of heat transfer were obtained at small Reynolds numbers ($\sim 10^2$). These differed markedly in magnitude and axial distribution to the measured values at moderate Re ($< 10^3$). It was considered necessary to show that such low coefficients were not simply indicative of some unacknowledged limitation on the means of measurement.

FIGURE 11.1

HYPOTHETICAL DESCRIPTION OF FLOW THROUGH A DIVERGENCE AND TYPICAL, LOCAL COEFFICIENTS OF HEAT TRANSFER.

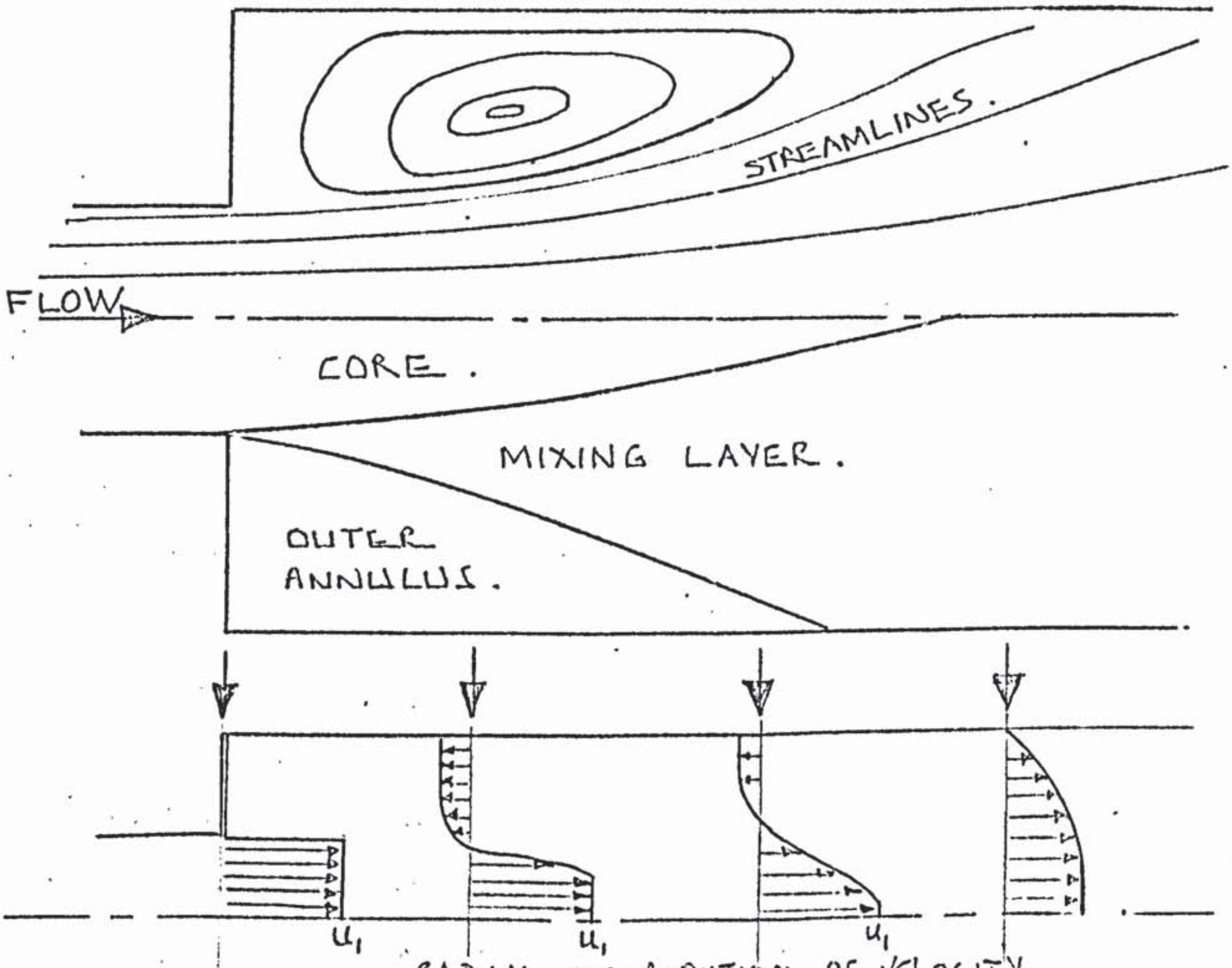

RADIAL DISTRIBUTION OF VELOCITY.

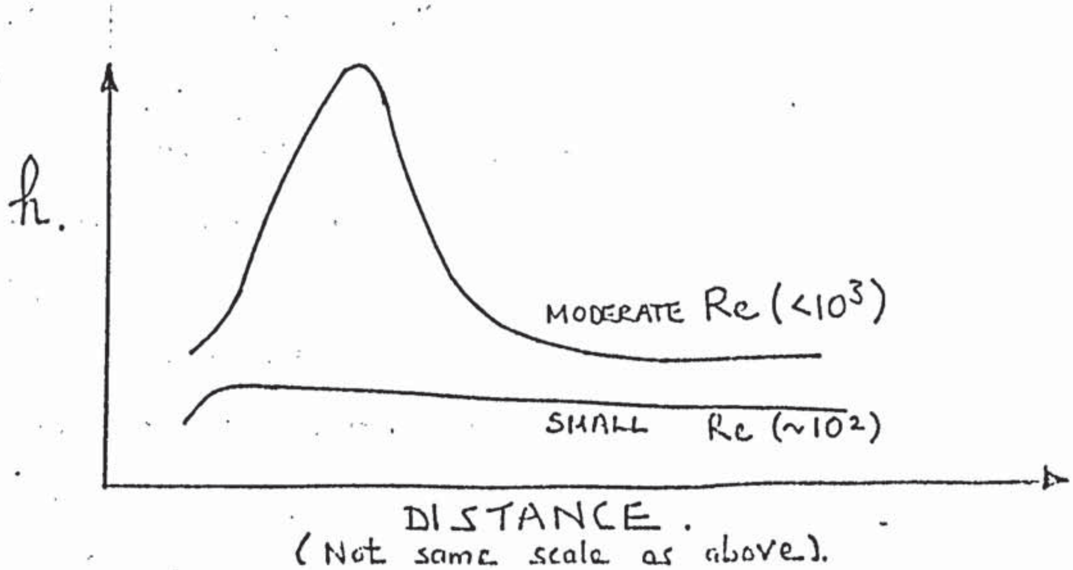

LOCAL COEFFICIENTS OF HEAT TRANSFER.

Figure 11.1 illustrates the probable flow development through a sudden divergence, and shows the axial distribution of the local coefficient of heat transfer in general terms. The flow pattern is similar to that proposed by Abramovitch for turbulent wakes behind enclosed, bluff bodies (Ref: K.7), but the diagram can be taken as applicable to both turbulent and laminar flows provided they are stable. Abramovitch envisaged a simple, boundary-layer model in which the initial part of the divergence was at constant pressure, and contained an inner, fast moving core having uniform velocity. A slow reverse flow occurred in the outer annulus, which also had a uniform, radial velocity distribution, and a mixing layer was positioned between the two uniform streams in which the shape of the velocity profile was assumed. Further downstream the velocity profile was supposed to flatten as the source of inertia in the core became depleted, and the mixing layer thickened. This region of the flow was solved by an inviscid analysis.

Omissions have been made in the above description for brevity, but a qualitative description is given for the way in which a standing eddy is formed downstream of a step. However, it is doubtful whether such boundary layer simplifications can be used to determine reliable temperature distributions in a divergence. A recent attempt by Filetti (Ref: H.8) to describe heat transfer to air in a divergence, indicated that such simplifications were unacceptable.

The analysis of a two-dimensional flow with recirculation invariably leads to a numerical solution of the momentum equations. This implies the finite-difference solution of two elliptic, partial differential equations. Until recently, the difficulty in obtaining a stable result, with recirculation present, limited such solutions to extremely small Reynolds numbers. The work of Gosman et al

(Ref: J.13) has made available a general procedure for solving such problems with the likelihood of a much improved stability.

The latter method was applied to the problem at hand, i.e. flow through a divergence with heat transfer. The ratio of upstream to downstream diameters was 1:2, but the computer programme discussed in this section can be used for other ratios with small modifications. An extensive theoretical investigation was not the objective of this analysis, but the mathematical procedure was utilised as a tool with which to explain the mechanisms of heat transfer.

In deriving the particular form of the momentum and energy equations required for a numerical solution (given in the next part 11.3(ii)) the operation described is simpler than the original explanation of Gosman (Ref: J.13). The reason for this is because the physical properties are assumed to be constant, and the system is specified at the outset as having 'cylindrical, polar co-ordinates'. The flow is further assumed to be axi-symmetrical.

11.3.(ii) The derivation of themomentum and energy equations.

11.3.(ii)a. The symbols used throughout are similar to those favoured by Gosman (Ref: J.13), so as to eliminate confusion when referring to the original source. These definitions are local to the present section 11.3. only.

Consider the co-ordinates below -

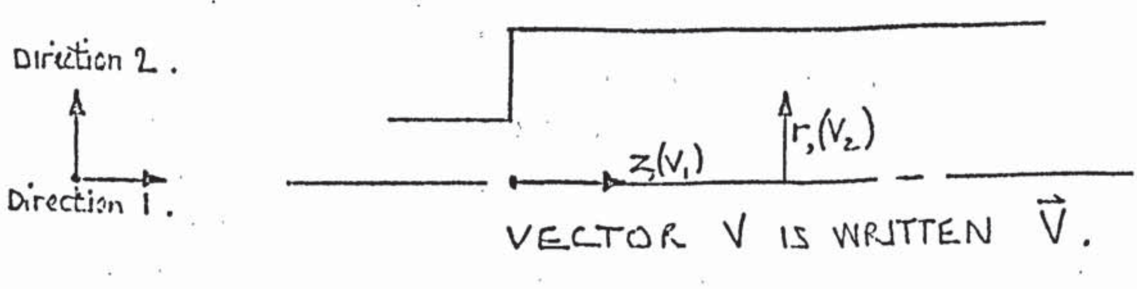

The nomenclature is first specified -

Programming Symbols.	Text Symbols	Meaning.
X1(I)	Z	axial distance
X2(J)	r	radial distance
NV1,NV2 *	V1,V2	axial, radial velocities
	p	pressure
NW *	(ω/r)	(vorticity/radius)
NF *	ψ	stream function
NT *	t	temperature
NRO *	ρ	density
NMU *	μ	viscosity
	C'	specific heat capacity
	K'	thermal conductivity
	ϕ	generalised dependent variable in text
	$a_\phi, b_\phi, c_\phi, d_\phi$	coefficients in generalised form of differential equation

A(I,J,K)	array for the general dependent variable
AE, AW, AN, AS.	the coefficients $A_j^!$ defined in text.
APP	The coefficient $a_{\phi P}$ in integrated form of general equation.
BE(I),BW(I), BN(J),BS(J)	the coefficients $B_j^!$ defined in text.
BPP	the coefficient $b_{\phi P}$ in integrated form of general equation.
CC	convergence criterion (maximum residual).
I	index for constant Z lines.
IE	number of differential equations to be solved.
IMAX(J), IMIN(J)	the I - indices denoting nodes adjacent to the wall and axis.
IN	total number of constant Z grid lines
INM	IN - 1
IP	number of successive printouts required
IV	number of variables to be output.
J	index for constant r lines
JN	total number of constant r grid lines.
JNM	JN - 1
NBEGIN	index of first variable to be output
NCORD	a number given to particular co-ordinate system.
NITER	number of iterations carried out.
NMAX	maximum number of iterations.

Programming Symbols.	Meaning.
NPRINT	number of iterations between printout
NTOTAL	number of variables output.
PR(K)	Prandtl number for variable K.
QK	(Heat flux)/(thermal conductivity).
R(J)	distance from axis.
RES	maximum residual for all ϕ equations.
ROREF	refernnce density.
RP(K)	relaxation parameters α, used in updating ϕ viz: $\phi = \alpha \phi^{(N)} + (1 - \alpha)\ \phi^{(N-1)}$, where $\phi^{(N)}$ and $\phi^{(N-1)}$ are values computed at consecutive iterations.
RS	residual, or $(1 - \phi_P^{(N)}/\phi_P^{(N-1)})$.
RSDU(K)	maximum value of RS for each ϕ.*
SOURCE	$-d_{\phi P}$ in generalised differential equation.
ZMUREF	reference viscosity.

* Index corresponding to K in array A.

11.3.(ii)b. The momentum equations in directions 1 and 2 can be written down

$$\operatorname{div}\left(\rho V_2\vec{V}-\vec{T}_1\right)+\frac{\partial p}{\partial Z}=0$$

$$\operatorname{div}\left(\rho \bar{V}_2\vec{V}-\vec{T}_2\right)+\frac{2\mu V_2}{r^2}+\frac{\partial p}{\partial r}=0$$

where $\operatorname{div}(\vec{f})=\frac{1}{r}\frac{\partial}{\partial r}(f_2 r)+\frac{1}{r}\frac{\partial}{\partial Z}(f_1 r)$,

and the stress components are

$$T_{1,1}=2\mu\frac{\partial V_1}{\partial Z}\quad,\quad T_{1,2}=\mu\left(\frac{\partial V_1}{\partial r}+\frac{\partial V_2}{\partial Z}\right)$$

$$T_{2,1}=T_{1,2}\quad,\quad T_{2,2}=2\mu\frac{\partial V_2}{\partial r}\ .$$

The continuity equation is written

$$\operatorname{div}\vec{V}=0\ .$$

The equations above are quoted in many standard text books and require no proof.

It is convenient to eliminate the pressure gradients by introducing vorticity into the equations, as defined by -

$$\omega=\frac{\partial V_2}{\partial Z}-\frac{\partial V_1}{\partial r}\ .$$

Differentiating the direction 1 euqation with respect to r, and the direction 2 equation with respect to Z, gives rise to similar pressure terms, which are eliminated by combining the equations thus

$$\rho\frac{\partial}{\partial Z}\left(\operatorname{div}(V_2\vec{V})\right)-\rho\frac{\partial}{\partial r}\left(\operatorname{div}(V_1\vec{V})\right)=\frac{\partial}{\partial Z}\left(\operatorname{div}\vec{T}_2\right)-\frac{\partial}{\partial r}\left(\operatorname{div}\vec{T}_1\right)-\frac{\partial}{\partial Z}\left(\frac{2\mu V_2}{r^2}\right),$$

or after introducing the vorticity

$$\rho r\left(\operatorname{div}\frac{\vec{V}\omega}{r}\right)=\frac{\partial}{\partial Z}\left(\operatorname{div}\vec{T}_2\right)-\frac{\partial}{\partial r}\left(\operatorname{div}\vec{T}_1\right)-\frac{\partial}{\partial Z}\left(2\frac{\mu V_2}{r^2}\right)=\Omega,\ \text{say.}$$

Expanding the right hand side of the equation, Ω , the following is obtained

$$\Omega = \frac{\partial}{\partial Z}\left\{\frac{\partial}{\partial Z}\left[\mu\left(\frac{\partial V_1}{\partial r} + \frac{\partial V_2}{\partial Z}\right)\right] + \frac{1}{r}\frac{\partial}{\partial r}\left[\mu r\left(\frac{2\partial V_2}{\partial r}\right)\right]\right\} -$$
$$-\frac{\partial}{\partial r}\left\{\frac{\partial}{\partial Z}\left[\mu\left(\frac{2\partial V_1}{\partial Z}\right)\right] + \frac{1}{r}\frac{\partial}{\partial r}\left[\mu r\left(\frac{\partial V_1}{\partial r} + \frac{\partial V_2}{\partial Z}\right)\right]\right\} -$$
$$-\frac{\partial}{\partial Z}\left\{\frac{\mu}{r}\left[2\frac{V_2}{r}\right]\right\}.$$

The first and third terms (denoted by a square bracket) can be combined to introduce vorticity; the second and fourth terms are combined in a similar way, hence

$$\mu^{-1}\Omega = \frac{\partial^2\omega}{\partial Z^2} + \frac{\partial}{\partial r}\left(\frac{1}{r}\frac{\partial}{\partial r}\left[\omega r\right]\right) + 2\left(\frac{\partial}{\partial Z}\left[\frac{1}{r}\frac{\partial V_2}{\partial r}\right] - \frac{\partial}{\partial r}\left[\frac{1}{r}\frac{\partial V_1}{\partial Z}\right] - \frac{\partial}{\partial Z}\left[\frac{V_2}{r^2}\right]\right).$$

The next step is to replace the remaining velocity terms on both sides of the equation by the stream function, which is an expedient to eliminate the continuity equation from the calculations. The velocities are $V_1 = \frac{1}{\rho r}\frac{\partial\psi}{\partial r}$, $V_2 = -\frac{1}{\rho r}\frac{\partial\psi}{\partial Z}$.

Now, the final form of the momentum equation is

$$r^2\left(\frac{\partial}{\partial Z}\left[\frac{\omega}{r}\frac{\partial\psi}{\partial r}\right] - \frac{\partial}{\partial r}\left(\frac{\omega}{r}\frac{\partial\psi}{\partial Z}\right]\right) - \frac{\partial}{\partial Z}\left(r^3\frac{\partial}{\partial Z}\left[\frac{\mu\omega}{r}\right]\right) - \frac{\partial}{\partial r}\left(r^3\frac{\partial}{\partial r}\left[\frac{\mu\omega}{r}\right]\right) = 0.$$

This rather complicated form of the momentum equation has close similarity to the energy equation, soon to be derived, hence its unconventional appearance.

The vorticity equation can be written in terms of the stream function $\frac{\partial}{\partial Z}\left(\frac{1}{\rho r}\frac{\partial\psi}{\partial Z}\right) + \frac{\partial}{\partial r}\left(\frac{1}{\rho r}\frac{\partial\psi}{\partial r}\right) + \omega = 0.$

11.3.(ii)c. The energy equation is simplified by neglecting the dissipation of mechanical energy into heat, hence

$$\frac{\partial}{\partial Z}\left(\rho C' V_1 t r\right) + \frac{\partial}{\partial r}\left(\rho C' V_2 t r\right) = \frac{\partial}{\partial Z}\left(K' r \frac{\partial t}{\partial Z}\right) + \frac{\partial}{\partial r}\left(K' \, r \frac{\partial t}{\partial r}\right).$$

Replacing the velocity by the stream function, then defining the exchange coefficient $\Gamma = K'/C'$, the equation becomes

$$\frac{\partial}{\partial Z}\left(t\frac{\partial \psi}{\partial r}\right) - \frac{\partial}{\partial r}\left(t\frac{\partial \psi}{\partial Z}\right) - \frac{\partial}{\partial Z}\left(\Gamma r \frac{\partial t}{\partial Z}\right) - \frac{\partial}{\partial r}\left(\Gamma r \frac{\partial t}{\partial r}\right) = 0.$$

11.3.(iii) The General Equation.

Three differential equations are to be solved in ω, ψ and t. The velocity components can be readily determined from this information. A single, elliptic, partial differential equation can be stated having a similar form to the three equations derived. This reduces the numerical procedure to the solution of only one equation, which is -

$$a_\phi\left\{\frac{\partial}{\partial Z}\left(\phi\frac{\partial \psi}{\partial r}\right) - \frac{\partial}{\partial r}\left(\phi\frac{\partial \psi}{\partial Z}\right)\right\} - \frac{\partial}{\partial Z}\left\{b_\phi r\frac{\partial}{\partial Z}\left(c_\phi \phi\right)\right\} - \frac{\partial}{\partial r}\left\{b_\phi r \frac{\partial}{\partial r}\left(c_\phi \phi\right)\right\} + r d_\phi = 0.$$

where the parameters are

ϕ	a_ϕ	b_ϕ	c_ϕ	d_ϕ
t	1	Γ	1	0
(ω/r)	r^2	r^2	μ	0
ψ	0	$(\rho r^2)^{-1}$	1	$-(\omega/r)$

11.3.(iv) Outline of the Mathematical Solution.

The numerical solution of the general equation - after Gosman (Ref: J.13) - will be described briefly.

The equation is integrated approximately over small, finite elements in the field of interest. Parallel grid lines intersect at nodal points, P, which are not necessarily equi-spaced. The notation is given below.

N, E, W. and S are adjacent nodes.

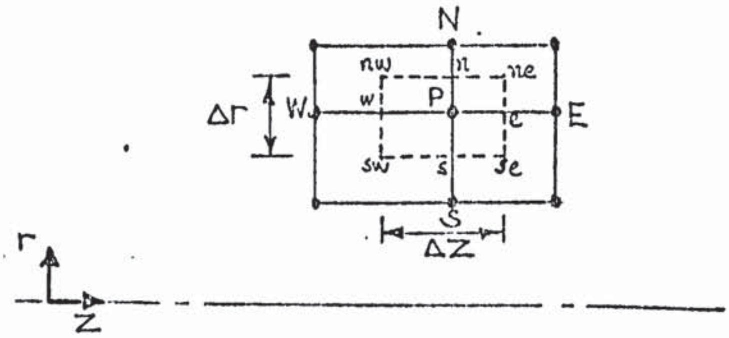

The integration required is

$$\int_{r_s}^{r_n}\int_{Z_w}^{Z_e} a_\phi \left\{ \frac{\partial}{\partial Z}\left(\phi \frac{\partial \psi}{\partial r}\right) - \frac{\partial}{\partial r}\left(\phi \frac{\partial \psi}{\partial Z}\right) \right\} dZ\,dr \; -$$

$$- \int_{r_s}^{r_n}\int_{Z_w}^{Z_e} \left\{ \frac{\partial}{\partial Z}\left(b_\phi r \frac{\partial}{\partial Z}\left[c_\phi \phi\right]\right) + \frac{\partial}{\partial r}\left(b_\phi r \frac{\partial}{\partial r}\left[c_\phi \phi\right]\right) \right\} dZ\,dr \; +$$

$$+ \int_{r_s}^{r_n}\int_{Z_w}^{Z_e} (r d_\phi)\, dZ\,dr \quad = \quad 0 \, .$$

To illustrate the process, one term of each integral is considered. The first part of the first integral, I_c, becomes

$$I_c = \int_{r_s}^{r_n}\int_{Z_w}^{Z_e} a_\phi \frac{\partial}{\partial Z}\left(\phi \frac{\partial \psi}{\partial r}\right) dZ\,dr \simeq \; a_{\phi P}\, \bar{\phi}_e (\psi_{ne} - \psi_{se})$$

where $\bar{\phi}$ is the value of ϕ upstream of the e-face, ie. ϕ_P or ϕ_E depending on the flow direction. Hence -

$$I_c \simeq \frac{a_{\phi P}}{2}\left[\phi_E\left\{(\psi_{ne} - \psi_{se}) - \left|\psi_{ne} - \psi_{se}\right|\right\} + \phi_P\left\{(\psi_{ne} - \psi_{se}) + \left|\psi_{ne} - \psi_{se}\right|\right\}\right]$$

The form of I_c ensures that upstream differences are always selected, and the stability of the solution improves considerably because of this. The inter-nodal values are approximated by

$$\psi_{se} \simeq (\psi_{SE} + \psi_E + \psi_P + \psi_S)/4 \, .$$

The first term of the second integral, I_d, is

$$I_d = \int_{r_s}^{r_n}\int_{Z_w}^{Z_e} \frac{\partial}{\partial Z}\left(b_\phi r \frac{\partial}{\partial Z}\left[c_\phi \phi\right]\right) dZ\,dr$$

$$\simeq \frac{(b_{\phi E} + b_{\phi P})}{2} \cdot \frac{(r_E + r_P)}{2} \cdot \frac{(c_{\phi E}\phi_E - c_{\phi P}\phi_P)}{(Z_E - Z_P)} \cdot \frac{(r_n - r_s)}{2}$$

The third integral, I_{SOR}, becomes

$$I_{SOR} = \int_{r_s}^{r_n}\int_{Z_w}^{Z_e} r\, d_\phi \, dZ\, dr \simeq d_{\phi P} V_P$$

where $$V_P = \frac{(Z_E - Z_W)}{2} \cdot \frac{(r_N - r_S)}{2} r_P$$

The general differential equation can now be replaced by an algebraic equation, as follows.

$$A_E(\phi_P - \phi_E) + A_W(\phi_P - \phi_E) + A_N(\phi_P - \phi_N) + A_S(\phi_P - \phi_S) -$$
$$- B_E(c_{\phi E}\phi_E - c_{\phi P}\phi_P) - B_W(c_{\phi W}\phi_W - c_{\phi P}\phi_P) - B_N(c_{\phi N}\phi_N - c_{\phi P}\phi_P) -$$
$$- B_S(c_{\phi S}\phi_S - c_{\phi P}\phi_P) + d_{\phi P}V_P = 0.$$

Where the coefficients of $\emptyset$ are as stated at the end of this section 11.3.(iv).

The algebraic equation is solved for $\emptyset_P$ by an iterative procedure, in which the field is scanned repeatedly updating the value of $\emptyset_P$ at each node. The order of scanning is - increasing Z then increasing r. Initially, a guess at the $\emptyset$ distribution is necessary, then the data from any five adjacent nodes is used to obtain a better value of $\emptyset_P$ at each position.

The form of the numerical equation must now be changed to permit the procedure to be implemented. Therefore

$$\underline{\emptyset_P = C_E\,\emptyset_E + C_W\emptyset_W + C_N\,\emptyset_N + C_S\emptyset_S + D}$$

where $C_E = (A_E + B_E c_{\phi N})/\sum_{AB}$, $C_W = (A_W + B_W c_{\phi W})/\sum_{AB}$,

$C_N = (A_N + B_N c_{\phi N})/\sum_{AB}$, $C_S = (A_S + B_S c_{\phi S})/\sum_{AB}$,

and $D = -d_{\phi P} V_P / \sum_{AB}$,

$$\sum_{AB} = A_E + A_W + A_N + A_S + c_{\phi P}(B_E + B_W + B_N + B_S), \quad V_P = \frac{r_P}{4}(Z_E - Z_W)(r_N - r_S).$$

The coefficients A are in terms of the stream function, and the coefficients B are in terms of spatial parameters only.

$$A_E = \frac{a_{\phi P}}{8}\left[\left(\psi_{SE} + \psi_S - \psi_{NE} - \psi_N\right) + \left|\psi_{SE} + \psi_S - \psi_{NE} - \psi_N\right|\right]$$

$$A_W = \frac{a_{\phi P}}{8}\left[\left(\psi_{NW} + \psi_N - \psi_{SW} - \psi_S\right) + \left|\psi_{NW} + \psi_N - \psi_{SW} - \psi_S\right|\right]$$

$$A_N = \frac{a_{\phi P}}{8}\left[\left(\psi_{NE} + \psi_E - \psi_{NW} - \psi_W\right) + \left|\psi_{NE} + \psi_N - \psi_{NW} - \psi_W\right|\right]$$

$$A_S = \frac{a_{\phi P}}{8}\left[\left(\psi_{SW} + \psi_W - \psi_{SE} - \psi_E\right) + \left|\psi_{SW} + \psi_W - \psi_{SE} - \psi_E\right|\right]$$

$$B_E = \frac{(b_{\phi E} + b_{\phi P})}{8} \cdot \frac{(r_N - r_S)}{(z_E - z_P)} \cdot (r_E + r_P)$$

$$B_W = \frac{(b_{\phi W} + b_{\phi P})}{8} \cdot \frac{(r_N - r_S)}{(z_P - z_W)} \cdot (r_W + r_P)$$

$$B_N = \frac{(b_{\phi N} + b_{\phi P})}{8} \cdot \frac{(z_E - z_W)}{(r_N - r_P)} \cdot (r_N + r_P).$$

$$B_S = \frac{(b_{\phi S} + b_{\phi P})}{8} \cdot \frac{(z_E - z_W)}{(r_P - r_S)} \cdot (r_S + r_P)$$

The complicated problem posed initially reduces to three solutions of the finite difference equation above.

In the original text (Ref: J.13) considerable space was devoted to the discussion of convergence, and of truncation errors. In this application it will simply be stated that small truncation errors are inevitable, but these have been minimised by the selection of small finite elements at the expense of considerable computer time.

No attempt was made to under or over-relax the solution, (i.e. correcting the updated values of ϕ_P by a multiple of the difference between successive iterations, the multiple being the relaxation parameter) and the relaxation parameter was set at unity.

Conditions at the boundary must be specified to define the specific problem. The next section deals with these conditions.

11.3.(v) Boundary conditions.

For uniform property flow through the divergence the boundary conditions, with uniform heat flux can be specified as in the diagram below.

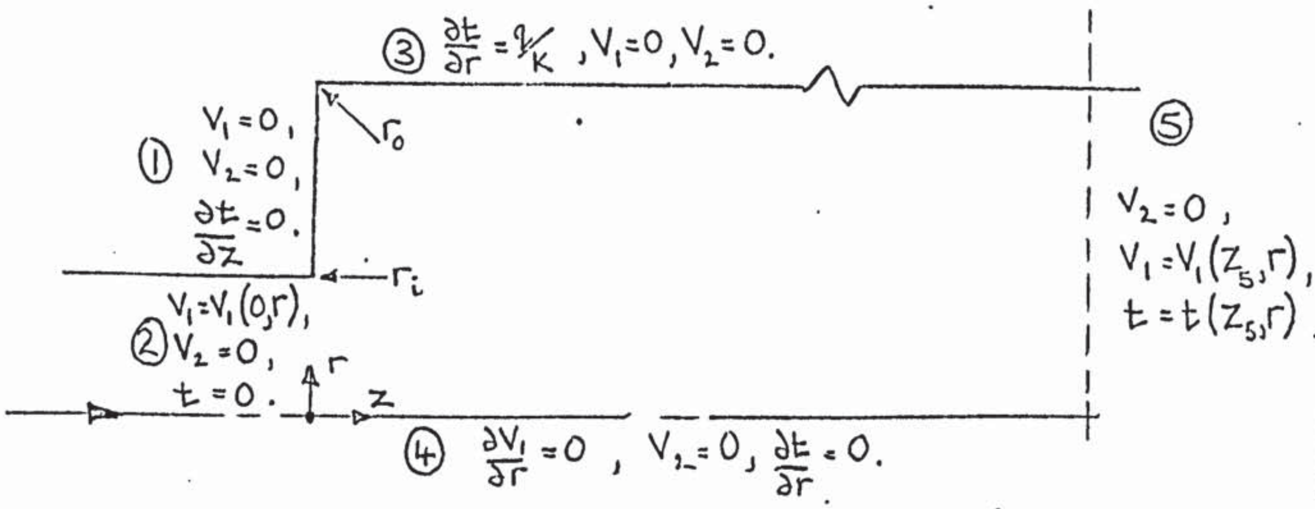

At the inlet (2) the velocity is specified as parabolic in r for laminar flow, or uniform in r for turbulent flow.

At the outlet (5), the boundary conditions are not critical because being far downstream they were unlikely a priori to affect the temperature and flow near to the divergence. The boundary values selected were found by experience to give a tolerable rate of convergence, whereas gradient-type conditions were found to be very slow. The temperature was put equal to the bulk temperature, and the flow was assumed to be fully developed (i.e. parabolic, axial velocity for laminar flow, and uniform velocity for turbulent flow).

The conditions posed are readily converted into vorticity and stream function, as follows:

At (1) $V_1 = \frac{1}{\rho r}\frac{\partial \psi}{\partial r}$ = therefore $\psi = \psi_I$, constant along the wall.

The vorticity at the wall is replaced by an equation relating vorticity to stream function -

Suppose that P is a wall-node, and NP is the nearest node to the wall. Linearising the vorticity near the wall gives

$$\omega_{NP} \cong \frac{A'(Z_{NP} - Z_P) + B'}{\mu}.$$

From the definition of stream function

$$(\psi_{NP} - \psi_P) = -\rho r_P \int_{Z_P}^{Z_{NP}}\int_{Z_P}^{Z_{NP}} \frac{A'(z-z_P)+B'}{\mu}\, dz\, dz ,$$

$$= \frac{-\rho r_P}{\mu}\left[\frac{A'}{6}(Z_{NP}-Z_P)^3 + \frac{B'}{2}(Z_{NP}-Z_P)^2\right]$$

Combining the two expressions

$$\left(\frac{\omega}{r}\right)_P = -\left(\frac{3(\psi_{NP}-\psi_P)}{\rho r_P^2 (Z_P - Z_{NP})} + \frac{\omega_{NP}}{2r_P}\right)$$

At (2) $V_1(o,r)$ is expressed in terms of stream function.

$$V_1(0,r) = V_1(0,0)\left[1-(r/r_i)^2\right]$$, for laminar flow,

so that

$$\psi = \rho V_1(0,0)\left[(r^2/2) - (r^4/4r_i^2)\right)$$

The vorticity is $\omega = -\partial V_1/\partial r$

therefore $$\left(\frac{\omega}{r}\right) = \frac{2V_1(0,0)}{r_i^2} .$$

At (3) the stream function is again $\psi = \psi_T$, and the vorticity equation is derived in the same way as at the shoulder (1).

Hence $$\left(\frac{\omega}{r}\right)_P = \left(\frac{3(\psi_{NP}-\psi_P)}{\rho r_P^2 (r_P - r_{NP})^2} + \frac{\omega_{NP}}{2r_P}\right)$$

At (4) the stream function is zero (any constant suffices) for symmetry, and the vorticity at the axis is found by approximating the axial velocity with a parabola. $V_1 = \bar{A}r + \bar{B}r^2$.

From the definition of stream function $\psi = V_1(0,0)\frac{r^2}{2} + \frac{\bar{B}r^4}{8}$,

and since $\omega = -\partial V_1/\partial r$,

$$\left(\frac{\omega}{r}\right)_P = \frac{8}{\rho}\left[(\psi_{NP1}/r_{NP1}^2) - (\psi_{NP}/r_{NP}^2)\right] \Big/ \left(r_{NP}^2 - r_{NP1}^2\right) ,$$

where NP and NPI are nodes which are once and twice removed from the axis.

The bulk temperature is given by

$$t_{bulk} = \left(\frac{4q}{K'}\Big/ Re\,Pr\right)Z .$$

11.3.(vi) The computer programme.

The programme for solving the equations described is given in this section. It is very similar to that proposed by Gosman, named ANSWER, therefore it is unnecessary to describe the general contruction. A step by step description of the component parts has been included in the programme itself, and the language ALGOL 60 has been utilised instead of the original FORTRAN IV. Close inspection of the programme would be necessary before modifying it to suit a different problem. The particular example given applies to laminar flow with uniform flux heat-transfer and constant physical properties. The computations were carried out on an ICL 1905 computer.

Before rewriting the equations in programming symbols the general substitution formula must be slightly altered, for convenience, by putting

$$\phi_P = \frac{\sum_{j=N,S,E,W} \left[A_j' + c_{\phi j}(b_{\phi j} + b_{\phi P}) B_j' \right] \phi_j - d_{\phi P}}{\sum_{j=N,S,E,W} \left[A_j' + c_{\phi P}(b_{\phi j} + b_{\phi P}) B_j' \right]}$$

where $$A_j' = A_j / V_P \quad ,$$

and $$B_j' = B_j / V_P (b_{\phi j} + b_{\phi P}) \; .$$

To improve the stability of the solution when a non-uniform grid is specified, the vorticity at the wall is eliminated from those calculations appertaining to the 'near wall' nodes. This is achieved by introducing another form of the substitution equation in which the vorticity at the wall is replaced by that boundary condition, (11.3.(v)) which relates vorticity to stream function. This is referred to in the programme itself.

In making use of the programme described, a converged solution was obtained after approximately 130 iterations, each requiring 6 seconds of the total time. The number of iterations could have been drastically reduced by selecting fewer nodes, with an ensuing loss of accuracy. The total number required for convergence was found to increase with Reynolds number and Prandtl number. It is generally known that comparatively slow convergence ensues when uniform flux is specified rather than uniform wall temperature, so substantial computing times were anticipated.

```
'BEGIN'
'COMMENT'    MESTF116      ANSWER;
'INTEGER'    IN,JN;
                           IN:=READ;      JN:=READ;
'BEGIN'

'COMMENT'    DECLARATION OF VARIABLES;
       'REAL' AE,AW,AN,AS,APP,BBF,BBW,BBN,BBS,BPP,CC,RES,ROREF,RS,SOURCE,
              ZMUREF,RE,QK,QKRP,H2,RX2,DELX2,C1,C2,Z,DX2,DX1,ANUM,ADNM,
              RISQ,ROP,RSQ,DX2SQ,TERM1,TERM2;
     'INTEGER' I,IE,INM,IP,IV,J,JNM,K,NBEGIN,NCORD,NW,NF,NT,NV1,NV2,NMU,
              NRO,NL,NITER,NMAX,NPRINT,NTOTAL,IL,IH,H1,RX1,P;
'REAL' 'ARRAY' A[1:IN,1:JN,1:8],CE,RW[1:IN],DN,RS[1:JN],PR[1:8],R[1:JN],
              RP,RSDU[1:9],X1[1:IN],X2[1:JN];
'INTEGER' 'ARRAY' IMAX,IMIN[1:JN];


'PROCEDURE' VISCOS(NMU);
'INTEGER' NMU;
'COMMENT'    COMPUTES EFFECTIVE VISCOSITY;
'BEGIN'      'FOR' J:=1 'STEP' 1 'UNTIL' JN 'DO'
             'FOR' I:=1 'STEP' 1 'UNTIL' IN 'DO'
                       A[I,J,NMU]:=ZMUREF;
'END' VISCOS;


'PROCEDURE' SORCE(SOURCE);
'REAL' SOURCE;
                        'COMMENT'  CALC SOURCE TERMS ;
'BEGIN'                'IF' K=2 'THEN'     SOURCE:=A[I,J,NW];
                       'IF' K'NE'2 'THEN' SOURCE:=0;
'END' SORCE;


'PROCEDURE' CONVEC(K);
'COMMENT'    CALC AE,AW,AN,AS;
'INTEGER' K;
'BEGIN'      'REAL' DV,G1PW,G1PE,G2PS,G2PN;
             'COMMENT' CALC MEAN MASS FLOW RATES THRO 4 TUBES OF ELEMENT;
              DV:=R[J]*(X1[I+1]-X1[I-1])*(X2[J+1]-X2[J-1]);
          G1PW:=(A[I,J+1,NF]-A[I,J-1,NF]+A[I-1,J+1,NF]-A[I-1,J-1,NF])/DV;
          G1PE:=(A[I,J+1,NF]-A[I,J-1,NF]+A[I+1,J+1,NF]-A[I+1,J-1,NF])/DV;
          G2PS:=(A[I-1,J,NF]-A[I+1,J,NF]+A[I-1,J-1,NF]-A[I+1,J-1,NF])/DV;
          G2PN:=(A[I-1,J,NF]-A[I+1,J,NF]+A[I-1,J+1,NF]-A[I+1,J+1,NF])/DV;
'COMMENT'    COMPUTE AE,AW,AN,AS;
                             APP:=1;
            'IF' K=NW 'THEN'  APP:=R[J]*R[J];
                         AE:=0.5*APP*(ABS(G1PE)-G1PE);
                         AW:=0.5*APP*(ABS(G1PW)+G1PW);
                         AN:=0.5*APP*(ABS(G2PN)-G2PN);
                         AS:=0.5*APP*(ABS(G2PS)+G2PS);
'END' CONVEC;
```

```
'PROCEDURE' BOUND(P/QK,QKRP);
'REAL' QX,QKRP;         'INTEGER' P;
'BEGIN'
'COMMENT'  COMPUTES ONE ITERATION OF BOUNDARY NODES NEEDING UPDATING;
           DX1:=X1[IN]-X1[INM];     DX2:=X2[JN]-X2[JNM];
'COMMENT'  COMPUTES  VORTICITY/RADIUS NEAR WALL,NEAR AXIS,THEN TEMP
                                    NEAR WALL,NEAR AXIS;
           'FOR' I:=2 'STEP' 1 'UNTIL' INM 'DO'
'BEGIN'    A[I,JN,NW]:= -3*(A[I,JNM,NF]-A[I,JN,NF])/A[I,JN,NRO]/
                      (X2[JN]*DX2)/(X2[JN]*DX2)-0.5*A[I,JNM,NW]*
                      X2[JN]/X2[JNM];
           A[I,1,NW]:= 8*(A[I,3,NF]/X2[3]/X2[3]-A[I,2,NF]/X2[2]/X2[2])/
                      A[I,1,NRO]/(X2[2]*X2[2]-X2[3]*X2[3]);
           A[I,JN,NT]:=A[I,JNM,NT]+QK*DX2;
           A[I,1,NT]:= A[I,2,NT];
'END';
'COMMENT'  NEXT DO OUTLET END STREAM FUNC,VORT/RADIUS,TEMP;
                      A[IN,JN,NT]:=A[INM,JN,NT];
'COMMENT' NEXT DO ALONG SHOULDER  VORT/RADIUS AND TEMP;
                 DX1:=X1[2];
           'FOR' J:=P 'STEP' 1 'UNTIL' JN 'DO'
'BEGIN'    A[1,J,NW]:= -3*(A[2,J,NF]-A[1,J,NF])/A[1,J,NRO]/
                      (X2[J]*DX1)/(X2[J]*DX1)-0.5*A[2,J,NW];
           A[1,J,NT]:= A[2,J,NT];
'END';
'END' BOUND;

'PROCEDURE' EQN(NW,NF,NT);
'COMMENT'  ITERATION SUBROUTINE;
'INTEGER' NW,NF,NT;
'BEGIN'
'COMMENT'  CALC EFFECTIVE VISCOSITY;
                      VISCOS(NMU);

'COMMENT'  VORTICITY SUBCYCLE  *****************;  K:=NW;
           'FOR' J:=2 'STEP' 1 'UNTIL' JNM 'DO'
'BEGIN'
                      IL:=IMIN[J];
                      IH:=IMAX[J];
           'FOR' I:=IL 'STEP' 1 'UNTIL' IH  'DO'
'BEGIN'
'COMMENT'  CALC SOURCE TERM ;      SORCE(SOURCE);
'COMMENT'  CALC AE,AW,AN,AS ;      CONVEC(NW);
'COMMENT'  CALC  BBE,BBW,BBN,BBS,IDENTICAL TO BJ/VP IN SUBST.FORMULA;
           RSQ:=R[J]*R[J];    BBE:=2*RSQ*BE[I];
                              BBW:=2*RSQ*BW[I];
                              BBN:=(R[J+1]*R[J+1]+RSQ)*BN[J];
                              BBS:=(R[J-1]*R[J-1]+RSQ)*BS[J];
           'IF' J'NE'JNM 'THEN' 'GOTO' FE ;
'COMMENT' WHEN J=JNM THE FOLLOWING TERMS ARE CALC.TO INTRO.IMPLIC.FORM;
'BEGIN'    DX2SQ:=(X2[JN]-X2[JNM])'**'2;
           TERM1:=-3*(A[I,JNM,NF]-A[I,JN,NF])/RSQ/DX2SQ/ROREF;
           TERM2:=0.5*(AN+A[I,J+1,NMU]*BBN);
                      'GOTO' FF;
```

```
'END';
EE:        TERM1:=A[I,J+1,NW];
           TERM2:=0;
FF:
'COMMENT'  CALC NUMERATOR AND DENOMR.OF VORT.SUBSTN.FORMULA;
           ANUM:=(AE+A[I+1,J,NMU]+BBE)*A[I+1,J,NW]+
                 (AW+A[I-1,J,NMU]+BBW)*A[I-1,J,NW]+
                 (AS+A[I,J-1,NMU]+BBS)*A[I,J-1,NW]+
                 (AN+A[I,J+1,NMU]+BBN)*TERM1+TERM2+SOURCE;
           ADNM:=AE+AW+AN+AS+A[I,J,NMU]*(BBE+BBW+BBN+BBS)+TERM2;
           'IF' ADNM<.0000001 'THEN' 'GOTO' GG;
'COMMENT'  STORE OLD VALUE VORT.,CALC NEW VALUE,CALC RESIDUAL;
                     Z:=A[I,J,NW];
                     A[I,J,NW]:=ANUM/ADNM;
                     RS:=1-Z/A[I,J,NW];
'COMMENT'  UNDER OR OVER RELAX AND STORE MAX RESIDUAL;
                     A[I,J,NW]:=Z+RP[NW]*(A[I,J,NW]-Z);
           'IF' ABS(RS)>ABS(RSDU[NW]) 'THEN'  RSDU[NW]:=RS;
GG: 'END';
'END';

'COMMENT'  STREAM FUNC.SUBCYCLE ****************;    K:=NF;
           'FOR' J:=2 'STEP' 1 'UNTIL' JNM 'DO'
'BEGIN'              IL:=IMIN[J];
                     IH:=IMAX[J];
           'FOR' I:=IL 'STEP' 1 'UNTIL' IH 'DO'
'BEGIN'              SORCE(SOURCE);
'COMMENT'  THE AVERAGE VALUE OF RADIUS IS USED IN COEFFS.
           OF BE,BW,BN,BS;
           RISQ:=1/R[J]/R[J];
           ROP:=A[I,J,NRO];
           BBE:=4/(A[I+1,J,NRO]+ROP)*RISQ*BE[I];
           BBW:=4/(A[I-1,J,NRO]+ROP)*RISQ*BW[I];
           BBN:=16/(A[I,J+1,NRO]+ROP)/((R[J+1]+R[J])'**'2)*BN[J];
           BBS:=16/(A[I,J-1,NRO]+ROP)/((R[J-1]+R[J])'**'2)*BS[J];
           ANUM:=BBE*A[I+1,J,NF]+BBW*A[I-1,J,NF]+BBN*A[I,J+1,NF]
                     +BBS*A[I,J-1,NF]+SOURCE;
           ADNM:=BBE+BBW+BBN+BBS;
           'IF' ADNM<.0000001 'THEN' 'GOTO' HH;
                          Z:=A[I,J,NF];
                          A[I,J,NF]:=ANUM/ADNM;
                          RS:=1-Z/A[I,J,NF];
                          A[I,J,NF]:=Z+RP[NF]*(A[I,J,NF]-Z);
                 'IF' ABS(RS)>ABS(RSDU[NF]) 'THEN'  RSDU[NF]:=RS;
      HH:
'END'
'END';

'COMMENT'  SUBCYCLE FOR OTHER VARIABLES**********;
                'IF' IE<3 'THEN' 'GOTO' RR;
                'FOR' K:=3 'STEP' 1 'UNTIL' IE 'DO'
'BEGIN'         'FOR' J:=2 'STEP' 1 'UNTIL' JNM 'DO'
'BEGIN'                IL:=IMIN[J];
                       IH:=IMAX[J];
                'FOR' I:=IL 'STEP' 1 'UNTIL' IH 'DO'
'BEGIN'                SORCE(SOURCE);
                       CONVEC(K);
          BPP:=A[I,J,NMU];
```

```
                       BBE:=(A[I+1,J,NMU]+BPP)/PR[K]*BE[I];
                       BBW:=(A[I-1,J,NMU]+BPP)/PR[K]*BW[I];
                       BBN:=(A[I,J+1,NMU]+BPP)/PR[K]*BN[J];
                       BBS:=(A[I,J-1,NMU]+BPP)/PR[K]*BS[J];
          ANUM:=(AE+BBE)*A[I+1,J,K]+(AW+BBW)*A[I-1,J,K]+(AN+BBN)*
                 A[I,J+1,K]+(AS+BBS)*A[I,J-1,K]+SOURCE;
          ADNM:=AE+AW+AN+AS+BBE+BBW+BBN+BBS;
             'IF' ADNM<.0000001 'THEN' 'GOTO' SS;
                       Z:=A[I,J,K];
                       A[I,J,K]:=ANUM/ADNM;
          'IF' A[I,J,K]>.0000001 'THEN'
                       RS:=1-Z/A[I,J,K];
                       A[I,J,K]:=Z+RP[K]*(A[I,J,K]-Z);
                 'IF' ABS(RS)>ABS(RSDU[K]) 'THEN' RSDU[K]:=RS;
          SS:
'END';
'END';
'END'; RR:

'COMMENT' UPDATE BOUNDARY NODES;
                       BOUND(P,QK,QKRP);
'END' EQN;

'PROCEDURE' PRINTS(NBEGIN,NTOTAL);
'COMMENT' OUTPUT RESULTS;
'INTEGER' NBEGIN,NTOTAL;
'BEGIN'
'INTEGER' JX,IX,L,M;
                                              JX:=1;
                                              IX:=1;
                            K:=NBEGIN;
                 'FOR' M:=1 'STEP' 1 'UNTIL' NTOTAL 'DO'
'BEGIN'          PAPERTHROW;
                 WRITETEXT('('DISTRIBUTION%OF%A(I,J')'); PRINT(K,1,0);
                 WRITETEXT('(')XAXIALLY%AT%GIVEN%RADIUS%'('2C')'')');
                 'FOR' L:=1 'STEP' JX 'UNTIL' JN 'DO'
'BEGIN'          J:=JN+1-L;
                             NEWLINE(2);
                 WRITETEXT('('RADIUS=')'); PRINT(X2[J],1,3);
          SPACE(5);  WRITETEXT('('J=')'); PRINT(J,3,0); NEWLINE(2);
             'FOR' I:=1 'STEP' IX 'UNTIL' IN 'DO'
'BEGIN'  WRITETEXT('('X1=')'); PRINT(X1[I],3,3); SPACE(3);
         PRINT(A[I,J,K],0,5);      SPACE(2); PRINT(I,3,0); SPACE(2);
'END';
'END';                      K:=K+1;
'END';
'END' PRINTS;

'COMMENT' BLOCK DATA    NUMERICAL DATA INPUT ;
          NU:=1; NF:=2; NT:=3; NV1:=4; NV2:=5; NMU:=6; NRO:=7; NL:=8;
          IE:=3; IV:=7;
          NMAX:=READ; NPRINT:=READ; IP:=READ; CC:=READ; PR[3]:=READ;
          'FOR' K:=1 'STEP' 1 'UNTIL' 9 'DO'
```

```
                RP[K]:=1;
                ROREF:=1,0;   7MUREF:=READ;
                'FOR' J:=1 'STEP' 1 'UNTIL' JN 'DO'
'BEGIN'         IMIN[J]:=2;              IMAX[J]:=IN-1;
'END';          QK:=READ;                    P:=READ;   NCORD:=2;

'COMMENT'       PROGRAM CONTROL *********************;
                       INM:=IN-1;            JNM:=JN-1;
'COMMENT'       GRID
                COMPUTE GRID COORDS:
                'FOR' I:=1 'STEP' 1 'UNTIL' IN 'DO'
                           X1[I]:=READ;
                X2[1]:=0;                  DX2:=1/JNM;
                'FOR' J:=2 'STEP' 1 'UNTIL' JN 'DO'
                X2[J]:=X2[J-1]+DX2;
                'FOR' J:=1 'STEP' 1 'UNTIL' JN 'DO'
                              R[J]:=X2[J];
'COMMENT'       CALC  BE,BW,BN,BS;
                'FOR' I:=2 'STEP' 1 'UNTIL' INM 'DO'
'BEGIN'                    DX1:=1/(X1[I+1]-X1[I-1]);
                BW[I]:=DX1/(X1[I]-X1[I-1]);
                BE[I]:=DX1/(X1[I+1]-X1[I]);
'END';
                'FOR' J:=2 'STEP' 1 'UNTIL' JNM 'DO'
'BEGIN'                    DX2:=0,5/(X2[J+1]-X2[J-1]);
                BS[J]:=(1+R[J-1]/R[J])/(X2[J]-X2[J-1])*DX2;
                BN[J]:=(1+R[J+1]/R[J])/(X2[J+1]-X2[J])*DX2;
'END';
'COMMENT'       PRINT  OUT  COORDS:
                WRITETEXT('('('1C')'DISTANCES%DIRECTION%X1'('1C')')');
                'FOR' I:=1 'STEP' 1 'UNTIL' IN 'DO'  PRINT(X1[I],4,3);
                WRITETEXT('('('1C')'DISTANCES%DIRECTION%X2'('1C')')');
                'FOR' J:=1 'STEP' 1 'UNTIL' JN 'DO'  PRINT(X2[J],2,3);
'COMMENT'  INIT:    SET UP INITIAL GRID VALUES AT INLET,SHOULDER,WALL AND

                   AXIS,OUTLET ;
                'FOR' K:=1 'STEP' 1 'UNTIL'  8 'DO'
                'FOR' J:=1 'STEP' 1 'UNTIL' JN 'DO'
                'FOR' I:=1 'STEP' 1 'UNTIL' IN 'DO'
                           A[I,J,K]:=0;
                'FOR' I:=1 'STEP' 1 'UNTIL' IN 'DO'
                'FOR' J:=1 'STEP' 1 'UNTIL' JN 'DO'
                           A[I,J,NRO]:=ROREF;
'COMMENT'  INLET ;         A[1,1,NV1]:=READ;
                'FOR' J:=1 'STEP' 1 'UNTIL' P 'DO'
'BEGIN'                    A[1,J,NV1]:=A[1,1,NV1]*(1-(X2[J]/X2[P])'**'2);
                           A[1,J,NT]:=0;
                           A[1,J,NF]:=A[1,J,NRO]*A[1,1,NV1]*X2[J]'**'2
                                  *0.25*(2-(X2[J]/X2[P])'**'2);
                           A[1,J,NW]:=2*A[1,1,NV1]/X2[P]/X2[P] ;
'END';
'COMMENT'  SHOULDER ;
                'FOR' J:=(P+1) 'STEP' 1 'UNTIL' JN 'DO'
```

```
'BEGIN'              A[1,J,NV1]:=0;     A[1,J,NF]:=A[1,P,NF];
'END';
'COMMENT'   WALL,AXIS ;
            'FOR' I:=2 'STEP' 1 'UNTIL' INM 'DO'
'BEGIN'     A[I,JN,NV1]:=0;     A[I,JN,NF]:=A[1,JN,NF];  A[I,1,NF]:=0;
'END';
'COMMENT'   REYNOLDS NO;
                RE:=X2[JN]*A[1,1,NV1]*ROREF/ZMUREF/(X2[JN]/X2[P])'**'2;
                     QKRP:=QK*4/RE/PR[3];
'COMMENT'   OUTLET:
            'FOR' J:=1 'STEP' 1 'UNTIL' JN 'DO'
'BEGIN'          A[IN,J,NF]:=X2[J]'**'2*(1-0,5*X2[J]'**'2);
                 A[IN,J,NW]:=4;
                 A[IN,J,NT]:=100*QKRP;
'END';
          'FOR' K:=1 'STEP'1'UNTIL'9'DO'  RSDU[K]:=0;

'COMMENT'   START ITERATION AND PRINT OUT -----------;
                 NITER:=0;
        XXX:     NITER:=NITER+1;
'COMMENT'   ONE CYCLE OF ITERATION CARRIED OUT;
                       EQN(NW,NF,NT);
'COMMENT'   TEST IF PRINTOUT REQUIRED;
'IF' ENTIER((NITER+NPRINT-IP)/NPRINT)'NE' ENTIER(NITER/NPRINT) 'THEN'
                 'GOTO' TT;
                 PRINTS(1,IE);
          WRITETEXT('('('('1P')'NO.OF%ITERATIONS%--RESIDUALS%A[1],A[2]
ETC.'('3C')')');
        TT:      NEWLINE(1);     PRINT(NITER,3,0);  SPACE(5);
             'FOR' K:=1 'STEP' 1 'UNTIL' IE 'DO'          'BEGIN'
                 PRINT(RSDU[K],0,4);  SPACE(4);           'END';
'COMMENT'   TEST FOR MAX.NO. ITERATIONS;
             'IF' NITER=NMAX 'THEN' 'GOTO' UU ;
                       RES:=0;
             'FOR' K:=1 'STEP' 1 'UNTIL' IE 'DO'
'BEGIN'    'IF' ABS(RES)<ABS(RSDU[K]) 'THEN' RES:=RSDU[K];
                       RSDU[K]:=0;
'END';
'COMMENT'   TEST CONVERGENCE (CC):
         'IF' ABS(RES)>CC 'OR' NITER<5 'THEN' 'GOTO' XXX;
'COMMENT'   LOOP ENDS                       ----------;
                 'GOTO' VV;
       UU:      WRITETEXT('('('('1C')'PROCESS%DID%NOT%CONVERGE'('1C')'
)');
       VV:

'COMMENT'   CALC.VELOC.DISTBNS.;
'COMMENT'   VELDIS.      COMPUTE VELOCITIES V1,V2
INTERIOR NODES:          'FOR' J:=2 'STEP' 1 'UNTIL' JNM 'DO'
'BEGIN'          H2:=(X2[J]-X2[J-1])/(X2[J+1]-X2[J]);
                 RX2:=R[J]*(X2[J+1]-X2[J-1]);
                 IL:=IMIN[J];
                 IH:=IMAX[J];
                 'FOR' I:=IL 'STEP' 1 'UNTIL' IH 'DO'
'BEGIN'
             H1:=(X1[I-1]-X1[I])/(X1[I+1]-X1[I]);
             PX1:=R[J]*(X1[I+1]-X1[I-1]);
   A[I,J,NV1]:=(A[I,J+1,NF]-A[I,J,NF])*H2+(A[I,J,NF]-A[I,J-1,NF])/H2;
```

```
                A[I,J,NV1]:=A[I,J,NV1]/RX2/A[I,J,NRO];
'END';
'END';
'COMMENT'    ON PLANE OF SYMMETRY;
             DELX2:=X2[2]-X2[1];
                            'FOR' I:=2 'STEP' 1 'UNTIL' IN 'DO'
             A[I,1,NV1]:=(A[I,2,NF]-A[I,1,NF])/DELX2/A[I,1,NRO];

'COMMENT'    FINAL PRINTOUT;
                            PRINTS(1,NV1);
                            PAPERTHROW;
WRITETEXT('('('1C')'REF%DENSITY%FOR%FLUID')'); PRINT(ROREF,2,2);
WRITETEXT('('('1C')'REF%VISCOSY%FOR%FLUID')'); PRINT(ZMUREF,3,2);
WRITETEXT('('('1C')'REF%REYNOLDS%NUMEER')');  PRINT(RE,5,0);
WRITETEXT('('('1C')'REF%PRANDTL%NUMBER')');    PRINT(PR[3],3,2);
WRITETEXT('('('1C')'RELAX.PARAMETERS')');
            'FOR' K:=1 'STEP' 1 'UNTIL' IE 'DO' PRINT(RP[K],2,2);
WRITETEXT('('('1C')'MAX.NO.ITERATIONS')');      PRINT(NMAX,3,0);
WRITETEXT('('('1C')'CONVERG.CRITERIA')');       PRINT(CC,1,5);
WRITETEXT('('('1C')'NO.COLUMNS%DIRECT.1')');    PRINT(IN,3,0);
WRITETEXT('('('1C')'NO.ROWS%%%%DIRECT.2')');    PRINT(JN,3,0);
            WRITETEXT('('('1P')'NUSSELT%NUMBERS'('3C')')');
            'FOR' I:=1 'STEP' 1 'UNTIL' IN 'DO'
'BEGIN'              PRINT(I,3,0); SPACE(2);
                     PRINT((2*X2[JN]*QK/(A[I,JN,NT]-QKRP*X1[I])),4,3);
                                NEWLINE(1);
'END';
'END';
'END';
```

11.3.(vii) STABLE, LAMINAR MOTION.

An investigation was carried out of stable laminar motion through a 1:2 divergence with the boundary conditions specified in 11.3.(v). The downstream section of tube was taken as 50 diameters in length, and the axial grid spacing was 0, 0.1, 0.25, 0.5, 0.75, 1.0, 1.5, 2, 3, 4, 5.5, 7, 8.5, 10, 12, 14, 16, 18, 20, 23, 26, 30, 40, and 50 diameters downstream. Fourteen evenly spaced radial increments were chosen.

A Reynolds number (for the larger tube) of 200 was considered suitable initially, because the experimental results were found to be unstable in this region, exhibiting the 'high' and 'low' values of Nu referred to in part 11.3.(i). Figure 11.19 shows the pattern of streamlines for Re = 200. A standing eddy is clearly indicated, the 'eye' of which occurs at 1.65 diameters. The recirculation zone is approximately 8 diameters in length. Axial velocity profiles are given in figure 11.20, these indicate that the reverse-flow in the outer annulus of fluid occurs at small axial velocity in comparison with the central core.

With a Prandtl number of 100, the temperature distribution was computed, and figure 11.19 shows the pattern of the isotherms. The recirculating flow carries 'hot' fluid to the 'cold', fast moving elements near the inlet causing a point of inflection in the radial temperature profile. The 'hot' outer layers are almost stagnant and tend to insulate the 'cold' core from the tube wall giving rise to low coefficients of heat transfer near the discontinuity.

A graph of Nusselt number versus distance (figure 11.21b) shows that Nu rises rapidly with increasing distance, from 9.6 at the discontinuity to 15.0 at approximately 8.5 diameters downstream. A slow diminution occurs as the distance increases further, until Nu $\simeq$ 10 near the outlet end. Since fairly large axial increments were selected close to the outlet, the numerical values of Nu in this region may not be very reliable. The value of Nu at large distances was of little interest, however, and the precise magnitude was not a prime objective.

The peak in the axial distribution of Nu almost corresponds to the point of boundary layer reattachment, the latter being defined by zero vorticity at the wall. The point of reattachment is at approximately 9.2 diameters, and $\hat{Nu}$ occurs at 8.5 diameters.

In figure 11.21b Nu is compared with the corresponding result for entrance-region heat-transfer in a short tube. Initially the local value of Nu is much greater for the short tube, but after 15 diameters the divergence-values converge to within 4% and it is probable that further downstream Nu can be closely estimated from short-tube theory.

Pr was increased for the same value of Re (200) in order to investigate whether a correlation of the kind $Nu \sim Pr^n$ was a valid method of presenting the experimental data at low Reynolds numbers.

Figure 11.24 shows that for Pr = 1,000, the axial Nu distribution is qualitatively similar to the previous case (Pr = 100). A peak occurs in the Nu function at the same position as before, (8.5 diameters) but throughout the length of tube Nu is much higher. At the discontinuity Nu = 15.6, rising to a maximum of 24.2, then falling to approximately 19 at the outlet.

In an attempt to form a unique function of distance, the relationship $Nu \sim Pr^n$ was investigated for Pr = 100 and 1,000. It was found that the exponent n would have to be a function of axial position to satisfy both sets of data. At small distances $Nu \propto Pr^{0.2}$ whereas near the outlet $Nu \propto Pr^{0.3}$. Figure 11.21a indicates that in plotting $(Nu/Pr^{0.2})$ versus (distance) considerable differences (approximately) 20% arise at large distances.

The effect of increasing Re on the flow pattern, and the subsequent distribution of Nu, was determined by setting Pr = 100 and Re = 1,000. The results obtained in this case were fairly crude estimates because of two practical limitations. First, the high value of Re led to considerable computing time, and convergence of the solution was truncated in the interests of economy. 150 iterations were carried out whereas an estimated 200 to 250 iterations would be required for complete convergence. The ensuing errors were probably quite small, and are indicated by a slight waviness in the 'Nu - distance' curve (figure 11.22). Second, in specifying the outlet boundary conditions a tube length far greater than 50 diameters was desirable. This implies the selection of many more axial increments. The point of reattachment was found to be well in excess of 50 diameters downstream, but this tube length was maintained, despite the artificiality of the system, so that some insight into the heat-transfer process could be gained.

Figure 11.23 shows that when Re is increased to 1,000 the resulting streamlines reveal an elongation of the standing eddy, such that the length of the recirculation zone is of the order 50 diameters. The computed Nusselt numbers given in figure 11.22, when compared with the values for Re = 200, indicate that substantial increases in Re cause a stretching of the 'Nu - distance' function without significantly increasing the magnitude. At small axial distances an increase in Re actually reduces Nu. The converse is found to be true at large distances.

A direct comparison between the theory and experimental results was unlikely to be meaningful, since stable laminar flow without a free convectional contribution was unlikely to occur in practice. Two typical sets of test results are shown in figure 11.24, both have Re $\simeq$ 200, with Pr = 230 and 408. Nu versus distance is plotted, and it is clear that the experimental results tended to be unstable. Reasonable agreement between theory and experiment is shown however, considering the limitations discussed and the existance of a flow regime associated with 'low' coefficients of heat transfer is established satisfactorily.

11.3.(viii) TURBULENT MOTION IN A DIVERGENCE.

In turbulent flows the kinetic energy associated with the eddying motion is either generated by frictional shear, or diffused from the regions of high intensity to the regions of low intensity. (A good description of the mechanisms is given in Ref: H.22). In most boundary-layer type flows the former mechanism predominates, but in stalled regions of a flow field the transport of turbulence energy by diffusion predominates.

With 'shear' flows the effective turbulent transport properties can be derived from Prandtl's 'mixing length' theory (as in part 11.2.(iv); an example would be the region of flow upstream of a divergence. Downstream of a divergence, at small distances, the field can be treated as 'diffused' flow. The high velocities upstream cause the discontinuity to act as a highly intense source of turbulence, and it can be argued that theeffective transport properties downstream differ only slightly from those upstream because the kinetic energy of turbulence is similar. It has been shown (p.175 Ref: K4) that free jets and wakes can be analysed with a constant value for the effective viscosity, as might be predicted from the hypothesis stated.

The properties required are the effective thermal conductivity and viscosity; these can be interrelated using Reynolds analogy ($Pr_{effective} = 1$). In prescribing the effective viscosity a single constant value was postulated which has been used successfully for analysing round turbulent jets (e.g. Ref: K.4) viz:

$$\text{effective viscosity } \mu_{eff} = 0.013\, \rho . V_1(0,0) . r_i$$

The equation appears to be a simplified form of Prandtl's mixing length theory in which the 'length' $\ell \sim 0.1\, r_i$; such a value is typical of turbulent shear flows in general.

An important conclusion can be derived from the above argument: when analysing turbulent flow through a given divergence it is possible to state an equivalent laminar Reynolds number Re_{eff} (a particular value) which will exhibit a similar flow pattern to any turbulent flow (arbitrary Re). The system is specified by the Reynolds number

$$\left(\frac{\rho\, \bar{V}_1\, 2r_o}{\mu_{eff}}\right) \equiv Re_{eff}$$

which has the value $154(r_i/r_o)$ from the definition of μ_{eff}. Initially, this was approximated for a 1:2 divergence by $Re_{eff} \simeq 80$, since the true value could only be derived by trial and comparison with experiment.

Along the tube-wall, turbulence must be damped by viscous action, Regions of high and low shear stress exist, so that diffusion and generation of turbulence energy takes place in a complex fashion, and the estimation of local effective properties becomes difficult. This thin 'viscous' layer which persists on the tube wall was ignored for convenience, and an investigation was carried out treating the boundary conditions in an identical way to the laminar analyses discussed previously.

It is reasonable to assume that the true wall-vorticity can be derived from the effective value by the following -

$$\omega_{wall} = \omega_{eff.wall}\left(\frac{\mu_{eff}}{\mu}\right)$$

because the region near to the wall can be treated as a constant shear-stress layer. To determine the temperature distribution near the tube wall it is essential to have a knowledge of the transition from the turbulent mainstream conductivity, K'_{eff} to the laminar wall value K'. No procedure could be found which enabled such functions to be determined reliably, so it was considered unfeasable to attempt calculating the coefficients of heat transfer.

From the preceding arguments it was postulated that turbulent flow patterns for a 1:2 divergence would resemble laminar flow with Re = 80. The stream function and vorticity were calculated, and the results are given in figure 11.25.

The standing eddy formed is short in length, the recirculation zone being 2 to 3 diameters long. The 'eye' of the eddy occurs at approximately ½ diameter downstream. The line of zero rotation ($\omega = 0$) approaches the tube wall at 2.45 diameters, and this corresponds to the point of boundary-layer reattachment.

The laminar results for Re = 200 indicated that the maximum in the 'Nu versus distance ' function occured at;92% of the distance to the point of reattachment. If the same holds true for the turbulent case then the maximum value of Nu would occur at 2.2 diameters downstream. In practice, it was found that the peak value of Nu corresponded to a distance of 1.8 to 2.0 diameters. The relatively small disparity is probably a consequence of the wrongful selection of Re_{eff}, which could only be reliably established after studying several different configurations and comparing the theoretical results with experimental work.

A graph of the effective wall vorticity ($\propto$ shear stress) versus distance is compared with the Nu distribution derived by experiment for a particular case (fig: 11.26). In general, Nu is seen to be inversely related to the modulus of the shear stress.

In the region of zero wall shear (approximately maximum Nu) turbulence energy is diffused from the mainstream to the wall without the generation of turbulence by shear. The local effective transport properties in this region must be a function of the mainstream turbulence level, the true viscous properties, and the distance from the wall. From the definition used for the effective viscosity it would seem that the maximum value of Nu is a function of Re upstream and Pr. The model therefore predicts that $\hat{Nu}$ is independent of the divergence ratio, provided the flow is turbulent throughout. The practical implications of this statement, and empirical justification is given in part 9.7. The argument was supported substantially, but there was a tendency for viscous action to damp the turbulence downstream at low Reynolds numbers, thereby causing a reduction in $\hat{Nu}$.

FIGURE. II.2

A PROGRAMME FOR SOLVING THE EQUATIONS FOR LAMINAR FLOW HEAT TRANSFER WITH DISSIPATION.

```
'BEGIN' 'COMMENT' MESTF116 DISSIPATON;
   'REAL' D,A,GGGG;
   'INTEGER' N,M,BBB;
   'REAL' 'ARRAY' Q,R[0:200],F[1:6,0:200],P,I[0:200];
             D:=.018;       BBB:=100;
       WW:
             'FOR' N:=2 'STEP' 1 'UNTIL' 200 'DO'
        'BEGIN' Q[N]:=2-2*(N-1)*(N-1)*D*D*D/3+2*(N-1)*D*D*D/3;
         R[N]:=2*(N-1)*(N-1)*D*D*D/3-1;
        'END';
             F[1,0]:=1;     F[1,1]:=1-D;
             F[2,0]:=1;     F[2,1]:=1;
             F[3,0]:=1;     F[3,1]:=1;
             F[4,0]:=1;     F[4,1]:=1;
             M:=1;
       PP:   A:=0;
             'IF' M=3 'OR' M=6 'THEN'
             A:=1;
             'FOR' N:=2 'STEP' 1 'UNTIL' 200 'DO'
        'BEGIN'
             GGGG:=Q[N];
          'IF' M=3 'OR' M=4 'OR' M=6 'THEN'
            GGGG:=Q[N]+2*(N-1)*D*D*D/3;
             F[M,N]:=GGGG*F[M,N-1]+R[N]*F[M,N-2]-A*D*D;
        'END';
             M:=M+1;
             'IF' M<5 'THEN' 'GOTO' PP;
             'IF' M=6 'THEN' 'GOTO' PP;
             'IF' M=7 'THEN' 'GOTO' JJ;
             F[5,0]:=1-F[1,200]/F[2,200];      F[5,1]:=F[5,0]-D;
             F[6,0]:=1-F[3,BBB]/F[4,BBB];      F[6,1]:=F[6,0];
             'IF' M=5 'THEN' 'GOTO' PP;
       JJ:   'FOR' N:=0 'STEP' 4 'UNTIL' 200 'DO'
        'BEGIN' NEWLINE(1);
             PRINT(N*D,2,4);
             SPACE(5);
             PRINT(F[5,N],1,6);
             SPACE(5);
             PRINT(F[6,N],1,6);
        'END';
             BBB:=BBB*1.25;
          'IF' BBB>160 'THEN' 'GOTO' EE;
       EE:
   'END';
```

FIGURE. 11.3

LAMINAR FLOW HEAT TRANSFER WITH DISSIPATION. THE FUNCTIONS "g" AND "γ."

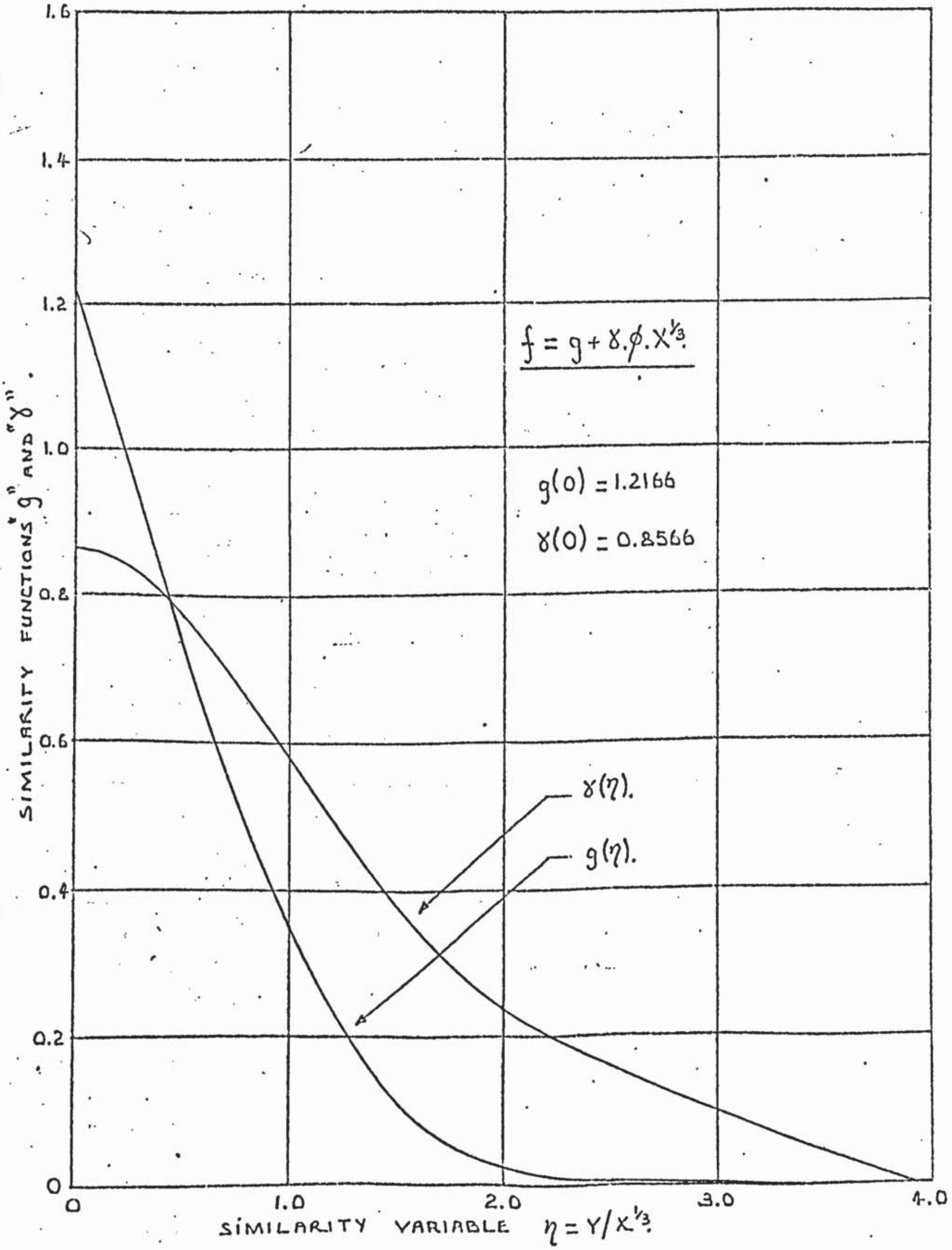

FIGURE. 11.4

CALCULATED NUSSELT NUMBERS FOR LAMINAR FLOW, ENTRANCE REGION HEAT TRANSFER, AT HIGH PRANDTL NUMBERS, WITH VISCOSITY VARIATION.

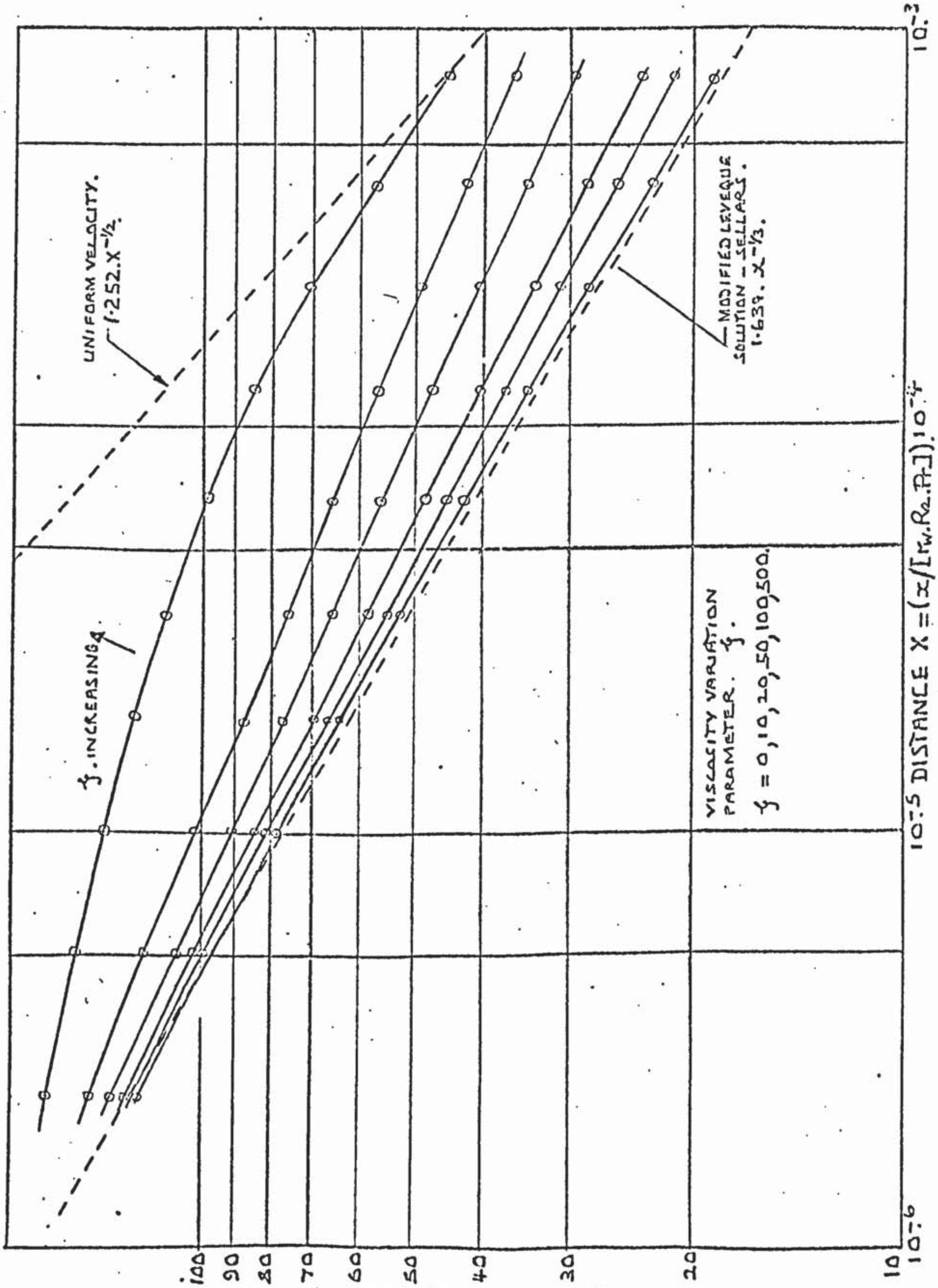

FIGURE 11.5 . .

LAMINAR FLOW HEAT TRANSFER WITH VARIABLE VISCOSITY. THE FUNCTIONS f_0 AND f_1.

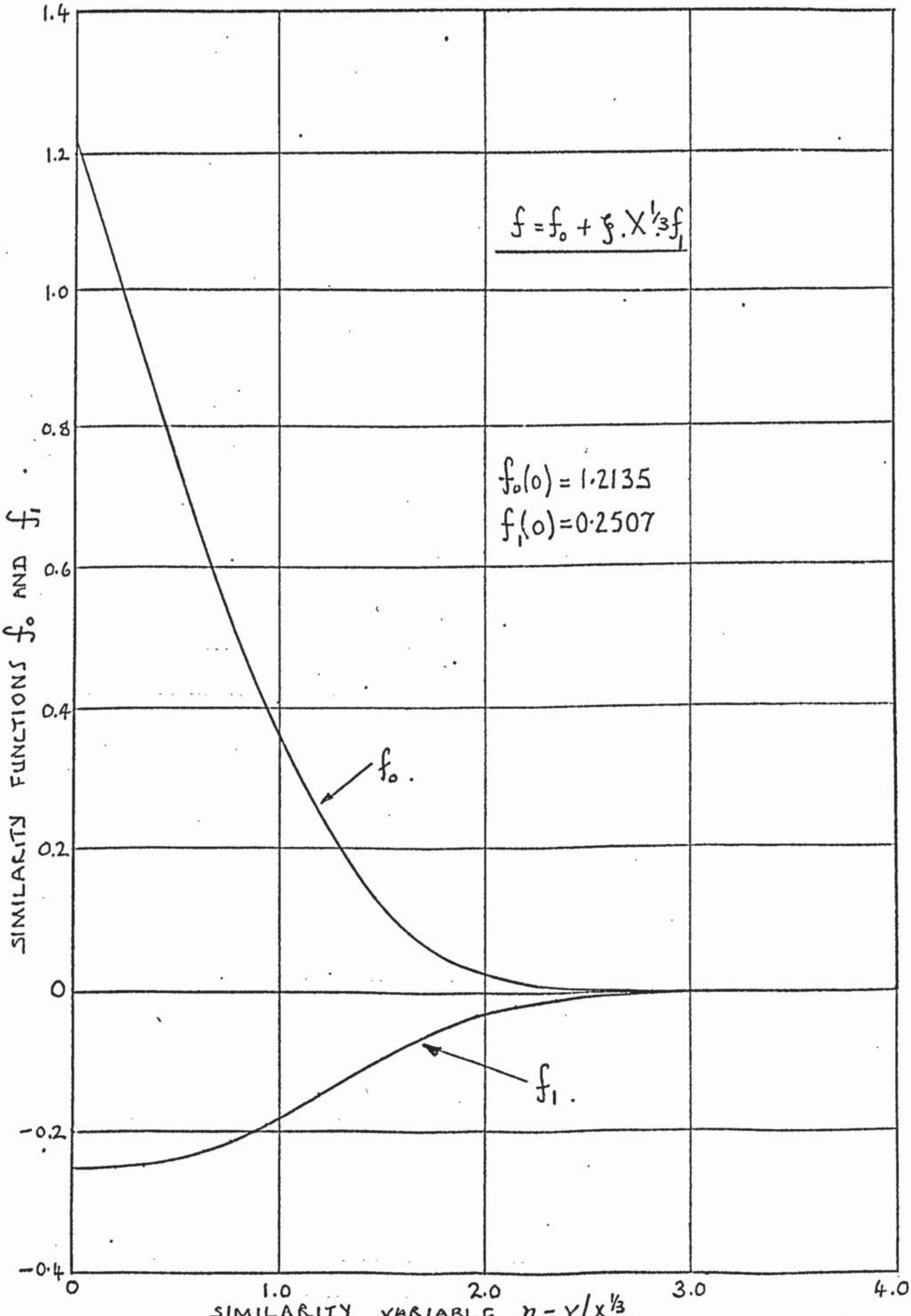

FIGURE. 11.6

TURBULENT FLOW HEAT TRANSFER IN THE ENTRANCE OF A TUBE.
THE FUNCTIONS "f_0" AND "f_1".

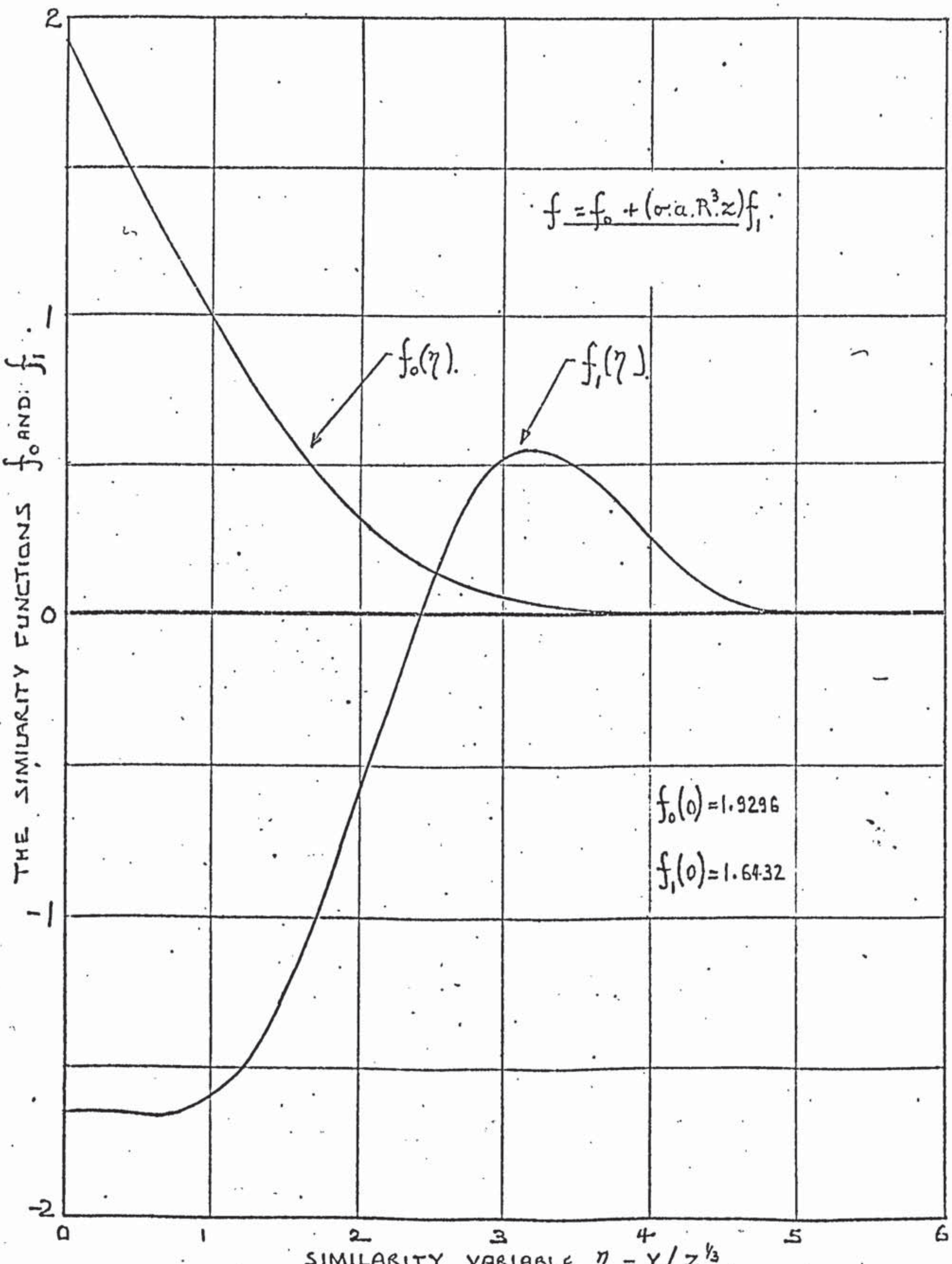

FIGURE . 11.7

THE EFFECTS OF DISSIPATION ON NUSSELT NUMBER AT THE ENTRANCE OF A TUBE WITH LAMINAR FLOW.

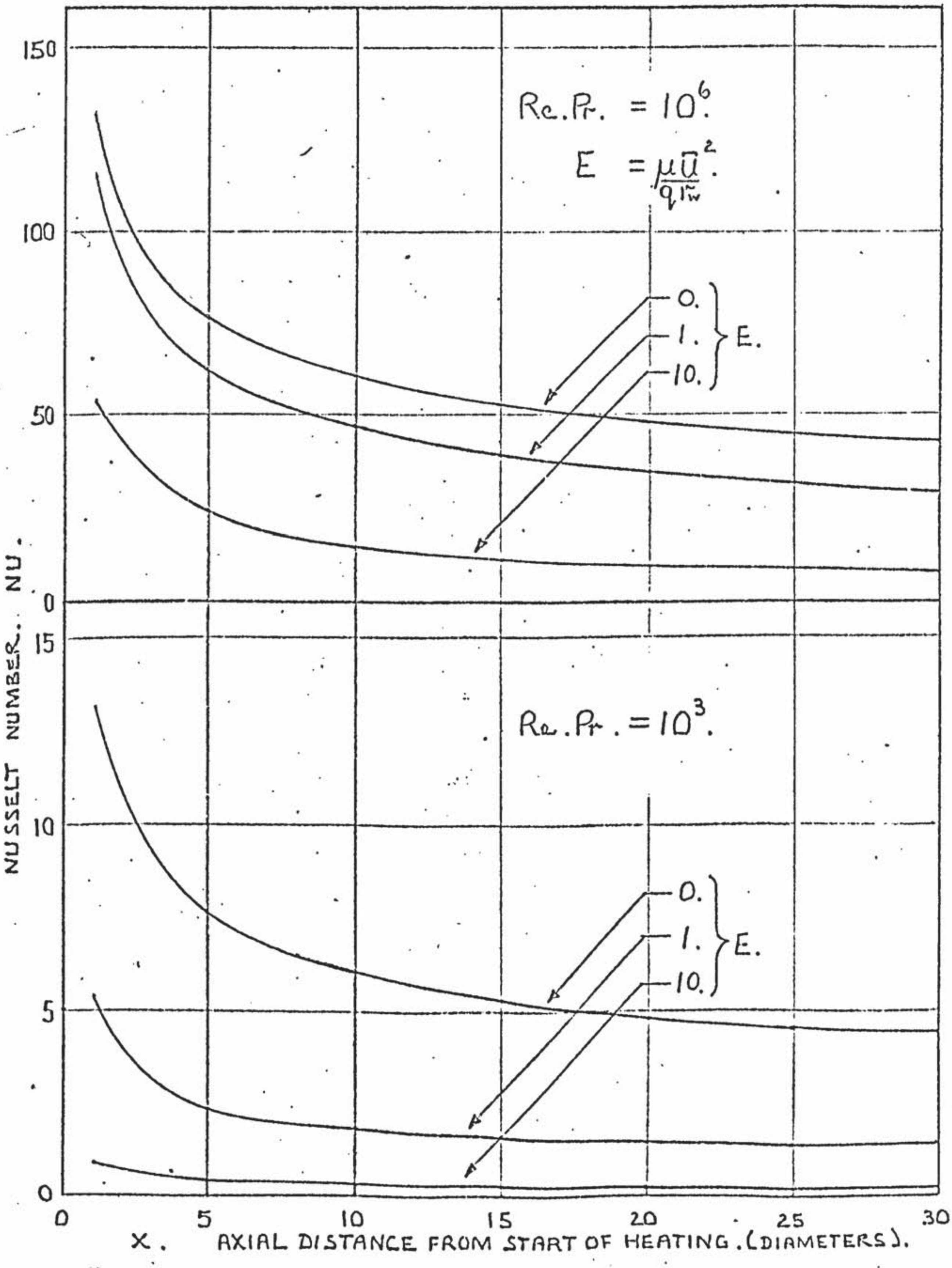

FIGURE. 11.8

THE EFFECTS OF DISSIPATION ON NUSSELT NUMBER AT GIVEN VALUES OF REYNOLDS NUMBER AND PARAMETER $E = \left(\frac{\mu . \bar{U}^2}{q . r_w}\right)$

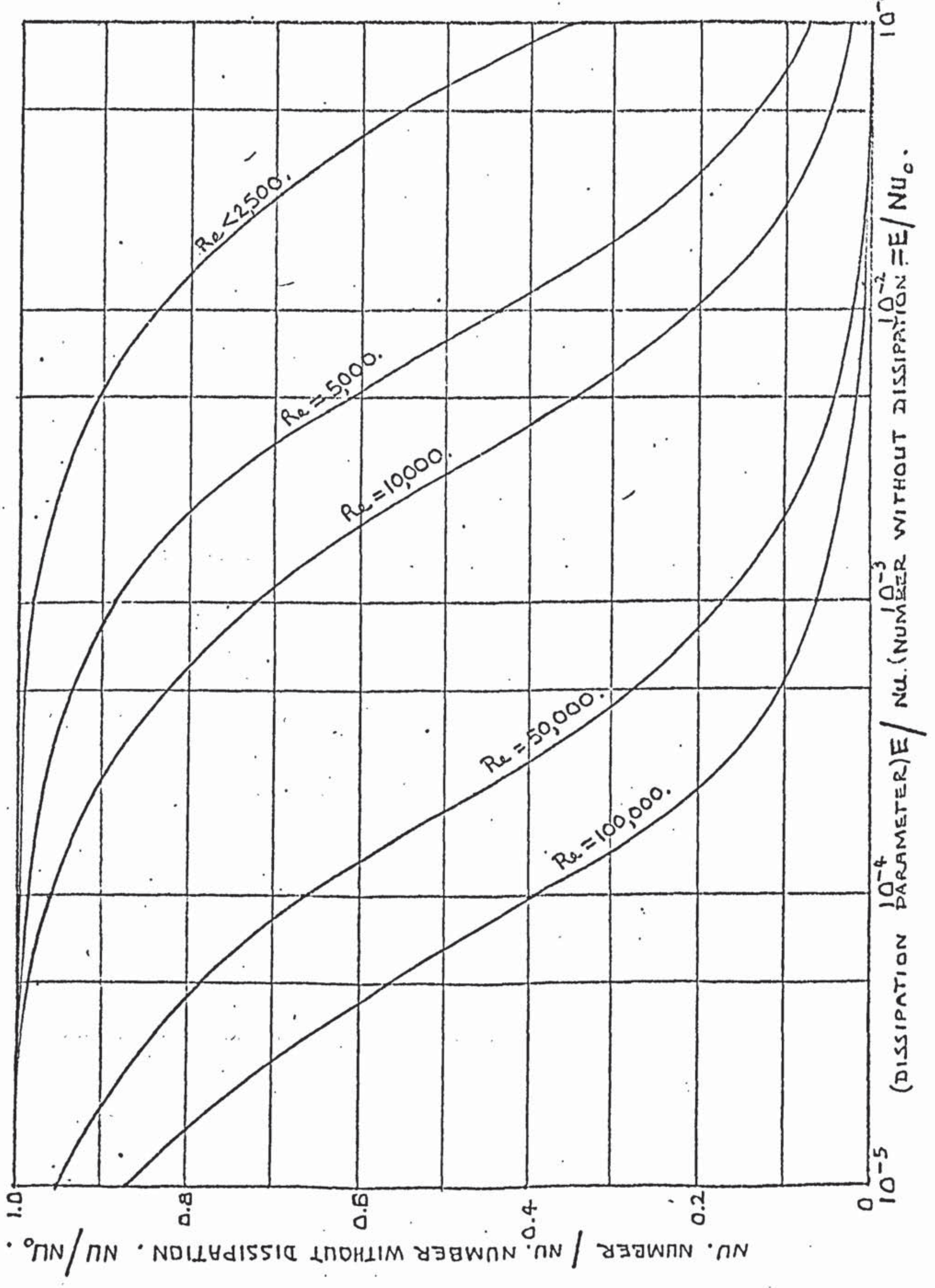

FIGURE: 11.9.

CALCULATED NUSSELT NUMBERS FOR VARIABLE VISCOSITY, LAMINAR FLOW.

VISCOSITY VARIATION PARAMETER ζ.	DIMENSIONLESS AXIAL DISTANCE $X = (x/r_w / Re.Pr.)$, FROM START OF HEATING.									
	2.320×10^{-6}	5.050×10^{-6}	1.002×10^{-5}	1.909×10^{-5}	3.560×10^{-5}	6.570×10^{-5}	1.205×10^{-4}	2.204×10^{-4}	4.024×10^{-4}	7.340×10^{-4}
0	122.0 1 1	96.54 1 1	77.97 1 1	63.40 1 1	51.70 1 1	42.20 1 1	34.45 1 1	28.12 1 1	22.95 1 1	18.74 1 1
10	124.8 1.023 1.17	99.45 1.030 1.22	80.92 1.039 1.28	66.38 1.047 1.35	54.68 1.058 1.44	45.15 1.070 1.56	37.36 1.084 1.71	30.97 1.101 1.91	25.72 1.121 2.18	21.42 1.143 2.54
20	127.4 1.044 1.37	102.2 1.059 1.48	83.75 1.074 1.61	69.23 1.092 1.78	57.50 1.112 2.00	47.94 1.136 2.30	40.08 1.163 2.71	33.60 1.195 3.29	28.25 1.231 4.12	23.81 1.27 5.36
50.	134.1 1.099 2.11	109.7 1.136 2.49	91.42 1.172 2.99	76.97 1.214 3.67	65.19 1.261 4.64	55.45 1.314 6.07	47.33 1.374 8.27	40.48 1.440 11.8	34.66 1.510 17.9	29.64 1.582 29.2
100	142.8 1.170 4.06	119.8 1.243 5.31	102.0 1.309 7.11	87.60 1.379 9.81	75.70 1.464 14.0	65.70 1.555 21.0	57.00 1.655 33.5	49.30 1.755 57.9	42.40 1.847 112.	36.00 1.921 260.
500	166.0 1.361 413.	150.7 1.561 763.	137.1 1.758 1467.	124.5 1.964 3076.	111.9 2.164 7582.	98.77 2.341 24940.	84.82 2.462 13.2×10^{4}	70.63 2.512 14.1×10^{5}	57.23 2.494 38.7×10^{6}	45.48 2.427 35.4×10^{8}

THE VALUES OF — Nu ; Nu / Nu_0 ; $M_{WALL} (= \mu_{ac}/\mu_{WALL})$.

FIGURE. 11.10

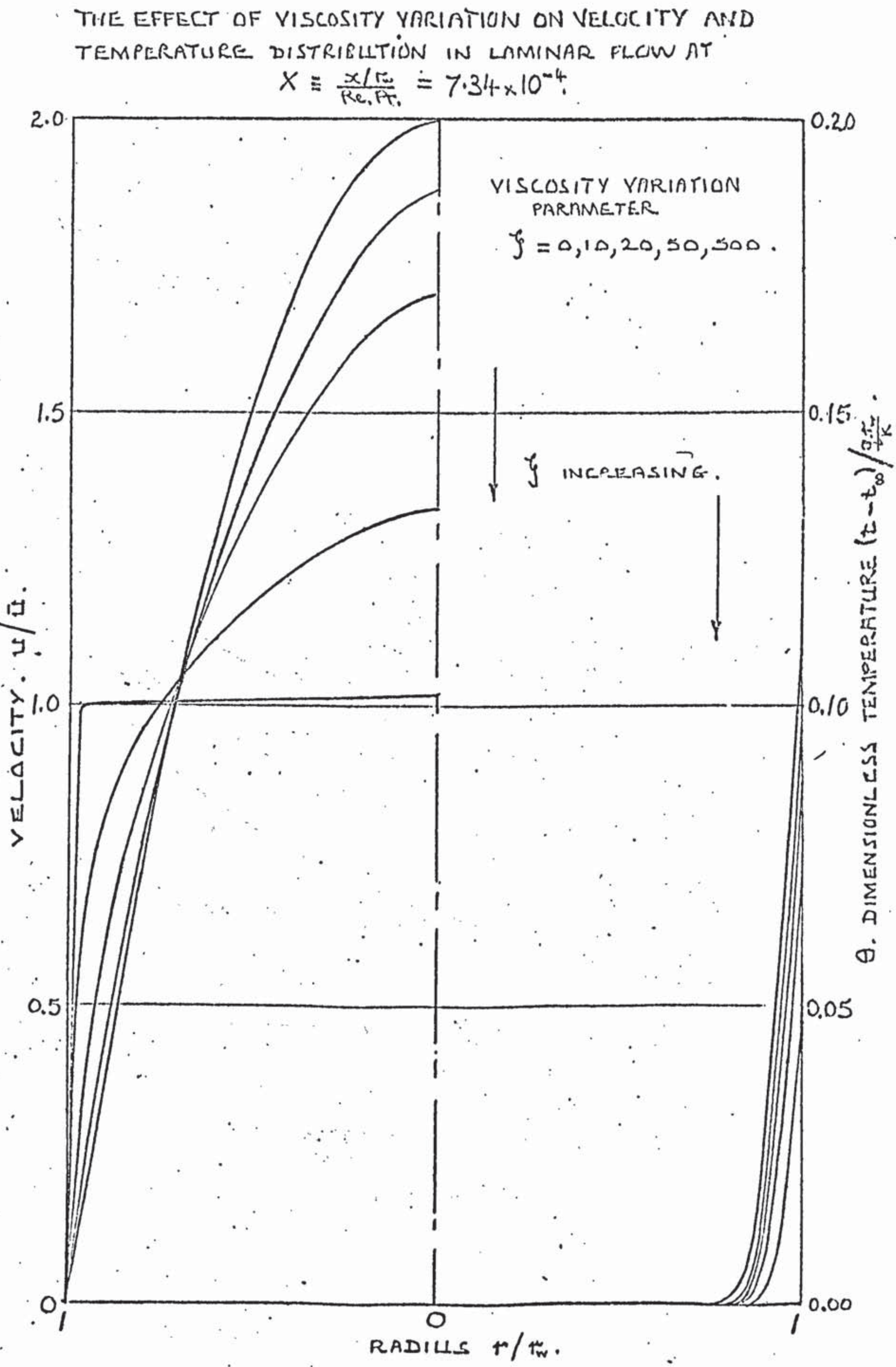
THE EFFECT OF VISCOSITY VARIATION ON VELOCITY AND TEMPERATURE DISTRIBUTION IN LAMINAR FLOW AT
$X \equiv \frac{x/r_w}{Re.Pr.} = 7.34 \times 10^{-4}$.
VISCOSITY VARIATION PARAMETER
$\zeta = 0, 10, 20, 50, 500$.
ζ INCREASING.
2.0
1.5
1.0
0.5
0
0.20
0.15
0.10
0.05
0.00
1
0
1
VELOCITY. $u/\bar{u}$.
θ. DIMENSIONLESS TEMPERATURE $(t - t_0)\Big/\frac{q.r_w}{k}$.
RADIUS r/r_w.

FIGURE. II.11

THE VARIATION IN NUSSELT NUMBER WITH DISTANCE FROM START OF HEATING, IN VARIABLE VISCOSITY, LAMINAR FLOW.

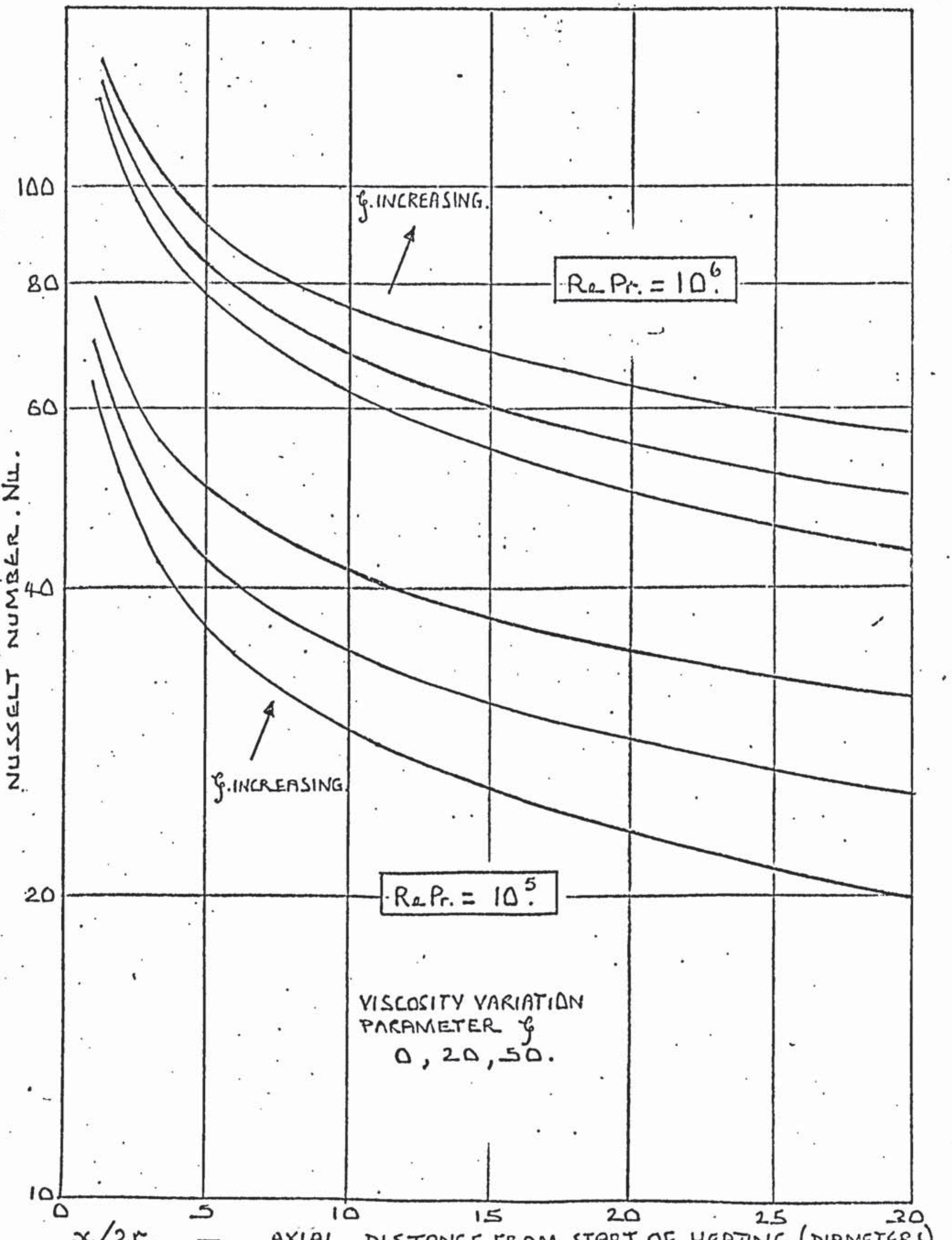

FIGURE . 11.12

THE EFFECT OF VISCOSITY VARIATION ON THE NUSSELT NUMBER FOR LAMINAR FLOW, ENTRANCE REGION HEAT TRANSFER, WITH MODERATE VALUES OF THE RATIO — VISCOSITY AT START OF HEATING/VISCOSITY AT THE TUBE WALL. (M_{WALL}).

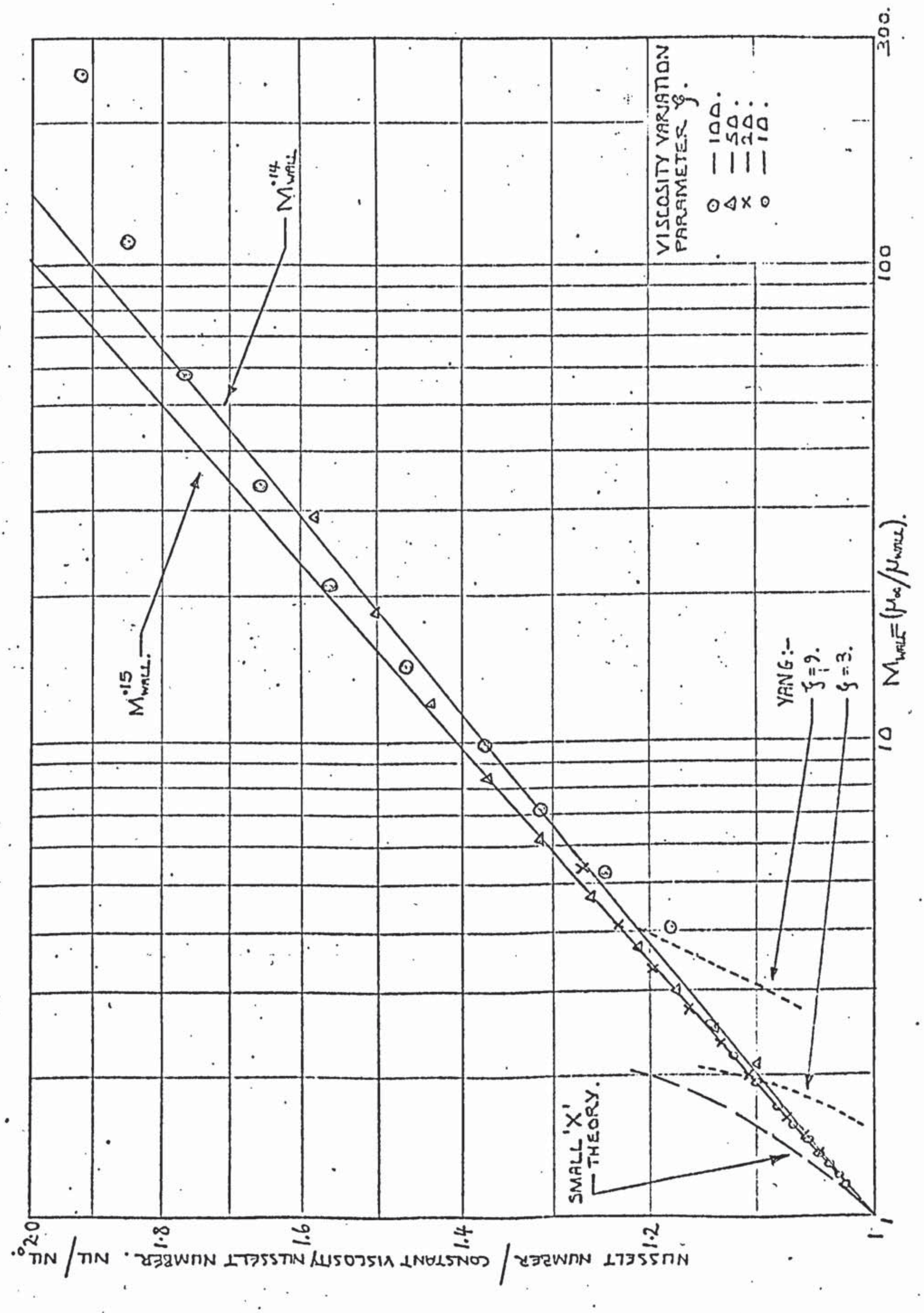

FIGURE. 11.13

A COMPARISON BETWEEN THE CALCULATED NUSSELT NUMBERS (NU) AND THE CONSTANT VISCOSITY VALUE, CORRECTED BY THE WALL VISCOSITY RATIO, ACCORDING TO SIEDER AND TATE. ($Nu_o . M_{WALL}^{0.14}$).

X = DIMENSIONLESS AXIAL DISTANCE / Ra. Pr.

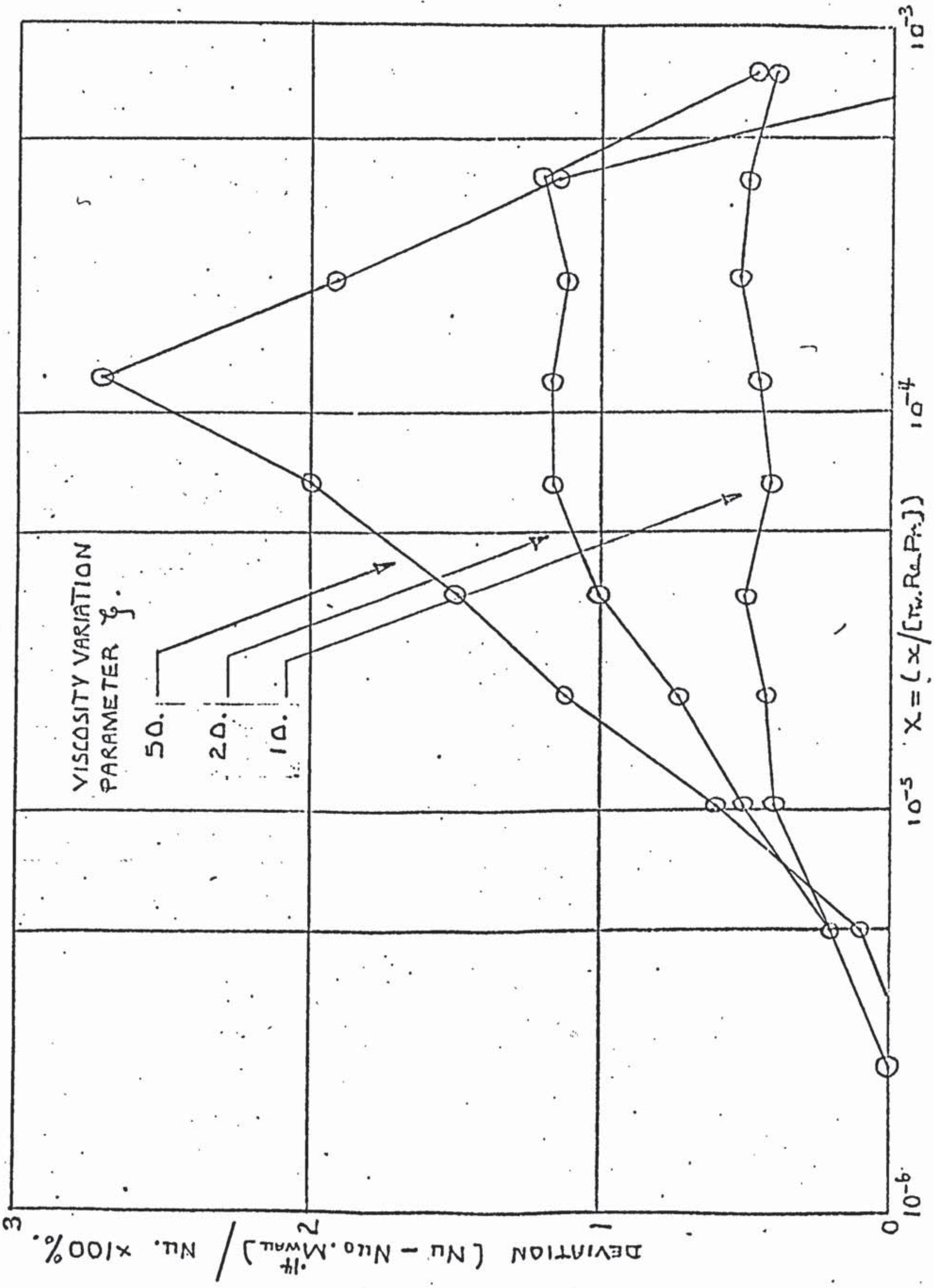

FIGURE. 11.14

THE EFFECT OF VISCOSITY VARIATION ON THE NUSSELT NUMBER FOR LAMINAR FLOW, ENTRANCE REGION HEAT TRANSFER, WITH VERY LARGE VALUES OF THE RATIO — VISCOSITY AT START OF HEATING / VISCOSITY AT THE TUBE WALL.

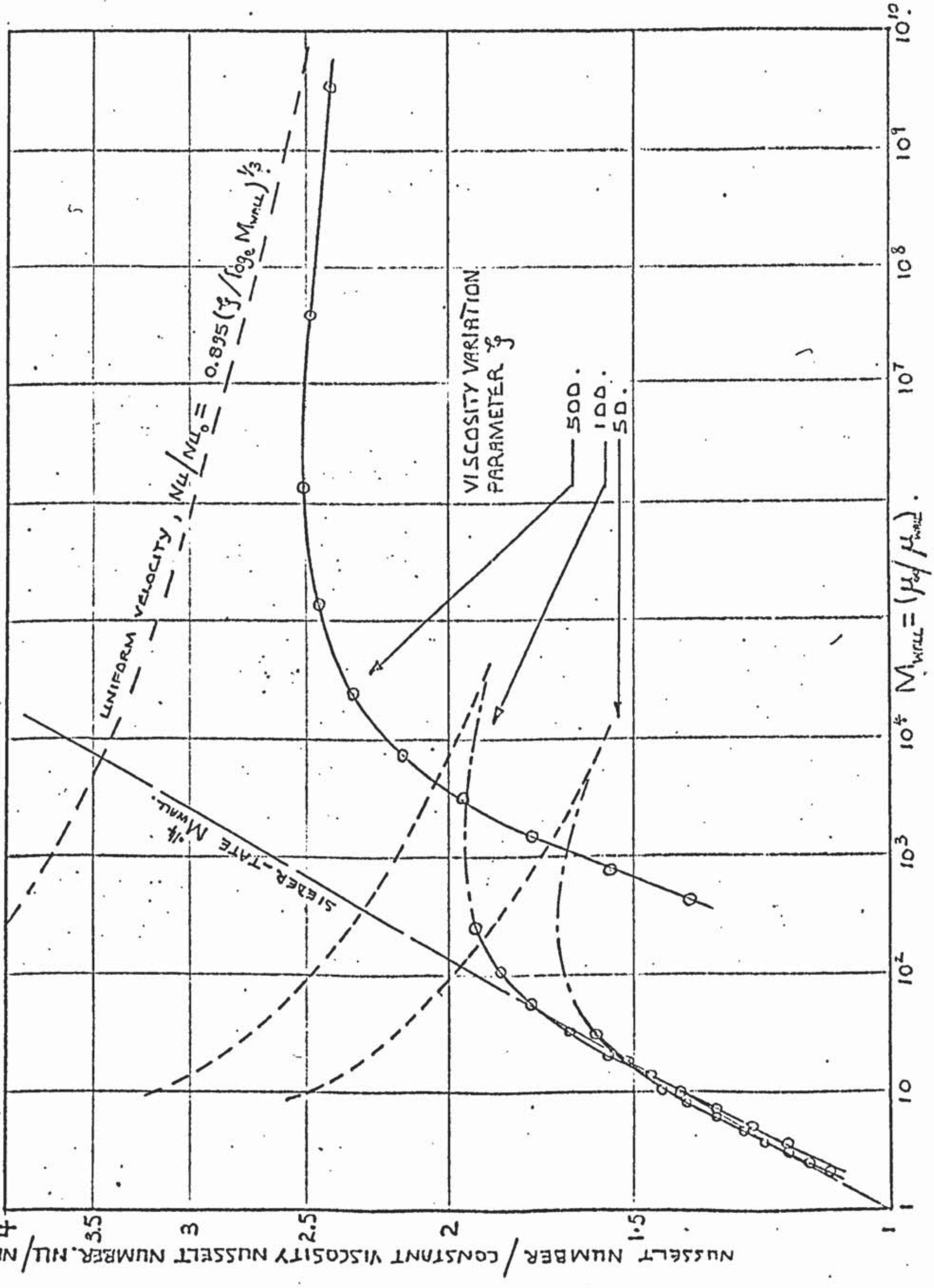

FIGURE. 11.15

THE DIMENSIONLESS VELOCITY GRADIENT AT TUBE WALL $\left(\frac{\partial V}{\partial Y}\right)_0$ AS A FUNCTION OF REYNOLDS NUMBER Re.

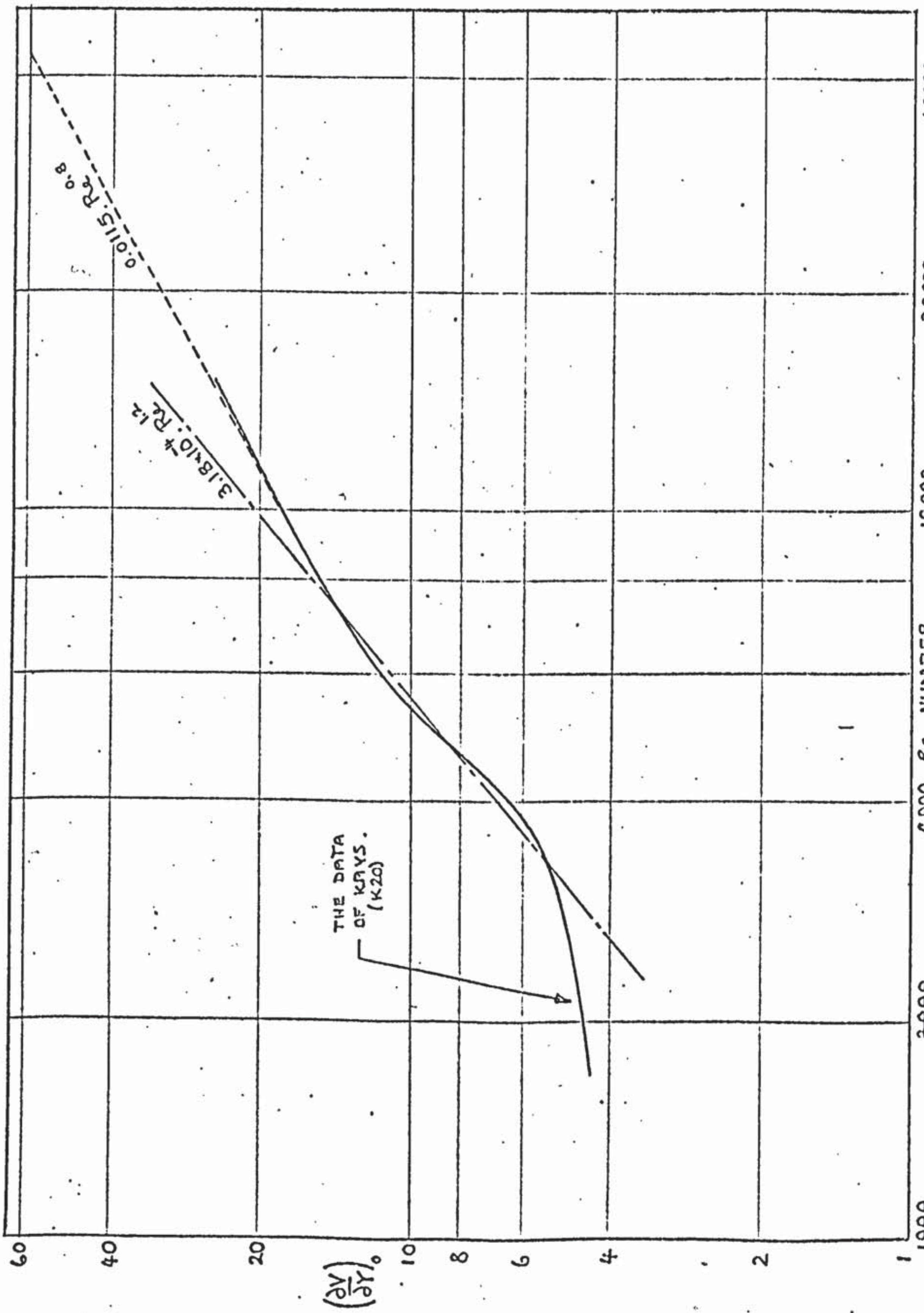

FIGURE. 11.16

A COMPARISON BETWEEN THEORETICAL AND EXPERIMENTAL NUSSELT NUMBERS, AT SMALL AND LARGE AXIAL DISTANCES, FOR TURBULENT FLOW IN A TUBE ENTRANCE REGION.

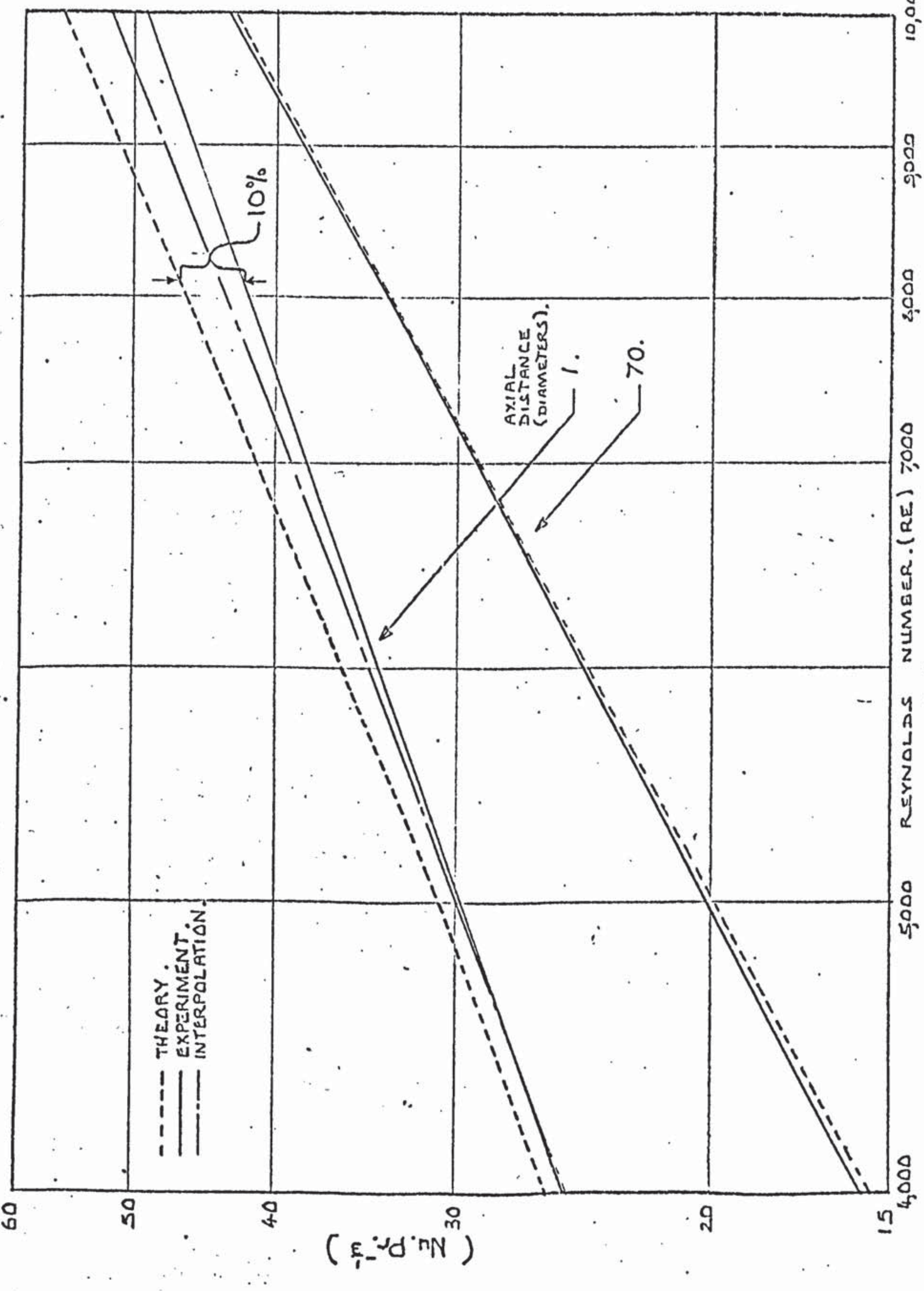

FIGURE. 11.17

THE VARIATION IN NUSSELT NUMBER WITH DISTANCE IN THE TURBULENT ENTRANCE REGION OF A TUBE. A COMPARISON BETWEEN THEORY AND EXPERIMENT.

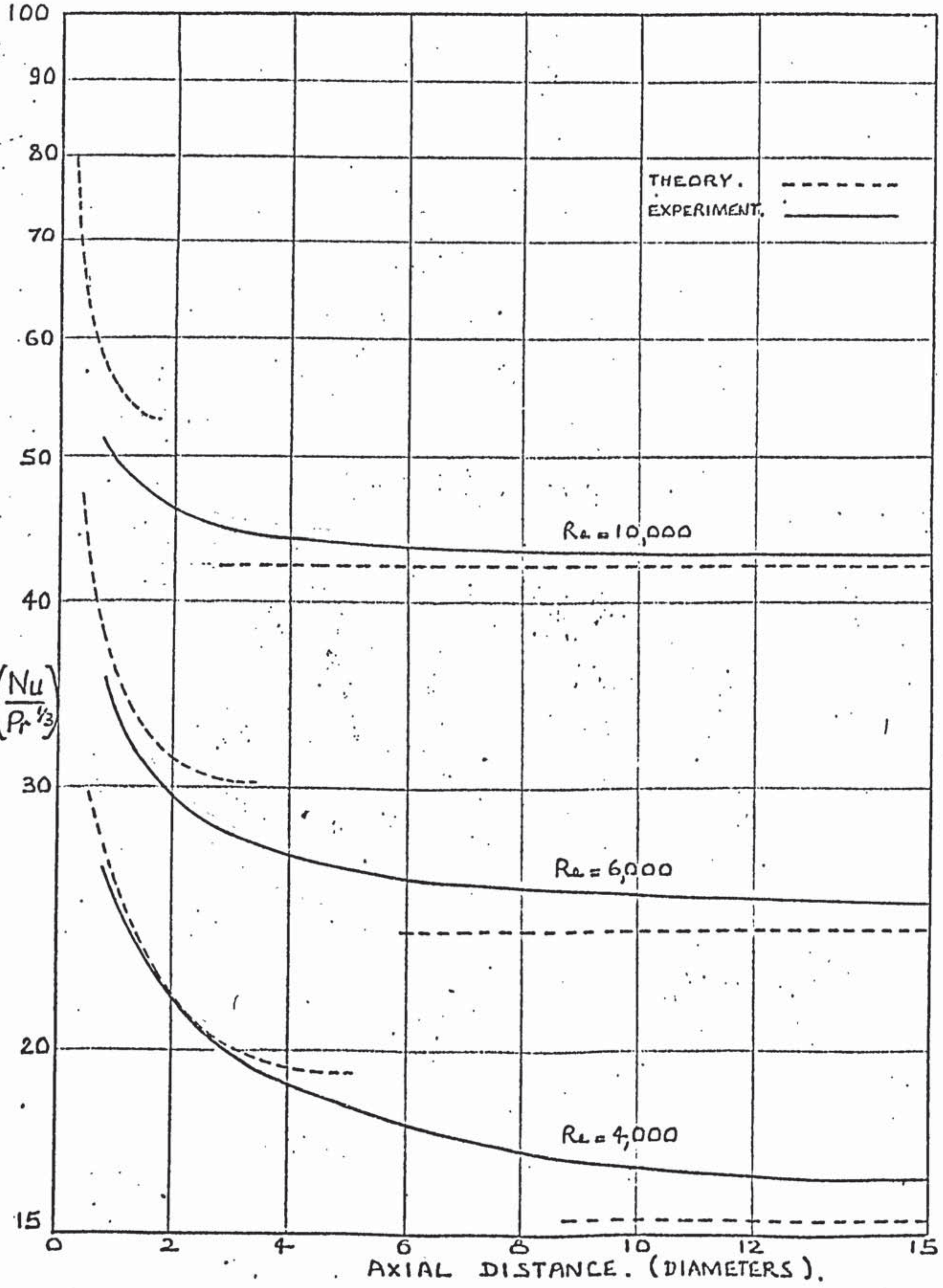

FIGURE. 11.18

THE VARIATION IN NUSSELT NUMBER WITH AXIAL DISTANCE IN THE TURBULENT ENTRANCE REGION OF A TUBE. A COMPARISON BETWEEN EXPERIMENT AND SEMI-THEORETICAL INTERPOLATION.

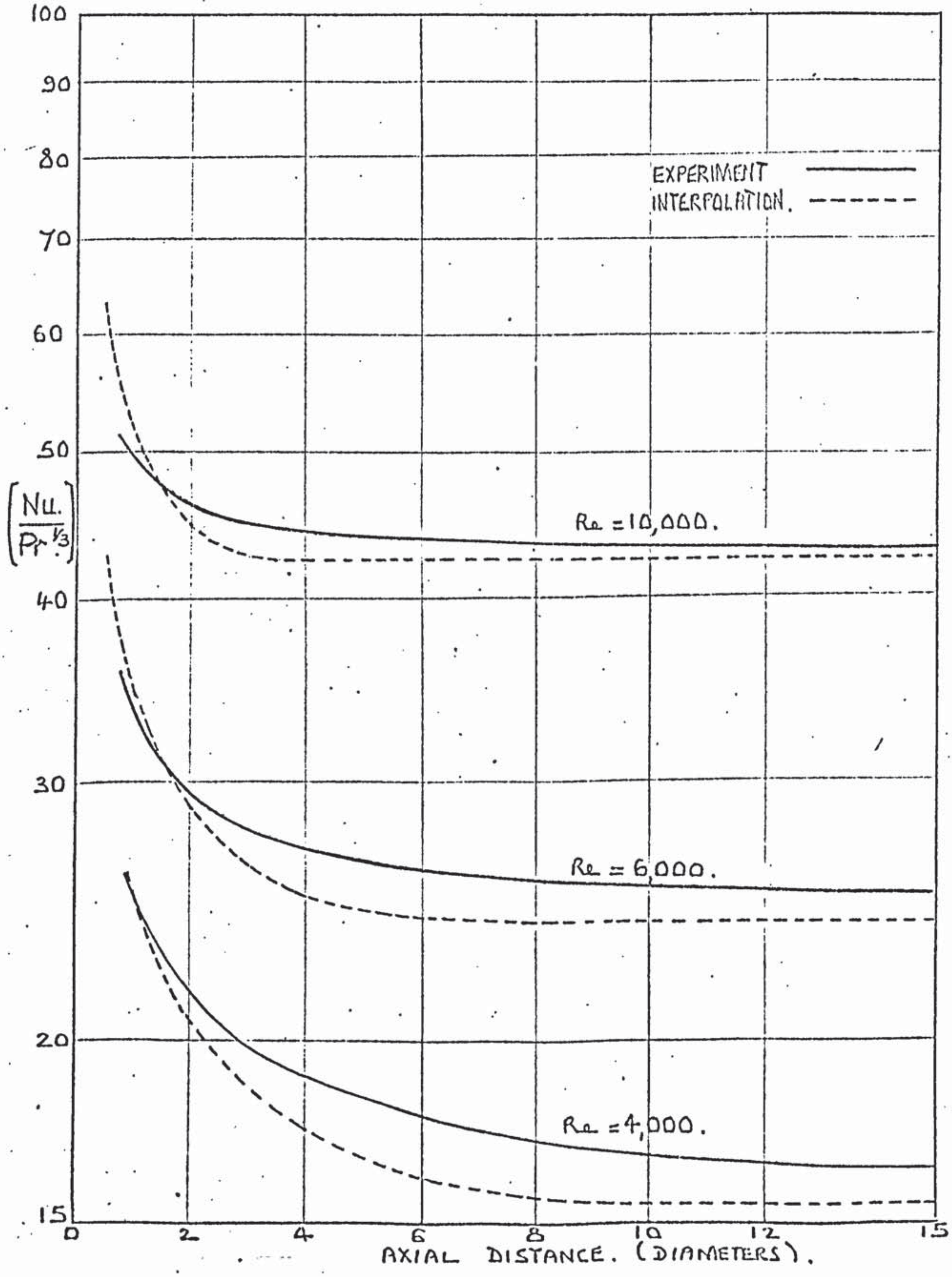

FIGURE 11.19.

COMPUTED STREAMLINES AND ISOTHERMS. 1:2 DIVERGENCE. Re=200 . Pr=100.

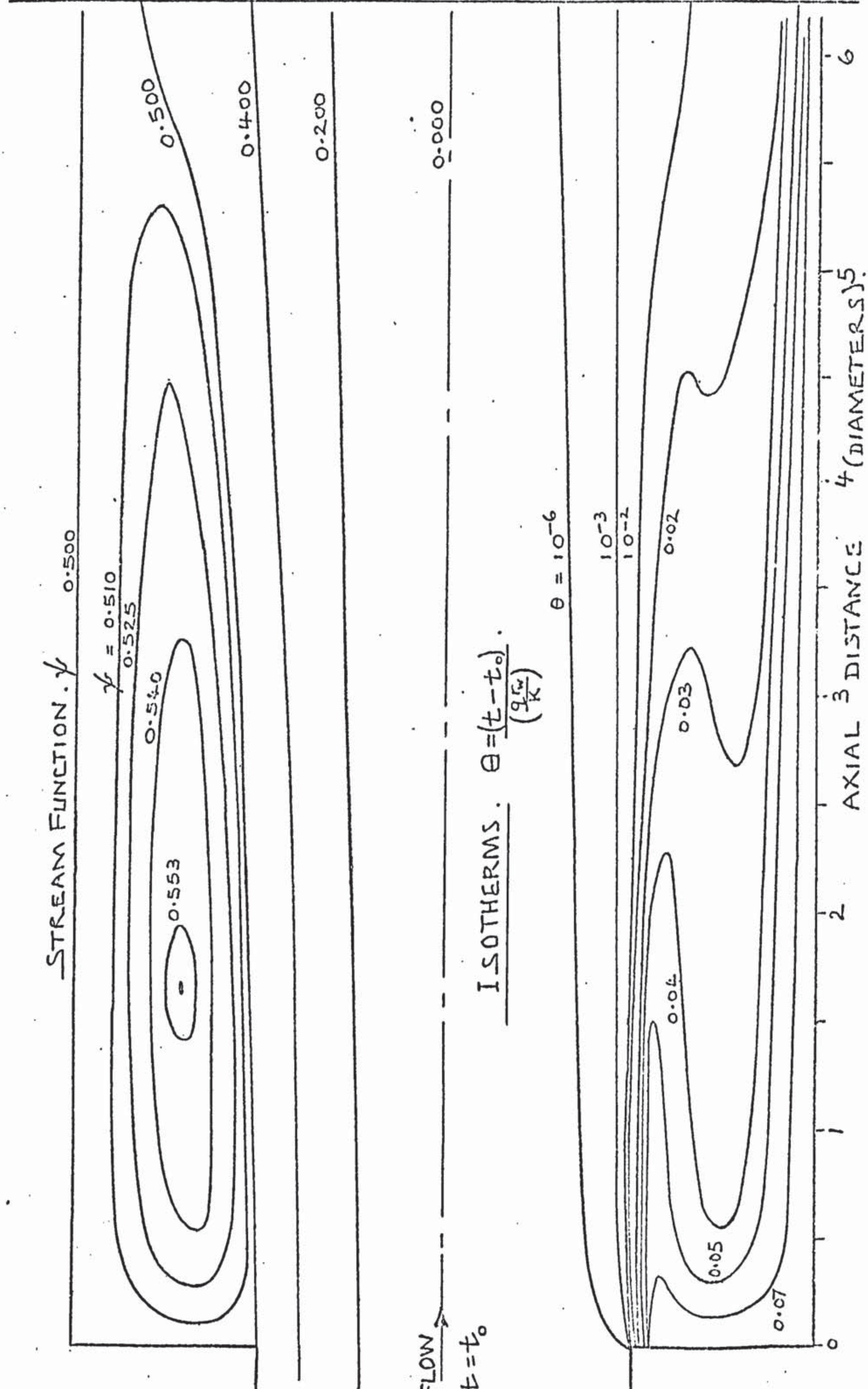

FIGURE 11.20.

AXIAL VELOCITY PROFILE FOR 1:2 DIVERGENCE.

Re = 200.

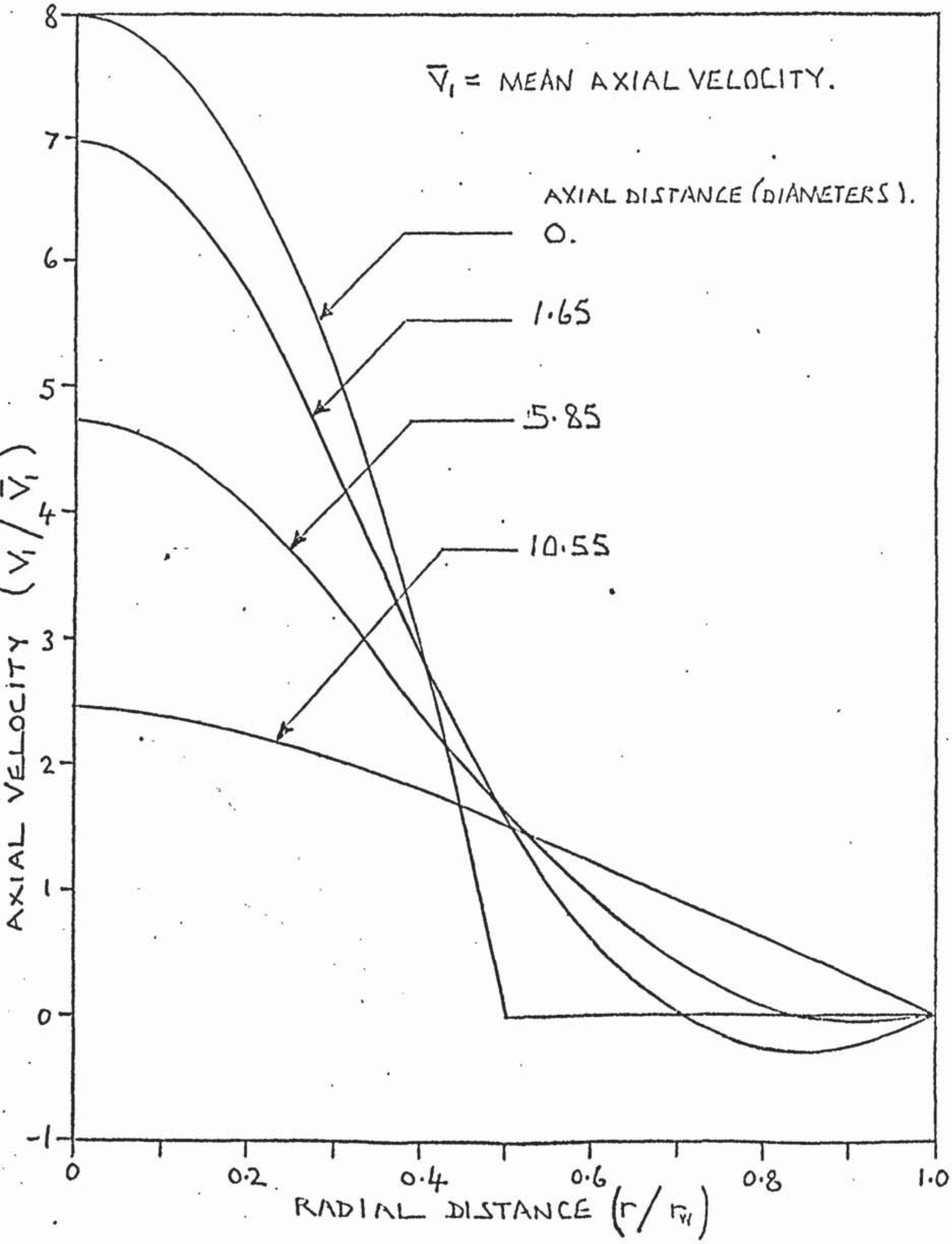

FIGURE 11.21a

(Nu / $Pr^{0.2}$) VERSUS AXIAL DISTANCE IN A DIVERGENCE. THE EFFECTS OF PRANDTL NUMBER FOR Pr = 100 AND 1,000.

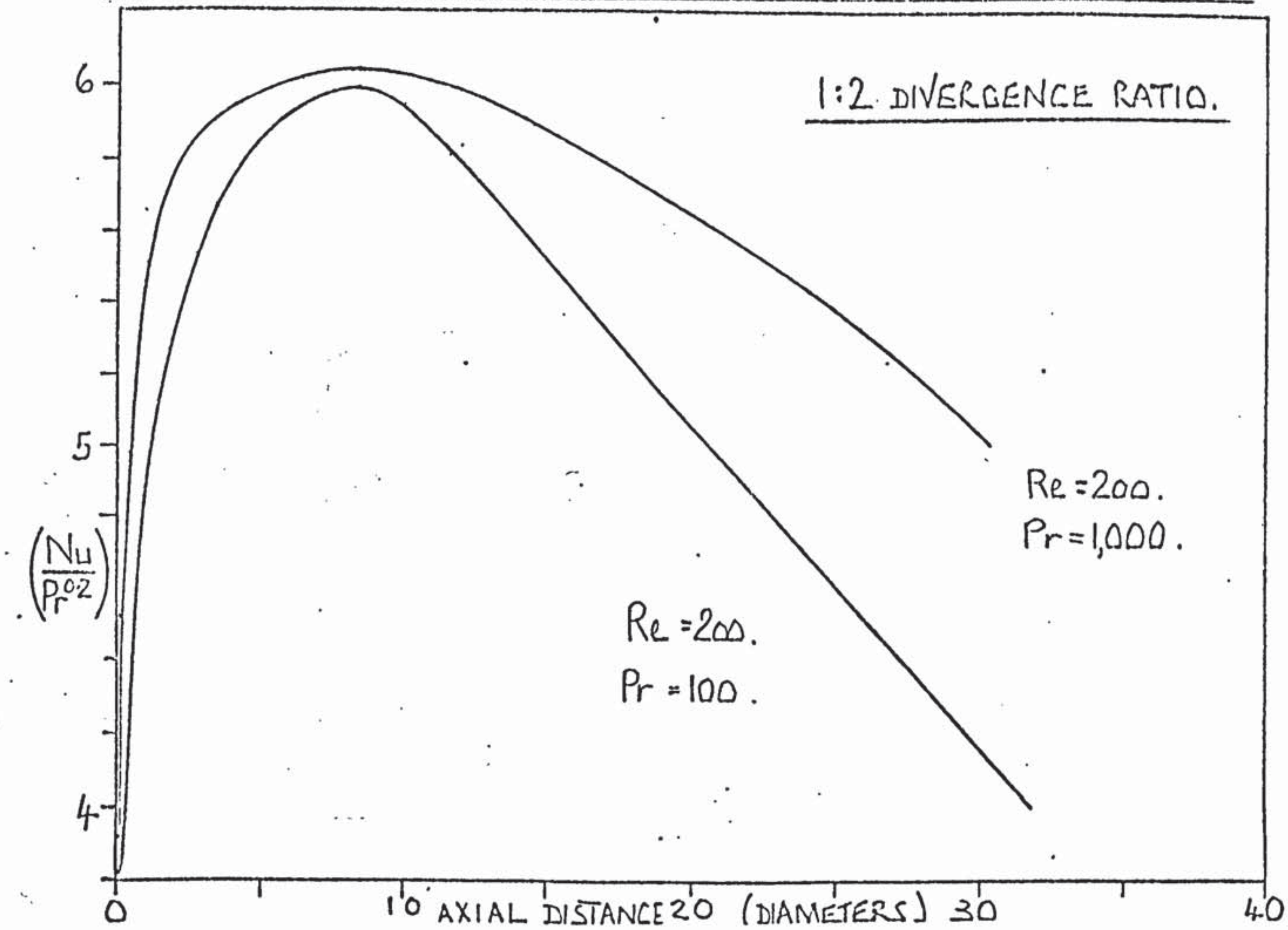

FIGURE 11.21b

NUSSELT NUMBER VERSUS DISTANCE. COMPARISON WITH SHORT TUBE THEORY.

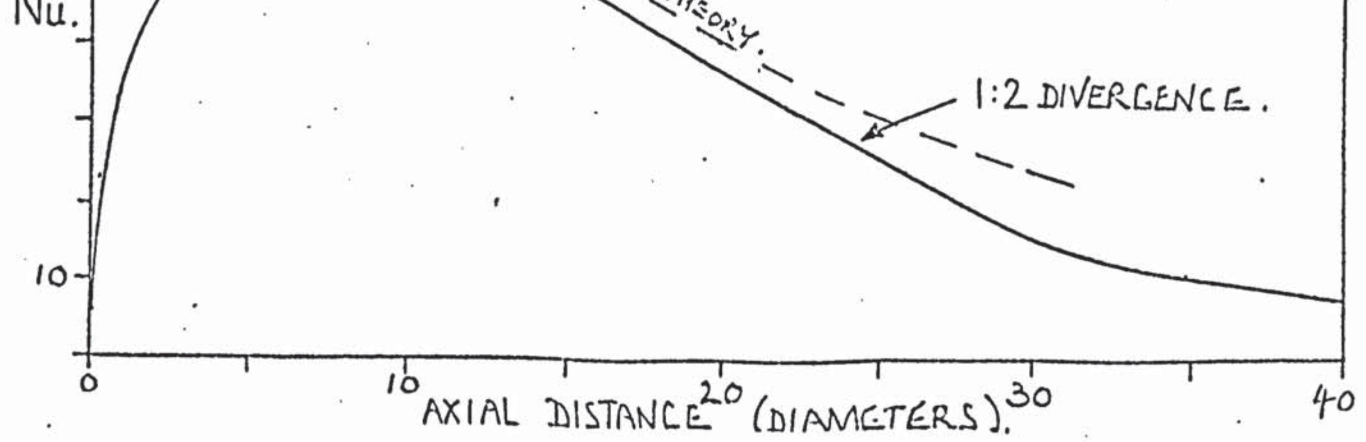

FIGURE 11.22.

NUSSELT NUMBER VERSUS DISTANCE FOR DIFFERENT VALUES OF REYNOLDS NUMBER.

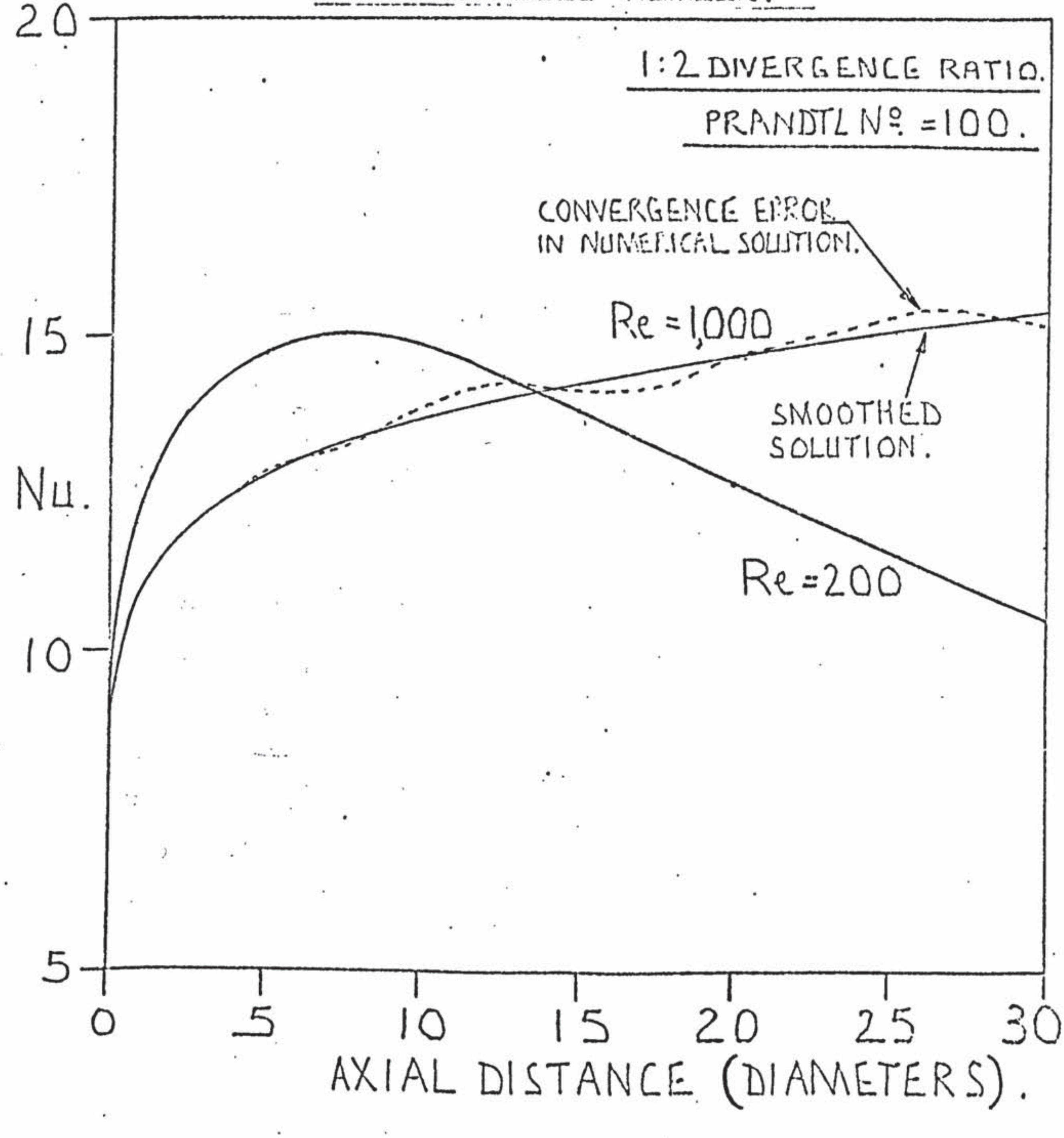

FIGURE 11.23..

COMPUTED STREAMLINES AND ISOTHERMS. 1:2 DIVERGENCE.

Re = 1000   Pr = 100.

STABLE LAMINAR FLOW.

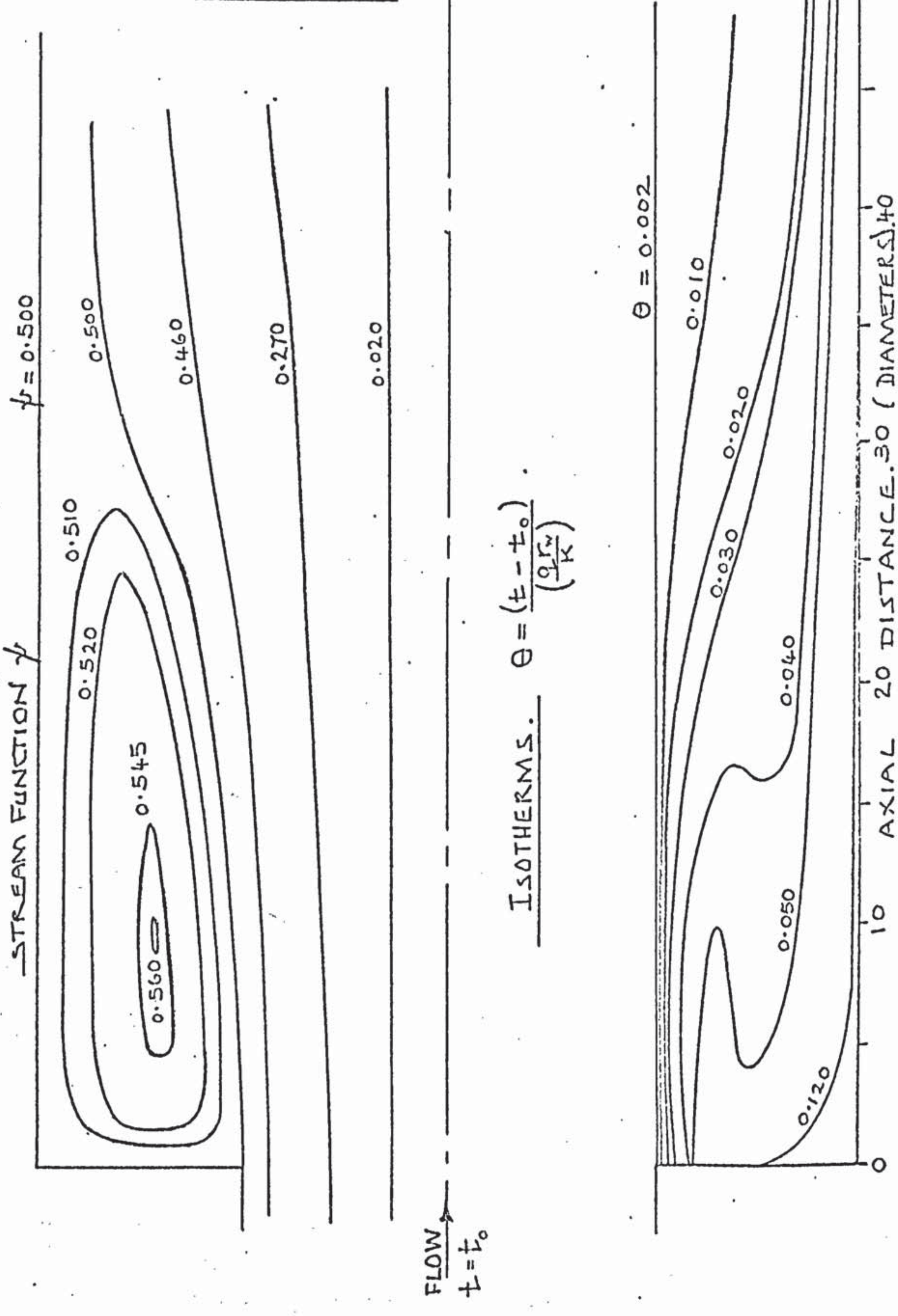

FIGURE 11.24.

COMPARISON BETWEEN THEORY AND EXPERIMENT FOR NUSSELT NUMBER IN A 1:2 DIVERGENCE. Re = 200 (LAMINAR) PRANDTL NUMBERS 100 AND 1,000.

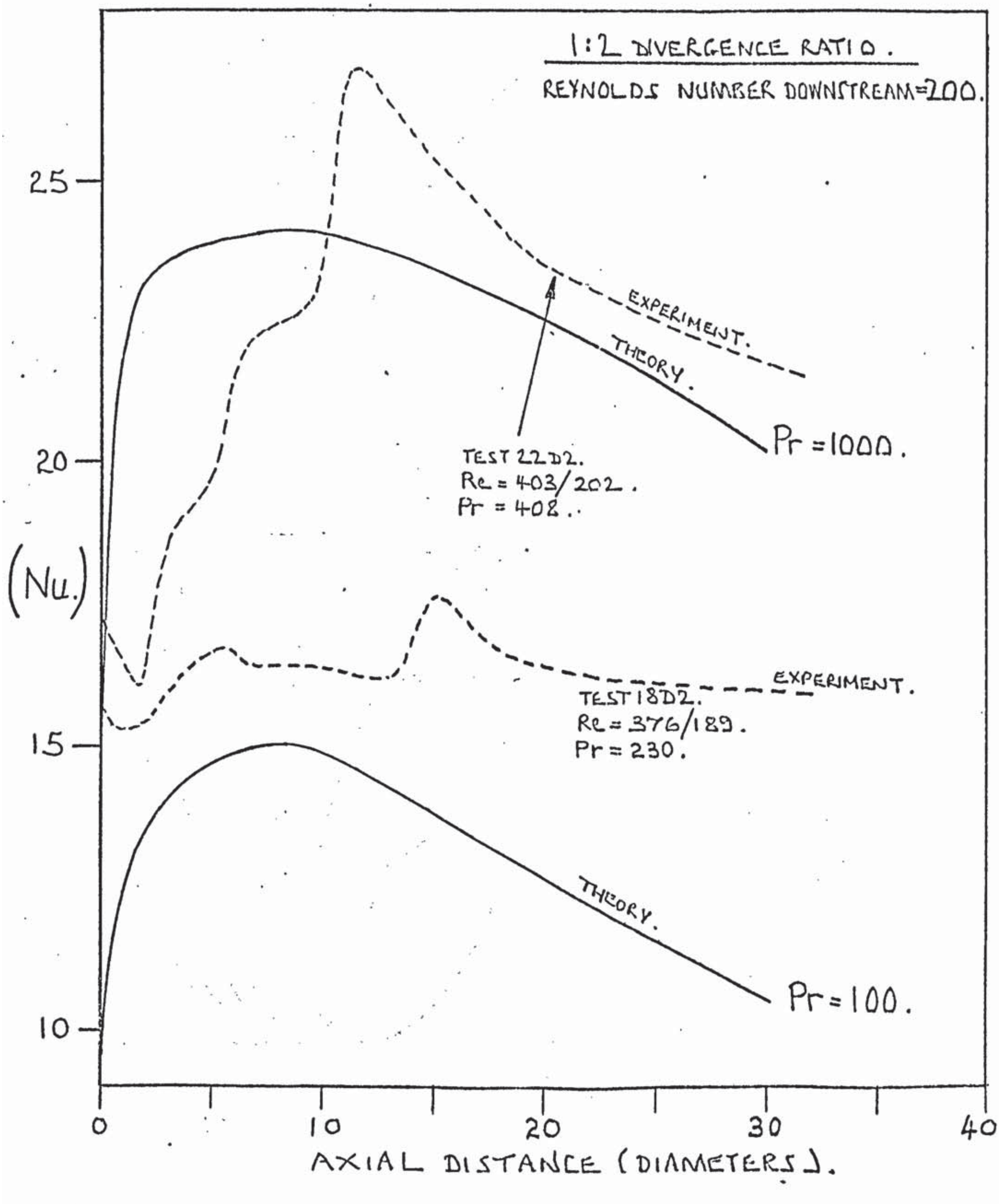

FIGURE 11·25

CALCULATED STREAMLINES (ψ) AND VORTICITY/RADIUS ($\frac{\omega}{r}$) FOR TURBULENT FLOW THROUGH A 1:2 DIVERGENCE.

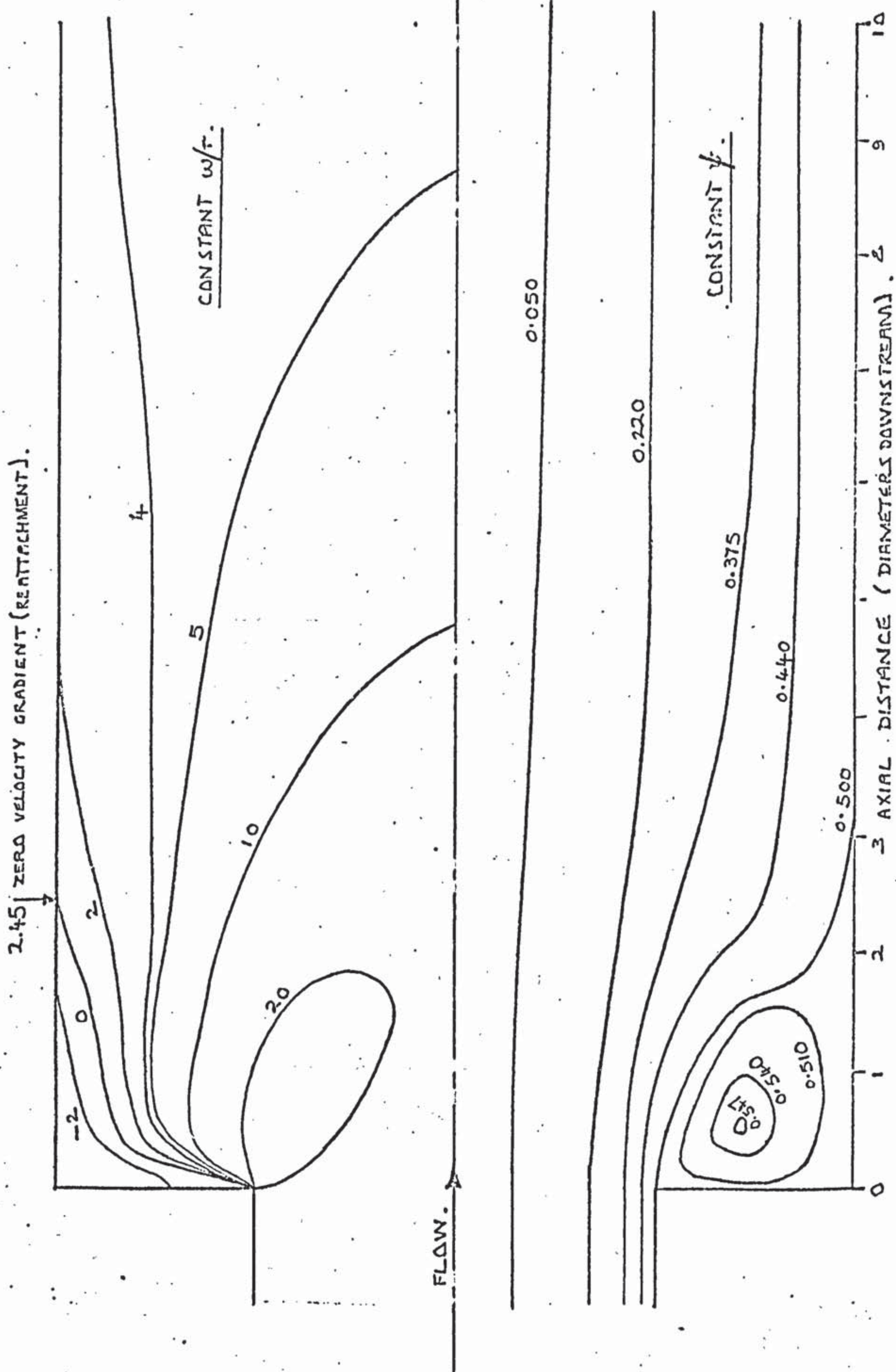

FIGURE 11.26.

VORTICITY AT WALL FOR TURBULENT FLOWS THROUGH 1:2 DIVERGENCE RATIO.

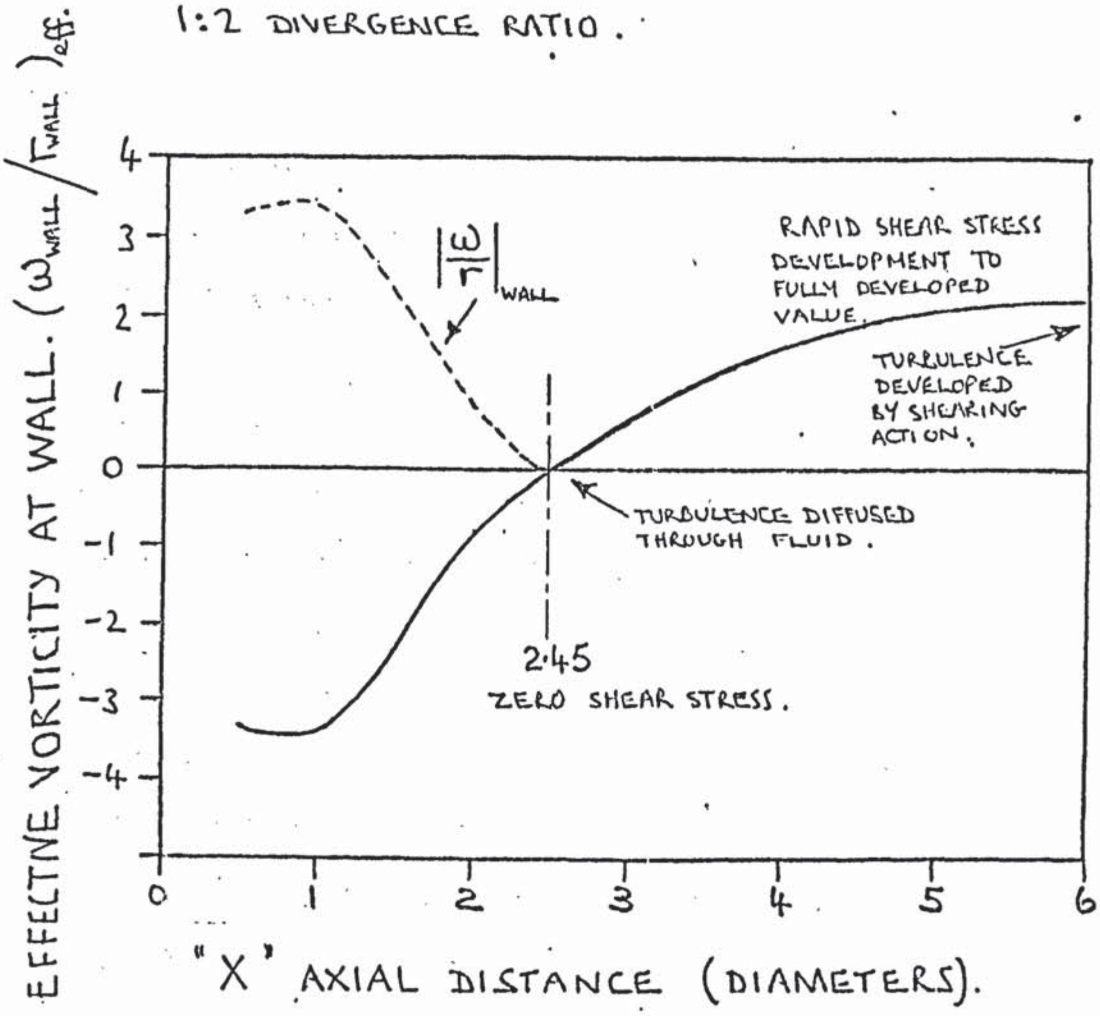

NOTE: TRUE VORITICITY AT WALL GIVEN BY – $\omega_{WALL} = \omega_{eff.WALL}\left[\frac{\mu_{eff}}{\mu}\right]$

WHERE – $\mu_{eff.} = 0.013.\rho.V_1(0,0).r_i$

HENCE – $\omega_{WALL} = \omega_{eff.WALL}\left(\frac{0.013}{2}.Re_{upstream}\right)$

NUSSELT NUMBER FOR TURBULENT FLOW.

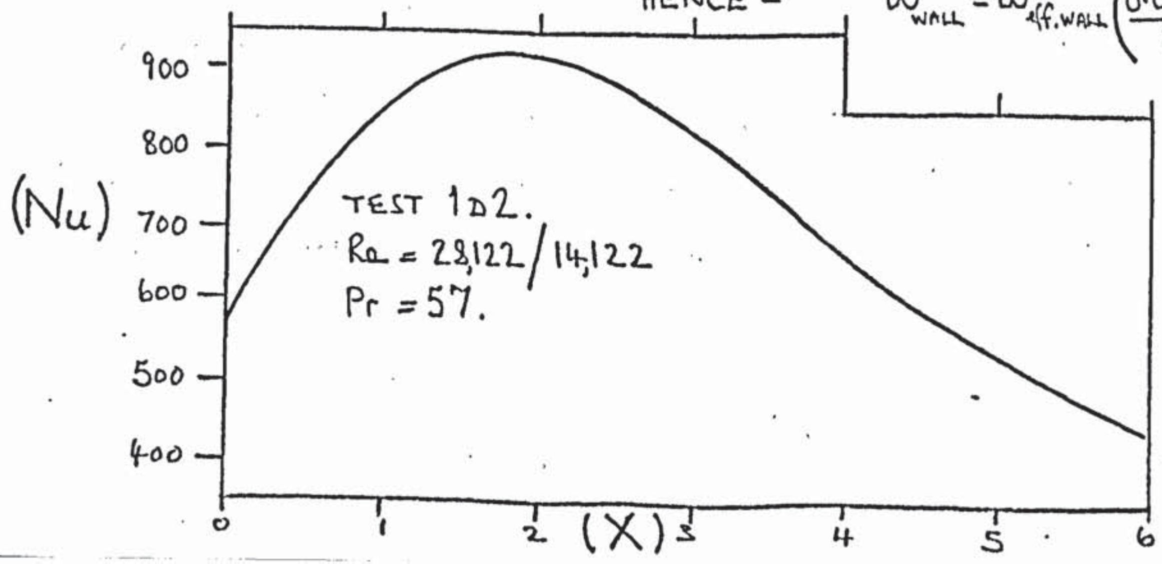

12. DISCUSSION OF THE RESULTS AND THEIR APPLICATION.

12.1 THE SHORT STRAIGHT TUBE.

The axial distribution of the local coefficient of heat transfer h in a short tube can be derived directly by interpolating the data presented in figures 9.16, 9.20, 9.24 and 9.26.
It is necessary to consider the contribution of viscous dissipation, variations in viscosity, and free convection to the value of h.

Viscosity variations are discussed in part 9.5., where h is shown to be proportional to $M_{wall}^{0.14}$. This parameter is readily determined once the tube and bulk fluid temperatures are known. If the heat flux is specified, the temperatures must be determined by an iterative procedure.

The theoretical appraisal of viscous dissipation in parts 11.1.(ii), (v) and (vii) showed that h is reduced in magnitude when the heat flux q is small. The effect on h is less than 10% when $q > 20(\mu\bar{u}^2/r_w)$ for laminar flow, or $q > 0.2\ (\mu\bar{u}^2/r_w)\mathrm{Re}^{0.7}\mathrm{Pr}^{-\frac{1}{3}}$ for turbulent flow. Several relationships are proposed in part 11.2. which may be used to correct the value of h if the above conditions are not satisfied.

Free convection was found to increase the value of h in laminar flows, and the criterion for determining whether such contributions were significant was as follows -
free convection was small if $\dfrac{(\mathrm{GrPr})^{\frac{1}{4}}}{(\mathrm{RePr})^{\frac{1}{3}}}\cdot\left(\dfrac{x}{2r_w}\right)^{\frac{1}{3}} < 2.5$

The corrected value of h can be determined from figure 9.18.

For some applications a detailed knowledge of the local values of h is not required. In such instances it is useful to have an 'effective increase in tube length', which is defined as follows -

$$\Delta L = \int_0^L \left(\frac{h}{h_\infty} - 1\right) dx ,$$

where h_∞ = the value of h at large axial distances.
L = tube length.

This concept enables a designer to visualize conditions near the entrance as being equivalent to an extra length of tube, when the flow regime is turbulent. In laminar flow a mean value of h is sometimes used, as follows: -

$$h_m = \frac{1}{L} \int_0^L h \; dx .$$

The latter result is easily obtained from the theoretical or experimental values of h discussed above, should the information be required. The value of ΔL is worthy of investigation however because of its physical interpretation.

The theoretical results of part 11.2.(vii) permitted the transitional and turbulent values of h/h_∞ to be given with reasonable accuracy by

$$h/h_\infty = \frac{33.4}{\gamma(1 - 2.87\ 10^{-6}\gamma^3)} ,$$

for $\gamma < 44.4$, where $\gamma = \left(\frac{x}{2r_w} Re^{1.1}\right)^{\frac{2}{3}}$

The value of ΔL becomes 22,100 $Re^{-1.1}$ diameters after integration, which is numerically 2.4 diameters at Re = 4,000, and 0.9 diameters at Re = 10,000 (when L exceeds the entrance length).

12.2. THE CONVERGENCE.

When a sudden reduction in tube diameter occurs, the local values of h can be derived from figures 9.27 to 9.38 . The magnitude of h was shown to be dependent on the Prandtl number and diameter ratio in a complicated way, so that it was impossible to define a unique relationship between h and Pr valid for all axial positions. A tedious but necessary procedure must be undertaken to interpolate the data provided, so that graphs of

$(Nu/Pr^{\frac{1}{3}})$ versus (distance) can be determined for a particular configuration and type of fluid. Although experiments were not carried out to assess the way in which Nu could be influenced by free convection, viscous dissipation, and variations in viscosity it would be reasonable, in the absence of further information, to assume that the methods suggested for application to the short tube configuration will give a fair estimate of such secondary effects. The similarity in the geometry and measured functions of Nu substantiate this suggestion.

If local values of h are not required for a given application it is recommended that for laminar flows h_m is calculated, and for transitional or turbulent flows ΔL is determined. A simple numerical integration of the $(Nu/Pr^{\frac{1}{3}})$ functions can be carried out as discussed in part 12.1.

12.3. THE DIVERGENCE.

Consider first the local coefficient of heat transfer in a divergence with Re_1(upstream leg) greater than 2,500. From the data presented in figures 9.48 to 9.62 it might be found useful to plot graphs of (h/h_∞) versus (distance) for a particular diameter-ratio, and for a range of Reynolds numbers (h_∞ can be assumed to be the value at 40 diameters downstream). This is possible because it has benn demonstrated that $Nu \propto Pr^{\frac{1}{3}}$ at large axial distances, and in the region of the maximum value of h. Alternatively, if local values of h are not required the value of ΔL can easily be determined as discussed in parts 12.1. and 12.2.

With $Re_1 < 2,500$ there is no simple method of estimating local coefficients of heat transfer reliably (for detailed discussion see part 9.7.). In the first instance, a transition region of Re_1 was shown to exist in the approximate range 700 and 2,800 for diameter-ratios up to 1:3.34. In this region the two extremes of turbulent and laminar flow could give rise to values of h differing by a factor of 5 to 7 times. The selection of appropriate data will obviously depend on the design criteria in the transition region. In the second instance, for all values of Re_1 less than 2,500 it was demonstrated that the shape and magnitude of the (Nu) versus (distance) functions were primarily dependent on Re_1 and Pr, but it was also observed that the functions were sensitive to the heat flux imposed. In view of the preceding arguments it is recommended that part 9.7. is understood before attempting to utilise the data presented in figures 9.48 to 9.62 .

12.4. GENERAL CONSIDERATIONS.

The applications for which it is particularly advantageous to have information on local coefficients of heat transfer are those in which the heat-transfer channels, or cooling passages, (in the present discussion circular ducting), comprise short lengths having uniform diameter. A typical example is illustrated below, for which it is difficult to imagine how a reliable rate of heat transfer per unit temperature difference could be estimated without the data presented herein. The configuration might represent a cooling passage in a piece of machinery, and the designer could be interested in the minimum number of such passages required to hold down the temperature of a component, there being a limit on the available space. Many similar applications can be envisaged where large variations in the value of h occur continuously with distance.

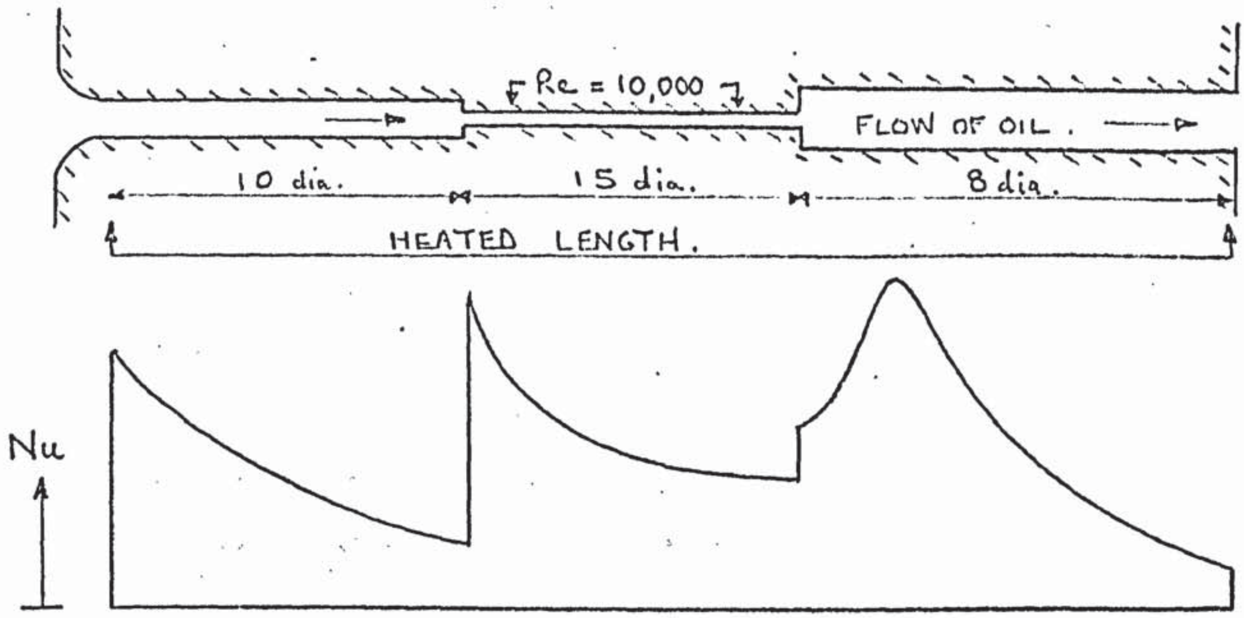

Other configurations will certainly arise where the engineer must use some discretion in applying the results of these tests. Typical cases might incorporate severe variations in the axial distribution of heat-flux, or the geometry of the system might not correspond closely with those included in this work, for example:

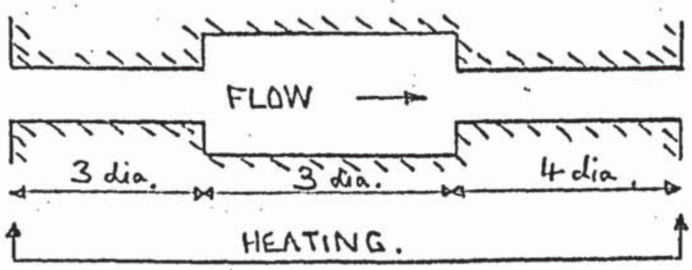

Unfortunately, no general guidance can be given for dealing with problems of this kind, each case must be considered independently. In the above diagram, the convergence nearest the outlet end might alter the flow pattern within the centre section substantially, although it is probable that the axial distribution of Nu in this region would be significantly different from the divergence results stated during laminar flow only.

13. CONCLUSIONS AND FUTURE WORK.

Measurements have been obtained of the local coefficient of heat transfer in short lengths of horizontal tube, and in the region of a discontinuity in tube diameter. Laminar, transitional and turbulent flows were investigated utilising several viscous fluids.

The effects of free convection, temperature dependent viscosity, and viscous dissipation on the heat transfer process were assessed with the proviso that such contributions were small in magnitude. In the latter case the assessment was purely theoretical, since dissipation was shown to play an insignificant role in the experiments carried out. Both theoretical and empirical analyses were instigated for the cases of free convection and variable viscosity.

In the experiments with the short tube it was first shown theoretically that Nu was proportional to $Pr^{\frac{1}{3}}$, then the group $(NuPr^{-\frac{1}{3}})$ was shown by experiment to be a unique function of axial position for particular Re. It is implied in the foregoing that no secondary effects (e.g. free convection) were present, and the flow was fully developed at the entrance of the tube. When the flow was undeveloped at the entrance, the parameter $(Nu/Pr^{\frac{1}{3}})$ was found to be a unique function, as described, only for the transitional and turbulent flow regimes. With laminar flow, $(NuPr^{-\frac{1}{3}})$ was found to be a weak function of Pr as well as Re and distance. The maximum difference between Nu-developed and Nu-undeveloped in these experiments was approximately 40% with $Pr \simeq 90$, and 20% with $Pr \simeq 500$. In general, the 'developed' correlations could therefore be used to give a reasonable estimate of 'undeveloped' coefficients of heat transfer when a viscous medium was utilised.

The axial distribution of Nu close to a sudden convergence in diameter was determined experimentally for four different Prandtl numbers. The parameter ($NuPr^{-\frac{1}{3}}$) was shown to be a function of the axial position and Re when turbulence was present in the section of tube downstream. With laminar flow downstream, the values of ($NuPr^{-\frac{1}{3}}$) close to the discontinuity were shown to increase as Pr was reduced, for a particular Reynolds number. With particular values of Re and Pr downstream, the Nusselt numbers measured close to the convergence were found to increase with the ratio (upstream diameter)/(downstream diameter). The magnitudes of Nu were found to be greater than the corresponding values obtained with a short tube having undeveloped flow at the entrance, provided the turbulent regime prevailed. With laminar flows the measured values of Nu were generally less than those obtained in the short tube experiments.

The separated region of flow, which occurred just downstream of a sudden divergence in diameter, gave rise to an axial distribution of Nu with a well defined peak-value near to the discontinuity. When the Reynolds number for the section of tube upstream was greater than 2,500 the flow regime close to the step could be described as turbulent. The axial distribution of Nu for such flows was expressible in the graphical form ($NuPr^{-\frac{1}{3}}$) as a function of axial distance, with Re constant. The position of maximum Nu was found to be invariant with Re for a particular diameter ratio. Some theoretical substantiation of this was derived.

For lower Reynolds numbers (than 2,500 upstream) a complicated flow pattern was evident which was investigated using flow visualization experiments and numerical analysis. Laminar flow was present when Re was of the order 100 and coefficients of heat transfer were measured which were relatively much lower than turbulent values. An intermediate flow regime was shown to exist in which either turbulence or lamination could occur, it was clear that there was no smooth transition from one regime to the other.

At the lower Reynolds numbers just described, the axial distribution of Nu was found to be dependent on the heat flux. Generally, the peak in the Nu - distance function moved upstream as the flux was increased.

A theoretical analysis indicated that the position of maximum Nu was just upstream of the point of boundary layer reattachment. It was shown also that a relationship of the kind $Nu \propto Pr^n$ was inadmissible as a means of correlating the experimental data at low Reynolds numbers because the exponent n would have to be a function of the axial position.

Certain aspects of these investigations could be extended still further to give an 'in depth' appreciation of the heat transfer mechanisms, and to provide information on a greater range of practical conditions than are covered herein. For example, the use of more highly viscous oils arises in practice, and extremely small Reynolds numbers (creeping flows) are likely to be encountered. In this thesis it has been indicated that a geometrical discontinuity can be used to prevent the occurrence of large coefficients of heat transfer at the entrance of a tube having low Reynolds number flow. Further, it became apparent that a geometrical discontinuity has a significant effect on Nu at large axial distances. The rate of heat transfer could easily be overestimated in these circumstances if one is led by intuition in the absence of recorded measurements.

Other types of fluid could be investigated to advantage, in particular the non-newtonian fluids. Comparatively, little experimentation has been carried out in this area of heat-transfer, and information on the effects of a sudden change in diameter would prove a valuable contribution. Initially, pseudoplastic, time-independent fluids (i.e. with a non-linear stress-strain relationship) should be considered since the results would have wide application in the process industries. A suitable dilute polymer solution might be considered initially.

Other topics which should be pursued are as follows - the investigation of a sudden divergence when the diameter ratio is large (not necessarily with viscous fluids), the theoretical analysis of laminar and turbulent heat transfer in a divergence or convergence, and heat transfer in two-phase flow through a discontinuous tube. The scope of the research could be increased by considering other practical geometrical configurations; changes in the flow direction such as occur in a helical tube would be a suitable subject.

APPENDIX (A)

SPECIFICATION AND DESCRIPTION OF APPARATUS.

(1) Pump and Motor

Drysdale and Co. Ltd. Type UniMac U14/25

Supply 415 v, a.c 3ph. 50 c/s.

Motor 25 h.p.

Centrifugal Pump 14 h.p. 100 lbf/in^2.

(2) Cooler

Serck Radiators Ltd. Type 509304.

Cast iron shell, alum-brass tubes.

Specification with oil-viscosity 72 cP.

Oil Side				
Flow rate lb/hr	Pressure drop lbf/in^2	Temperature °F in	out	diff
32,000	7	104	100	4
Water Side				
3,000	2	70	-	-
Heat Transferred = 135,000 Btu/hr.				

(3) Filters

Birfield Filtration Ltd.

One type 620 ST, with 80 mesh monel gauze strainer

One type FC1, with 5 micron filter cartridge.

(4) Flowmeters

Meterflow Ltd.

Frequency meter, type M707, 0 - 2,000 c/s.

Turbine flowmeter, type M2/1500/B150, 0 - 150 gal/min.

Turbine flowmeter, type M2/0625/B15, 0 - 15 gal/min.

Meters calibrated on water, Aeroshell, and Tellus 27.

(5) Thermocouple selector switches

The Croydon Precision Instrument Co.

3 - 100 way selector switches, type SP2.

(6) Calibrated shunt

The Cambridge Instrument Co. Ltd.

N.P.L. calibrated shunt.

Resistance $50\mu\Omega \begin{smallmatrix} +0.025 \\ -0 \end{smallmatrix}$ at 20°C with 200-2,000A.

(7) Potentiometer

H. Tinsley & Co. Ltd.

Vernier potentiometer type 4025A.

(8) Voltage controller

Midland Transformer Co. Ltd.

On load power regulator type RDCAM 50/250

Input 415 v   0 - 50A

Output 0 - 415 v   50A

(9) Rectifier and smoothing unit

Hackbridge and Hewittic Electrical Co. Ltd.

Rectifier transformer type 106029A

Primary 415 v,   103A

Secondary 26 v, 1640A

Metal rectifier type 11L2

Output 30 v,   2000A.

APPENDIX (B).

HEAT TRANSFER IN SLUG FLOW USING THE LEVEQUE PROCEDURE AS MODIFIED BY SELLARS.

The problem is to determine the axial distribution of Nu, in a tube passing fluid at uniform velocity, when a constant heat flux is applied downstream of a point x = 0. When utilising Sellars' procedure (Ref: C.13) a solution must first be obtained for the case of constant tube temperature, then this becomes a particular solution which can be modified to suit other boundary conditions.

The energy equation is written

$$\frac{d\Theta}{dX} = 2\,\frac{d^2\Theta}{dY^2}$$

where t_w = tube wall temperature,

t_∞ = the inlet temperature,

$$\Theta = \frac{(t - t_\infty)}{(t_w - t_\infty)} \,,$$

$$X = \frac{x}{r_w \mathrm{RePr}} \,, \qquad Y = \frac{y}{r_w} \,.$$

Now choosing the similarity variable $\eta = \frac{Y}{X^{\frac{1}{3}}}$, so that $\Theta(X,Y) = \theta(\eta)$, the equation becomes,

$$\theta'' + \frac{\eta}{4}\,\theta' = 0 \,,$$

$$\text{or} \qquad \frac{d}{dZ}\left(e^{\eta^2/8} \cdot \theta'\right) = 0 \,.$$

Integrating with $\theta(\infty) = 0$, $\theta(0) = 1$, gives

$$\theta = \left(\int_Z^\infty e^{-\eta^2/8}\, d\eta\right) \Big/ \left(\int_0^\infty e^{-\eta^2/8}\, d\eta\right).$$

The Nusselt number at constant temperature is found from

$$\mathrm{Nu}_{temp} = 2\,\frac{d\Theta}{dY}\bigg|_{Y=0} = 2\,\frac{d\eta}{dY}\,\theta'(0) \,,$$

$$\text{hence} \qquad \mathrm{Nu}_{temp} = 2\,X^{-\frac{1}{3}}\;\theta'(0).$$

$\theta'(0)$ is as follows

$$\theta'(0) = \left[\int_0^\infty e^{-\eta^2/8}\, d\eta\right]^{-1}$$

$$= \frac{8^{\frac{1}{2}}}{4.\Gamma(\frac{1}{2})}$$

so that $\underline{Nu_{temp} = 0.798\, X^{-\frac{1}{2}}}$

To obtain a similar result for uniform heat flux, Nu_{heat}, the following integral is utilised.

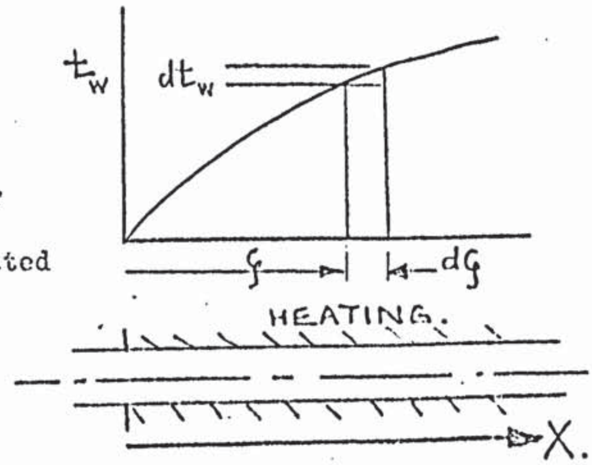

$$q = \int_{\xi=0}^{X} h'\,(X,\xi)\; dt_w$$

Where h' = coefficient of heat transfer for a step in temperature, with ξ unheated length, or $\left(\frac{2h'\, r_w}{K}\right) = 0.798(X-\xi)^{-\frac{1}{2}}$.

Rewriting,

$$1 = \frac{0.798}{2}\int_{\xi=0}^{X} (X-\xi)^{-\frac{1}{2}}\; \frac{d\bar{\theta}_w}{d\xi}\; d\xi, \text{ where } \bar{\theta}_w = \frac{(t_w - t_\infty)}{\frac{q r_w}{K}}\,.$$

Suppose $Nu_{heat} = AX^{-\frac{1}{2}}$, and constant A is to be determined. The wall temperature is given by $\bar{\theta}_w = 2/Nu_{heat}$, so that

$$\frac{d\theta_w}{d\xi} = (A\xi^{\frac{1}{2}})^{-1}\,.$$

Putting this into the integral

$$\frac{2A}{0.798} = \int_{\xi=0}^{X} (X-\xi)^{-\frac{1}{2}}\;\xi^{-\frac{1}{2}}\, d\xi$$

$$= \frac{\Gamma(\frac{1}{2}).\Gamma(\frac{1}{2})}{\Gamma(\frac{1}{2}+\frac{1}{2})}\,.$$

Therefore $A = 1.252$

or $\underline{Nu_{heat} = 1.252.X^{-\frac{1}{2}}}$.

BIBLIOGRAPHY.

The following references are classified under eleven main subject headings. In some instances a paper contains information on more than one subject, in such cases a particular subject has been selected as being the most relevant.

(A) Heat transfer in long tubes - experimental.

(1) A.J. EDE, Int.J.Heat Mass Transfer, 1961, 4, 105-110.

(2) P. SACHS, Jour. Mech. Eng. Sci, 1962, 4, 78-84.

(3) H. KRAUSSOLD, Die Warme, 1939, 267-268.

(4) W.L. FRIEND, A.B. METZNER, A.I.Ch.E.J., 1958, 4, 393-403.

(5) F.H. MORRIS, W.G. WHITMAN, Ind. Eng. Chem., 1928, 20, 234-240.

(6) H. HAUSEN, Allg. Warmetechnik, 1959, 9, 75-79.

(7) T.K. SHERWOOD, Ind. Eng. Chem., 1932, 24, 736-745.

(8) A.P. COLBURN, Trans. A.I.Ch.E., 1933, 29, 174-210.

(9) R.H. NORRIS, M.W. SIMS, Trans. A.I. Ch. E., 1942, 38, 469-492.

(10) W. BUHNE, Die Warme, 1938, 162-165.

(11) J. BOHM, Die Warme, 1942, 20, 221-228.

(12) K. WINKLER, Forsch. Ing-Wes., 1935, 6, 261-268.

(B) Heat transfer in short tubes - local measurements.

(1) J.A. MALINA, E.M. SPARROW, Chem, Eng. Sci., 1964, 19, 953-692.

(2) J.P. HARTNETT, Trans.A.S.M.E. J. Heat Transfer, 1955, 77, 1211-1220.

(3) J.R. STONE, NASA Tech. Note TN.D - 3098, 1965.

(4) W. LINKE, H.KUNZE, Allg. Warmetechnik, 1953, 4, 73-79.

(5) I.T. ALAD'EV, Izv.Akad. Nauk SSSR 1954, 11, 1669-1681.

(6) V.C. DAVIES, M.ALARABI, Proc. I. Mech E, 1955, 169.

(7) P.D. BERGMAN, LB KOPPEL, A.I.Ch.E.J., 1966, 12 (4), 648-655.

(8) H. WOLF, Trans. A.S.M.E. J. Heat Transfer, 1959, 81, 267-279.

(9) C.A. DEPEW, Trans.A.S.M.E.J. Heat Transfer, 1962, 84, 186-188.

(10) R.W. ALLEN, E.R.G. ECKERT, Trans. A.S.M.E.J. Heat Transfer, 1964, 86, 301-310.

(11) G. GRASS, Allg. Warmetechnik, 1956, 7, 58-64.

(12) A.F. MILLS, J. Mech. Eng. Sci., 1962, 4, 63-77.

(13) C. SCOTT, G.E. EGGLESTON, W.L. SIBBITT, A.S.M.E. paper number 55....SA..17, 1955.

(14) A. CHOLETTE, Chem. Eng. Prog., 1948, 44, 81-88.

(15) J.P. HARTNETT, A.S.M.E. Paper number 54...A..184, 1954.

(c) Theoretical heat transfer in tubes.

(1) W.M. KAYS, Technical report No. 20, Dept. Mech. Eng., Stanford University, California, 15th Oct. 1953.

(2) R.G. DEISSLER, Trans. A.S.M.E. J. Heat Transfer, 1955, 77(8), 1221-1233.

(3) R.G. DEISSLER, Trans.A.S.M.E.J. Heat transfer, 1951, 73, 101-107.

(4) E.M. SPARROW, T.M. HALLMAN, R. SIEGEL, App. Sci. Res., 1958, A7, 37-52, and 386 - .

(5) T. Von KARMAN, Trans. A.S.M.E.,1939, 61, 705-710.

(6) L.M.K.BOELTER, R.C. MARTINELLI, F. JONASSEN, Trans. A.S. M.E., 1941, 63, 447-455.

(7) A.McD.MERCER, Appl. Sci, Res., 1960, 9, 450-456.

(8) R. MANOHAR, Int. J. Heat Mass Transfer, 1969, 12, 15-22.

(9) R.R. HUNZIKER, Journ.Franklin Institute, 1958, 265, 205-225.

(10) T.J. HANRATTY, Engineering Experiment Station, University Illinois, 1957, Tech. report No. 4.

(11) H.F. POPPENDIEK, Oak Ridge National Lab., 1951, ORNL-913 and 1952, ORNL-914.

(12) D.N. ROY, Trans.A.S.M.E. Jour. Heat Transfer, 1965, 87, 425-426.

(13) J.SELLARS, M. TRIBUS, J. KLEIN, A.S.M.E. Paper No. 55..SA.66 1955.

(14) M. TRIBUS, J. KLEIN, University of Michigan, Heat transfer symposium 1952, 211-235.

(15) W.C. REYNOLDS, A.S.M.E. Paper No. 59..HT.13, 1959.

(16) C.S. YIH, J.E. CERMAK, Civil Eng. Dept., Colorado Agricultural and Mechanical College, Report No. 5 Project 137, 1951.

(17) C. TIEN, R.A. PAWELEK, App. Sci. Res. 1963, 13, 317-331.

(18) J. LEVEQUE, Annales des Mines, 1928, 13(12).

(19) M. HISHIDA, Bull J.S.M.E., 1967, 10, 113-123.

(20) R.D. HABERSTROH, L.V. BALDWIN, Trans. A.S.M.E. J. Heat transfer, 1968, 90, 191-200.

(21) D.BUTTERWORTH, T.D.HAZELL. 4th Int. Heat Trans. Conf; Heat Transfer 1970 (Elsevier, Amsterdam).

(D) <u>The effect on heat transfer of viscosity variations with temperature.</u>

(1) E.N. SIEDER, G.E. TATE, Ind. Eng. Chem., 1936, 28, 1429-1435.

(2) B.S. PETUKHOV, E.A. KRASNOSHCHEKOV, L.D. NOL'DE, Teploenergetika, 1956, 3, 41-47.

(3) K.T. YANG, A.S.M.E. paper No. 61..WA.166, 1961.

(4) G.I. MAIKAPAR, Izv. Akad. Nauk, SSSR. July 1958, 108-114.

(5) F.L.TEST, A.S.M.E. paper No. 67..WA/HT.8, 1967.

(6) L.B. KOPPEL, J.M.SMITH, Trans. A.S.M.E. J. Heat transfer 1962, 84, 157-163.

(7) C.F. KETTLEBOROUGH, A.S.M.E. paper No. 66..WA/FE.22.

(8) D.E. ROSENBERG, J.D. HELLUMS, I & E.C. Fundls., 1965, 4, 417-432.

(9) R.G. DEISSLER, N.A.C.A. Tech. Note T N-2410, 1951.

(10) R.L. SHANNON, C.A. DEPEW, A.S.M.E. paper No. 68..WA/HT.20 1968

(11) H.F. POPPENDIEK, Oak Ridge Nat. Lab. report 54-11-37, 1954.

(E) <u>Combined forced and free convection with forced flow predominating.</u>

(1) S.T. McCOMAS, E.R.G. ECKERT, Trans. A.S.M.E. J. Heat Transfer, 1966, 88, 147-153.

(2) D.Q. KERN, D.F. OTHMER, Trans. A.I.Ch. E., 1943, 39, 517-555.

(3) D.R. OLIVER, Chem. Eng. Sci., 1962, 17, 335-350.

(4) R.C. MARTINELLI, C.J. SOUTHWELL, G. ALVES, H.L. CRAIG, E.B. WEINBERG, N.F. LANSING, L.M.K. BOELTER, A.I.Ch. E.J., 1942, 38, 493-530.

(5) G.A. KEMENY, E.V. SOMERS, A.S.M.E. paper No. 61..WA.161, 1961.

(6) A.R. BROWN, MA THOMAS, J. Mech. Eng. Sci., 1965, 7, 440-448.

(7) R.L. SHANNON, C.A. DEPEW, Trans. A.S.M.E. J Heat Transfer, 1968, 90, 353-357.

(8) B.R. MORTON, J. Me ch Applied Math., 1959, 12, 410-420.

(9) Y. MORI, K. FUTAGAMI, S. TOKUDA, M. NAKAMURA, Int. J. Heat Mass Transfer, 1966, 9, 453-463.

(10) Y. MORI, K. FUTAGAMI, Int J. Heat Mass Transfer, 1967, 10, 1801-1813.

(11) I.T. ALADEV, MA MIKHEEV, O.S. FEDYNSKII, Izv. Akad. Nauk. SSSR, OTN, 1951, 1, 55-67.

(12) B.S. PETUKHOV, A.F. POLYAKOV, B.K. STRIGIN, Heat Transfer - Soviet research, 1969, 1, 24-31.

(13) E.L. RODIONOV, Thermal Eng., 1965, 12, 106-111.

(14) T.W. JACKSON, J.M. SPURLOCK, K.R. PURDY, A.I.Ch.E.J., 1961, 7, 38-42.

(15) J.J. MARTIN, M.B. CARMICHAEL, A.S.M.E. paper No. 55..A.30, 1955.

(16) C.K. BROWN, W.H. GAUVIN, Canad. J. Chem. Eng., 1965, 43, 306-318.

(17) W.T. LAWRENCE, J.C. CHATO, Trans. A.S.M.E. J. Heat Transfer, 1966, 88, 214-222.

(18) T.W. JACKSON, W.B. HARRISON, W.C. BOTELER, Trans. A.S.M.E., 1958, 80, 739-745.

(19) E.R.G. ECKERT, A.J. DIAGUILA, Trans. A.S.M.E., 1954, 76, 497-504.

(20) G.A. KEMENY, E.V. SOMERS, Trans. A.S.M.E.J. Heat Transfer, 1962, 84, 339-346.

(21) J. MADEJSKI, Bull. Acad. Polonaise des Sciences, 1961, 9, 633-637.

(22) G.A. OSTROUMOV, Zh. Tek. Fiz., 1950, 20, 750-757.

(23) C. NARASIMHAN, W.H. GAUVIN, Canad. J. Chem. Eng., 1968, 46, 141-142.

(24) K.C. CHENK, G.J. HWANG, Trans. A.S.M.E. K. Heat Transfer, 1969, 91, 59-66.

(F) The effect on heat transfer of mechanical dissipation.

(1) L.I. KUDRYASHEV, V.M. GOLOVIN, Tr. Kuibyshevsk. Aviats. Inst., 1962, 15, 27-36.

(2) L.I. KUDRYASHEV, V.M. GOLOVIN, Tr. Kuibyshevsk. Aviats. Inst., 1962, 15, 37-45.

(3) V.P. TYAGI, Trans. A.S.M.E.J. Heat Transfer, 1966,88,161-169.

(4) A.H. ERASLAN, W.T. SNYDER, Trans. A.S.M.E.J. Heat Transfer, 1966, 88, 330-331.

(G) Conduction of heat in the heated surface.

(1) V.G. CHAKRYGIN, P.P. SEVERYANINA, Thermal Eng., 1964, 2, 87 - 91.

(2) J.SCHENK, J.M.DUMORE, App.Sci.Res., 1955, 4, 39 - 51.

(H) Separated flows and heat transfer.

(1) A.J.EDE, R.MORRIS, E.S.BIRCH, N.E.L. Report No. 75, 1962, East Kilbride, Glasgow: National Engineering Laboratory.

(2) A.J.EDE, CI HISLOP, R.MORRIS, Proc. I.Mech.E, 1956, 170, 1113 -1126.

(3) A.J.EDE, N.E.L.Report Heat 162, 1958.

(4) A.J.EDE, N.E.L. Report Heat 165, 1959.

(5) E.S.BIRCH, I.W.S. MACKAY, R.MORRIS, N.E.L. Report Heat 142, 1957.

(6) W.H.EMERSON, N.E.L. Report No. 182, 1965.

(7) W.H.EMERSON, N.E.L. Report No. 256, 1966.

(8) E.G.FILETTI, W.M.KAYS, Trans.A.S.M.E.J. Heat transfer, 1967, 89, 163 - 168.

(9) K.M.KRALL, EM.SPARROW, Trans. A.S.M.E.J. Heat transfer, 1966, 88, 131 - 136.

(10) D.D.LANGREN, E.M.SPARROW, Trans. A.S.M.E.J. Basic Eng., 1967, 89, 233 -236.

(11) R.A.SEBAN, Trans.A.S.M.E.J. Heat transfer, 1964, 86, 259 -264.

(12) P.P.ZEMANICK, PhD thesis, Mech. Eng. Dept. University of Pittsburgh, 1968.

(13) R.A. SEBAN, A.EMERY, A.LEVY, J.Aerospace Sci, 1959, 26, 809 - 814.

(14) D.E.ABBOTT, S.J.KLINE, Trans. A.S.M.E.J. Basic Eng, 1962, 84, 317 - 325.

(15) L.M.K.BOELTER, G.YOUNG, H.W.IVERSON, NACA Tech. note No. 1451, 1948.

(16) R.D.MILLS, J. Mech.Eng.Sci., 1968, 10, 133 - 140.

(17) E.O.MACAGNO, T.HUNG, J. Fluid Mech., 1967, 28, 43 - 65.

(18) J.R.LLOYD, E.M.SPARROW, Int.J. Heat Mass Transfer, 1966, 9, 693 - 695.

(19) L.H.BACK, P.F.MASSIER, R.F.CUFFEL, Int. J. Heat Mass Transfer, 1969, 12, 1 - 13.

(20) H.K.LARSON, J. Aerospace Sci., 1959, 26, 731 - 738.

(21) D.R. CHAPMAN, NACA Tech. note TN 3792, 1956.

(22) D.B. SPALDING, J. Fluid Mech., 1967, 27, 97 - 109.

(23) M. WOLFSHTEIN, Int. J. Heat Mass Transfer, 1969, 12, 301 - 318.

(24) G. GRASS, Atomkernenergie, 1958, 3, 328 - 31.

(I) Other topics.

(1) G.W. MORGAN, W.H. WARNER, On heat transfer in laminar boundary layers at high Prandtl number, J. Aeron.Sci., 1956, 23, 937 - 948.

(2) R. SIEGEL, A.H.SHAPIRO. The effect of heating on boundary layer transition for liquid flow in a tube. A.S.M.E. paper No. 53-A-178, 1953.

(3) T.K.SHERWOOD, KA.SMITH, P.E. FOWLES. The velocity and eddy viscosity distribution in the wall region of turbulent pipe flow. Chem. Eng. Sci., 1968, 23, 1225 - 1236.

(4) J.S.SON, T.J. HANRATTY, Limiting relation for the eddy diffusivity close to a wall. Trans.A.I.Ch.E., 1967, 13, 689 - 696.

(5) A.T.POPOVICH, R.L.HUMMEL. Experimental study of the viscous sublayer in turbulent pipe flow. Trans. A.I.Ch.E., 1967, 13, 854 - 860.

(6) E.R.vanDRIEST. On turbulent flow near a wall. J. Aeron. Sci., 1956, 23, 1007 - 1011 and 1036.

(7) S.V. PATANKAR, D.B. SPALDING. Acalculation procedure for heat transfer by forced convection through two-dimensional uniform-property turbulent boundary layers on smooth impermeable walls. Proc. 3rd Internaltional heat transfer conf. I.Mech.E. 1966, 2, 50 - 63.

(8) D.W.HUBBARD, E.N.LIGHTFOOT. Correlation of heat and mass transfer data for high Schmidt and Reynolds numbers. I & E.C. Fundls., 1966, 5, 370 - 379.

(9) P.HARRIOTT, R.M. HAMILTON. Solid-liquid mass transfer in turbulent pipe flow. Chem. Eng. Sci. 1965, 20, 1073 -1078.

(10) H. REICHARDT. Complete representation of turbulent velocity distribution in smooth pipes. Z.Angew.Math.Mech., 1951, 31, 208.

(J) Recent works.

(1) P.P.ZEMANICK, R.S.DOUGALL, Local heat transfer downstream of abrupt circular expansion, Trans.A.S.M.E.J. Heat Transfer 1970, 92, 53 - 60.

(2) YE.P.DYBAN, E.YA.EPIK, Heat Transfer - Soviet research 1970, 2, 11 - 16.

(3) N.V.ZOZULYA, B.L.KALININ, Effect of velocity and turbulent pulsation fields at a plate with a rectangular step, Heat transfer - Soviet research, 1970, 2, 46-50.

(4) J.COSTELLO, Flow and heat transfer processes at abrupt expansions, 1969 PhD dissertion, University of Aston in Birmingham.

(5) H.C.REYNOLDS, T.B.SWEARINGEN, D.M.McELGOT. Thermal entry for low Reynolds number turbulent flow. Trans.A.S.M.E.J. Basic Eng., 1969, 91, 87 - 94.

(6) C.A. BANKSTON, D.M. McELIGOT. Turbulent and laminar heat transfer to gases with varying properties in the entry region of circular ducts. Int.J. Heat Mass Transfer, 1970, 13, 314 -344.

(7) E.J.DAVIS, W.N.GILL. The effects of axial conduction in the wall on heat transfer with laminar flow. Int. J. Heat Mass Transfer, 1970, 13, 459 - 470.

(8) T.MIZUSHINA, F.OGINO. Eddy viscosity and universal velocity profile in turbulent flow in a straight pipe. J. Chem. Eng. Japan. 1970, 3, 166 - 170.

(9) A.E. BERGLES, R.R.SIMONDS. Combined forced and free convection for laminar flow in horizontal tubes with uniform heat flux. Int.J. Heat Mass Transfer, 1971, 14, 1989 - 2000.

(10) D.P.SIEGWARTH et.al. Effect of secondary flow on the temperature field and primary flow in a heated horizontal tube. Int.J. Heat Transfer, 1969, 12, 1535 - 1552.

(11) G.N.FARIS, R.VISKANTA. An analysis of laminar combined forced and free convection heat transfer in a horizontal tube. Int. J. Heat Mass Transfer, 1969, 12, 1295 - 1309.

(12) P.H.NEWELL, A.E.BERGLES. Analysis of combined free and forced convection for fully developed laminar flow in horizontal tubes. Trans.A.S.M.E.J. Heat Transfer, 1970.

(13) A.D.GOSMAN, et.al. Heat and mass transfer in recirculating flows. Academic Press, London and New York (1969.)

(14) B.W.MARTIN, D.FARGIE. Effect of temperature dependent viscosity on laminar forced convection in the entrance region of a circular pipe. Heat and Fluid Flow, 1972, 2, 84 - 93.

(K) General references.

(1) H.SCHLICHTING, Boundary layer theory. 4th edn. McGraw-Hill, New York (1960.)

(2) W.H.McADAMS, Heat transmission. 3rd edn. McGraw-Hill, New York (1954.)

(3) J.G.KNUDSEN, DL.KATZ, Fluid dynamics and heat transfer, McGraw-Hill. New York (1958).

(4) C.C.LIN, Turbulent flows and heat transfer. Oxford University Press (1959).

(5) W.M.KAYS, Convective heat and mass transfer. McGraw-Hill New York (1966).

(6) S.S.KUTATELADZE, Fundamentals of heat transfer, E. Arnold, London (1965).

(7) G.N.ABRAMOVICH. The theory of turbulent jets. M.I.T. press, Massachusetts (1963).

(8) J.A.OWCZAREK. Introduction to fluid mechanics. Int. text-book co. Pennsylvania (1968).

(9) M.R.SHAFER, Performance characteristics of turbine flowmeters. Trans.A.S.M.E.J. Basic Eng., 1962, 84, 471-485.

(10) W.F.Z. LEE, H.KARLBY. A study of viscosity effect and its compensation on turbine type flowmeters. Trans. A.S.M.E. J. Basic Eng., 1960, 82, 717 - 728.

(11) H.M.HOCHREITER. Dimensionless correlation of coefficients of turbine type flowmeters. Trans. A.S.M.E., 1958, 80, 1363 - 1368.

(12) M.R. SHAFER, F.W. RUEGG. Liquid flowmeter calibration techniques, Trans. A.S.M.E., 1958, 80, 1369 - 1379.

(13) P.JEPSON, P.G.BEAN. Effect of upstream velocity profiles on turbine flowmeter registration. NEL report. The National Engineering Laboratory, East Kilbride, Glasgow.

(14) ENGINEERING SCIENCES DATA UNIT, LONDON. Forced convection heat transfer in circular tubes, Parts I, II and III, Item Nos. 67016, 68006, 68007.

(15) G.P.CURME. Glycols. Reinhold publish. corp., New York, (1953).

(16) R.W.GALLANT. Hydrocarb. processing, 1967, 46, 201 - 205.

(17) D.T.JAMIESON, J.S.TUDHOPE, NEL Report No. 435, 1969, East Kilbride, Glasgow: National Engineering Lab.

(18) O.K.BATES, G.HAZZARD, Ind.Eng.Chem., 1945, 37, 193 - 195.

(19) L.RIEDEL, Chemie. Ingr. Tech., 1951, 23, 465 -469.

(20) W.M.KAYS, Compact Heat Exchangers. McGraw-Hill. New York. 1964.